IMPACT OF LIGHTING CONDITIONS ON THE DEVELOPMENTAL PHYSIOLOGY OF ATLANTIC SALMON (*Salmo salar*)

BENJAMIN GREGORY JAMES CLOKIE

July 2017

THESIS SUBMITTED FOR THE DEGREE OF DOCTOR OF PHILOSOPHY

INSTITUTE OF AQUACULTURE, UNIVERSITY OF STIRLING

I. Abstract

The Atlantic salmon (*Salmo salar*) lifecycle is punctuated by distinct ontogenic stages which are routinely manipulated commercially by photoperiod regimes to enable year-round production. As such, light plays a critical role throughout the production cycle, however, it remains poorly characterised and light spectrum and intensity have not been defined optimally yet. This thesis was therefore set out to test the effects of narrow bandwidth light (Blue-$\boldsymbol{\lambda}_{(max)}$ 444 nm, Green-$\boldsymbol{\lambda}_{(max)}$ 523 nm, Red-$\boldsymbol{\lambda}_{(max)}$ 632 nm and White) and intensity in freshwater (FW). Fry-parr development, out-of-season smoltification and ocular and vertebral health were examined as was the long-term effects of FW light regimes on seawater (SW) growth and muscle structure. In addition, the impact of photoperiod regimes on out-of-season smolts following transfer to SW was investigated.

Major findings from the trials conducted show that light spectrum and intensity influence parr development with lower intensities performing better than higher intensities. Both the initiation and duration of smoltification was impacted by spectrum. Importantly, this doctoral work showed that daily changes in light intensity, from low during the scotophase to high during the photophase applied for the duration of a standard out-of-season smoltification regime was capable of providing a sufficient cue for the induction of smoltification. Historic FW light exposure impacted SW performance and post-transfer SW photoperiod had significant impact upon growth and maturation development. Results based on changes to the gonadosomatic index provide important guidance for suitable post-transfer photoperiods for smolt transferred to SW around the winter solstice. Importantly, from the parameters tested, exposure to different spectrum or light intensities did not adversely affect vertebral or ocular health.

This thesis did not only focus on the physiological effects of light but also aimed to characterise better the pathways involved in light perception and integration. To do so, the neural response to both broad spectrum white light, darkness and Red and Blue light was investigated through deep brain insitu-hybridisation and high throughput sequencing (NGS) of the pituitary gland. Results showed substantial spectral and light/ dark changes in the both the deep brain and pituitary transcriptome. Overall, this research provides both scientifically interesting and commercially relevant guidance for the optimisation of lighting systems for use in captive salmon aquaculture.

II. Acknowledgments

I would like to extend my sincere gratitude to my supervisors, Prof Herve Migaud and Dr John Taylor for their patience, support and reasoned arguments throughout this project whose guidance and acceptance of my sometimes leftfield approach has been invaluable. Their contribution to discussions, practical sampling expertise, and considered feedback mean that there is a thesis here to read. I would also like to express my gratitude and thanks to my sponsors Philips Lighting represented by Cristina, Rainier and Michiel whose contribution has been illuminating.

I would like to thank the Reproduction group members past and present for their help, support and endurance during the many, many sampling trips that this project required. Achieving this would not have been possible without the help of Yehwa, Sarah-Louise, Thomas, Robyn, Elsbeth, Lynn, Andrew Preston and Stefano. Reasoned conversations with Dr Andrew Davie, Dr John Taggart and Bernat have proven very helpful and for that I am grateful.

I would like to acknowledge the technical help and guidance with several of the analytical techniques from Dr. John Taylor, Dr Elsbeth McStay, Dr Naomi Brooks and Dr Michael Bekeart.

I would like to extend my thanks to the technical and support staff in particular Brian, Debbie, Fiona, Charlie, Jane and Gillian. I would like to thank those involved in the husbandry aspects of this project, especially Rob, Alastair, John and Iain for their freshwater expertise and Bill, Cam, Andy and Simon for the sea water support. In addition, the help and assistance of Davie, Ken and Ronnie at Ardnish needs to be acknowledged.

The friendship and close support of Marie, Mikey, and Lucas must be celebrated, the importance of scientific discussion in closely related fields should not be underestimated.

The love, support and encouragement of my mum Jill (don’t worry, there are no more muscle fibre pictures to trace) has been immeasurable and for that I am truly grateful.

In addition, Ian's rational guidance and clear headed review has been greatly appreciated. I would like to thank my dad Julian for his reasoned contemplation, encouragement and broad scientific viewpoint not just during this PhD but in life in general. Thanks also to Martha, Ollie and Sam who have endured many conversations about the fineries of aquaculture, analytical approaches and provided considerable encouragement. I also extend my sincere love and thanks to Jane-Ann and Duncan for their support and love throughout this endeavour.

A PhD, is, by its very nature, a truly selfish enterprise. Achieving this enterprise with the support of someone who is selfless has made the selfish possible.

For Jo, Sula and Matilda, whose love and support has been unending.

III. Contents

IV. List of Figures

V. Glossary and List of Commonly Used Abbreviations

AC/DC	Alternating Current / Direct Current
ACTH	Adrenocorticotropic Hormone
Alevin	Hatched salmon egg prior to first feeding
ANOVA	Analysis of Variance
B	Blue
bFCR	Biological feed conversion ratio
BLAST	Basic Local Assignment Search Tool
BW	Body weight
cDNA	Complementary DNA
CFL	Compact Fluorescent Lamp
CG	Compensatory Growth
cGMP	cyclic guanosine monophosphate
Circadian	occurring within a 24-hour period
Circannual	occurring within an annual period
cm	Centimeter
CRF	Coticotropin Releasing Factor
CV	Coefficient of variation
CWT	Coded Wire Tag
DALI	Digital Addressable Lighting Interface
Diurnal	occurring daily
DNA	Deoxyribonucleic acid
DO	Dissolved Oxygen
ELISA	Enzyme-Linked Immunosorbent Assay
FC	Fold change
FCR	Feed conversion ratio
FL	Fork Length
FPKM	Fragments per kilobase of transcript per million mapped reads
Fry	Juvenile salmon from first feeding to 1 g
FT	Flow Through
FW	Freshwater

G	Green
GH	Growth Hormone
GR	Glucocorticoid Receptors
Grilse	Male salmon that has fully matured after 1 sea winter
GSI	Gonadosomatic Index
HPI	Hypothalamic Pituitary
IGF	Insulin-like Growth Factor
igf-1	Immunoglobulin factor -1
INL	Inner Nuclear Layer
ipRGCs	Intrinsically Photosensitive Retinal Ganglion Cells
ISH	*In-situ* Hybridisation
jack	Male salmon that has matured before 1 sea winter
K	Condition Factor
KEGG	Kyoto Encyclopedia of Genes and Genomes
kg	Kilogram
l	litre
$\lambda_{(max)}$	lambda max
LBP	Light-Brain-Pituitary Axis
LD	Long Day
L:D	Light Dark
LED	Light Emitting Diode
LL	Continuous Light
lme	Linear mixed effects model
Mel	melanopsins layer
ml	Milliliter
mlm	Mixed Linear Model
MMERL	Machrihanish Marine Environment Research Laboratory
MPC	Muscle Progenitor cell
MR	Mineralocorticoid Receptor
mRNA	Messenger RNA
Mya	Million years ago
n =	Number of samples

NDR	Natural Daylight Replication
NGS	Next Generation Sequencing
NKA	Na^+-K^+-ATPase pump
NKAe	Referring to the Na^+-K^+-ATPase pump enzyme
NKCC	Na-K-Cl Cotransporter
NL	Netherlands
NLT	Nucleus Lateralis Tuberis
nm	Nanometers
OCT	Optimal Cutting Compound
ONL	Outer Nuclear Layer
Out-of-season	Smolts that are produced out with the timings experienced in the natural lifecycle.
p-value	Probability value set at 0.05
Parr	Juvenile salmon from 1g to smolt
PCR	Polymerase Chain Reaction
pde	Phosphodiesterase
pdf	Probability Density Function
Photophase	Light period of a photoperiodic cycle of light and dark
PIT	Passive Integrated Transponder
PNES	Photoneuroendocrine System
POA	Pre-optic Area
POMC	Proopiomelanocortin
ppm	parts per million
Q1	Smolts transferred to SW in 1st quarter of the year
Q2	Smolts transferred to SW in 2nd quarter of the year
Q3	Smolts transferred to SW in 3rd quarter of the year
Q4	Smolts transferred to SW in 4th quarter of the year
qPCR	Quantitative polymerase chain reaction
R	Red
RAS	Recirculating Aquaculture System
REML	Restricted Maximum Likelihood
Rhythm	Pertaining to an endogenous cycle
RNA	Ribonucleic acid

RPi	Raspberry Pi Computer
S0	Smolt produced ~6 months prior to a natural smolt (S1)
S1	Smolt produced in line with natural photoperiod
SCN	Suprachiasmatic Nucleus
Scotophase	Dark period of a photoperiodic cycle of light and dark
SD	Short Day
SFR	Specific Feed Rate
SI	Smolt Index
Smolt	SW adapted juvenile salmon
SNP	Simulated Natural Photoperiod
SubWin	Subjective Winter induced through a change in light intensity relative to pre-and post smolt induction
SW	Seawater
SWC	Seawater Challenge
Sys	System
TGC	Thermal Growth Coefficient
TH	Thyroid Hormone
TSH	Thyroid Stimulating Hormone
UK	United Kingdom
USA	United States of America
VA Opsin	Vertebrate Ancient Opsin
W	White
W/m^2	Watts per meter square
WS	Water surface
°C	Degrees Celsius
°Days	Degree Days

1 Introduction

1.1 Commercial Aquaculture of Atlantic Salmon

The Atlantic salmon (*Salmo salar* (L.) is an animal of enormous biological intrigue and high economic value. In 2015, culture of this species accounted for 7.3 % of the total value of global aquaculture through the production of 2.25 % of the total tonnage (FAO.org 2017). Production in Scotland contributes 7.2 % to the total global Atlantic salmon production and 8.2% of the value (FAO.org 2017). The Scottish government has set ambitious targets to raise production from 180 000 tonnes in 2015 to 210 000 tonnes by the year 2020 (The Scottish Government 2017). The significant contribution that salmon aquaculture makes to both the rural and export economy are key drivers behind these aims (The Scottish Government 2017). Meeting such targets requires significant investment in developing both scientific and commercial knowledge identified as production bottlenecks (Bostock et al., 2016).

Challenges which currently face the industry can be broadly dissociated into two separate but intrinsically linked factors: salmon biology and production protocol. Balancing the often-complex consumer demands of size, quality, and environmental and welfare considerations, requires considerable control over both factors (Bostock et al., 2016); achieving these goals whilst maintaining economic competitiveness adds a further complexity. A shortage of natural freshwater (FW) and seawater (SW) sites has increased the uptake of land based recirculating aquaculture systems (RAS) (Bergheim et al., 2009; Terjesen et al., 2013). RAS mediates both space and environmental concerns by recycling water and capturing organic waste (Terjesen et al., 2013). RAS offers the ability to manage environmental conditions in a tightly controlled fashion, facilitating the manipulation of salmon physiology to meet specific requirements. Currently, however, very little is known regarding the optimal photic conditions for such systems. As a result, there is clear need to characterise how lighting conditions impact upon the developmental physiology of the Atlantic salmon. As RAS requires considerable capital and ongoing financial commitment, production efficiencies in terms of both energy and productivity must be maximised. The development of physiologically optimised lighting systems offers potential to help achieve these goals.

1.2 Salmon Life cycle

1.2.1 Overview

Atlantic salmon belong to the family Salmonidae and the Teleostei infraclass of the Actinopterygii (the ray-finned fish). Teleost fish, of which there are around ~29000 species, comprise the largest class of the Actinopterygii and account for ~96% of all fish species (Björnsson and Bradley 2007). The native distribution of Atlantic salmon spans from 40 to 70 °N of the North Atlantic Ocean and within the rivers of the associated land masses. (MacCrimmon and Gots 1979). Within these latitudes, a strong photoperiod rhythm is experienced with which the life cycle is broadly synchronised.

Atlantic salmon are found in three forms: anadromous, partly anadromous and non-anadromous landlocked populations. It is the anadromous form which is most important for commercial salmon aquaculture owing to the accelerated growth in SW compared to FW. Anadromous salmon spawn in FW, fertilised eggs hatch into alevins and develop firstly into fry and then parr (Fig. 1.1). Upon attaining appropriate physiological attributes such as length (Skilbrei 1988; McCormick, 2007), somatic status (Duston and Saunders 1995) and genetic disposition (Handeland et al., 2003), environmental stimuli such as photoperiod (McCormick et al., 1987) and water temperature (Jonsson and Rudd-Hansen, 1985) induce smoltification preparing the animal for life in SW. Following smoltification, fish traverse estuarine habitats and reach the sea whereupon a period of rapid growth occurs. In SW a combination of environmental, physiological and genetic factors combine to initiate a return to FW after 1-5 years in order to spawn in natal stream and complete the lifecycle.

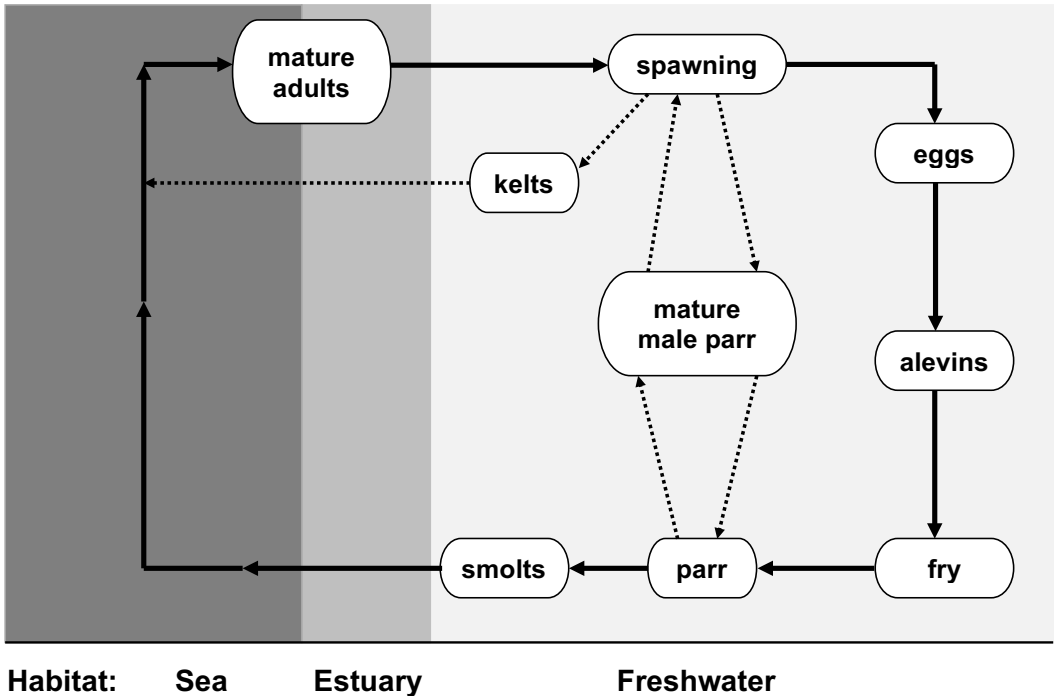

Figure 1.1. Outline of the anadramous natural lifecycle of the Atlantic salmon. Spawning leads to the release of eggs in freshwater (FW). Following hatch, alevins start first feeding and develop into fry (1g), parr (>1g) and remain in FW until smoltification. Fish traverse the esturine envirnoment and mature in seawater before returning to FW to spawn.

1.2.2 Spawning and Freshwater Development

Eggs are deposited in nests, redds, built in the gravel river beds of shallow streams with moderate velocity (Fleming 1996) by sexually mature individuals. Redds feature an indentation within which eggs and milt are deposited whereupon the female covers the contents with gravel using the tail fin. Eggs remain in relative darkness and undergo two distinct metamorphic developments. Progression of development is temperature sensitive and cumulative degree days (°Days), i.e. the number of days multiplied by the mean daily temperature in °C, provides a robust estimation of the timing of development. During an initial period of approximately 220-250 °Days eggs become water hardened and initial embryogenesis occurs. As the pigment of the eye becomes visible, ova are classed as “eyed eggs” and development continues for a further 220-250 °Days (RSPCA 2015). Alevins hatch from the eggs retaining a yolk-sac and remain in the gravel until most of the sac is absorbed (McCormick et al., 1998). During this stage, the alevins are non-feeding. Alevins gradually travel through the

gravel (Leaniz et al., 1993), emerging over a period of a few weeks (Marty and Beall 1989). Light intensity appears to play a permissive role for the emergence of parr and higher numbers leave when light intensity is low (Gustafson-Marjanen and Dowse, 1983; Crisp and Hurley, 1991; Leaniz et al., 1993).

As the yolk sac continues to disappear first feeding starts and alevins become classed as fry. Once fry reach 1 gram, the yolk sac has been completely absorbed and the fish are classed as parr for the remaining duration of FW development prior to the onset of smoltification (Adams 1989). Atlantic salmon parr are aggresivly territorial, defending areas of gravel dictated by the availability of food, substrate characteristics and current velocity (Kalleberg, 1958; Grant et al., 1998). Feeding occurs through visual recognition and parr remain sheltered, darting out to feed (Keenleyside, 1962; Stradmeyer and Thorpe, 1987). As water temperatures drop during winter, feeding changes from crepuscular to nocturnal and parr inhabit crevices which are dimly lit. This adaptation is suggested as a response to increased sluggishness at lower water temperatures which aids predator avoidance (Fraser and Metcalfe, 1997).

1.2.3 Smoltification

The end of parr, which can occur at range of body sizes (Hoar 1988), is marked by the start of smoltification in preparation for survival in SW (Hoar, 1976). Smoltification leads to changes in behaviour; fish become less aggressive and shoaling behaviour replaces the territorial behaviour seen during parr growth (Hoar 1988). Crystalline purines, guanine and hypoxanthine, change the external phenotype improving camouflage for SW (Folmar and Dickhoff 1980). Body length, relative to weight, increases and significant changes in condition factor occur (Folmar and Dickhoff 1980).

Photoperiod and temperature provide the main environmental cues, “zeitgeber”, which initiate this process (Fjelldal et al., 2011). In the Atlantic salmon, photoperiod is considered the major cue (McCormick et al., 1998). Seasonal cues are entrained via annual changes in the duration of the photophase and scotophase. The seasonal change from long to short daylength initiates the process and finalisation occurs in coordinated response to the rising spring photoperiod (McCormick et al., 1998; Mccormick et al., 1987.

Adaptations during smoltification occur temporally (Stefansson et al., 2008) and nutritional status (Duston and Saunders 1995) and size (minimum length of 12-13cm) (McCormick et al., 2007) play important and permissive roles (Kristinsson et al., 1985; Rowe et al., 1991) (Fig. 1.2). Salmon residing in slow growing, high latitude locations can take 4 years to meet such thresholds whereas fast growing, lower latitude fish can undergo smoltification in just 1 year (Wedemeyer et al., 1980; Hutchings and Myers 1994; Thorpe et al., 1998). Smoltification may also be influenced by temperature as photoperiod cues are mitigated below <3 ºC (McCormick et al., 1995) whilst high water temperatures increase the rate and progression of smoltification (Zydlewski 1997).

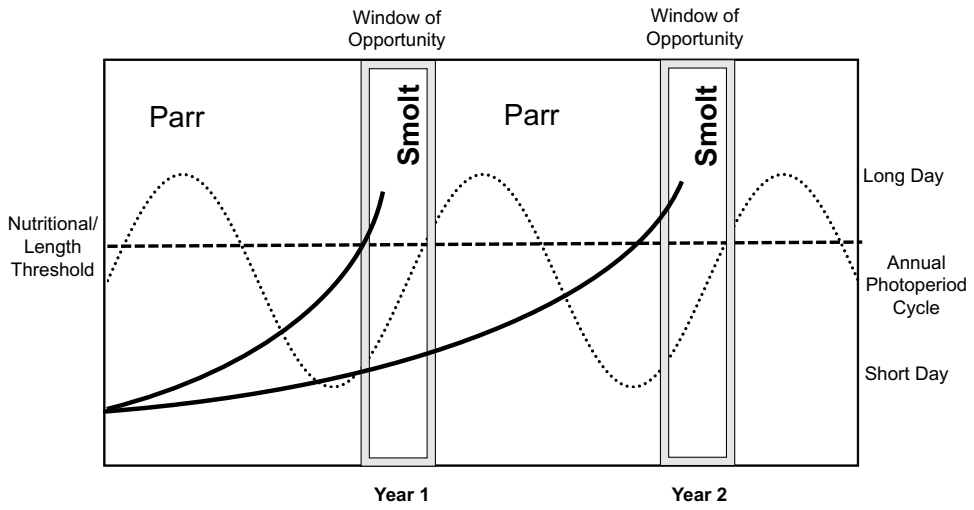

Figure 1.2. Seasonal cycles of long and short day provide a cue with which smoltifcation can be initiated. The decision also requires that nutritional and length (McCormick et al., 2007) thresholds are attained before the smoltification window is entered, failure to do so will result in a delay until the following year.

Smoltification results in structural changes in the brain which lead to the alteration of the endocrine system and initiates the observed behavioural and physiological adaptations (Ebbesson et al., 2011). Feedback mechanisms driven by neuroendocrine and metabolic signalling are thought to direct gated decisions (Duston and Bromage 1988) and 'confirm' readiness to start smoltification. Size constraints may be linked to a direct physical requirement to develop pineal and retinal innervation of the hypothalamus in order to convey photoperiod and endocrine signalling (Ebbesson et al., 2003). Incident light stimulates the light brain pituitary (L-B-P) axis

(Holmqvist et al., 1992; Holmqvist et al., 1994) which develops prior to the phenotypic responses, acting in a permissive manner though enhanced production of hormones that drive downstream cascades (Holmqvist et al., 1994; Holmqvist and Ekström 1995; Holloway and Leatherland 1998). Retinal innervations of the preoptic area (POA), stimulated by day length, relay photoperiod information directly to the brain, stimulating neurogenesis of corticotrophin releasing factor CRF neurons which occurs continually until the corticotropic axis is complete (Ebbesson et al., 2011).

Stimulation by CRF ultimately upregulates cortisol and growth hormone (GH) via the pituitary gland, increasing lipolysis resulting in the characteristic reduction of condition factor (Stefansson et al., 2008). Substantial skeletal remodelling occurs and length increases significantly. During this remodelling, environmental parameters such as low light intensity (Handeland et al., 2013) and elevated temperatures (Fjelldal et al., 2006), may impact the reorganisation leading to vertebral malformation. Energy reserves during smoltification become reduced as lipids and glycogen present in the liver and muscle tissue are mobilised (Sheridan 1989). A reduction in growth similar to that seen during periods of stress is brought about by an increase in circulating corticosteroids (Barton et al., 1985; Dickhoff et al., 1997; Barton 2002) that reduce feed intake and utilisation (Mommsen et al., 1999). As cortisol levels increase towards the end of smoltification, the major hormone involved in FW ion uptake, prolactin, becomes inhibited allowing salts to be excreted in SW (McCormick 2012). Osmoregulation maintains plasma chloride at approximately 130nM in both FW and SW environments (Folmar and Dickhoff, 1981; Arnesen et al., 2003). Osmoregulation is performed by ion transporter cells in the kidney, salt gland and general epithelium, however, it is the gills that play the most significant role (McCormick and Saunders, 1987). Owing to the close proximity to the aqueous environment and high blood flow required for oxygen transportation. (Doyle and Gorecki, 1961) the gills are ideally adapted for this role. SW adaptations in a FW environment are energetically expensive and if seawater is not reached then desmoltification occurs (Hoar 1988; Duston et al., 1991). This period of maximum suitability for reaching SW is known as the smolt window (McCormick 1998) and has been demonstrated to dramatically influence seawater survival (Thorpe, 1994) .

1.2.4 Maturation and Spawning

After reaching SW a period of extended growth occurs before Atlantic salmon become sexually mature. Maturation occurs with considerable plasticity mediated through a range of parameters such as growth rate (Hutchings and Jones., 1998), genetic disposition (Garcia de Leaniz et al., 2007) and environmental influences (Thorpe 2007). Such plasticity results in a wide range of body sizes and year classes breeding during each spawning season, increasing genetic variation of the offspring (Johnstone et al., 2013). Salmon return to their natal streams in order to reproduce and spawn. Photoperiod plays a significant role in the timing of the onset of gametogenesis and subsequent egg maturation. In direct opposition to the onset of smoltification, initiation occurs through an increase in daylength seen during January to April whilst the decreasing photoperiod during October to December leads to completion of gametogenesis and spawning (Taranger et al., 1999; Pankhurst ad Porter., 2003).

Female maturation requires significant basal somatic reserves, limiting early maturation (Gjerde 1984). Conversely, male maturation exhibits considerable plasticity. Male parr may become sexually mature, “precocious”, in FW, returning to the original spawning sites without ever going to sea (Buck and Youngson 1982; Myers et al., 1986). Sperm in precocious parr is viable and mating may occur directly with large anadromous females (Hutchings and Myers 1994) or through “sneaking”, gazumping larger males (Jones and King 1952). Such behaviour is suggested to help maintain genetic fitness through cross generational breeding (Johnstone et al., 2013). Maturation in males may also occur immediately after reaching seawater, becoming jacks and returning to the natal streams after a short period (Duston and Saunders, 1997). Finally, fish that have been at sea for one seawinter may also mature, becoming grilse and returning early in comparison to generational cohorts. Seasonal cues synchronise the main female and male spawning run to coincide with high spring and autumn water volumes, facilitating access over barriers such as waterfalls as fish return to natal streams (Jensen et al., 1986).

1.2.5 Photoentrainment

Photoentrainment, driven by photoperception, thus plays a significant role in each developmental stage of the Atlantic salmon. In temperate regions, the area between the polar circles and the tropics, daylength fluctuates with strict annual rhythmicity.

The seasonal change in daylength (Fig. 1.3) provides a proximate environmental cue for the timing of physiological adaptations such as smoltification (Hoar 1976) and breeding and spawning (Bromage et al., 2001; Pankhurst and Porter, 2003) allowing the greatest chance of survival (Sumpter 1990). In addition to annual rhythms, daylength (Bjornsson et al., 1989) and photoperiod history play important permissive roles with the contrast between long and short and short and long days initiating different developmental changes.

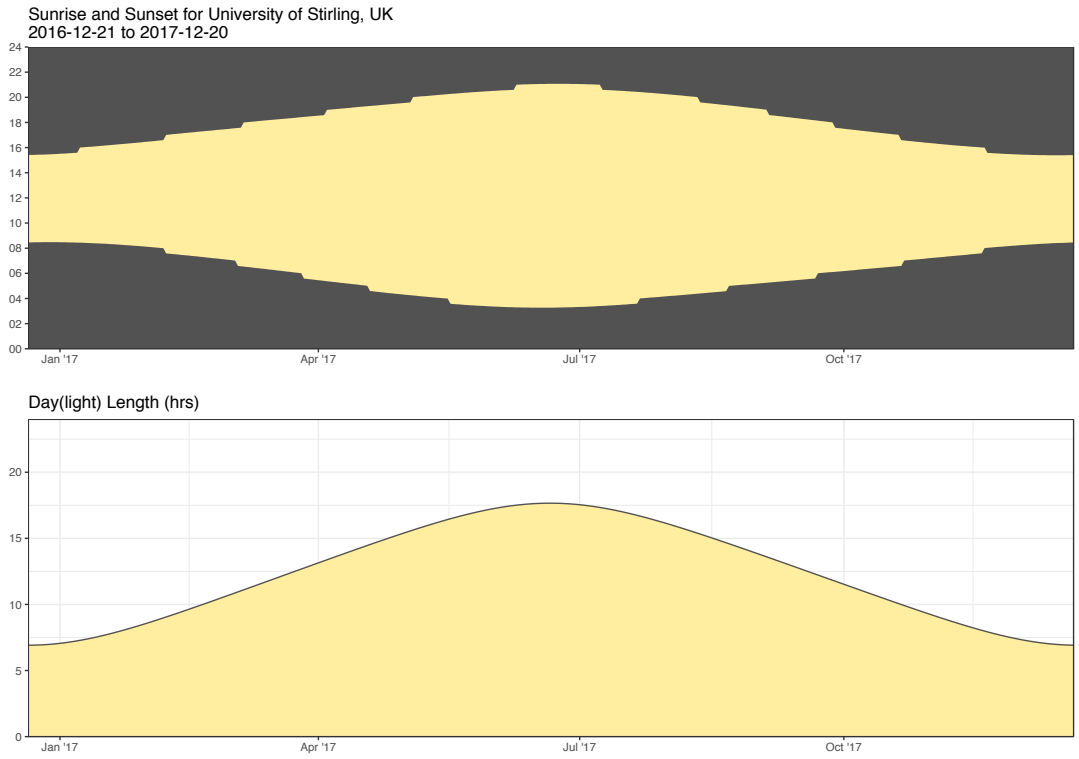

Figure 1.3. Annual changes in daily photoperiod occur in a predictable manner each year.

1.3 Properties of light and Photoperception Physiology

1.3.1 Light

The detection of light, which drives photoentrainment, occurs when incident light falls upon specialised cells, photoreceptors, which initiate phototransduction pathways. Light is generally referred to as the visible portion of the optical spectrum, defined as the section of the electromagnetic spectrum that obeys the laws of optics (Douglas and Djamgoz 1990) and which spans from ultraviolet to infra-red. The wavelength of

visible light ranges from 380 to 740 nanometres (Fig. 1.4) (Douglas and Djamgoz 1990). Light is composed of photons which can vary in both wavelength and energy dictating the colour and intensity perceived by the eye (Nicol 1989).

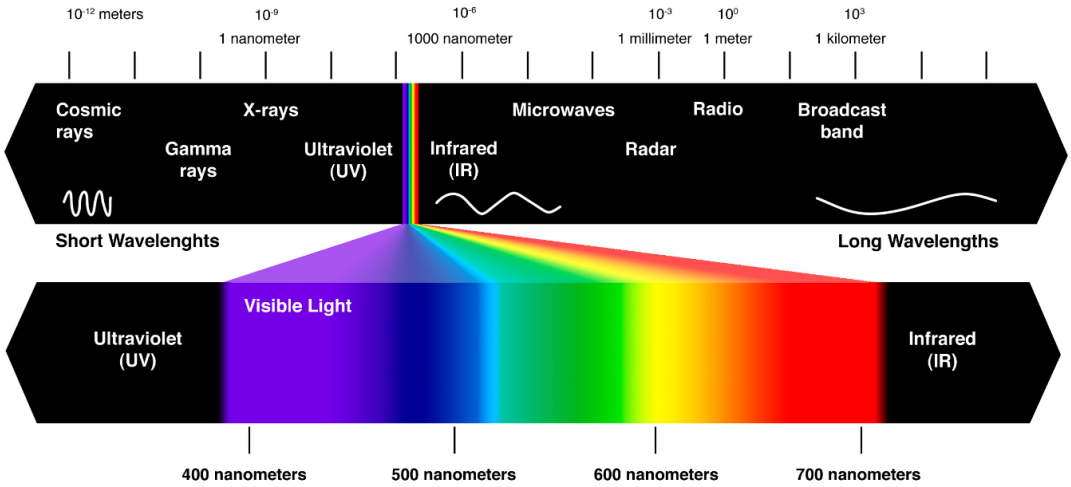

Figure 1.4. The optical spectrum represents a portion of the electromagnetic spectrum. The visual spectrum sits within this range from ~380 to 740nm. (image source: GlobalSpec.com 2017)

1.3.2 The Underwater Photic Environment

Light transfer through the atmosphere and the water column are broadly homologous and highly complex (Douglas and Djamgoz 1990). Solar radiance from the stars and moon travels through the atmosphere where it is subjected to scattering and absorption which, dependent upon its wavelength and path, becomes attenuated and loses some of its intensity (Douglas and Djamgoz 1990). The distance of the path affects the attenuation, as does the wavelength. Shorter wavelengths are subjected to greater scatter and reduced intensity (Monteith and Unsworth 2013). Although attenuation is experienced, many scattered photons still reach the earth's surface. The loss in intensity through the earth's atmosphere is highly variable depending on environmental conditions and this is the same in aquatic environments. In addition, the underwater photic environment is also influenced by both the angle of incident light and surface undulations which reflect a portion of the light back from the surface. Some light however travels into the water, becoming refracted giving rise to a compressed field of view of 48.5 degrees under perfect conditions according to Snell's law (Douglas and Djamgoz 1990). The impact of Snell's law is to create a dark

surround out with this angle whereby light received is reflected back into the water column which increases prey detection for aquatic organisms (Lythgoe 1972).

The absorption coefficient, dictated by wavelength, results in longer and shorter wavelengths being absorbed more readily and travelling shorter distances (Douglas and Djamgoz 1990). As light penetrates water, suspended materials may also influence spectrum; gilven, a common degradation product from plants reduces blue light through absorption (Hoge et al., 1995).

One of the challenges in reviewing published literature is the use of measurement units for light intensity. Many studies have used lux as a unit for determining light intensity (e.g. Hansen 1989; Oppedal et al., 1997; Johnston 2003). Lux, however, is a measurement of light in the visible spectrum weighted to the sensitivity of the human eye rather than a measurement of physical power. The weighting is referred to as the luminosity function. Lux meters are also not designed to detect light in the ultraviolet or infra-red spectrum, both of which are known to be perceptible to aquatic organisms (Sontag 1971; Douglas and Djamgoz 1990; Sabbah et al., 2013). Interestingly the very use of lux for mammalian studies is starting to be questioned as recent literature on mammalian photoreceptors suggest sensitivities to wavelengths not previously considered (Lucas et al., 2014). Using a photometric unit for measuring irradiance such as Wm^{-2} is more appropriate when trying to characterise the power being received by the subject. Comparing values of lux with values of W/m^{-2} is far from easy as the conversion between photometric to radiometric units requires the exact wavelength profile of the light to be known in order for appropriate weighting to be given to each wavelength. It is thus challenging to cross compare published intensity information in the field due to environmental and technical differences.

1.3.3 Photoreceptive Tissue

Incident light of sufficient intensity acts upon photosensitive cells to drive two distinct, but mechanistically similar, receptor networks involved in visual and non-visual processes (Peirson et al., 2009) (Fig. 1.5). The eye is the sensory organ where visual perception occurs. Unparalleled in evolutionary complexity (Lamb 2013), the eyes pass information regarding absorbance and reflectance to the brain. Between 600 and 500 Mya the chordate eye went through its most profound developments in terms of body plan (Erwin et al., 2011) resulting in a structure highly conserved within all extant

jawed vertebrates (Lamb 2013) featuring high numbers of localised photoreceptors. The development of the eye is linked to the 'Cambrian explosion', (Parker 2011; Lamb 2013). Interestingly, the development of extraocular muscles and a lens proceeded the development of the photosensitive retina as highlighted by the similarities between invertebrate and vertebrate vision (Lamb 2013). Lenses, extraocular muscles and a mechanism for controlling aperture are common in all extant vertebrates (Pat et al., 2005).

Unlike mammals and birds, fish lack palpebra (Ferguson et al., 1989). Instead melanin granules and positional shifts of photoreceptors help to mitigate the impact of incident light (Ferguson et al., 1989). Susceptibility to retinal damage however is high (Vera and Migaud 2009). In humans, long term exposure to short wavelength light has been shown to induce ocular damage (Taylor et al., 1992) however in salmon the retina is capable of significant regeneration throughout the life cycle via the differentiation of stem cells which repair damage and facilitate ocular growth (Fernald 1985; Johns and Easter, 1977). Photoreceptor cell bodies form the outer nuclear layer (ONL) and processing neurons such as bipolar cells, Muller glia and amacrine cells form the inner nuclear layer (INL). Regeneration originates from cone pre-curser stem cells within both the INL and the ONL. INL progeny undergo mitotic division before migrating into the ONL to replenish rod precursor populations (Julian et al., 1998). Pluripotent circumferential germinal zone cells residing in the retinal margin provide additional replacement retinal cell types (Vera and Migaud 2009) whilst multipotent Muller glia cells provide replacement retinal neurons (Bernardos et al., 2007).

In contrast to ocular perception, non-ocular perception entrains oscillating circadian clocks with daily and seasonal information to facilitate the timings of physiological responses (Falcón et al., 2010; Migaud et al., 2010). In mammals, non-visual photoperception occurs in specialised intrinsically photosensitive retinal ganglion cells (ipRGCs) which comprise around 1-5% of the ocular photoreceptors (Bellingham et al., 2006; Schroeder and Colwell 2013; Lucas et al., 2014). ipRGCs feature melanopsin which has a rhabdomeric structure phylogenetically and structurally closer to the opsins found in invertebrates (Hattar et al., 2002). Phototransduction cascades occur through depolarisation rather than hyperpolarisation (Lucas et al., 2014) and photoentrainment is achieved through prolonged responses to high intensity and duration (Peirseen et al., 2009). ipRGCs project into all major retinorecipient brain areas including the olivary pretectal nucleus,

the neural area responsible for pupil reflex (Baver et al., 2008) and the hypothalamic suprachiasmatic nucleus (SCN), stimulating central pacemaker clocks regulating processes to a circadian and circannual level (Yau and Hardie 2009).

Whereas the network of non-visual photosensitive cells within higher vertebrates is reasonably well described, organisation within lower vertebrates such as the teleost fish species is considerably more diverse. Work by Whitmore et al., 2000 and Kaneko et al., 2006 identified that almost all tissues, from whole blood to the heart, possess fully photoentrainable circadian pacemakers. Exposing immortal cell lines derived from a variety of tissues to prolonged dark periods results in an arrhythmic expression of key circadian genes (Whitmore et al., 2005). However, a short pulse of light, 15 minutes, is capable of resynchronising all cells such that a clear circadian rhythm can be observed. In addition to the circadian clock genes, a range of other genes involved in DNA repair, mitochondrial function, heme metabolism and oxidative stress are also demonstrated to be strict circadian transcriptional control (Gavriouchkina et al., 2010; Weger et al., 2011). Zebrafish circadian regulation can be demonstrated prior to the formation of any neural cells in the developing larvae suggesting that the traditional model of neural regulation of circadian rhythmicity is incomplete (Whitmore et al., 2000).

Despite responses being clearly demonstrable, identifying the photopigment by which the detection occurs is not (Davies et al., 2015). To date 42 distinct genes have been described in zebrafish involved in photodetection, 10 classical visual photopigments and 32 non-visual opsins. Analysis of the elctrophysical and spectral responses demonstrate that these newly described opsins form functional photopigments with specific and unique chromophore binding and wavelength specific behaviour (Davies et al., 2015). Identifying how these photopigments interact with the circadian machinery and how the circadian machinery interacts across an organism is an active area of research (Davies et al., 2015). Non-visual photoperception is clearly highly complex and significantly more complicated than traditional models suggest. The discovery in zebrafish suggests that similar diversity may be found in other less well described vertebrate species.

Elucidating the physiological function of photopigments is also challenging. Exposure of zebrafish fertilised eggs and the corresponding larvae to narrow bandwidth light can dramatically influence development (Villamizar et al., 2014). Exposure to blue and purple light has been shown to lead to increased growth and

elongation whereas exposure to red light leads to significantly reduced growth and the proliferation of deformities (Villamizar et al., 2014). Recently specific neurotransmitters have been attributed to distinct brain regions (Hang et al., 2016), if stimulation of these regions is spectrally selective then understimulation through the use of narrow spectrum light may induce such changes in growth characteristics. A relationship between photopigment specificity, opsin stimulation and subsequent initiation of biological pathways thus seems likely although is still hypothetical (Villamizar et al., 2014). In the Atlantic salmon, the characterisation of spectrum and development is currently unknown however such interactions have particular pertinence for production in captive systems where artificial lighting is used, especially given the limited spectral range of LED lighting.

Current understanding of non-visual photoperception in salmonids is built around a model of a broad range of loosely interconnected photoreceptive units such as the pineal complex (Falcón et al., 2010; Migaud et al., 2010), the deep brain (Hang et al., 2016), saccus vasculosus (Nakane et al., 2013) and the dermis (Chen et al., 2014), in addition to the retina (Philp et al., 2000). Some of these tissues have a significant distance for light to travel before stimulation of the receptors occurs. This raises important questions regarding what light intensities are required to deliver the entrainment of photoperiod and stimulate development.

1.3.4 Photon Capture and Receptor Physiology

Two broad classes of photoreceptors exist, classified by the manner in which they were formed: ciliary (C-type) and rhabdomeric (R-type) (Lamb 2013). Photon capture, regardless of type, is remarkably conserved. Opsins are bound to the membranes of a series of disks within the outer segment of the photoreceptor. Formed from a 348 amino acid peptide chain arranged in a 7 alpha helix structure the opsin traverses the lipid bilayer. Embedded on the 296th amino acid is a prosthetic group formed from an aldehyde of vitamin A bound via a Schiff base linkage (Palczewski et al., 2000). The aldehyde, termed chromophore, has different structures dependent upon whether it was derived from vitamin A1 or A2. The major chromophore in visual photoreception is 11-cis retinal derived from vitamin A1. In non-visual photoperception and in invertebrates 3-dehydroretinal, a vitamin A2 derivative is the predominant chromophore (Tombran-tink and Barnstable 2008).

Incident light provides energy for the conversion of 11-cis retinal to an all-trans form which after repeated stimulation changes the alpha helix structure at the 5^{th} 6^{th} and 7^{th} helix. The conformational change opens a pocket enabling the catalysation of transducin which is held in close proximity on the membrane (Arshavsky et al., 2002). The activated opsin catalyses the alpha GDP subunit on the transducin molecule to alpha GTP causing it to dissociate. Several hundred transducin molecules can be catalysed via a single activated opsin offering considerable amplification. Alpha GTP interacts with the effector molecule phosphodiesterase (PDE) by binding to two gamma subunits on the PDE. The remaining alpha and beta subunits, now activated, break down cyclic guanosine monophosphate (cGMP) into 5'-GMP (Bowler et al. 1994).

In an inactivated state, cGMP maintains receptor membrane bound cyclic nucleotide-gated ion channels (CNG) open by binding to the four subunits surrounding the channel. Binding allows Ca^{++} and K^{+} ions inside the cell. The production of cGMP by a dimer of guanylate cyclase protein converts GTP into cGMP and regulates CNG activity in the resting cell. Regulatory control over guanylate cyclase occurs via guanylate cyclase activator proteins (GCAP). Ion transfer though the CNG combined with NaK/ATPase pumps in the inner segment and membrane bound Na^{+}/Ca^{+}-K^{+} exchangers (NCKX) channels maintain a negative basal membrane potential (Fig. 1.6) (Arshavsky et al., 2002).

The arrival of light closes the CNG as described, preventing the influx of Ca^{++} and K^{+} ions leading to hyperpolarisation. Hyperpolarisation inhibits the release of the neurotransmitter glutamate in a graded response to light (Tombran-tink and Barnstable 2008). Glutamate signaling stimulates the bipolar cells and removal leads a signal transduction cascade whereby ganglion cells interact with myelinated axons giving rise to series of action potentials (Arshavsky et al., 2002). The amplitude and frequency convey signal strength to the requisite processing centres in the brain. Deactivation of the photoreceptor requires the phosphorylation of the opsin molecule followed by the binding of an arrestin protein. Transducin also requires deactivation and it is catalysed by the enzyme regulator of G-protein signaling 9 (RGS9) which hydrolyses the alpha GTP subunit so that it can rebind to the transducin molecule (He et al., 1998).

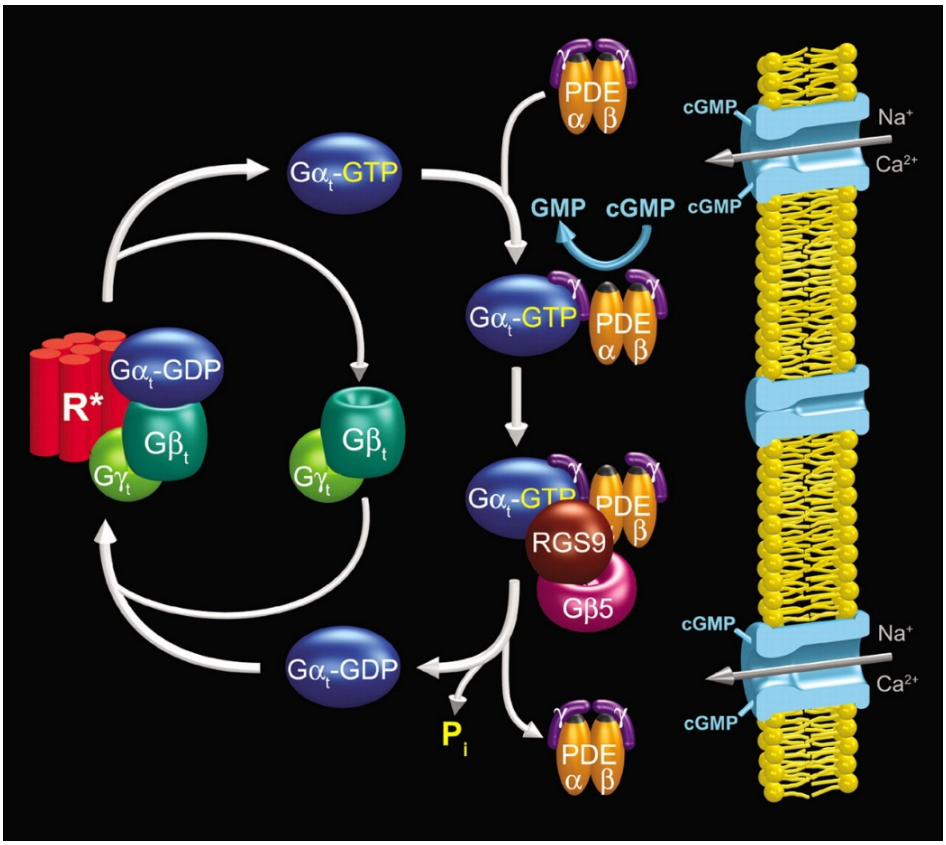

Figure 1.5 G-protein activation and inactivation. Activated rhodopsin (R*) rapidly exchanges the GDP on the bound $G\alpha_t$ transducin molecule which dissociates. $G\alpha_t$-GTP activates the phosphodiesterase (PDE) by binding to the gamma subunits which had previously inhibited the catalytic ability by binding to the catalytic site. Activated PDE reduces cytoplasmic cGMP concentration causing the closure of the CNG channel, reducing the flow of Na^+ and CA^{++} ions into the cell and inhibiting glutamate production at the photoreceptor terminal. Binding of RGS9 and Gβ5 deactivates the transducin molecule by releasing a phosphate group allowing transducin to become available again. (Figure from: (Arshavsky et al., 2002)

1.3.5 Spectral Sensitivity

Photoreceptor sensitivity, the lambda max, is derived from the amino acid arrangement of the opsin and the chromophore group (Douglas and Djamgoz 1990). Vitamin A1 derived chromophores have a double bond in the carbon ring which results in a longer lambda max compared to 3-dehydroretinal (Mehta and Cheng 2013). The chromophore also influences sensitivity through the regeneration pathways. Converting all-trans retinal to the 11-cis form occurs via the retinoid enzymatic

pathway in neighbouring cells, a slow process that can lead to bleaching of the photoreceptor due to a lack of naive 11-cis retinal (Chellappa et al.,, 2014). 3-dehydroretinal is regenerated in-situ by additional incident light (Isoldi et al., 2005; Panda et al., 2005) which can result in a bistable photopigment regenerated through long-wavelength light (Mure et al., 2009). This adds an extra level of sensitivity as the opsin can interact with different signalling pathways in either state, allowing greater spectral discrimination to occur (Piersen et al., 2006).

Initial investigations regarding visual spectral sensitivity in vertebrates was centred around behavioural studies (Walls 1942). Visual acuity is determined by the proportion of short wave sensitive (SWS), medium wave sensitive (MWS) and long wave sensitive (LWS) opsins (Beatty 1966; Folmar and Dickhoff 1981). Environmental photic conditions likely dictate spectral sensitivities (Karakatsouli et al., 2007; Vera et al., 2010; Shcherbakov et al., 2013) which may change depending upon ontogenic stage (Lamb 2013) and time of year (Fraser and Metcalfe 1997). In addition, feeding strategy, nocturnal, diurnal or crepuscular leads to adaptations that are highly specialised (Shcherbakov et al., 2013). Adaptation to a particular mechanism of feeding may come at the cost of reduced sensitivity of other detection parameters (Ullmann et al., 2011). Fish residing in FW are generally reported to be more responsive to red and yellow light whereas heightened blue sensitivity is reported in SW species (Levine and MacNichol 1979). In 1959, a series of experiments examining spectral sensitivity of Atlantic salmon using electrophysical techniques was published observing the position of retinal elements in response to different spectra deriving spectral sensitivity to range between 364 and 690 nm (Ali 1959).

In addition to the visible spectrum some species may be able to detect other parts of the optical spectrum. Atlantic salmon are predicted to detect UV due to the presence in early ontogeny of UV sensitive (UVS) corner cones (Harosi and Hashimoto 1983; Bowmaker and Kunz 1987; Parkyn et al., 2000) that form a double-cone structure with the membranes acting as a dichroic mirror (Randall 1988). UVS cones are replaced with blue sensitive cones as fry grow suggesting a shift from tetrachromic to trichromic vision (Kamermans and Hawryshyn 2011). Changes are linked to differences in feeding mechanisms between FW and SW (Hawryshyn et al., 2010). Polarised light may also be able to be detected by some species though linear dichroism (Kamermans and Hawryshyn 2011). Initially, it was thought that the apparent random orientation of teleost retinal receptors prevented such sensitivity,

however, Roberts and Needham (2007) successfully used laser tweezers to manipulate medium wavelength sensitive (MWS) cones in goldfish (*Carassius auratas*) to initiate a polarisation response. Polarised perception may increase edge definition, de-blurring and the removal of redundant information (Flamarique and Browman 2001; Kamermans and Hawryshyn 2011). Changes in ontogenic retinal architecture may suggest that lighting requirements change during different ontogenic stages to ensure appropriate development and consideration must be made to these if culture occurs out with natural systems.

1.3.6 Photoneuroendocrine System

A multitude of physiological responses are initiated and mediated through the photoneuroendocrine system (PNES) (Scharrer 1964; Migaud et al., 2010). Salmon development, as discussed, is highly responsive to daily and seasonal photoperiodic changes (Duston and Saunders 1992). Following assimilation of photoreceptor signals in the hypothalamus, hypothalamic neurons either terminate in close proximity to or make direct synaptic contact with pituitary adenohypophysial cells, releasing secretions that act upon the pituitary and stimulate downstream pathways (Mayer et al., 1997). Neurosecretion may also reach the adenohypophysis through the vascular plexus of the neurohypophysis representing a dual stimulatory mechanism of vascular (indirect) and neural (direct) connection (Falcón et al., 2010). However, evidence is controversial due to the lack of median eminence-like primary plexus connecting to a portal vein as seen in mammals. Synchronisation of photic entrainment is proposed to be under locally produced autocrine control of melatonin (Falcón et al., 2010). At least four areas have been identified that receive pineal and retinal information in the diencephalon contributing to the regulation of pituitary output in response to photic information: the SCN, lateral tuberal nucleus, ventromedial thalamic nucleus and the rostral pre-optic area highlighting the complexity of the neural networks involved.

A major component of the PNES is the pituitary gland which is involved a wide range of endocrine responses including the Hypothalamic-Pituitary-Interrenal (HPI) axis (Bernier and Peter 2001). Stimulation of the HPI leads to the initiation of a hormonal cascade whereby corticotrophin releasing factor (CRF) from the hypothalamus stimulates the upregulation of a multipeptide prohormone, pro-opiomelanocorticotropin (POMC) (Madaro et al., 2015). Post-translational modification

cleaves POMC into adrenocorticotropic hormone (ACTH) which leads to enhanced cortisol production by the interrenal gland. Cortisol forms a powerful corticosteroid, binding to both mineralocorticoid (MR) and glucocorticoid (GR) receptors (Jiao et al., 2006). Cortisol is a major component of the stress response that occurs during exposure to adverse conditions (Pankhurst 2011) and its integration with the PNES means a natural collaboration whereby adverse photic conditions can directly stimulate ACTH production and cortisol release.

1.3.7 Melatonin Signalling

The major timekeeping hormone in vertebrates is considered to be melatonin and production occurs in a rhythmical response to light and dark (Klein et al., 1981; Collin et al., 1986). Multiple physiological changes are associated with increased melatonin level such as food intake, skin pigmentation, shoaling and vertical migration, osmoregulation (Falcón et al., 2010; Migaud et al., 2010; Ekstrzm and Meissl 1997). Plasma and cerebrospinal melatonin originate in the pineal gland where specific pineal opsins are found (Mano and Fukada 2007). Production also occurs in the deep brain and retina (Falcón et al., 2003) where it is thought to act as a paracrine agent. Its stimulatory effect appears to be wide ranging with receptors found in an array of brain tissues involved in information receiving and integration such as the telencephalon, diencephalon, cerebellum and olfractive bulbs (Falcón et al., 2010). The diencephalon may be directly photosensitive as opsins, transducin and arrestin, are all present (Falcón et al., 2010).

Regulation is well described (Klein 2009). The amino acid tryptophan is taken up by the pineal gland where enzymatic hydroxylation produces hydroxytryptophan which in turn undergoes decarboxylation. The resultant product, serotonin is converted to N-acetylserotonin by the enzyme arylkylamine N-acetyltransferase (AANAT). Hydroxyindole-O-methyltransferase (HIOMT) completes the final conversion to melatonin (Falcón 1999). Ca^{++} and cAMP accumulate during the night period and receptor depolarisation leaves voltage gated Ca^{++} channels open (Falcón 1999). Ca^{++} and cAMP phosphorylate, and increase, AANAT2 activity which in turn increases the production of melatonin (Falcón et al., 2001). In response to light, pineal photoreceptors are hyperpolarized and cAMP and gated channels are closed. Inhibition is dose dependant (Migaud et al., 2006) and spectrum may play a role as

seen in the rainbow trout (*Oncorhynchus mykiss*) which is highly sensitivity to short wavelengths (Max and Menaker 1992). Feedback control in teleost fish species is poorly understood, however, local neurotransmitters / neuromodulators such as adenosine and γ-Aminobutyric acid (GABA) which have been related to specific clusters of photoreceptors in the deep brain (Hang et al., 2016), alternatively glucocorticoids or sex steroids (Falcón et al., 2010) may play a role.

1.3.8 Clock Genes

Diurnal rhythms stimulate a heterodimer molecular feedback loop that drives an oscillating internal circadian clock in concert with melatonin to entrain time (Darlington et al., 1998; Davie et al., 2009). Light dependant expression of clock genes and the resultant products instigate an auto regulatory feedback loop driven by transcription and translation (Darlington et al., 1998). An estimated 10% of all mammalian genes are under pacemaker control in peripheral tissues (Reppert and Weaver 2002). Two repressors, PER and CRY and two activators BMAL and CLOCK drive the expression of, amongst other genes, *Aanat2*. By transcribing *Aanat2* into mRNA during the day and early evening transcripts are available for rapid AANAT production at the onset of true night (Reppert and Weaver 2002). In the morning, the clock is reset and AANAT activity is inhibited. Atlantic salmon exposed to short day and long day lighting produce differing levels of expressed clock genes in direct response to the lighting schedule (Davie et al., 2009). Despite circadian regulation being well described, the mechanism by which photoperiod history and circannual rhythmicity are perceived are presently not understood. Understanding such mechanisms is an active area of research with particular relevance to commercial aquaculture production (Migaud et al., 2010).

1.4 Commercial Application of Light

Photoperception and photoentrainment have clear and significant impacts upon salmon physiology. The commercial production of Atlantic salmon utilises supplementary light throughout the production cycle in order to manipulate physiology and provide the market with fish of desirable size year-round (Fig 1.7). Given this importance, surprisingly little is known regarding the detailed parameters of photic conditions throughout the production cycle in terms of both spectrum and intensity during each ontogenic stage.

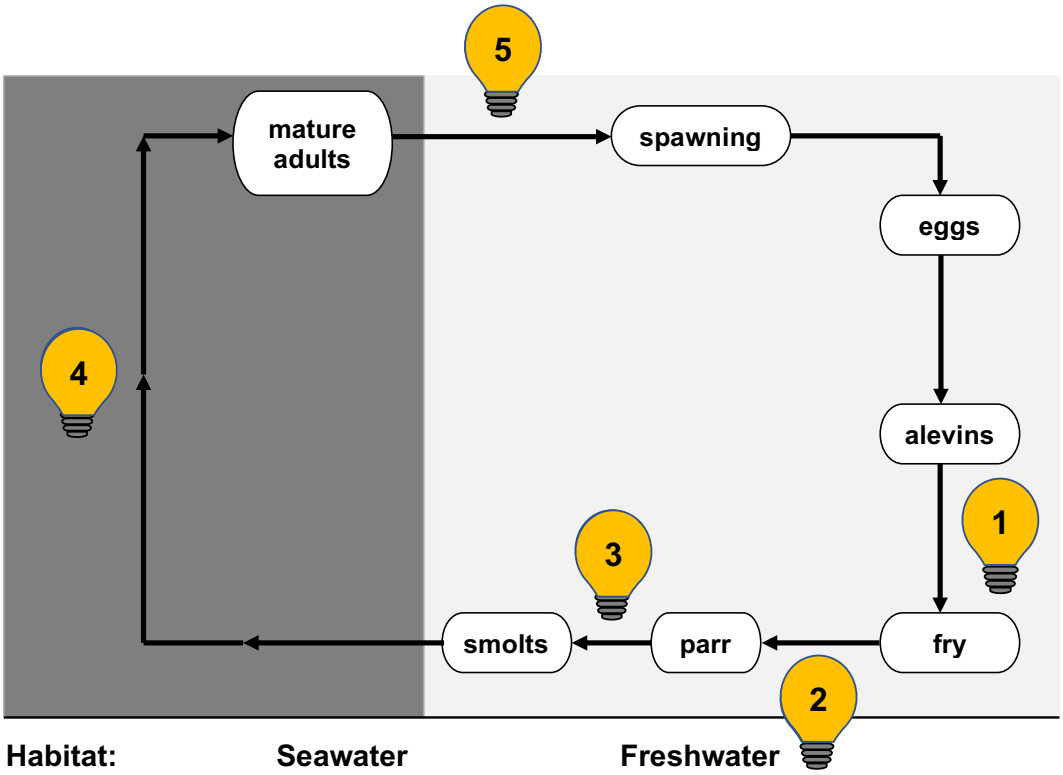

Figure 1.6. Stages of commercial salmon production in which supplementary lighting may be utilised in order to manipulate physiological traits. Growth enhancement during alevin to fry (1) and fry to parr (2). Photoperiod manipulation for the progression or retardation of smoltification and the control of parr maturation (3). Growth enhancement and maturation control in SW (4 and 5).

1.4.1 Captive Freshwater Production

During early freshwater production, supplementary lighting may be applied to alevins through to the end of parr development. LL enhances growth rates resulting in nutritional and size (e.g. 40g+) thresholds being attained earlier than in ambient conditions. Maximising growth rates ensures fish are suitable for inducing smoltification both in and out of phase with ambient conditions (Bergheim et al., 2009). Currently, the impact of spectrum and intensity on FW parr growth are unknown, identifying optimal photic conditions may have potential to achieve benefits in growth.

During FW, fish are graded with larger fish separated for out-of-season smolt induction using an artificial photoperiod regime. Induction protocols manipulate day length and photoperiod history in order to induce smoltification. Smaller cohorts are retained on an ambient photoperiod. The photoperiod cue, whether replicating

ambient conditions or advancing seasonal adaptations is typically provided through artificial light sources. During the infancy of commercial production smolts were produced at 6 month advances or delays relative to the natural cycle (S1) leading to S0+, S1, S1.5, S2 and S2.5 (Bergheim et al., 2009). However, photoperiod manipulation and modern production systems are reshaping supply, enabling year-round smolt production to meet customer demand (Bergheim et al., 2009). Smolts may thus be characterised by the quarter of the year in which they are stocked i.e. Q1, Q2, Q3 and Q4 (Personal comms Dr J Taylor).

Out-of-season regimes are applied when water temperature is elevated relative to spring conditions via ambient river water in flow through (FT) or artificially with recirculating aquaculture systems (RAS). Progression is measured in degree days, (ºDays) resulting in the photoperiod being compressed relative to that which occurs within natural conditions. Provision of the short day (SD) photoperiod must present an abrupt shift relative to the long day (LD) photoperiod (Taranger et al., 1998). An appropriate short day (SD) cue can be achieved using a LD12:12 photoperiod for 400 ºDays (Duncan and Bromage 1998). Returning fish to a long day photoperiod (e.g. LL) initiates the completion of SW adaption which occurs after a further ~400 ºDays (Duncan and Bromage 1998). Smolt production protocols must achieve a homogenous response within the population to ensure optimal post-transfer performance (Duston et al., 1991). Both sub-optimal SD cue (Duncan and Bromage 1998) and post-SD duration (Handeland et al., 2003) can lead to desynchrony, compromising post-transfer smolt performance (Sigholt et al., 1998; McCormick et al., 1999).

Smoltification is thus a critical stage in the commercial production of salmon. As discussed, optimal light conditions are currently poorly characterised. Protocols must ensure a suitable cue for initiation of a synchronised smoltification response occurs. In addition, it would be useful to identify parameters for both the photophase and scotophase. Production must occur predictably and if possible the smolt window should be as long as possible. Intriguingly, the impact of spectrum and intensity on these changes and the duration of the smolt window in RAS salmon smolts is currently uncharacterised. Understanding such parameters would provide vital guidance for industrial FW production protocols.

1.4.2 Controlling Maturation During On-growing

Following successful smoltification fish are transferred to SW for on-growing. Depending upon the time of year transfer occurs, fish will typically be harvested after one, or two, seawinters. Farmed salmon generally start to initiate puberty after 12 to 18 months in saltwater when a body size of 2 to 5kg is reached (Taranger et al., 2010); however optomised nutrition and culture conditions can act to induce maturation earlier. Maturation leads to the development and subsequent ripening of gonads in preparation for reproduction (Randall et al., 1987). Management of maturation prior to harvest has been a problem since the start of the industry and selective breeding for late maturing strains has been undertaken since the early 1970s (Gjedrem 2012) with an estimated improvement of 3% per generation after consideration regarding farming practice and nutrition has been given (Gjedrem 2012). Photoperiod, however, offers farmers a more immediate approach for managing this problem.

Smolts transferred to SW in line with ambient conditions will typically experience one seawinter before reaching market size. In these groups, the change in photoperiod from a short to long (spring) day initiates maturation after around 9 months in SW. Maturation initiates a hormonally induced growth spurt during the spring months (Cotter et al., 2002; Kadri et al., 1996; Hansen et al., 1992). In such groups, harvest will occur before major maturation occurs in the population. Smolts transferred either out of synch with the natural photoperiod cycles or the smaller cohorts of in-synch year classes typically experience two seawinters. This is problematic as fish become exposed to two seasonal cycles with each providing a cue to induce maturation. In addition, out-of-season smolts are selected from the faster growing cohorts within a year class. Thorpe (1896) proposed a model whereby a photoperiod cue in addition to genetically determined thresholds regarding somatic reserves and growth rate induce maturation. As a result, out-of-season fish are predisposed to early maturation. Pre-harvest maturation is problematic as flesh and growth characteristics become negatively affected (Saunders and Harmon 1988; Krakenes et al., 1991; Hansen et al., 1992; Taranger et al., 2010) and market value is reduced (McClure et al., 2007).

To prevent economic losses, photoperiod manipulation provides an effective tool for controlling maturation (Porter et al., 1999). Enhancing photoperiod duration relative to ambient conditions is capable of overriding seasonal information (Randall

et al., 1998) as long as the timing is appropriate (Taranger et al., 1999) (Fig. 1.8). Shifting the perceived season prevents nutritional thresholds from being attained resulting in maturation being delayed (Duston and Bromage 1988; Bromage et al., 2001; Taranger et al., 2010; Rowe et al., 1991; Thorpe et al., 1988). Supplementary lighting is typically applied during the second sea-winter in sea cages. In addition to this, Leclercq et al., (2010) showed that top-crop grading throughout the production cycle allows the removal of the cohorts most likely to mature as these fish are typically bigger than non-maturing cohorts. Identification and removal prior to a reduction in organoleptic properties ensures the highest market price is achieved (Leclercq et al., 2011). Surprisingly low light levels have been shown to be efficient at preventing maturation. A mean irradiance of $0.012 Wm^{-2}$ supplied to 12% of the rearing environment has been demonstrated to be sufficient (Leclercq et al., 2011) suggested to be due to the positive phototactic nature of salmon (Juell et al., 2003; Juell and Fosseidengen 2004; Oppedal et al., 2007).

Photoperiod history plays a large part in the decision to mature and so both the duration and timing of supplementary lighting is critical, extending a summer signal too long can induce maturation as fish attain thresholds and meet somatic gateways (Bromage et al., 2001). More recently, evidence has emerged regarding the effect of photoperiod on different sexes with male fish exposed to high water temperatures and continuous light achieving a 6 month shift in maturation whereas no such change in females is seen (Fjelldal et al., 2011). Although prolonged periods in SW initiate maturation, enhanced growth during FW stimulated by high temperature and continual lighting can also impact SW maturation rates (Fjelldal et al., 2011) and induce jacking (Imsland et al., 2014). Fish raised in RAS systems may be more prone to jacking as advancement of smoltification produces fish that are transferred to ambient conditions capable of providing a photoperiod cue. Enhanced somatic reserves combined with the abrupt change in photoperiod relative to the hatchery increase the likelihood of early maturation in smolts (King et al., 2004). The mechanism appears to be the same that triggers grilsing later in SW and again stems from the plastic nature of seasonality in the Atlantic salmon. Research into understanding how post-transfer photic conditions can mediate the impact of prior culture conditions is becoming increasingly relevant and requires urgent consideration within the context of industrial practices.

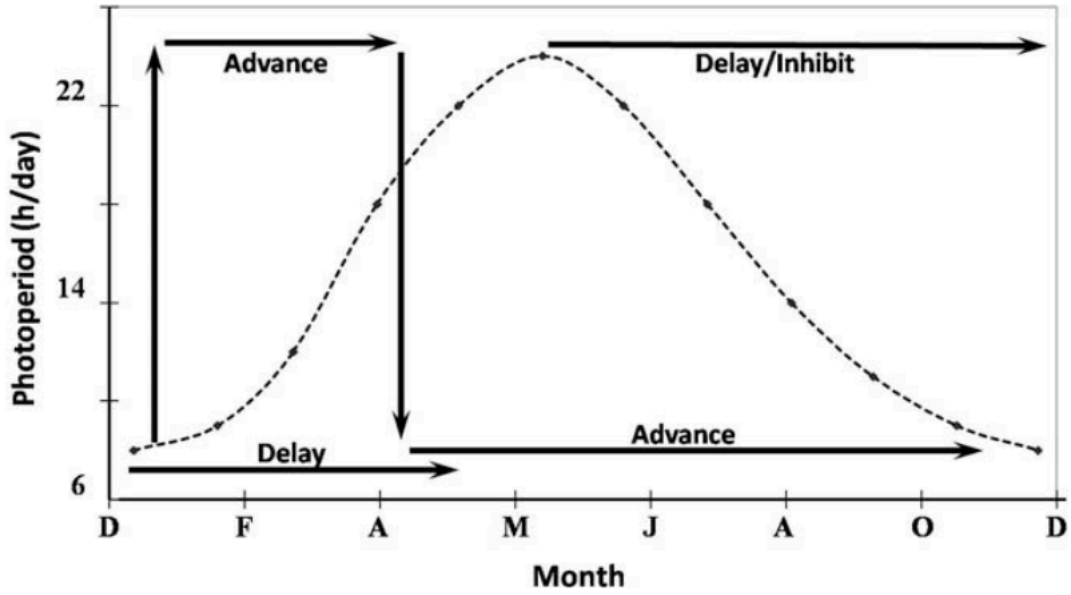

Figure 1.7. Model showing the effect of photoperiod on the advancement or delay of the onset of puberty in Atlantic salmon. By applying LL throughout December to April, puberty can be advanced however somatic reserves may be insufficient for puberty to complete resulting in a delay to maturation. Application of LL from mid-summer delays the cue required to start maturation, extending the growing period before the onset of puberty. (Figure from: Taranger et al., 2010).

1.4.3 Broodstock Management

Whereas post-SW transfer photoperiods aim to prevent maturation, controlling manipulation in broodstock allows further control over smolt production by increasing the availability of eggs. Advancing eggs production by 6 months can be achieved by using continuous light from March and changed to L:D8:16 in May (Taranger et al., 1998). High water temperature plays an important role initially however fish spawn when moved to low water temperatures (Taranger and Hansen 1993). Maintaining fish under LL from mid-summer delays the decision to mature offering the ability to push eggs production later in the year (Taranger et al., 1998). RAS is ideally suited for this type of manipulation and protocols are currently being developed to enable year-round production (Mommens et al., 2016). The concept is proven by Stofnfiskur, an Icelandic egg production company that uses pumped geothermal water to heat indoor tanks allowing the provision of sufficient thermal cues (Hansen et al., 2015).

1.4.4 Growth

In the Atlantic salmon, somatic development is primarily under the control of the hypothalamus via the release of pluripotent GH from the pituitary. GH production is mediated in response to feed intake (Johnsson and Björnsson 1994), environmental stimuli (Björnsson et al., 1994) and receptor density (Björnsson 1997; Reinecke et al., 2005). Daylength also directly influences the production of pituitary somatotrophs such as GH (Komourdjian et al., 1976) which acts synergistically with the growth promoting peptide insulin like growth factor 1 (IGF-1) in a dual-effector mechanism (Isaksson et al., 1987; Daughaday and Rotwein 1989; Widmaier et al., 2008). IGF-1 synthesis is stimulated by the binding of GH. Receptor density is very high in the liver (Jiao et al., 2006) and so most IGF-1 is hepatically derived (Johnston et al., 2011). Other versions of IGF are also found amongst other tissues produced via the cleavage of the E-domain, to date, these remain relatively unexplored both functionally and structurally (Company et al., 2001). IGF-1 acts as both an endocrine and paracrine agent (Reinecke et al., 2005; Stefansson et al., 2007) with known roles in regulating osmoregulation, reproduction and hypoxia responses (Wood et al., 2005). IGF-1 stimulation leads to the breakdown of glycogen into glucose and gluconeogenesis from non-carbohydrate precursors in the liver (Widmaier et al., 2008) which provides energy for anabolic functions (Widmaier et al., 2008).

During FW and SW increasing daylength also increases the opportunity to feed (Boeuf and Le Bail 1999) and fish raised under continuous light achieve enhanced growth, at least initially (Nordgarden et al., 2003). Increased feed intake enhances the production of IGF*1* and fibroblast growth factor 2 *(FGF2)* mRNA expression (Chauvigné et al., 2003). In addition, the myogenic growth factors myostatin (MSTN) and scatter factor hepatocyte growth factor (HGF) also become elevated (Johnston 2003). HGF is a potent stimulator of myogenic cell proliferation (Tatsumi et al., 1998) and the density of the HGF receptor c-met provides a useful indicator for determining myogenic cell proliferation and c-met positive cells increase in direct response to LL (Johnston 1999; Johnston 2003; Brodeur 2003).

Whereas mammalian growth occurs through post-natal hypertrophy of fibres formed during gestation (Rowe and Goldspink 1969) Atlantic salmon growth occurs through the combined actions of hypertrophy and the formation of new muscle fibres (recruitment) (Stickland 1983). Muscle progenitor cells (MPCs) differentiate into

proliferating myoblasts destined to undergo terminal differentiation. Differentiation leads either to absorption into existing muscle fibres to fuel hypertrophy and maintain nuclear to cytoplasmic ratios or fuse to form strings of cells that ultimately form new fibres (Rowe and Goldspink 1969). It is thought that determination of the differentiation is under local paracrine control (Johnston 1999). Muscle is predominantly comprised of two fiber types arranged longitudinally. Slow muscle uses aerobic metabolism to provide rhythmical undulations required for sustained swimming whilst fast muscle, fueled by anaerobic metabolism, drives rapid burst locomotion (Dunn and Johnston 1986; Johnston 1991). Slow muscle fibres typically constitute less than 10% of the muscle network (Johnston 1999), however, the tissue is rich in fatty acids and together with fast muscle act as an essential store of peptides and fatty acids that can be mobilised during periods of fasting or remodelling during smoltification or gonadal recruitment (Venugopal and Shahidi 1996).

Muscle fibre recruitment in Atlantic salmon varies depending upon the animal age, life history and time of year. A rapid and synchronised proliferation of fibres are reported to occur in response to changes in water temperature and photoperiod prior to smoltification (Johnston 2003). Fish exposed to continuous light (LL) have been shown to recruit an average of 4400 fibres day^{-1} per cross section of myotome compared to 200 fibres day^{-1} in ambient cohorts (Johnston 2003). This increase occurred for a short period of 40 days' post LL, after which 900-1000 fibres day^{-1} were recruited in both treatments. There is some debate regarding the impact of higher muscle fibre numbers and future growth potential and it appears to be related to ontogenic stage (Macqueen et al., 2008). However, significant correlation is seen between high fibre numbers and fillet taste, appearance and firmness (Johnston et al., 2000). Fewer, larger, fibres allow light to scatter, preventing penetration and giving the appearance of a pale colour, large numbers of small fibres have the opposite effect as scattering is reduced and the colour appears darker and more desirable to the consumer. It is this light scattering, rather than the total pigment content which influences pigment perception (Johnston et al., 2000).

Little is known about how spectrum and intensity may interact with the recruitment of fibers. However, in chickens (*Gallus gallus*) blue light is suggested to play a role in muscle deposition during later stages of development (Rozenboim et al., 2004) whereas green light is suggested to enhance early development (Rozenboim et al., 1999). A similar myostatic role of green light in barfin flounder (*Verasper moseri*)

has been proposed (Yamanome et al., 2009). Thus, the use of coloured light on growth presents an exciting area for research requiring careful analysis of muscle structure.

Unintended growth enhancement has been frequently reported in trials looking to inhibit maturation in SW. A model suggesting the advancement of endogenous seasonal growth cycles has been proposed (Oppedal et al., 1999; Oppedal et al., 2006; Nordgarden et al., 2003). In salmon raised under natural photoperiods (or simulated natural photoperiod (SNP) in tank production), accelerated growth and development is seen during spring and summer months and decreases during autumn and winter (Johnston et al., 1999). Fish exposed to LL initially grow much faster compared to SNP due to the perception of a long day signal similar to that experienced during spring/summer. However, weights obtained over a production cycle are reported not to differ between LL and SNP groups (Nordgarden et al., 2003). As an alternative to the advancement of seasonal cycles, direct photostimulation on muscle fibre recruitment has been suggested to explain observed differences (Johnston et al., 2003). Elucidation between these proposals requires a comparative study examining SNP vs LL growth and muscle structure in SW. Performing this with fish with known photic history would further to elucidate the mechanisms behind observed differences. Such information may help to guide lighting protocols and spectral profiles.

1.4.5 Recirculating Aquaculture Technology

Perhaps the greatest recent advancement in salmon aquaculture is the widespread adoption of recirculating aquaculture systems (RAS) which allows the culture environment to be optimised. Manipulation of water temperature combined with artificial seasonal photoperiods remove biological strictures on the timing and progression of smoltification (Bergheim et al., 2009). Much of the original literature regarding smolt induction was based upon a final smolt weight of between 45-70g (e.g. Sigholt et al., 1995; Thrush et al., 1994). Such sizes are no longer relevant as smolt size is increasing rapidly especially in RAS, reported at 140-170g by Bergheim et al., in 2009. The aim of producers is to increase this further in order to reduce the duration of SW on-growing (FishFarmingExpert.com 2016). The influence of elevated water temperature, increased body size and accelerated smoltification regimes on post-transfer survival, growth performance and maturation remains to be explored. Concerns regarding significant changes in adiposity and the likelihood of meeting the

somatic thresholds that control key physiological development earlier are starting to be discussed (Imsland et al., 2014). The transfer of large smolts to out of phase photoperiods may compound developmental decision (Stefansson et al., 2008) and compromise the effectiveness of RAS grown smolts and as such this is an area requiring urgent research.

The role of photic parameters has particular relevance to such systems. Typically, RAS systems feature clear water with high light penetration allowing a much broader spectrum of light to reach the fish, unlike native conditions (Douglas and Djamgoz 1990). How the major attributes of light, spectrum and intensity, interact with salmon physiology during early development and smoltification under stable RAS conditions are unknown. From an evolutionarily standpoint, adaptations are tuned for redds and freshwater rivers. Early feeding mechanisms and aggressive territorial behaviour (Keenleyside 1962; Wańkowski 1981), compared to placid shoaling during the parr-smolt development may mean that conditions need to be adapted throughout captive rearing. The latent impact of FW photic composition on SW development is also currently unknown and unexplored. Advances in lighting technology have seen the introduction of highly efficient LED lighting systems with long serviceable life offering high levels of spectral and intensity control (Pimputkar et al., 2009). Such technology provides an ideal tool to examine these questions with results having direct implications for the design of lighting systems for RAS.

1.4.6 Stress and Welfare in RAS Systems

In addition to impacting upon growth and the timing of physiological adaptations, spectrum and intensity are demonstrated to act upon the previously discussed stress axis (Migaud et al., 2007; Vera et al., 2010). Trials examining photoperiod manipulation in FW were predominantly conducted using FT (e.g. Saunders et al., 1985; Mccormick et al., 1987) and incandescent lighting (e.g. Stefansson et al., 1989; Thrush et al., 1994). Despite lower intensity, photic composition would be similar to that experienced in native rivers (Fraser and Metcalfe 1997). In RAS systems, spectral quality and intensity differ considerably (Kristensen et al., 2009) and photic conditions that are successful in FT may not be suitable for RAS. An understanding of the influence of spectrum and intensity during each stage is required to identify potential problems. Poor growth performance (Wendelaar et al., 1997) and disease

susceptibility are associated with stressed fish (Barton 2002). The measurement of plasma cortisol is widely used as a proxy for stress status (Pottinger 2010) owing to its early role in the stress response which is gradual and allows basal levels to be identified (Mommsen et al., 1999; Ellis et al., 2012). Cortisol can be measured easily using standard ELISA type kits (Gesto et al., 2015) however elevated cortisol occurs throughout changes in ontogenic stage i.e. smoltification or maturation (Barton et al., 1985; Pankhurst et al., 2008) and results may be misleading. Sub-optimal rearing conditions will typically manifest in changes in growth rates and long term growth studies provide arguably a better indication of the impact of environmental conditions on the developmental physiology. In addition, information must be gained to ensure welfare attributes such as vertebral deformities and ocular structure are not impinged by photic parameters.

1.5 Aims

Recent changes in production system and lighting technology have resulted in the ability to fine tune the culture environment in order to maximise commercial salmon production. Exploiting these technologies requires understanding how parameters such as intensity and spectrum impact upon salmon development throughout the three broad ontogenic stages of freshwater, smoltification, and on-growing. Investigating this requires detailed assessment of an array of developmental traits, many of which are specific to each stage, in order to fully determine the impact of lighting conditions on developmental physiology. Thus, the thesis overall aims were to:

- Determine how light specific spectrum and intensity parameters impact upon growth attributes during freshwater development
- Investigate how exposure to narrow spectrum light impacts upon the induction of smoltification and the duration of SW adaptations
- Explore the role of intensity on smoltification and the impacts on SW adaptation
- Assess the long-term implications of exposure to narrow spectrum light on welfare traits such as vertebral formation, eye structure, and the stress axis
- Explore the impact of long term exposure to narrow bandwidth light on somatic growth and muscle structure

- Examine how prior photic history and post-transfer photoperiod regimes impact upon SW growth and sexual maturation in fish transferred out-of-season
- Identify the neural and pituitary response to assimilated light perception in response to different spectra

The trials presented in this thesis thus aim to elucidate how altering the composition of the photic environment influences major physiological development within a commercially relevant setting. By combining relevant physiological assessment with an exploration of the fundamental perception in the deep brain and pituitary, a framework is provided with which to base parameters for the development of successful artificial lighting systems.

2 Materials and Methods

2.1 Tank system

All freshwater trials were conducted in the Temperate Aquarium, University of Stirling, UK (56°N, 4°W). Development from a bare room with a waterproof floor, drain, and sterile area occurred in the initial phase of this project. Two bespoke 12 tank recirculation aquaculture systems (RAS) (Fig. 2.1) with independent water temperature and filtration controls were built and developed on site. Each system (System 1 and System 2) was designed to maximise available space.

General Layout

Each tank system comprised of two levels with six top tanks immediately above 6 bottom tanks. Tanks were supported on a custom built hot dip galvanised frame with fixed staircase and walkway.

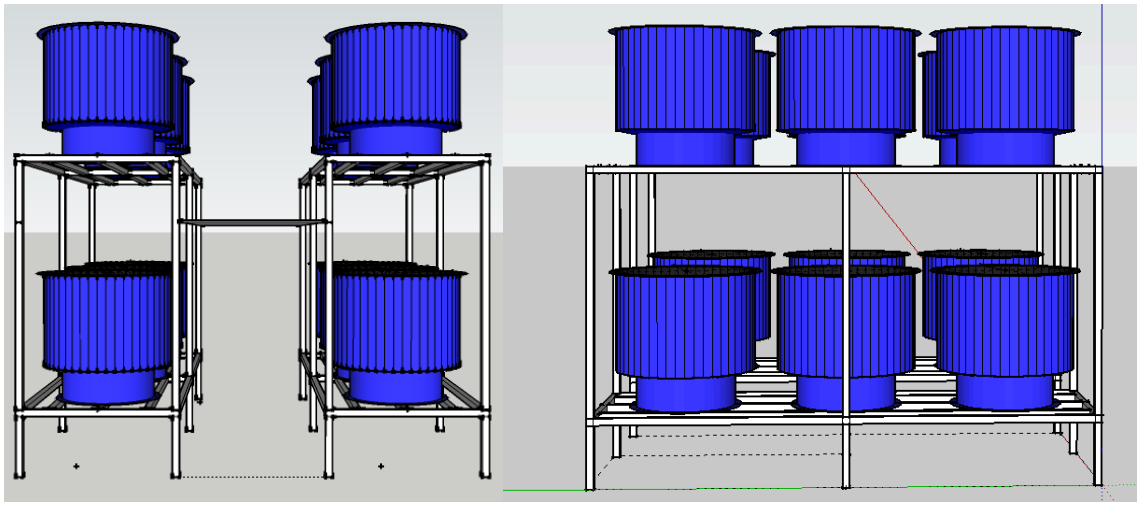

Figure 2.1. Tank layout- Each system comprised of 12 tanks, six on the upper and six on the lower level. Upper tanks accessed via fixed walkway and staircase.

Room Environment Control

Two large air conditioning units were installed to allow room temperature to be controlled between 8ºC and 30ºC ±1ºC. Adjustment of air temperature reduced the workload of water chillers and provided redundancy for any problems regarding the chillers.

Water Temperature Control

Teco TC500 (Teco, Italy) aquarium heater/chillers, provided the ability to manipulate individual system water temperature with a temperature range of 5ºC-35ºC.

Tank Sizes

Each system comprised of 12 no., 300 litre (o.d. 94cm x 55cm height), glass reinforced plastic tanks (Purewell, England with an interior and exterior gel coat. The colour of the exterior gel coat was different between systems. Internally all tanks were coloured black. The bottom of each tank was fitted with a 2inch polyvinyl chloride (PVC) elbow fitment bonded during manufacturer which facilitated connection to the main drain. A 25cm circular collar on the bottom provided support and space for drain connections.

Top Nets

Tanks were fitted with 0.6 cm hexagonal mesh top net (Norfine Nets, Norfolk, UK) secured using bungee cord to prevent jumping and fish loss. This net obscured ~25% of incident light. Light values are reported below the net.

Stand Pipes

Water volume was controlled initially using an external standpipe design. This design was chosen to facilitate feed waste collection and worked by trapping waste feed between the fitting bonded into the tank floor and the overflow pipe. Waste feed was extracted by draining the pipe through a ½ inch ball valve connected to the bottom of the external standpipe. In addition to feed other waster material was also collected reducing waste return to the sump. External traps were cleaned daily and rodded from the top of the external standpipe to the inside of the tank.

A stub standpipe, 15cm X 2inch diameter PVC pipe with slots cut and covered with mesh was initially used to prevent fish loss and facilitate pellet removal. The risk of blockage and tank overflow was negated through the placement of holes in the pipe.

Following the first full trial it was deemed necessary to change the configuration to allow better control of water volume. The external standpipe was reduced in height and volume was controlled by an internal standpipe sleeved with a section of 3-inch pipe to induce a venturi to remove excess feed and waste. A 15 cm stainless steel perforated cylinder was designed and manufactured (Fig. 2.2) to encompass both the collar and internal standpipe (Plastok, Merseyside, UK). The cylinder socketed into a

circular mesh plate bonded onto the tank floor using CT-1 sealant adhesive certified for use in potable applications (C-Tec, Newry, Norther Ireland). The top of the cylinder was held in place with a stabiliser support made from PVC foam. Perforated cylinders with 0.4 cm and 0.8 cm holes were manufactured to facilitate pellet clearing and good water transfer as the fish grew.

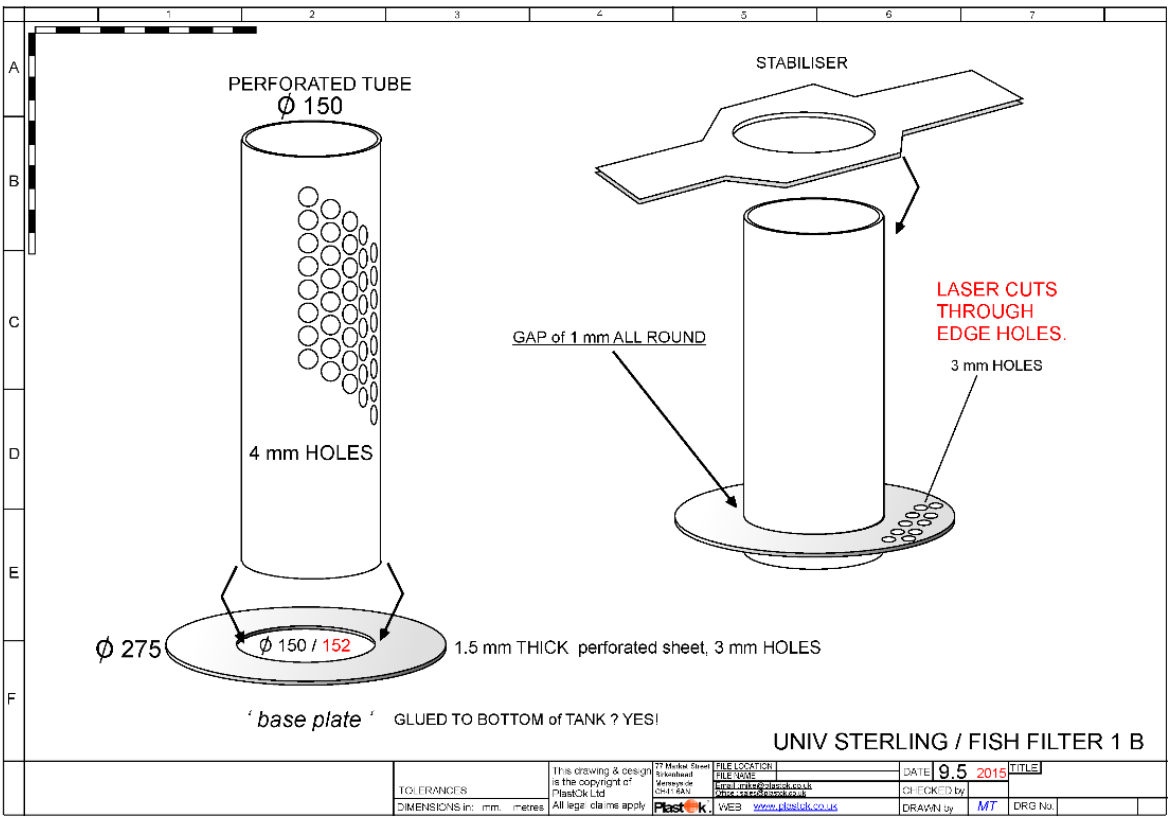

Figure 2.2. Design of internal steel mesh filter. and base plate to allow cleaning and prevent fish loss.

System Sumps

A sump acted as a reservoir, buffering between circulating water and return water. The sump tank was made from an insulated pallet container fitted with an ABS plastic grid. The grid supported a trickle filter, protein skimmer, UV filter and biological filter allowing a head of pressure to return water to the system.

Aeration

A compressed fresh air supply was produced by a BVC Unijet 75 (BVC, Havant, UK) which supplied individual air stones in each tank to aid surface agitation to prevent the

accumulation of surface film owing to external standpipe design. In addition, air was required to provide 'lift' in the fluidised bed bio filters attached to each system.

Low Water Alarm

Each sump was installed with a low water level alarm connected to a GSM autodialer.

Pumps and Water Flow

Two distinct pipe networks were serviced by separate pumps. A supply pump (Argonuat AV-150, Denmark) circulated water into each tank whilst a recirculation pump (Argonuat AV-200, Denmark) was used to direct water through the chiller/heater and the filtration system. Pumps were self-priming and designed for continual use. A bypass on both networks allowed control of pump pressure by returning excess capacity to the sump.

Prior to reaching the tanks water, supply water was passed through a UV filter (UV PU10, 500W, TMC, UK).

Tank Supply

Above each set of three tanks was a loop of pipework designed to negate linear pressure differences in flow. Tank flow was controlled ¾ inch gate valve.

Mechanical Filtration

Waste water retuned to the sump via two large 4-inch drain pipes connected to a collection unit fitted with four filter socks for mechanical extraction of solids. Sock filter size varied depending upon solid loading (50-500 microns) and could be removed and interchanged as required All socks were removed and cleaned twice daily.

Protein Skimmer

System one was fitted with a skimmer for removing proteinaceous compounds from the water. A tall plastic column with a venturi air inlet was attached to the recirculation pump. Water in the column was continually aerated with fine bubbles from the venturi, bubbles coagulated compounds in the water column and formed a thick foam. At the top of the column an upside-down funnel allowed bubbles to travel over the lip and be transferred to a drain, the collection area was fitted with a timer operated spray mechanism to backflush the funnel.

Biofilters

Biological filtration occurred in two separate filters: a sump mounted sand filter and a sump mounted trickle filter. An 800-litre water tank fitted with an air supply circulated K1 type plastic media provided additional filtration added after the first complete trial to aid the conversion of nitrogenous system waste. Water was delivered via the recirculating pump into the top of the filter before passing through the fluidised filter media and returning to the sump via a screened outlet.

Water Quality Monitoring

Daily water quality assessment was performed for ammonia, nitrites, pH, dissolved oxygen and chloride. Latterly an Oxygaurd system (Oxygaurd, Denmark) provided alarm notification for dissolved oxygen, carbon dioxide, pH and water temperature.

Water quality was assessed using a Palintest 7500 photometric test kit (Palintest, UK) according to manufacturer's guidelines for individual tests.

Power Redundancy

Electrical redundancy was provided via an emergency backup generator. In the event of a mains power failure all systems automatically restarted. The self-priming nature of the pumps ensured that the water would continue to flow.

Temperature Monitoring

A bespoke temperature logging system provided both a record of water temperature and an alarm to alert for water temperature out with set norms. DS18B20 temperature probes were connected to a Raspberry Pi (Raspberry Pi Foundation, UK) with a script installed which used the google API to connect to a shared spreadsheet updated every 15 minutes. Within the script a simple logic statement assed temperature range. An errant temperature resulted in an email being sent both to interested parties and to an SMS gateway (Textlocal, UK) to alert the change in temperature via text message.

2.2 Tank Lighting

Light Meter

In all trials light level was recorded using a Skye Instruments (UK) W/m^2 light meter. The meter was fitted with two heads depending upon intensity being recorded. The light meter was calibrated to the national physics laboratory (UK) standard.

As photoreceptors are effectively photon counters several authors have reported intensity using photon flux, measured in micromoles per square meter per second (μmoles/m^2/s). Using a conversion factor, it is possible to change W m-^{2} into this unit allowing comparisons between published light levels. All values in the current thesis are reported in W/m$^{2.}$

2.2.1 LED System 1 General Information

System 1 was installed with a bespoke LED lighting system supplied by Philips as part of the project (Philips Lighting, Eindhoven, Holland). Each luminaire was installed with one of four LED modules and capable of producing either: Blue, Green, Red or White light (Fig. 2.3).

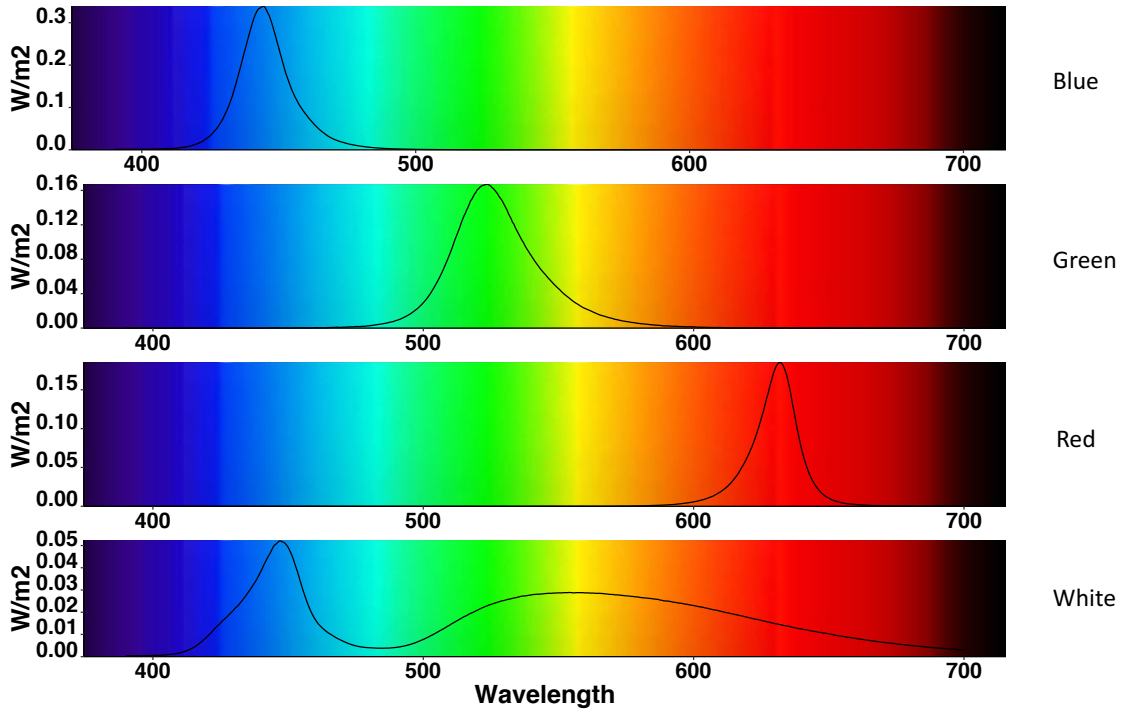

Figure 2.3. Spectrographs of the output from the LED lights used in each trial.

Light Proofing

To prevent light leaching between tanks solid partitions were erected on three sides (left, right and rear) made from white PVC foam board to form a three-sided box. The upper 60cm section of box, inclusive of slightly below the tank lip, was wrapped in E3 grade MC-PET. MC-PET is a highly reflective (97%) plastic used for making light reflectors. Hung from the steel frame was a fourth sheet to enclose the tank on four sides. To reduce the risk of light contamination between tanks, a curtain comprising thick black plastic suspended from a length of 2.2 cm electrical conduit was affixed to the steel support frame. Each curtain was weighted down with a piece of electrical conduit filled with sand acting as a weight.

Bracket System for Lights

A stainless-steel u shaped channel was bolted to a twin slot channel cantilever bracket to provided support for the wheels of the luminaires. Brackets fixed into slotted channels fixed onto stainless steel struts that ran the length of the steel tank support frame. This system was rated to hold 45kg per cantilever, sufficient for the weight of the lights even at the furthermost extremity of the support.

Luminaire Design

Luminaires featured a large driver box on one side to provide power and control the LEDs (Fig. 2.4). The LED modules were suspended off a large heatsink and protected using glass. Lights were installed with wheels to allow them to be moved for tank access.

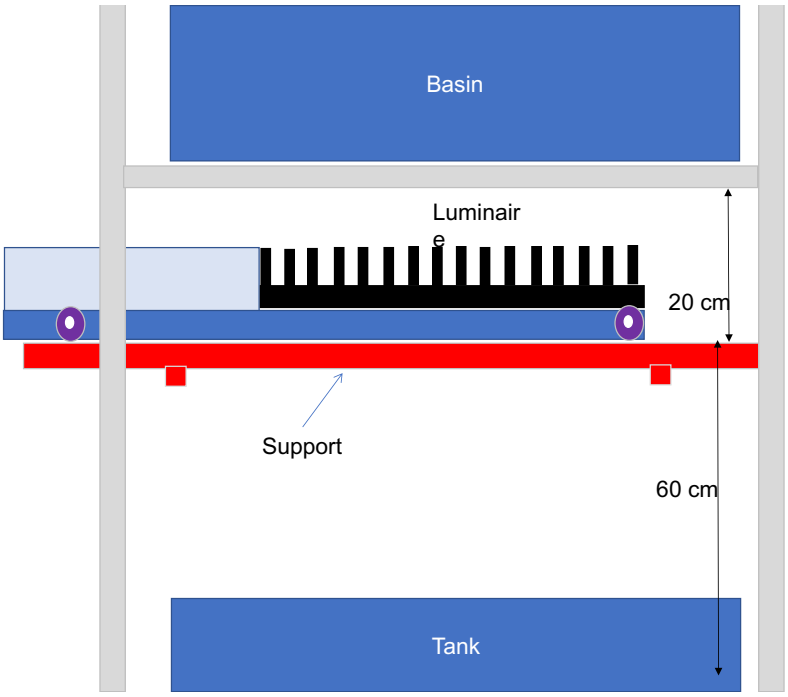

Figure 2.4. LED luminaire support and design

Lighting Controls

Light intensity was manipulated though a program written in LabView (NI Instruments, USA). The lights were supplied with a Digital Addressable Lighting Interface (DALI) interface control through an IP control box which communicated with the luminaires. The program used a series of logic cases to move from one state to another (Fig. 2.5).

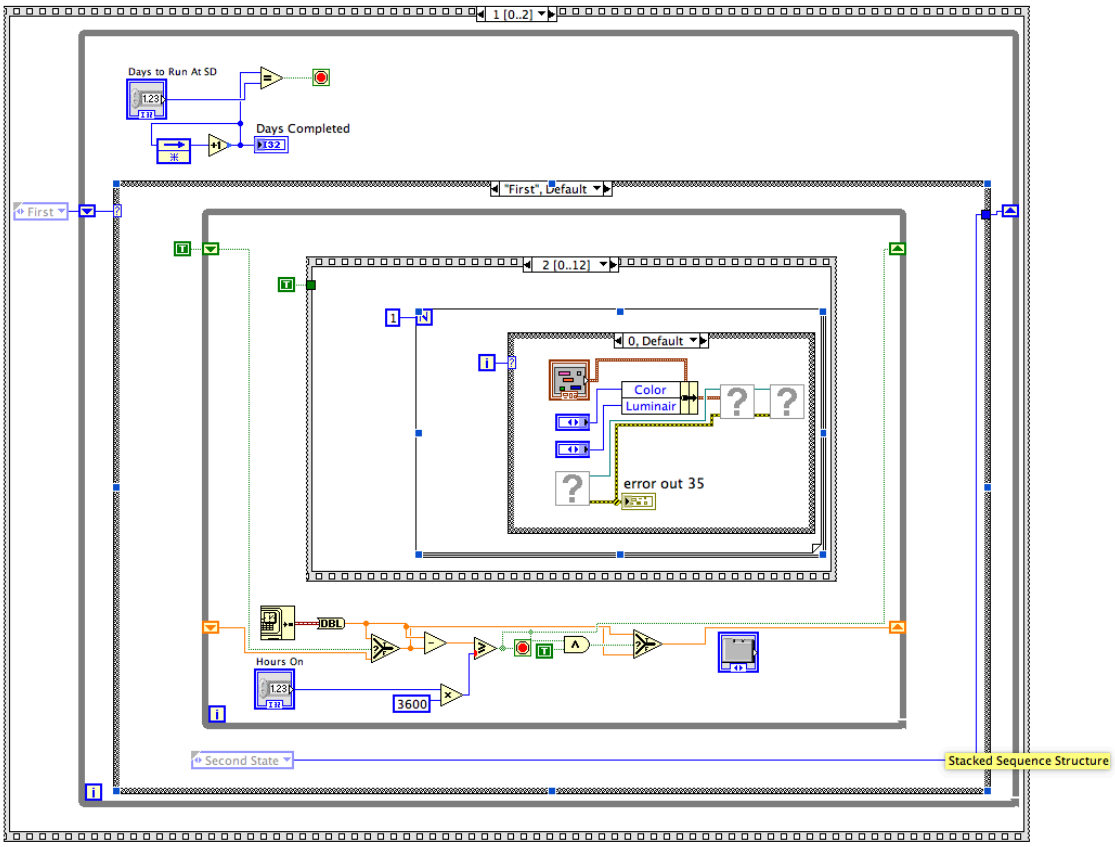

Figure 2.5. Outline of case structure used to implement day and night control in Labview

Setting Light Intensity and Duration

Manipulating the photophase during the three periods of an out-of-season smoltification regime was attained by configuring three separate tabs. Each tab had a separate field for each set of three luminaires and light intensity was adjusted within these fields (Fig. 2.6). Duration was set on the 'Hours' and 'Days to Run' fields. Once these parameters were satisfied the program then moved to the next tab where the scotophase was defined before moving finally to the last tab where the spring/summer photoperiod was defined.

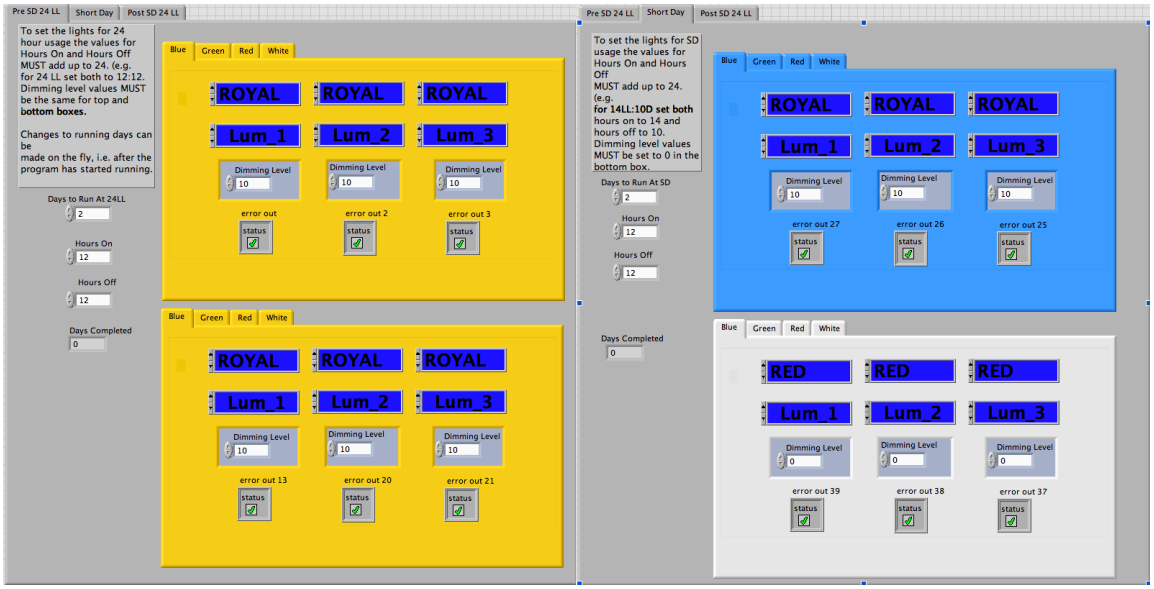

Figure 2.6. Light control software for LED luminaires

Locating Luminaires

Each luminaire was centred to the standpipe in the centre of the tank using a plumb bob. (Fig. 2.7). Position on the runners was marked using tape to allow future relocation.

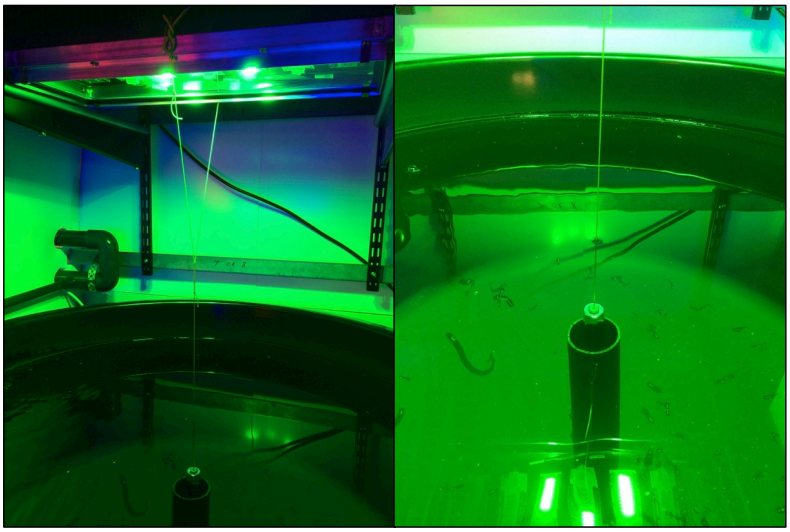

Figure 2.7. Each luminaire was positioned in the centre of the tank using a plumb bob to ensure equal light distribution across tanks.

Physical Setup of the Tank Space

Illuminance was measured at A, B and C. Position A is above the water surface so this value is only recorded in air. Position B and C are under the water. Position C is the standpipe socket which the grid for the light meter was adapted to fit into (Fig 2.8).

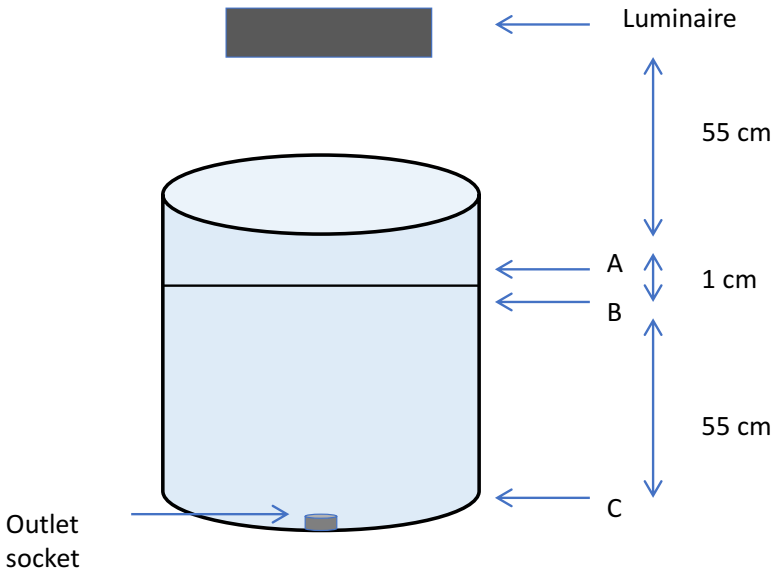

Figure 2.8 Arrangement of tank and where measurements were recorded.

Intensity Output and Light Distribution

Following installation, light distribution from each luminaire was tested. A plastic grid was made from transparent polycarbonate with holes cut every 10cm as per figure 9. Luminaire output was tested using a light meter placed into the grid in each position as represented by a dot (Fig. 2.9).

Figure 2.9. Grid locations and start position (1) and end position (52) for assessment of the distribution of light output for each colour.

All light intensity readings were carried out in the same orientation (Table 2.1). The walkway is on the first row of each graph. The values on each graph are presented as a physical X, Y co-ordinate with reading 1 being located on C, A.

Table 2.1. Grid Positions for determining light intensity distribution

H			49	50	51	52		
G		43	44	45	46	47	48	
F	35	36	37	38	39	40	41	42
E	27	28	29	30	31	32	33	34
D	19	20	21	22	23	24	25	26
C	11	12	13	14	15	16	17	18
B		5	6	7	8	9	10	
A			1	2	3	4		
	A	**B**	**C**	**D**	**E**	**F**	**G**	**H**

Intensity is presented as I_X where X is the percentage output of the luminaire as determined by the DALI driver. In addition to the surface values a value at 41cm below the surface was also acquired and is presented as I_X_41. This depth is close to where the tank starts to taper towards the stand pipe socket and was chosen as the deepest location to place the light meter without the bottom hindering the probe holder (Fig. 2.10).

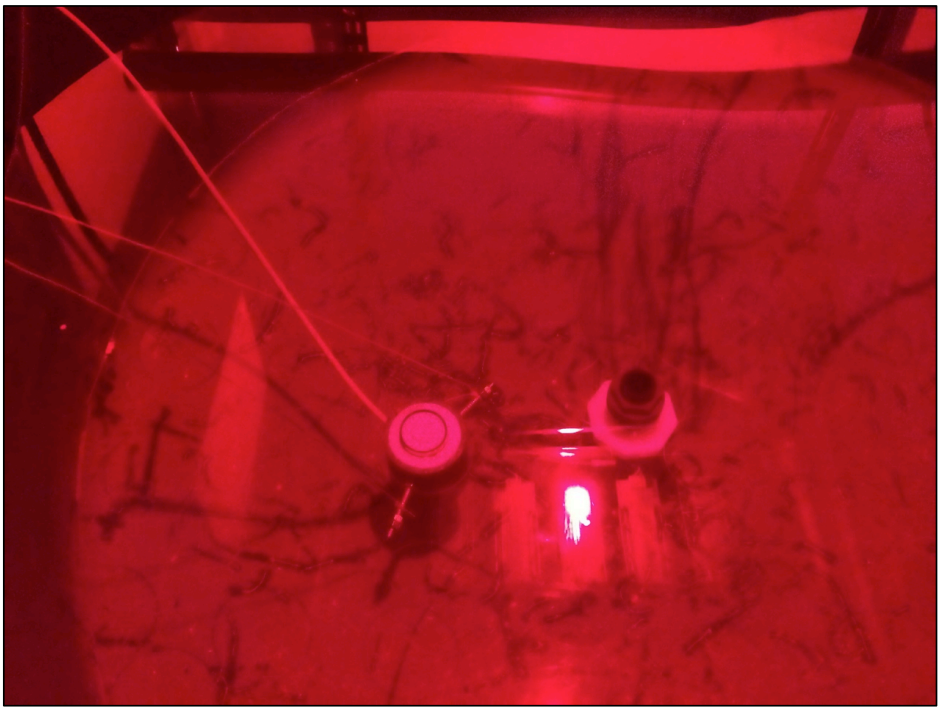

Figure 2.10. Recording light values. Light meter positioned on clear grid at 41cm below the water surface, the grid is fixed in place using a section of pipe with an adaptor to fit into the standpipe socket.

Light Distribution

To determine light distribution each reading was normalised against the maximum value for that intensity and depth.

The maximum, minimum and mean for each intensity and depth is also reported in the first two tables below the graphs. The percentage loss due to the light travelling 41cm into the water column is presented calculated by:

$$\text{Percentage Loss} = 100 - \left(\frac{\text{Value at 41 cm below water surface}}{\text{Value just below the water surface}}\right) \text{X } 100$$

Recorded values were then plotted using a relative gradient with 100% being the light colour and 0% being black. Figures 2.11, 2.12, 2.13 and 2.14 shows the distribution of light at both the surface and at 41cm. Whilst lower in intensity the light distribution became more even at depth for each of the luminaires tested. Each luminaire produced a different light intensity when the percentage of maximum light output was selected (Tables 2.2, 2.4, 2.6, 2.8).

A comparison of light loss between the water surface and the bottom of the tank (41cm) was performed (Table 2.3, 2.5, 2.7, 2.9). Loss between the surface and 41cm was highest under Red light (Table 2.7). A similar light distribution was seen in the Blue, Green and White lights. Distribution was most even at 41cm in all colours. The rear (furthest away but parallel to the walkway) was consistently brighter than the walkway side. A slight skew in the White light was observed towards the position of the LED modules which was identifiable in the intensity readings (Fig. 2.14).

Blue

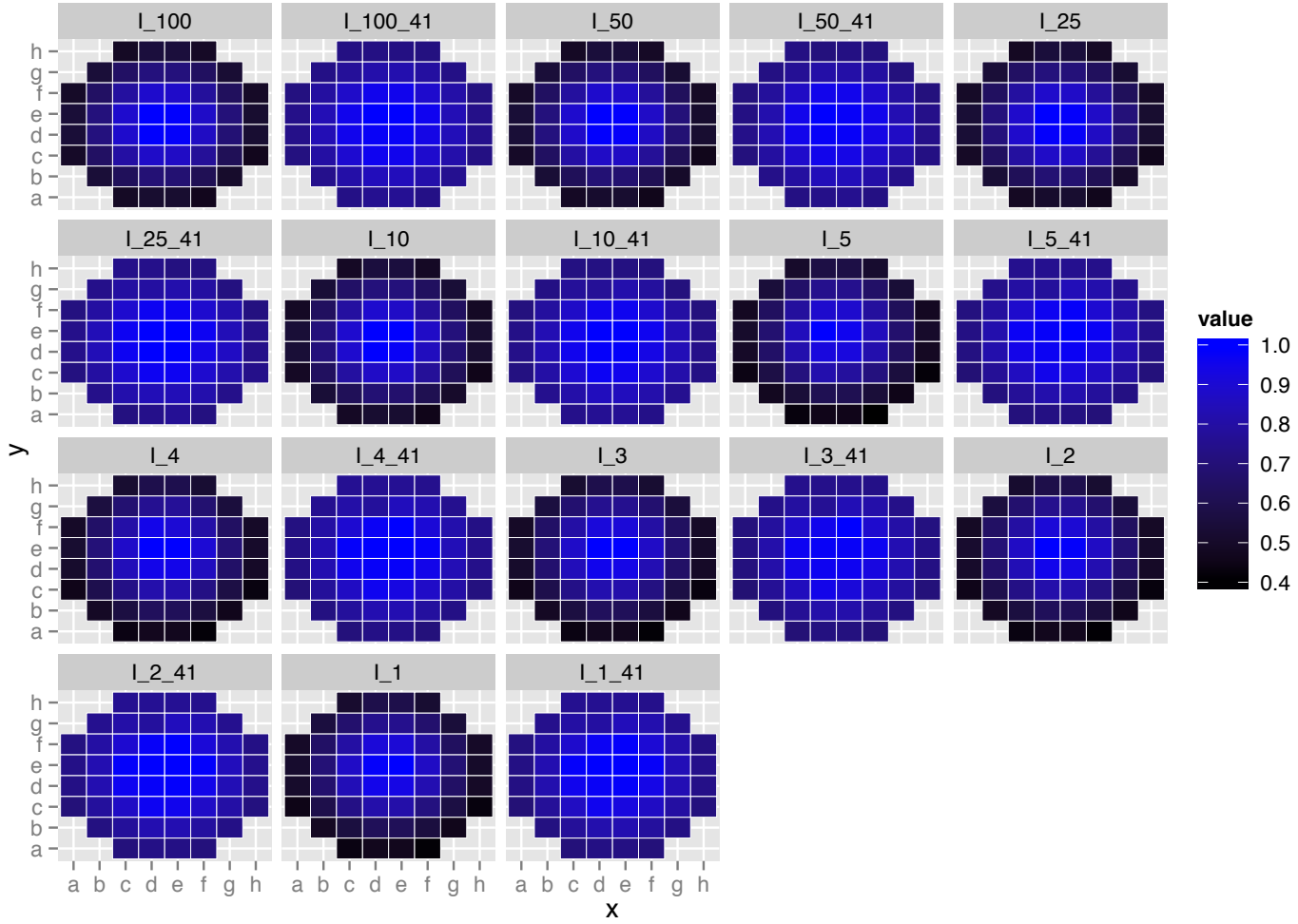

Figure 2.11. Distribution of Blue light with I_**X** representing the percentage (%) of maximum luminaire output. I_X vs I_X_41 provides comparison between water surface and 41 cm below at each output. Values presented as relative proportion of highest output.

Table 2.2. Maximum, minimum and mean value for Blue light at A. Surface (I_X) and B. 41cm (I_X_41) below the surface. Values are presented as W/m^2 and are recorded based on the percentage of maximum output of each luminaire i.e. I_100 is at 100% of output compared to I_25 which is a 25% of the maximum output that the luminaire is capable of producing.

(A)	I_100	I_50	I_25	I_10	I_5	I_4	I_3	I_2	I_1
Max	446.00	247.00	134.00	58.00	28.00	22.00	17.10	12.00	10.40
Min	204.00	112.00	61.00	26.00	11.05	8.97	6.93	4.84	4.20
Mean	300.9	165.96	89.87	39.00	17.95	14.54	11.24	7.84	6.80

(B)	I_100_41	I_50_41	I_25_41	I_10_41	I_5_41	I_4_41	I_3_41	I_2_41	I_1_41
Max	131.00	73.00	39.00	16.96	7.88	6.32	4.98	3.41	2.98
Min	94.00	52.00	28.00	12.06	5.45	4.41	3.42	2.39	2.07
Mean	108.50	59.98	32.42	14.03	6.46	5.24	4.06	2.83	2.46

Table 2.3. Percentage of Blue light lost between surface and 41 cm

% Loss	I_100	I_50	I_25	I_10	I_5	I_4	I_3	I_2	I_1
Max	70.6	70.4	70.9	70.8	71.9	71.3	70.9	71.6	71.3
Min	53.9	53.6	54.1	53.6	50.7	50.8	50.6	50.6	50.7
Mean	63.9	63.9	63.9	64.0	64.0	64.0	63.9	63.9	63.8

Green

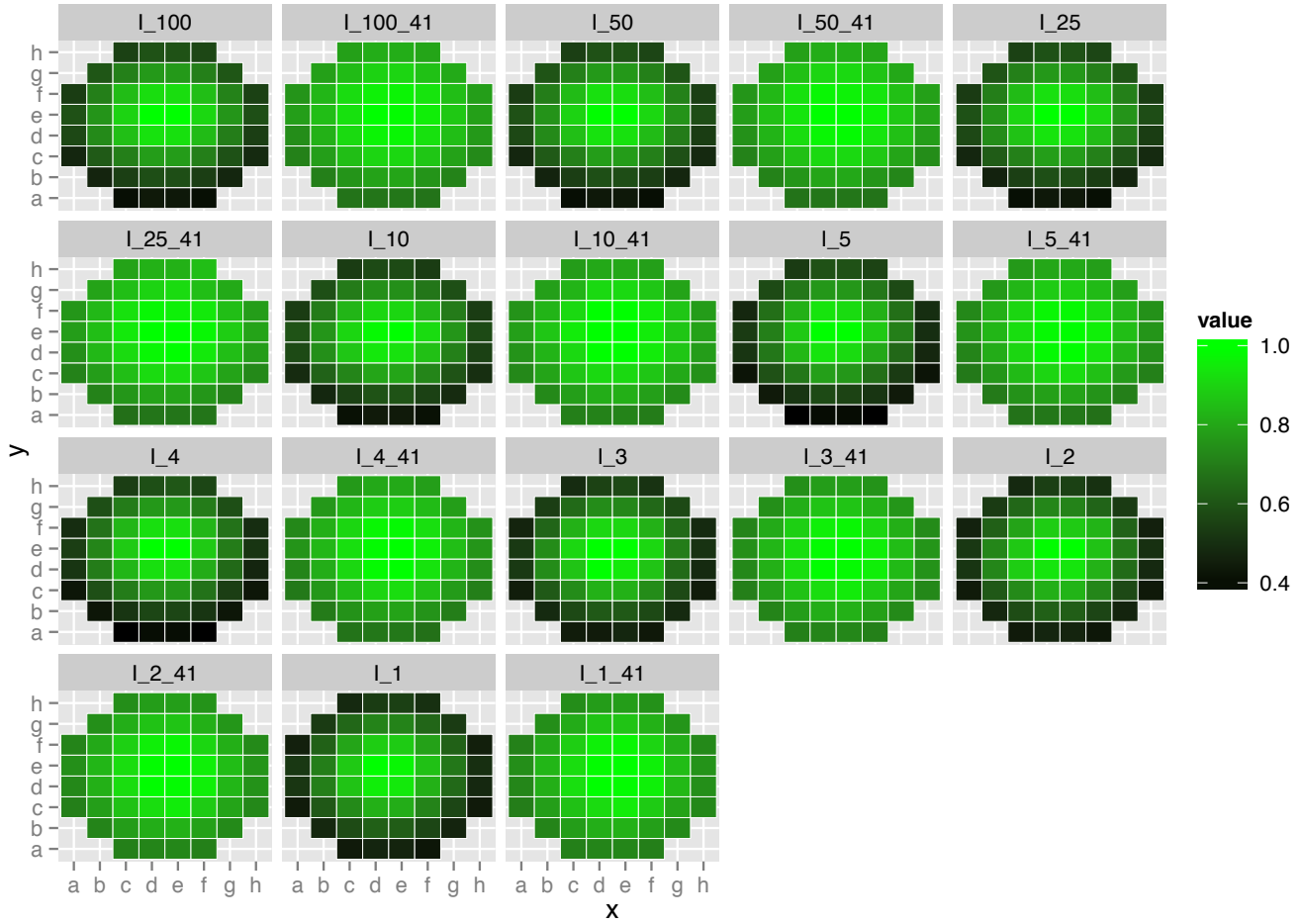

Figure 2.12. Distribution of Green light with I_**X** representing the percentage (%) of maximum luminaire output. I_X vs I_X_41 provides comparison between water surface and 41 cm below at each output. Values presented as relative proportion of highest output.

Table 2.4. Maximum, minimum and mean value for Green light at A. Surface (I_X) and B. 41cm (I_X_41) below the surface. Values are presented as W/m^2 and are recorded based on the percentage of maximum output of each luminaire i.e. I_100 is at 100% of output compared to I_25 which is a 25% of the maximum output that the luminaire is capable of producing.

(A)	I_100	I_50	I_25	I_10	I_5	I_4	I_3	I_2	I_1
Max	559.00	352.00	206.00	79.00	51.00	43.00	23.00	18.00	10.90
Min	222.00	140.00	82.00	32.00	19.00	16.00	9.78	7.55	4.56
Mean	376.58	236.71	138.69	53.21	32.85	27.85	15.17	11.69	7.05

(B)	I_100_41	I_50_41	I_25_41	I_10_41	I_5_41	I_4_41	I_3_41	I_2_41	I_1_41
Max	173.00	108.00	63.00	24.00	14.98	12.59	6.79	5.23	3.15
Min	117.00	73.00	42.00	16.78	10.04	8.43	4.79	3.69	2.21
Mean	144.37	90.62	52.94	20.27	12.34	10.38	5.62	4.33	2.60

Table 2.5. Percentage lost between surface and 41 cm below

% Loss	I_100	I_50	I_25	I_10	I_5	I_4	I_3	I_2	I_1
Max	69.1	69.3	69.4	69.6	70.6	70.7	70.5	70.9	71.1
Min	47.3	47.9	48.8	47.6	47.2	47.3	51.0	51.1	51.5
Mean	61.7	61.7	61.8	61.9	62.4	62.7	62.9	63.0	63.1

Red

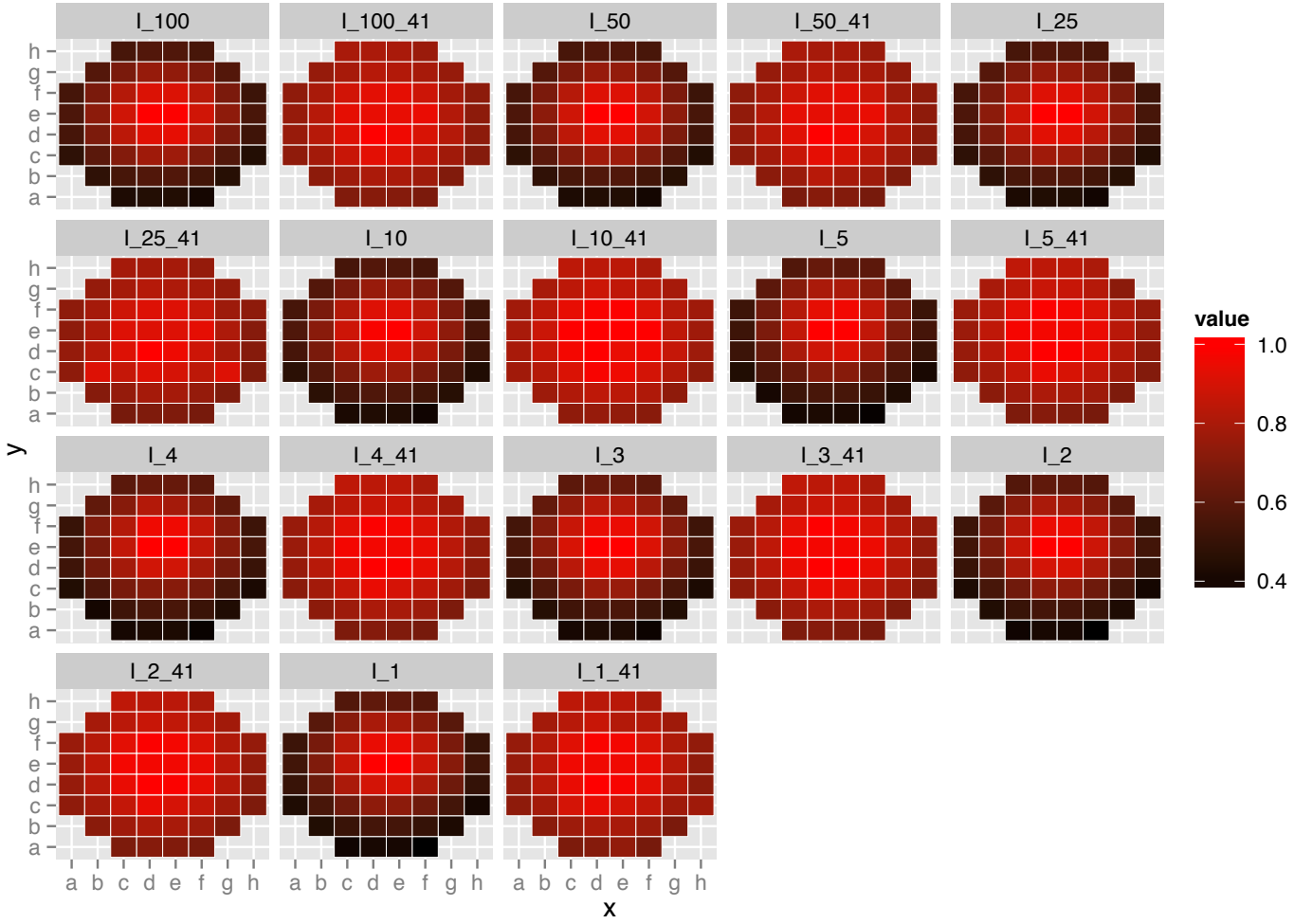

Figure 2.13. Distribution of Red light with I_**X** representing the percentage (%) of maximum luminaire output. I_X vs I_X_41 provides comparison between water surface and 41 cm below at each output. Values presented as relative proportion of highest output.

Table 2.6. Maximum, minimum and mean value for Red light at A. Surface (I_X) and B. 41cm (I_X_41) below the surface. Values are presented as W/m^2 and are recorded based on the percentage of maximum output of each luminaire i.e. I_100 is at 100% of output compared to I_25 which is a 25% of the maximum output that the luminaire is capable of producing.

(A)	I_100	I_50	I_25	I_10	I_5	I_4	I_3	I_2	I_1
Max	705.00	375.00	191.00	78.00	35.00	28.00	21.00	14.59	7.34
Min	278.00	147.00	74.00	30.00	12.90	10.43	7.90	5.26	2.64
Mean	465.04	247.63	126.06	51.06	22.56	18.25	14.05	9.42	4.73

(B)	I_100_41	I_50_41	I_25_41	I_10_41	I_5_41	I_4_41	I_3_41	I_2_41	I_1_41
Max	189.00	101.00	52.00	20.00	9.07	7.34	5.54	3.70	1.86
Min	129.00	68.00	35.00	14.38	6.13	4.94	3.74	2.49	1.25
Mean	154.27	82.04	42.08	17.15	7.56	6.10	4.62	3.08	1.54

Table 2.7. Percentage lost between surface and 41 cm below

% Loss	I_100	I_50	I_25	I_10	I_5	I_4	I_3	I_2	I_1
Max	73.2	73.1	72.8	74.4	74.1	73.8	73.6	74.6	74.7
Min	53.6	53.7	52.7	52.1	52.5	52.6	52.7	52.7	52.7
Mean	66.8	66.9	66.6	66.4	66.5	66.5	67.1	67.3	67.4

White

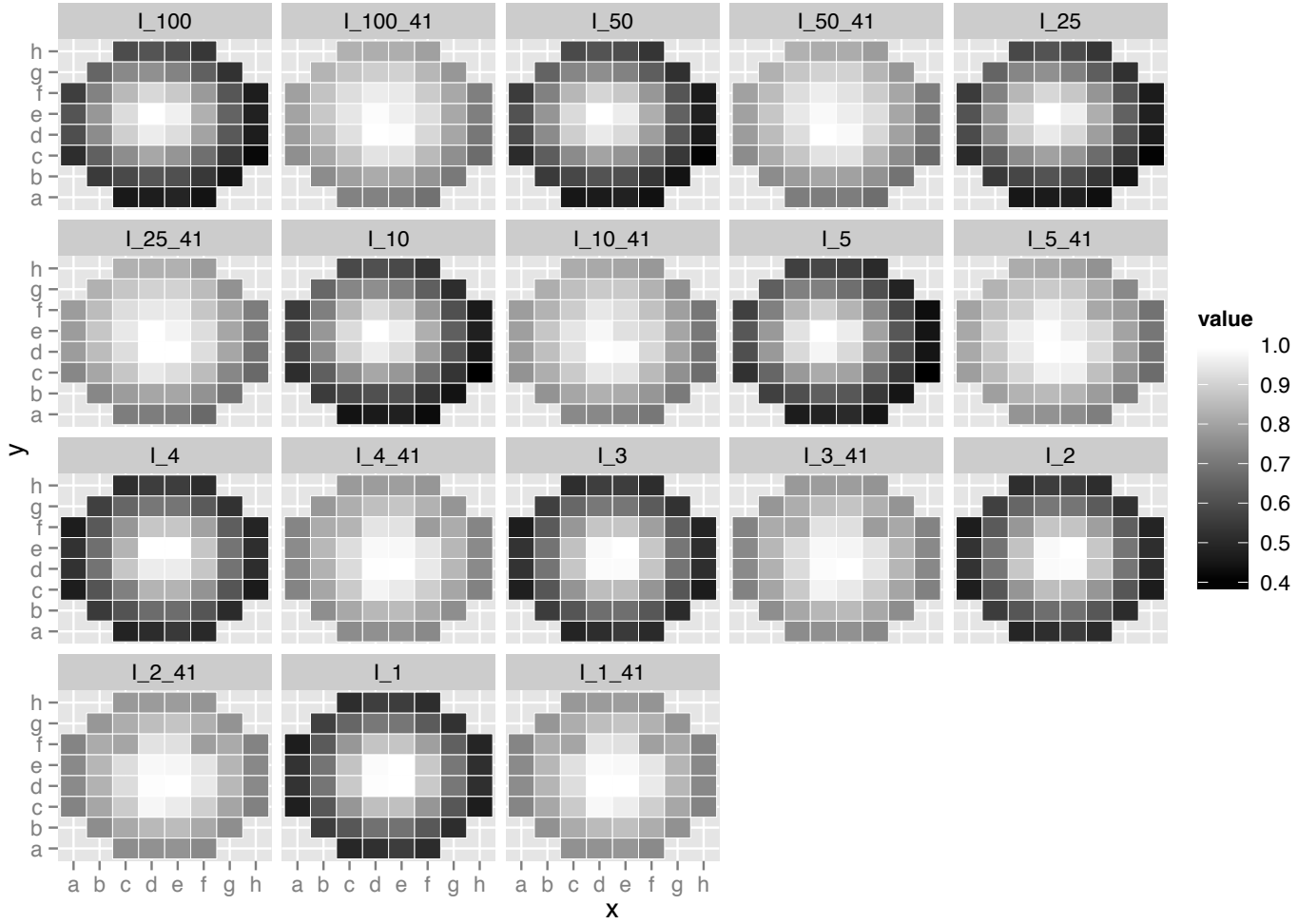

Figure 2.14. Distribution of White light with I_**X** representing the percentage (%) of maximum luminaire output. I_X vs I_X_41 provides comparison between water surface and 41 cm below at each output. Values presented as relative proportion of highest output.

Table 2.8. Maximum, minimum and mean value for White light at A. Surface (I_X) and B. 41cm (I_X_41) below the surface. Values are presented as W/m^2 and are recorded based on the percentage of maximum output of each luminaire i.e. I_100 is at 100% of output compared to I_25 which is a 25% of the maximum output that the luminaire is capable of producing.

(A)	I_100	I_50	I_25	I_10	I_5	I_4	I_3	I_2	I_1
Max	531.00	288.00	144.00	53.00	50.00	25.00	18.78	12.64	7.41
Min	218.00	116.00	58.00	21.00	19.86	11.46	8.64	5.81	3.42
Mean	354.79	190.94	95.46	35.12	32.98	16.64	12.60	8.48	4.99

(B)	I_100_41	I_50_41	I_25_41	I_10_41	I_5_41	I_4_41	I_3_41	I_2_41	I_1_41
Max	156.00	84.00	42.00	15.92	14.51	7.22	5.47	3.68	2.16
Min	105.00	56.00	28.00	10.75	9.77	5.24	3.96	2.66	1.57
Mean	130.58	70.00	35.00	13.25	12.20	6.03	4.55	3.07	1.81

Table 2.9. Percentage lost between surface and 41 cm below

% Loss	I_100	I_50	I_25	I_10	I_5	I_4	I_3	I_2	I_1
Max	70.6	70.8	70.8	70.0	71.0	71.1	70.9	70.9	70.9
Min	51.8	51.7	51.7	48.8	50.8	54.3	54.2	54.2	54.1
Mean	63.2	63.3	63.3	62.3	63.0	63.8	63.9	63.8	63.8

2.2.2 MMERL –Tank Lighting

Light supplied in the flow through system at the Machrihanish Marine Environment Research Laboratory (MMERL) was produced using a Philips Master PL-S 9W/840/2P 1CT (Philips, Eindhoven, NL) compact fluorescent lamp rated at 9W. The spectral profile is a presented in figure 2.15.

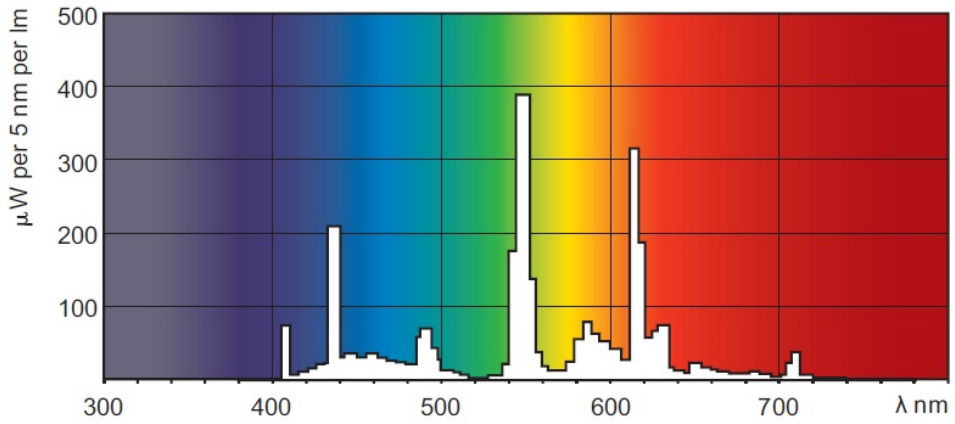

Figure 2.15. Spectral profile of lights used for the SW on-growing trial at Machrihanish produced by a Philips Master PL-S 9W/840/2P 1CT.

2.3 Bespoke Feeding System

In order to feed fish with sufficient frequency a bespoke feeding system was built using modified twin screw feeders (Eheim, Germany). Feeders required modification (Fig. 2.16) due to their intention for the home aquarium market which limits 6 inputs a day of a minimum delivery of 1 turn of the auger screw that delivers the food. Feeders were located on the tank lip in a plastic wall mounted patress box which keeps the feeder safe whilst positioning it close to the water surface to exploit surface tension to distribute the feed.

Figure 2.16. Adapted EHEIM twin screw feeder with direct connections soldered onto the mottors. Connectors enables feeders to be changed as required.

Feeders were attached to custom built timing box. A series of interface cards connected to a Raspberry Pi (RPi) running Raspbian, a variation of Debian Linux operating system was used to control relays. Each interface card was addressable allowing the control of feeding by switching on and off for controlled amounts of time. 6 cards each with two relays provided the control of 12 feeders (Fig. 2.17).

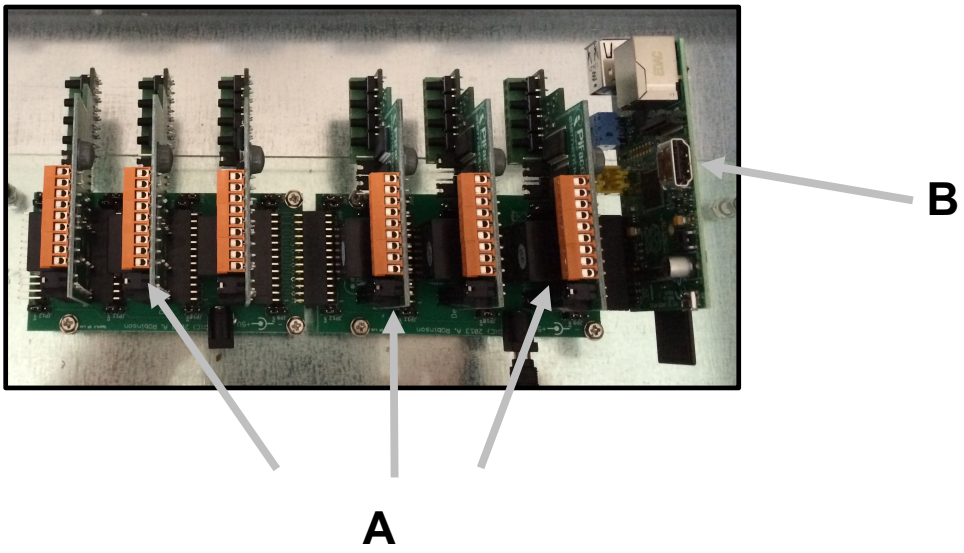

Figure 2.17. Raspberry pi (B) with interface cards (A) connected in series. Each interface card features two relays and each relay is connected to a single feeder.

Control Box

The controller was housed in a large waterproof box (Fig. 2.18). Each two interface cards were supplied with a shared adjustable AC-DC power supply. Eheim feeders were modified by wiring both motors into a lever based connection block. The connection block allowed the feeder to be changed quickly should the need arise. From the connector block the wire (0.05 cm 2-core) attached to a relay on the interface card.

Figure 2.18. Main control box pre and post assembly.

Software and Scripts

A script installed on the RPi controlled the duration of feed auger turn and feed delivery. A record was written to a log file when the script has been run indicating that feed has been delivered.

The inbuilt scheduler called Crontab was used to control how often feed was delivered. Briefly, Cron scripts work through a prescribed syntax and when installed will re-actuate even after a power outage. A simple web page provided accesses to the log file and displayed the timestamp recorded when the feeder delivered. To make this work an Apache webserver and myPhP was installed. A telnet session via SSH allowed the RPi to be controlled whilst running headless.

Calibration

Feeders were calibrated through a series of repeat runs of seconds or parts thereof to obtain consistent feed delivery (Fig 2.19). A repeat loop for 100 runs was followed by weighing the feed delivered. Differences occurred between feeders so it is important that each one was calibrated accordingly. Unlike a drum type system feed delivery was more variable owing to voltage losses and quality differences between motors, the design of the feeder from the manufacturer incorporated an electromechanical switch to determine a complete turn of the auger so precision was not required within the motor component. Modification with a stepper motor would provide a considerable

improvement in performance. In this application over feeding was required so feed volume was checked weekly by weight and visual and pinch feeding assessment ensured adequate ration.

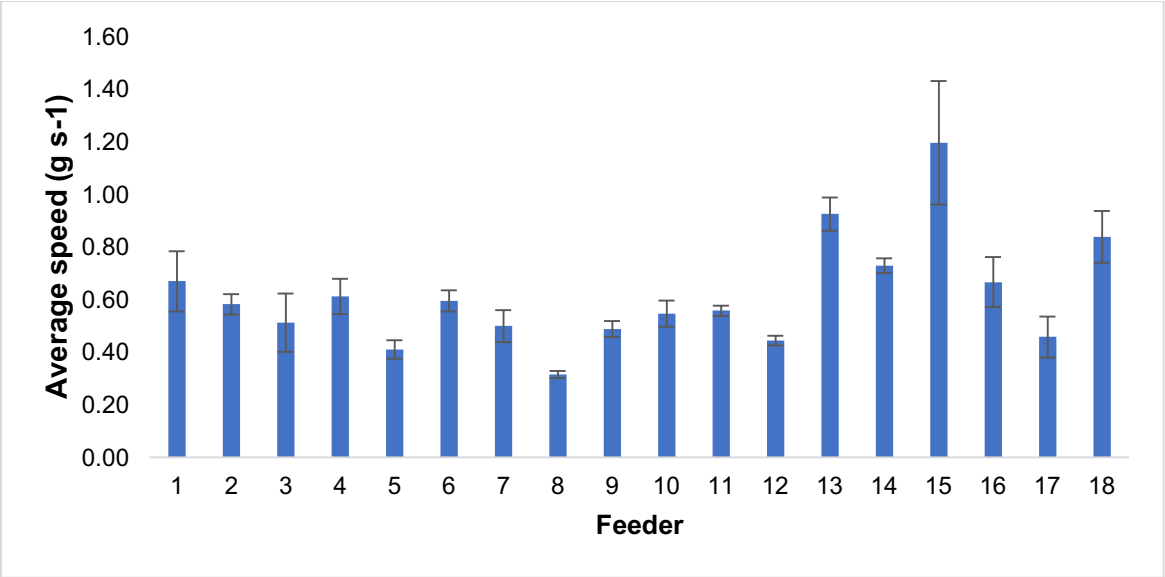

Figure 2.19. Example of feeder calibration using steps of 0.1S repeated 100 times

2.4 Sampling Materials and Methods

2.4.1 Fish Handling

Anaesthesia

In all cases, anesthesia was prepared by dissolving 5 grams of MS222 (Pharmaq, UK) in 1 litre of dH_2O to get a concentration of 5 mg/ ml. The solution was then buffered using1 g $NaHCO_3$ (Cat. No S6297, Sigma-Aldrich) and the pH adjusted to 7 with NaOH. To prevent degradation by light the solution was wrapped in tin foil.

A working solution was then prepared using 10 ml of stock solution (5 mg/ ml) to 990 ml litre of system water (fresh water) to achieve 50 mg/litre**.** The progression of anaesthesia was checked in line with Home office guidelines whereby fins were pinched to identify the conscious state of the animal.

Euthanasia

Euthanasia of fish was conducted using a concentration of 400mg/litre produced by adding 80 ml of stock solution anaesthetic prepared as above at 5 mg/ ml added to

960 ml of system water (fresh water). Following cessation of vital signs fish were removed from the anaesthetic and a percussive blow to the head and severing of the gill aorta was performed in accordance with schedule 1 Home Office procedure

2.4.2 Fish Identification

Fin clipping

Facilitation of visual external identification of tagged and non-tagged fish was achieved through fin clipping. Following tagging (CWT or PIT) the adipose fin was removed using 0.8 cm curved sprung scissors (World Precision Instruments, catalogue number 14127).

Coded Wire Tags (CWT)

A single shot tag injector was used to implant a 0.22 cm coded wire tag (CWT) (Northwest Marine Technologies (NMT), WA, USA) inter-muscularly (IM) in the nape below the 2-3rd fin ray on the dorsal fin and half way between the dorsal fin and lateral line in fish that had been anesthetised as described **(chapter 2.4.1)**. During sampling fish were scanned with a metal detector (Blue Hand Held Detector, NWT, WA, USA)

Tagged fish were removed, euthanised as described **(chapter 2.4.1)** and BW (± 0.1 g) and FL (± 0.1 cm) recorded. Tags were removed (Fig. 2.20) and metrics matched to original records.

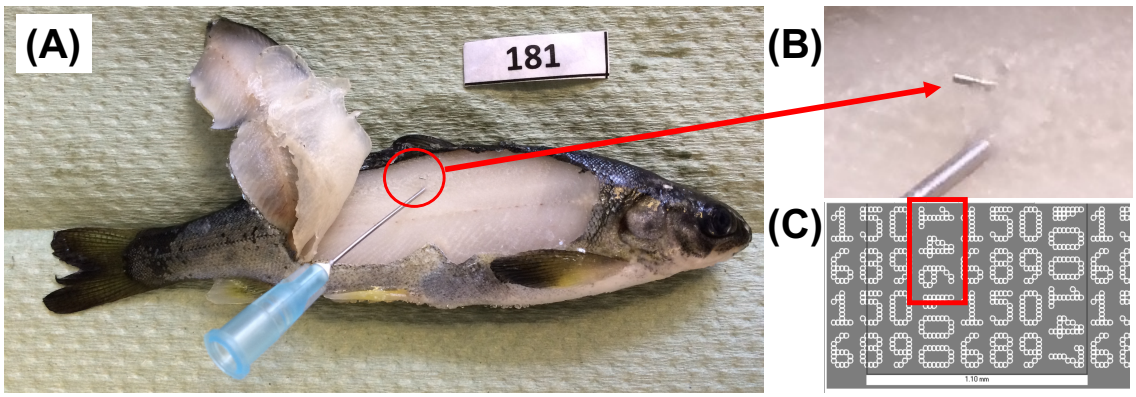

Figure 2.20 Coded wire tag (CWT) location and removal. The CWT is removed post mortem by slicing thin layer of tissue from the flank (A) in order to reveal the tag (B). The tag is then removed and a microscope used to read the code which is sequentially numbered (C). The tag contains a range of information written over the 0.11 cm length. The fish number was used in this trial which in example (C) would be 146.

Passive Integrated Transponder (PIT) Tags

Identification of larger individual fish (>50g) was achieved by using PIT tags (Trovan, USA) inserted intramuscularly into the nape directly below the 2-3rd fin ray on the dorsal fin in anesthetised fish. A single angled needle point injector 12G (Biomark, USA) was used to insert the PIT tag.

A portable PIT tag reader (Model R-560, Trovan, USA) was used to determine the code and fish identification and checked against a pre-identified database in Excel (Microsoft, USA).

2.4.3 Blood Sampling

Needle Gauges

Blood sampling was performed on euthanised fish. Blood was removed using a suitable gauge of needle (<150g: 25G, 150g > 500g: 23G, 500g + 21G Terumo, Japan) and either 1ml or 5 ml disposable plastic syringe.

Heparinised Syringes

Where required porcine heparin was used to prevent coagulation. Heparinised syringes were produced by drawing heparin solution at 4mg/ml made by dissolving 0.08g in 20ml of dH_2O into a syringe before evacuating the syringe. The remaining residue sufficient to prevent coagulation. Needles were not heparinised to prevent immediate blood loss form the site of needle puncture.

2.4.4 Growth Metrics

Weight

Weights for fish were obtained by removing anesthetised fish from the water and placing upon a weighing scale of suitable range.

Length

The length of fish was obtained by placing anesthetised fish onto a measuring board ("fish stick") and recoding the length from the snout to the tail fork to the nearest 0.1 cm.

Condition Factor

BW and FL data was used to calculate Fulton's condition factor (K).

$$\text{Condition factor (K)} = \frac{\text{Weight (g) x 100}}{\text{Total Length (cm)}^3}$$

Growth Model Comparisons

Care must be taken when using models to assess growth performance (Dumas et al., 2010). SGR models typically account for growth as a linear trend and fail to take into account condition factor. To avoid these limitations TGC has been used for comparisons in growth performance. Assignation of a regression coefficient of 3 (Jobling 2003) results in TGC with a high convergence with FW growth profiles in salmonids (Cho 1992). Further, concerns raised by Joblin 2003 regarding accuracy of TGC at the extremities of the temperature range for Atlantic salmon are negated as temperatures in these trials were well within the biological optima (Austreng et al., 1987; Forseth et al., 2001) and thus further model corrections as suggested by Elliott and Hurley 1997 were deemed unnecessary.

Thermal Growth Co-efficient

TGC was calculated as follows:

$$\text{TGC}_{\text{weight}} = \frac{\left(\sqrt[3]{\text{weight}_{\text{end}}} - \sqrt[3]{\text{weight}_{\text{start}}}\right) \text{X } 1000}{\text{degree days}}$$

2.4.5 Smoltification Assessment

A number of methodologies were used throughout the thesis to asses the process of parr smolt transformation. These included external phenotyping, assessment of osmoregulation capacity using direct measurement and genomic approaches. The rationale for the application of a given assessment method is provided in each respective experimental chapter.

Smolt Index

To assess smoltification status fish were assessed using a smolt index (SI) scale assessed via the criteria. A scale where: 1= parr; 2 - parr marks visible but some silvering; 3- full silvering with some parr marks; and 4 = smolt where no parks were visible was recorded (Sigholt et al., 1995).

After the initial assessment at 0 °Days it became clear that the colour of the fish was influenced by the tank photic conditions with fish under Red light becoming very yellow and those under Blue being very blue in colour. Figure 2.21 shows a comparison between two smolts of the same age and stage, one raised under Red and one under Blue. Fish under Green and were broadly similar to each other and reflected a more natural skin tone. As a result, smolt index was not used for any comparisons and was dropped as an assessment from future trials.

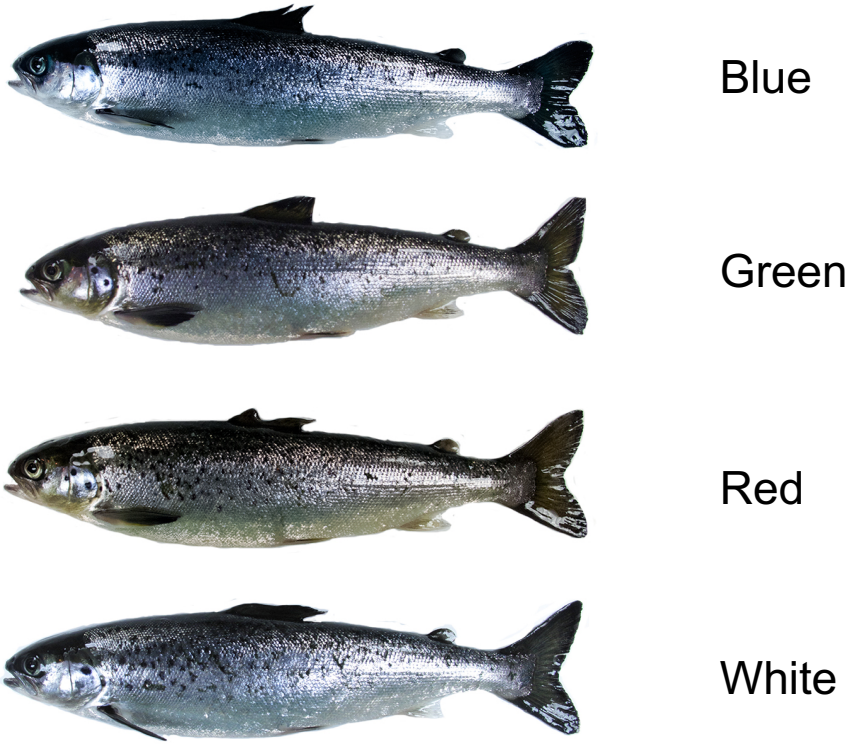

Figure 2.21. Smolt colour under different photic conditions. Blue light (top), Green second, Red third and White at the bottom as observed at 500 °Days post winter solstice. Photos show differences in external pigmentation following sampling highlighting the difficulty in using a phenotype smolt index to assess smoltification in fish exposed to coloured lighting.

NKA Enzyme Assay

Gill samples for NKA enzyme analysis were processed according to McCormick 1993. Four to six gill filaments were removed using curved fine point scissors from above

the septum of the second gill arch on the left-hand side of the fish. Immediately, filaments were placed in ice chilled SIE buffer (150 mM sucrose, 10 mM EDTA, 50 mM imidazole, pH 7.3) held in a 0.5ml Eppendorf microcentrifuge tube. Samples were immediately snap frozen in liquid nitrogen and stored at -70 until required.

Once all samples had been attained samples were processed in a random order to reduce the impact of inter-assay variation. Immediately prior to assay, samples were thawed with all reagents kept on ice throughout the procedure. SEID buffer (50 µl; 0.15 g sodium deoxycholic acid in 50 ml SEI buffer) was added to each sample. Samples were homogenised using a hand-held homogeniser. Samples were then centrifuged for 5 min at 12,000 *g* at 4 °C and were added in quadruplet to a 96-well clear bottom plate. Assay mixture (solution A) contained 4 U lactate dehydrogenase (LDH) ml -1, 5 U pyruvate kinase (PK) ml -1, 2.8 mM phosphoenolpyruvate (PEP), 0.7 mM adenosine triphosphate (ATP), 0.22 mM nicotinamide adenine dinucleotide (reduced form, NADH), and 50 mM imidazole (pH 7.5) (all biochemical reagents from Sigma-Aldrich, UK). Assay solution B was as above but also contained 0.5 mM ouabain. Solution A was added (200 µl) to half of the wells, and solution B to the other half. Na+, K+-ATPase activity was determined at 26 °C and read at a wavelength of 340 nm for 10 min (Multiskan Ex, Labsystems; Finland). Protein content was measured using a bicinchoninic acid (BCA) protein assay kit (Sigma-Aldrich, UK). The principles regarding BCA are the reduction of Cu^{2+}, formed under alkaline conditions, to Cu^{1+}. A purple-blue complex is formed between BCA and Cu^{1+} resulting in a colour change which is directly proportional to the amount of protein present. Results were read at 562nm (Multiskan Ex, Labsystems; Finland). Na^+, K^+-ATPase activity was calculated as the difference in ATP hydrolysis in the presence and absence of ouabain, expressed as micromoles of ADP per milligram of protein per hour.

Quantitative qPCR assessment of gill NKA α1a and NKA α1b

Random Sample Selection

Three gill samples per replicate (n=3) were selected for analysis by qPCR. Samples were chosen at random using a random number generator in excel and ranked in numerical order. The lowest numbered three samples from each group of five were selected resulting in 9 samples per treatment.

RNA Extraction, DNase Treatment and cDNA Synthesis

Gill samples were removed from the RNA stabilisation medium and dried on a paper towel. Tissue was macerated using a scalpel blade and immersed in Tri-reagent (Sigma-Aldrich, St Louis, MO USA) with a 10:1 reagent to tissue ratio. Samples were incubated on ice for one hour and homogenised at maximum speed for 1 minutes using a mini bead-beater (Biospec, Bartlesville, OK, USA). Following homogenization samples were extracted using the manufacturers protocol for Tri-reagent.

Post extraction the RNA pellet was dissolved in the appropriate volume of nanopure nuclease free H_2O to achieve a concentration of between 1000 and 1500 ng/**µ**l. A nanodrop spectrophotometer ND-1000 (Labtech Int., East Sussex, UK) was loaded with the appropriate volume of dissolved RNA and the concentration adjusted accordingly. A 260/280 ratio of between 1.8 and 2.0 was used to assess RNA was of sufficient quality for analysis. A random subset was checked using gel electrophoresis using 500 ng of concentrate on a 1 % agarose RNA denaturing gel.

Following extraction and quantification a DNase enzyme (DNA-free™: Applied Biosystems, UK) was used to treat 5μg of RNA according to manufacturer's instructions. DNase treated sample was re quantified using nanodrop. A 1 µg volume of DNase treated RNA was reverse transcribed into cDNA using a high capacity reverse transcription kit (Applied biosystems, UK) observing the manufacturer's instructions. Prior to qPCR all samples were diluted to 1/10.

Generation of Plasmids for Absolute Quantification

To perform absolute quantification using a qPCR assay each gene was cloned using the appropriate PCR reaction in order to generate plasmids of known concentrations.

The expression of specific Na^+,K^+ - ATPase alpha subunits 1a and 1b was the target of these assays. Primer pairs were designed according to regions displaying enough difference between the subunits and that would allow identification of specific products by sequencing. The α1b primers were designed to identify both the α1bi and α1bii isoforms as differentiation between them failed using a SYBR green assay. Bi and bii shared 98% nucleotide identity and differentiation between them was not possible using SYBR green chemistry.

Initially PCR products for cloning were purified using Thermo genejet PCR purification kit (Thermo Scientific, UK) following the manufacturers protocol. Cloning

of the resulting products was carried out using the pGEM®-T Vector System (Promega) kit and plasmids harvested used a GenElute™ Plasmid Miniprep Kit (Sigma Aldrich, St Louis, USA) according to manufacturer's instructions. The resultant plasmid for each gene was sequenced via SUPREMErun^{TM} sequencing (GATC, Cologne Germany) to confirm identity. To develop standards for use in qPCR plasmids were linearized using a serial dilution in Lambda DNA buffer for each gene from 10^8 copies to 10.

qPCR

Absolute quantification was performed using qPCR analysis performed where possible in accordance with the Minimum Information for Publication of Quantitative Real-Time PCR Experiments (MIQE) guidelines (Bustin et al. 2009). qPCR was conducted in 384 well format using a Light Cycler 480 (Roche) and using Luminaris Colour Hi Green Master Mix Sybr green (Thermo Scientific). Intra time point variation between treatments was of particular interest in this assay so plates were arranged as follow: Plate 1: -400, - 100, 0, 100, 200 ºdays; Plate 2: 300, 400, 500, 600, 800 ºdays; Plate 3: 1000 ºdays, Post Saltwater Transfer SNP treatment, Post Saltwater Transfer LL Treatment. Each time point had 3 samples per replicate, 3 replicates per treatment (n=9) and 4 treatments per time point (n=36/treatment). In addition to the samples a series of non-template controls (H_2O) and line standard were run. To achieve quantification a parallel set of reactions using standards previously generated was also run. All samples were run in duplicate.

The assay was constructed with a total volume of qPCR reaction was 10 µl comprised of primer pairs (Table 2.1) at a concentration of 3 pica moles, 2.5 µl of cDNA (1/10), 1.9 µl DNA/RNA free H2O and 5 µl of Luminaris Colour Hi Green qPCR Master mix) (Thermo scientific). In accordance with the manufacturer's instructions an initial denaturation at 95 °C for 10 minutes was conducted followed by 40 cycles of 3 temperature steps: 95 °C for 15 s anneal X°C (see Table 3.2 for target specific annealing temperatures) for 15 s and 72 °C for 30 s. A final temperature ramp from 60-90 °C provided data for melt-curve analysis to verify no primer-dimer artefacts were present and that only one product was generated from each qPCR assay. Efficiency for all assays was between 1.95 and 2. The reference gene ß-actin was used to provide a reference to facilitate normalization as described by Yada et al. (2012).

Cross assay normalization was carried out using four internal template controls run in duplicates from mixed tissue cDNA.

Table 2.10. Annealing Temperatures for qPCR Analysis

Primer	Sequence	Ascension Number	Annealing Temperature
ATP1α1aF	5'AGACACGTACTCCGGATTTCTC'3	Kj756510 (bi) KJ756511.1 (bii)	59 °C
ATP1α1aR	3'GCTATAGGCGTCTTCCCACC'5	Kj756510	59 °C
ATP1α1bF	5'CCCAAACTCGTAGTCCCGATTTTA'3	KJ175156.1(a)	68 °C
ATP1a1bR	3'AATTCCGAGAGGCGTCTGCC'5	KJ175156.1	58 °C
β-Actin F	5'ATCCTGACAGAGCGCGGTTACAGT'3	AF012125	60 °C
β-Actin R	3'TGGACTTTGAGCAGGAGATGGGCA'5	AF012125	60 °C

Seawater Challenge

Saltwater challenge (SWC) fish were placed in a 0.3 m x 1 m x 1 m tank, separated with 4 dividers and supplied with aerated saltwater for 24 hours (Blackburn and Clarke 1987). The system comprised of a 1000 l sump to ensure homogenous conditions for all test subjects. Seawater was artificially manufactured using TMC Pro Reef (TMC, UK) salt mix with a final salinity of 35 ppt measured using a refractometer (TMC V2, UK). Saltwater was replaced after each challenge. A Panjet needless injector (Wright Health Group, Dundee, UK) filled with Alcian blue (1.63 g dissolved in 25 ml) was used to mark replicates from each treatment using ventrally located dots denoting replicate number (1,2,3). All sampling was conducted between 10:00 and 11:00 a.m. to reduce any diurnal variation.

After 24 hours SWC fish were euthanised using a lethal dose of tricaine methanesulphonate (400 ppm MS222, Pharmaq, UK) before a percussive blow to the head and severing of the gill aorta in accordance with schedule 1 Home Office procedure. Blood samples were collected from the caudal vein using heparinised syringes. Whole blood was centrifuged at 2500 rpm for 15 mins at 4 °C and plasma retained for immediate plasma chloride analysis.

Plasma Chloride Analysis

Plasma chloride was analysed using a chloride analyser model no. 926 (Sherwood Scientific, Cambridge, UK). This method uses a coulometric titration where donor silver electrodes are reduced through passing a current between them and the resulting solution provides the reagent for analysis. Differences in solution conductivity are recorded as silver ions bind to form silver chloride and the conductivity. The subsequent availability of silver ions and resultant conductivity change provides the end point for the titration. Results are then calculated and expressed as mmolCl/l.

Blood was removed from the caudal vein and centrifuged at 2500 rpm for 15 min at 4 °C. Serum was removed and stored at −80 °C until analysis whereby 50µl of plasma was pipetted into 15ml of acid buffer reagent combined with 0.3ml of gelatine reagent. Reading were generated within 5 seconds and recorded.

2.4.6 Welfare Assessments

Several methodologies were adopted throughout the thesis to assess fish welfare including physical assessment of eyes and skeletal formation and molecular approaches. The rationale for the application of particular assessments is provided in each experimental chapter respectively.

Cortisol Analysis

Cortisol was analysed using an IBL Cortisol ELISA kit (RE50261, IBL, Germany) according to the manufacturer's instructions. Briefly, 20 µl of sample was mixed with 200 µL of conjugate enzyme and incubated for 60 minutes, the excess was washed off using wash buffer and 100 µL of TMB substrate solution was added to each well. Following 15 minutes of incubation a TMB stop solution was added and the optical density read using a spectrophotometer (model) at 450 nm. Recorded optical density was compared to a concentration gradient curve created at the same time and values extrapolated using the R/DRC package (Ritz et al., 2015).

Cataract Assessment of Eyes

Assessment for cataracts was performed using a handheld ophthalmoscope. The severity was recorded according to a previously published scoring index (Wall and

Bjerkas, 1999). Severity is based upon the percentage of opacity of the lens area: 1 = <10%; 2 = 10-50%; 3 = 50-75% or 4= >75%.

Histological Examination of Eyes

The right eye was removed and a small incision made in the sclera, 90 º to the right of the choroid fissure before placing in Bouin's fixative for 24 hours. The solution was replaced with 70 % ethanol every 24 hours until clear (3 washes) and stored at 4 ºC according to Vera and Migaud (2009).

Following preservation samples were prepared for sectioning using a standard protocol whereby samples were firstly places in a dehydration alcohol series followed by a clearing step using xylene. Samples were then impregnated with wax before being embedded in wax for sectioning on a microtome. Sections of 7µm were cut and stained using a standard H and E protocol. Sections were digitalised using a slide scanner (Zen AxioScan, Zeiss, Germany). Assessment of layer thickness was conducted using ImageJ (vs. 2.0.0.-rc-54/1.51g, NIH, USA). The following measurements were recorded in 10 locations on the dorsal, lateral and ventral planes: the thickness of the photoreceptor layer not including the outer nuclear later, the retinal pigment epithelium (RPE), the outer nuclear layer thickness, the melanin granules layer within the RPE.

Vertebral Radiological Assessment

Radiological assessment was performed on whole fish at the relevant sample point as described later in each chapter. Samples were collected and frozen flat. Parr/Smolt samples were x-rayed using a Faxitron PathVision (Faxitron, USA) mammography x-radiography unit. Samples at the end of the seawater trial were x-rayed using an Agfa DX-D40 (Agfa, Belgium) digital direct radiography unit coupled with an x-ray generator. Images were analysed using OsirixLite 8.0.1. Vertebrae (V) were counted and only fish with the same number of vertebrae compared. The spine was divided into 4 regions with region 1 encompassing V1-V8; region 2 V9-V30, region 3 V31-49 and region 4 the remaining vertebrae. Classification of gross malformation mas made in accordance to Witten et al 2009 and results calculated as a total of identified deformities per region. Where appropriate, the total count of deformities was recorded across all regions and the percentage of fish samples with each total deformity count is presented.

2.4.7 Insitu-Hybridisation Methods

Identification of neural stimulation in response to light of different spectral content was performed as described in Chapter 6 using *in situ* hybridisation. Sampling consisted in vascular perfusion following anesthesia with buffered MS-222 (50/mg^{-1}) with 4% paraformaldehyde as described in Sandbakken et al. (2012). The brains, one per time point, were dissected out and prepared for *in situ* hybridization on cryo-sections (Sandbakken et al., 2012). The ISH was carried out under similar conditions for all sampling points. The sampling followed the local animal care guidelines and was given ethical approval by the Norwegian Veterinary Authorities (Application number: 6918).

Identification of *c-fos* Paralogue Genes

The salmon database Ssa_ASM_3.6.scaf.fasta at ViroBLAST (http://marineseq.imr.no/salmon2014/viroblast/viroblast.php) was searched with a query sequence of Atlantic halibut *c-fos* (Accession number: KF941297) giving two relevant contigs (ccf1000000124_0-0 and ccf1000000152_0-0). Alignment of the query sequence and subject (contig) indicated two potential *c-fos* genes. Based on the alignment the exons were predicted and primers located in the potential UTR's were designed for the two genes. Primers are listed in Table 2.11.

Table 2.11. Primer ID, sequences and accession id for c-fos paralogue genes

Primer name	Sequence (5'–3')	Accession ID
cfos124F1	GGATCACTTGACTTTGACAGC	MF685241
cfos124R1	TGCGCTGAAGAACAAGTCAAC	MF685241
cfos152F1	GGGATCACTTGACTTTGACAAC	MF685242
cfos152R1	GCTTCCTGGTTGTGCGAGTC	MF685242

Molecular Cloning

Total RNA isolation, DNase treatment and cDNA synthesis was performed according to Grassie et al. (2013). The two Atlantic salmon *c-fos* genes were cloned by amplification of the genes by PCR using a pool of DNase treated cDNA of Atlantic salmon brains. PCR was run with annealing temperature of 63°C for *c-fos124* and

62°C for *c-fos152* and 35 cycles were used. The primer pairs for both of the genes generated a PCR product of approximately 1500 bp. The PCR products were separated on an agarose gel and the relevant bands were cut out and extracted from the agarose gel by QIAEX II Gel Extraction kit (Qiagen, Germany). The PCR products were ligated into StrataClone PCR cloning vector pSSC-A-amp/kan (Agilent Technologies, CA) and sequenced at the University of Bergen Sequencing Facility. The nucleotide sequences were deposited into GeneBank with the accession number MF685241 (*c-fos124*) and MF685242 (*c-fos152*).

Synthesis of RNA Probe for *c-fos*, Melanopsin and VA Opsin

For the synthesis of RNA probes, PCR product was used as template for the reaction and primers were designed for *c-fos*, melanopsin and VA opsin as described in (Thisse and Thisse 2008). The primers for *c-fos* were designed to be specific for both paralogues by making them degenerative, ensuring a probe specific for both genes. For melanopsin three probes were synthesized and used together, *opn4m1a1* (specific for JN210547), *opn4xa1* (specific for JN210546) and *opn4x1b1/2* (specific for both JN210544 and JN210545) ensuring to detect all the functional photopigments of melanopsin. For VA opsin the probe primer was designed based on NM_001123626. Synthesis of DIG-labelled RNA probe for *c-fos* and the melanopsins and DIG and FITC-labelled RNA probe for VA opsin was done following the manufacturer's instructions (Roche Diagnostics, Germany). The synthesized probes were precipitated by LiCl and EtOH together with tRNA (Roche Diagnostics, Germany).

In situ Hybridization and Nissl Staining

Parallel sectioning (10µm) was performed on a Leica CM 3050S cryostat and, before storage at 20°C, the tissues were air dried for 1 hour at room temperature and for 30 minutes at 65°C. *In situ* hybridization was carried out as described by Sandbakken et al. (2012). One parallel of the sectioned brain was Nissl-stained with 0.5% cresyl fast violet (Chroma-Gesellschaft, Germany), and the other parallel was stained by *in situ* hybridization (ISH).

2.4.8 Pituitary Sequencing using Next Generation Sequencing (NGS)

RNA Extraction

Pituitary gland was removed from the RNA stabilisation medium and dried on a paper towel. Tissue was macerated using a scalpel blade and immersed in Tri-reagent (Sigma-Aldrich, St Louis, MO USA) with a 10:1 reagent to tissue ratio. Samples were incubated on ice for one hour and homogenised at maximum speed for 1 minutes using a mini bead-beater (Biospec, Bartlesville, OK, USA). Following homogenisation, samples were extracted using the manufacturers protocol for Tri-reagent.

Post extraction RNA samples were treated with RNase-free DNase Miniprep (Qiagen), RNA pellet was dissolved in nanopure nuclease free H_2O. A nanodrop spectrophotometer ND-1000 (Labtech Int., East Sussex, UK) was loaded to determine concentration and each sample was checked using gel electrophoresis using 500 ng of concentrate on a 1% agarose DNA denaturing gel.

Sequencing

Samples were sent to the sequencing centre (Theregen Etex Bio Institute, Korea) in two batches. Firstly, the dark versus light extractions (Da/Li) were sent to ensure that the sequencing was of a suitable quality for analysis. This initial set of samples were extracted using a TruSeq extraction protocol poly-A chemistry as described.

Following successful sequencing, the second set of samples, Blue versus Red were shipped. During quality control at the sequence centre the quality was found to be degraded with one sample failing quality control entirely. A new sample was sent and on the advice of the sequencing centre libraries were prepared using a Ribo-Zero rRNA removal kit. The use of two different library preparation techniques prevent comparisons ‘between’ the two groups however results ‘within’ groups are valid.

Libraries were prepared for 100 bp paired-end sequencing using either the Poly-A TruSeq RNA Sample Preparation Kit (Illumina, CA, USA) or the Ribo-Zero rRNA removal kit, as per the manufacturer’s instructions. Namely, mRNA molecules were purified and fragmented from 2 µg of total RNA using oligo (dT) magnetic beads. The fragmented mRNAs were synthesized as single-stranded cDNAs through random hexamer priming. By applying this as a template for second strand synthesis, double-stranded cDNA was prepared. After sequential processes of end repair, A-tailing and adapter ligation, cDNA libraries were amplified with 8-10 cycles of PCR (Polymerase Chain Reaction). Quality of these cDNA libraries was evaluated with the Agilent 2100 BioAnalyzer (Agilent, CA, USA). They were quantified with the KAPA library quantification kit (Kapa Biosystems, MA, USA) according to the manufacturer’s library

quantification protocol. Following cluster amplification of denatured templates, sequencing was progressed as paired-end (2×100 bp) using Illumina HiSeq2500 (Illumina, CA, USA).

Transcription Assembly

For each RNA-Seq sample the reads were mapped to the *S. salar* genome (NCBI Assembly GCF_000233375.1) using HISAT2 v2.0.5 (Kim, Langmead, and Salzberg, 2015). StringTie v1.3.0 (Pertea et al., 2015) was subsequently used to assemble the read alignments into potential transcripts. During mapping of reads, the reference annotation information (NCBI Assembly GCF_000233375.1) was used and a non-redundant set of transcripts observed in all the RNA-Seq samples was then built following the protocol by Pertea et al., 2016. Finally, for each RNA-Seq sample, an estimate of each transcript abundance was generated with StringTie. Cuffdiff v2.2.1 (Trapnell et al., 2012) and R/cummeRbund v2.7.2 (Edwards, 2016) were used to perform various statistical analyses for differential expression and generate plots.

Confidence values are presented as corrected p-value (q-values). The q-value accounts for the for the false discovery rate induced through multiple tests. Significant differentially expressed genes (DEX) is determined by a q-value limit of <0.05.

Functional Annotation

Kyoto Encyclopaedia of Genes and Genomes (KEGG) Automatic Annotation Server (Moriya, Itoh, Okuda, Yoshizawa, and Kanehisa, 2007) was used to provide functional annotation of assembled transcriptome against the manually curated KEGG GENES database. The result contains KO (KEGG Orthology) assignments and automatically generated KEGG pathways. R (Ritz, Baty, Streibig, and Gerhard, 2015), R/pathview v1.16.1 (Luo and Brouwer, 2013) and R/clusterProfiler v3.4.4 (Yu, Wang, Han, and He, 2012) were used to Visualise the KEGG pathways. Following the analysis some genes were associated with ribosomal RNA and where apparent these were removed from the lists, as they are likely to be technical artefacts.

2.4.9 Assessment of Sexual Maturation

Gonadosmatic index

Gonadaosamatic index (GSI) was calculated by:

$$GSI = \frac{Weight\ of\ gonad}{Weight\ of\ fish}\ X\ 100$$

GSI distributions are presented using violin plots whereby a kernel density is calculated and presented perpendicular to the X axis and mirrored to illustrate the distribution of all values.

Histological examination of gametes

Samples selected for histological examination of gametes were fixed in Bouin's fluid for a period of 48 hours and washed three times in (24 hours each time) in 70 % ethanol before long term storage at 4 ºC. Upon selection, samples underwent further fixation, decalcification and wax embedding before being sectioned (7 μm) and stained using a standard H and E staining protocol. Slides were scanned (AxioScan Z1, Zeiss, Germany) and images were assessed according to Grier (2009).

2.4.10 Muscle Fiber Histology and Quantification

Muscle Fibre Sample Processing

From each sample a 0.3-0.4 cm fillet from the truncal region anterior to the dorsal fin was removed, photographed against a scale, and a 0.5 cm X 0.5 cm section attached to a cork disk using optimal cutting temperature compound (O.C.T.). The cork disk was inverted and placed in a beaker of 2-methylbutane previously cooled to close to freezing point (-159 ºC) by submerging in a bowl-shaped Dewar vessel of liquid. Adequate temperature was gauged by the opalescent characteristic that occurs when 2-methylbutance is close to its freezing point. Samples were stored in airtight 25 ml Nalgene cryovials in a -70 ºC freezer and cut within 14 days.

Prior to sectioning, tissue was warmed to -18 ºC in a cryostat (CM1950, Leica Biosystems, USA) before sectioning at 7 μm and allowing to air dry at room temperature. Unfixed cut sections were stained using a standard H and E stain (Cellpath, UK) before mounting in Pertex.

After drying, slides were scanned (AxioScan, Zeiss, Germany and a fixed sized (2000 μm x 1000 μm) representative region of interest (R.O.I.) was removed from 7 separate areas, four from the epaxical and three from the hypaxical myotome blocks.

R.O.I. images were then split into RBG channels and the red channel retained. Images were resized ensuring aspect ratio was maintained and the contrast adjusted (Photoshop CS4, Adobe, USA). Images were printed and outlines traced using copy paper. A total of 7 sections per fish and 3 fish per replicate (n=3) were traced and the outlines rescanned and digitised, the resulting image was thresholded using the built in Robust Automatic Threshold Selection tool and analysed using the Analyse Particles plugin in Fiji (Fiji 1.5g, NIH, USA).

Images of the fillet obtained during the process were printed and traced using copy paper (Fig. 2.22). Using the accompanying scale for reference the area of each fillet was calculated using the same Analyse Particles plugin (Fiji 1.5g, NIH, USA) as used for the muscle fibres.

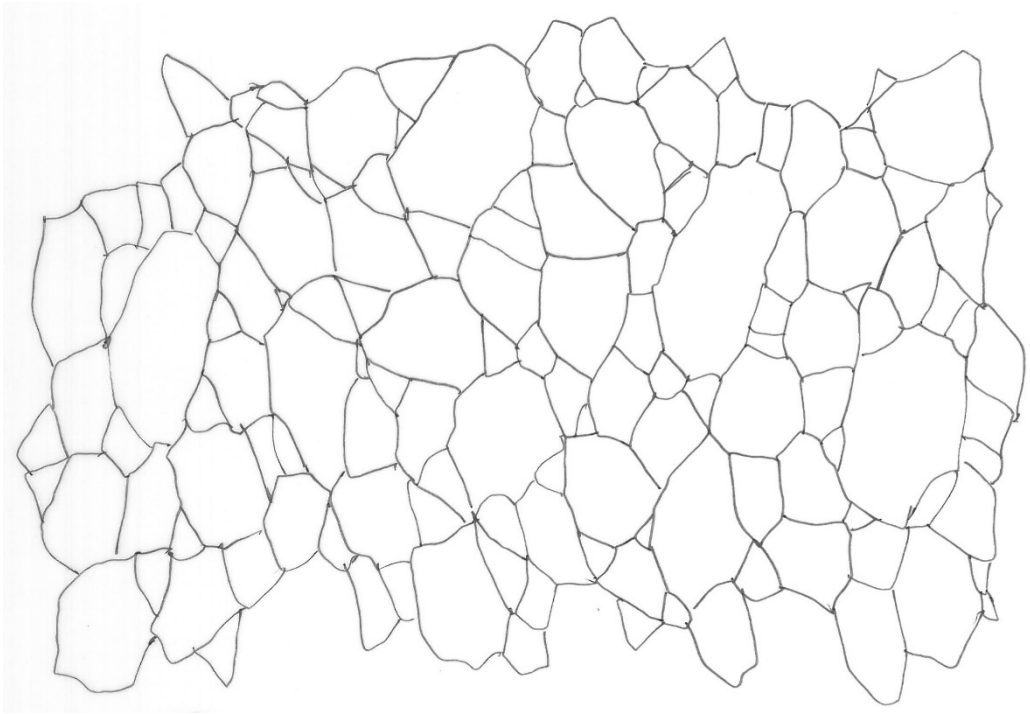

Figure 2.22. Tracing of muscle fiber section prior to digitalisation.

Muscle Fibre Analysis

Digitised muscle fibre data was analysed in accordance with the detailed method from Johnston et al. (1999). Following digitalisation of traced fibres, the diameter of each fibre was calculated. Fibre number varied per fish but was in the range of 900-1100 for parr and smolt sample points, 500-600 for fish exposed to SNP and 350-450 for fish exposed to LL. The number of fibres assessed varied for each sample point due to changes in mean population diameter.

Muscle fibre distributions were then assessed by applying a smooth kernel probability density function (PDF) to each value. The kernel density estimate allows missing data points to be surmised by applying a weighted curve (kernel) to each known value, here a Gaussian distribution was used to estimate missing values as used by Johnston et al. (1999). Missing values were determined through evaluating the tails of the curve between known data points. The width of the tails, and also the shape of kernel, allowed the power of neighbouring data points to be controlled. If too wide a tail is used then the curve becomes over smoothed, if too short then the curve becomes jagged. Here, H, the width of the curve (in effect binwidth) was calculated based on the mean data from each sample point to ensure comparison between treatments was equivalent.

Having applied the kernel the weight of all values under the distribution were calculated and the value was used to provide a density estimate curve with a resolution of all data points. Using a histogram would lose data resolution as bin size is fixed. The need for using this technique stems from the unique mechanisms by which salmon muscle develops (i.e. through mosaic hypertrophy). The mean PDF was plotted against the individual PDFs in order to assess variability (Fig. 2.23).

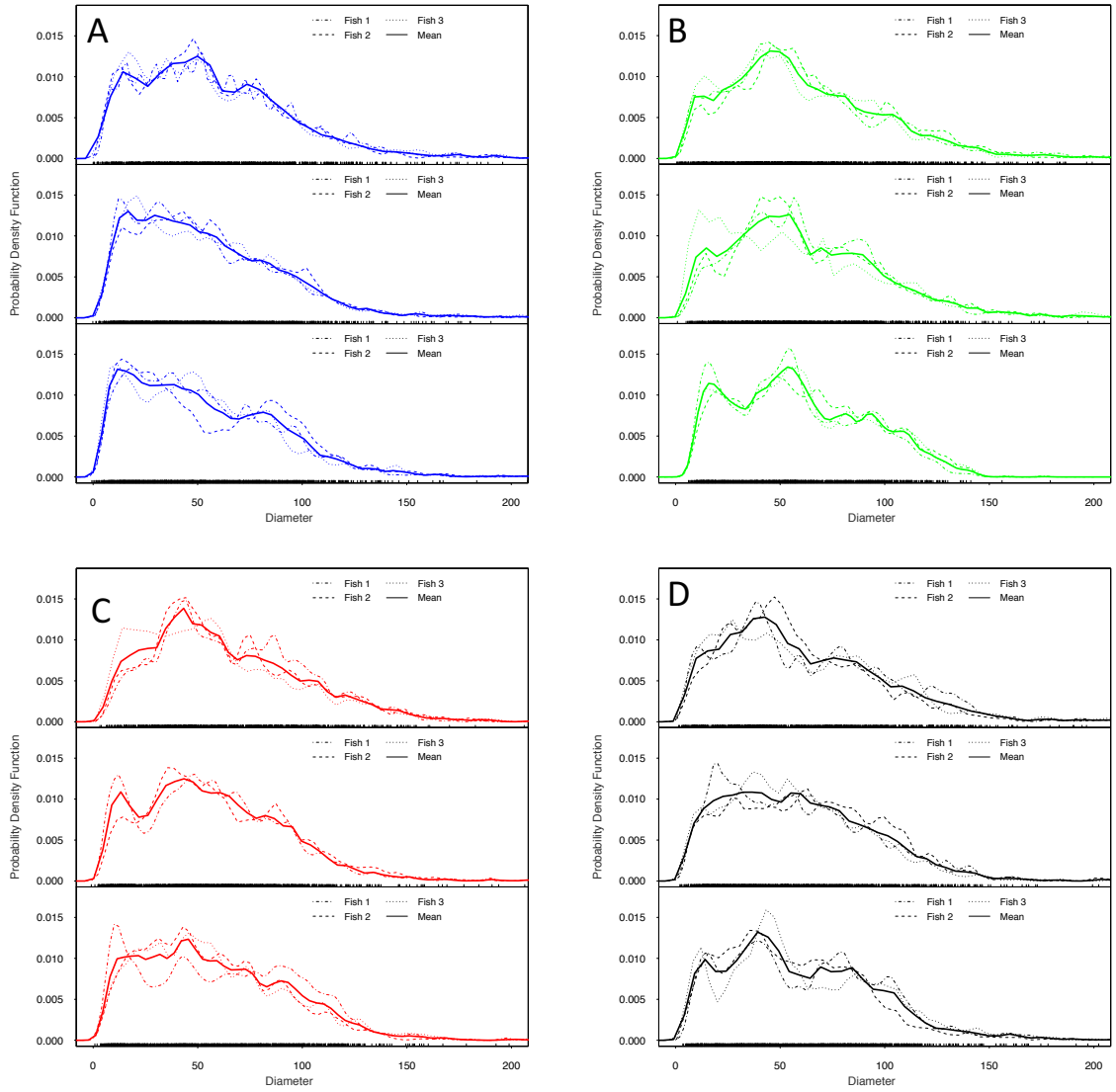

Figure 2.23. Example of individual versus mean probability density function from Atlantic salmon exposed to continuous coloured light from ~0.75g and sampled immediately prior to the induction of smoltification using an out-of-season regime. A. Blue; B. Green; C: Red and D: White.

The continuous nature of this data prevents standard deviations from being derived. To gain an insight into the variation within each treatment a PDF using a 500 repeat bootstrap subsample with replacement was carried out on grouped replicate data for each treatment. Each bootstrap PDF was overlaid and the mean PDF was also plotted. A variation band of 95% of the values was overlaid as a dotted line. Arrows in Figure 2.24 highlight differences in fiber distribution between the Blue and Green treatments with a higher number of smaller fibers present in the Blue compared to the Green groups.

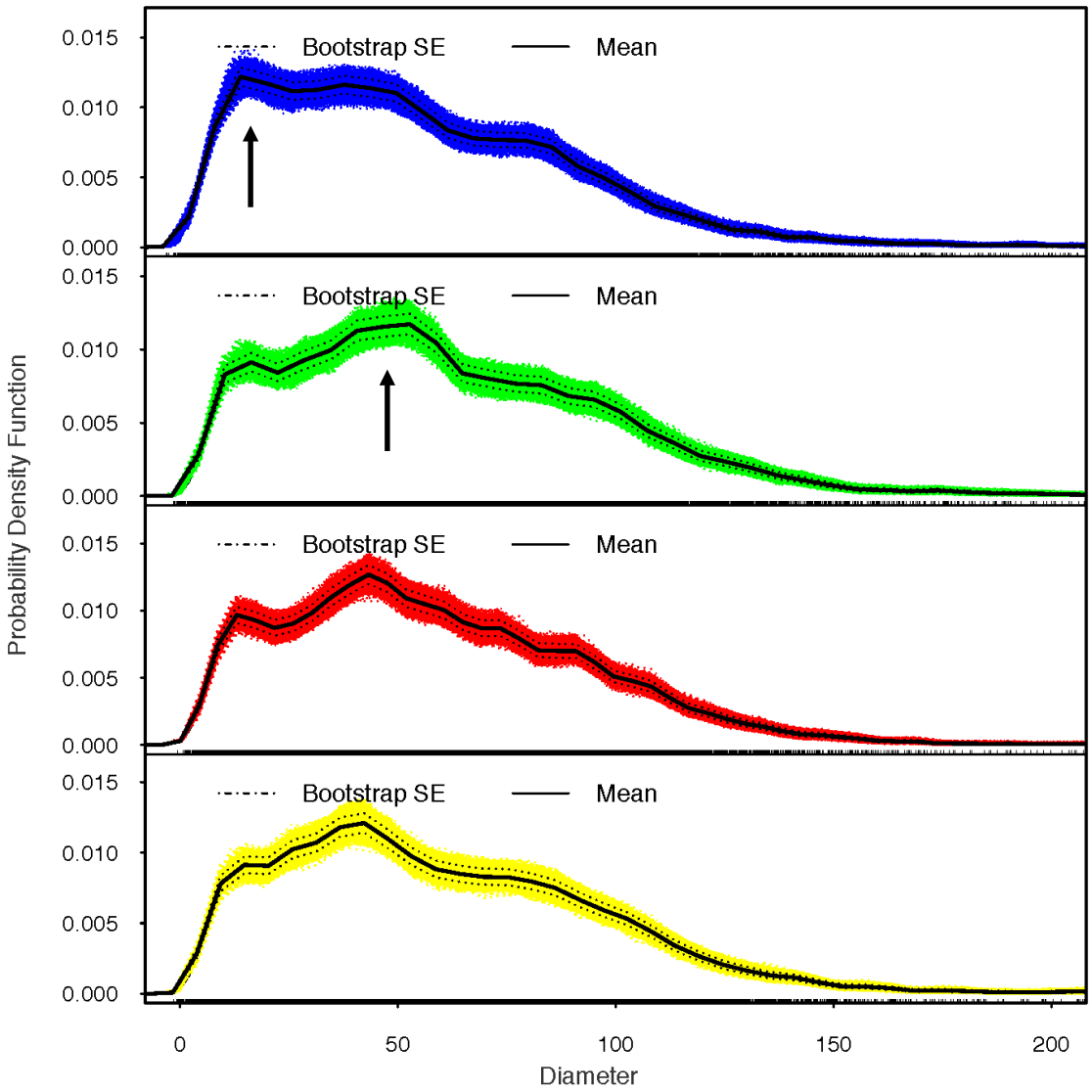

Figure 2.24 Successive bootstrap PDF function obtained from each dataset for each colour. Individual plots are overlaid and the mean value plotted as a solid black line and the 95% values plotted as dotted lines. Arrow highlights the difference in distribution between treatments with a clear skew towards smaller sizes seen in the Blue compared to the Green treatment.

To assess differences between overall distributions a Kolmogorov-Smirnov test was applied to repeated bootstraps from the population using the Matching package in R (Sekhon 2011). The test calculates an empirical cumulative distribution using ordered data points $\mathbf{Y_1, Y_2, \ldots Y_n}$,:

$$E_N = n(i)/N$$

Where ***n(i)*** is the number of points less than $\mathbf{Y}_i$ and that data $\mathbf{Y}_i$ is in numerical order form the smallest to the largest value. The maximum difference between plots is derived, the outcome of which is the D test statistic.

$$D = \max_{1 \le i \le N} (F(Y_i) - \frac{i-1}{N}, \frac{i}{N} - F(Y_i))$$

Where F is the theoretical cumulative distribution of the distribution being tested. The value D is tested against a critical value table.

Whilst Kolmogorov-Smirnov shows that population distributions are different it does little to show where these might lie. To this aim two approaches were used, firstly the 5th, 10th, 50th, 95th and 99th percentile was calculated for each replicate using base R and compared using a Kruskall-Wallace test:

$$H = \frac{12}{n(n+1)} \sum_{i=1}^{k} \frac{R_i^2}{n_i} - 3(n+1)$$

where n_i (i = 1, 2, .., k) represent the sample size of each of the K samples (groups) The combined sample is then ranked and R_i = is the sum of the ranks for each group i. H is then calculated and if it is greater than the chi-square percent point function then it is considered significant. A Dunn's post-hoc test allowed multiple comparisons (Dinno 2016)

The second approach was to plot a variability band (Fig. 2.25) from the two populations of fibres being contrasted and then to plot the distribution of each treatment individually. In areas where the individual plots fall outside of the variance band then differences may be attributed to that part of the fibre distribution.

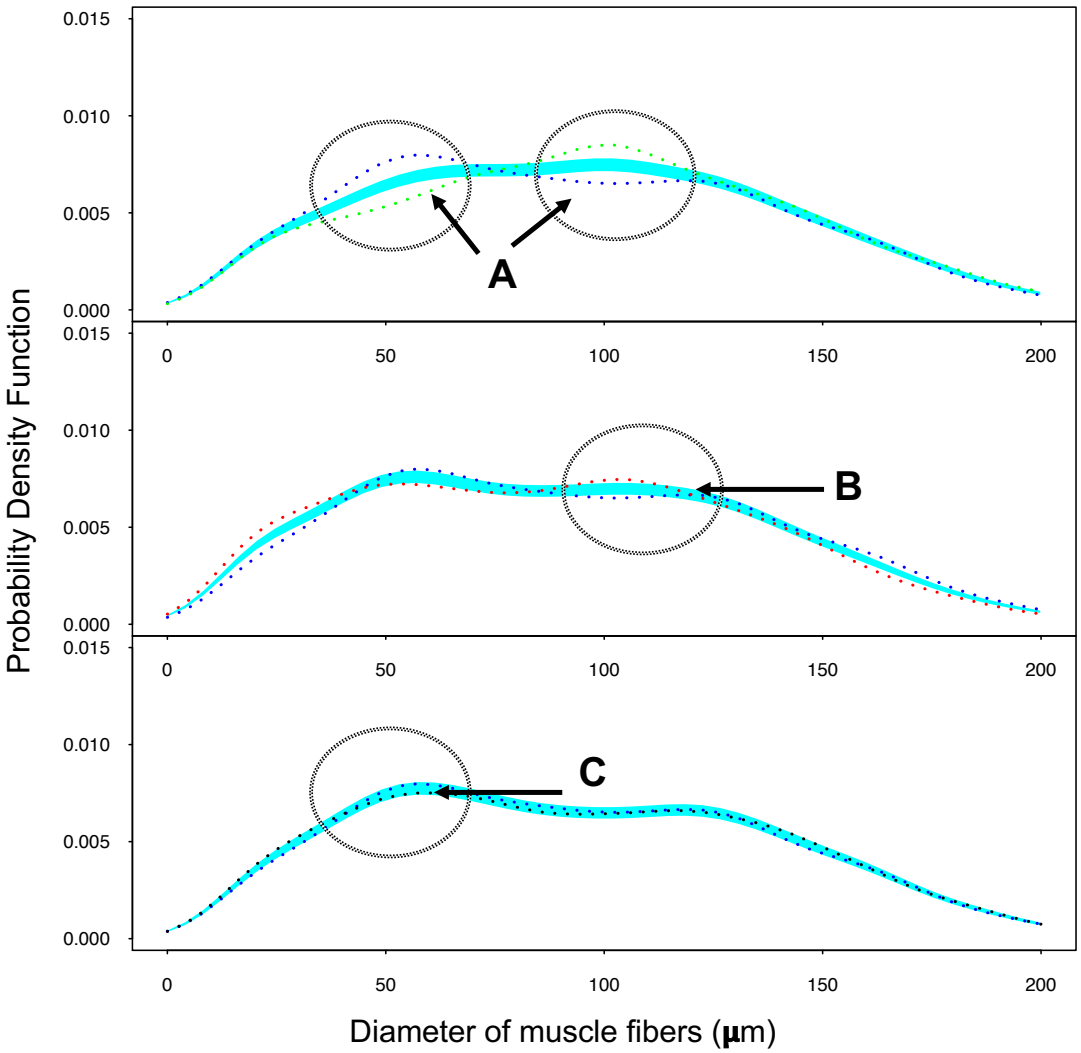

Figure 2.25 Visual comparison between muscle fibers diameters recorded from each treatment. The values for both treatments being compared are plotted as single dataset (the blue shaded area). The individual datasets are then plotted as a single line. Where the lines fall outside the shaded area (e.g. A) a statistical difference regarding the distribution can be assumed. Where differences are small (e.g. B) differences may be considered small. Where lines fall within the shaded area (e.g. C) no statistical differences are assumed.

Mean Fibre Size

The mean muscle fibre diameter was calculated:

$$Mean\ Fiber\ Diameter = \frac{Sum\ of\ all\ fiber\ diamaters}{Number\ of\ fibers}$$

2.5 Statistical Analysis

All analysis was performed within the R-studio environment (vs 1.0.44) (R Core Team 2016) using R version 3.3.2. Mixed linear model was performed with the nlme package (vs. 3.1-128) (Pinheiro et al., 2016), statistical comparisons were performed using TukeysHSD post-hoc lsmeans package version 2.25 (Lenth 2016) and compact letter significance determined using the multcompView package (vs. 0.1.7) (Graves et al. 2015). Random sampling for population data was carried out using the dplyr package (version 0.5.0) (Wickham and Francois 2016). All graphics were created using the graphics package ggplot2 (vs. 2.2.1) (Wickham 2009).

2.5.1 Estimation of the mean

Populations means are calculated using the sample or arithmetic mean, ($\overline{X}$) to estimate the population mean μ.

Arithmetic mean $\overline{X} = \frac{\sum X}{n}$

Where $\sum X$ = sum of observed samples

n = the number of observations

The arithmetic mean is presented with the standard error of the mean (SEM) unless otherwise stated at ± 1 SEM to give a representation of sample distribution.

Standard error of the mean (SEM) = $\frac{s}{\sqrt{n}}$

Where s = sample standard deviation = $\sqrt{\frac{\sum x^2 - \frac{(\sum x)^2}{n}}{n-1}}$

2.5.2 Coefficients of Variation

The coefficient of variation (CV) is used to report the relative variance within a sample, thus it can be used to compare populations with different means.

$$CV = \frac{(s \times 100)}{\overline{X}}$$

Where s= sample standard deviation and $\overline{X}$ is arithmetic mean.

2.5.3 Pearson Correlation

Correlations are calculated using the Pearson correlation calculated as follows:

$$r = \frac{\sum(x - m_x)(y - m_y)}{\sqrt{\sum(x - m_x)^2 \sum(y - m_y)^2}}$$

Where x and y are two vectors of length n, m_x and m_y corresponds to the means of x and y respectively.

The p-values of the correlation is determined by calculating the t value as follows:

$$t = \frac{r}{\sqrt{1 - r^2}} \sqrt{n - 2}$$

And compared with a t-distribution table to determine p.
Pearson correlation require several assumptions to be met:

- covariation must be linear
- x and y must follow a normal distribution

Covariation was checked visually by plotting data (Fig. 2.26) to determine potential relationships between metrics.

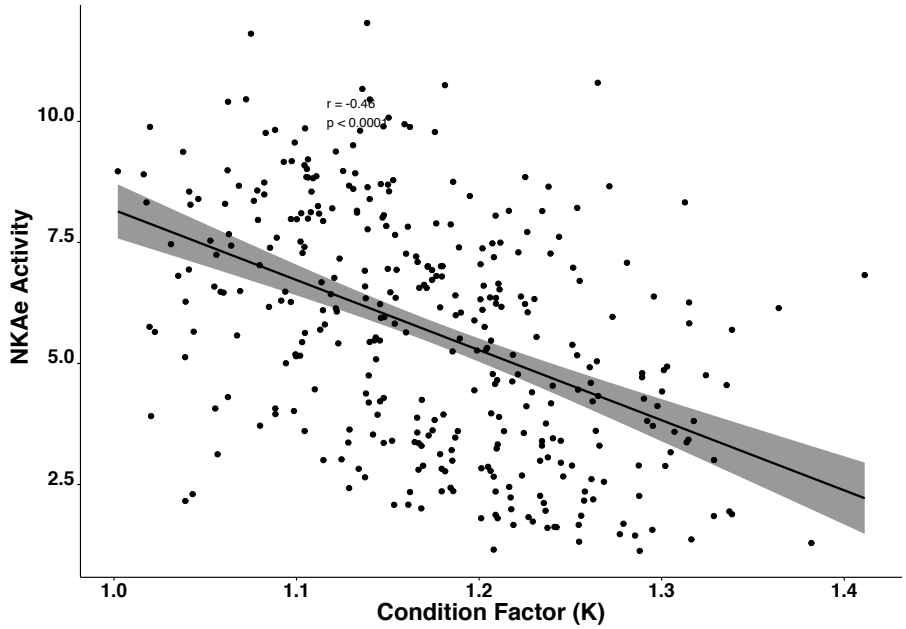

Figure 2.26. Example of testing coefficient of variation for linearity

A value of -1 or +1 signify a strong relationship whereas a value of 0 shows no such relationship. The test values (r) are then compared against a Gaussian distribution to determine the reported P-value.

2.5.4 Shapiro-Wilk Test for Normality

Normal distribution of x and y was checked using the Shapiro-Wilk test in base R. This test calculates a W statistic to determine whether a random sample comes from a normal distribution.

$$W = \frac{(\sum_{i=1}^{n} a_i x_{(i)})^2}{\sum_{i=1}^{n} (x_i - \overline{x})^2},$$

Where $x_{(i)}$ are the ordered samples and $x_{(1)}$is the smallest and the a_i are constants generated from the variances, means and covariance's of a sample of size n from a normal distribution.

ANOVA

Two approaches were used to determine statistical significance between groups and treatments. When sample number was equal parametric comparisons between groups within individual time points were conducted using a one-way ANOVA. Parametric comparisons between groups and time points were carried out using a two-way ANOVA.

Homogeneity of variance was tested before each analysis of variance test (ANOVA). Levene's test works by accessing data for homoscedasticity. Significant for p for the test was set at 0.05. Statistical transformations, either log or sqrt were performed where necessary. Proportion data was corrected using an arcsine transformation where n was equal between subjects and in accordance with the limitation set out by Warton and Hui 2011.

2.5.5 Tukey's HSD

Post-hoc multiple comparisons were conducted using Tukeys HSD test for all factor/interactions. This method compares group means to form calculate a test-statistic.

$$\overline{y}_{i.} - \overline{y}_{j.} \pm \frac{1}{\sqrt{2}} q_{\alpha;r,N-r} \hat{\sigma}_{\epsilon} \sqrt{\frac{2}{n}} i, j = 1, \dots, r; i \neq j.$$

2.5.6 Mixed-effect Linear Model Analysis

Repeat measure longitudinal data such as those from the PIT and CWT tagged fish in addition to data with unequal numbers per sample point was analysed using a mixed effect linear model. Model testing ascertained that allowing random intercept and slopes for each individual accounted for the greatest variation within the dataset.

The model has two levels, the first accounts for the fixed effect factors such as time and treatment. The second level takes into account random effect factors such as replicate and variation within time point. Maximum likelihood was calculated using Restricted Maximum Likelihood (REML) to account for unequal sample size. Briefly, REML calculates a series of contrasts from the original dataset and these contrasts provide the probability distribution with which the maximum likelihood function is calculated. Contrasts were then performed used an orthogonal matrix accounting for variance in time (ar1).

The model took the form:

$$\begin{aligned} &\text{Level 1} \\ &Y_{ij} = \beta_{0j} + \beta_{1j}t_{ij} + R_{ij} \\ &\text{Level 2} \\ &\beta_{0j} = \gamma_{00} + \gamma_{01}TX_j + U_{0j} \\ &\beta_{1j} = \gamma_{10} + \gamma_{11}TX_j + U_{1j} \end{aligned}$$

With: $$\begin{pmatrix} U_{0j} \\ U_{1j} \end{pmatrix} \sim \mathcal{N}\left(\begin{pmatrix} 0 \\ 0 \end{pmatrix}, \begin{matrix} \tau_{00}^2 & \tau_{01} \\ \tau_{01} & \tau_{10}^2 \end{matrix}\right),$$

and

$$R_{ij} \sim \mathcal{N}(0, \sigma^2)$$

The model was built as follows: firstly, a straight line was applied to the data, this was proceeded by adding random intercepts and slopes for each dependent variable and comparing results using an ANOVA until a significant improvement in fit was not attained. At this stage, the simplest number of model additions was used. In all models, random intercepts and slopes were used as this provided the best fit (Winter 2013; Winter 2015; Doncaster and Davey 2007).

2.6 Trial Timetable

Trials were conducted in an order that enabled obtaining fish of a suitable size for each life stage being investigated. An overview of the trials and the chapters that each trial is discussed is given in Figure 2.27

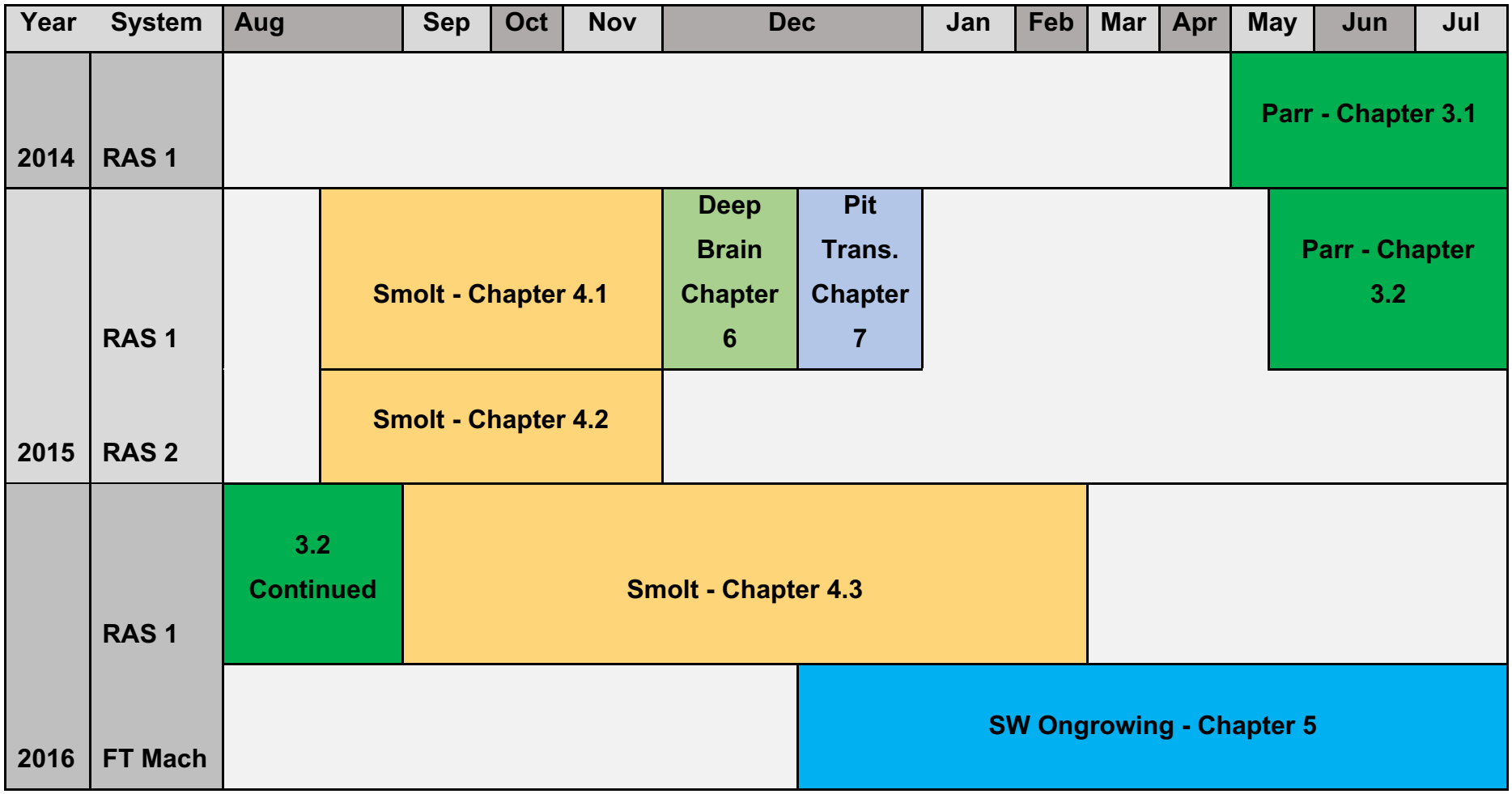

Figure 2.27 Trial timing and duration of each trial is shown in addition to the chapter in which the results are discussed. Are shown. The system that the trial was conducted within is also presented.

3 The Development of Atlantic Salmon Fry in Response to Different Photic Conditions

3.1 Introduction

The production of Atlantic salmon (*Salmo salar*) parr, the freshwater stage from 1g to when smoltification is induced, occurs in freshwater cages, indoor rearing tanks using either flow through (FT) or recirculating aquaculture systems (RAS) (Bergheim et al., 2009). The limited availability of freshwater sites and a desire to maximise production levels whilst mitigating environmental concerns are driving the adoption of RAS (Bostock et al., 2016) in both Norway and Scotland (Bergheim et al., 2009; Dalsgaard et al., 2013). Water quality parameters such as ammonia (Kolarevic et al., 2013), nitrite (Van Rijn et al., 2006; Lewis and Morris, 1986), nitrate (Freitag et al., 2015), dissolved oxygen (Kolarevic et al., 2013, 2014), carbon dioxide (Summerfelt et al., 2015; Moran, 2010), suspended solids (Pedersen et al., 2015; Liao and Mayo, 1972), temperature (Colt 2006) in addition to system design (Terjesen et al., 2013) all have a direct impact on fish welfare and growth performance and require careful management. Significant energy debts are incurred from pumping, heating and cooling water and reducing energy usage benefits both economic and environmental costs (Terjesen et al., 2013).

Utilising recent advances in lighting technology may help reduce these costs. LED lights may offer energy savings by using, either wholly or by adjusting the composition in white light, colours that are more energetically efficient to produce i.e. blue (Akasaki 2007). Alternatively, using narrow bandwidth light of specific colours may offer growth or manipulation benefits, increasing control and decreasing production costs. Energy usage may be further reduced by the provision of biologically relevant light intensities (Pimputkar et al., 2009). Achieving this requires an understanding of how photic conditions, determined by intensity and spectrum, influence the developmental physiology of the Atlantic salmon. Requirements may also differ at each ontogenic stage to reflect changes feeding strategies (Damsgård and Arnesen, 1998). For example, small parr display aggressive, territorial behaviour and a preference for dimly lit areas whereas salmon smolts are passive and shoal (Stradmeyer and Thorpe, 1987). Using more energy efficient spectra requires identifying how, and if, spectrum impacts growth rates and fish welfare. Care must be taken to ensure that welfare attributes such as vertebral and ocular health are not impinged. Extended exposure to short wavelengths in humans leads to macular

degeneration (Taylor et al., 1992), in a visual feeder such as salmon this could be detrimental to both growth and welfare. Currently little is known regarding how either intensity, or spectrum, effect development during any stage of salmon production, including freshwater rearing.

Knowledge regarding salmonid photosensitivity comes predominantly from examining wild fish (Ali 1959; Beatty 1966; Douglas and Djamgoz, 1990). Atlantic salmon vision is considered generalist owing to its anadromous life strategy (Parkyn et al., 2000). Vision displays considerable plasticity capable of adapting to the broad range of photic conditions that occur between freshwater (FW) and seawater (SW) (Smith and Baker, 1981; Morel et al., 2007). Plasticity is required to allow switching between these complex photic environments twice, as fish return to spawn (Hawryshyn et al., 2010). Salmon are visual feeders and as such, light perception, especially spectral sensitivity, is of great importance. Photic sensitivity, describing both the limits at which light can be detected, and the spectral range that elicits a response, is mediated through the composition and density of rods for low intensity detection and cones for photopic vision (Wheeler 1982; Allen and Munz, 1983; Coughlin and Hawryshyn, 1995; Flamarique and Hawryshyn, 1996; Cheng et al., 2006). Currently the absolute scotopic threshold in Atlantic salmon is unknown, however, brown trout (*Salmo trutta)* and Arctic charr (*Salvelinus fontinalis)* have been shown to respond to a light stimulus of 1.1 $\mu mol/m^{-2}/s^{-1}$ and other closely related species like rainbow trout (*Oncorhynchus mykiss)* and Yellowstone cutthroat trout (*Oncorhynchus clarki bouvieri)* exhibit thresholds of approximately twice this value (Rader et al., 2007). It is likely that the Atlantic salmon are around these values.

Visual photoperception occurs in the eye, as with higher vertebrates, however non-visual photoreception, mediating processes like seasonal entrainment, occurs in a wide range of photoreceptive tissue loosely connected by neurons and peptigenic signalling (Philp et al., 2000; Soni et al., 1998). Distinct neurochemical messaging, diurnal rhythmicity and direct photosensitivity can be localised to discrete areas of the brain (Hang et al., 2014). Thus, neural networks may play discrete physiological roles beyond seasonal entrainment. The spectral sensitivity of these brain clusters is currently unknown (Migaud et al., 2006). Research has, however, been performed on the pineal gland. Vera et al. (2010) examined whether the pineal complex in three aquaculture species exhibited spectral sensitivity. The pineal gland is perhaps the best described of the non-visually photosensitive tissues in teleosts and threshold

sensitivity in salmon occurs between 3.8 X 10^{-4} and 3.8 X 10^{-5} W/m^2, substantially lower than 3.8 X 10^{-5} and 3.8 X 10^{-6} in European seabass (*Dicentrarchus labrax*) (Migaud et al., 2006). By measuring the inhibition of melatonin production *ex vivo,* no spectral sensitivity was determined in either European seabass (all spectra 3.8 X10^{-3} W/m^2) or Atlantic cod (*Ghadus morhua*) (all spectra 3.8 X10^{-5} W/m^2). However, the sensitivity of the Atlantic salmon pineal varied depending on light colour (blue/green between 3.8 X10^{-2} W/m^2 and 1.2 X10^{-3} W/m whilst melatonin output in response to red light, was statistically higher than blue/green in the range of 1.2 X 10^{13} and 1.2 X 10^{12} photons s^{-1} cm^{-2} (Vera et al., 2010) and results indicate that spectrum may influence endocrine signalling.

Spectrally specific endocrine responses have been suggested in several other species. In the damsel fish (*Chrysiptera cyanea*), stimulation of deep brain photoreceptors leads to increases in ovarian development (Bapary et al. 2011). Exposure to red wavelengths for 45 days out with the breeding season led to 100% of the 10 fish examined exhibiting vitellogenic oocytes compared to 0 out of 10 exposed to White LED (Bapary et al. 2011). Takemura et al., 2011 examined this further, identifying activation in the deep brain of a specific red light sensitive opsin and proposed a functional relationship between red light and ovarian development. Conversely, Adatto et al., (2016) demonstrated reduced fecundity in zebrafish *(Danio reiro*) exposed to errant light from a red emergency exit sign compared to a green sign. Contrasting effects may stem from differences between species, or trial design, and highlight the difficulties in determining the impact of spectrum on fish development. Coloured lights may alter desirable production traits such as somatic growth as reported for barfin flounder (*Verasper moseri*) exposed to green light (Yamanome et al., 2009). In the early stages of the Atlantic salmon production cycle, somatic growth is essential for ensuring that parr reach an appropriate size for inducing smoltification. Understanding how the deposition and the structure of myogenic development are influenced by narrow bandwidth light may help to determine future growth potential (Johnston 1999). Currently, environmental manipulation of temperature and photoperiod are used to accelerate FW growth. This, however, has been suggested to increase the prevalence of vertebral deformities (Fjelldal et al., 2006; Handeland et al., 2013) with melatonin (Fjelldal et al., 2004) and thyroxin (FT4) inhibition (Handeland et al., 2013) cited as effectors. FW conditions, then, can elicit long term effects on

growth potential and welfare considerations. Careful examination of how spectrum and intensity affect both of these metrics is required.

In this chapter, results of two different trials are presented. The overall aim of this work was to investigate the effects of different spectral profiles and light intensities on juvenile Atlantic salmon growth and development. The first trial was designed to provide preliminary data on the combined effect of a range of intensities and spectra on growth and development of Atlantic salmon parr. The second trial tested the effects of exposure of salmon juveniles to a fixed intensity of narrow bandwidth light, following progression until the end of parr growth.

3.2 Trial I – Preliminary Testing of a Combination of Light Intensities and Spectra on Juvenile Atlantic Salmon Growth and Development

3.2.1 Trial I - Materials and Methods

Fish Stocks and Rearing Conditions

On the 15th of May, 2014 ~6000 fry (mean weight 1.4 ± 0.22 g) of the Aquagen strain were transferred from Howietoun Hatchery, Scotland (56°N, 4°W) into a recirculating aquaculture system at the University of Stirling. Prior to receiving the fish fry had been maintained under LL since hatch. Upon receipt, each tank (94 cm outside diameter x 75 cm tall with a working volume of 300 litres) was stocked with ~500 fish corresponding to an initial stocking density of 2.1 kg/m^3. Water temperature was maintained at 11.5 ± 0.5 ºC. Fish were fed a standard salmon diet (EWOS Micro, Scotland) according to BW, initially 1P size followed by 5P and 10P at the end of the trial adjusted according to sample weights and in accordance with manufacturer guidelines (daily SFR ranged from 1.7 - 2.5 %). Satiation was verified through pinch feeding and observation of waste feed at the tank bottom. Eheim twin-screw feeders were programmed to deliver feed every two hours 24 hours a day and based upon manufacturers feed table (EWOS, Scotland). Adequate ration was verified by weighing feed at the start and end of each week. Initially waste feed recovery was performed to calculate bFCR. The system was installed with feed traps on the outflow, however, the design was insufficient to ensure complete capture of uneaten food and so this was stopped after 14 days. The data is not presented.

Throughout the trial, dissolved oxygen was checked daily and maintained above 80 %. System biofiltration was not fully mature at the start of the trial and resulted in elevated ammonia throughout the trial, ranging between 0.2 and 0.47 ppm (average 0.34 ± 0.11 ppm) in addition to elevated nitrite which ranged between 0.2 - 1.74 ppm (average 0.57± 0.38 ppm). Daily water changes were performed (replacing 30 % of the system water) to reduce ammonia loading and the system was dosed daily with sodium chloride (average 200 g^{-day} average salinity 94.6 ± 12.1 ppm) to reduce the potential impact of high nitrites. pH was maintained at between 6.3 and 7.23, (average 6.71 ± 0.24). Daily dosing with sodium bicarbonate (175 g/day) was performed via a continual drip.

Experimental Design and Sampling

The experimental setup (Fig. 3.1) consisted of 12 tanks (500 fish / tank) each corresponding to one of four spectral profiles provided by a bespoke LED lighting system (Philips, Eindhoven, Holland) controlled through in-house software as described (Chapter 2.2.1). Spectra emitted were Blue ($\boldsymbol{\lambda}_{(max)}$ 444 nm), Green ($\boldsymbol{\lambda}_{(max)}$ 523 nm), Red ($\boldsymbol{\lambda}_{(max)}$ 632 nm) and White (W) at one of three light intensities – 0.5 W/m^2 (0.5), 5 W/m^2 (5) and 35 W/m^2 (35) (Fig. 3.1). Light intensity was measured in the middle of the tank at the water surface (below 1 cm of water) and with top nets fitted using a light meter (Skye Instruments Ltd, UK) calibrated to the National Physics laboratory (UK) standards. Light spectrum and intensity remained constant for each tank for the duration of the trial.

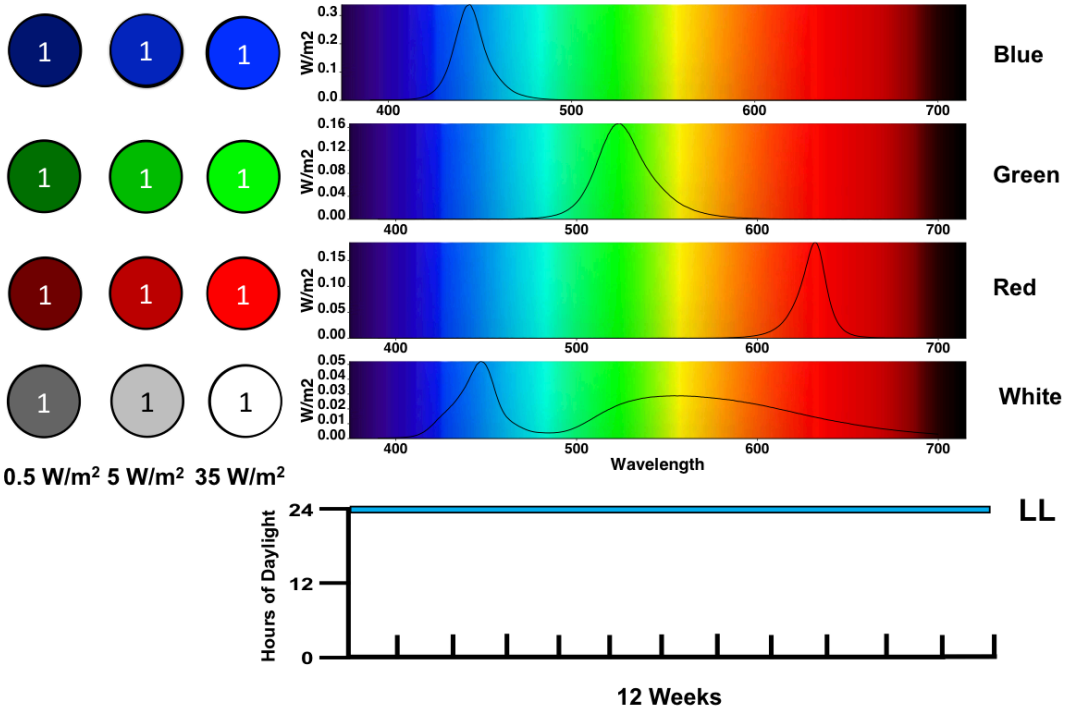

Figure 3.1. Trial I trial design. The trial consisted of 12 tanks each randomly assigned either Blue ($\lambda_{(max)}$ 444 nm), Green ($\lambda_{(max)}$ 523 nm), Red ($\lambda_{(max)}$ 632 nm) and White (W) LED at one of three light intensities – 0.5 W/m^2 (0.5), 5 W/m^2 (5) and 35 W/m^2 (35) lit under continual lighting for a period of 12 weeks. A single treatment was performed per colour / intensity combination.

Due to limitation in tank availability, no replication could be tested in this first preliminary trial with one tank for each spectrum-intensity combination. However, a sub-population of each tank was tagged to allow for pseudo replication as described below. Treatments are referred to as Blue-0.5, Green-0.5, Red-0.5, White-0.5, Blue-5, Green-5, Red-5, White-5, Blue-35, Green-35, Red-35, White-35. Each tank was exposed to continuous light (LL) for 12 weeks. Photic conditions were assigned randomly regarding both spectrum and intensity.

One day after stocking the initial 500 fish, 50 fish per tank were removed, briefly anesthetised and implanted with a coded wire tag (CWT) (Northwest Marine Technologies (NMT), WA, USA) as described in chapter 2.4.2. Fork length (± 0.1 cm), and weight (± 0.1 g) were recorded and the adipose fin was removed from each tagged fish to facilitate external identification of the tagged fish. Tagged fish acted as pseudo

replicates for statistical tests and to give an overview of individual growth performance in relation to photic composition.

At the start and then approximately every four weeks (06/06/2014, 23/06/2014, 21/07/2014 and 04/08/2014), fish were scanned with a metal detector (Blue Hand Held Detector, NWT, WA, USA) and the first 30 non-tagged individuals sampled for BW (± 0.1 g) and FL (± 0.1 cm). The trial was performed as a preliminary trial with a defined period and the trials discussed in Chapter 4.1 and 4.2 immediately followed this one, termination was conducted based on assigned period as opposed to any biometric targets.

The trial concluded on the 5th of August 2014 after 12 weeks. Tagged fish were removed, euthanised and BW (± 0.1 g) and FL (± 0.1 cm) recorded. Tags were removed (Chapter 2.4.2) and final metrics matched to original records. Recovery of CWT was complex resulting in varying percentages of recovery, on average 11 % of tagged fish were not recovered. Recovery details are presented in Table 3.1.

Table 3.1 Number of coded wire tags initially implanted and subsequently recovered per treatment.

Tank	Tagged	Recovered	Treatment	Tagged	Recovered
Blue 0.5	50	40	**Red 0.5**	50	45
Blue 5	50	46	**Red 5**	50	46
Blue 35	50	48	**Red 3.5**	50	44
Green 0.5	50	47	**White 0.5**	50	38
Green 5	50	47	**White 5**	50	46
Green 35	50	41	**White 35**	50	47

Remaining un-tagged fish were graded using a manual box grader. All tanks were graded with a bar size of 0.9 cm (weight cut off 8.7 g) derived from the median value of a test sample. Graded fish were bulk weighed and counted to determine the number and weight of upper and lower cohorts.

Statistics

All statistics were performed using R studio (R Core Team, 2016). Transformations and analysis were performed using base packages unless otherwise stated.

Trial 1- Statistical Approach

As mentioned, Trial I constituted a general comparison of a wide range of intensities and spectra. Due to restraints on the number of tanks it was not possible to run this trial with replication. As a result, values for each treatment are determined on the data recorded from individual tagged fish which act as pseudo-replicates. The data analysed meets the assumptions for using a linear mixed effects model (LME) (i.e. normal distribution, homogeneity of variance) and the model allows for repeat measures of the same individuals and changes in sample number owing to mortality or tag loss. The use of individual fish as pseudo-replicates in studies which have replication has been heavily criticised (see Thorarensen et al., 2015 for a review) mainly due to the high probability that “tank-effects” (differences attributable to the tank rather than the treatment) and interactions between individuals contribute to observed differences as opposed to the treatment being applied. In this study water quality parameters and spectrum output were maintained relatively consistent owing to the use of shared water though a RAS system and identical lighting modules verified for spectral output. Despite these similarities, we cannot rule out interactions within each population, environmental perturbation by tank location or tank specific influences. Thus, caution must be given to the reported statistical differences and results should be interpreted with the limitations of this experimental design fully in mind, i.e. whilst the statistical value is correct as reported, the effects may be due to confounded factors (tank and treatment).

All growth data was transformed using the natural logarithm to meet parametric assumptions. No transformation was applied to condition factor or to TGC data.

Cumulative Distribution Functions

Individual weight distributions are reported using the empirical cumulative distribution function in the R package ggplot2 (Wickham 2009). Data is ranked in order of value and the cumulative count is recorded. This approach allows greater interpretation of the distribution of individual sizes as all values are presented. A non-parametric

assessment using a Kolmogorov-Smirnov was performed to determine differences between distribution for each intensity.

3.2.2 Trial I - Results

CWT data is used to present changes in BW, FL and K from trial I for each combination of spectrum and intensity. The comparative effect of intensity within each colour on the impact on the distribution of weights is shown. A breakdown of fish by size class (top or bottom) is presented based on the remaining non-tagged population. Mortality across all tanks was 3.2 ± 2.5%.

Trial I – Assessment of Development within the Population

Trial I – Coded Wire Tag (CWT) Body Weight

Individual initial weights of tagged fry ranged from 0.71 to 2.11 g in all tanks with a mean of 1.51 ± 0.11 g. BW values at initial stocking and at the final sample point were compared using an LME model taking into account random variation within each tank. Following 12 weeks' exposure all groups had increased significantly in weight [all p-values <0.001] however no significant differences were observed at either sample point between treatments (Fig.3.2) although Blue-35 and Red-35 appeared to be lighter however differences were not significant.

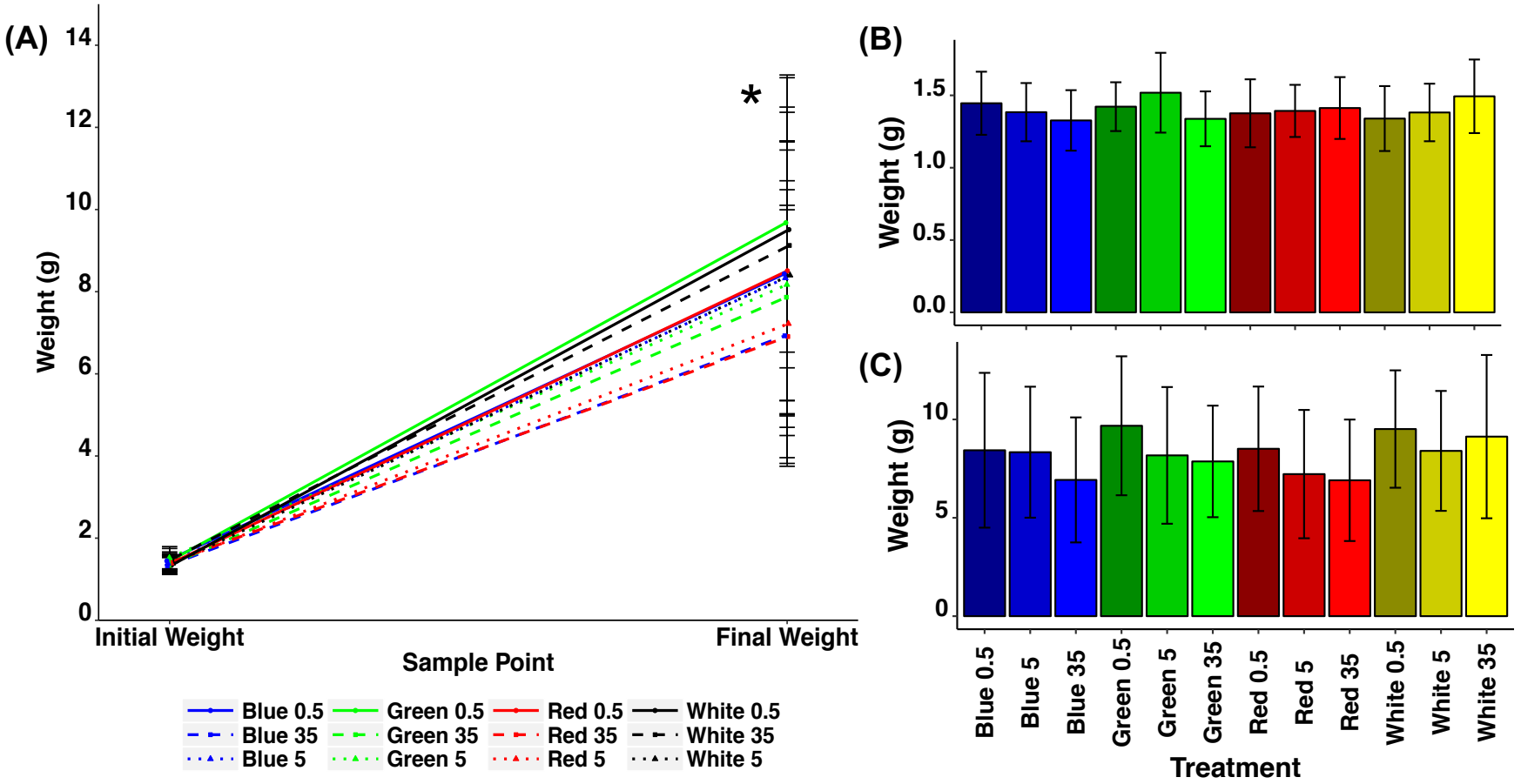

Figure 3.2. Initial (15th of May, 2014) and final (5th of August, 2014) weight of tagged juvenile Atlantic salmon (initial n= 50; final n range= 38 to 48) exposed to LL either Blue, Green, Red or White at one of three intensities – 0.5, 5 and 35 W/m^2 for 82 days. Data presented as mean ± SD. Significant differences between treatments within time points where present are shown as upper case superscripts (Mixed-linear model, $p<0.05$), significant changes between time points are denoted by an asterisk.

Trial I – Coded Wire Tag (CWT) Lengths

Individual initial lengths of tagged fry ranged from 4.5 to 6.0 cm in all tanks, mean 5.29 ± 0.26 cm. After 12 weeks, fork length in all groups had increased significantly [all p-values <0.001]. Values between tanks was compared at initial and final sample using an LME model taking into account the random tank variation (Fig. 3.3). No significant differences between tanks was observed at either sample point. Blue-35 and Red-35 appeared to be shorter however differences were not significant.

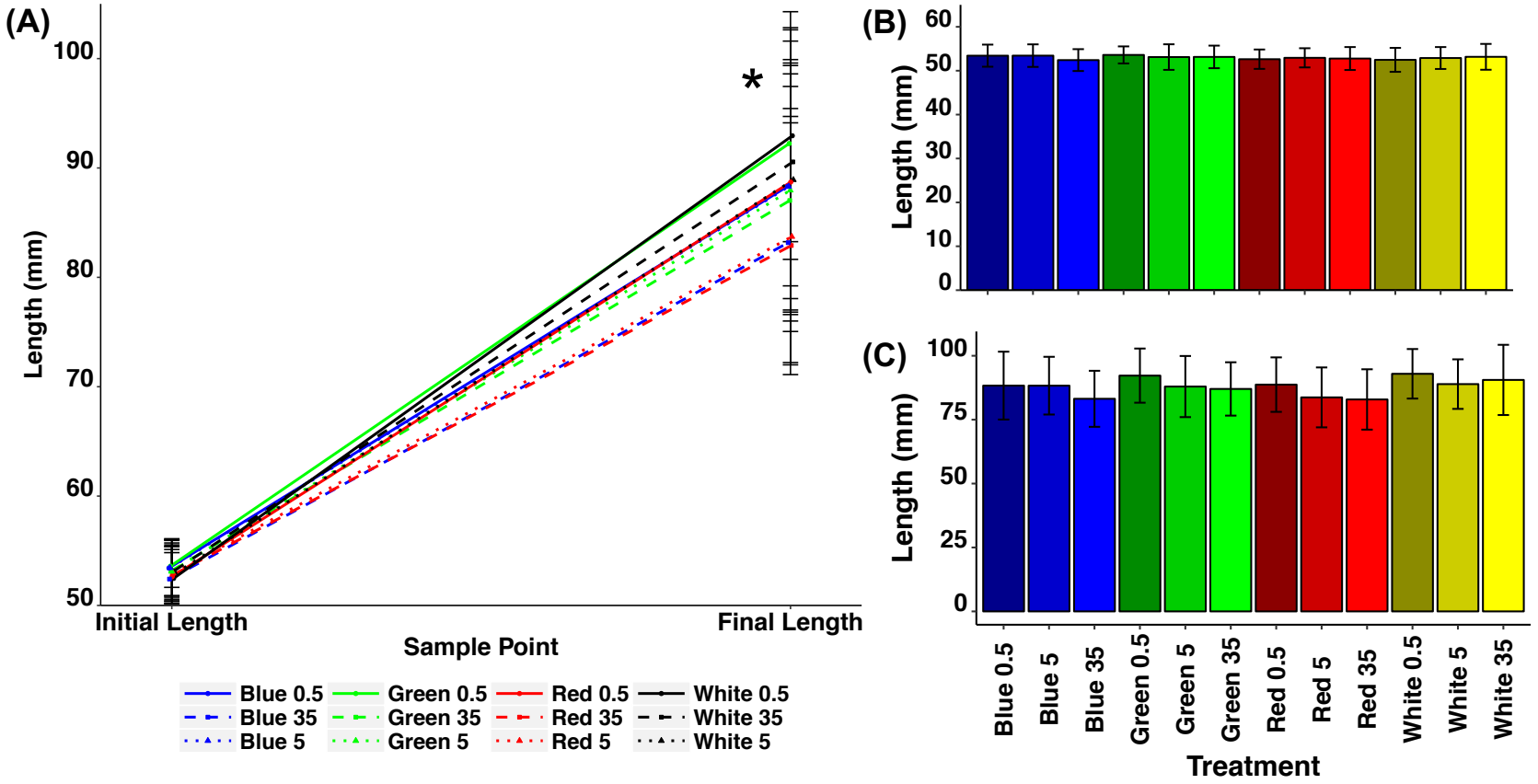

Figure 3.3. Initial (15th of May, 2014) and final (5th of August, 2014) lengths of tagged juvenile Atlantic salmon (initial n= 50; final n range= 38 to 48) exposed to LL either Blue, Green, Red or White at one of three intensities – 0.5, 5 and 35 W/m^2 for 82 days. Data presented as mean ± SD. Significant differences between treatments within time points where present are shown as upper case superscripts (Mixed-linear model, $p<0.05$), significant changes between time points are denoted by an asterisk.

Trial I – Coded Wire Tag (CWT) Condition Factor (K)

Individual initial condition factor of tagged fry ranged from 0.88 to 1.76 in all tanks with a mean of 1.14 ± 0.07. Values at initial stocking and at the end of the trial were compared using an LME model taking into account random variation within each tank. K showed significant variation between Green 35 and Green 0.5 [p=<0.001]. K increased significantly with time for all groups {all p-values <0.001]. No significant differences between tanks at the trial termination. (Fig. 3 4).

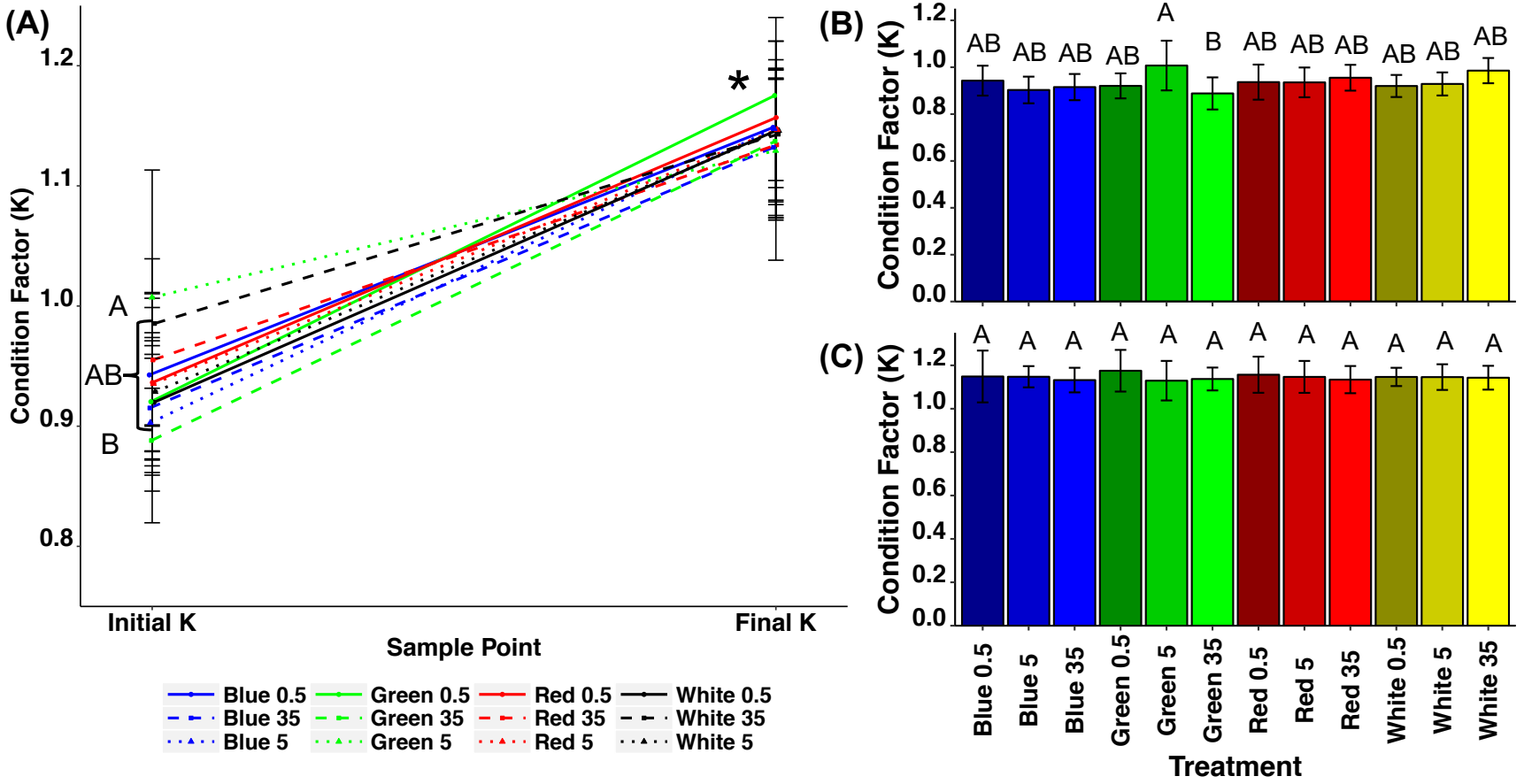

Figure 3.4. Initial (15th of May, 2014) and final (5th of August, 2014) condition factor of tagged juvenile Atlantic salmon (initial n= 50; final n range= 38 to 48) exposed to LL either Blue, Green, Red or White at one of three intensities – 0.5, 5 and 35 W/m^2 for 82 days. Data presented as mean ± SD. Significant differences between treatments within time points where present are shown as upper case superscripts (Mixed-linear model, $p<0.05$), significant changes between time points are denoted by an asterisk.

Trial I – Coded Wire Tag (CWT) - Thermal Growth Coefficient (TGC)

Individual TGC were calculated and SD derived from values for each tank (Fig 3.5) Values were tested using an LME accounting for variation within each tank and no significant differences were determined between any treatments. Fish exposed to Green, Red and White light all exhibited a trend for decreasing TGC relative to intensity. Fish exposed to Blue showed less of a response to increasing intensity.

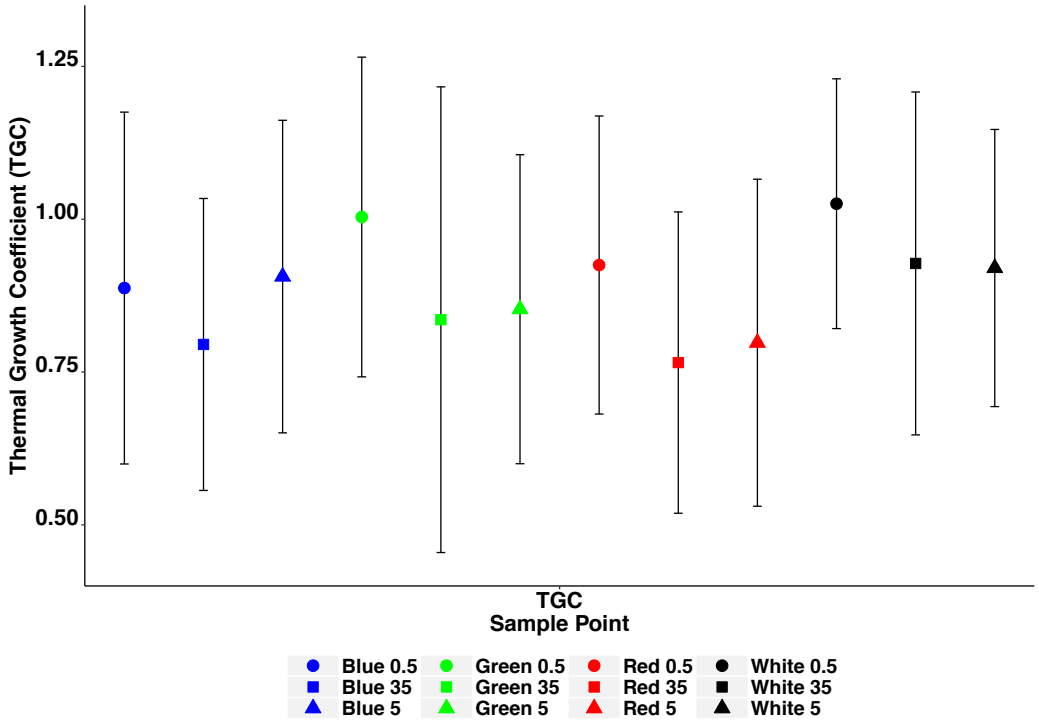

Figure 3.5. Thermal growth coefficient of tagged juvenile Atlantic salmon (initial n= 50; final n range= 38 to 48) exposed to LL of either Blue, Green, Red or White at one of three intensities – 0.5 W/m^2, 5 W/m^2, 35 W/m^2 for a period of 82 days between 15th of May, 2014 and 5th of August, 2014. No significant differences were recorded.

Trial I – Coded Wire Tag (CWT) Cumulative Distribution of Fry Length

Exposure to Blue-35 resulted in a significantly different distribution of sizes compared to Blue 5 with a greater number of small length fish in Blue-35 compared to Blue 5 (Fig. 3.6A). The distribution of lengths within all other treatment groups showed no significant differences (Table 3.2) however distributions show a general pattern of greater lengths in response to lower intensities (Fig. 3.6B-D).

Table 3.2. Kolmogorov-Smirnov two sample test outcomes for contrasts between the length of fish exposed to each intensity within each spectral profile group.

	35W/m^2 - 5W/m^2		**35W/m^2 - 0.5W/m^2**		**5 W/m^2 - 0.5 W/m^2**	
	D-Value	**P-Value**	**D-Value**	**P-Value**	**D-Value**	**P-Value**
Blue	0.29	0.03	0.24	0.17	0.15	0.68
Green	0.17	0.55	0.23	0.19	0.23	0.15
Red	0.11	0.94	0.26	0.10	0.24	0.16
White	0.19	0.37	0.18	0.47	0.29	0.07

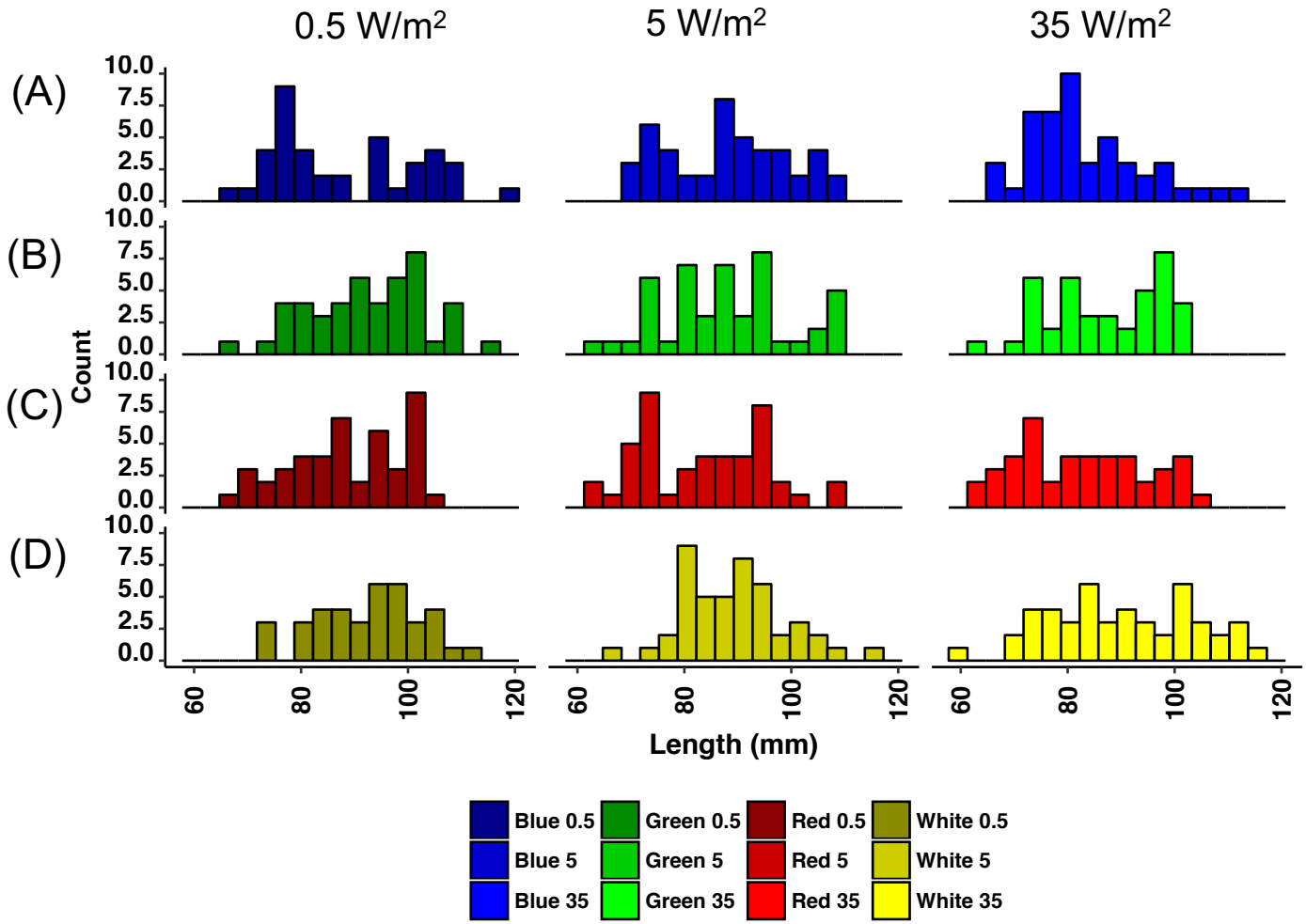

Figure 3.6. Distribution of individual lengths of tagged juvenile Atlantic salmon exposed to LL of either Blue (A), Green (B), Red (C) or White (D) at one of three intensities – 0.5 W/m^2, 5 W/m^2 and 35 W/m^2.

Population Growth

Using bulk weights (Fig. 3.7) to track developmental changes no significant differences were seen at initial stocking. Following four weeks of exposure significant differences in weight were identifiable with W-0.5 being significantly heavier than all treatments with the exception of the White-5 and Blue-35. Exposure to Red-35 reduced growth and this was significant compared to all other treatments except Red-5. Upon completion of the trial White-0.5, White-5 and White-35 were significantly heavier than Red-5 and Red-35.

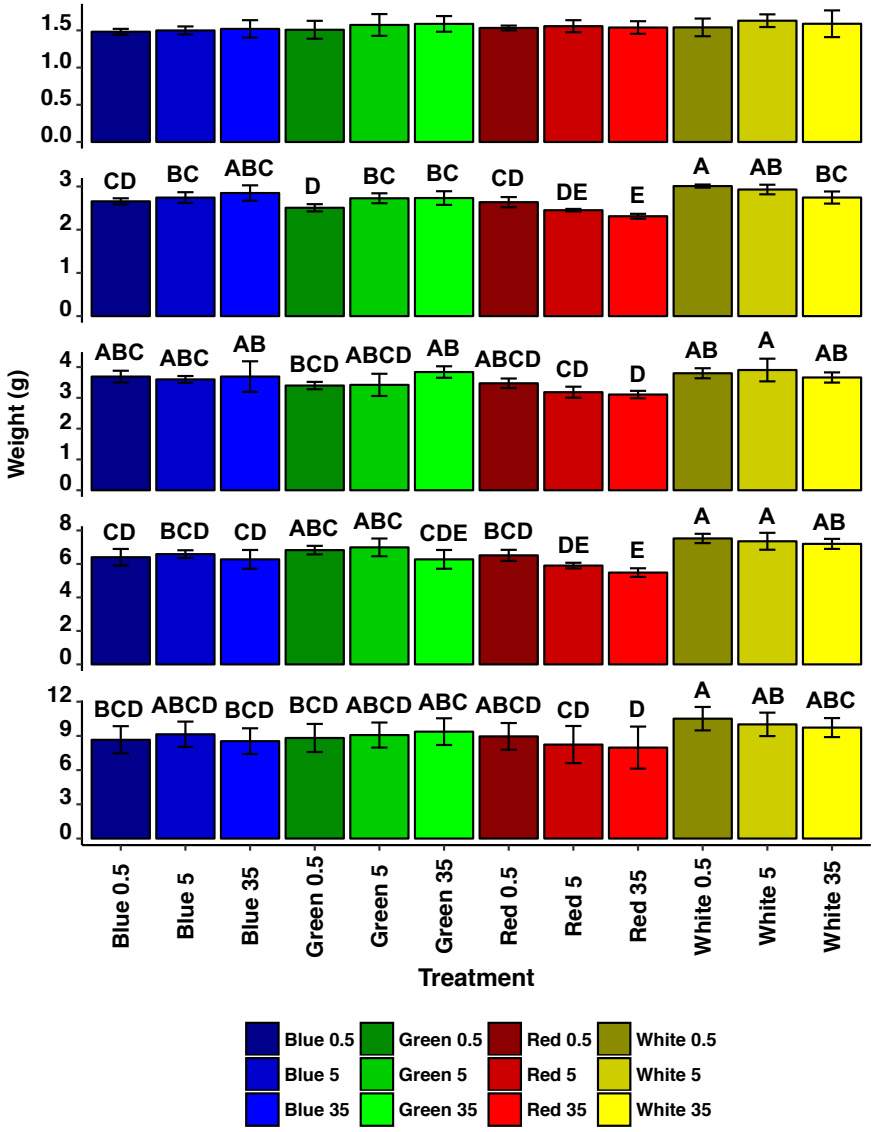

Figure 3.7. Weight of juvenile Atlantic salmon (n=30) exposed to LL of either Blue, Green, Red or White at one of three intensities – 0.5 W/m^2, 5 W/m2, or 35 W/m^2 for a period of 12 weeks. Data presented as mean ± SEM. Significant differences between treatment are denoted by lower case superscripts (Mixed-linear model, $p<0.05$).

Trial I – Population Grading

Splitting each tank population into either top or bottom grade fish based upon weight and separated using a grading bar with a size threshold of 8.7g selected by taking the median value of a random sample of 50 fish, showed differences between treatment groups although without replication only a general overview can be observed (Fig. 3.8). The percentages of fish classed as top and bottom showed that Red groups were influenced most by intensity and White least.

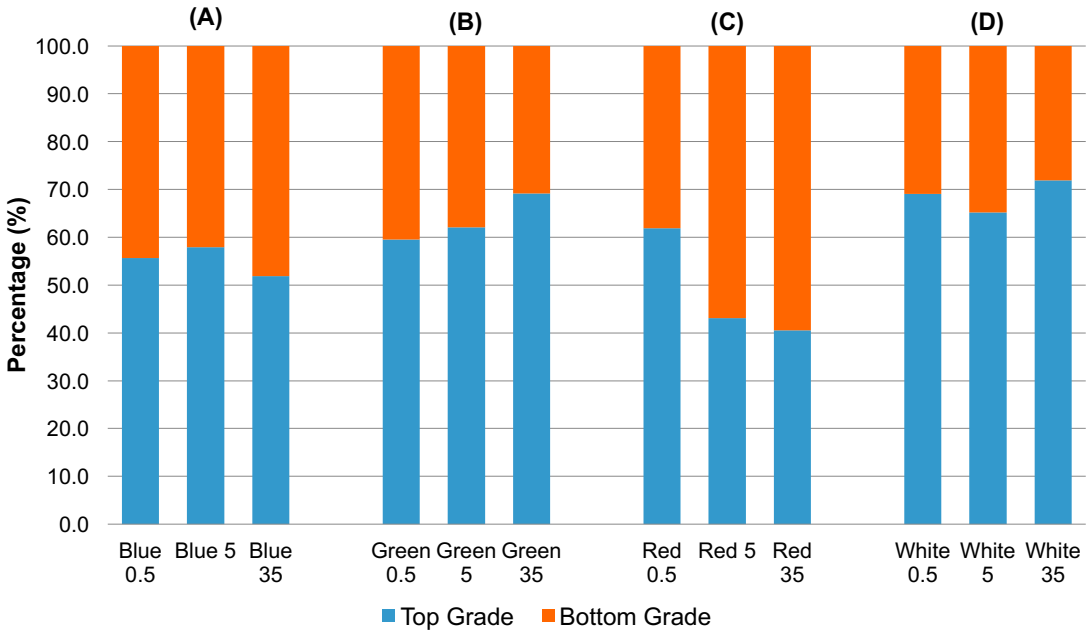

Figure 3.8. Percentage of juvenille Atlantic salmon exposed to LL of either Blue, Green, Red or White at one of three intensities – 0.5, 5 and 35 W/m^2 for a period of 4 months and graded into smaller (bottom grade) and larger (top grade) groups with a size threshold of 8.7 g derived from the median value from a random sample.

3.3 Trial II - Impact of Exposure to Low Intensity Light of Different Spectral Composition until the end of Parr Development

3.3.1 Trial II - Materials and Methods

Fish Stocks and Rearing Conditions

On the 26th of May 2015, 5460 fish (1.05 ± 0.02 g) from the Aquagen strain were transferred from Howietoun Hatchery, Scotland into the same recirculation aquaculture system (RAS) as for trial I and distributed equally between the 12 tanks (455 fish / tank). Prior to receiving the fish fry had been maintained under LL since

hatch. Water temperature was maintained at 12.5 ± 1.0 °C for the duration of the trial. A standard salmon diet (Micro, EWOS, Scotland) was fed according to manufacturer feed tables and the ration delivered over 24 hours. Pellet size was adjusted according to sample weight and manufacturer feed table and ranged from an initial size 1P to size 20P at the end of the trial. As pellet size changed, specific feed rate was adjusted and SFR ranged from an initial 2.4 % to 1.1 %/day. Feed was delivered via an automated feeding system (Arvotec, Sweden) and adjusted daily using an integrated feeding algorithm for water temperature and DO at outflow. Periodic sample weights were used to update the feeding protocols in the feeding software (Arvo-Pro, Arvotec, Sweden). Tank flow was maintained at 10 l/min.

Water quality parameters (ammonia, nitrite and chloride concentration) were checked daily. Ammonia ranged from 0.3-1.68 ppm (0.62 ± 49 ppm) and nitrite from 0.07-1.1ppm (average 0.52 ± 41 ppm). System was dosed with sodium bicarbonate using a continual drip (163 g/day) and with $NaCl^-$ (350 g/day) assessed and maintained at a concentration of 100 ppm. DO was recorded at tank outflow and maintained above 80 %. pH was maintained between 6.32 and 7.0 (average 6.7 ± 0.17).

Experimental Design and Sampling

The trial consisted of exposing 12 tanks (455 fish / tank) for 17 weeks to one of four narrow bandwidth light spectra in triplicate, Blue (B – $\boldsymbol{\lambda}_{(\max)}$ 444 nm), Green (G – $\boldsymbol{\lambda}_{(\max)}$ 523 nm), Red (R – $\boldsymbol{\lambda}_{(\max)}$ 632 nm) and White (W) (broad spectrum) (Fig. 3.9). The light intensity for this trial was based upon results presented in **Chapter 4.3.2** where fish exposed to LL White light at 0.04 W/m^2 during a subjective winter appeared to grow more quickly than the higher intensities tested (results not significant). Although this was a smolt trial fish dialed to smolt so data was extrapolated to suggest that fish were still parr. Light intensity of 0.05 W/m^2 was measured using a light meter (Sky Instruments, UK) calibrated to the National Physics Laboratory (UK) in the tank center under 1 cm of water. Light output was adjusted using control software developed in house and neutral density filters and adjusted to account for the top net and spectra. Each tank was exposed to continuous light (LL).

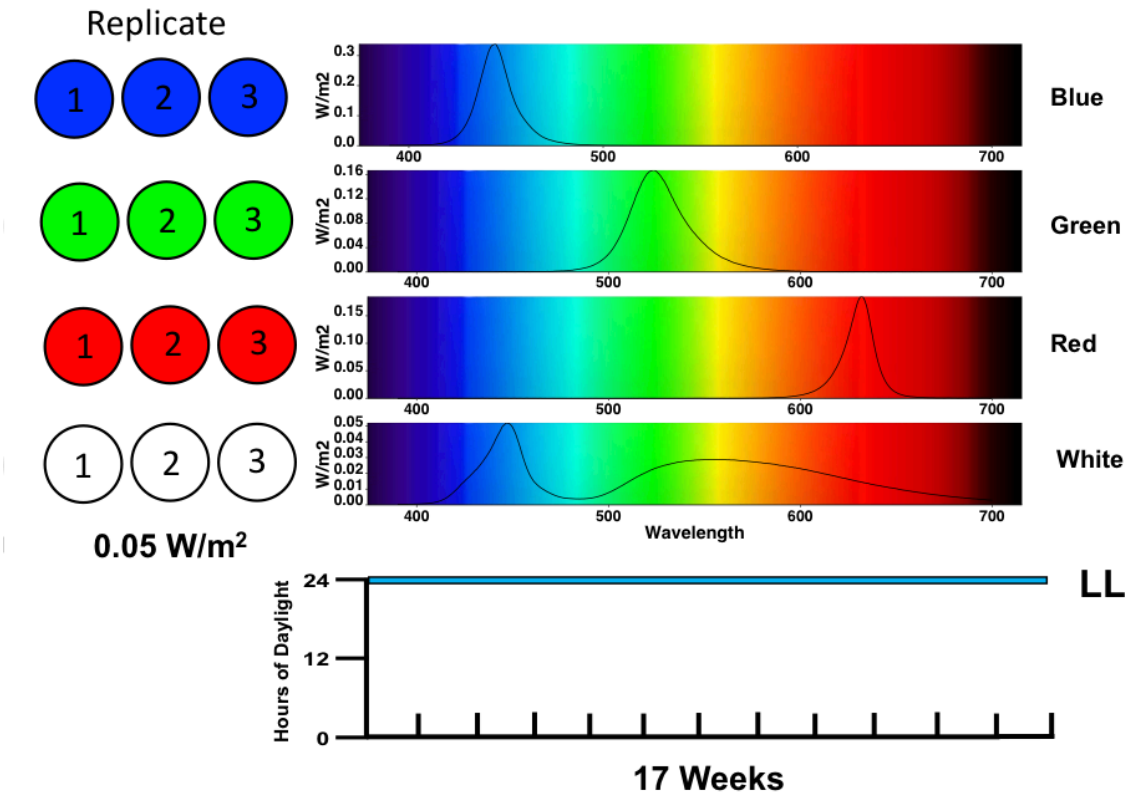

Figure 3.9. Trial II trial design. The trial consisted of 12 tanks each randomly assigned either Blue ($\lambda_{(max)}$ 444 nm), Green ($\lambda_{(max)}$ 523 nm), Red ($\lambda_{(max)}$ 632 nm) and White (W) LED in triplicate at 0.05 W/m^2. Light was applied continually for a period of 17 weeks.

Population Growth

At the start, after one week and then every subsequent 4 weeks until the 25th of September, 50 fish per replicate (n=3) were randomly selected, euthanised using a lethal dose of buffered tricaine methanesulphonate (400 ppm MS222, Pharmaq, UK) before a percussive blow to the head and severing of the gill aorta was performed in accordance with schedule 1 Home Office procedure, and BW (± 0.1 g) and FL (± 0.1 cm) recorded. Fish from this trial are the same fish that are discussed in Chapter 4-Trial III and Chapter 5 on smoltification and on-growing respectively. On the 25th of September mean sample weight across all tanks had reached ~40 g. At this point fish were determined suitable for S0+ induction and the juvenile FW phase of the trial concluded. A final biomass assessment (fish weight and number) was performed on all tanks and in doing so, it became apparent that the Green Replicate 1 tank had been

overstocked by 50 fish during initial fish allocation. The data from this tank has therefore been disregarded from all analysis.

Vertebral Assessment

On the 25th of September, at the end of parr growth and immediately prior to the implementation of an out-of-season smoltification regime (S0), 15 fish per replicate (n=3) were euthanised as described previously and stored flat at -20 ºC for future x-radiological assessment of vertebrae formation.

Ocular Assessment

At the end of 17 weeks 10 fish per replicate (n=3) were terminally sampled as described for in chapter 2.4.6. Five eyes from each group of 10 were randomly selected using a random number generator (Microsoft Excel, USA), ranked in order of value and the eyes corresponding to the lowest 5 values selected for histology. Samples underwent embedding in paraffin wax (Chapter 2.4.6). The following measurements were recorded in 10 locations on the dorsal, lateral and ventral planes: the thickness of the photoreceptor layer not including the outer nuclear later, the retinal pigment epithelium (RPE), the outer nuclear layer thickness, the melanin granules layer within the RPE.

Trial II – Statistical Approach

Data in trial II was simpler to deal with as there was triplication. Again, an LME model was used as this allowed using unequal replicate numbers due to Green Rep 1 being dropped from the study as discussed earlier. As for Trial I the approach allows the use of unequal sample numbers and replicate numbers by adjusting the F-test using a Kenward-Rodgers correction (see Chapter 2.5.6 for a full explanation).

In Trial II the natural logarithm of weight was using in model predictions. K was untransformed and TGC was transformed using an arcsine transformation using Excel (Microsoft, USA).

3.3.2 Trial II- Results

BW, FL and K for each sample point during fry development is presented along with the distribution of fish sizes at each sample point. A summary of radiological and ocular assessment is then given.

Trial II – Weight

No significant initial variation in weight was observed between groups (Fig. 3.10). Weight increased significantly over time for all treatments. Weight of fish exposed to Red light were significantly lower than fish exposed to White by the 31/07/2015. At the following sample point (28/08/2015), fish weights in Red treatment were still lower however differences were not significant. At the final sample point fish weights in response to Red light were significantly lower than fish exposed to Blue. No other statistical differences were evident between treatments.

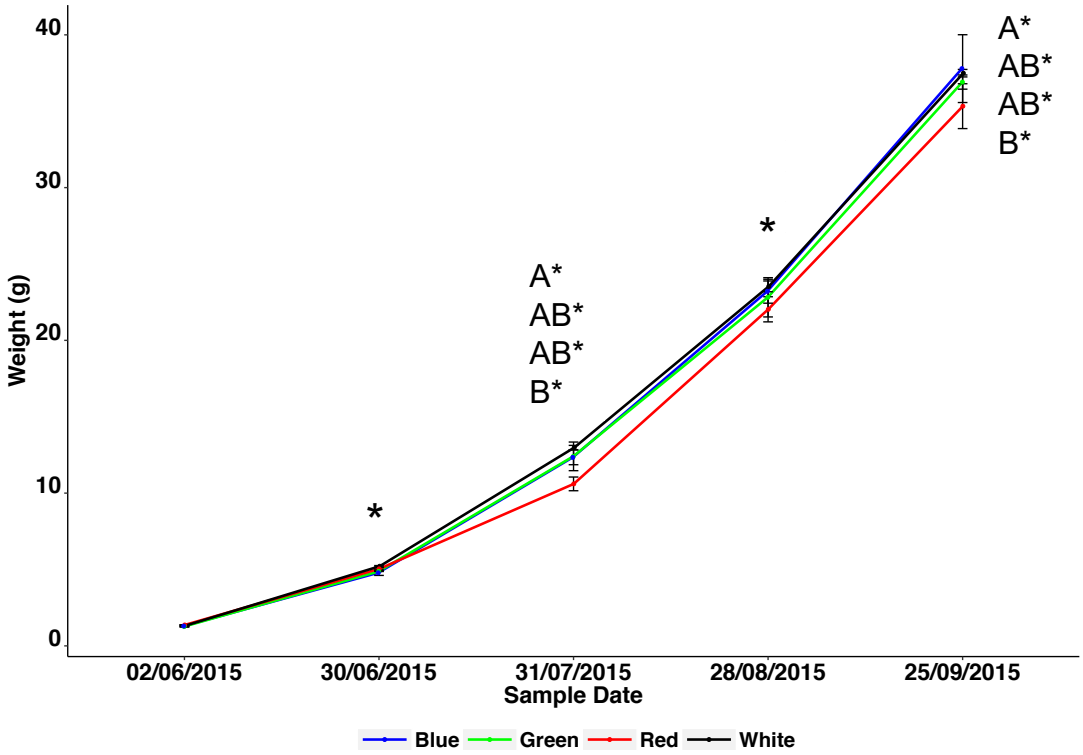

Figure 3.10. Weight of juvenile Atlantic salmon exposed to LL of either Blue, Green, Red or White at an intensity of 0.05 W/m^2 from the 2nd of June 2015 to the 25th of September 2015 (115 days). Mean value of 50 fish ± SEM (n=3 except for Green where n=2) per sample point is reported. Significant differences between treatments

within time points where present are shown as upper case superscripts (Mixed-linear model, $p<0.05$), significant changes between time points are denoted by an asterisk.

Trial II - Length

No significant differences in length were observed at the start of the trial. On the 31/07/2015 fish exposed to Red were significantly shorter than all other groups. At the following and final sample points, no significant differences between groups were apparent (Fig. 3.11)

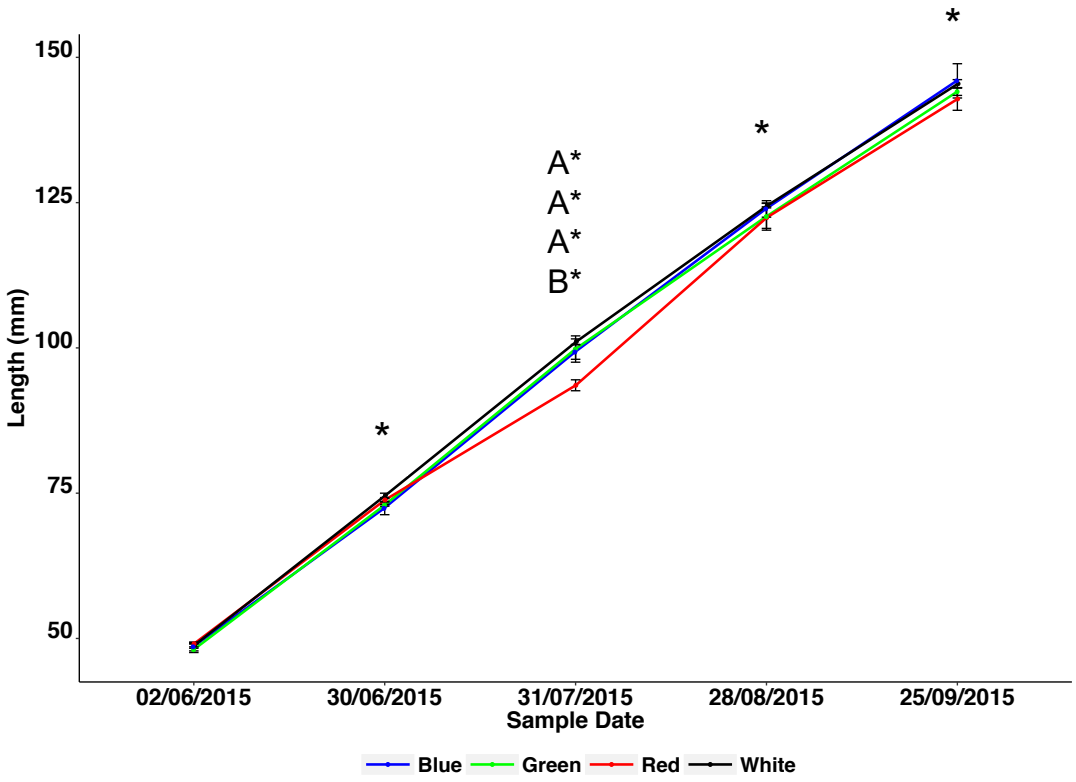

Figure 3.11. Length of juvenile Atlantic salmon exposed to LL of either Blue, Green, Red or White at an intensity of 0.05 W/m^2 from the 2nd of June 2015 to the 25th of September 2015 (115 days). Mean value of 50 fish ± SEM (n=3; Green n=2) per sample point is reported. Significant differences between treatments at each time point is denoted by lower case superscripts, significant differences between the time point and the previous time points is marked with an asterisk (Mixed-linear model, $p<0.05$).

Trial II - Condition Factor (K)

Condition factor increased significantly for all groups between 02/06/15 and 30/06/15 (Fig. 3.12). No significant change in K was exhibited by fish exposed to Blue or Green

light over the course of the trial. K in the Red groups was significantly higher at the start of the trial than the Blue and White groups and significantly lower on the 28/08/15 (1236 ºDays) and K decreased significantly between 31/07/15 and the 28/08/15 (886 to 1236 ºDays). In groups exposed to White light a significant decrease in K was also observed between 31/07/15 and the 28/08/15 (886 to 1236 ºDays) and K was not significantly different from the other 3 treatments.

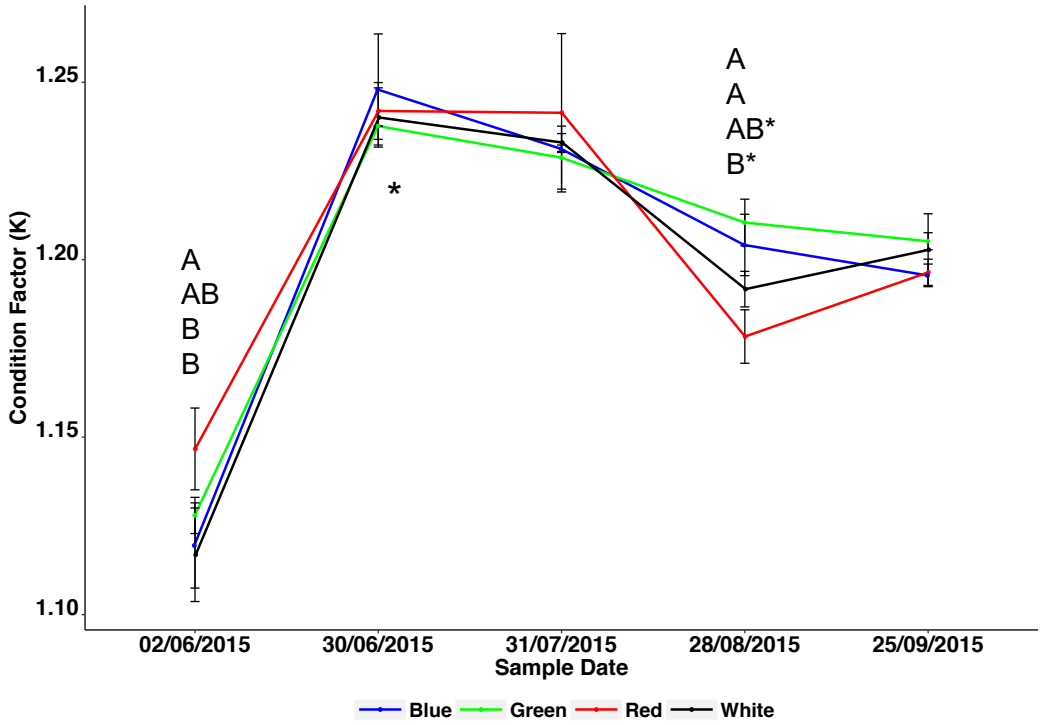

Figure 3.12. Condition factor of juvenile Atlantic salmon exposed to LL of either Blue, Green, Red or White at an intensity of 0.05 W/m^2 from the 2nd of June 2015 to the 25th of September 2015 (115 days). Mean value of 50 fish ± SEM (n=3; Green n=2) per sample point is reported. Significant differences between treatments at each time point is denoted by lower case superscripts, significant differences between the time point and the previous time points is marked with an asterisk (Mixed-linear model, p<0.05).

Trial II – Thermal Growth Coefficient

No significant changes in TGC were recoded for either the Blue, Green or Red groups over the duration of the trial (Fig. 3.13). TGC for the Red groups was significantly lower on the 31/07/15 (886 ºDays) [p= <0.005] and significantly higher on the 28/08/15 (1236 ºDays) [p=<0.001] than the three other treatment groups. The only treatment to show significant changes in TGC was the Red groups which increased significantly between

31/07/15 and the 28/08/15 (886 to 1236 ºDays) and decreased significantly between 28/08/15 and 25/09/15 (1236 ºDays to 1586 ºDays).

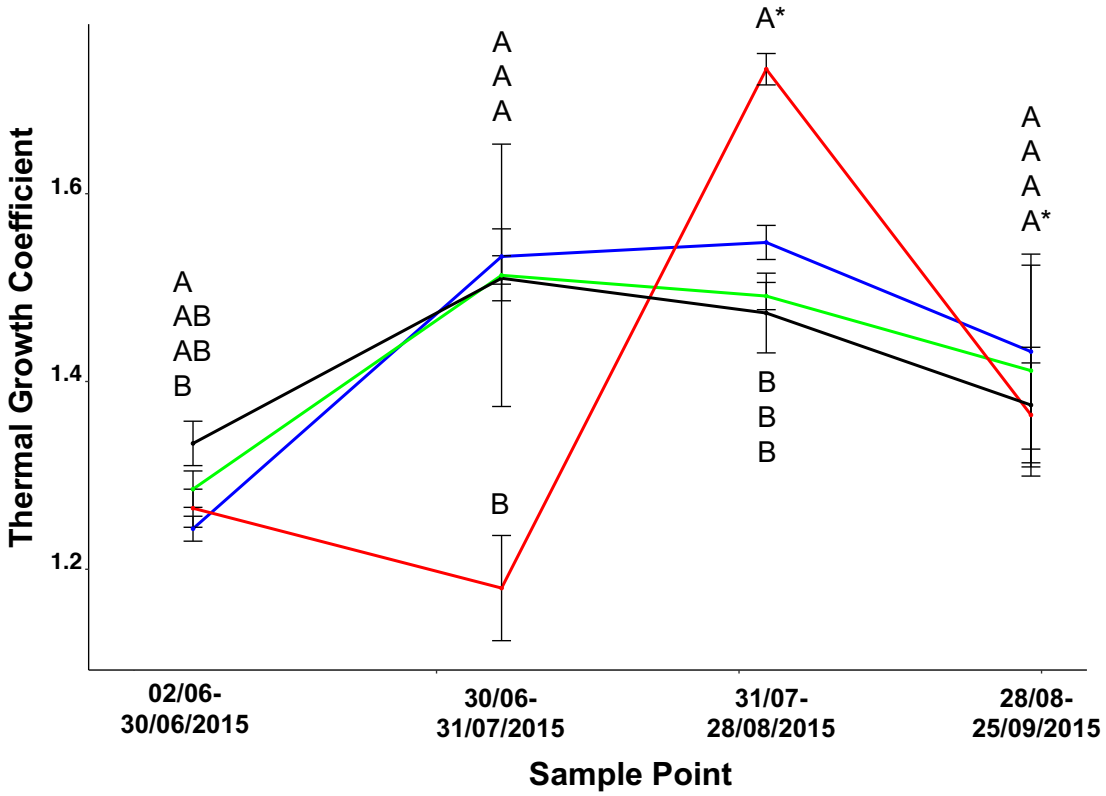

Figure 3.13. TGC of juvenile Atlantic salmon exposed to LL of either Blue, Green, Red or White at an intensity of 0.05 W/m^2 from the 2nd of June 2015 to the 25th of September 2015 (115 days). Mean value of 50 fish ± SEM (n=3; Green n=2) per sample point is reported. Significant differences between treatments at each time point is denoted by lower case superscripts, significant differences between the time point and the previous time points is marked with an asterisk (Mixed-linear model, $p<0.05$).

Trial II - Cumulative Distribution of Fry Lengths

The distribution of lengths within each population in response to spectral treatments over time showed clear differences between the Red groups and the Blue, Green and White (Fig. 3.14). From 56 Days Red groups exhibited a greater proportion of smaller fish. Length distribution under Blue, Green and White light treatments were all similar at both 56 and 115 Days. Kolmogorov-Smirnov backed up the visual observations. No significant differences were seen at the start of the trial between any group however at both 56 and 115 Days (Table 3.3) Red was significantly different a greater proportion of longer fish present in the Blue, Green and White groups

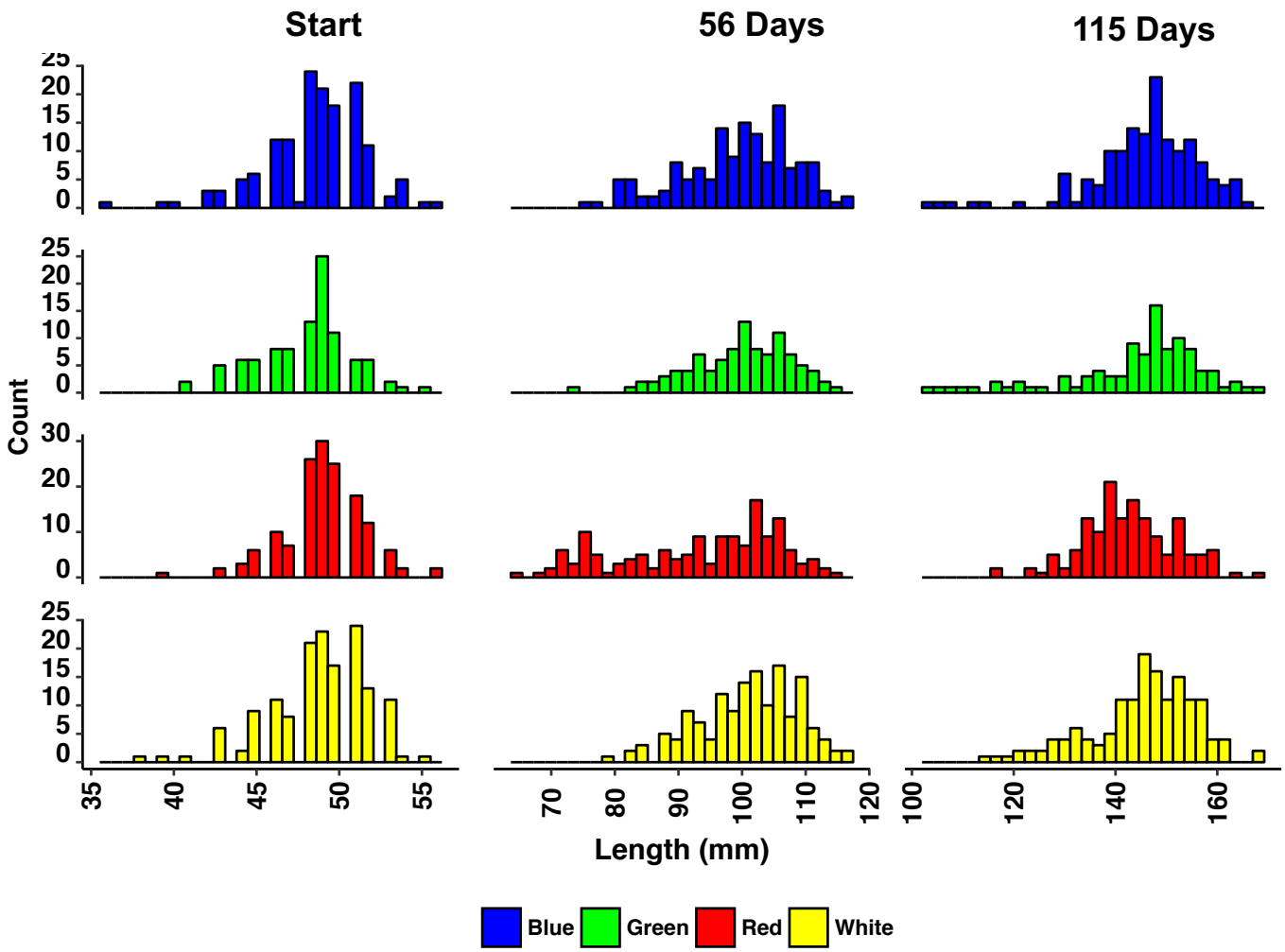

Figure 3.14. Distribution of individual lengths of 150 (Green = 100) juvenile Atlantic salmon exposed to LL of either Blue, Green, Red or White at 0.05 W/m^2. At the start of the trial, 56 days and 115 days.

Table 3.3. Kolmogorov-Smirnov 2-tailed test comparisons between the distribution of juvenile Atlantic salmon sizes exposed to either Blue, Green, Red or White. Results are presented from the start, middle (8 weeks) and end (16 weeks) of the trial. The test statistic D is reported derived from the maximum distance between cumulative distributions. Significant values are highlighted in bold.

Contrast			
Treatment vs Treatment			
Start		**D**	**P-value**
Blue	Green	0.13	0.26
Blue	Red	0.11	0.36
Blue	White	0.06	0.95
Green	Red	0.16	0.08
Green	White	0.18	0.05
Red	White	0.07	0.89
8 weeks			
Blue	Green	0.06	0.98
Blue	Red	**0.21**	**<0.01**
Blue	White	0.11	0.36
Green	Red	**0.24**	**<0.01**
Green	White	0.11	0.46
Red	White	**0.27**	**<0.01**
16 Weeks			
Blue	Green	0.08	0.80
Blue	Red	**0.24**	**<0.01**
Blue	White	0.06	0.95
Green	Red	**0.25**	**<0.01**
Green	White	0.07	0.90
Red	White	**0.25**	**<0.01**

Trial II – Vertebral Assessment – Parr

Radiological examination of juvenile salmon at the end of parr stage and immediately prior to the application of an out-of-season smoltification regime appeared to show a higher percentage of deformities in region 4 compared to regions 1, 2 and 3 (Fig 3.15). However, differences between treatments were not significant. Comparison between the Green and White in region four had the lowest p-value [p=0.15].

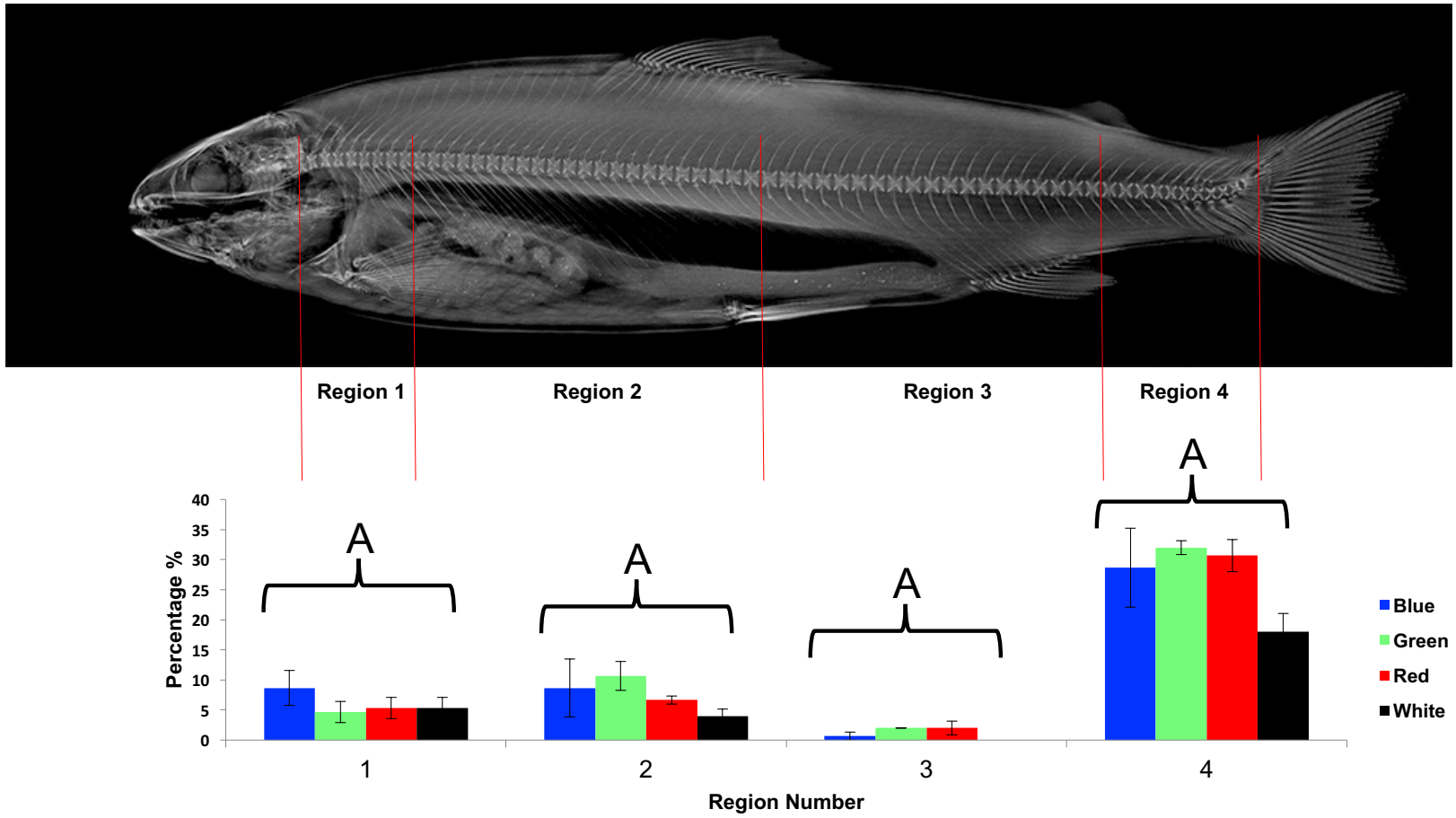

Figure 3.15. X-ray of juvenile Atlantic salmon (36.4 ± 10.6 g) after 16 weeks (115 days) in FW immediately prior to smoltification. The vertebral column is divided into four regions and each vertebra was assessed according to Witten et al. (2009). Results showed no significant differences between regions.

Percentage of Vertebral Deformity

Fig. 3.16 shows the breakdown of the prevalence of deformity between treatments. In the Blue treatment, the highest recorded number was seven deformed vertebrae which was reported in one fish. For both the Green and Red treatments the highest number was 6 and in the White the highest number was in the White groups where 8 deformed vertebrae where recorded.

No.	% Blue	% Green	% Red	% White
1	25	25	15	11
2	9	9	9	9
3	4	4	7	1
4	1	1	2	2
5	0	1	1	0
6	1	1	1	1
7	1	0	0	0
8	0	0	0	1
9	0	0	0	0

Figure 3.16. The percentage of fish with the number of deformed vertebrae (n=45) recorded per treatment.

Trial II – Cataract and Retina Layer Composition

At the end of the 17 weeks, 10 fish per colour replicate (n=3) were assessed for cataracts as previously described. No significant differences were observed between the treatments (data not shown). Assessment of the melanin and photoreceptor inner segments, melanin, outer nuclear layer, outer plexiform layer, inner nuclear layer, inner plexiform layer at the dorsal, ventral and lateral orientation also showed no significant differences between treatments (Fig. 3.17).

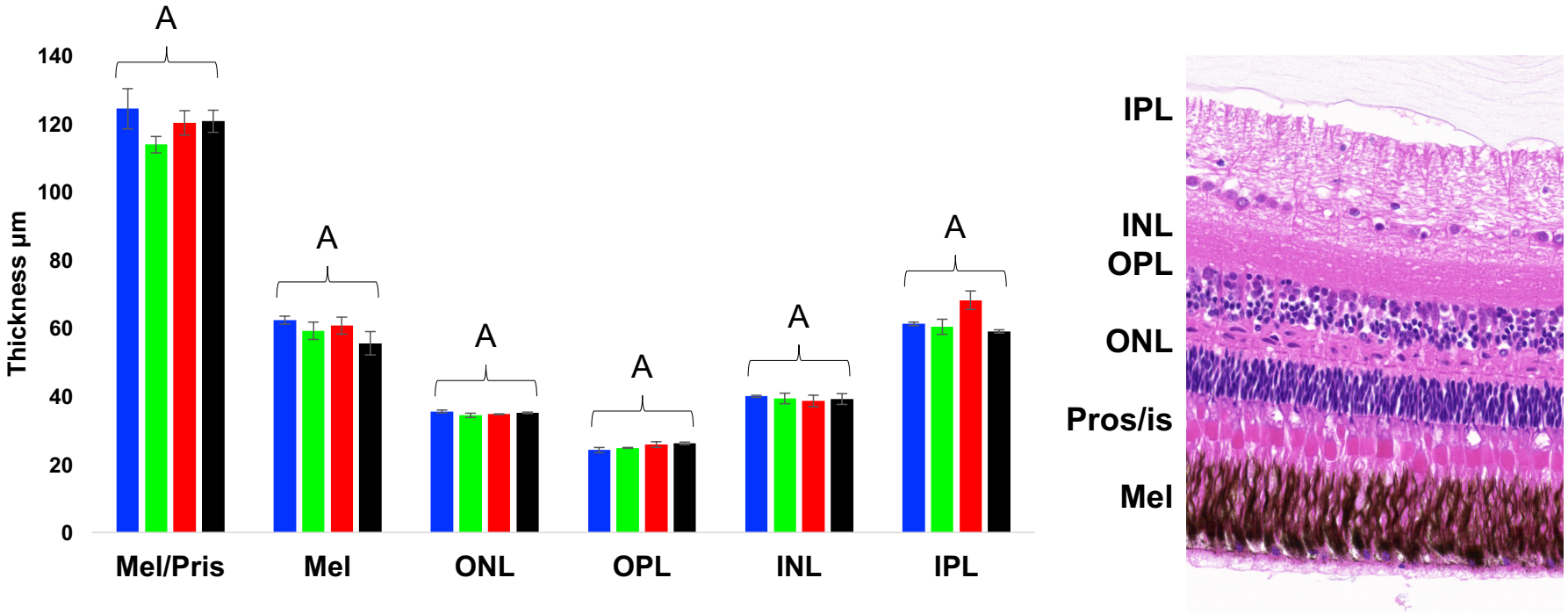

Figure 3.17. Examination of the melanin and photoreceptor inner segments (Mel/Pros/is), melanin (Mel), outer nuclear layer (ONL), outer plexiform layer (OPL), inner nuclear layer (INL), inner plexiform layer (IPL) were performed in ten locations at the dorsal, ventral and lateral orientation. Samples were collected after 16 weeks (115) days of exposure to either Blue, Green, Red or White Led light. No significant differences were observable between groups.

Muscle Fibre Histology

Muscle fibre samples collected at the end of 17 weeks of exposure to narrow bandwidth light showed significant differences between the overall distributions for each of the treatments (Table 3.4). Evaluation using probability density functions (Fig. 3.18) showed a clear difference in the distribution of small muscle fibres in the Blue treatments. Repeat bootstrap values (Fig. 3.19) showed the same pattern of distributions. No such differences were apparent when comparing quantiles (Table 3.5).

Table 3.4. Kolmogorov-Smirnov non-parametric bootstrap test for comparison of muscle fibre distribution between groups exposed to Blue (fB), Green (fG), Red (fR) and White (fW) treatment during freshwater. Fish were sampled at the end of parr prior to the induction of out-of-season smoltification.

Contrast: Treatment vs Treatment		**End of Parr**	
		D	***P*-value**
fB	**fG**	0.030	0.001
fB	**fR**	0.052	<0.000
fB	**fW**	0.022	0.021
fG	**fR**	0.070	<0.000
fG	**fW**	0.021	0.038
fR	**fW**	0.058	<0.000

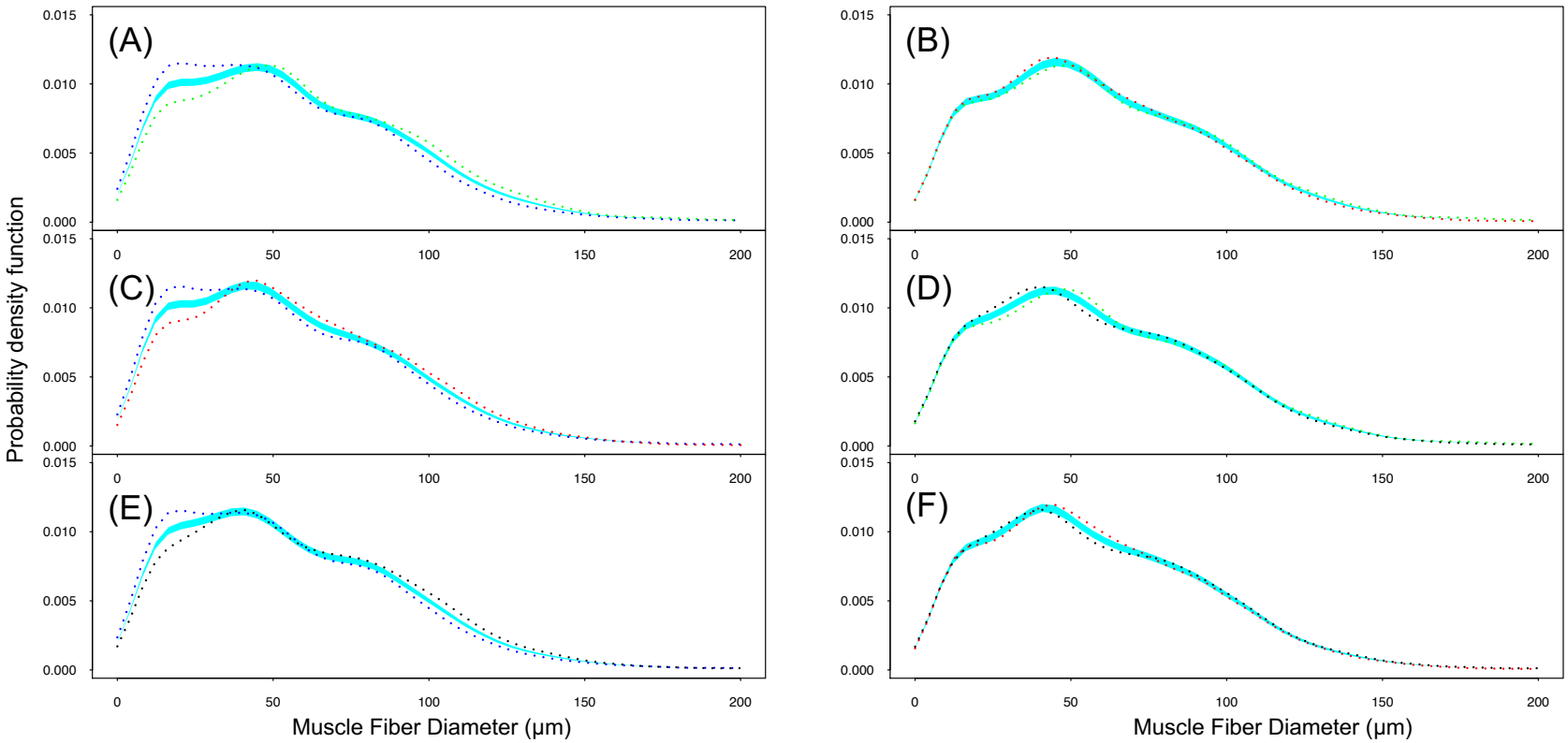

Figure 3.18. Comparison of muscle fibre distribution in post-smolt Atlantic salmon immediately after an out-of-season smoltification regime under four different spectra (White (black lines): Blue; Green or Red) reflected by line colours. Shaded area shows combined probability density plot (PDF) for both treatments being contrasted. Coloured dashed lines are the PDF of each individual treatment. A: Blue vs Green; B: Green vs. Red; C: Blue vs Red; D: White vs Green; E: Blue vs White; F: Red vs White.

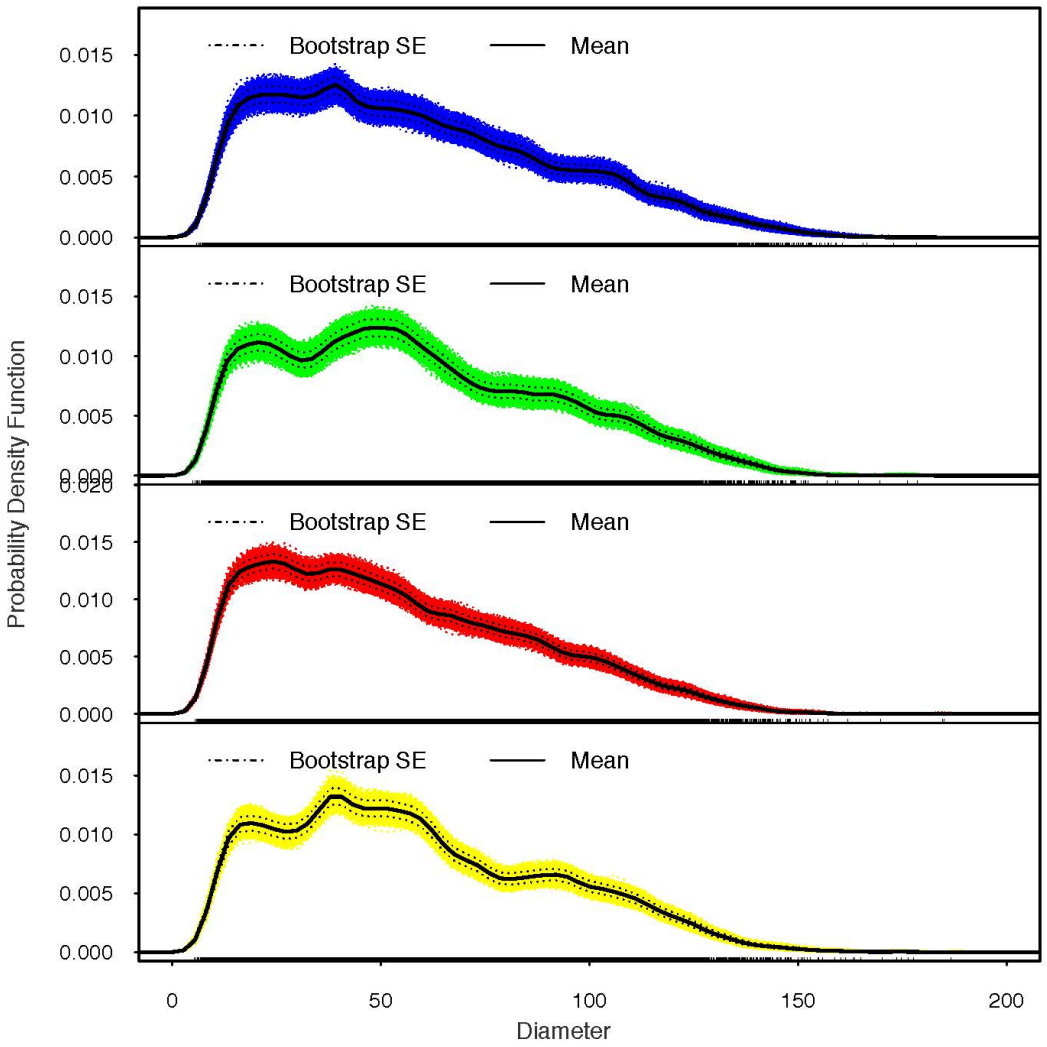

Figure 3.19. Variability band and mean (black line) of repeated bootstrapped probability density functions of muscle fibre diameter in Atlantic salmon parr. Fish were exposed to four different spectra (White; Blue; Green or Red) indicated by line colours.

Table 3.5. Comparison of values determined from the percentiles of mean muscle fibre diameter in fish exposed to Blue (fB), Green (fG), Red (fR) and White (fW) during freshwater and smoltification and subsequently following exposure to either a simulated natural photoperiod (SNP) or continuous lighting (LL) using White light. Fish were sampled at the end of parr, at smolt transfer and trial termination.

Sample Point	**Percentile**	**Kruskall-Wallace *P*-value**	**Percentile for fB**	**S.E.M.**	**Percentile for fG**	**S.E.M.**	**Percentile for fR**	**S.E.M.**	**Percentile for fW**	**S.E.M.**
End of parr	5%	0.70	14.64	0.97	14.07	0.17	13.54	0.39	14.53	0.70
	10%	0.86	19.09	1.18	18.67	0.62	17.70	0.62	19.13	1.21
	50%	0.13	53.67	1.21	54.36	0.83	49.25	1.51	53.19	1.73
	95%	0.07	120.53	0.89	118.61	1.27	112.40	0.87	116.94	1.96
	99%	0.08	141.02	2.03	136.86	2.01	131.08	1.57	135.59	3.25

3.4 Summary of chapter results

Trial I – Preliminary testing of a combination of light intensities and spectra on juvenile Atlantic salmon growth and development

- No significant differences between groups regarding spectrum or intensity
- Increasing light intensities resulted in lower growth under Red light than the other colours tested
- A non-significant but general trend was identified where fish exposed to lower intensities (e.g. 0. 5 w/m^2) grew better than those exposed to higher light intensities

Trial II - Impact of exposure to low intensity light of different spectral composition until the end of parr development

- Significant differences in weight were apparent at the end of the 17 weeks between fish reared under Red light compared to Blue
- Fish exposed to Red light appeared to exhibit a period of enhanced growth after 8 weeks
- Long term exposure to 0.05 W/m^2 resulted in no significant differences in length or K at the end of the trial
- No significant differences in ocular histology were observed following 17 weeks' exposure to narrow bandwidth light compared to controls
- No significant differences were observed regarding vertebral deformity between treatment groups
- Blue light appeared to influence the number of small muscle fibers

3.5 Discussion

Identification of the best lighting conditions for optimal freshwater growth and development is critical for the longer-term performance of salmon in the production cycle. Findings from the initial trial suggested that fish exposed to lower intensities, in general, performed better than high intensities and that spectrum appeared to influence development. Using these findings, trial II applied the same four spectra at a lower intensity and confirmed similar effects of narrow bandwidth lights as seen in trial I. No spectral effects on either vertebral deformity or ocular structure were observed. Interestingly, a higher number of smaller muscle fibres were identified in response to the Blue light treatment which may impact on the longer-term growth potential.

Growth Rates Between Trials

Compared to trial II growth rates were substantially lower in trial I with an average TGC of ~0.9 compared to 1.4 in Trial II. Trial II TGC is very similar to that reported in other trials examining parr growth (Bendiksen et al., 2002). Several confounding issues may explain why growth rates were so low in trial I. Firstly, the RAS system was very new and the filter naïve, this lead to compromised water quality as seen in the values reported for ammonia and nitrites. A considerable effort was made daily to reduce this however it remained an issue throughout the trial. It became apparent after this trial that the supplied biofiltration towers, even when mature would be provide inadequate filtration. Subsequently these were replaced such that by trial II the system was performing considerably better. In the second trial feed was delivered using a commercial feeding system. In trial I, off-the-shelf feeders designed for home aquaria were used which were only programmable for 6 feeds per day although these were reset daily to allow 12 feeds. Feed delivered in large doses has been reported to result in feeding hierarchies (Thorpe et al., 1990) within the population leading to small fish receiving very little food. This is reflected in the CWT data with some fish exhibiting a very low TGC (0.2- 0.4, data not shown). For subsequent trials and prior to investing in a commercial system, these feeders were adapted to allow feeding to be performed every 5 minutes as described in Chapter 2.5. Given these restrictions and the lack of replication results from trial one must be interpreted carefully, however challenges were consistent for all tanks. The final major reason for observed differences in growth

rates stems from the light intensity trialled which was another order of magnitude lower than that trialled in trial I and was determined by growth results from chapter 4 trial II.

Light Spectrum

Fry growth across both trial I and trial II showed consistent responses to spectra with Red light hindering BW in both trials. Using a triplicated design and extended time period in trial II (17 vs 12 weeks), fish exposed to White, Blue and Green treatments showed similar growth performances (BW, FL and K). However, fish exposed to Red light had a significantly reduced BW compared to fish reared under Blue and this was reflected in the TGC; although both FL and K were similar to the other groups. The impact of Red light on BW was immediate and differences were apparent after 4 weeks of exposure in both trials although not significant until 8 weeks in trial II.

An examination of the population structure through the distribution of weights in trial II showed a transient change from equal or greater initial size to consistently smaller at the end of the trial in comparison to other groups. Little has been published to date regarding the impact of spectrum on growth although several studies have examined the impact of prey colour/background on feed intake (Ali 1961; Ginetz and Larkin, 1973; Clarke and Sutterlin, 1985). Browman and Marcotte (1987) showed increased ingestion of prey in response to the contrast between dyed prey and coloured tank walls and it is possible that this may account for differences in growth observed in the present trial. Unfortunately, such a hypothesis could not be confirmed in the present trials due to the lack of feed recovery and therefore further studies are required to confirm feed intake levels in response to spectral compositions.

In trial II a period of accelerated growth occurred after 8 weeks which led to a significantly higher TGC under Red light compared to the other treatments. This increase lasted for 4 weeks before levels reduced to that seen in the other treatments. Such an adaptation and then comparative growth may be as a result of an adaptive response to the spectrum. Salmonids have been demonstrated to change relative proportions of porphyropsin (A2) and rhodopsin (A1) in order to adjust spectral sensitivity (Dartnall et al., 1961; Beatty 1966; Allen and Munz, 1983). Prolonged exposure of guppies (*Poecilia reticulate*) to orange 600 nm light also lead to an adaptive response and an upregulation of long wave sensitive photoreceptor expression (Sakai et al., 2016). The ability to adapt is well described and concurs with the anadromous nature of the Atlantic salmon which is exposed to a multitude of

spectral conditions throughout the life cycle (Douglas and Djamgoz, 1990). The plasticity of adaptive visual responses was also seen in trials examining the spectral and UV sensitivity in juvenile salmonids with contrasting results attributed to different light sources, ontogenic stages, stocks and culture conditions (Douglas and Hawryshyn, 1980). Adaptation can result in growth increase however, by the end of trial II the Red treatment was still significantly different. This data demonstrates how important the early growth phase is regarding future growth.

Light Intensity

As lighting technology advances, greater levels of light control become available to producers. Identifying the optimal intensity for a given physiological process is complex and differences in production systems will undoubtedly affect photic perception and requirements. Trial I sought to screen prospective intensities to select for in trial II. Results suggested that lower intensities perform better however clearly there must be a scotopic limit where feed detection becomes adversely hindered. In Chapter 4.2 the lowest intensity light, which was an order of magnitude below the lowest trialled in trial I (this chapter) achieved the highest growth rates. As a result, an intensity of 0.05 W/m^2 in trial II (this chapter) was used. Although 4.2 was examining smoltification, full SW adaptation did not occur so results where extrapolated to apply to parr. Replication in trial I could not be achieved and therefore results must be interpreted with caution however data from CWT fish showed a general inhibitory effect of 35 W/m^2 on BW in fish exposed to Blue, Green and Red treatments. While this did not come as a surprise given that such intensity is far above what commercial fish would experience in RAS aquaculture, unexpectedly, fish exposed to White light appeared to be less affected and growth was generally higher. The general effect on the population weights also showed strong convergence with the CWT weights and greater growth at lower intensities being recorded. Results from trial I agreed with findings reported by Mitchel (1986) who showed low intensity light (from 0.001 – 0.014 W/m^2) resulted in higher growth rates in 30 g parr when compared to 1.28 W/m^2. Observation by Migaud et al. (2007) identified a lower sensitivity to Blue light than White light when examining stress responses via plasma glucose and cortisol. Such stress responses may lead to reduced feed intake or feed utilisation and subsequently growth (Barton 2002). Differential growth observed in tank studies examining light intensity and tank colour for Eurasian perch (*Perca fluviatalis*) and FCR data showed

that ingestion rather than utilisation in response to brighter light conditions was the reason for lower growth (Strand et al., 2007).

Despite being unable to draw firm conclusions from trial I, all groups increased in weight over time. Ali 1961 reported a minimum light intensity threshold of 0.004 W/m^2 as the minimum threshold required for feed intake in salmonids (Ali 1961). However, despite the ability of salmonids to detect very low light intensities (Rader et al., 2007), Fraser and Metcalf (1997) reported that only 50 % of parr exposed to 1 lux exhibited feeding behaviour and suggested that higher light intensities are required to ensure optimal feed intake. High light intensity however increases aggression and territorial behaviour (Valdimarsson and Metcalfe, 2001) and so photic conditions must balance feed intake with aggression. Long term, photoreceptor expression changes both in response to high light intensities (Taylor et al., 2015) and low light intensities where elongation of the outer segment of cones and variation in photopigment increases the bandwidth of photon capture by individual photoreceptors (Allen et al., 1973). Such adaptation to intensity may help to mediate the influence of photic intensity and spectrum. In spite of this, identifying optimal photic conditions remains essential to optimise productivity and energy efficiency.

Light Impact on Fry Muscle, Eye and Vertebral Physiology

Significant differences between colour light treatments were seen in the overall muscle fiber distribution at the end of parr development in trial II. Examination of the PDFs showed higher fiber numbers below 30 µm in fish exposed to Blue light compared to Green, Red and White and this was also supported by the bootstrap results. Very few trials have examined the importance of early muscle fiber development on future growth with the exception of one study on thermal imprinting (Johnston et al., 2000). Results showed that exposure of salmon prior to first feeding to cooler water temperatures enhanced the proliferation of muscle satellite cells increasing fiber recruitment and hypertrophy and increasing future growth (Johnston et al., 2000). Identification of fiber number in this trial suggested that future growth may be affected by observations in fiber number related to light treatment. The longer-term impact of observed differential fiber recruitment is investigated in the Chapters 4 and 5.

Concerns regarding welfare, both in term of maximum (Vera and Migaud, 2009) and minimum (Thrush et al., 1994; Handeland et al., 2013) light levels were addressed through morphometric assessment. Retinal damage caused by short wavelengths are

well known in humans (Taylor et al., 1992) however no such impact was seen in the present study. The lack of differences in ocular physiology however are perhaps not surprising given both the protective and regenerative capabilities of fish retina thought to stem from a lack of palpebra (Ferguson 2006), high levels of reactive oxygen species (Boulton et al., 2001) and indeterminate growth (Stenkamp 2007). Adaption occurs though the alteration of melanin granules filtering incident light on the photoreceptors. In addition, photoreceptors within the retina can undergo contraction or elongation, raising or decreasing the distance light travels before contacting the receptor and altering sensitivity (Ferguson 2006). A remarkable regenerative ability, in stark contrast to the gliotic response of damaged mammalian retina (Stenkamp 2007), stems from two sources of pluripotent stems cells found within the eye, circumferential retinal cells and cone pre-curser stem cells within the INL capable of replacing required constituent retinal cells types. Vera and Migaud (2009) showed these responses in salmon exposed to a very high light intensity where a ~25% reduction in the Pro/is visual receptor layer, destruction of the melanin layer and disorganization of the ONL were fully repaired 30 days after exposure. No such changes in structure were found in this trial which suggests that the intensity tested in trial II was below the threshold required to induce damage and that the spectra tested were safe for the early FW development. Identifying the impact of short wavelengths is important given the spectral output of LED White lights which typically have a reduced spectral range compared to incandescent or metal halide bulbs.

Vertebral deformities at the end of parr growth showed characteristically higher prevalence of individual vertebra deformed in the tail region as described by Fjelldal et al. (2007). No differences were seen between the other regions or between any colour treatments. The samples reported here came immediately before the onset of an out-of-season smtoltification regime during which substantial remodelling occurs and when light intensity appears to impact upon malformation (Handeland et al., 2013). Fjelldal et al. (2004) reported vertebral deformities occurring as a result of pinealectomy and suggested that this was related to the production of melatonin although such an invasive procedure can undoubtedly lead to other unknown effects and as such the relationship between light and deformities requires further investigation.

Conclusions

The optimisation of photic conditions for successful growth and development of juvenile Atlantic salmon relies upon improving our understanding of the roles of intensity and spectrum during early FW development. Trial I results suggested that both intensity and spectrum can impact on growth at an early developmental stage however results were not significant between treatments. Utilising 0.05 W/m^2 for an extended period in Trial II resulted in substantially better TGC than in trial I although this was likely influenced by serval additional factors. Observations showed no discernible differences between Blue, Green or White in either trial. White is predominated by blue and green wavelengths so White results are perhaps not surprising. The exclusive use of Red light even at low intensities may negatively impact growth as seen in the final weights recorded in Trial II however results regarding other growth metrics were not consistent or conclusive. Results highlight the extraordinary plastic nature of photic perception in salmonids. Given the range of narrow bandwidth lights across a broad range of intensities the lack of a response is remarkable. In addition, no differences regarding vertebral or ocular health were seen. The use of Blue light appeared to promote the differentiation of a greater numbers of smaller muscle fibres however the impact this has on future development remains to be elucidated especially given the plasticity of fish growth. The impact of these narrow bandwidth lights at low intensity on future smoltification and on-growing performances will be presented in the proceeding chapters.

4 Assessing the Role of Spectrum and Intensity on An Out-Of-Season Smoltification Regime in Atlantic Salmon

4.1 Introduction

Out-of-season smoltification regimes are used to meet yearlong customer demand by manipulating photoperiod to induce temporal adaptations required for life in seawater (SW). The same market forces that dictate year-round supply also dictate efficient and responsible production (Klinger and Naylor 2012; Bostock et al., 2016). In reaction to this, freshwater (FW) production on land is increasingly being moved away from flow through (FT) systems and into large recirculating aquaculture systems (RAS) where environmental concerns can be mitigated and the environmental conditions of production systems manipulated (Dalsgaard et al., 2013). A relationship, although not significant, between intensity and fry growth was seen in the previous chapter with faster somatic development occurring in response to lower intensities. Responses reflected known visual photoreceptor sensitivity (Parkyn et al., 2000) and comparatively lower intensities in Red and Green resulted in reductions in growth compared to Blue which has known reduced ocular sensitivity (Douglas and Djamgoz 1990; Parkyn et al., 2000). The effects of spectrum during smoltification, however, are currently unknown.

Out-of-season smolt production typically takes the largest cohort from a population and enhances growth through exposure to continuous light (LL) exploiting the naturally higher ambient temperatures in FT or artificially created in RAS. An artificial short day (SD), or 'winter' period, is applied before returning to LL. Body size (McCormick 2012) and energetics (Berrill et al., 2006) play a key role in successful initiation and completion. Identification of the optimal time for SD application received considerable attention in the infancy of the industry (Thrush et al., 1994; Duston et al., 1985; Duncan and Bromage 1998) as has the duration of lighting during both the SD and LL stages. Once fish have reached a suitable size, a widely-used protocol is LL from hatch followed by a 12:12 SD for 400 ºDay and returning to LL for 400 ºDays prior to SW transfer (Handeland and Stefansson 2001). A synchronised smoltification response within the population is essential to ensure post-seawater transfer growth is maximised (Arnesen et al., 2003). Completion of smoltification can be predicted using a combination of accumulated degree days based upon historic temperature exposure (Bromage 1998) and analytical tools such as measuring gill NKA enzymatic activity

(Mccormick 1993) or gene expression (Nilsen et al., 2007; Loncoman et al., 2015). Physiological adaptations reach an optimal state, the 'smolt window', during which fish must be transferred to SW. Adaptations are so extreme that osmoregulation in FW is compromised and so de-smolting occurs if SW is not reached (Arnesen et al., 2003). The duration of the smolt window has been determined under ambient temperature regimes at around 350 ºdays (Stefansson et al., 1998; McCormick et al., 1999) however, little is known about the impact of higher temperatures frequently used in RAS systems where growth and development are driven at the economic optima to reduce operating costs.

Seasonal cues are demonstrably interpreted through a network of non-visual photoreceptors. Originally observed in enucleated minnows (*Phoxinus phoxinus*) through the continued display of seasonal developmental traits (Frisch 1911), photoreceptors have been localised in the pineal (Ekström et al., 1987; Fjelldal et al., 2004), deep brain (Sandbakken et al., 2012a; Sandbakken et al., 2012b; Hang et al., 2016) and the retina where functionality has been linked to both circadian and pupillary reflexes (see Lamb 2013 for a comprehensive review). To date over 35 different opsins have been identified in non-visual photoreceptors with spectral sensitivity varying depending upon the structural configuration (Hang et al., 2016). Given the wide range of opsins identified to date it is not unreasonable to postulate that different spectra may elicit different physiological responses regarding the interpretation of seasonal cues. Identifying the impact of spectrum will provide valuable information for designing efficient aquaculture lighting owing to the enhanced efficiencies of some LED spectral outputs compared to others. Concern has been raised regarding minimum light intensity with a value of 43 lux suggested to mitigate vertebral malformation (Handeland et al., 2013), as the visual system exhibits clear spectral sensitivity regarding perception, the impact of different spectra must be investigated to ensure that signals delivered meet biological requirements.

LL fails to provide a seasonal cue and inhibits retinal innervation of the preoptic area, a mechanism suggested to prevent smoltification (Ebbesson et al., 2007). Little is known regarding minimum and maximum light intensities during the scotophase and whether values change dependant on spectrum. Historically red light has been used for night observation and sampling owing to restrictions in the far red visual sensitivity in fish (Allen and Munz 1983), however recently red light from emergency exit signs have been shown to negatively impact on zebrafish (*Danio Rerio*) maturation showing

both perception and interpretation to have occurred (Adatto et al., 2016). In hatcheries, general tank maintenance is avoided during the scotophase of smoltification regimes however emergency lighting in addition to alarm situations requiring tank access may disrupt the scotophase and so the identification of maximum acceptable light levels and spectrum would provide useful guidance for such situations.

The parr-smolt transformation induces both osmoregulatory mechanisms and phenotypic adaptation to facilitate life in SW. Osmoregulation maintains ionic homeostasis such that plasma chloride is around 130nM in both FW and SW environments (Folmar and Dickhoff 1981; Arnesen et al. 2003). Salt balance is driven by the presence in the kidney, salt gland and general epithelium of ion transporter cells. The major excretory organ however are the gills. Given the close proximity to the aqueous environment and high blood flow these organs are ideally situated for high levels of exchange (Doyle and Gorecki 1961).

In the gill lamellae two populations of chloride cells can be differentiated using insitu-hybridisation (McCormick 2007) and related to either a FW or a SW environment. Structurally very similar, columnar in shape with a highly convoluted tubular structure at one end and a large apical crypt, cells are continuous with the basolateral membrane and rich with mitochondria (McCormick 1995). Three key transporter proteins responsible for salt secretion reside on the membrane of these cells, the Na^+-K^+-ATPase (NKA) or sodium pump, Na^+-K^+-$2Cl^-$ cotransporter (NKCC) and cystic fibrosis transmembrane conductance regulator (CFTR). Two major discrete NKA alpha isoforms, NKAα1a and NKAα1b have been described (McCormick et al. 2009). Kinetics of NKAα1a and NKAα1b are optimised for FW and SW respectively and cell population vary dependent upon the aqueous environ (Nilsen et al. 2007). Cells containing NKAα1b rapidly expand upon contact with SW maximising ion transport (McCormick 2012).

In saltwater, an ionic gradient is created through a constant efflux of Na^+ ions and a constant influx of K^+ ions with a 3:2 stoichiometry driven by NKA. Hydrolysis of ATP powers as many as 10^8 sodium pumps in a single chloride cell (Karnaky et al. 1977). The ionic gradient overrides the membrane electrical potential allowing K+ ions to exit the cell through Kir (inward rectifier K+) channels. As a result, a transmembrane electrical potential of ~100 mv^{-1} (Loretz 1995) can be achieved. This potential is used by the NKCC to move 1 Na^+, 1 K^+ and crucially $2Cl^-$ into the cell which can be excreted

by the apically situated CFTR. Na^+ in the gills transfers to the interstitial lumen into paracellular pathways via claudins, a family of tight junctions, again driven by the transepithelial potential (Tipsmark et al. 2008). Several claudins have been identified with 10e playing the most important role in salt excretion. Confirmation of the importance of the excretory components is highlighted by the upregulation of NKCC1, CFTR1 and claudin 10e mRNA after exposure to SW (Nilsen et al. 2007; Tipsmark et al. 2010). Further evidence of the distinct roles of the two isoforms is seen in the RNA transcripts, NKAα1b mRNA expression rates in S1 smolts is highly elevated prior to SW transfer whereas NKAα1a stays relatively consistent (Nilsen et al. 2007; Stefansson et al. 2007). As such, analysis of both NKA enzyme activity and the expression of NKA genes provide a strong indication of likely saltwater adaptiveness and are a useful indicator for producers to determine where in the 'smolt window' their stock is.

In this chapter results from three trials are presented exploring the impact of spectrum and intensity on smolt development when using an out-of-season smoltification regime. The aims from each trial are summarised as:

Trial I. Identify the impact of narrow bandwidth light on the initiation of smoltification by altering the perception of an artificially induced seasonal cue.

Trial II. Examine physiological responses to a continuous light photoperiod where the short day "winter" photoperiod of an out-of-season smoltification regime is replaced with a single intensity drop to deliver a subjective winter.

Trial III. Determine whether an appropriate seasonal cue can be perceived using continuous light with a daily intensity change in response to three spectra.

In addition, trial III aimed to identify whether long-term exposure to narrow spectrum light influenced muscle histology.

Collectively, these trials sought to determine the duration of the smolt window for out-of-season smolts of current commercial relevancy in response to both standard and novel photic regimes using a combination of classical and molecular techniques.

4.2 Trial I - The Impact of Narrow Spectrum Light on Smoltification using a Traditional Photoperiod

4.2.1 Trial I - Material and Methods

Fish Stocks, Rearing Conditions and Photoperiod Regimes

On the 8th of September, 2014, 960 fish (mean weight of 48.4 ± 3.2 g) of the Aquagen strain were transferred from the University of Stirling Hatchery, Scotland (56°N, 4°W) into a recirculating aquaculture system at the University of Stirling. Prior to transfer fish had been maintained under LL white compact fluorescent light (CFL) from first feeding. Fish were distributed equally between 12 tanks (80 fish per tank) with a working volume of ~300 l. Water temperature prior to transfer was 14 ºC, RAS water temperature was maintained at 13.5 ± 1.0 °C for the duration of the trial. Fish were fed a standard salmon diet (EWOS Micro 20P, Scotland) during the photophase according to manufacturer's guidelines (daily SFR ranged from 1.1-1.4 % depending upon biomass and body weight). Feed was weighed at the start and end of each week to ensure adequate ration. Satiation was verified through pinch feeding and the accumulation of excess pellets at the tank outflow. Feed was delivered every 5 minutes using adapted Eheim twin screw feeders (Eheim, Germany) controlled through an in-house developed control system as described in Chapter 2.3. Tank flow was set at 10 l min^{-1}. Throughout the trial outflow oxygen was checked periodically and maintained above 80 %. pH was maintained at 6.78 ± 0.46. Ammonia varied from 0.04 to 0.64 ppm (average 0.24 ppm) and nitrite from 0.06 to 1.2 ppm (average 0.52 ppm). The sump was dosed daily with sodium bicarbonate (mean 128 g^{-day}) via a continual drip.

Experimental Design and Sampling

The trial consisted of triplicated tanks (80 fish / tank) and each tank was acclimated for 200 degree days (ºday) to LL of either Blue ($\lambda_{(max)}$ 444 nm), Green ($\lambda_{(max)\ 523}$ nm), Red ($\lambda_{(max)}$ 632 nm) and White LED (Fig. 4.1). Illumination was delivered at 5 W/m^2 based on results from Chapter 3- Trial I where 5 W/m^2 elicited a response in all spectra tested. Intensity was measured directly below the luminaire under 1 cm of water. Illumination and timings were provided by a bespoke LED lighting system (Philips, Holland) as described in Chapter 2.2.1. Light spectrum remained constant for each

tank for the duration of the trial, standardised between tanks using a light meter (Skye Instruments Ltd, UK) calibrated to the National Physics laboratory (UK) standards.

The photoperiod followed industry norms for out-of-season smolt production whereby a square-wave photoperiod was applied with a short day (SD, LD12:12) period of 400 ºdays used to simulate a subjective winter. During the SD period tanks were lit from 08:00 to 20:00 and kept in darkness from 20:00 to 08:00. During the night period, all external lighting within the room was switched off. After 400 ºdays all tanks were returned to continuous lighting (LL) for a further 500 ºdays.

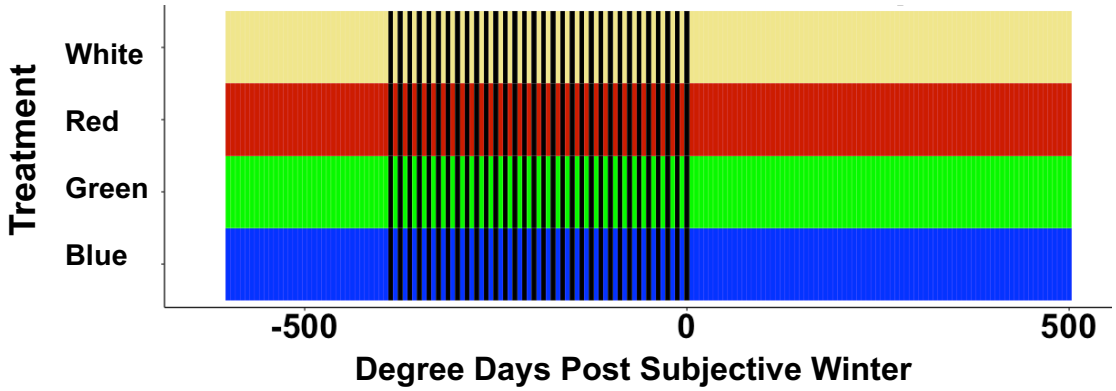

Figure 4.1. Photoperiod regime used for induction of out-of-season smoltification (LD12:12 “winter” -400 ºdays to 0 ºdays; LL “summer” 0-500 ºdays) where photophase was provided by one of four differing spectral compositions (White; Blue; Green; or Red). Fish were acclimated to each treatment for 200 ºdays and returned to LL post subjective winter.

Population and Smoltification Assessment

Two distinct datasets were recorded throughout this trial for assessment of photic influence on a population as a whole and another for examining smoltification.

Population Metrics

Growth metrics, including values from fish terminally sampled for NKA enzyme activity at 0 ºdays and 500 ºdays, were recorded for 20 individuals per tank at -400 ºdays, 25 per tank at 0 ºdays and 20 per tank at 500 ºdays with the exception of White Rep 1 where 16 individuals remained at the end of the trial. Fish were briefly anesthetised using buffered tricaine methanesulphonate (50 ppm MS222, Pharmaq, UK) and body

weight (BW) to the nearest 0.1 g and fork length (FL) to the nearest 0.1 cm recorded. Growth data from SWC fish was not included in the population metrics.

Smoltification Metrics

At 0, 100, 200, 300, 400 and 500 ºdays post SD completion application 5 fish per replicate per treatment (n = 3) were removed for a 24 h saltwater challenge (SWC). The following day a further 5 fish per tank were removed for gill Na^+-K^+-ATPase (NKA) enzyme activity assessment (NKAe). SWC and NKA enzyme sampling protocols are described in the materials and methods chapter (Chapter 2.4.5). All terminal samples had BW and FL recorded (Chapter 2.4.4).

4.2.2 Trial I - Results

Throughout the trial there was no mortality in any tank.

Trial I – Population Growth Performance

Trial I - Body Weight

At 0 ºdays all treatments had increased in weight from the start weights (-400 ºdays) (Fig. 4.2) and no significant differences were recorded between treatments. At 500 ºdays fish under White were significantly heavier than Blue, but there were no significant differences in smolt weight between fish exposed to Blue, Green or Red.

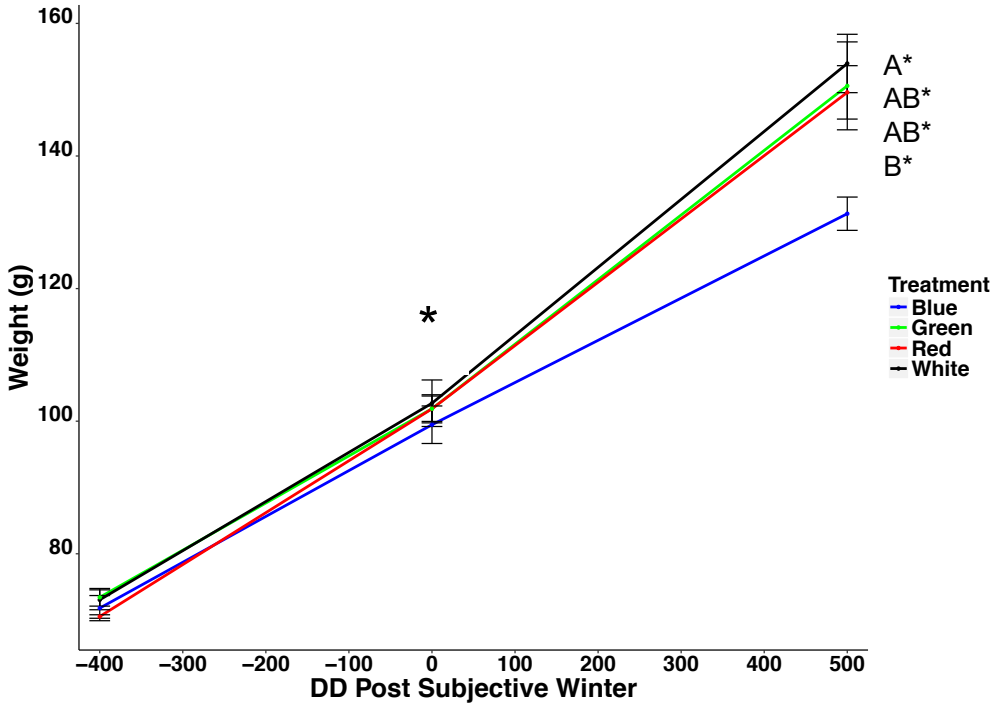

Figure 4.2. Weight increase (Mean ± SEM, n = 3) of juvenile Atlantic salmon subjected to an out-of-season photoperiod regime (LD12:12 "winter" -400 ºdays to 0 ºdays; LL "summer" 0-500 ºdays) provided by one of four differing spectral compositions (White; Blue; Green; or Red). Significant differences between treatments within time points where present are shown as upper case superscripts (Mixed-linear model, $p<0.05$), significant changes between time points are denoted by an asterisk.

Trial 1 – Length

At 0 ºdays all treatments had increased in weight from the start weights (-400 ºdays) (Fig. 4.3) and no significant differences were recorded between treatments. At 500 ºdays fish under White were significantly longer than Blue, but there were no significant differences in smolt weight between fish exposed to Blue, Green or Red.

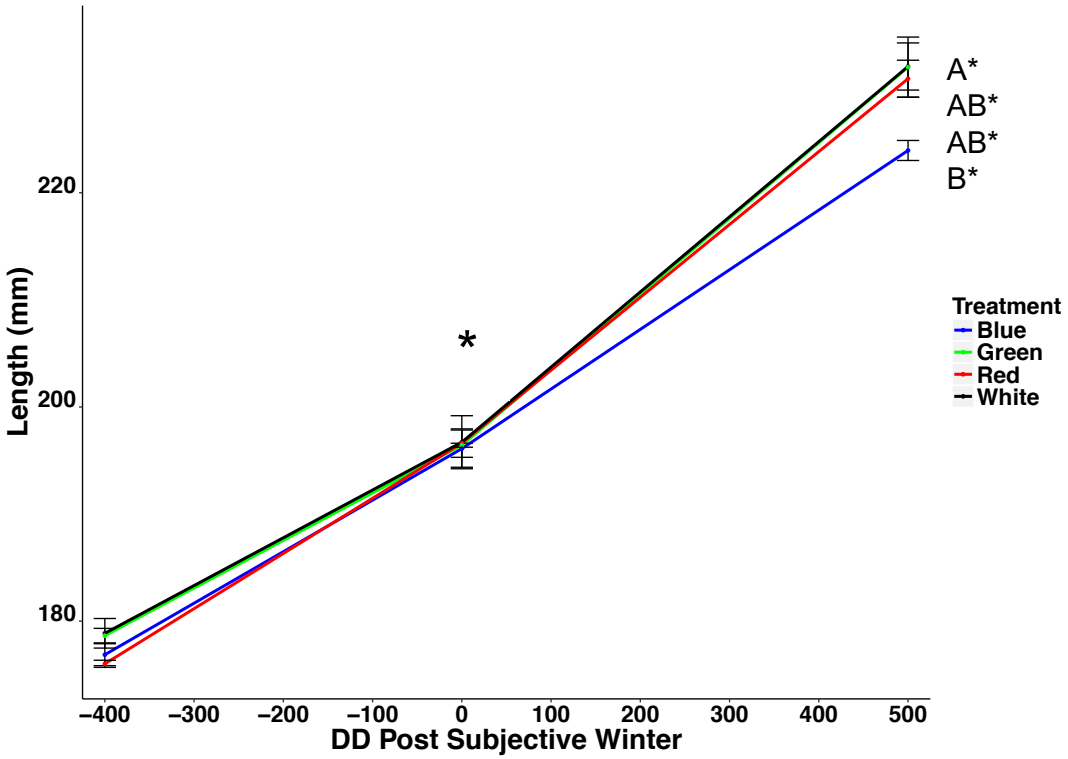

Figure 4.3. Length increase (Mean ± SEM, n = 3) of juvenile Atlantic salmon subjected to an out-of-season photoperiod regime (LD12:12 "winter" -400 ºdays to 0 ºdays; LL "summer" 0-500 ºdays) provided by one of four differing spectral compositions (White; Blue; Green; or Red). Significant differences between treatments within time points where present are shown as upper case superscripts (Mixed-linear model, $p<0.05$), significant changes between time points are denoted by an asterisk.

Trial I - Condition Factor

Condition factor did not change significantly during SD except for fish exposed to the White treatment which showed a significant increase [p=<0.01] (Fig. 4.4). Following application of LL (0-500 ºdays), condition factor decreased significantly for all treatments. No significant differences were observed between treatments at each sample point.

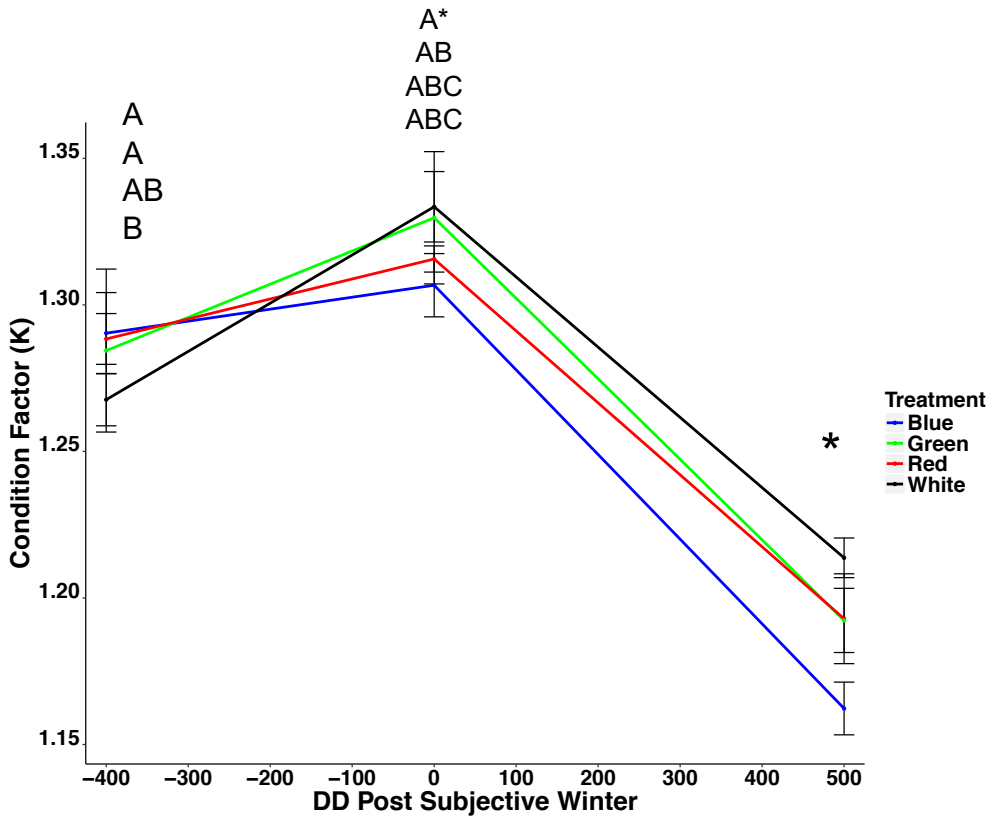

Figure 4.4. Change in condition factor (Mean ± SEM, n = 3) of juvenile Atlantic salmon subjected to an out-of-season photoperiod regime (LD12:12 "winter" -400 ºdays to 0 ºdays; LL "summer" 0-500 ºdays) provided by one of four differing spectral compositions (White; Blue; Green; or Red). Significant differences between treatments within time points where present are shown as upper case superscripts (Mixed-linear model, $p<0.05$), significant changes between time points are denoted by an asterisk.

Smolt Development

Trial I - Weight During Smoltification

After exposure to the SD "winter" photoperiod all groups increased significantly in weight over the next 500 ºdays (Fig. 4.5). Significant differences between treatments were seen at 100 ºDays where the BW of fish under Red light was significantly lower than the Blue (Fig 4.5.A). Exposure to White light led to a significant increase in weight between 100 ºdays and 400 ºdays (Fig. 4.5B**).** In response to Blue light no significant increase in fish weight was observed between 100 ºdays and the end of the trial (Fig 4.5C). Green treatments increased fish weight significantly between 100 and 400 ºdays (Fig. 4.5D) and in response to Red light significant increases in fish weight was observed between 100 and 500 ºdays (Fig. 4.5E).

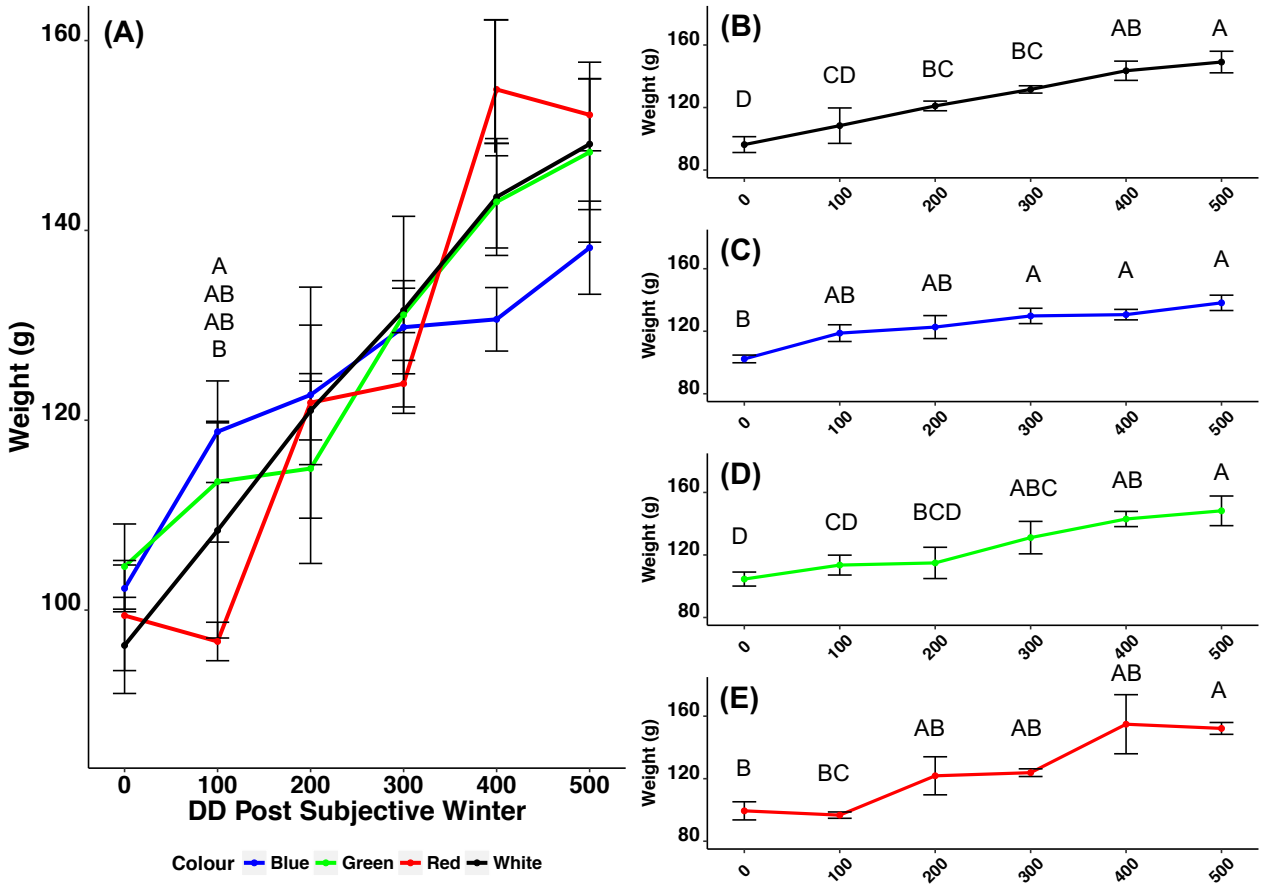

Figure 4.5. Weight increase (Mean ± SEM, n = 3) of juvenile Atlantic salmon sampled for NKA enzyme activity after subjection to an out-of-season photoperiod regime (LD12:12 “winter” -400 ºdays to 0 ºdays; LL “summer” 0-500 ºdays) provided by one of four differing spectral compositions (B-White, C-Blue, D-Green and E-Red) reflected by line colour. Significant differences between treatment where present are shown in **(A)**. Significant differences within treatment over time are shown in **(B) - (E** (1-Way ANOVA, $p<0.05$).

Trial I - Condition Factor During Smoltification

Condition factor (K) decreased significantly between 0 and 500ºdays after the application of SD “winter” (Fig. 4.6). At 300 ºDays the condition factor in fish exposed to Red light was significantly higher than those exposed to Blue (Fig 4.6A). K of fish exposed to White and Blue light (Fig. 4.6B and 4.6C) exhibited a significant decrease between 0 and 300 ºdays. Fish Exposed to Green and Red light exhibited a significant decrease from starting values after 400ºdays (Fig. 4.6D and 4.6E). Final condition factor in all treatments ranged between 1.08 and 1.12 having dropped significantly from a starting value of ~1.22.

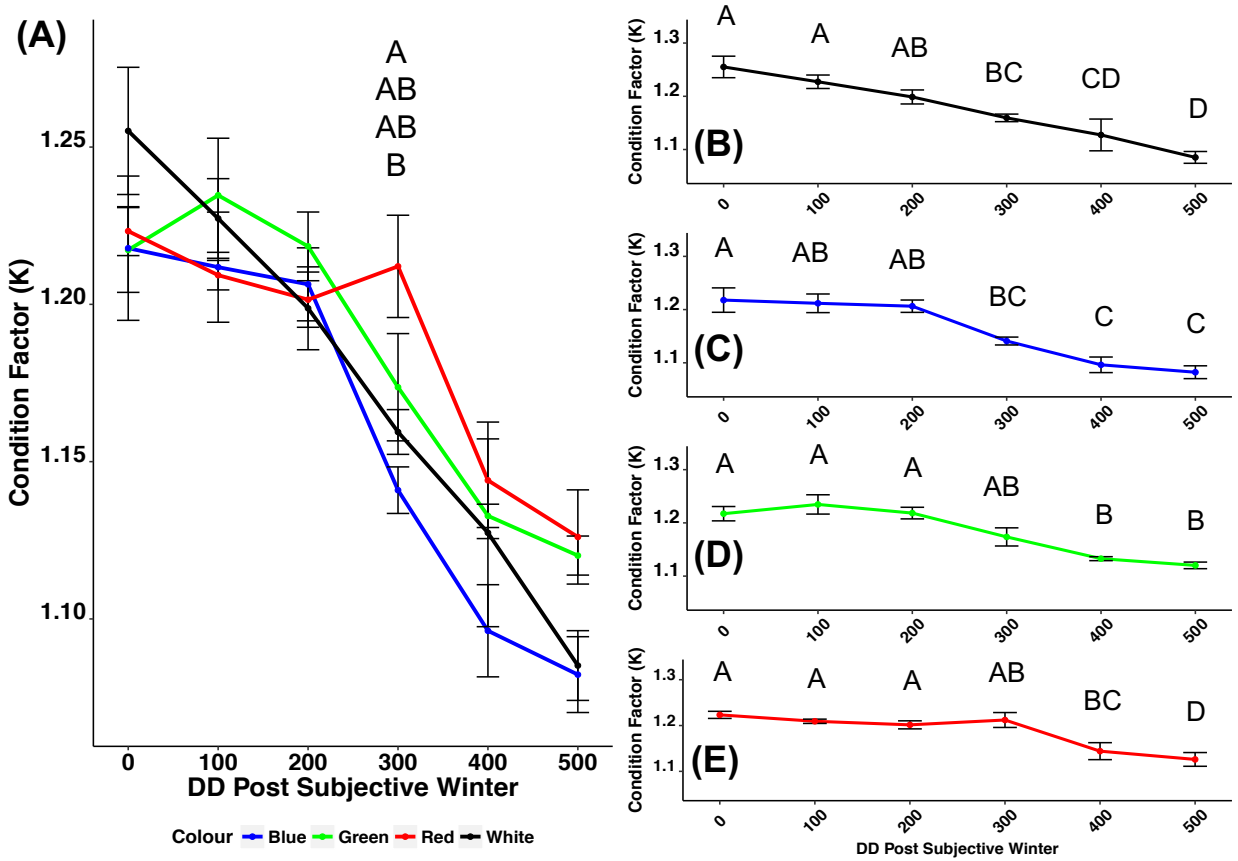

Figure 4.6. Changes in condition factor (Mean ± SEM, n = 3) of juvenile Atlantic salmon sampled for NKA enzyme activity after subjection to an out-of-season photoperiod regime (LD12:12 “winter” -400 ºdays to 0 ºdays; LL “summer” 0-500 ºdays) provided by one of four differing spectral compositions spectral compositions (B-White, C-Blue, D-Green and E-Red) reflected by line colour. Significant differences between treatment where present are shown in **(A)**. Significant differences within treatment over time are shown in **(B) - (E)** (1-Way ANOVA, $p<0.05$).

Trial I – NKA

Gill NKAe Enzymatic reduction assay (NKAe)

NKAe activity in fish exposed to Green and Blue was significantly higher at 200 ºDays than in fish exposed to Red light [p=0.001 and p=0.003 respectively] (Fig. 4.7A). At the same time point NKAe activity in fish exposed to White light appeared lower, but not significantly and higher than the fish under Red. At 400 ºDays fish exposed to Red light exhibited significantly higher NKAe activity than fish under Green light [p=0.017]. Exposure to White resulted in significantly higher NKAe at 200 ºdays from initial values (Fig. 4.7B) and values increased significantly at 300 and 400 ºdays compared to 200 º Days. This pattern was the same for both the Red and White groups. It was not until 300 ºDays that a significant increase from the initial value was seen in response to Red light (Fig. 4.7E). NKA enzyme activity increased significantly (by 3-fold) in all treatments between 0 and 400 ºdays (Fig. 4.7B-E). NKAe remained steady between 400-500 ºDays except in fish under Blue light which showed a significant drop (Fig. 4.7B).

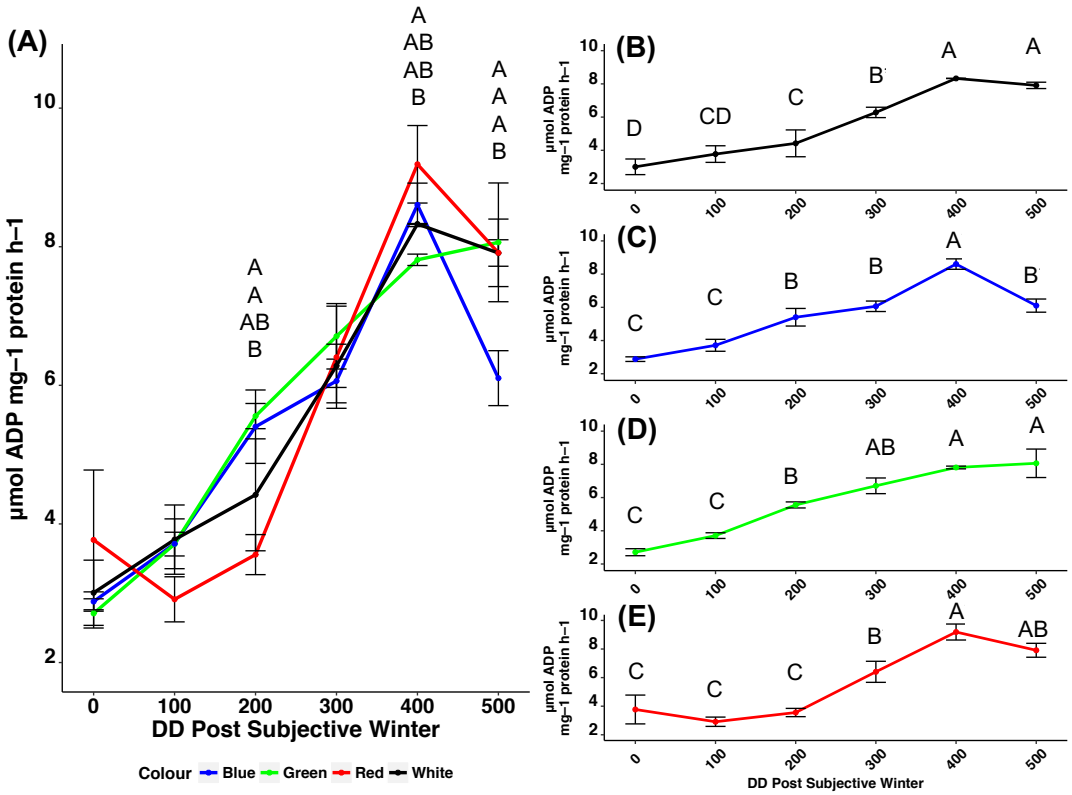

Figure 4.7. Changes in NKA enzymatic activity (Mean ± SEM, n = 3) of juvenile Atlantic salmon sampled for NKA enzyme activity after subjection to an out-of-season photoperiod regime (LD12:12 "winter" -400 ºdays to 0 ºdays; LL "summer" 0-500 ºdays) provided by one of four differing spectral compositions (A-White, B-Blue, C-Green and D-Red) reflected by line colour. Significant differences between treatment where present are shown in **(A)**. Significant differences within treatment over time are shown in **(B) - (E)** (1-Way ANOVA, $p<0.05$).

Trial I - NKA Activity Correlations

In all treatment groups a significant correlation was observed between decreasing condition factor and NKA enzyme activity (Table 4.1).

Table 4.1 Pearson correlations coefficients between NKAe and growth metrics of Atlantic salmon exposed to an out-of-season smoltification regime (LD12:12 “winter” -400 ºdays to 0 ºdays; LL “summer” 0-500 ºdays) provided by one of four differing spectral compositions (White; Blue; Green; or Red).

		Blue		**Green**		**Red**		**White**	
Metric	**Metric**	**Cor.**	**p-value**	**Cor.**	**p-value**	**Cor.**	**p-value**	**Cor.**	**p-value**
BW	**FL**	0.96	<0.01	0.97	<0.01	0.97	<0.01	0.96	<0.01
BW	**NKAe**	0.30	<0.01	0.49	<0.01	0.35	<0.01	0.46	<0.01
FL	**NKAe**	0.39	<0.01	0.58	<0.01	0.42	<0.01	0.56	<0.01
K	**NKAe**	-0.38	<0.01	-0.56	<0.01	-0.40	<0.01	-0.54	<0.01

Trial I – Saltwater Challenge (SWC)

At each time point tested using a SWC no mortality was observed in any group.

Trial I – Plasma Chloride

Plasma chloride was significantly lower in fish exposed to Blue light at 0 ºDays compared to both White and Red treatments (Fig 4.8A). This was the only time point where significant differences were identified. The profile of fish exposed to Red light closely matched that of fish under White (Fig. 4.8E), decreasing significantly between 0-100, 100-200 and 200-300 ºdays and not increasing significantly by 500 ºdays. Plasma chloride values for fish exposed to all light treatments reduced significantly from 0 ºDays to 200 ºDays (Fig. 4.8B-E) and was maintained until 500 ºDays.

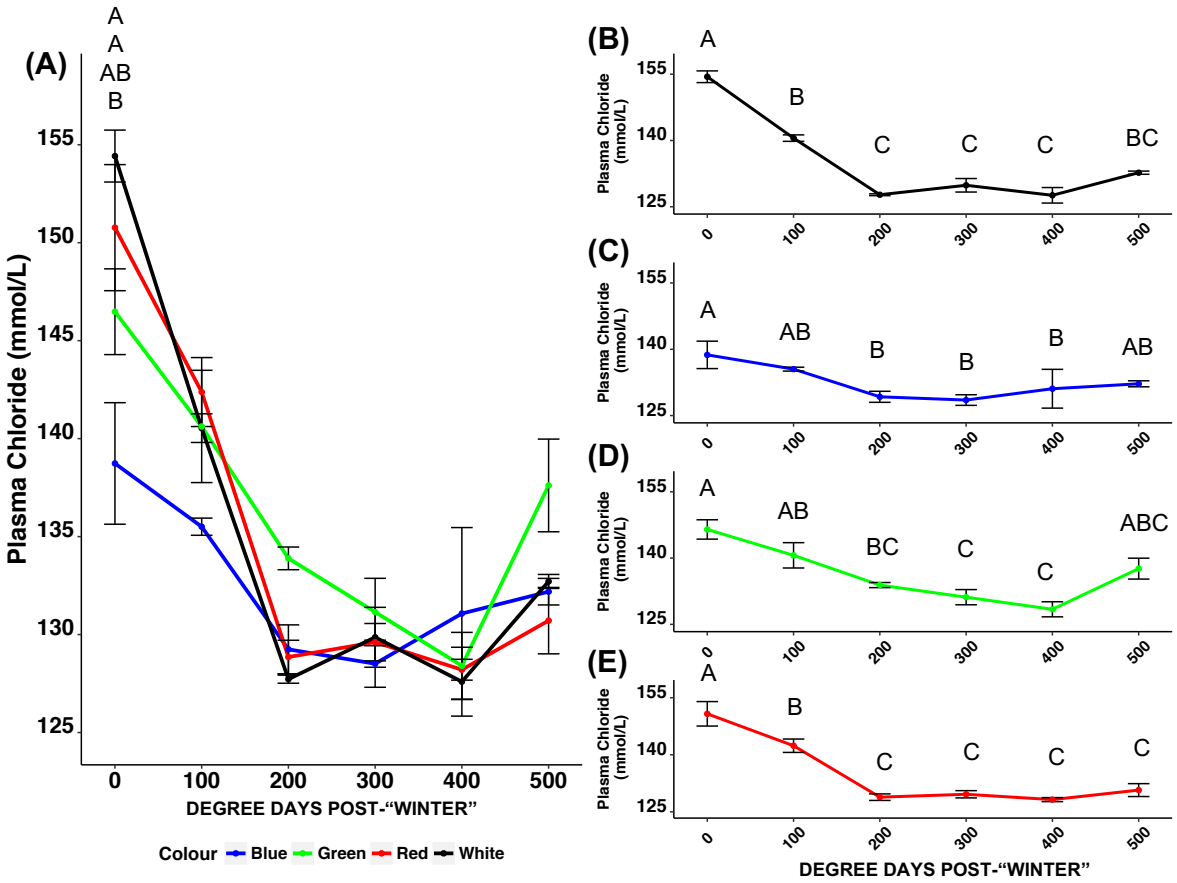

Figure 4.8. Changes in plasma chloride concentration (Mean ± SEM, n = 3) of juvenile Atlantic salmon sampled for NKA enzyme activity after subjection to an out-of-season photoperiod regime (LD12:12 "winter" -400 ºdays to 0 ºdays; LL "summer" 0-500 ºdays) provided by one of four differing spectral compositions (A-White, B-Blue, C-Green and D-Red) reflected by line colour. Significant differences between treatment where present are shown in **(A)**. Significant differences within treatment over time are shown in **(B) - (E)** (1-Way ANOVA, $p<0.05$).

Trial I - Plasma Chloride Correlations

Both BW and FL showed a strong negative correlation under all treatments. The relationship was stronger in fish under both Red and White lights (Table 4.2). As K decreased so did plasma chloride. This relationship was stronger for fish exposed to Red and White light and as observed in Fig. 4.8. These two colours shared similar plasma chloride profiles.

Table 4.2 Pearson correlations coefficients between plasma chloride and growth metrics

		Blue		Green		Red		White	
Metric	**Metric**	**Cor.**	**p-value**	**Cor.**	**p-value**	**Cor.**	**p-value**	**Cor.**	**p-value**
BW	**FL**	0.96	<0.01	0.97	<0.01	0.97	<0.01	0.96	<0.01
BW	**Chloride**	-0.35	<0.00	-0.37	<0.00	-0.60	<0.00	-0.53	<0.00
FL	**Chloride**	-0.34	<0.00	-0.33	<0.00	-0.58	<0.00	-0.60	<0.00
K	**Chloride**	0.07	0.53	0.14	0.21	0.16	0.15	0.27	<0.01

4.3 Trial II – Investigating the Impact of Replacing Diurnal Scotophase/Photophase Fluctuations with a Reduced LL Intensity during the Winter Period of an Out-Of-Season Smoltification Regime

4.3.1 Trial II - Materials and Methods

Fish Stocks, Rearing Conditions and Photoperiod Regimes

On the 8th of September, 2014, 960 fish (mean weight 48.4 ± 3.2 g) of the Aquagen strain were transferred into a recirculating aquaculture system at the University of Stirling from the University of Stirling Hatchery, Scotland (56°N, 4°W). Fish were distributed equally between 12 tanks (80 fish per tank) with a working volume of ~300 l. Water temperature for 21 days prior to transfer was 14 ºC, RAS water temperature was maintained at 13.5 ± 1.0 °C for the duration of the trial. Prior to transfer fish were maintained under continual (LL) white compact fluorescent light (CFL) from first feeding. A standard salmon diet (EWOS Micro 20P, Scotland) was fed according to manufacturer's guidelines (daily SFR% ranged from 1.1-1.4 % depending upon biomass and body weight) and feed was delivered to all tanks during the photophase of the control treatment. Water quality parameters, feed delivery, weight, and satiation was managed as described for trial I.

Experimental Design and Sampling

The trial consisted of triplicated tanks (80 fish / tank) with illumination provided through dual bulb external grade flood light luminaires (Philips, Holland) installed directly above the tanks. Natural daylight replication compact fluorescent (CFL) bulbs (Viva-Lite, Germany) were used to provide illumination (Fig. 4.9). Initial intensity was measured 1 cm below the water surface in the centre of the tank using a light meter (Skye Instruments Ltd, UK) calibrated to the National Physics laboratory (UK) standards and fine tuning of intensity was made by changing the proximity of the light source in relation to the water surface.

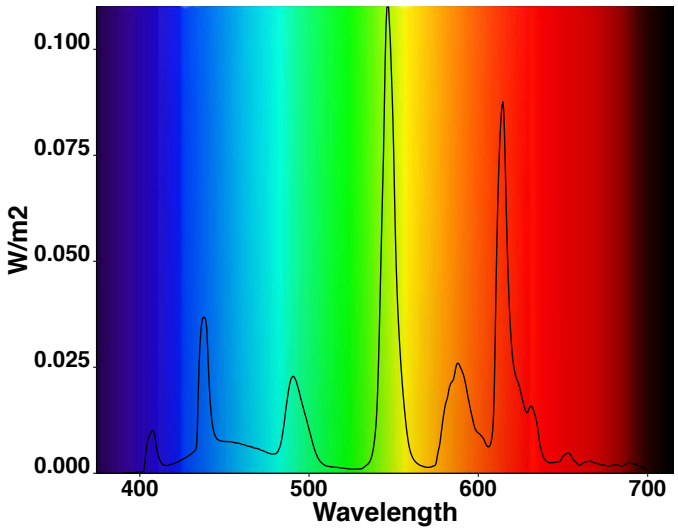

Figure 4.9. Spectral profile of light emitted from compact fluorescent (CFL) daylight bulbs (Viva-Lite, Germany).

Fish were acclimated to LL applied at 5 W/m^2 for a period of 200 ºdays whereupon each tank was randomly assigned one of four intensities for 400 ºdays providing a period of altered intensity under continuous illumination termed 'subjective winter' (SubWin): 5 W/m^2 (control); 1 W/m^2; 0.2 W/m^2 and 0.04 W/m^2 (Fig. 4.10). Each intensity step represents a 5-fold decrease in intensity. Light intensity was manipulated using neutral density 'gel' filters (Lee Filters, Hampshire, UK) to maintain the spectral profile whilst reducing the intensity delivered. Upon completion of the 400 ºday altered intensity, filters were removed and light intensity returned to 5 W/m^2.

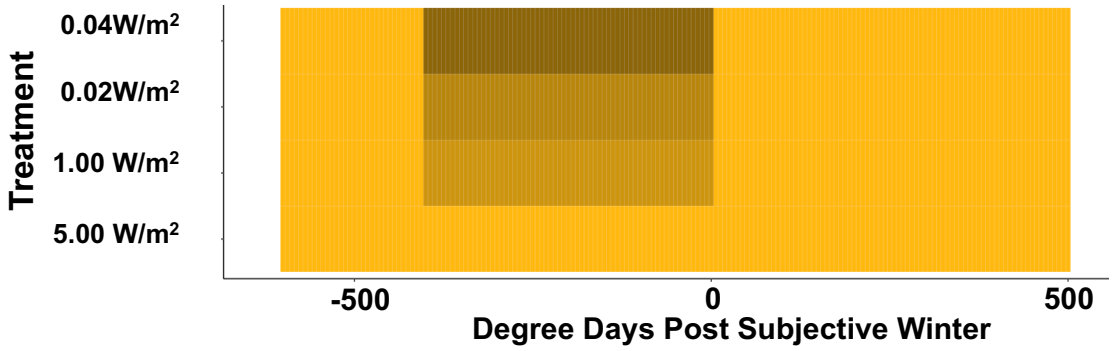

Figure 4.10. Photoperiod regime used for an out-of-season photoperiod regime whereby a "subjective winter" photoperiod (-400 to 0 ºdays) was provided by constant light (LL) at one of four intensities (5, 1, 0.2, 0.04 W/m^2). Tanks were acclimated for

200 ºdays before regime induction and returned to 5W/m^2 following 400 ºdays of subjective winter.

Population and Smoltification Assessment

Two distinct datasets were recorded throughout this trial for assessment of photic influence on a population as a whole and another for examining smoltification.

Population Metrics

Growth metrics, including values from fish terminally sampled for NKA enzyme activity at 0 and 500 ºdays, were recorded for 20 individuals per tank at -400 ºdays, 25 individuals at 0 ºdays and 20 at 500 ºdays. Fish were assessed as described in trial I. Population metrics were contrasted against a "control" (LL-LD12:12-LL) White treatment from trial I.

Smoltification Metrics

At 0, 100, 200, 300, 400 and 500 ºdays post subjective winter 5 fish per replicate (n=3) were removed for a 24h saltwater challenge. The following day a further 5 fish per tank were removed for gill Na^+-K^+-ATPase (NKA) enzyme activity (NKAe). Both SWC and NKA enzyme sampling protocols are described in the materials and methods chapter (Chapter 2.4.5). All terminal samples were assessed for BW and FL in addition to smoltification metrics.

Smoltification results were contrasted against a "control" (LL-LD12:12-LL) White treatment from trial I. Analysis was conducted as described previously in section 4.3.5

4.3.2 Trial II - Results

No mortality was recorded throughout the trial.

Population Growth Performance

Trial II - Body Weight

Fish weight in all groups increased significantly during the trial (Fig. 4.11). No significant differences were observed between group weights at -400 ºdays. After subjective winter (SubWin), groups exposed to 0.04 W/m^2 were significantly heavier

than both the control and 1 W/m^2 treatments. At 500 ºdays no significant treatments differences were observed for weight.

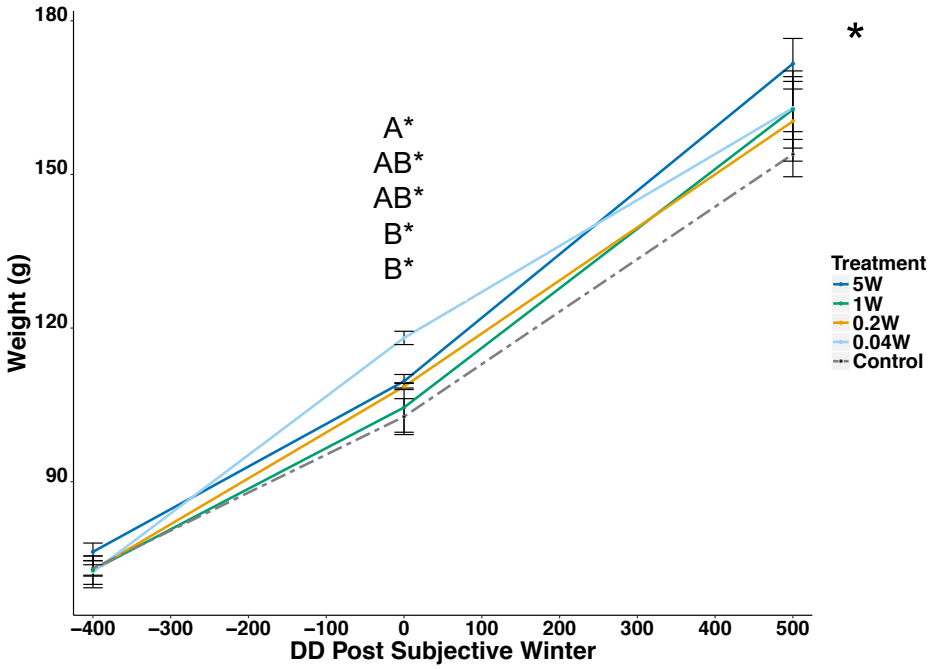

Figure 4.11. Change in weight (Mean ± SEM, n = 3) of juvenile Atlantic salmon subjected to an out-of-season photoperiod regime whereby a subjective "winter" photoperiod (-400 to 0ºdays) was provided by constant light (LL) at one of four intensities (5, 1, 0.2 and 0.04 W/m^2) in relation to a control population that received an LD12:12 photoperiod during the same period. Significant differences between treatments within time points where present are shown as upper case superscripts (Mixed-linear model, $p<0.05$), significant changes between time points are denoted by an asterisk.

Trial II – Length

All groups increased in length significantly over time (Fig. 4.12). Length of control fish was significantly lower at the end of SubWin compared to the 0.04 W/m^2 group. At 500 ºdays no significant differences were observed between treatments.

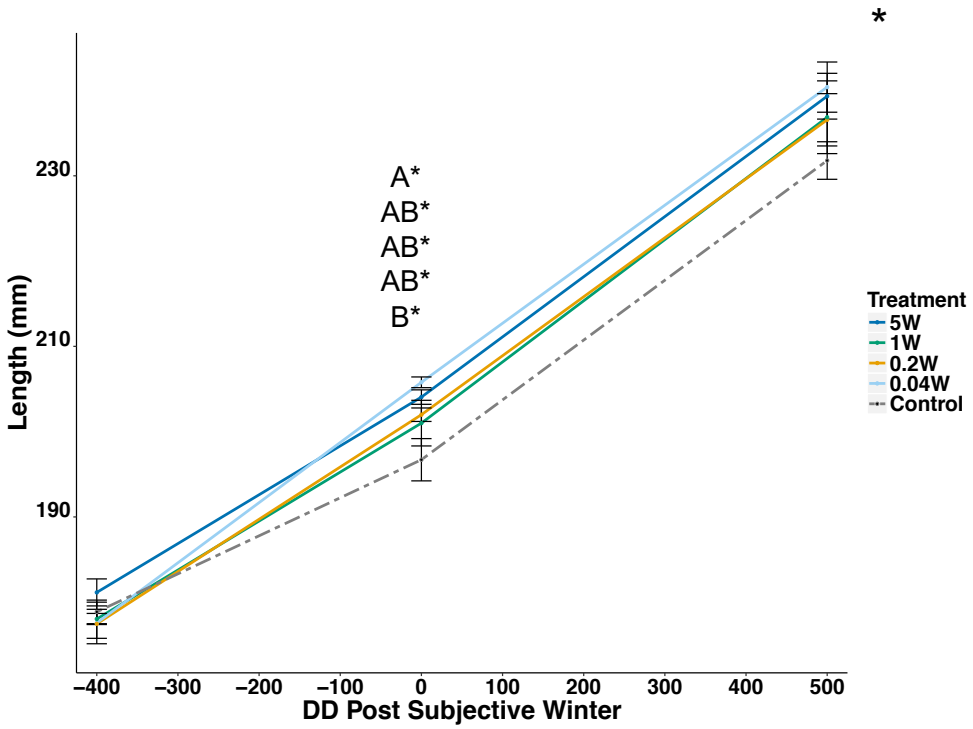

Figure 4.12. Change in length (Mean ± SEM, n = 3) of juvenile Atlantic salmon subjected to an out-of-season photoperiod regime whereby a subjective "winter" photoperiod (-400 to 0 ºdays) was provided by constant light (LL) at one of four intensities (5, 1, 0.2 and 0.04 W/m^2) in relation to a control population that received an LD12:12 photoperiod during the same period. Significant differences between treatments within time points where present are shown as upper case superscripts (Mixed-linear model, $p<0.05$), significant changes between time points are denoted by an asterisk.

Trial II – Condition Factor

No significant differences were seen in condition (K) factor at -400 ºdays (Fig. 4.13). K increased significantly between -400 and 0 ºdays in the control group. K in fish exposed to 5, 1, 0.2 and 0.04 W/m^2 did not increase significantly between -400 and 0 ºdays. At 0 ºdays both the control and 0.04 W/m^2 treatments had significantly higher K than the 5 W/m^2 and 1 W/m^2 groups. All treatments exhibited a significant decrease by 500 ºdays. At 500 ºdays, K was significantly lower in the 0.04 W/m^2 treatment than 5, 1 W/m^2 and control groups [all p-values <0.01].

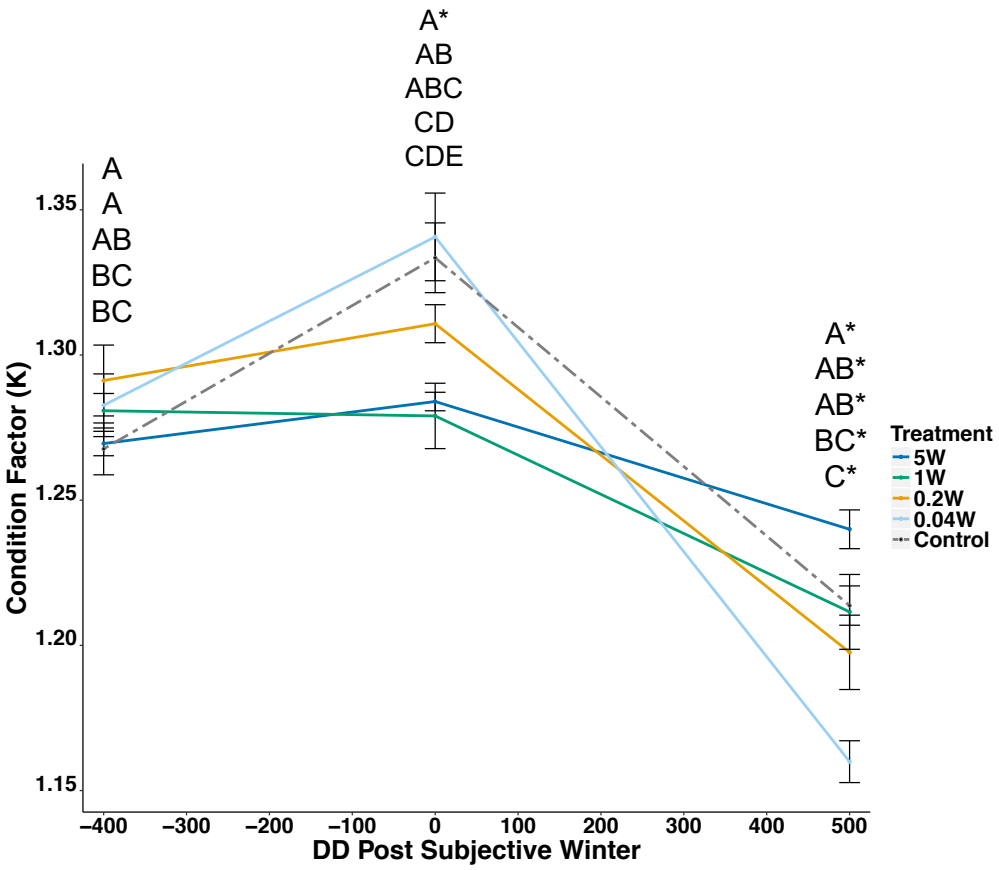

Figure 4.13. Change in condition factor (Mean ± SEM, n = 3) of juvenile Atlantic salmon subjected to an out-of-season photoperiod regime whereby a subjective "winter" photoperiod (-400 to 0ºdays) was provided by constant light (LL) at one of four intensities (5, 1, 0.2 and 0.04 W/m^2) in relation to a control population that received an LD12:12 photoperiod during the same period. Significant differences between treatments within time points where present are shown as upper case superscripts (Mixed-linear model, $p<0.05$), significant changes between time points are denoted by an asterisk.

Trial II – Weight During Smoltification

Weight increase in all fish sampled for NKAe between 0 and 500 ºdays were broadly comparable for all treatments (Fig. 4.14B-F). At 100ºDays the control group was significantly lower than the 5, 1 and 0.5 W/m^2 treatments (Fig. 4.14A).

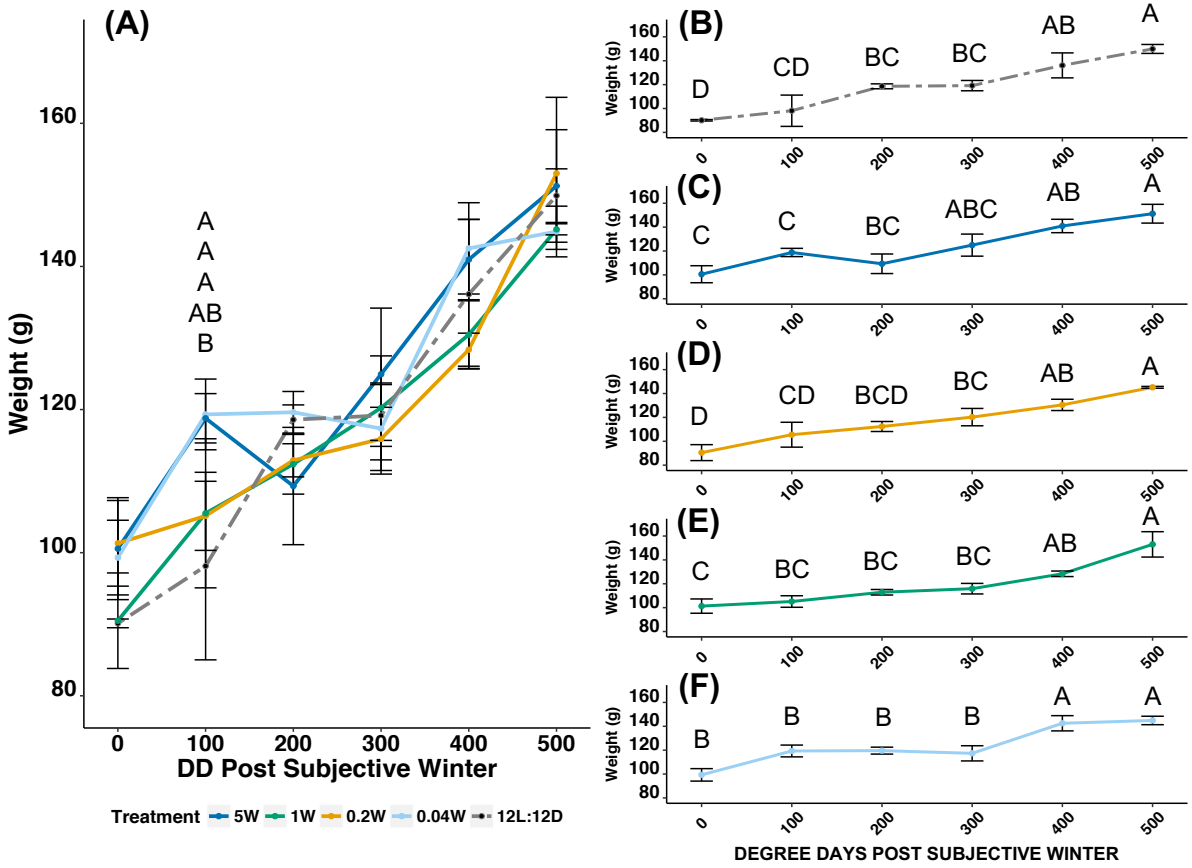

Figure 4.14. Change in weight (Mean ± SEM, n = 3) of juvenile Atlantic salmon sampled for NKA enzyme activity and subjected to an out-of-season photoperiod regime whereby a subjective "winter" photoperiod (-400 to 0 ºdays) was provided by constant light (LL) at one of four intensities (C-5, D-1, E-0.2 and F-0.04 W/m^2) in relation to a control population (B) that received an LD12:12 photoperiod during the same period. Significant differences between treatment where present are shown in **(A)**. Significant differences within treatment over time are shown in **(B) - (F)** (1-Way ANOVA, $p<0.05$).

Trial II - Condition Factor During Smoltification

Changes to condition factor varied depending upon the intensity of exposure during the subjective winter photoperiod (Fig. 4.15). Control K decreased throughout each sample point with a significant reduction between start and 300 ºdays and 300 to 500 ºdays (Fig. 4.15A). In contrast, no significant changes in K were observed throughout the sample points for fish exposed to either the 5 W/m^2 (Fig. 4.15B) or 1 W/m^2 (Fig. 4.15C). In both the 0.2 W/m^2 (Fig. 4.15D) and 0.04 W/m^2 (Fig. 4.15E), K was significantly lower after 200 ºdays compared to starting values. At 400 ºdays K of fish exposed to 5, 1, and 0.2 W/m^2 treatments was significantly higher than the 0.04 W/m^2. At 500 ºdays the control treatment was significantly lower than the 5 W/m^2 and 1 W/m^2 groups.

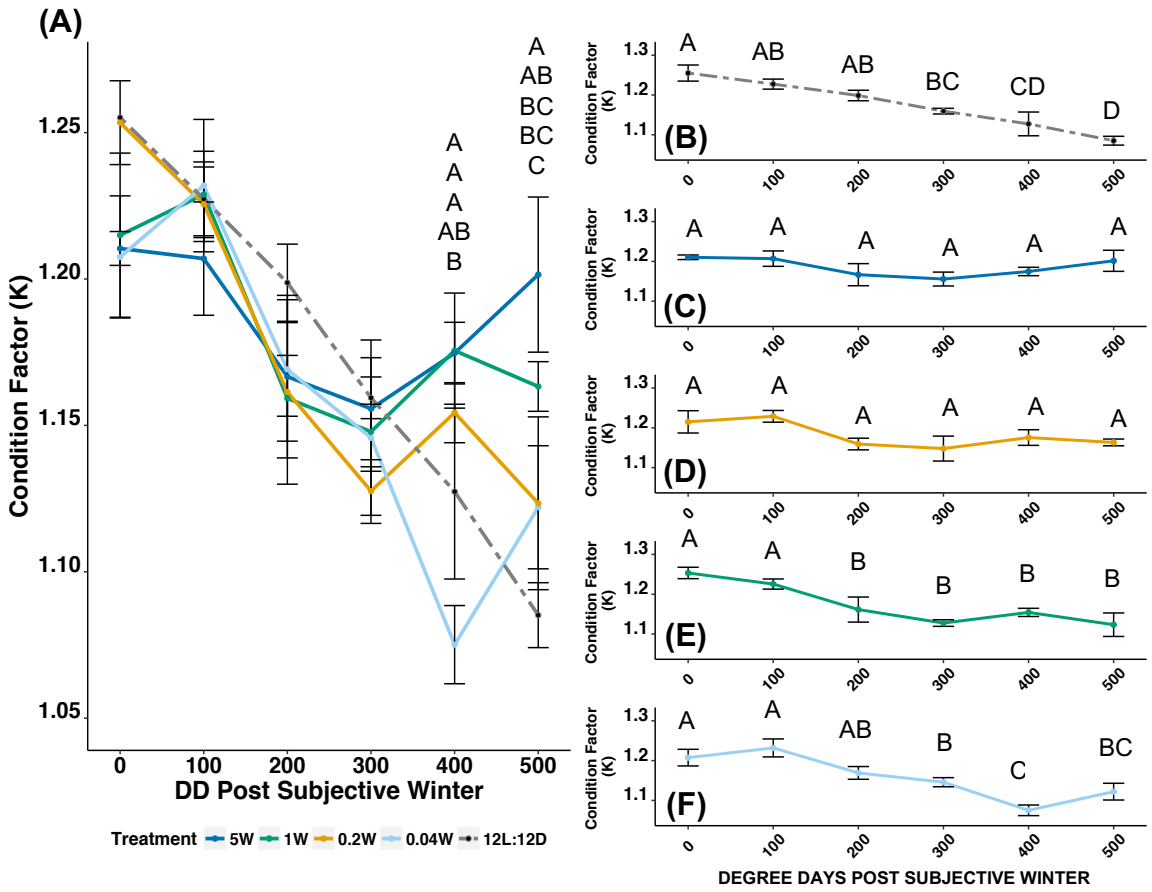

Figure 4.15. Change in condition factor (Mean ± SEM, n = 3) of juvenile Atlantic salmon sampled for NKA enzyme activity and subjected to an out-of-season photoperiod regime whereby a subjective "winter" photoperiod (-400 to 0ºdays) was provided by constant light (LL) at one of four intensities (C-5, D-1, E-0.2 and F-0.04 W/m^2) in relation to a control population (B) that received an LD12:12 photoperiod during the same period. Significant differences between treatment where present are shown in **(A)**. Significant differences within treatment over time are shown in **(B) - (F)** (1-Way ANOVA, $p<0.05$).

Trial II – NKA Activity

Gill NKAe Enzymatic reduction assay (NKAe)

At 0 ºdays both the control and 5 W/m^2 treatments were significantly lower than the 1 W/m^2. At 400 ºdays, NKAe in control fish was significantly higher than in the 0.04 W/m^2 treatment (Fig. 4.16A).

With the exception of the 0.2 W/m^2 treatment NKA activity showed a rise in all treatments between 0 and 500 ºDays. (Fig. 4.16A). Activity in fish exposed to the Control photoperiod increased significantly between 0 and 200 ºdays, increasing significantly at 300 and 400 ºdays (Fig. 4.16B). 500 ºdays NKAe activity did not change significantly from 400 ºdays. In fish exposed to 5 W/m^2, a significant increase in activity was seen between 0 and 300 ºdays with no further increase until the end of the trial (Fig. 4.16C). Fish exposed to 1 W/m^2 showed no significant increase throughout the trial duration (Fig. 4.16D). NKAe activity in response to 0.2 W/m^2 increased significantly between 0 and 400 ºdays (Fig. 4.16E) and exposure to 0.04 W/m^2 saw a significant increase from 0 to 500 ºdays (Fig. 4.16F).

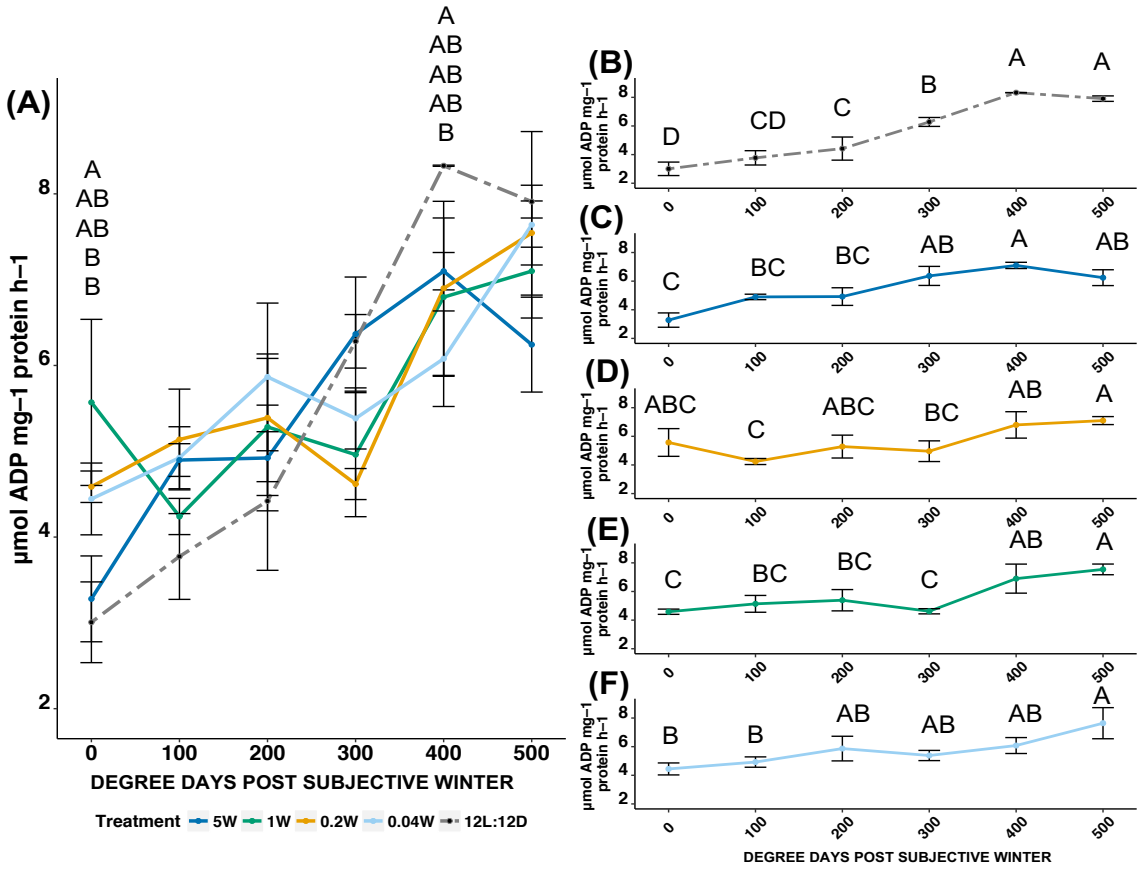

Figure 4.16. Change in NKA enzyme activity (Mean ± SEM, n = 3) of juvenile Atlantic salmon subjected to an out-of-season photoperiod regime whereby a subjective "winter" photoperiod (-400 to 0 ºdays) was provided by constant light (LL) at one of four intensities (B-5, C-1, D-0.2 and E-0.04 W/m^2) in relation to a control population (A) that received an LD12:12 photoperiod during the same period. Significant differences between treatment where present are shown in **(A)**. Significant differences within treatment over time are shown in **(B) - (F)** (1-Way ANOVA, $p<0.05$).

Trial II – NKAe Correlations

Under control (White) conditions and 0.04 W/m^2, NKAe correlated with decreasing condition factor (Table 4.3).

Table 4.3 Pearson correlations coefficients of NKAe and growth metrics juvenile Atlantic salmon subjected to an out-of-season photoperiod regime whereby a subjective "winter" photoperiod (-400 to 0 ºdays) was provided by constant light (LL) at one of four intensities (5, 1, 0.2 and 0.04 W/m^2) in relation to a control population that received an LD12:12 photoperiod during the same period.

		Control		**5 W/m^2**		**1 W/m^2**		**0.2 W/m^2**		**0.04 W/m^2**	
Metric	**Metric**	**Cor.**	**p-value**	**Cor.**	**p-value**	**Cor.**	**p-value**	**Cor.**	**p-value**	**Cor.**	**p-value**
BW	**FL**	0.96	<0.01	0.96	<0.01	0.97	<0.01	0.96	<0.01	0.96	<0.01
K	**NKAe**	**-0.06**	**<0.01**	-0.06	0.60	-0.14	0.21	-0.15	0.15	**-0.30**	**<0.04**

Trial II – Saltwater Challenge (SWC)

No mortality was observed in any group at any time point.

Trial II – Plasma Chlorides

A sharp reduction in plasma chloride values attained in the control group resulted in significant differences at 300 [p=0.015] and 400 ºdays [p=0.015] compared to the 5 W/m^2 treatment (Fig. 4.17A).

Plasma chloride concentrations decreased over time in all treatments (Fig. 4.17). By 500 ºdays, plasma chlorides of all treatment groups were significantly lower than their starting values (Fig. 4.17). The profile of the control group was markedly different in comparison to all other groups and decreased rapidly from 0 to 200 ºdays and did not increase significantly for the rest of the trial (Fig. 4.17B). Both the 1 (Fig. 4.17D) and 0.2 W/m^2 (Fig. 4.17E) groups were significantly lower at 400 ºdays than start values whereas this was not the case until 500 ºDays for the 5 and 0.4 W/m^2 treatments.

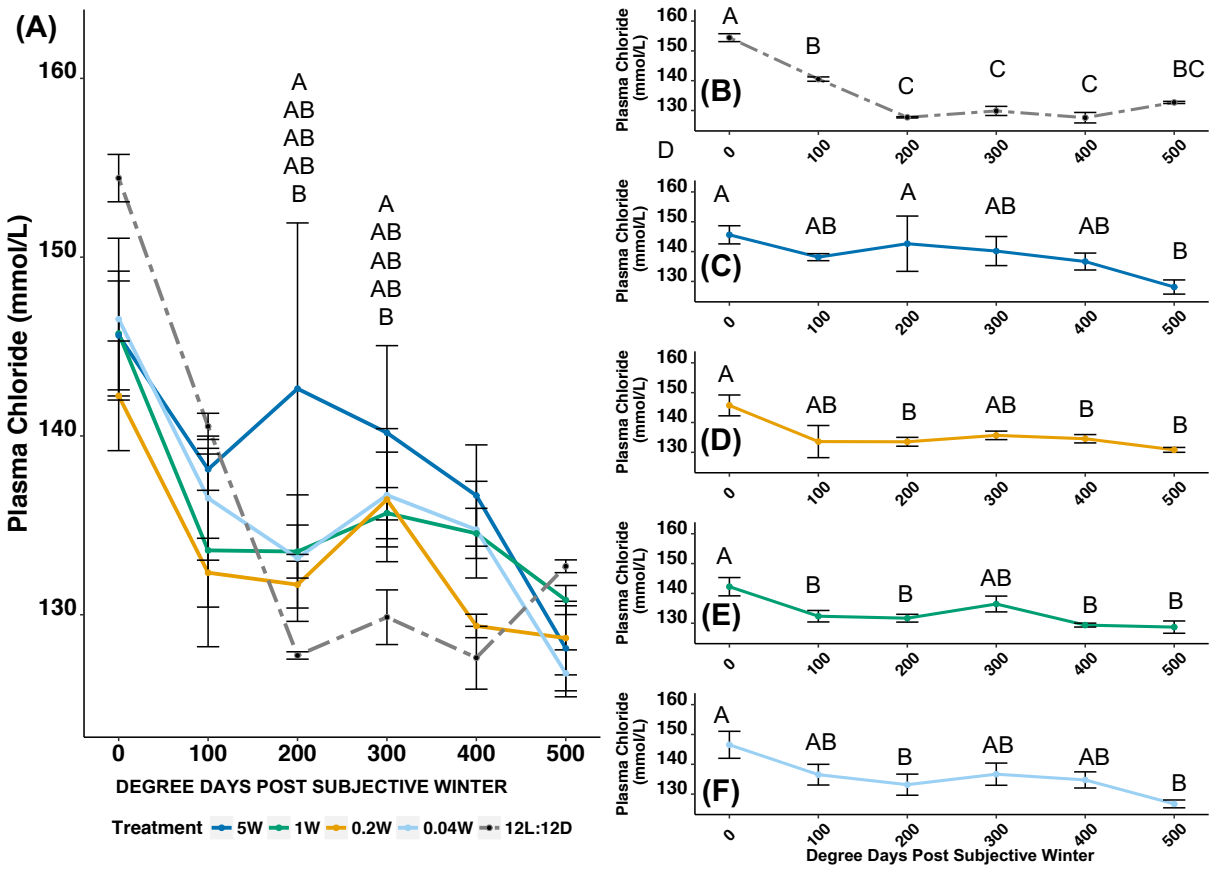

Figure 4.17. Change in plasma chloride concentration (Mean ± SEM, n = 3) of juvenile Atlantic salmon subjected to an out-of-season photoperiod regime whereby a subjective "winter" photoperiod (-400 to 0 ºdays) was provided by constant light (LL) at one of four intensities (B-5, C-1, D-0.2 and E-0.04 W/m^2) in relation to a control population (A) that received an LD12:12 photoperiod during the same period. Significant differences between treatment where present are shown in **(A)**. Significant differences within treatment over time are shown in **(B) - (F)** (1-Way ANOVA, $p<0.05$).

Trial II – Plasma Chloride Correlations

Significant negative correlation was observed in all treatments between BW or FL and plasma chloride (Table 4.4). The control treatment showed significant correlation between changes in K and plasma chloride concentrations and this was also evident in the 0.2 W/m^2 treatment.

Table 4.4 Pearson correlations coefficients of plasma chloride concentration and growth metrics juvenile Atlantic salmon subjected to an out-of-season photoperiod regime whereby a subjective "winter" photoperiod (-400 to 0 ºdays) was provided by constant light (LL) at one of four intensities (5, 1, 0.2, 0.04 W/m^2) in relation to a control population that received an LD12:12 photoperiod during the same period.

		Control		**5 W/m^2**		**1 W/m^2**		**0.2 W/m^2**		**0.04 W/m^2**	
Metric	**Metric**	**Cor.**	**p-value**	**Cor.**	**p-value**	**Cor.**	**p-value**	**Cor.**	**p-value**	**Cor.**	**p-value**
BW	**FL**	0.96	<0.01	0.96	<0.01	0.98	<0.01	0.97	<0.01	0.96	<0.01
BW	**Chloride**	-0.53	<0.01	-0.48	<0.01	-0.32	<0.01	-0.44	<0.01	-0.43	<0.01
FL	**Chloride**	-0.60	<0.01	-0.48	<0.01	-0.31	<0.01	-0.42	<0.01	-0.42	<0.01
K	**Chloride**	0.27	0.01	-0.02	0.87	0.15	0.17	0.24	0.03	0.06	0.60

4.4 Trial III – Assessing the Impact of Replacing the Scotophase of an S0+ Regime with Continuous Light of Reduced Intensity

4.4.1 Trial III - Materials and Methods

Fish Stock and Husbandry

Fry to Parr

Fry to Parr development occurred under conditions reported in **chapter 3 – Trial II**.

Parr to Smolt

On the 6th of October 2015, parr exposed to different narrow spectrum light under LL, as previously described, had reached a suitable size for S0+ induction (population mean weight of 43.5 g ± 9.0). From a population of ~220 per tank, 150 fish were randomly netted and retained. To assess the impact of FW history on post-SW transfer growth 85 fish were selected for future transfer to SW. These fish were vaccinated with 0.05 ml (Alphaject Micro 6, Pharmaq, UK) and PIT tagged (Trovan, USA) and the adipose fin removed as per chapter 2.4.2. No grading was carried out in order to preserve the population structure of fast and slow growing individuals.

Experimental Design, Sampling and Light Regimes

The trial consisted of triplicated tanks (150 fish / tank). Tank were illuminated using either Blue (444 nm peak), Green (523 nm peak), Red (632 nm peak) and White LED as per chapter 2.2.1. Following a recovery period of 6 days post-vaccination, light intensity was gradually increased from 0.1 to 5 w/m^2 over a period of seven days (Day 1 at 0.1 w/m^2, Day 2 at 0.2 w/m^2, Day 3 at 0.4 w/m^2, Day 4 at 0.8 w/m^2, day 5 at 1.6 w/m^2, day 6 at 3.2 w/m^2, day 7 at 5 w/m^2) until the light intensity under 1 cm of water in the centre of each tank reached 5.0 w/m^2. All tanks were acclimated to 5 W/m^2 for 175 ºdays prior to application of the experimental photoperiod regimes.

The photoperiod using to induce out-of-season smoltification replaced the scotophase of short day (SD) with a reduced intensity of the same narrow bandwidth (Fig. 4.18). Pre-SD (-575 to -400 ºDays) all tanks were exposed to LL at 5 W/m^2. During SD (-400 to 0 ºDays) a 12:12 photoperiod was used and Blue, Green and Red treatments were exposed to 5 W/m^2 during the day and 0.05 W/m^2 during the

subjective night. Post-SD (0 to 1000 ºDays) all tanks were exposed to LL at 5 W/m^2. The night period in the Control White tanks was a true dark period. The intensity used for the subjective night (0.05 W/m^2) was selected based upon the results from Trial II which showed fish exposed to the lowest intensity (0.04 W/m^2) exhibited several characteristic changes associated with smoltification. The difference is explained by technical limitations when normalising across spectra to the same intensity.

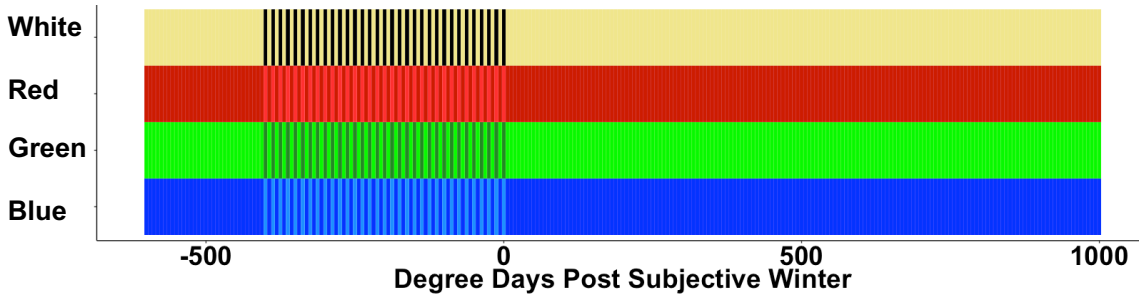

Figure 4.18. Photoperiod regime for out-of-season smoltification replacing the scotophase of short day (SD) with continuous light of reduced intensity. Pre-SD (-575 to -400 ºDays) all tanks were exposed to LL at 5 W/m^2. During SD (-400 to 0 ºDays) a 12:12 photoperiod was used and Blue, Green and Red treatments were exposed to 5 W/m^2 during the day and 0.05 W/m^2 during the 'night'. Post-SD (0 to 1000 ºDays) all tanks were exposed to LL at 5 W/m^2. Control White tanks were exposed to a true dark night period during short day.

Following smoltification which was verified in house using gill Na+,K+,ATPase activity, PIT tagged fish, ~85 per tank with a mean weight of 155 ± 8 g, were transferred to the Marine Environmental Research Laboratory (MERL), Machrihanish, Scotland (55°N, 6°W) for on-growing in seawater under fluorescent white lighting provided at 1 w/m2 in the tank centre below the water surface using a Philips Master PL-S 9W/840/2P 1CT (Philips, Eindhoven, NL) compact fluorescent lamp rated at 9W as described in chapter 2.2.2. A summary of light conditions for each group is found in Table 4.5.

Table 4.5. Photic conditions for fish in trial III. For the duration of the trial the initial spectrum assigned was maintained.

Post SD Light Regime				
	DD	Colour	Photophase Intensity	Scotophase Intensity
Long Term FW Group	1000	Blue	5 W/m^2	5 W/m^2
	1000	Green	5 W/m^2	5 W/m^2
	1000	Red	5 W/m^2	5 W/m^2
	1000	White	5 W/m^2	5 W/m^2
PIT Tagged LL Fish	400FW 240SW	White (LED) White (CFL)	1 W/m^2	0 W/m^2
PIT Tagged SNP Group	400FW 240SW	White (LED) White (CFL)	1 W/m^2	1 W/m^2

Each replicate was randomly divided in half and assigned either a simulated natural photoperiod or LL. After a period of 240 ºdays (4 weeks) post-transfer, 5 fish per replicate (n=3) from each FW colour treatment were removed and sampled for gill Na+,K+,ATPase activity and NKA gene expression. All remaining fish had their length and weight recorded for assessment of post-transfer growth performance.

Non-tagged fish were retained in FW under LL conditions for an additional 600 ºdays (total of 1000 ºdays post SD application) to examine the duration of the smolt window.

At the start of SD, a fish loss (27 fish) occurred due a failure of the standpipe in Red replicate 1 which resulted in reduced numbers available for smolt window NKA enzyme and PCR assessment so these values were omitted from 700, 900 and 1000 ºdays data points.

Population Data and Smoltification Assessment

Two distinct datasets were recorded during this trial for population performance and smoltification progression

Population Metrics

The PIT tag fish data was used to assess the population as a whole. At -400, 0 and 400 ºdays tagged individuals were removed, briefly anesthetised in 50 ppm buffered tricaine methanesulphonate and the BW (± 1 g) and FL (± 0.1 cm) was recorded as per chapter 2.4.4.

Smoltification Assessment

A random sample of 5 untagged fish per tank (n=3) was removed at -400, -100, 0, 100, 200, 300, 400, 500, 600, 700, 800, 900 and 1000 ºdays post SD and terminally sampled for gill NKA enzyme activity analysis and NKA qPCR analysis.

From the second gill arch, 6-9 gill filament tips were removed centrally, divided in half and each half stored in chilled SEI buffer or RNA stabilisation solution. NKA enzyme samples were immediately snap frozen in liquid nitrogen in a dry shipper before being stored at -70 °C for future analysis (McCormick 1993). RNA samples were stored at 4 ºC for 48 hours and stored at -24 ºC for future qPCR analysis.

NKA enzyme and NKA qPCR assessment of gill NKA was conducted as described in chapter 2.4.5. Due to facility restraints, no SWC assessment was conducted.

Muscle Fibre Distributions

At SW transfer 3 fish from each replicate were selected at random those sampled for NKAe, and NKA qPCR for muscle fibre analysis. A fillet was removed from the truncal region, anterior to the dorsal fin and data was analysed according to Johnston et al. (1999) as described in chapter 2.4.10.

Trial III - Statistics

BW and FL were used to calculate Fulton's condition factor (K) as described in 2.6.3. Start and end weight and ºDays were used to calculate Thermal growth coefficient as described in chapter 2.5.

Population Body Weight and Condition Factor

All statistical tests were performed using R Studio (R Core Team 2016). Normality was tested using a Shapiro-Wilk test as described in chapter 2.5 and homogeneity of variance was tested using Levene's test.

Data was assessed using an additive linear mixed effect model (LME) (Pinheiro et al., 2016) model to identify the interaction of time and treatment. The model uses restricted maximum likelihood to account for unequal sample size whereby a series of contrasts are calculated from the original dataset, contrasts provide the probability distribution with which the maximum likelihood function is calculated. The natural logarithm of body weight was used as the dependant variable and colour and replicate were nested as random factors within the treatments, time was added as a continuous variable and variance owing to time was model using a first order autoregressive function (Ar01). This approach models individual fish variability to fully account for the data structure and allows the use of an unbalanced design owing to mortality throughout the trial (Thorarensen et al., 2015). Condition factor was modelled using the same approach but without transforming the data.

An additive approach was used to determine best fit, firstly a straight line was applied to the data, this was proceeded by adding random intercepts and slopes for each variable and comparing results using an ANOVA until a significant improvement in fit was not attained. At this stage, the simplest number of model additions was used. In all models, random intercepts and slopes were used as this provided the best fit. Determination of the F-test calculated by the model uses the Kenward-Rogers modification of F-tests which adjusts F-value and degrees of freedom depending on the size of the tank effect, thus when tank variation is low then the statistical power is increased (Thorarensen et al., 2015). Post-hoc comparisons were then performed using least-square means and Tukeys-HSD to determine significant comparisons.

Comparisons of NKA-Body Weight, NKA- Condition factor, NKAe and Plasma Chlorides

Data was compared using a one-way ANOVA comparing the natural logarithm of BW and untransformed K, NKAe and Plasma Chloride. Progression through time was compared across time points using a single treatment. Comparison of treatments at individual time points was tested using a one-way ANOVA. In Trial III NKAα1a and NKAα1b were arcsine transformed prior to analysis with a one-way ANOVA.

qPCR Data Analysis

qPCR data was analysed using a modified version the $2^{-\Delta\Delta Ct}$ method as described by Livak and Schmittgen 2001. This method was supplemented by adjusting for slope

efficiency for each cycle of PCR (Pfaffl 2001) to normalise intra-assay variation. Analysis of each gene required 3X 384 plates, internal controls were run on plate one and two and plate values normalised against the mean values of controls. Plate three had repeated analysis of White -100 to 800 ºDays and for these values the mean was calculated and data corrected against the correction factor derived from these values. The mean of the White run 1 and run 2 were then used for the data analysis. Data is presented relative to the -400 ºdays White sample as a calibrator and β-actin was used as an internal control.

Correlations

Correlations were performed using Pearson correlations coefficient to measure the linearity between variables X and Y as both X and Y were measured (chapter 2.5). A value of -1 or +1 signify a strong relationship whereas a value of 0 shows no such relationship. The test values (r) are then compared against a Gaussian distribution to determine the reported P-value.

4.4.2 Trial III – Results

Results With the exception of the accidental fish loss in Red replicate 1, there was no mortality during the trial.

Trial III – Population Growth and Development

Trial III – Body Weight

All treatments increased significantly in weight over time (Fig. 4.19). Weights at -400 ºdays were significantly different between fish under White and Green light treatments [p=<0.001]. At 0 ºdays, fish exposed to Blue was significantly heavier than fish exposed to Green and Red treatments [p=<0.001]. At 400 ºdays Blue treatments were still significantly heavier than those under Red [p=<0.001].

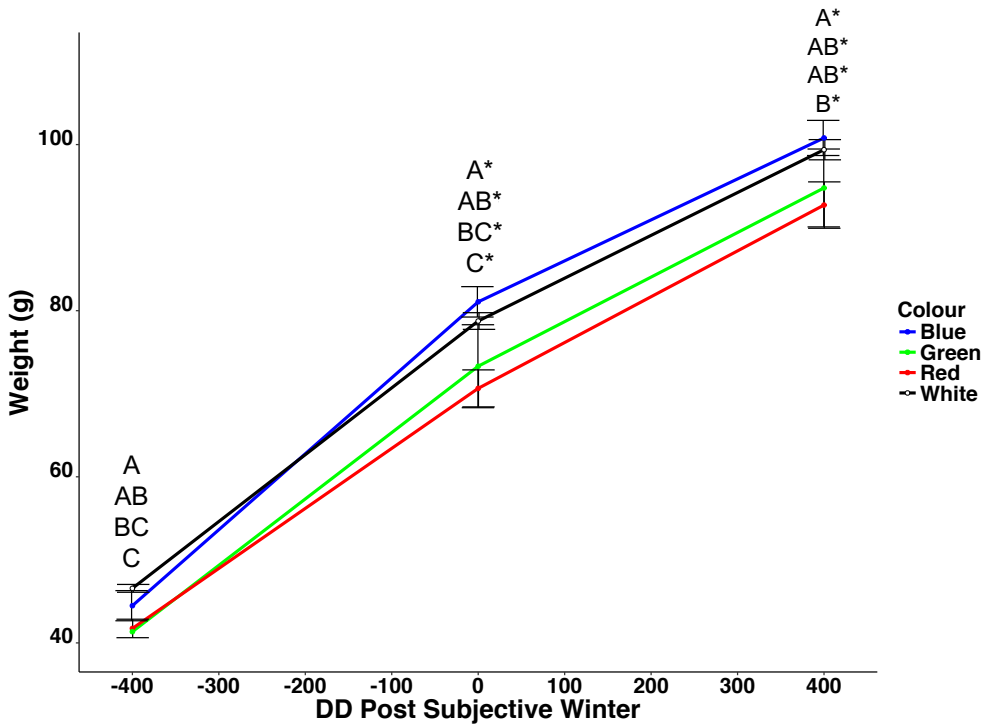

Figure 4.19. Weight increase (Mean ± SEM, n = 3) of PIT tagged juvenile Atlantic salmon (85 fish /tank) subjected to an out-of-season photoperiod regime whereby a subjective "winter" photoperiod (-400 to 0 ºdays) was provided by replacing the scotophase with a reduced intensity from the photophase for the Blue, Green and Red treatments (5 W/m^2 daytime and 0.05 W/m^2 nigh time) in relation to a control population that received an LD12:12 photoperiod during the same period. Significant differences between treatments within time points where present are shown as upper case superscripts (Mixed-linear model, $p<0.05$), significant changes between time points are denoted by an asterisk.

Trial III – Fork Length

Fork length increased significantly over time (Fig. 4.20). At -400 ºdays, fish exposed to White were significantly longer than those exposed to Green light [p=<0.001]. At 0 ºdays fish under both Blue and White lights were significantly longer than those exposed to Red. Fish under Blue where was also significantly longer than those under Green. At 400 ºdays both fish exposed to Blue and White where significantly longer than those exposed to Red light and again fish under Blue light was significantly longer than those under Green treatment [all p values <0.001].

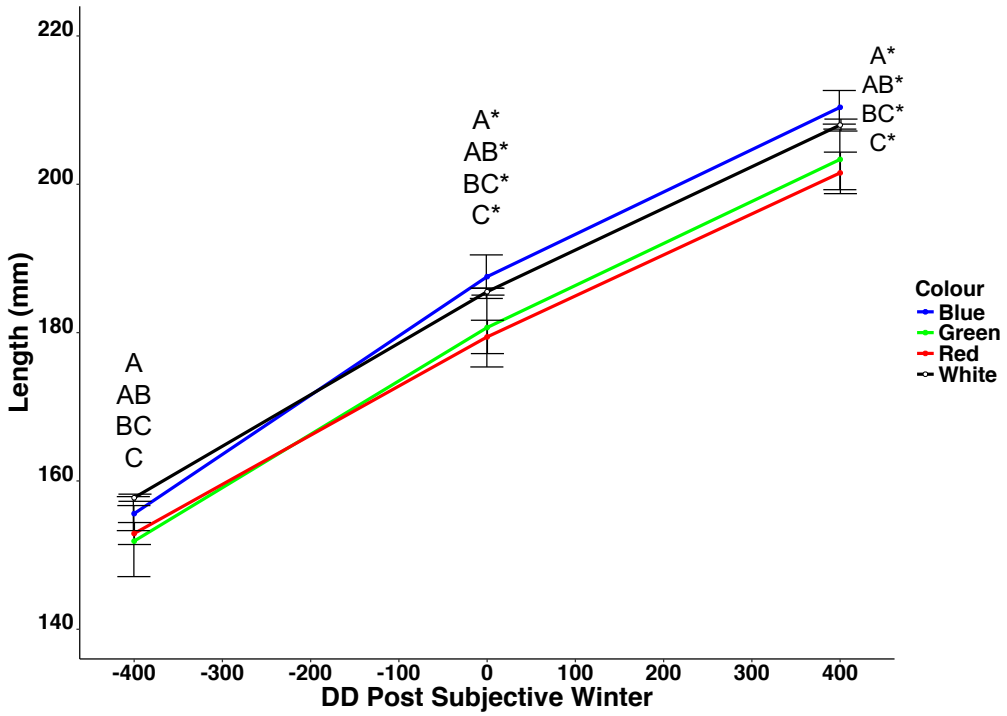

Figure 4.20. Length increase (Mean ± SEM, n = 3) of PIT tagged juvenile Atlantic salmon (85 fish / tank) subjected to an out-of-season photoperiod regime whereby a subjective "winter" photoperiod (-400 to 0ºdays) was provided by replacing the scotophase with a reduced intensity from the photophase for the Blue, Green and Red treatments (5 W/m^2 daytime and 0.05 W/m^2 nigh time) in relation to a control population that received an LD12:12 photoperiod during the same period. Significant differences between treatments within time points where present are shown as upper case superscripts (Mixed-linear model, $p<0.05$), significant changes between time points are denoted by an asterisk.

Trial III – Condition Factor

No significant differences were seen between treatments at -400 and 0 ºdays. At 400 ºdays fish exposed to both the Red and Green treatments had significantly higher K than those exposed to the White and Blue treatments (Fig. 4.21) [p-values <0.001]

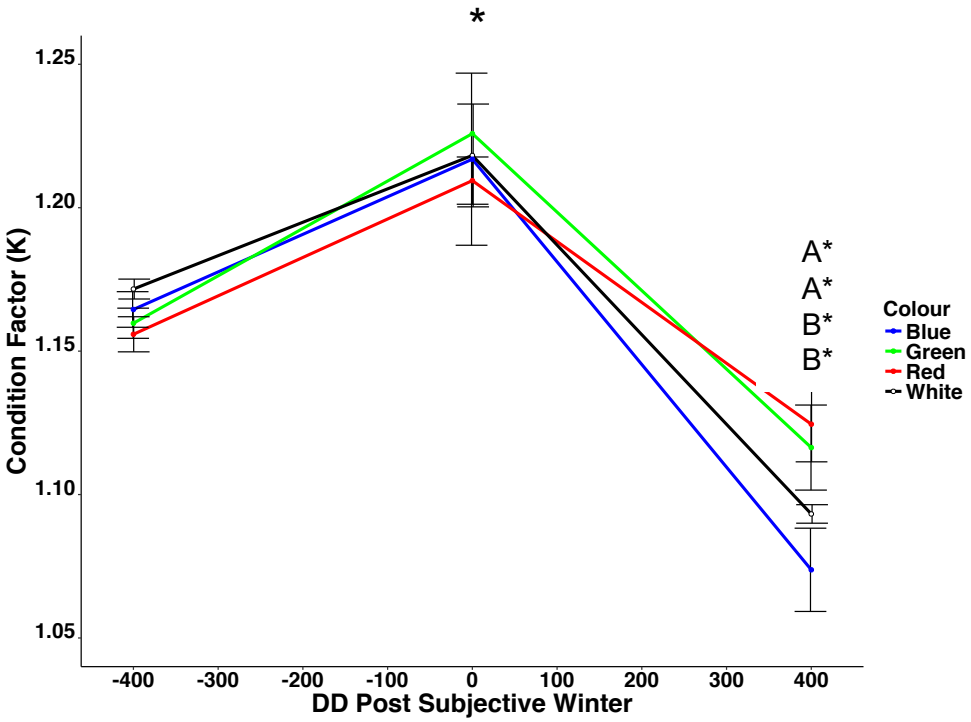

Figure 4.21. Condition factor (K) changes (Mean ± SEM, n = 3) of PIT tagged juvenile Atlantic salmon (85 fish /tank) subjected to an out-of-season photoperiod regime whereby a subjective "winter" photoperiod (-400 to 0 ºdays) was provided by replacing the scotophase with a reduced intensity from the photophase for the Blue, Green and Red treatments (5 W/m^2 daytime and 0.05 W/m^2 nigh time) in relation to a control population that received an LD12:12 photoperiod during the same period. Significant differences between treatments within time points where present are shown as upper case superscripts (Mixed-linear model, $p<0.05$), significant changes between time points are denoted by an asterisk.

Trial III –Thermal Growth Coefficient

TGC in fish under the Blue treatment was significantly higher between -400 and 0 ºdays than all other treatments [p values = <0.001]. In addition, TGC of fish under Green was also significantly higher than Red but not White. From 0 to 400 ºdays, fish under both the Green and Red treatments had significantly higher TGC than under Blue [G-B p=<0.001; R-B p=<0.001] and White treatments [G-W p=0.001; R-W p=0.001] (Fig. 2.22).

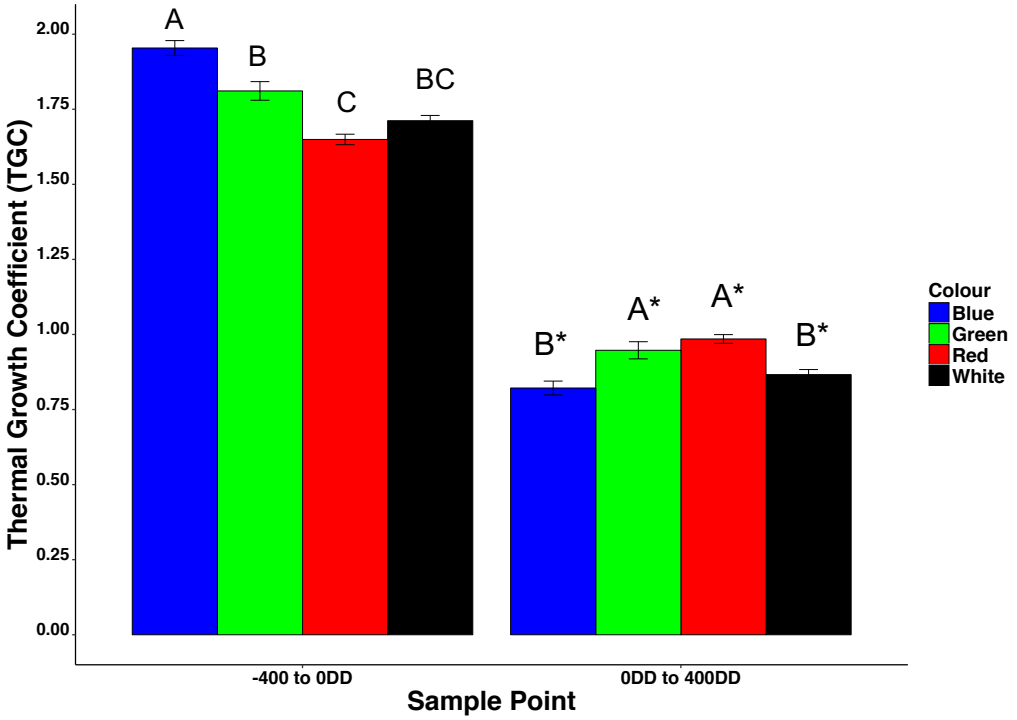

Figure 4.22. Thermal Growth Coefficient (TGC) (Mean ± SEM, n = 3) of PIT tagged juvenile Atlantic salmon (85 fish / tank) subjected to an out-of-season photoperiod regime whereby a subjective "winter" photoperiod (-400 to 0 ºdays) was provided by replacing the scotophase with a reduced intensity from the photophase for the Blue, Green and Red treatments (5 W/m^2 daytime and 0.05 W/m^2 nigh time) in relation to a control population that received an LD12:12 photoperiod during the same period. Coloured bars reflect colour of exposure during the whole trial. Significant differences between treatments within time points where present are shown as upper case superscripts (Mixed-linear model, $p<0.05$), significant changes between time points are denoted by an asterisk.

Trial III – Weight During Smoltification

Weight in all treatment groups increased significantly over time. Between treatment comparisons showed that the control was significantly heavier than the Green at -100 ºdays [p=0.026] and 300 ºdays [p=0.026]. At 500 ºdays weights recorded from the Blue treatment were significantly heavier than the Green. At 1000 ºdays White treatment was statistically heavier than all other treatments [W-B p=0.003; W-G p=0.003; W-R p= 0.008] however this may be due to sampling error.

Growth under the control photoperiod increased significantly from -400 to 0 ºdays (Fig. 4.23A). From 0 to 400 ºdays weight did not change significantly. A significant increase in weight was seen between 400 and 800 ºdays and between 800 and 1000 ºdays. In fish exposed to Blue light, weights increased significantly between -400 and 0 ºdays but not between 0 and 400 ºdays, a further 400 ºdays saw a significant increase in weight (Fig. 4.23B). In fish exposed to Green light, weight increased significantly between -400 and 0 ºdays, between 0 and 600 ºdays and 600 to 800 ºdays (Fig. 4.23C). In the Red treatment, fish weigh increased significantly between -400 and 0 ºdays with significant increases in weight also evident at 600 and at 900 ºdays (Fig. 4.23D).

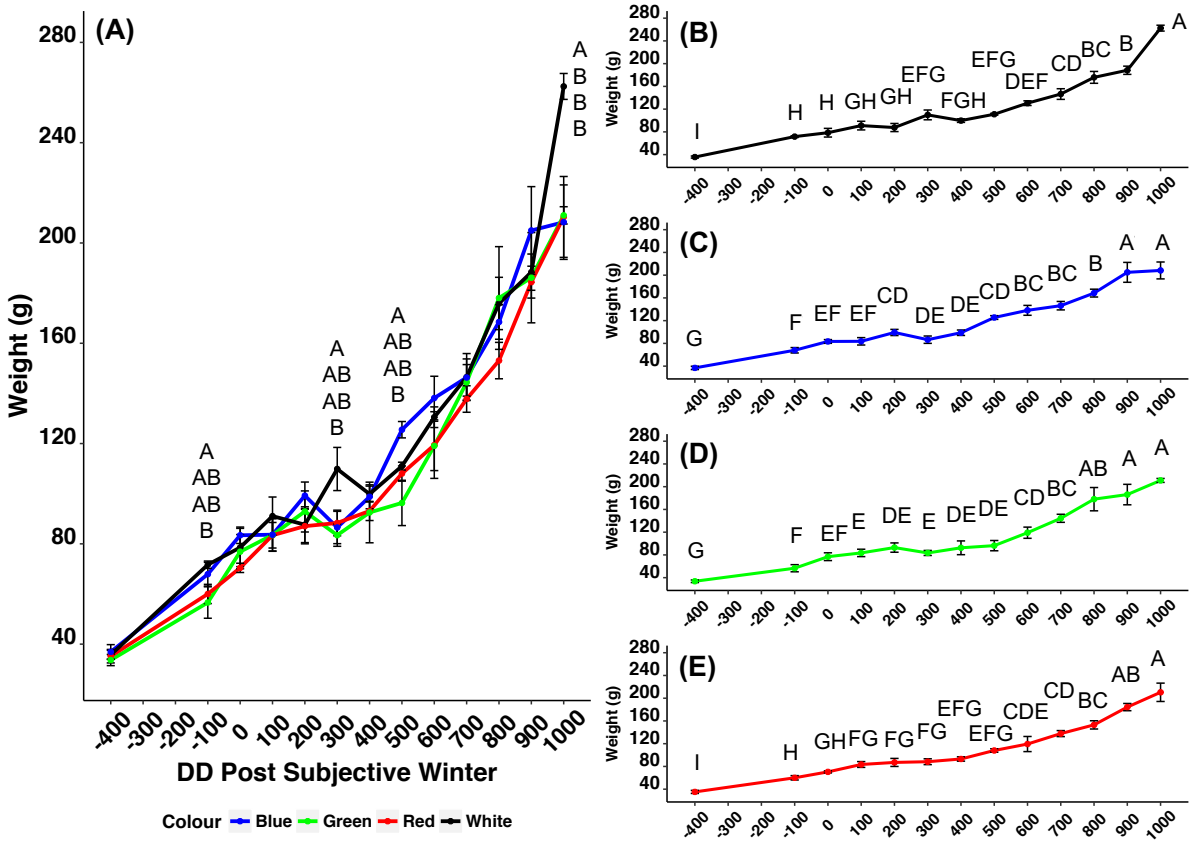

Figure 4.23. Weight increase (Mean ± SEM, n = 3) of juvenile Atlantic salmon sampled for NKA enzyme activity and subjected to an out-of-season photoperiod regime whereby a subjective "winter" photoperiod (-400 to 0 ºdays) was provided by replacing the scotophase with a reduced intensity from the photophase for the Blue, Green and Red treatments (5 W/m^2 daytime and 0.05 W/m^2 nigh time) in relation to a control population that received an LD12:12 photoperiod during the same period. Significant differences between treatment where present are shown in **(A)**. Significant differences within treatment over time are shown in **(B) - (E)** (1-Way ANOVA, $p<0.05$).

Trial III – Length During Smoltification

All treatments increased significantly in length over time. Significant differences between White and Red groups were apparent at -100 and 300 ºdays as in the weight data. Blue groups were significantly longer than the Green at 500 ºdays and the Red at 600 ºdays (Fig. 4.24A).

Fish exposed to the control photoperiod experienced a significant increase in length from -400 to 0 ºdays, 0 to 400 ºdays, 400 to 800 ºdays and 800 to 1000 ºdays (Fig. 4.24B). Under Blue light, length increased significantly from -400 to 0 ºdays, 0 to 400 ºdays, and 400 to 800 ºdays (Fig. 4.24C). In response to Green light similar changes as seen in Blue were observed with no significant increase between 800 and 1000 ºdays (Fig. 4.24D). Red light again led to significant increases from -400 to 0 ºdays, 0 to 400 ºdays, 400 to 800 ºdays and 800 to 1000 ºdays (Fig. 4.24E).

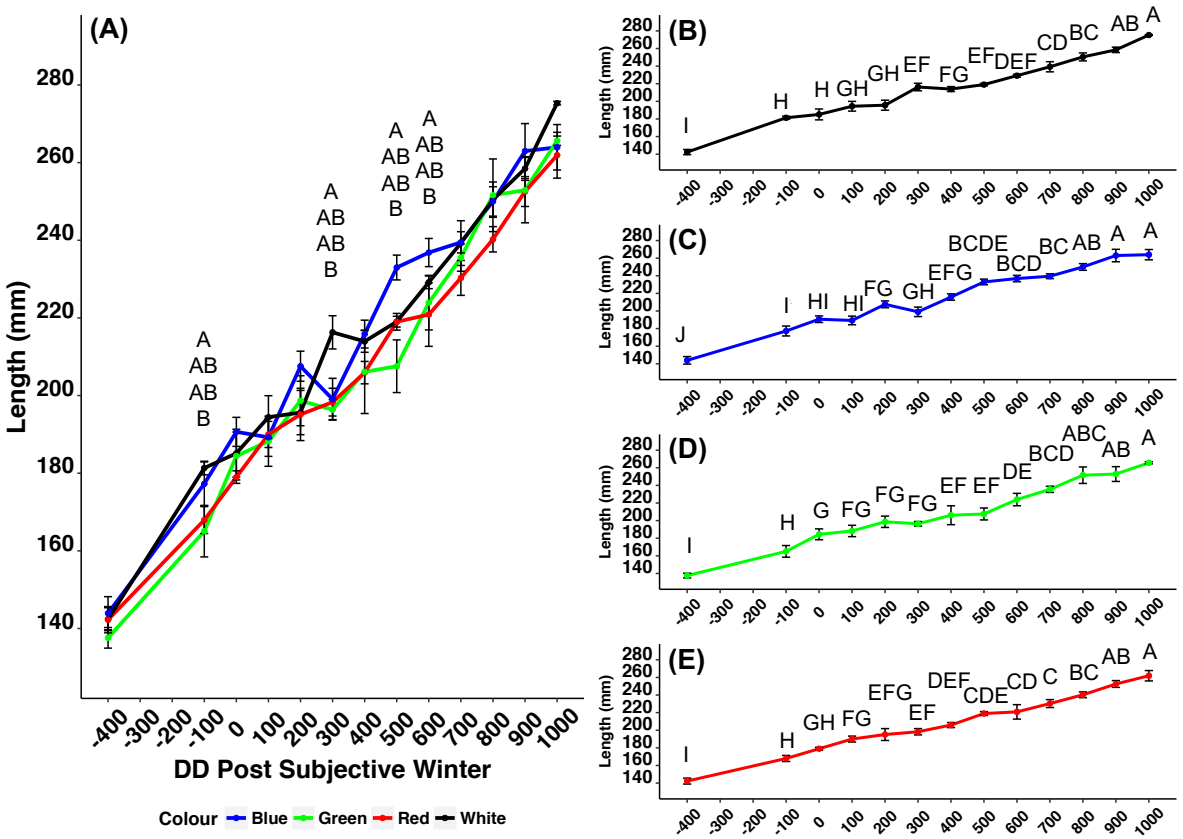

Figure 4.24. Length increase (Mean ± SEM, n = 3) of juvenile Atlantic salmon sampled for NKA enzyme activity and subjected to an out-of-season photoperiod regime whereby a subjective "winter" photoperiod (-400 to 0 ºdays) was provided by replacing the scotophase with a reduced intensity from the photophase for the Blue, Green and Red treatments (5 W/m^2 daytime and 0.05 W/m^2 nigh time) in relation to a control population that received an LD12:12 photoperiod during the same period. Significant differences between treatment where present are shown in **(A)**. Significant differences within treatment over time are shown in **(B) - (E)** (1-Way ANOVA, $p<0.05$).

Trial III – Condition Factor During Smoltification

Between -400DD and 0 ºDays no significant decrease in condition factor was observed under any light conditions. From 0 ºDays to 400 ºDays all treatments exhibited a significant decrease in K. Under control White photoperiod (Fig. 4.25B) K did not change significantly until 1000 ºDays. Condition factor under Blue light (Fig. 4.25C) was maintained from 400DD to 600 ºDays and was significantly higher by the 1000 ºDays. From 400 ºDays until the trial termination no significant change in condition factor K was observed under Green light (Fig. 4.25D). K in response to Red light (Fig. 4.25E) remained significantly similar until 1000 ºDays.

K in fish exposed to Blue light was significantly lower than the Red and Green treatments at 400DD and significantly lower than Green at 500DD and Red at 600DD (Fig. 4.25A). Final K under White light was significantly higher than the Blue, Green and Red treatments.

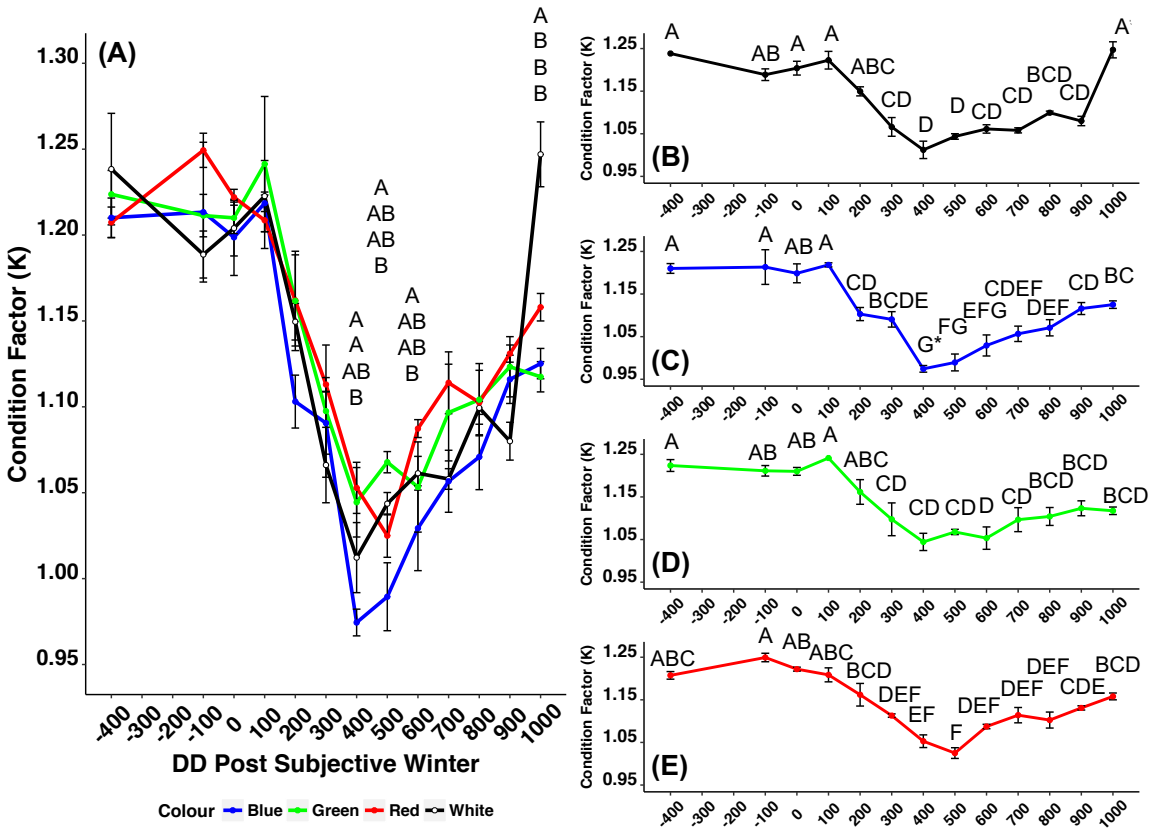

Figure 4.25. Changes in to condition factor (K) (Mean ± SEM, n = 3) of juvenile Atlantic salmon sampled for NKA enzyme activity and subjected to an out-of-season photoperiod regime whereby a subjective "winter" photoperiod (-400 to 0 ºdays) was provided by replacing the scotophase with a reduced intensity from the photophase for the Blue, Green and Red treatments (5 W/m^2 daytime and 0.05 W/m^2 nigh time) in relation to a control population that received an LD12:12 photoperiod during the same period. Significant differences between treatment where present are shown in **(A)**. Significant differences within treatment over time are shown in **(B) - (E)** (1-Way ANOVA, $p<0.05$).

Trial III –NKA Activity

Trial III- Gill NKAe Enzymatic Reduction Assay - Freshwater

At 0 ºdays, NKAe in fish under Blue light was significantly higher than those under either the White, Green or Red treatments (Fig. 4.26A). At 200 ºdays exposure to Blue treatment led to significantly higher NKAe activity than in the White treatment. Peak NKAe for all groups was achieved at 400-500 ºdays.

NKA enzyme activity (NKAe) in fish exposed to control (White) photoperiod decreased significantly between -100 and 100 ºdays (Fig. 4.26B). A significant increase was observed between 100 and 300 ºdays and no significant decrease was apparent until 1000 ºdays. In fish under Blue light NKAe increased significantly between -400 and 200 ºdays but no significant decrease was evident until 900 ºdays (Fig. 4.26C). Exposure to Green light showed a significant increase in NKAe from -400 to 100 ºdays and did not decrease significantly until 900 ºdays (Fig. 4.26D). NKAe activity in fish under Red increased significantly from -400 to 300 ºdays and decreased significantly by 900 ºdays (Fig. 4.26E). In all groups 1000 ºdays NKAe values were significantly similar to starting NKAe values.

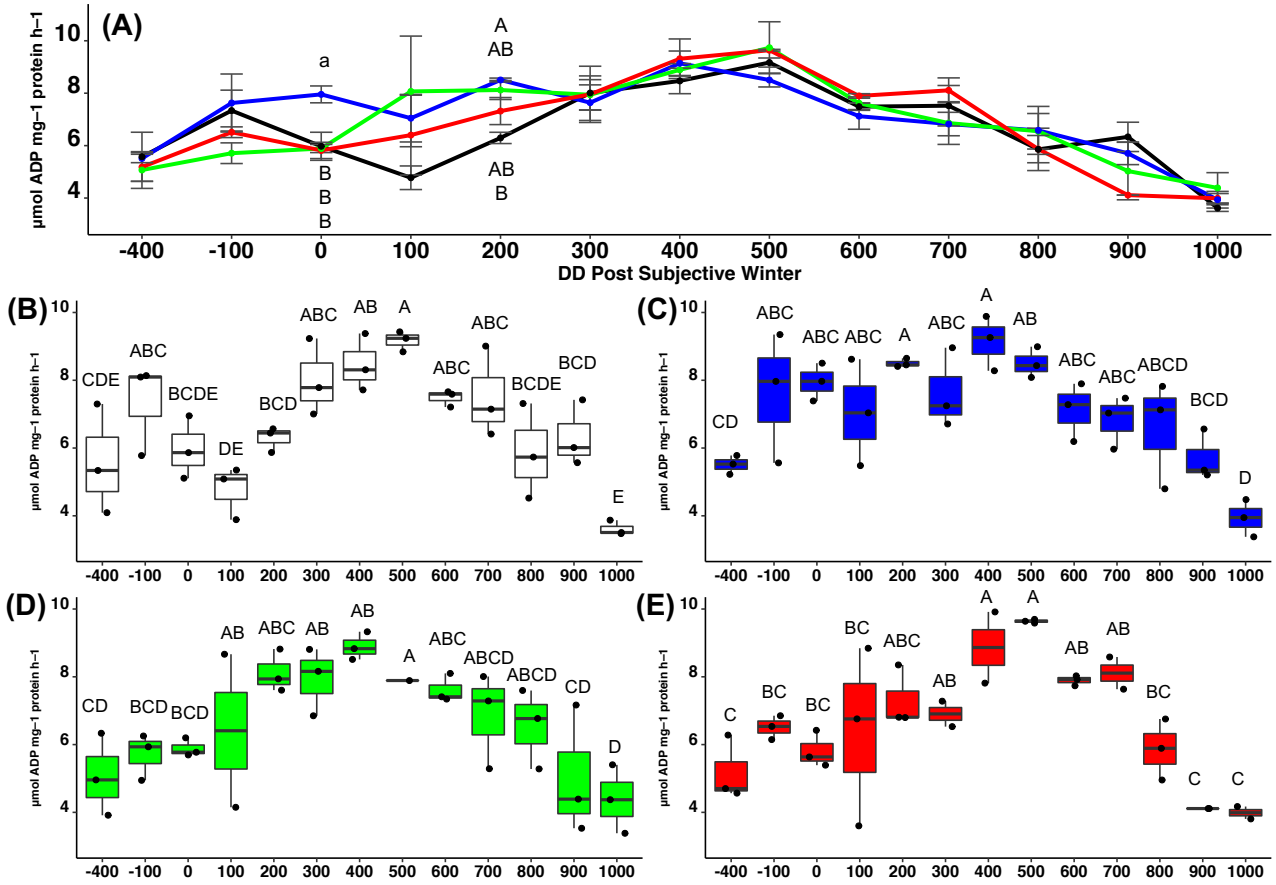

Figure 4.26. NKA enzyme activity (Mean ± SEM, n = 3) of juvenile Atlantic salmon (5 fish / tank) subjected to an out-of-season photoperiod regime whereby a subjective "winter" photoperiod (-400 to 0 ºdays) was provided by replacing the scotophase with a reduced intensity from the photophase for the Blue, Green and Red treatments (5 W/m^2 daytime and 0.05 W/m^2 nigh time) in relation to a control population that received an LD12:12 photoperiod during the same period. Significant differences between treatment where present are shown in **(A)**. Significant differences within treatment over time are shown in **(B) - (E)** (1-Way ANOVA, $p<0.05$).

Trial III - Gill NKAe Enzymatic Reduction Assay - Post Seawater Transfer

NKAe activity in fish exposed to a simulated natural photoperiod (SNP) post-SW transfer was maintained in fish previously exposed to the control (White) photoperiod and Green treatment (Fig. 4.27A). NKAe activity decreased significantly in fish exposed to Blue and Red treatments previously during freshwater. No significant change in NKAe was observed in fish transferred to LL for any group (Fig. 4.27B).

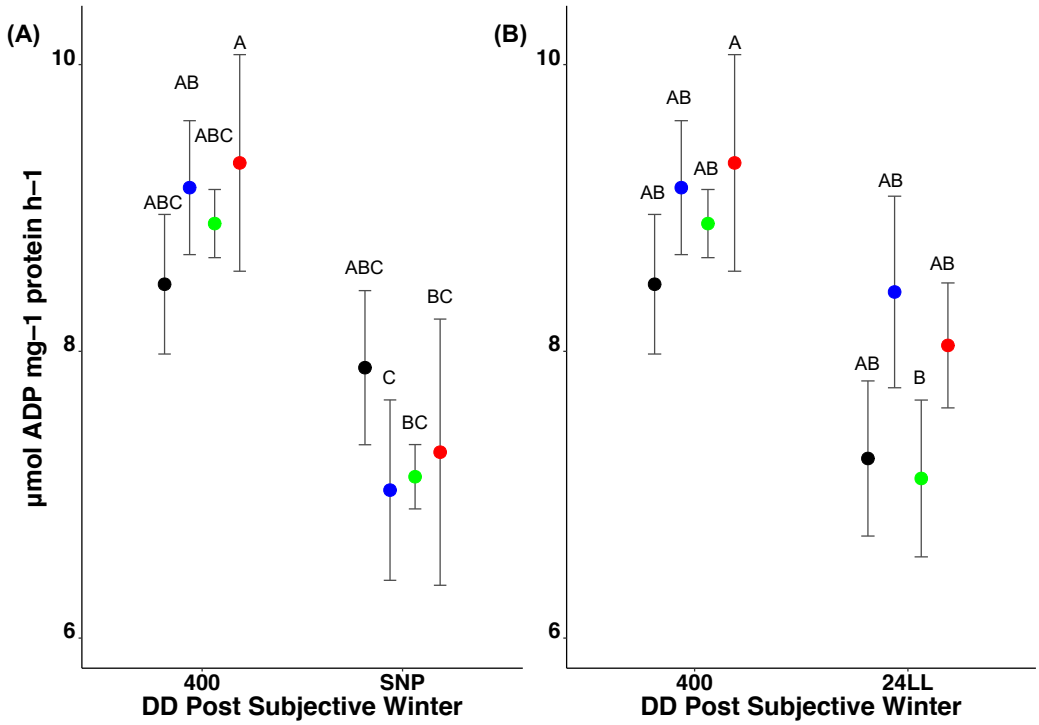

Figure 4.27. Comparison of gill NKAe activity levels at transfer and after 220 ºdays (4 weeks) in SW under either SNP (A) or LL (B) fluorescent white light conditions. Coloured dots represent colour of exposure prior to transfer. Values (n=3) are presented ± SEM. Significant differences between treatments are denoted by different upper case superscript (1-Way ANOVA, $p<0.05$).

Trial III – NKAα1a PCR - Freshwater

Significant differences between treatments were only observed at 600 ºdays where the control (White) expression was significantly higher than the fish under the Blue, Green and Red treatments [W-B p=0.009; W-G p=0.003; W-R p=0.010] (Fig. 4.28A). NKAα1a expression showed no significant variation between -400 and 1000 ºdays in fish exposed to the control photoperiod (Fig. 4.28B) or to the Blue treatment (Fig. 4.28C). Under the Green light, a significant decrease was observed between 0 and

300 ºdays and a significant increase was evident between 600 and 800 ºdays [p=0.026] (Fig. 4.28D). Fish exposed to Red light showed a significant decrease in expression between -100 and 300 ºdays and increased significantly from 300 to 400 ºdays [p=0.011] (Fig. 4.28E).

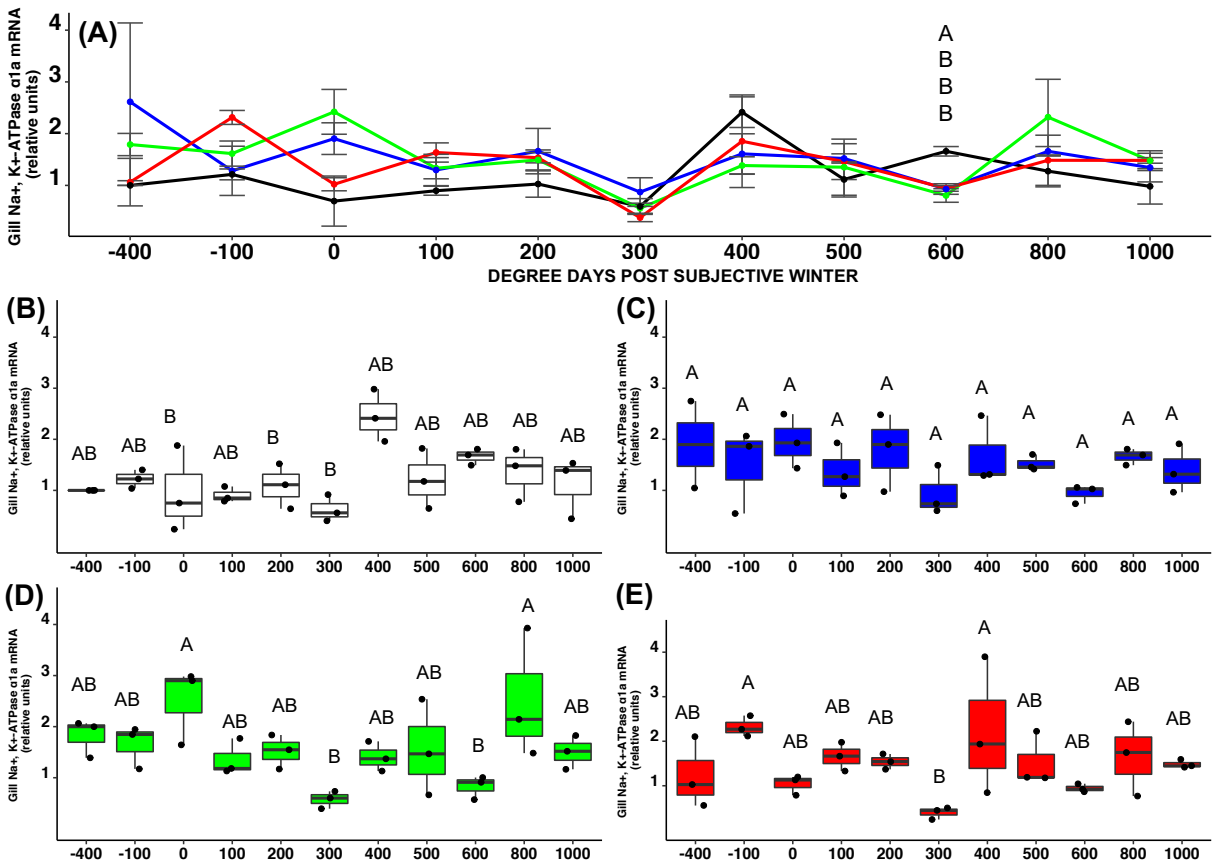

Figure 4.28. Gill NKAα1a expression levels as relative units (Mean ± SEM, n = 3) of juvenile Atlantic salmon (5 fish / tank) subjected to an out-of-season photoperiod regime whereby a subjective "winter" photoperiod (-400 to 0 ºdays) was provided by replacing the scotophase with a reduced intensity from the photophase for the Blue, Green and Red treatments (5 W/m^2 daytime and 0.05 W/m^2 nigh time) in relation to a control population that received an LD12:12 photoperiod during the same period. Significant differences between treatment where present are shown in **(A)**. Significant differences within treatment over time are shown in **(B) - (E)** (1-Way ANOVA, $p<0.05$).

Trial III – NKAα1a Expression - Post Seawater Transfer

NKAα1a expression decreased significantly between 400 ºdays in FW after four weeks in seawater for fish transferred to both SNP (Fig. 4.29A) and LL (Fig. 4.29B).

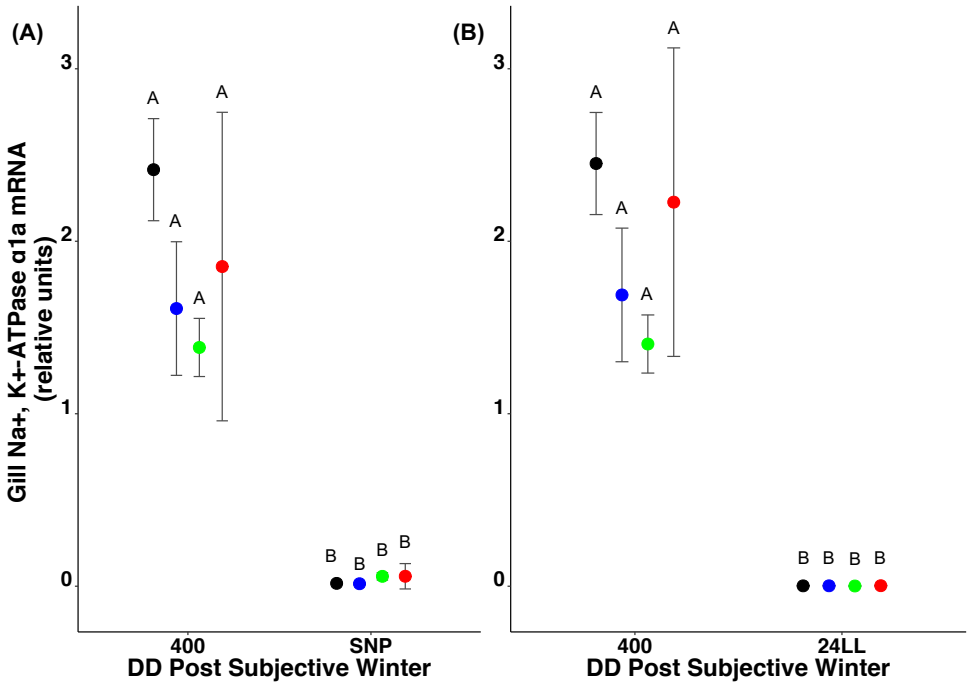

Figure 4.29. Comparison of gill expression of NKAα1a at transfer and after 220 ºdays (4 weeks) in SW under either SNP (A) or LL (B) fluorescent white light conditions. Coloured dots represent colour of exposure prior to transfer. Values (n=3) are presented ± SEM. Significant differences between treatments are denoted by different upper case superscript (1-Way ANOVA, $p<0.05$).

Trial III - NKAα1b PCR - Freshwater

NKAα1b expression in response to the White control photoperiod showed no significant variation from -400 to 1000 ºdays (Fig. 4.30B). Exposure to Blue light resulted in a significant increase in expression between 400 and 500 ºdays which then decreased significantly between 400 and 500 ºdays (Fig. 4.30C). A similar significant increase between 400 and 500 ºdays was observed in fish exposed to Green light (Fig. 4.30D) and Red light (Fig. 4.30E) with a subsequent significant fall between 500 and 600 ºdays. NKAα1b expression was significantly lower under Green light at -400 ºdays in comparison to all other treatments [G-B p= 0.016; G-R p=0.015]. At 0 ºdays control group expression was significantly lower than the Blue.

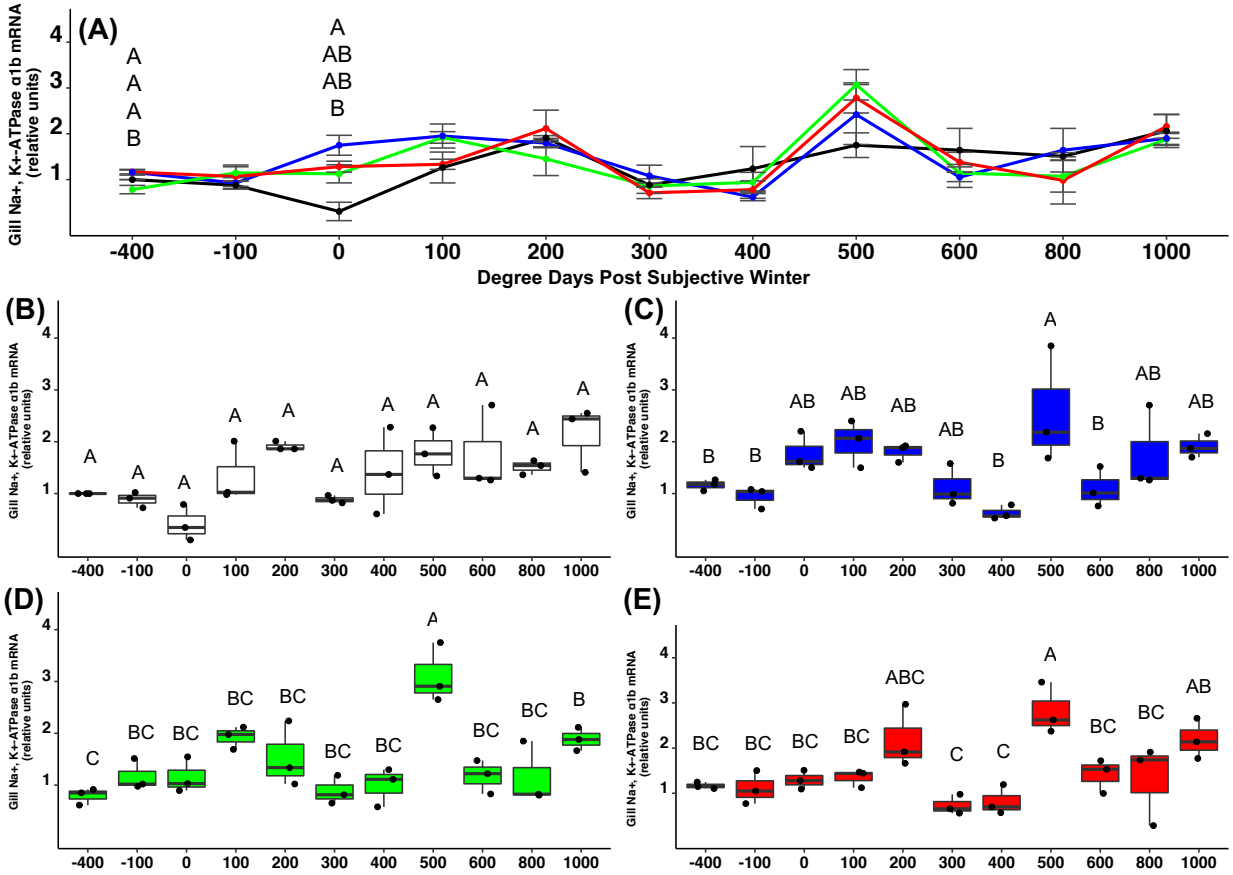

Figure 4.30. Gill NKAα1b expression levels as relative units (Mean ± SEM, n = 3) of juvenile Atlantic salmon (5 fish / tank) subjected to an out-of-season photoperiod regime whereby a subjective "winter" photoperiod (-400 to 0 ºdays) was provided by replacing the scotophase with a reduced intensity from the photophase for the Blue, Green and Red treatments (5 W/m^2 daytime and 0.05 W/m^2 night time) in relation to a control population that received an LD12:12 photoperiod during the same period. Significant differences between treatment where present are shown in **(A)**. Significant differences within treatment over time are shown in **(B) - (E)** (1-Way ANOVA, $p<0.05$).

Trial III – NKAα1b Expression Post Seawater Transfer

NKAα1b expression following transfer to SW in all groups exposed to either SNP or LL exhibited a significant increase in expression (Fig. 4.31A and B).

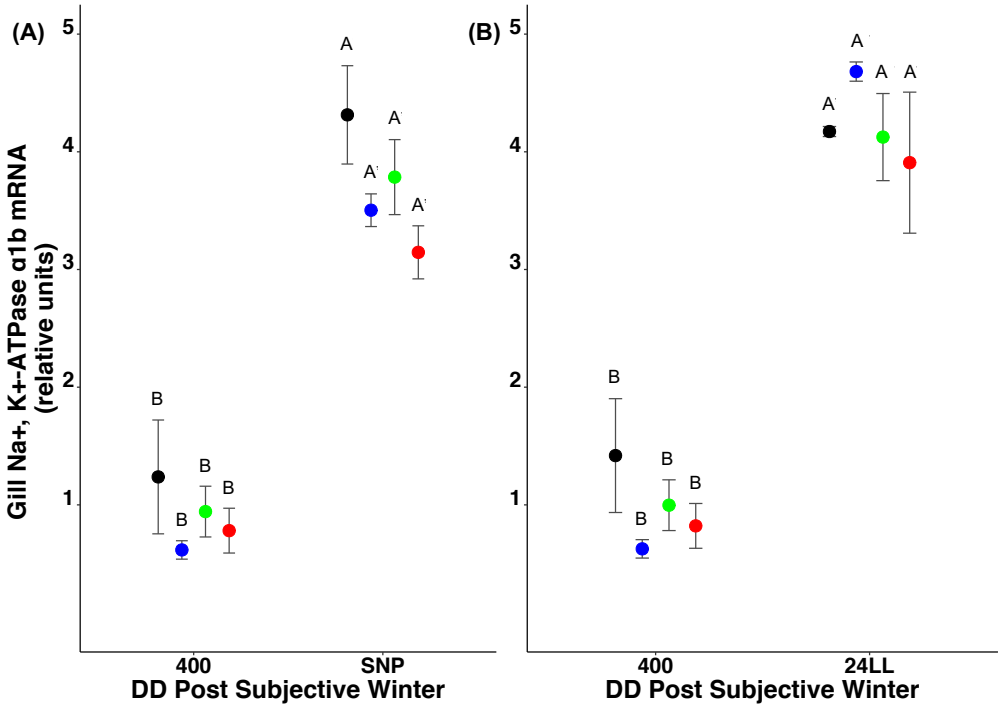

Figure 4.31. Comparison of gill expression of NKAα1b at transfer and after 220 ºdays (4 weeks) in SW under either SNP (A) or LL (B) fluorescent white light conditions. Coloured dots represent colour of exposure prior to transfer. Values (n=3) are presented ± SEM. Significant differences between treatments are denoted by different upper case superscript (1-Way ANOVA, $p<0.05$).

Trial III – NKAe, NKAα1a, NKAα1b Correlations

A significant negative correlation was observed between condition factor and NKAe between the short day "subjective winter" photoperiod until SW transfer (Table 4.6). The control (White) treatment was the only treatment to show a correlation between NKAα1a and NKAe. NKAα1b showed a significant positive correlation with increasing NKAe activity in all treatments. A significant negative correlation between NKAα1a and NKAα1b was observed for the fish exposed to the Blue, Green and Red treatments but not for the control (White) group which showed a significant positive correlation.

Table 4.6 Pearson correlations coefficients for growth metrics vs measures of smoltification from 0-400 ºdays.

		Blue		Green		Red		White	
Metric	**Metric**	**Cor.**	**p-value**	**Cor.**	**p-value**	**Cor.**	**p-value**	**Cor.**	**p-value**
Weight	Length	**0.98**	**<0.00**	**0.98**	**<0.00**	**0.99**	**<0.00**	-0.12	0.22
K	NKAe	**-0.31**	**<0.00**	**-0.31**	**<0.00**	**-0.41**	**0.00**	**-0.28**	**<0.00**
K	sqrtNKAα1a	-0.01	0.88	0.16	0.12	0.02	0.83	0.00	0.97
NKAe	sqrtNKAα1a	-0.03	0.79	-0.05	0.65	-0.09	0.37	**-0.35**	**<0.00**
NKAe	sqrtNKAα1b	**0.26**	**<0.01**	**0.33**	**<0.00**	**0.34**	**<0.00**	**-0.42**	**<0.00**
sqrtNKAα1a	sqrtNKAα1b	**-0.29**	**0.00**	**-0.37**	**<0.00**	**-0.22**	**<0.02**	**0.21**	**<0.03**

Muscle Fibre Recruitment

Significant differences were apparent between all treatments (Table 4.7). Recruitment in response to Blue light was significantly different to the other treatments (Table 4.8) resulting from an increase in small fibres (Fig. 4.33). The distribution of muscle fibre sizes in fish exposed to Green and Red treatments were similar and this is true to a lesser extent in fish exposed to White light (Fig. 4.34). Fish exposed to the Blue treatment differed with a more consistent distribution between 0 and 50 µm compared to the other treatments during smoltification. There were no mature muscle fibres identifiable in any treatment groups throughout these stages.

Table 4.7 Kolmogorov-Smirnov non-parametric bootstrap test for comparison of muscle fibre distribution between groups exposed to Blue (fB), Green (fG), Red (fR) and White (fW) treatment during freshwater and smoltification.

Contrast: Treatment vs Treatment		**End of Smoltification**	
		D	***P*-value**
fB	**fG**	0.087	<0.000
fB	**fR**	0.072	<0.000
fB	**fW**	0.062	<0.000
fG	**fR**	0.033	<0.000
fG	**fW**	0.034	<0.000
fR	**fW**	0.020	0.038

Table 4.8 Comparison of values determined from the percentiles of mean muscle fibre diameter in fish exposed to Blue (fB), Green (fG), Red (fR) and White (fW) since first feeding and until the completion of S0+ smoltification.

Sample Point	Percentile	Kruskall-Wallace *P*-value	Percentile for fB	S.E.M.	Percentile for fG	S.E.M.	Percentile for fR	S.E.M.	Percentile for fW	S.E.M.
Smolt Transfer	5%	0.13	9.94	0.62	11.55	0.17	11.83	1.14	11.31	0.08
	10%	0.09	13.81	0.78	17.03	0.96	16.89	1.78	16.55	0.39
	50%	**0.05**	**48.70**	1.36	55.55	0.49	54.16	0.97	53.80	0.70
	95%	0.38	119.08	3.58	128.39	1.77	121.03	5.27	123.88	2.78
	99%	0.13	169.29	9.92	175.99	2.31	154.90	6.58	164.27	6.96

.

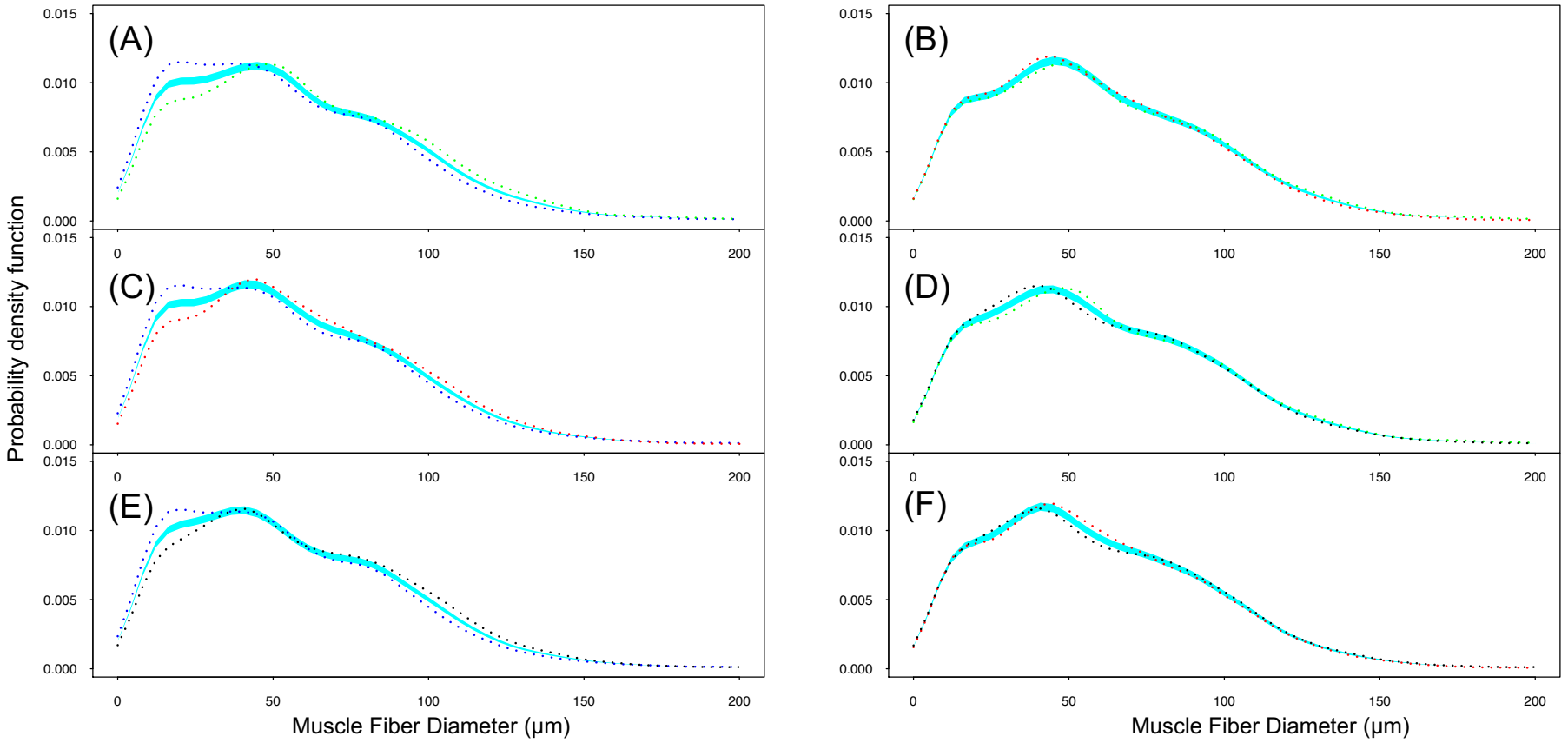

Figure 4.32. Comparison of muscle fibre distribution in post-smolt Atlantic salmon immediately after an out-of-season smoltification regime under four different spectra (White (black lines): Blue; Green or Red) reflected by line colours. Shaded area shows combined probability density plot (PDF) for both treatments being contrasted. Coloured dashed lines are the PDF of each individual treatment. A: Blue vs Green; B: Green vs. Red; C: Blue vs Red; D: White vs Green; E: Blue vs White; F: Red vs White.

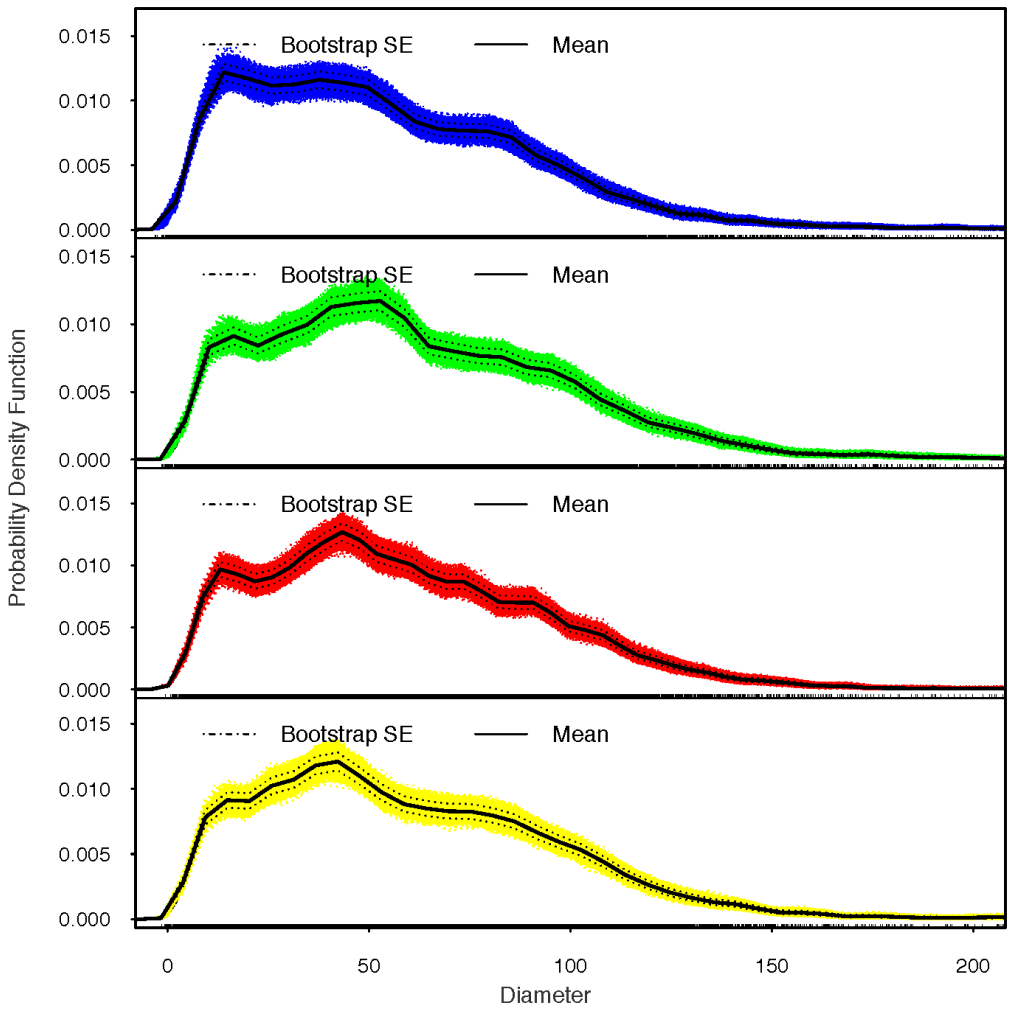

Figure 4.33. Variability band and mean (black line) of repeated bootstrapped probability density functions of muscle fibre diameter in Atlantic salmon at following application of an out-o-season smoltification regime (400 ºDays LD12:12 “winter”, LL “summer” 0-400 ºDays). Fish were exposed to four different spectra (White; Blue; Green or Red) indicated by line colours.

4.5 Summary of Chapter Results

Trial I - The Impact of Narrow Spectrum Light on Smoltification using a Traditional Photoperiod

- All wavelengths tested resulted in successful synchronised smoltification,

- Peak NKAe levels were attained for all treatments at 400 ºdays post application of LL following short-day suggesting that optimal SW transfer would occur at this time point,
- Effective reduction in plasma chloride was achieved after 200 ºdays application of LL following short-day,
- NKAe in response to Blue and Green photic conditions was significantly higher at 200 ºdays than the Red suggesting a possible earlier smolt induction in response to these photic conditions,
- NKAe and plasma chloride profiles for Red and White light regimes showed strong similarities.

Trial II - Investigating the Impact of Replacing Diurnal Scotophase/Photophase Fluctuations with a Reduced LL Intensity during the Winter Period of an Out-Of-Season Smoltification Regime

- Replacing SD with LL of decreased intensity relative to the pre-and post-SubWin photophase intensity led to a decrease in K for all groups,
- K changes in fish exposed to 0.04 W/m^2 closely resembled the control,
- Growth was highest in groups exposed to 0.04 W/m^2 during the subjective winter period,
- All treatments exhibited a rise in NKAe activity and a drop in plasma chlorides however, Control profiles were significantly different to all LL treatments,
- NKAe values showed significant correlation with K in both the Control group and 0.04 W/m^2 groups.

Trial III – Assessing the Impact of Replacing the Scotophase of an S0+ Regime with Continuous Light of Reduced Intensity

- All treatments exhibited clear signs of smoltification regardless of wavelength and in line with the control group,
- TGC for Blue was significantly higher than those exposed to Green and Red during SD,
- Following application of the winter photoperiod Red and Green TGC was significantly higher,
- Three period of development were observable for weight: SD, Post SD to 400 ºdays and 400 to 1000 ºdays,
- The smolt window, as determined by NKAe activity and K appeared to last from 300 to 600 ºdays post SD application,
- Gill NKAα1a and NKAα1b peaked at 400 ºdays and 500 ºdays respectively.
- At 0 ºdays exposure to Blue resulted in higher initial values for NKAe activity and NKAa1b expression and suggests earlier smoltification
- Following 4 weeks in SW, NKAα1a expression had decreased significantly in all treatments groups while expression of NKAα1b significantly increased for all treatment groups

4.6 Discussion

The aim of the experimental trials in the current chapter was to test the effects of light intensity and spectrum throughout a commonly used out-of-season smoltification regime. The spectrum and intensity profiles of trial I and III appeared to provide sufficient cues for inducing smoltification. Clear physiological changes were identified in fish exposed to the lowest light intensity when replacing a diurnal photophase and scotophase with a period of LL at reduced intensity relative to pre and post-SD periods. This led to the third trial where a low light intensity replacing the scotophase during SD was tested together with different spectra and the effects on growth and development were assessed. Results based upon NKA enzyme activity and gene

expression clearly showed that smoltification occurred successfully using these new regimes. Whilst the wavelength with which a successful cue was perceived appeared to be relatively plastic, some consistent differences were identified between trials. Collectively, these results suggest that the light intensity values tested for both the photophase and scotophase provided a sufficient cue to induce out-of-season smoltification. This chapter also raised interesting questions regarding light perception, inhibition of the photoneuroendocrine axis, and the process of smoltification in out-of-season smolts. A surprising but consistent result from the initial two trials was a lack of mortality in fish exposed to seawater before the supposed completion of smoltification which may indicate the potential for alternative photoperiod regimes to be used in commercial settings.

Spectral Influence on Smoltification

Smoltification in both S1 and S0 Atlantic salmon requires the perception of seasonal photoperiod cues (Bromage 1998). A minimum 'winter' period of 350 ºdays in S1 fish (Handeland et al., 2003) or a general 6-8 weeks are considered to be optimal for farmed salmon production (Sigholt et al., 1995; Duncan and Bromage 1998). Winter, or short-day (SD), is followed by a spring/summer period during which substantial physiological remodelling occurs between 0 and 400 ºdays allowing the fish to survive in SW (Sigholt et al., 1995; Sigholt et al., 1998). Concomitant changes in NKAe and K (Lubin et al., 1991; Berge et al., 1995; Duston and Saunders 1995) such as those in trials I and III observed between 400 and 500 ºdays are indicative of these changes. Different spectra appeared to influence the timing of smoltification as fish exposed to both Blue and Green light treatments achieved significantly higher NKAe activity after 200 ºdays than the Red treatment in trial I. In trial III, NKAe was also elevated earlier for these treatments at 100 ºdays for the Green and 0 ºdays for the Blue. The duration of elevated NKAe has been shown to be limited (McCormick et al. 1998) and the earlier increase in Blue NKAe was matched by an earlier decrease in response to Blue light. NKAe activity reduces plasma chlorides values (Mccormick et al., 1987; Handeland and Stefansson 2001) and homeostatic concentration is maintained between 110 and 135 mmol (Folmar and Dickhoff 1980). All treatments in trial I showed a sharp reduction by 300 ºdays however, under Blue light, chloride values were already low at 0 ºdays and remained low throughout the trial. Plasma chlorides showed a strong relationship to fish size (Duston and Saunders 1990) however no significant

differences in size were recorded between groups at this early stage again suggestive of the earlier smoltification in these groups. In addition, trial III showed a relationship between higher NKAe activity and gene expression in both the Green and Blue treatments compared to White and Red regimes. Taken together, results suggest that it may be possible to alter the timing of smoltification using different photic conditions and the application of this required further investigation.

Spectrum also appeared to influence weight gain which varied considerably during short day between trial I and III. The abrupt fluctuations of light and dark phase transition used in trial I have previously been shown to heighten oxygen consumption indicating a stress response (Folkedal et al., 2010). Each treatment experienced the same shifts and resulting growth was approximately equal. Replacing the scotophase with a reduced night intensity resulted in significantly higher TGC in Blue compared to Green and Red treatments. Salmonid sensitivity to Blue light is low (Parkyn et al., 2000) and small changes in intensity failed to elicit a measurable stress response (Migaud et al., 2007). Photosensitivity varies in response to wavelength and the method of stimulus, short and long exposures, such as those provided during SD in trial III are known to elicit increased electrical signalling from the optic nerve (Parkyn et al., 2000). Rainbow trout (*Oncorhynchus mykiss*) exposed to both sudden flashes of green light and long term exposure to red light elicited similar electrical responses at the optic nerve (Parkyn et al., 2000). Such responses may be responsible for the significantly lower TGC in these treatments. Removing the diurnal stressor initiated a significant increase in TGC and growth during 0-400 ºdays and was significantly higher in both the Green and Red treatments. Earlier TGC gains under Blue light however resulted in significantly higher transfer weights than those exposed to Red light. Transfer weights have an important impact on long term performance as restocking studies for brook trout (*Salveliinus fontinalis*) (McCormick and Naiman 1984), Coho salmon (*Oncorhynchus kisutch*) (Bilton et al., 1982) masu salmon (*Oncorhynchus masou*) (Miyakoshi et al., 2001) and Atlantic salmon (Lundqvist et al., 1994) all demonstrated.

Role of Intensity

Intensity, as shown in Chapter 3, plays an important role in somatic development and this was again apparent in trial II where exposure to low intensity lighting during the subjective winter resulted in a significant increase in weight compared to the control.

A photoperiod cue is required to induce smoltification (Eriksson and Lundqvist 1982), however, all treatments in trial II showed some characteristic changes normally related to smoltification. Fish exposed to 0.04 W/m^2 during the subjective winter decreased rapidly in weight once returned to 5 W.m^2 and exhibited a concomitant decrease in condition factor indicative of smoltification (Hoar 1988). A correlation between K and NKAe was apparent and a transient rise in NKAe activity and reduction in plasma chlorides all indicated the onset of parr-smolt transformation (Handeland and Stefansson 2001). Stefansson et al. (2007) examined the influence of continuous lighting on S1 smolts and described a similar increase in activity despite the supposed inhibitory action of LL. NKAe values reported were substantially higher than those reported here (30 vs. 9 µmol ADP mg^{-1} protein h^{-1}) and potentially point to fundamental differences in NKAe production in response to a compressed out-of-season photoperiod compared to the longer time periods experienced under ambient photoperiod conditions. Imsland et al. (2014) reported similar findings and determined that water temperature was providing a smoltification cue. No such signal was provided here due to the use of RAS and historic water temperatures pre-transfer varied by just ~0.5 ºC over the preceding 21 days. Here, a cue may instead have been provided by the sudden changes in intensity at the start of SD, sufficient to initiate smoltification but insufficient to provide the long-term cues required to fully induce smoltification.

Given the importance of smoltification in achieving year-round salmon production, surprisingly little research has examined photophase and scotophase threshold light levels for either S1 or S0+ smolts. Light levels have a demonstrable impact on endocrine signalling as evidenced with plasma melatonin levels in response to intensity (Meissl and Ekstrom 1988; Porter et al., 2001). Stefansson et al. (1991) demonstrated successful S1 smoltification using a reduced night intensity relative to day (27 lx night: 1400 lx. Daytime). By replacing the scotophase with a reduced intensity in trial III similar positive results on smoltification were achieved. Thus, the use of 5 W/m^2 12L:12D with Blue, Green, Red and White was sufficient to provide the “winter” cue for inducing smoltification. By replacing the SD photoperiod by LL with high (5 w/m2) and low (0.05 w/m2) intensity during the subjective day and night respectively, smoltification was successfully controlled.

This raises some intriguing questions regarding the photoneuroendocrine system and circadian perception and several postulations can be formed as to why

smoltification was successful. Detection may be asymmetric between the visual and non-visual system with 0.05 W/m^2 light sufficient to facilitate the visual detection of food, as evidenced through the high growth rates in trial II, but insufficient to be detected as day. Receptor sensitivity, or the location of the pineal and deep brain photoreceptors below the skull known to block ~2 % of transferred broad spectrum light (Migaud et al., 2007) may account for the observed asymmetry between visual and non-visual systems. The presence of non-visual photosensitive neural ganglion cells in the eye and the apparent detection of light by the eye in these trials could imply a compartmentalised functional role of non-visual photoreceptors in different tissue types performing distinct roles regarding seasonal perception. In addition, the unknown mechanism that inhibits neural innervation may be directly photosensitive with 0.05 W/m^2 being insufficient to induce inhibition. Alternatively, the contrast between daytime and night time light intensity may have been sufficient to override the mechanisms that inhibit smoltification.

Assessment of S0+ success

Smoltification leads to a characteristic change in the weight to length ratio with changes in condition factor acting as a reliable proxy for smoltification (Folmar and Dickhoff 1981). Decreases in growth result from hepatically and myotomally devolved energy reserves in the form of lipids and glycogen being mobilised (Sheridan 1989). Increased circulating corticosteroids involved in the transformation lead to concomitant decreases in feed intake and utilisation as seen during stress responses (Barton et al., 1985; Dickhoff et al., 1997; Mommsen et al., 1999; Barton 2002). Changes in condition factor, indicative of smoltification, were evident in all groups in trial II, however, other smoltification metrics did not support successful SW adaptation. Sub-optimal SW transfer leads to reduced growth performance even if no mortality occurs (Saunders et al., 1985). Assessing smoltification readiness is thus an important requirement for producers and a variety of metrics such as Na^+K^+-ATPase enzyme activity (NKAe) (Mccormick 1993), plasma chloride and more recently gene expression (Nilsen et al., 2007) are used.

Peak NKAe levels in trial I occurred at 400 ºdays which is in line with previously published studies at comparable water temperatures (Stefansson et al., 1998). The high energetic cost of maintaining SW osmoregulation in a FW environment (Hoar 1988; Duston et al., 1991) leads to de-smoltification as observed in trial III if the marine

environment is not reached within an appropriate time (Stefansson et al., 1998). Exposure to a salinity of 10 ppt was shown to retain SW adaptation and prevent reversal (Mortensen and Damsgård 1998), reflecting natural downstream brackish conditions. Peak NKAe levels occurred inversely with transient decreases in K in both trial I and III and despite lacking a suitable photoperiod cue in trial II both the control and the 0.04 W/m^{-2} treatments displayed very similar reductions in K factor. Operational constraints may lead producers to transfer fish to SW after peak NKAe has been achieved and McCormick (1997) suggested a period of 500 ºdays to re-attain parr activity levels. In the current study, a period of 300 ºdays was identified, in line with Handeland et al. (2004). Smolt size, however, may be influencing the current study results as Arnesen et al. (2003) found that the largest cohort of fish in their trials exhibited the shortest period of peak smolt status.

The NKA enzyme occurs in several isoforms with two specific to osmoregulation identified by double simultaneous immunofluorescence (Nilsen et al., 2007; McCormick et al., 2009; Imsland et al., 2011; Handeland et al., 2013). High levels of NAKα1a are localised to the basolateral membrane of filamentous and lamellar chloride cells in freshwater whereas NKAα1a resides in proximally arranged pavement cells (McCormick et al., 2009). SW adaptation has been shown to result in a concomitant rise in both NKAα1b and NKAe (Nilsen et al., 2007) and this was evident in trial III for NKAα1b following 4 weeks post SW transfer. Of note, a significant decrease in NKAe was observed in both the Blue and Red groups transferred to SNP. Expression of NKAα1a after 4 weeks in SW were significantly lower compared to FW at transfer. By contrast, all treatments exhibited a rise between 300 and 400 ºdays. This may stem from either a preparatory upregulation of FW NKAα1a to facilitate reversion of SW adaptation or point towards an unexplored functional role in SW. Only the control treatment showed a significant negative correlation between the expression of NKAα1a and NKAe indicating that NKAα1a expression may be linked to a true dark period. Peak expression of NKAα1b and NKAe activity occurred at 500 ºdays and may reflect that observed in post-smolts following 4 weeks at sea. Pavement cells expand rapidly following transfer to SW (McCormick 2012) and so increases in expression levels may be a pre-emptive response to this expansion. As such, correlation between NKAα1b expression and NKA activity levels in all treatments was significant within trial III.

Optimal Smolt Transfer

The duration whereby smolts can be successfully transferred to sea, the “smolt window”, has received surprisingly little attention for out-of-season smolts (Arnesen et al., 2003). The NKAe profiles from trial III provides the clearest elucidation of the smolt window for S0+ fish to date. An intriguing rise in NKAe prior to the end of SD in trial III has been shown previously in S1 fish of the same strain (Handeland et al., 2003) and suggests preliminary adaptation may be occurring during SD. NKAe then reached a peak at 400 ºdays which was maintained until ~800 ºdays. This peak duration of 400 ºdays is directly comparable to trials on S1 smolts (Stefansson et al., 1998; McCormick et al., 1999), however, the actual time within the NKAe window for optimal transfer has been the source of frequent debate. Sigholt et al. (1995) proposed optimal transfer to occur whilst NKA levels are increasing whereas both Handeland and Stefansson (2001) and Arnessen et al. (2003) both advocated transfer immediately post peak NKA activity. Based on the current study findings, the NKAα1a and α1b expression profiles suggest that transferring after peak NAKe would be more appropriate as substantial upregulation is still occurring at this time point.

An intriguing result from both trial I and trail II is the lack of mortality of fish that were transferred to SW at the end of the short-day photoperiod and SubWin when smoltification may be considered to be incomplete. Results may suggest an important interplay between physical size and SW survival as exploited in the rainbow trout industry where given sufficient size fish can be directly transferred to SW (Johnsson and Clarke., 1988). A hypothesis incorporating photoperiod, nutrition and water temperature has been suggested to account for these differences. However, in 2003 Arnesen reported similar low mortalities when examining smoltification in S0+ small versus large fish (15-45 g vs 30 -60 g). Size may not be the critical factor explaining survival, instead, a possible explanation may stem from changes that occurred during the “winter” period which allows the fish to adapt rapidly to SW, even if fish have not received the appropriate LL signal post SD or in the SubWin experienced in trial II. This has exciting potential for extending the smolt window of out-of-season fish. Further work needs to be carried out to assess the performance of fish transferred at this point versus those transferred after 400DD. Such analysis may offer producers greater flexibility for transferring fish to SW.

Impact of Smoltification on Muscle Fibre Distributions

Smoltification resulted in significant muscle fibre recruitment especially in the Blue treatment. Populations of small muscle fibres represent future growth potential as hypertrophy leads to the enlargement of fibres (Johnston et al., 1999). Both recruitment and growth are driven through the proliferation of muscle progenitor cells (Hollway et al., 2007). Interestingly recruitment was high despite a significantly lower TGC during the period 0 to 400 ºDays compared to the Red and Green groups. Although both Blue and White exhibited significantly higher growth compared to other treatments during the period -400 to 0 ºDays, the population structure was very different between these groups suggesting that this period did not induce the observed changes. Results suggested a stimulatory effect of recruitment in response to Blue light and suggested that future growth will be accelerated within this group.

Conclusions

Delivering a photoperiodic cue with which to induce successful smoltification is both predictable and adaptable. Collectively, these trials provide evidence to suggest that at sufficient intensity, the effects of specific wavelengths appear to be negligible when using standard smoltification assessments. However, consistent differences between wavelengths raised interesting questions regarding photoperception and also the role of light intensity. Ultimately, results will help to guide producers in optimising photic conditions in the hatchery whilst raising some key physiological questions requiring further investigations. The impact of replacing the scotophase with a period of reduced intensity, shown for the first time, needs to be assessed through longer term seawater performance. This is presented in detail in the next chapter.

5 The Interaction of Freshwater Photic History and Seawater Post Transfer Photoperiod on Atlantic Salmon Post-Smolts Growth and Maturation

5.1 Introduction

The somatic development of Atlantic salmon follows seasonal patterns related to water temperature and appetite (Kadri et al., 1996) with photoperiod being the main zeitgeber providing seasonal cues (Falcón et al., 2010). Smoltification, sexual maturation and growth can be manipulated by altering photoperiod resulting in the transfer of smolts to sea out-of-season (Duston and Saunders 1995; Thrush et al., 1994) and the suppression of early maturation during the first year at sea (Endal et al., 2000). In both situations, a growth enhancing effect of continuous light has been reported (Liu and Duston 2016; Oppedal et al., 2006; Johnston et al., 2004).

In out-of-season smolts (S0+), elevated ambient water temperatures or artificially heated RAS systems (Bergheim et al., 2009) leads to enhanced growth during this stage of development compared to smolts growing under ambient photoperiods (S1+) (Kolarevic et al., 2014). Out-of-season smolts produced in RAS systems are reported to initially perform poorly after SW transfer in comparison to S1+ fish. Slow growth in seawater (SW) may be attributable to transfer during a time of the year when growth is typically reduced (Late autumn/winter) or by the radical changes in environment (Mørkøre and Rørvik 2001). In addition, freshwater (FW) growth appears to impact greatly on seawater performance. In Atlantic salmon growth rates during on-growing in SW are influenced by early FW development. Similarly, in the marine species Atlantic cod (*Gadus morhua*), compromised growth during early development impacts future growth (Imsland et al. 2007; Imsland et al. 2014). The identification of different growth stanzas in rainbow trout (*Oncorhynchus mykiss*) highlights differential ontogenic development (Dumas et al., 2007).

FW Chapters 3 and 4 showed that photic conditions during parr and smoltification appeared to influence muscle fibre structure leading to greater numbers of small fibres in the Blue treatments. Accounting for ~60% of the carcass, and comprising the economic portion, the salmon myotome undergoes indeterminate growth until senescence or mortality prevails (Johnston et al., 2011). Early manipulation of growth rates using temperature has been shown to have a lasting impact on final fibre numbers (Macqueen et al., 2008). The spatial arrangement of myotome muscle blocks, separated by collagenous sheets of myocommata, enables undulations

required to produce swimming force (Johnston and Strugnell 1999) which manifests itself in the chevron pattern seen in fillets. In higher vertebrates, myogenesis occurs exclusively through the enlargement of muscle fibres which are recruited during early ontogenesis. Somatic growth in Atlantic salmon, however, occurs both through enlargement and through the addition of new fibres via recruitment whereby mononuclear myoblasts, termed myogenic progenitor cells (MPC), fuse to form multinucleated syncytial fibres (myotubes) (Johnston et al., 1999).

New muscle fibres <10μm (Johnston et al., 2003), are enlarged through hypertrophy where additional MPCs are absorbed until the fibres reach maturity at ~200μm (Johnston et al., 1999; Suresh and Sheehan 1998). Maximum size is limited by diffusional constraints of body mass, temperature and metabolic functions (Johnston 2003) and the need to maintain cytoplasmic/nuclear ratios (Koumans et al., 1991). Muscle fibre recruitment occurs until the second winter at sea and is a trait that can be selected for in salmon breeding programs (Johnston et al., 2004). MPC abundance directly influences both hypertrophy and recruitment (Johnston et al., 2003). Proliferation varies in response to photoperiod with a reduction in daylength inhibiting propagation (Johnston 2003) whilst continual lighting increases proliferation of MPC numbers resulting in an increase (23%) in final muscle fibre number as shown by Johnston et al. (2004). Supplementary lighting applied during the second sea winter was shown to maintain fibre number advantage (Johnston et al., 2004). Elucidation of the mechanisms behind why thermal imprinting leads to prolonged effects suggests that the generation of a self-renewing population of MPCs once accrued is maintained, continually contributing to the development of new muscle (Johnston et al., 2000). Fibre number is important as it is related to reduced gaping scores and improved organoleptic properties in the final fillet (Johnston et al., 2006).

In addition to transferring fish into a period of seasonally slow growth, the change in photoperiod from hatchery to SW in the late autumn or winter is at the highest annual extreme and days are short. Using LL to enhance S0+ growth in FW means that fish are exposed to long day photoperiods. Transfer to SW out-of-season effectively induces a change from long day to short day, a well described mechanism for inducing maturation (King et al., 2004). In the past, smolt size was small and fish were unlikely to meet key body size and adiposity thresholds. However, RAS fish are frequently large and there have been reports of high levels of early maturation in male post-smolts (Imsland et al., 2014) The use of LL inhibits maturation as it advances the

season to the next decision making window and the key thresholds are not sufficient to progress (Taranger et al., 2010). This trial examined this period to determine whether late application of light was capable of either progressing seasonal growth cycles or changed the decision to mature. The prevention of maturation during a grow out cycle of salmon is critical to ensure optimal productivity and profitability. Initially maturation results in a period of enhanced growth rate in both male and female fish due to the growth stimulating effects of sex steroids (Kadri et al., 1996). Long term, recrudescence leads to the redirection of somatic reserves, induces pubertal anorexia, and negatively impacts growth and flesh quality (Sloat et al., 2014) culminating in significant downgrading at harvest, and have a deleterious impact on stock welfare (Liu and Duston 2016; Leclercq et al., 2010; Taranger et al., 2010; Imsland et al., 2007; McClure et al., 2007). Advanced growth is postulated to occur from the advancement of endogenous growth cycles (Randall et al. 1998) however little is known regarding when in the year these can be induced given an appropriate switch in photoperiod.

Abrupt changes in daylength, rather than seasonal changes in photoperiod per se, are capable of inducing seasonality (Taranger et al., 1998). The duration of altered photoperiod can be short, as seen in the previous chapter where 400 ºDays provided sufficient duration of ‘winter’ and ‘summer’ cue to successfully advance smoltification. Over recent years, smolt size has increased dramatically (from 60-80g to >150g) mainly due to the use of RAS system providing optimal thermal conditions for growth (Bergheim et al., 2009), in addition to selective breeding for growth and improved diets (Kolarevic et al., 2014; Kadri et al. 1996; Rowel et al., 1991). Increasing temperature and daylength in RAS has the potential to result in premature maturation in both freshwater and during early grow out in sea water as somatic gateways are achieved earlier (Imsland et al., 2014; Fjelldal et al., 2011). It is particularly true for males which are capable of diverse life-strategies, leading to early maturation at several life stages: mature parr are precocious; mature smolts are jacks and fish maturing following one sea winter are grilse (Fleming 1996). Changes during gonadogenesis provide an important proxy with which to assess gonadal recrudescence, however, other metrics such as changes absolute forklength have been identified as key indicators of maturing cohorts within a stock population (Kadri et al., 1997). Given the impact of prior photic history on growth during FW it is possible that SW on-growing will be affected by historic photic conditions.

To date very few trials have studied the impact of FW light history on growth following out-of-season transfer to SW. Additionally, the use of supplementary lighting post SW-transfer received little attention in S0+ smolts compared to spring smolts (Oppedal et al., 1999; Taranger et al., 1998; Hansen et al., 1992). The aims of this trial were therefore to assess the impact of freshwater photic history and seawater photoperiodic regime post-transfer on growth, the number and size of muscle fibres and early maturation. As described in Chapter 3 fry were exposed to LL with narrow bandwidth lights (Blue (B), Green (G), Red (R) or White (W)). Once parr reached an appropriate size (~40g) smoltification was induced using a change in light intensity (Chapter 4.3) rather than true light dark for Blue, Green and Red groups versus a traditional light dark regime for the White group. The impact of FW history was investigated on future growth and development. In addition, two photoperiodic regimes were tested at sea, simulated natural photoperiod (SNP) or continuous light (LL) and populations were switched from one photoperiod to the other after 12 weeks in SW to determine effects on growth and sexual maturation.

5.2 Materials and Methods

Fish Stocks and Rearing Conditions

On the 16th of December 2015, 985 fish (BW 97.7 ± 7.2 g) were transferred from the Temperate Aquarium, University of Stirling, Scotland (56°N, 4°W) to the Machrihanish Marine Environmental Research Laboratory (MMERL), Scotland (55°N, -6°W). A standard commercial salmon diet (Inicio CPK, Biomar, UK) was used to feed the fish throughout the trial and feed was delivered for the same 8-hour period daily to each tank via an automated feeding system (Arvotec, Sweden) using an integrated feeding algorithm set at an initial 1.2 % Body Weight per day and hand fed to 1.5 % to ensure satiation. Feed was adjusted throughout the trial based on periodic sample weights. DO was continually monitored and maintained above 80% at all times.

During FW and prior to transfer, fish were maintained at 12.0 ± 1.0 ºC. Seawater tanks were supplied using pumped SW, temperature reflected ambient seasonal conditions and ranged from 6.5 to 15.3 ºC (Fig. 5.1).

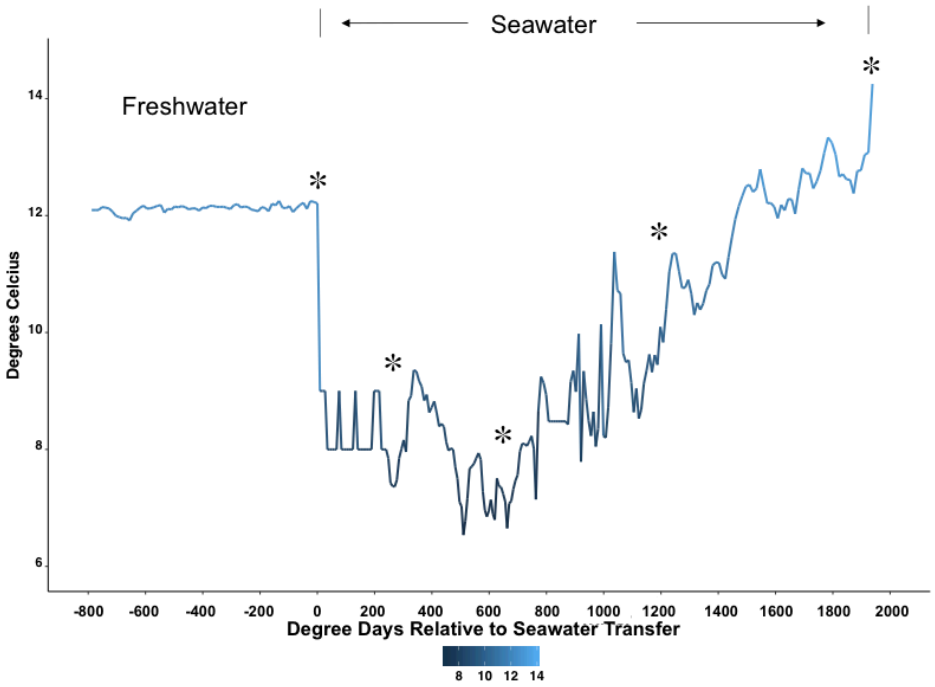

Figure 5.1. Water temperature (ºC) during FW and post SW transfer. Asterisks denote sample points discussed in this chapter.

Experimental Design and Sampling

Prior to smoltification, fish were PIT tagged intramuscularly using RFID tags (Trovan Ltd, USA) as described in chapter 2.4.2. Smoltification was induced out-of-season via either a control or experimental photoperiod as described in chapter 4.4.1 and fish were transferred at 400 ºDays post subjective winter.

Upon arrival to MMERL, 480 fish (mean weight 101.7 ± 8.8 g) (40 fish from each of B, G, R and W light treatments, n=3) were transferred into a 6.4 m^3 circular tank (3.0 x 0.9 m) exposed to a LL light regime and 523 (mean weight 95.3 ± 5.8 g) fish (~43 fish from B, G, R and W, n=3) transferred to a 6.4 m^3 circular tank (3.0 x 0.9 m) exposed to simulated natural photoperiod (SNP). Illumination was provided by a CFL bulb (Master PL-S 9W, Philips, Eindhoven, NL) producing an intensity during the photophase of 1 W/m^2 at the water surface.

Lighting Regime Post-Seawater Transfer

Timing reported in this trial are described as ºDays post seawater transfer. All fish in both SNP and LL tanks were maintained under their respective photoperiods from SW transfer until 1213 ºDays (146 days) whereupon 50 % of each population from each FW replicate were transferred to the opposing photoperiod treatment resulting in four

treatment groups: SNP, SNP-LL, LL, LL-SNP. The trial terminated at 1937 ºDays (207 days) post SW transfer (Fig. 5.2).

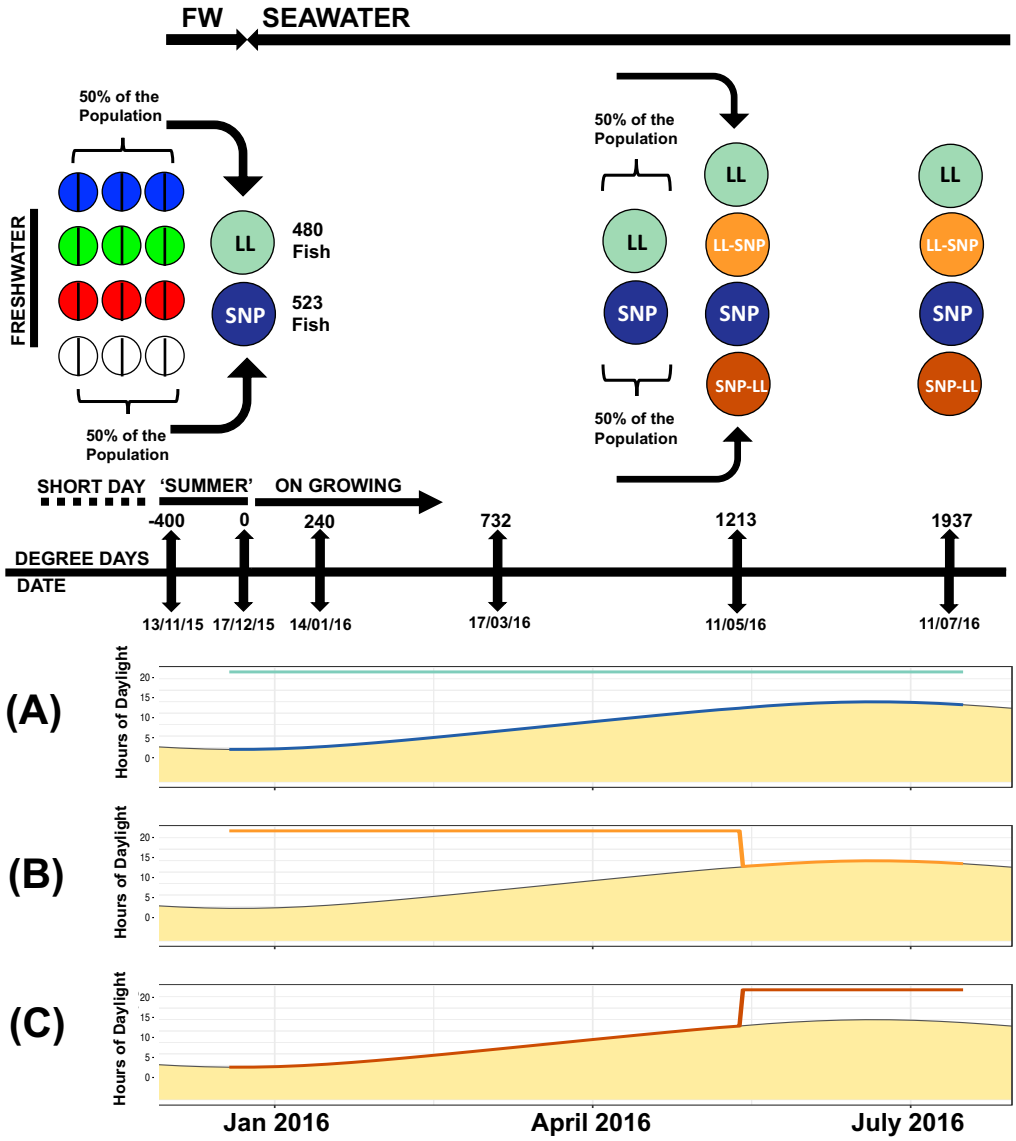

Figure 5.2. Overview of trial design. In FW, 90 fish (n=3) were exposed to either White, Blue, Green or Red light from first feeding. Out-of-season smoltification was induced via a 400 ºDays "winter / SubWin" followed by a "summer" period of 400 ºDays (13/11/15 – 17/12/15). At 0 ºDays (17/12/15) 45 from each replicate were transferred to SW and randomly assigned either a simulated natural photoperiod (SNP) or continuous lighting (LL) (**A**). After 1213 ºDays (11/05/16), based on historic FW photic conditions, half (~22) from the SNP were transferred to LL (**B**) and half from the LL transferred to SNP (**C**) giving four treatments groups (SNP, LL, SNP-LL and LL-SNP) until the trial terminated at 1937 ºDays (11/07/16).

Biomass

Stocked biomass for the beginning and end of each SW period were as reported in Table 5.1.

Table 5.1 Start and end stocking densities for the 6.4m^3 seawater tanks

Treatment	Start Date	Start Weight (kg/m^3)	End Date	End Weight (kg/m^3)	DD
SNP	17/12/2015	6.1	11/05/2016	26.3	1213
LL	17/12/2015	5.91	11/05/2016	38.4	1213
SNP- SNP	11/05/2016	13.0	11/07/2016	23.0	724
SNP-LL	11/05/2016	13.3	11/07/2016	23.8	724
LL-LL	11/05/2016	19.0	11/07/2016	31.8	724
LL-SNP	11/05/2016	19.4	11/07/2016	32.2	724

Population Metrics

BW and FL was related to individual fish via PIT tag ID. In Chapter 4 PIT tag data is presented for the entire group of fish exposed to a particular wavelength. In this chapter, the post-SW transfer group (i.e. the split group) is related back to performance in FW to determine how each group performed prior to transfer. BW and FL were assessed for all individuals in each treatment tank at 240 ºDays (16th of January, 2016) and then at 732 ºDays post-SD (17th of March, 2016) and 1213 ºDays post-SD (10th of May, 2016). A final assessment was conducted at the trial termination (1937 ºDays, 4th of July, 2016). Population metrics are presented as mean for the three FW replicates per treatment with error bars presented as standard error of the mean for these values.

Growth metrics for Condition Factor (K), Thermal-Growth Coefficient (TGC), Coefficient of Variation (CV) and Pearson's Correlation were calculated as described in chapter 2.5.

Gonadosomatic Index and Histological Examination

At the trial termination 13 fish were randomly selected from each FW replicate based upon the prior FW photic history from each of the SNP, SNP-LL, LL and LL-SNP tanks.

Gonads were dissected, removed, and weighed to calculate gonadosomatic index (GSI %) and sex recorded as described in chapter 2.4.9. GSI was used to assess maturation state. A value of greater than 0.2 % was used to determine a male undergoing pubertal recrudescence as described by (Kadri, Metcalfe, et al. 1997). Developmental stage of female gonads was assessed by using a selection of gonads from those collected from across all female fish regardless of FW treatment. Based upon the recorded GSI, six gonads per 0.1 % bracket ranging from 0.05 % (min value) to 0.6 % (max value) were used for histological examination. State of maturation was assessed according to Grier (2009).

Muscle Fibre Assessment

Samples for assessment of muscle cellularity as discussed in this chapter were collected at 1937 ºDays. At the trial termination 3 individuals from each replicate of each freshwater treatment from the SNP and LL tanks were collected. No samples were collected from the SNP-LL or LL to SNP tanks due to limitations in the ability to collect and store sample. Sample protocol involved liquid nitrogen and this was not available on site and had to be transported with a limited shelf life.

A fillet was removed from the truncal region, anterior to the dorsal fin, processed and the data was analysed according to Johnston et al. (1999) as described in chapter 2.4.10.

Vertebral Assessment

At the final SW sample point, 10 fish per historical freshwater replicate (n=3) X 2 treatment groups (SNP and LL) were placed on ice for a period of 2 days to ensure completion of rigor mortis prior to freezing flat at -20 ºC for future x-radiological examination. Radiological assessment was conducted as described in chapter 2.4.6 and vertebrae characterised according to Witten et al. (2009).

Statistics

BW and FL were used to calculate Fulton's condition factor (K), start and end weight and ºDays were used to calculate Thermal growth coefficient as described in chapter 2.5.

Population Body Weight and Condition Factor

All statistical tests were performed using R Studio (R Core Team 2016). Base R function were used unless stated otherwise. Normality was tested using a Shapiro-Wilk test and homogeneity of variance was tested using Levene's test.

To examine interactions of treatment and time a linear mixed model (LME) (Pinheiro et al. 2016) was applied to analyse differences at each sample point either between treatments, over time for each treatment or the interaction of the two were presented. PIT tag data comprises of longitudinal repeat measurements on the same fish and as such the statistical approach must account for variance of n. LME models used in this analysis allow for this by calculating restricted maximum likelihood (REML) as described in chapter 2.5. To meet assumptions regarding normality and homogeneity of variance square root transformation of all weight data was conducted, an arcsine transformation was applied to TGC data and no transformation on K was conducted. Once assumptions regarding homogeneity of variance and normality were met, the measured variable was used as the dependent variable and colour and replicate as a random factor, time was added as a continuous variable and variance owing to time was modelled using a first order autoregressive function (Ar01). An additive approach was used to determine best model fit. Post-hoc comparisons were performed using least-square means and Tukeys-HSD to determine comparisons.

Correlations

Correlations were performed using Pearson correlations coefficient to measure the linearity between variables X and Y as both X and Y were measured (chapter 2.5).

Kruskall-Wallace/ Dunns Test

The 5^{th}, 10^{th}, 50^{th}, 95^{th} and 99^{th} quantiles were calculated using base R from the distribution of GSI% and muscle fibres. Once calculated a non-parametric comparison between treatments for each given quantile was performed using a Dunn's test of multiple comparisons using rank sums (Dinno 2016). This test reports the results amongst multiple pairwise comparisons after a Kruskall-Wallace test for stochastic dominance amongst groups has been applied.

5.3 Results

PIT tag data from all individuals within the SNP and LL is used to present changes in BW, FL and K for initial SW transfer stage until 1213 ºDays (146 days) post SW transfer. Following photoperiod switch, PIT tag data for the period between 1213 ºDays and 1937 ºDays (61 days) is then presented to compare effects of the four photoperiodic groups (SNP, SNP-LL, LL and LL-SNP) on growth and physiological development. Treatment groups are defined based upon FW history thus each treatment is suffixed with the colour during FW, i.e. SNP-Blue. Data collected from the final sampling point is presented for muscle fibre structure, maturation, gonadal development and associated growth and performance in these groups. Mortality across all tanks was 4.8 ± 0.18 %.

Growth from SW transfer to 1213 ºDays

Weight

Weight increased significantly over time throughout the trial for all groups (Fig. 5.3). Growth rate, measured by TGC (Fig. 5.4) during the -800 to -400 ºDays (SubWin) ranged between 1.63 to 1.97. BW increased significantly but TGC was significantly lower for all treatments during -400 to 0 ºDays (summer LL regime) and values ranged between 1.63 to 1.97. TGC increased significantly for all groups between 0 and 240 ºDays and 240 to 732 ºDays. In all groups exposed to LL TGC decreased significantly during the period 732 to 1213 ºDays. From the groups exposed to SNP, a significant decrease in TGC was seen in the White and Red groups but not the Green and Blue.

At -800 ºDays, no significant differences in weight between any of the SNP and LL colour pairs (i.e. SNP-Blue and LL-Blue) were seen. SNP-Green and SNP-Red weighed significantly less than all other groups.

At -400DD, again no significant differences were between any colour pair. SNP and LL Red were both significantly lighter than both SNP and LL Blue, and SNP and LL White. No significant difference in TGC were seen between colour pairs. during the same period (-800 to -400 ºDays). TGC was significantly lower in both SNP and LL Red compared to SNP and LL Blue and SNP-Red was significantly lower than the LL-Green.

At 0 ºDays there were significant differences in weight between colour pairs. The weight of the SNP-Red group was significantly lower than the LL-Blue. -400 to 0

ºDays TGC showed no significant differences in any colour pairs. SNP and LL Blue, SNP and LL White and had a significantly lower growth rate than both the SNP and LL Red. SNP and LL Green were also both significantly lower than LL-Red.

At 240 ºDays White and Blue colour pairs showed no significant differences. SNP –Green and SNP Red were significantly lighter than their LL counterparts. SNP-Red was significantly lighter than LL –Blue, LL-Green, LL-Red and SNP and LL White. SNP-Green was significantly lighter than LL-Blue, LL-Green and LL Red. For the period 0-240 ºDay all TGCs had increased significantly compared to the previous period. growth rates supported changes in weight and no significant differences between the White and Blue pairs were identified. SNP-Blue, SNP-Green, SNP-Red and SNP-White were significantly lower than both LL-Green and LL-Red. Both LL-Blue and LL-White had significantly lower TGC than SNP-Red.

At 732 ºDays, Every SNP colour was significantly lower than the LL counterpart. No significant differences in weight between any LL treatment was seen. Within the SNP group, SNP-Red was significantly lighter than SNP-White or SNP-Blue, SNP-Green was significantly lighter than SNP –White. For the period 240-732 ºDays growth rate was again significantly higher than the previous period for all treatments. The growth rate in all SNP treatments was significantly lower than LL groups. SNP-Red was significantly lower than both SNP-Blue and SNP-White.

At 1213 ºDays, BW was significantly lower in all SNP groups. Within the SNP group Red was significantly lighter than SNP-Blue and SNP-White. SNP-Green was also significantly lighter than SNP-Blue. For the period 732 to 1213 ºDays, the growth rate for all fish exposed to LL decreased significantly and no significant differences were seen within those exposed to LL. In response to SNP both the SNP-Green and SNP-Red had significantly lower growth rates than SNP-Blue. TGC for the SNP-White and SNP-Red groups decreased significantly from the previous period.

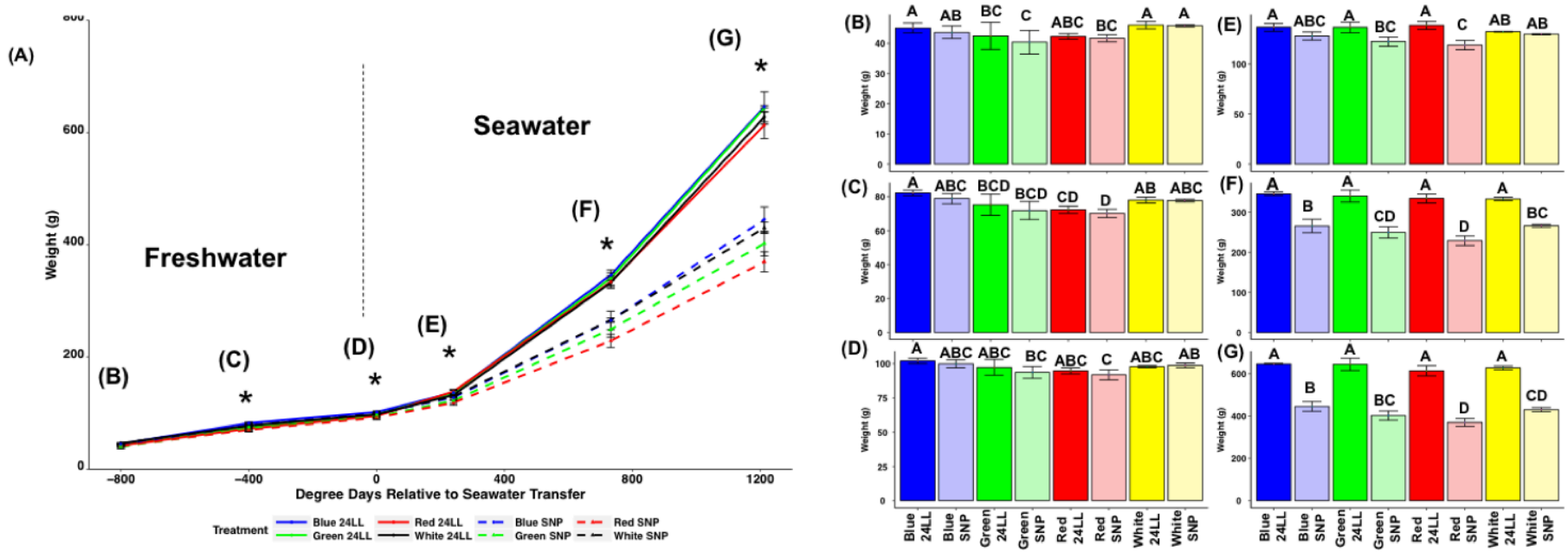

Figure 5.3. Weight (Mean derived from FW treatment ± SEM) of Atlantic salmon transferred to communal SW tanks illuminated using white light and subjected either to a simulated natural photoperiod (SNP - dashed line, pale colour bars) or continuous lighting (LL - solid line, dark coloured bars). During the FW phase, fish were exposed to four different spectra (White; Blue; Green or Red) reflected by colours. Line plot shows progression of weight through time with asterisks denoting significant change from previous time point. Bar plots (**B**)-(**G**) relate to period denoted by letters on figure (**A**). Significant differences between treatments within each time point are denoted by upper case superscript (Linear-mixed effects model, P =<0.5).

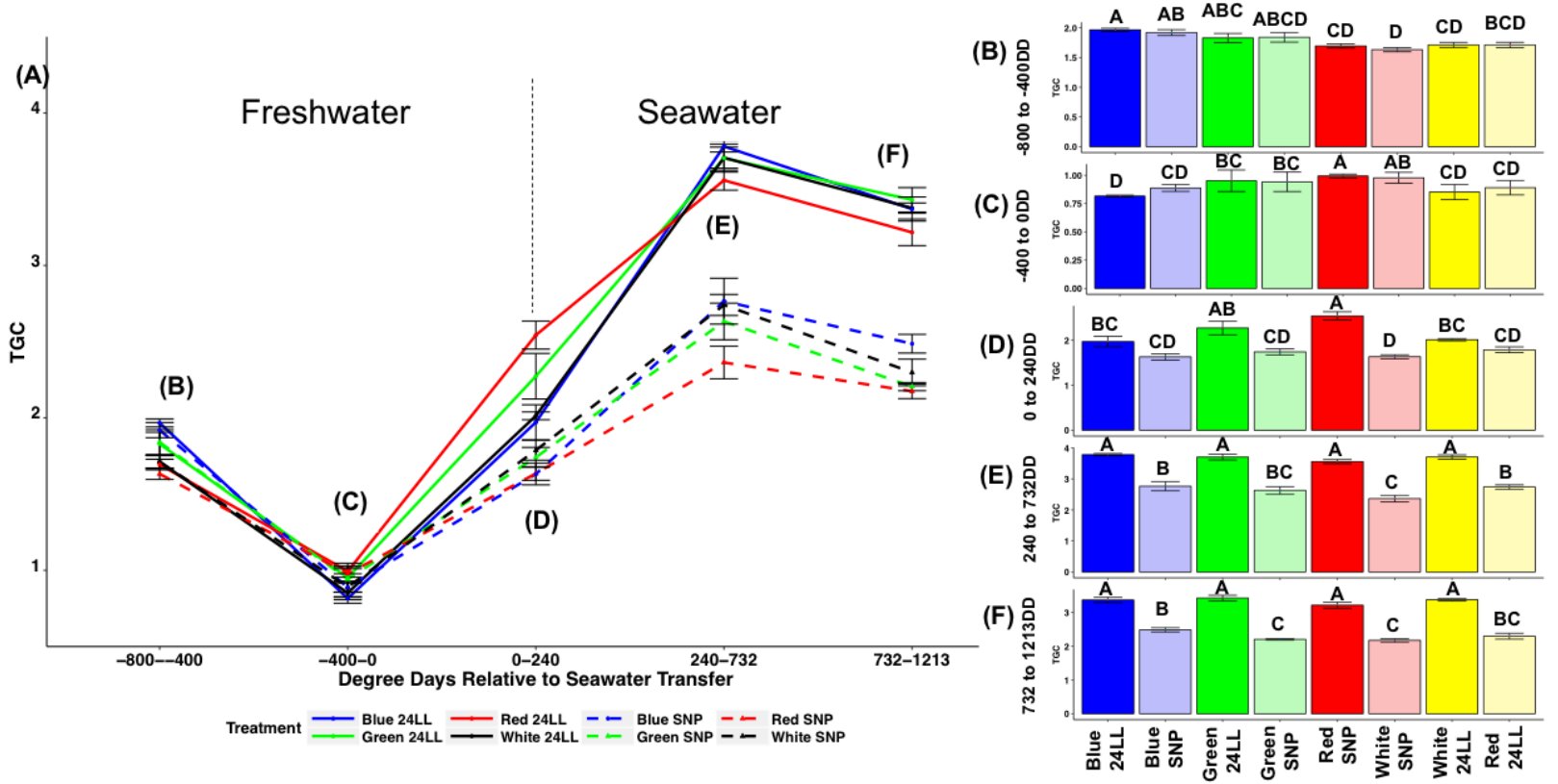

Figure 5.4. Thermal growth coefficient (TGC) (Mean derived from FW treatment ± SEM) of Atlantic salmon transferred to communal SW tanks illuminated using white light and subjected either to a simulated natural photoperiod (SNP - dashed line, pale colour bars) or continuous lighting (LL - solid line, bright coloured bars). During the FW phase, fish were exposed to four different spectra (White; Blue; Green or Red) reflected by colours. (**A**) Line plots including statistics for the final presented time point, (**B-F**) Bar plot for each time point marked (**B**)-(**F**) on figure (**A**) with significant differences between treatments within time point denoted by upper case lettering (Linear-mixed effects model, P =<0.5).

Condition (K)

Smoltification resulted in a significant drop in K factor by 0 ºDays as discussed in the previous chapter 4. K of fish exposed to SNP post SW transfer continued to decrease between transfer time and 240 ºDays irrespective of spectra in FW. No reduction in K was seen for all fish exposed to LL post SW transfer. K then increased in all treatments between 240 and 732 ºDays with only fish previously exposed to Green light having a significantly higher K than White irrespective of photoperiod post SW transfer [p=0.03] **(**Fig. 5.5**)**. Between 732 and 1213 ºDays, K differed significantly between photoperiodic groups with LL fish showing a significantly higher K than SNP fish irrespective of FW spectra except for LL-White being reduced compared to LL-Green [P=<0.001].

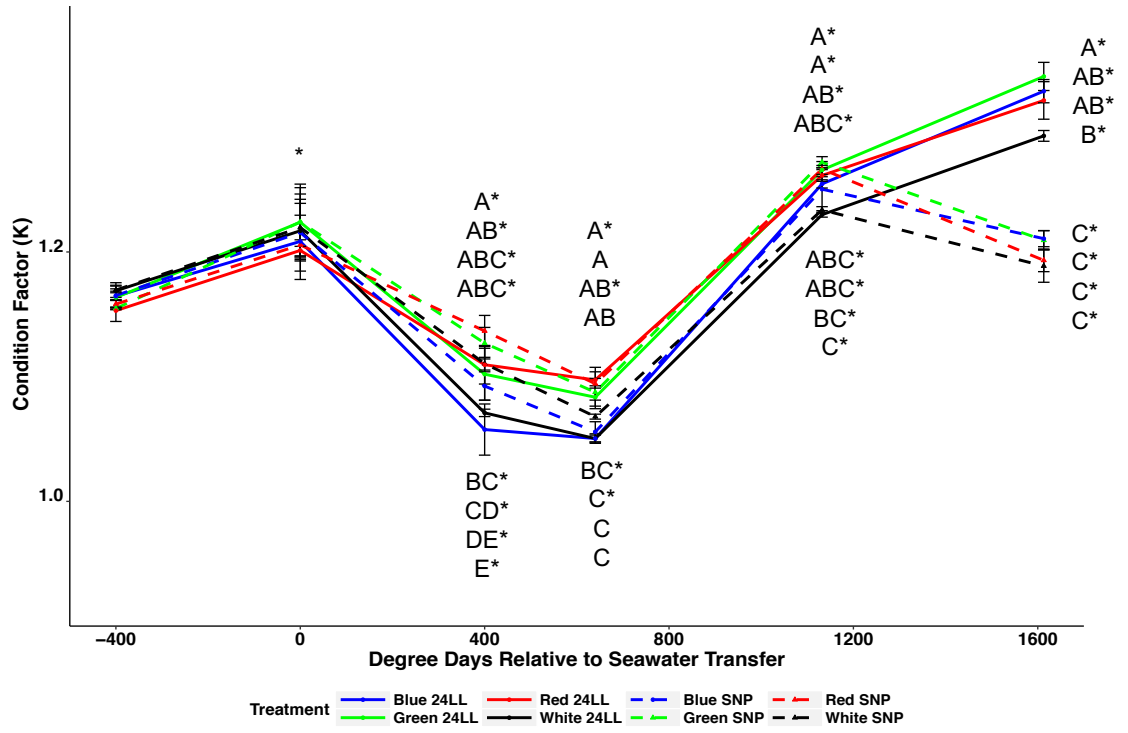

Figure 5.5. Condition factor (Mean derived from FW treatment ± SEM) of Atlantic salmon transferred to communal SW tanks illuminated using white light and subjected either to a simulated natural photoperiod (SNP- dashed line) or continuous lighting (LL-solid line). During the FW phase, fish were exposed to four different spectra (White; Blue; Green or Red) reflected by line colours. Significant differences between treatments within time points where present are shown as upper case superscripts (Linear mixed effects model, p<0.05), significant changes between time points are denoted by an asterisk.

Final Seawater Period – from 1213 to 1937 ºDays

Weight - 1213 to 1937 ºDays

Between 1213 and 1937 ºDays, all groups increased significantly in weight. At 1937 ºDays both SNP-Red and SNP-LL-Red weighed significantly less than the SNP-LL-Blue and SNP-White [all p-values=<0.001] (Fig. 5.6.A). In comparison to the SNP groups, tanks maintained under LL or switched to SNP all showed similar increase in weight such that there were no differences in final weight (Fig. 5.6.B).

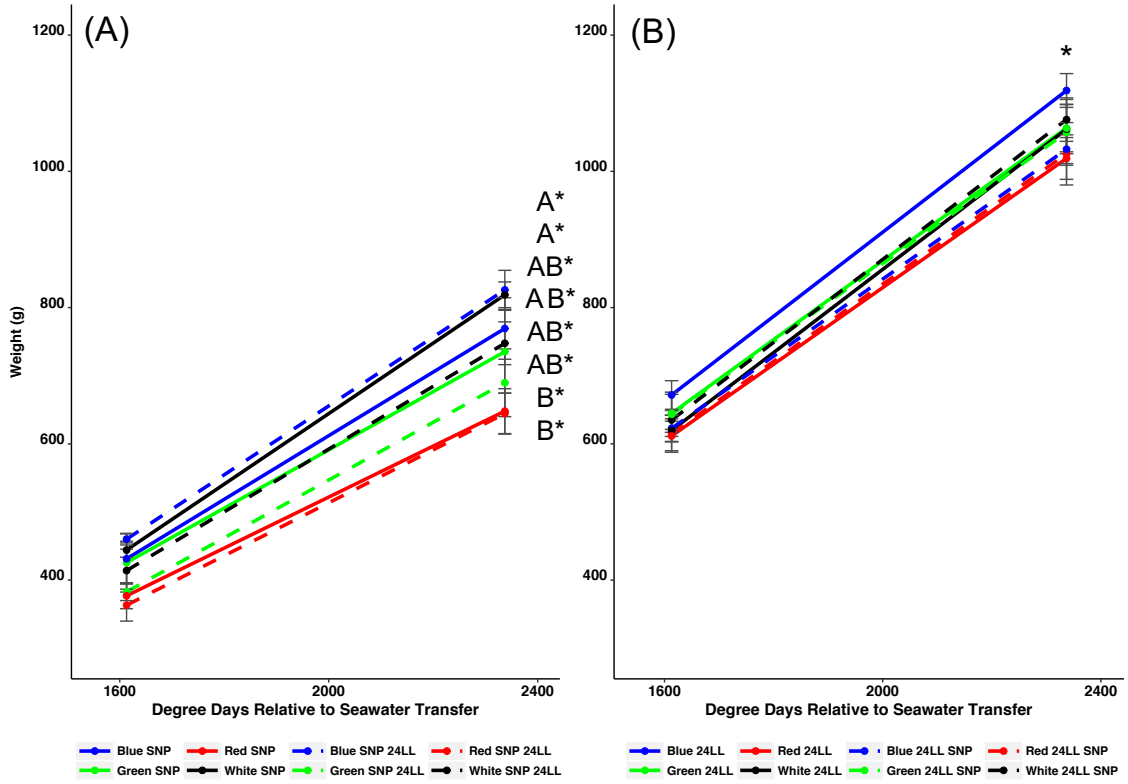

Figure 5.6. Weight (Mean derived from FW treatment ± SEM) following change in photoperiod at 1213 ºDays. Solid line represents continuation of previous light treatment either SNP (A) or LL (B). Dashed lines represent switched light treatments (A) SNP-LL and (B) SNP-LL. During FW fish were exposed to four different spectra (White; Blue; Green or Red) reflected by line colours. Significant differences between treatments within time points where present are shown as upper case superscripts (Linear mixed effects model, $p<0.05$), significant changes between time points are denoted by an asterisk.

Condition Factor - 1213 to 1937 ºDays

Condition factor (K) within the SNP treatment showed no significant differences between any group at 1213 ºDays (Fig. 5.7.A) however continued exposure to 1937 ºDays led to a significant increase in K for the White treatment. Switching fish to LL maintained similar values to those recorded at 1213 ºDays except for the Red treatment which appeared to decrease (Fig. 5.7.B). Continuous exposure to LL from 1213-1937 ºDays resulted in no significant changes in K. Switching to SNP caused a significant drop for all spectral treatments: LL-SNP-White [p=0.014], LL-SNP-Blue [p=0.001], LL-SNP-Green [p=<0.001] and LL-SNP-Red [p=<0.001].

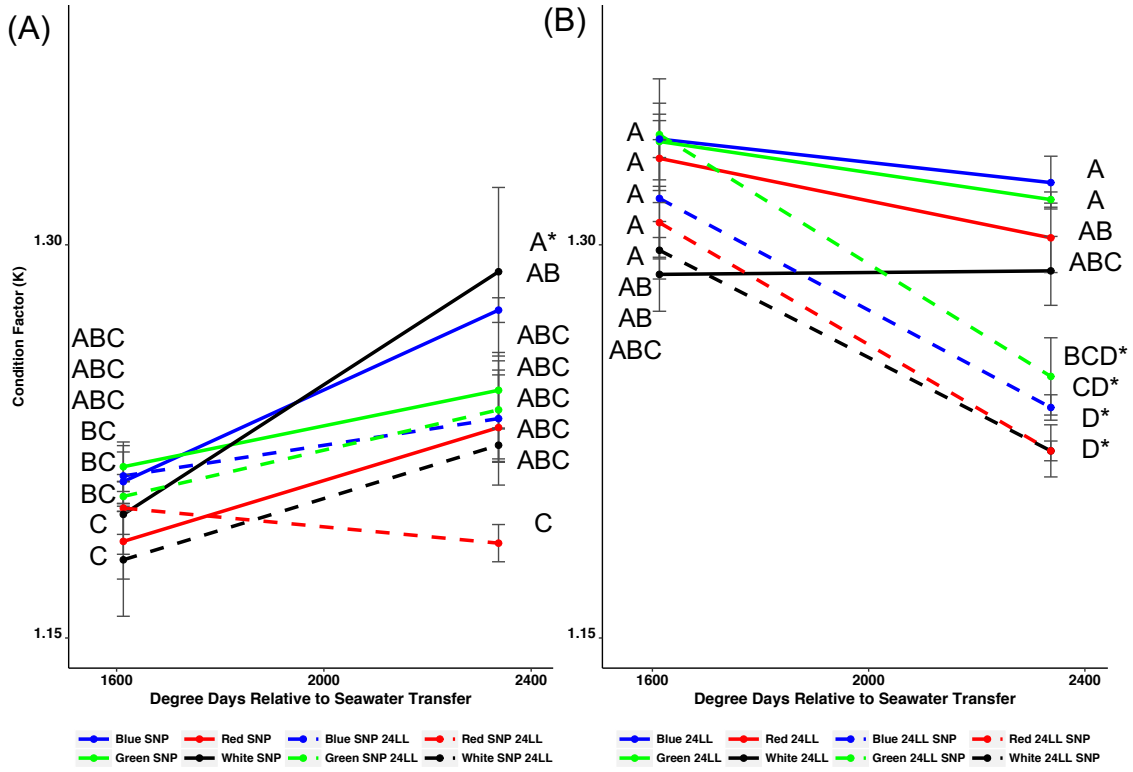

Figure 5.7. Condition factor (K) (Mean derived from FW treatment ± SEM) following photic 'switch' at 1213 ºDays. Solid line represents continuation of previous light treatment either SNP (A) or LL (B). Dashed lines represent switched light treatment (A) SNP-LL and (B) SNP-LL. During FW fish were exposed to four different spectral compositions (White; Blue; Green or Red) reflected by line colours. Significant differences between treatments within time points where present are shown as upper case superscripts (Linear mixed effects model, $p<0.05$), significant changes between time points are denoted by an asterisk.

Thermal Growth Coefficient - 1213 to 1937 ºDays

No significant differences in TGC were determined for the final sample period for any treatment group (data not shown).

Maturation

Maturation prevalence was higher in all male populations in each photoperiod treatment in comparison to female. 3 females across all treatment groups were classed as maturing (GSI% >0.5) (Fig. 5.8). Combined maturation based on male and female values ranged from 28 to 41 % for SNP groups and 28 to 50 % for the SNP-LL group. Combined maturation in groups exposed to LL ranged from 3 to 15 % and for the LL-SNP maturation ranged between 3 and 11 %. Maturation had a significant effect on weight as a CV of 35 % in SNP and 33 % in SNP-LL was observed compared to 19 % and 21 % in LL and LL-SNP, respectively. In general, recrudescence led to an increase in weight in response to SNP and SNP-LL photoperiods whereas a reduction in weight was observed under LL and LL-SNP conditions (Fig. 5.8).

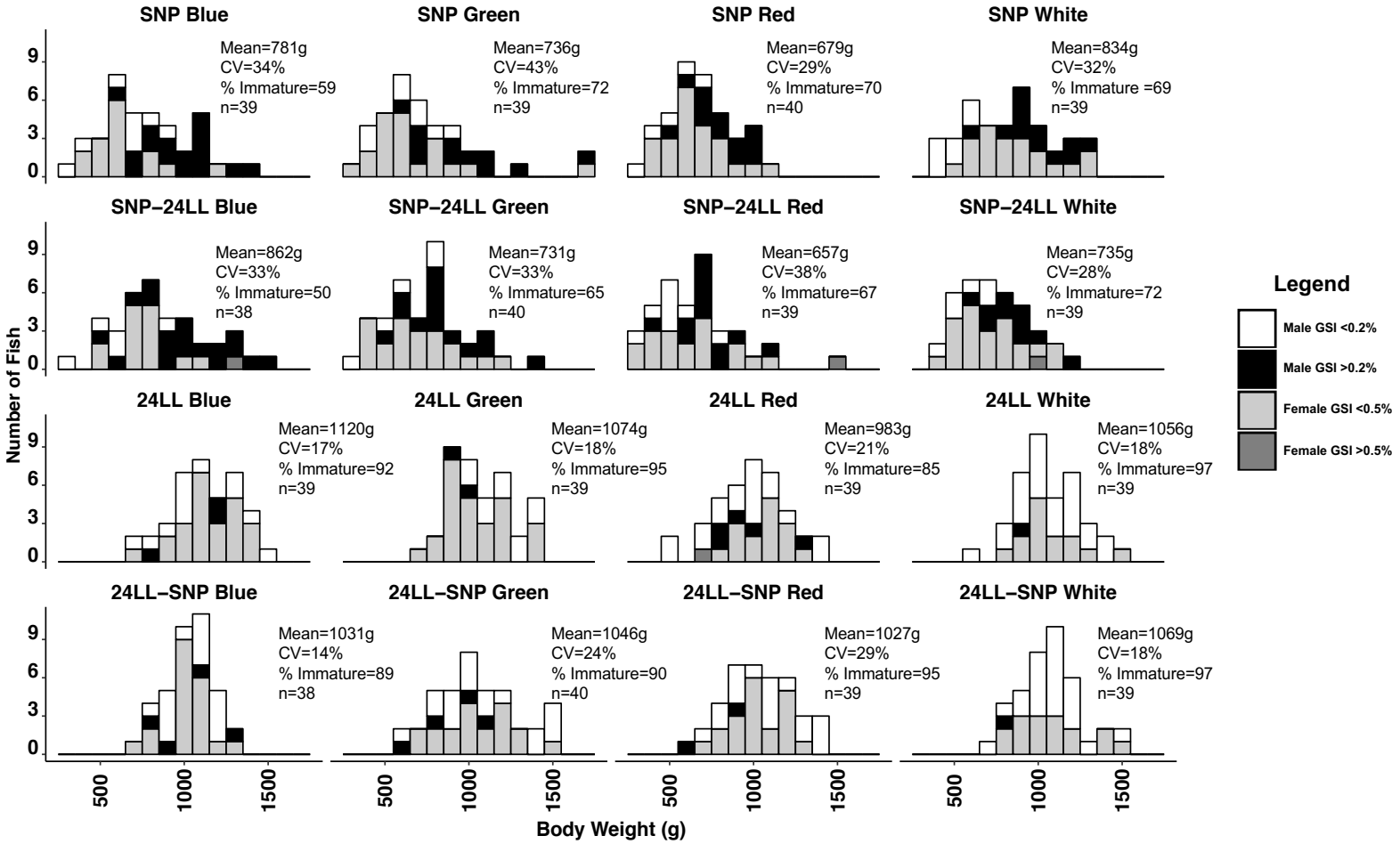

Figure 5.8. Final body weight distribution of post SW transfer reared Atlantic salmon exposed to either SNP, LL or switched to the opposing photoperiods after 1213 ºDays (bin size=100 g). Data is divided by treatment, gender and GSI. Mean is pooled, CV (coefficient of variation) within the treatment, %immature is derived from both genders. Shaded area represents gender and GSI: Light Grey – Male GSI <0.2 %; Black - Male GSI >0.2 %; Dark Grey – Female GSI <0.5 %; White- Female GSI >0.5 %.

Sexually Dimorphic Growth

Differential growth between immature sexes was examined over the duration of the trial to determine sexually dimorphic growth. Under all conditions with the exception of SNP no significant differences between sexes could be determined at any point. Under SNP White Females were significantly heavier than White Males at 1937 ºDays [p-value = 0.01] (Table 5.2).

Table 5.2. Mean final weights of immature males and females by light treatment. Threshold for maturing male GSI > 0.2%, female is GSI >0.5%. Significant differences between treatments are shown as upper case superscripts (ANOVA, p<0.05).

	Male		Female	
Final Mean Weight	Weight	SEM	Weight	SEM
Blue SNP	563.4 ^{A}	98.1	636.9 ^{A}	30.1
Green SNP	695.5 ^{A}	71.3	641.5 ^{A}	64.3
Red SNP	545.1 ^{A}	70.9	649.3 ^{A}	32.2
White SNP	**515.6** ^{B}	**9.2**	**836.3** ^{A}	**81.7**
Blue SNP-LL	588.0 ^{A}	69.9	734.2 ^{A}	44.1
Green SNP-LL	619.3 ^{A}	114.4	688.7 ^{A}	61.6
Red SNP-LL	484.8 ^{A}	67.8	617.0 ^{A}	88.9
White SNP-LL	609.1 ^{A}	68.2	725.0 ^{A}	61.2
Blue LL	1026.4 ^{A}	96.0	1139.7 ^{A}	27.3
Green LL	1195.1 ^{A}	46.9	1040.3 ^{A}	24.2
Red LL	932.9 ^{A}	32.7	1043.4 ^{A}	42.4
White LL	1059.0 ^{A}	28.9	1059.1 ^{A}	29.0
Blue LL-SNP	1056.3 ^{A}	39.9	1031.3 ^{A}	24.8
Green LL-SNP	1104.7 ^{A}	52.0	1036.4 ^{A}	43.3
Red LL-SNP	1092.2 ^{A}	97.6	1025.4 ^{A}	37.6
White LL-SNP	1074.1 ^{A}	30.0	1079.9 ^{A}	49.5

Gonadal Development in Response to SNP and SNP-LL

Changing photic conditions from SNP to LL resulted in a change to the distribution of GSI **(**Fig. 5.9 A-B**)**. By comparing the 5th, 10th, 50th, 95th and 99th percentiles (Table 5.3), significant differences in the upper distribution were seen in the SNP-Blue to SNP-LL-Blue and SNP-Green to SNP-LL-Green. In the White group, a similar change

in distribution was apparent although not significant. Within Red treatments, GSI was not significantly different.

In response to LL and LL-SNP, GSI was generally very low (Fig. 5.9 C-D). The highest single values of GSI from all of the treatments were found in the LL and LL-SNP groups. Examination of the percentiles (Table 5.4), as performed with the SNP and SNP-LL groups, shows differences in the lower 5th and 10th percentile distribution between the Green and White pairs (i.e. LL vs LL-SNP). No other significant differences were detected.

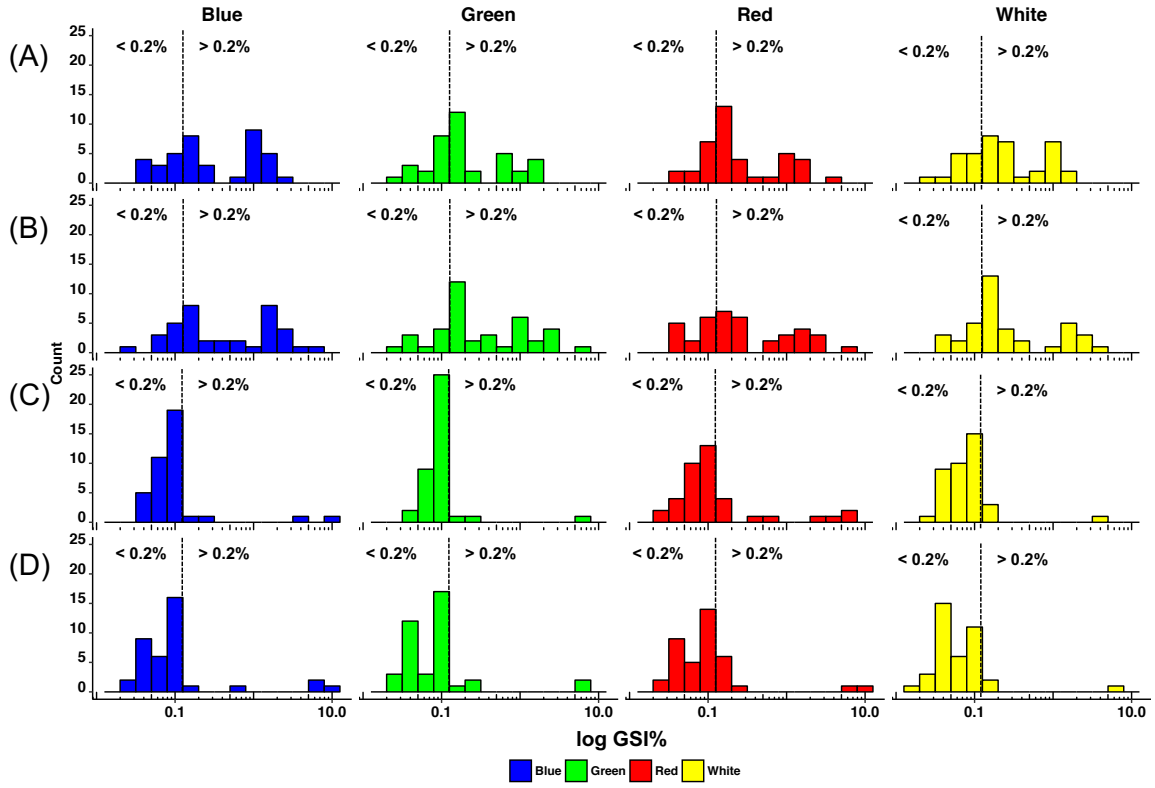

Figure 5.9. GSI distribution of male Atlantic salmon transferred to SW and (A) exposed to simulated natural photoperiod (SNP); (B) switched from SNP to continuous light (SNP-LL) after 1216 ºDays in SW; (C) exposed to continuous light (LL) or (D) switched from continuous LL to SNP. During the FW phase, fish were exposed to four different spectra (White; Blue; Green or Red) reflected by plot colours. GSI was determined at the end of the trial (1937 ºDays).

Table 5.3. Kruskall-Wallis comparison of percentiles from the distribution of GSI values from post-SW smolts exposed to SNP until 1213 ºDays and then exposed to either LL or maintained under SNP until 1937 ºDays. D= D statistic from Kruskall-Wallis test, P= p-value, significance <0.5

	Percentile	**5**		**10**		**50**		**95**		**99**	
Comparison		**D**	**P**	**D**	**P**	**D**	**P**	**D**	**P**	**D**	**P**
Blue SNP	Blue SNP-LL	0.12	0.45	0.00	0.50	-1.27	0.10	-1.62	0.05	-1.62	0.05
Green SNP	Green SNP-LL	0.35	0.36	0.23	0.41	-1.27	0.10	-2.08	0.02	-2.08	0.02
Red SNP	Red SNP-LL	1.56	0.06	1.79	0.04	-0.17	0.43	-0.75	0.23	-0.75	0.23
White SNP	White SNP-LL	-0.52	0.30	-0.29	0.39	-1.79	0.04	-1.44	0.07	-1.33	0.09

Table 5.4 Kruskall-Wallis comparison of percentiles from distribution of GSI values from post-seawater smolts exposed to LL for 1216 ºDays then exposed to SNP for a further 725 ºDays (sample point 1937 ºDays). D= D statistic from Kruskall-Wallis test, P= p-value, significance <0.5

	Percentile	**5**		**10**		**50**		**95**		**99**	
Comparison		**D**	**P**	**D**	**P**	**D**	**P**	**D**	**P**	**D**	**P**
Blue LL	Blue LL-SNP	1.15	0.12	1.56	0.06	-0.29	0.39	0.23	0.41	0.58	0.28
Green LL	Green LL - SNP	2.89	**0.00**	2.83	**0.00**	0.92	0.18	-0.40	0.34	-0.40	0.34
Red LL	Red LL-SNP	0.98	0.16	0.87	0.19	-0.35	0.36	-0.29	0.39	-0.52	0.30
White LL	White LL-SNP	1.91	**0.03**	1.67	**0.05**	1.21	**0.11**	-0.12	0.45	0.00	0.50

Overall Maturation

The level of maturation in fish exposed to both SNP (ranged 28-41%) and SNP-LL (range 28 to 50%) was considerably higher than fish exposed to LL (range 3-15%) or LL-SNP (range 3-11%) post SW transfer (Fig. 5.8). No significant differences were seen between fish classed as mature or immature under within the LL or LL-SNP groups.

Male Maturation

In groups exposed to LL, male maturation did not have a significant effect on weight (Table 5.5). In contrast, male maturation increased weights in groups exposed to SNP. In both the SNP-Blue (981 ± 170 g vs. 563 ± 105 g) and SNP-White (1017 ± 121 g vs. 516 ± 16 g) maturing males with a GSI >0.2% were significantly heavier. There was no statistical difference between either Green or Red males. In the SNP-LL group, fish previously exposed to Blue light with a GSI >0.2% were significantly heavier (996± 83 g vs. 588 ± 121g). No differences were seen in SNP-LL Green, Red or White.

No significant differences were seen in the numbers of fish that became either mature or immature in response to SNP. In the SNP to LL treatment, significantly more male fish became mature in the SNP-LL-Blue (78 % vs. 22 %) and SNP-LL-Green (74 % vs. 26 %) groups compared to remaining immature.

In response to LL, the LL-White group (4 % vs. 96 %) had a significantly lower proportion of maturing males. In groups exposed to LL-SNP, significant differences in the number of maturing males where recorded in response to LL-SNP-Red (89 % vs. 11 %) and LL-SNP-White (96 % vs. 4 %). No significant differences were seen in the other treatments. Again, the difference was significant in terms of the number of non-maturing fish. Results, particularly those based on the LL groups are derived from very small sample size and must be interpreted with this in mind.

Table 5.5 Weight of male Atlantic salmon with a GSI above and below a threshold value of 0.2 % indicative of pubertal recruitment (Leclercq et al. 2011). Maximum GSI is derived from highest value for each group. Percentages calculated as total per overall treatment group. Significant differences between GSI% and weight within GSI grouping (GSI < 0.2% or GSI > 0.2%) are denoted by upper case letters (Linear-mixed effects model, P =<0.5). Weight ± Stdev

Treatment	Total Fish	Total Males	GSI <0.2 %			GSI>0.2%			Maximum GSI%	Mean Male Population Weight
			No.	%	Mean Wt.	No.	%	Mean Wt.		
SNP Blue	39	24	8	33^{A}	563 ± 170^{C}	16	67^{A}	981 ± 105^{A}	2.2	772 ± 79
SNP Green	39	18	8	44^{A}	696 ± 124^{BC}	11	56^{A}	932 ± 162^{AB}	1.7	814 ± 203
SNP Red	40	17	5	29^{A}	545 ± 100^{C}	12	71^{A}	778 ± 65^{ABC}	3.3	662 ± 146
SNP White	39	19	7	37^{A}	516 ± 16^{C}	12	63^{A}	1017 ± 121^{A}	1.8	767 ± 48
SNP-LL Blue	38	23	5	22^{B}	588 ± 121^{BC}	18	78^{A}	996 ± 83^{A}	5.2	792 ± 116
SNP-LL Green	40	19	5	26^{B}	619 ± 198^{BC}	14	74^{A}	823 ± 144^{AB}	5.3	721 ± 167
SNP-LL Red	39	20	8	40^{AB}	485 ± 117^{C}	12	60^{AB}	770 ± 135^{ABC}	5.4	627.5 ± 22
SNP-LL White	39	15	6	40^{AB}	609 ± 118^{AB}	10	60^{AB}	838 ± 51^{AB}	4.3	724 ±16
LL Blue	39	15	12	80^{AB}	1026 ± 166^{AB}	3	20^{AB}	1113 ± 163^{AB}	9.3	1070 ± 129
LL Green	39	12	10	83^{AB}	1195 ± 66^{A}	2	17^{B}	961 ± 74^{AB}	5.9	1078 ± 143
LL Red	39	23	18	78^{AB}	933 ± 57^{B}	5	22^{AB}	947 ± 7^{AB}	7.7	940 ± 38
LL White	39	25	24	96^{A}	1059 ± 50^{AB}	1	4^{B}	891^{AB}	4.8	975 ± 56
LL-SNP Blue	39	18	14	78^{AB}	1056 ± 69^{A}	4	22^{CD}	1019 ± 222^{A}	8.2	1038 ± 68
LL-SNP Green	40	21	17	81^{AC}	1105 ± 90^{A}	4	19^{BCD}	958 ± 228^{A}	7.0	1032 ± 120
LL-SNP Red	39	19	17	89^{AB}	1092 ± 169^{A}	2	11^{cD}	768 ± 197^{A}	8.9	930 ±191
LL-SNP White	39	23	22	96^{A}	1290 ± 139^{A}	1	4^{D}	833 ± 51^{A}	6.8	1062 ± 31

Summary of male data - Thermal Growth Coefficient (TGC)

The influence of maturation on growth rates was evident in some groups immediately following SW transfer. The growth rate of Male fish with a final GSI <0.2% (Fig. 5.10 A) decreased significantly during the period -400 to 0 ºDays of the smoltification regime and increased significantly between the 0 to 240 ºDays, and 240 to 720 ºDays whereupon growth plateaued. In fish with a final GSI of >0.2 a similar pattern was identified. A decrease in TGC was observed for all groups during the period -400 to 0 ºDays whereupon growth rates increased in all groups until 732 ºDays where again growth plateaued.

In fish with a final GSI <0.2%, growth during -800 to -400 ºDays was significantly lower in SNP-Red compared to LL-Blue. In the following period -400 to 0 ºDays, growth in the SNP-White, SNP-Blue and LL-Blue groups was significantly lower than LL-Red. In the period 0 to 240 ºDays SNP-White and SNP-Blue and SNP-Red where significantly lower than LL-Green and LL-Red. Between 240 to 732 ºDays all SNP values were significantly lower than all LL values and no differences were seen within either SNP or LL groups, this was the same for the final period 732 to 1213 ºDays.

In fish with a final GSI >0.2 % for the period between -800 to -400 ºDays LL-White was significantly lower than LL-Blue. For the next two periods, -400 to 0 ºDays and 0 to 240 ºDays no significant differences in growth rate was seen between any group. For the period between 240 and 732 ºDays, SNP-White, SNP-Red were significantly lower than all of the LL treatments, SNP-Green was significantly lower than LL-White, LL-Blue and LL-Green and SNP-Blue was significantly lower than LL-Blue. For the sample period 732 to 1213 ºDays TGC was significantly lower in SNP-White, SNP-Green and SNP-Red compared to LL-Blue and LL-Green. No difference was seen between the remaining groups.

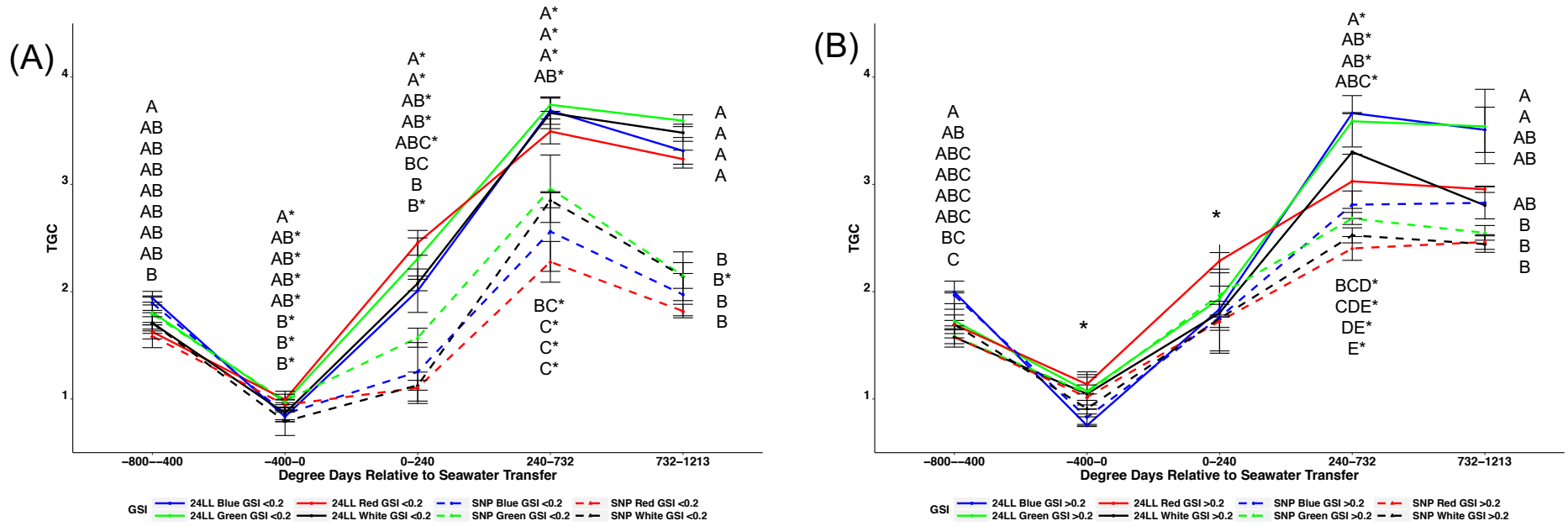

Figure 5.10. TGC (Mean ± SEM, n=3) of male Atlantic salmon transferred to SW tanks and illuminated using white light and subjected either to a simulated natural photoperiod (SNP- dashed line) or continuous lighting (LL-solid line). (**A**) shows individuals with a final GSI <0.2 % and (**B**) >0.2 %. During FW fish were exposed to four different spectral compositions (White; Blue; Green or Red) reflected by line colours. Significant differences between treatments at a given time are denoted by upper case letters, significant differences between times for a given treatment are denoted by an asterisk (Linear-mixed effects model, P =<0.5).

Individual TGC

Plotting individual TGC showed that growth rates where more variable in groups exposed to SNP and SNP-LL (Fig. 5.11A and B) than LL and LL-SNP (Fig. 5.11C and D). Reduced TGC in FW during SD (-800 to -400 ºDays) was observed in all groups. SNP and SNP-LL resulted in broadly linear growth post-SW transfer in both males and females whereas fish exposed to LL showed a sharp increase between SW transfer and 732 ºDays post-transfer before decreasing.

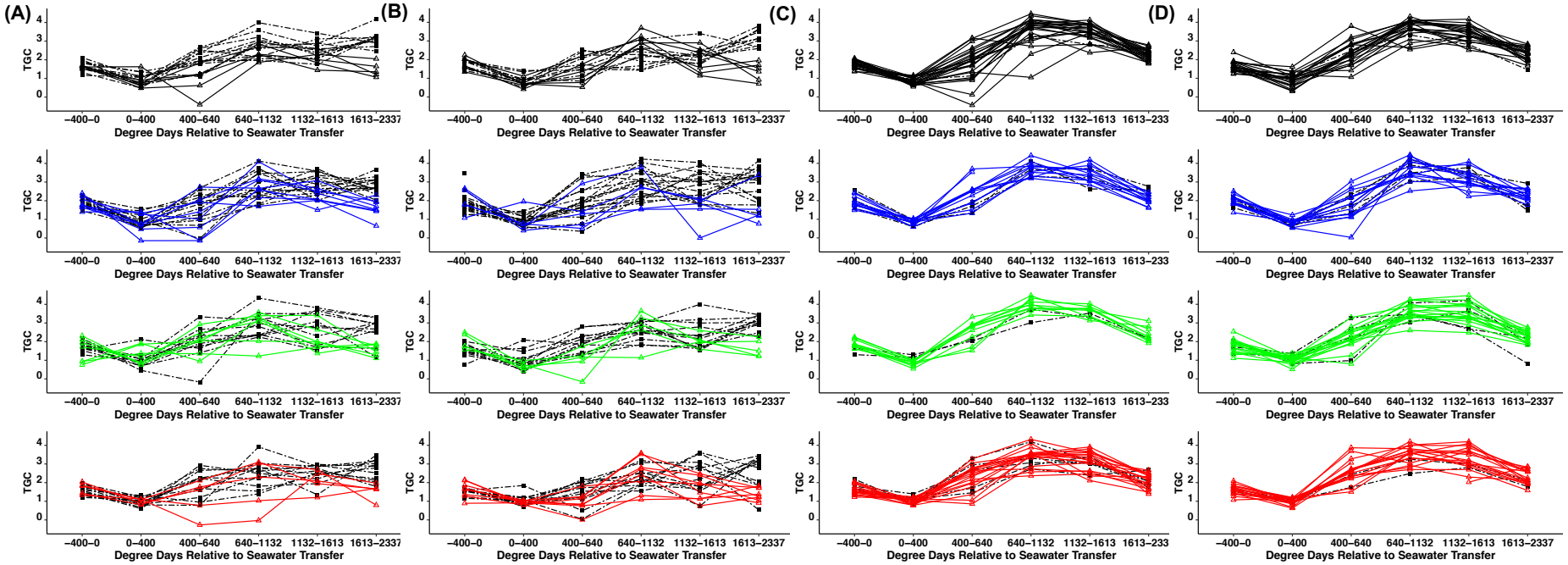

Figure 5.11. Individual Thermal growth coefficient (TGC) profile of Atlantic salmon transferred to SW and exposed to a simulated natural photoperiod (SNP) or switched to continuous light (LL) from 1213-1937 ºDays. Within each treatment males with a GSI >0.2 % are indicated by grey lines. (**A**) SNP males; (**B**): SNP-LL Males; (**C**): LL Males; (**D**): LL-SNP Males. During the FW phase, fish were exposed to four different spectra (White; Blue; Green or Red) reflected by line colours.

Summary of male data - Individual growth performance- Males

The weight of Male fish with a GSI >0.2 % (grey lines) grown under both SNP (Fig. 5.12A) and SNP-LL (Fig. 5.13.A) exhibited higher growth trajectories than those with a sub 0.2 % GSI (coloured lines). In response to LL, fish with a GSI >0.2 % were distributed more evenly within the population and no such trend could be identified based upon GSI (Fig 5.12B and 5.13B).

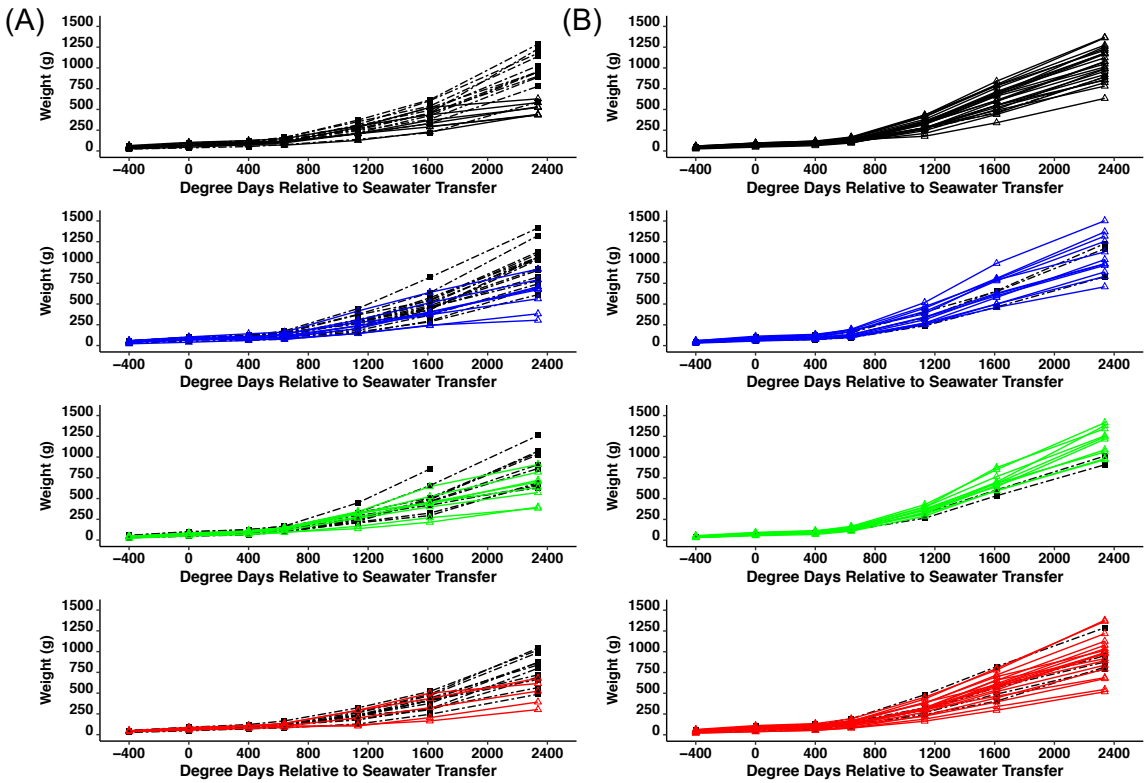

Figure 5.12. Weight of individual male fish exposed to white light during: (**A**) Simulated natural photoperiod (SNP); (**B**): continuous LL. During the FW phase, fish were exposed to four different spectra (White; Blue; Green or Red) reflected by line colours. GSI was determined at the end of the trial at 1937 ºDays, fish with a GSI >0.2 % are indicated by grey lines.

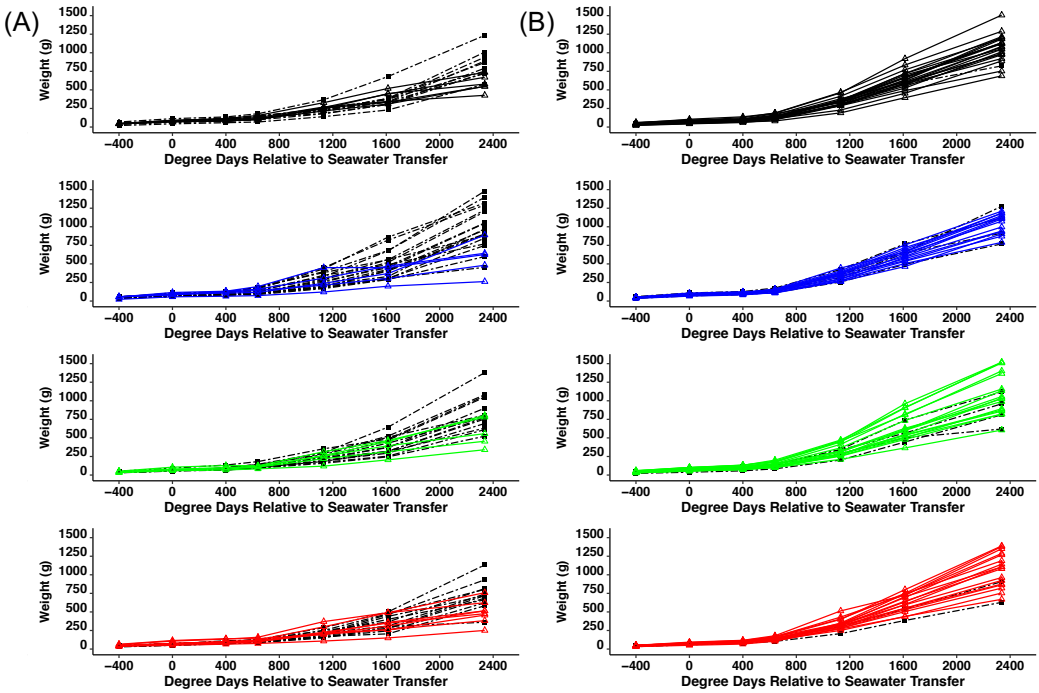

Figure 5.13. Weight of individual male fish exposed to white light during: (**A**) Simulated natural photoperiod (SNP and changed to continuous light from 1213 ºDays (LL); (**B**) continuous LL changed to SNP at 1913 ºDays. During the FW phase, fish were exposed to four different spectra (White; Blue; Green or Red) reflected by line colours. GSI% was determined at the end of the trial at 1937 ºDays, fish with a GSI >0.2 % are indicated by grey lines.

Summary of the Impact of GSI on Growth

Grouping fish by GSI showed significant differences between fish with a <0.2 % GSI exposed to either the SNP or SNP-LL photoperiod or LL and LL-SNP photoperiod (Fig. 5.14A) whereas no significant differences were observed between final weights of fish with a GSI >0.2 % for either the SNP or SNP-LL photoperiod or LL and LL-SNP photoperiod (Fig. 5.14B). Earlier differences are not shown.

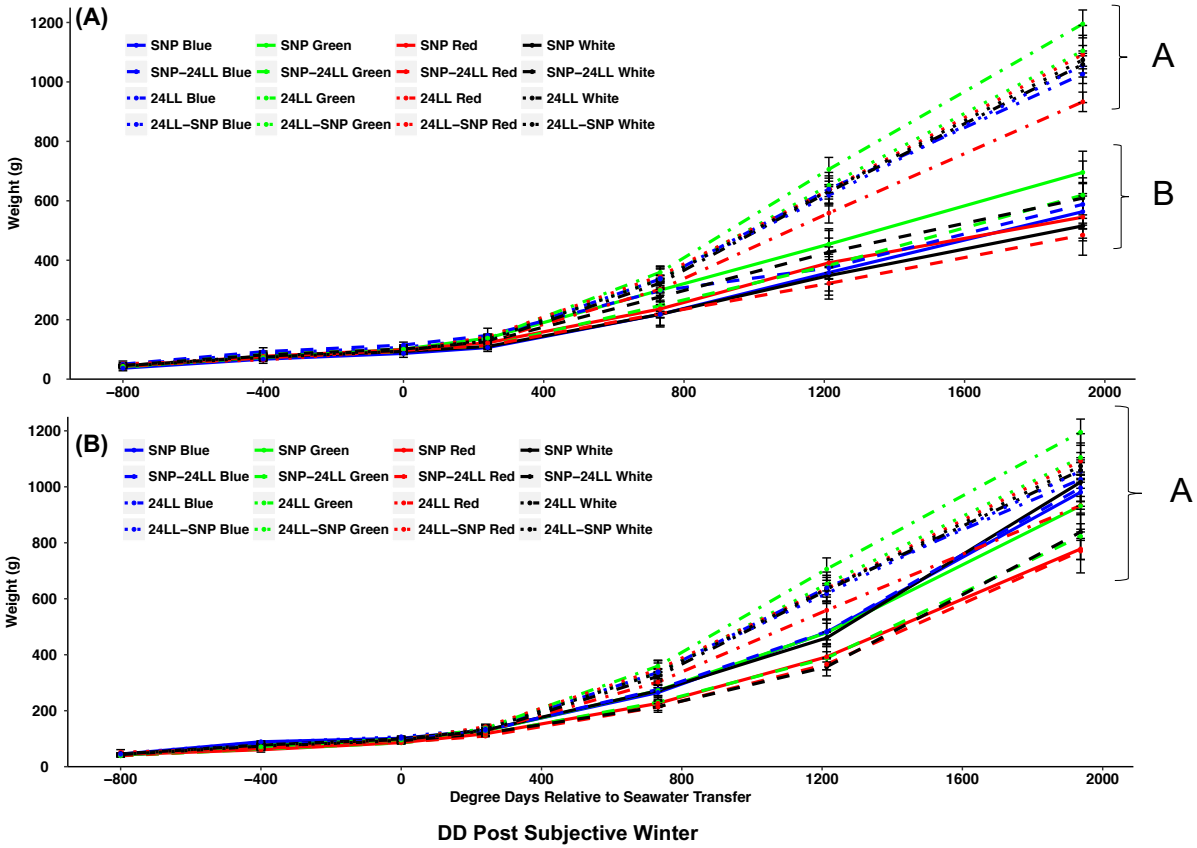

Figure 5.14. Weight (Mean ± SEM) of male Atlantic salmon transferred to SW and exposed either to Simulated natural photoperiod (SNP); SNP to continuous lighting (LL); LL or LL-SNP. Weight of male fish with a GSI <0.2 % (**A**) or a GSI >0.2 % (**B**) are shown. During the FW phase, fish were exposed to four different spectra (White; Blue; Green or Red) reflected by line colours. GSI was determined at the end of the trial at 1937 ºDays. Significant differences between treatments are shown only for the final time point and are denoted by upper case superscripts (Linear-mixed effects model, P =<0.5).

Predicting Maturation using BW, FL and TGC

GSI impacted both weight and growth rates throughout the SW period. To identify how early in development changes become apparent the distribution of males and females with final GSI% of <0.2% or > 0.2% are plotted as histograms (Fig. 5.15 and 5.16). The first sample point at which cohorts could be identified was at 1213 ºDays (Fig. 5.16B). At the end of the trial, male fish exposed to SNP with a GSI >0.2% were clearly clustered. Under LL, no such relationship was observed, maturing male fish were spread evenly throughout the population. In fish switched to the opposing photoperiod, a similar pattern was seen, SNP-LL closely resembled SNP and LL-SNP closely resembled LL (data not shown).

Correlation between TGC and GSI and Weight and GSI (Table 5.6) shows a significant positive correlation between TGC for the period -400 to 0 ºDays and 400 ºDays to 640 ºDays however this is not seen in the SNP group. These periods were prior to being switched to the opposing photoperiod. Between 1132 to 1613 ºDays and 1613 to 2337 ºDays both the SNP and SNP-LL treatment groups show a positive correlation between weight and GSI. A negative correlation is seen in the LL-SNP group for the period between 1613 ºDays and 2337 ºDays and this is also seen in the weight – GSI correlations for this group and time point. In both the SNP and SNP-LL groups a significant positive correlation between GSI and weight is seen at 2337 ºDays.

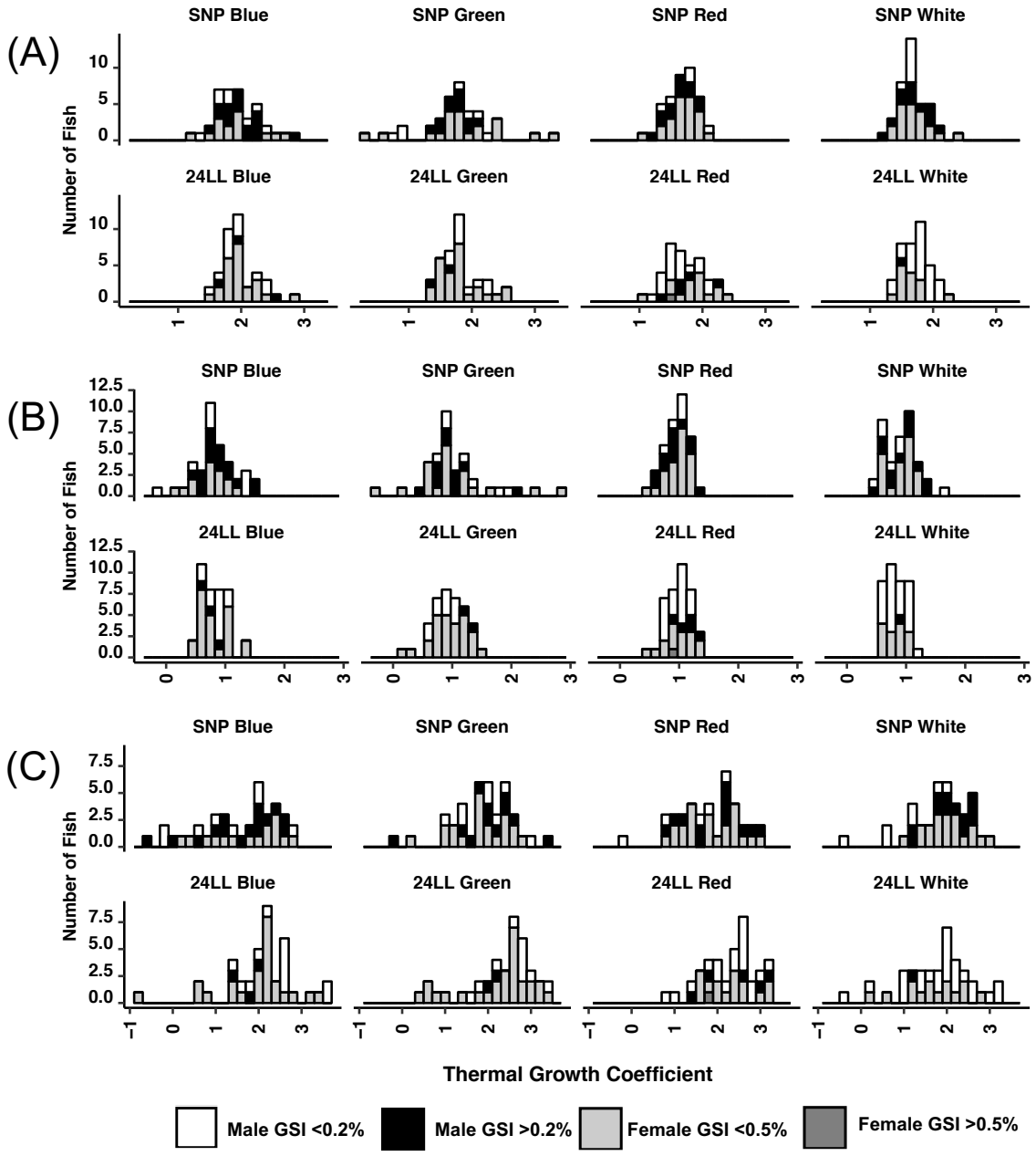

Figure 5.15. Thermal Growth Coefficient of male Atlantic salmon transferred to SW and exposed to simulated natural photoperiod (SNP) or continuous light (LL). Males are pooled from post-transfer photoperiod regime. A: minus 400 ºDays (FW), B: 0 ºDays (SW); C: 240 ºDays (SW).

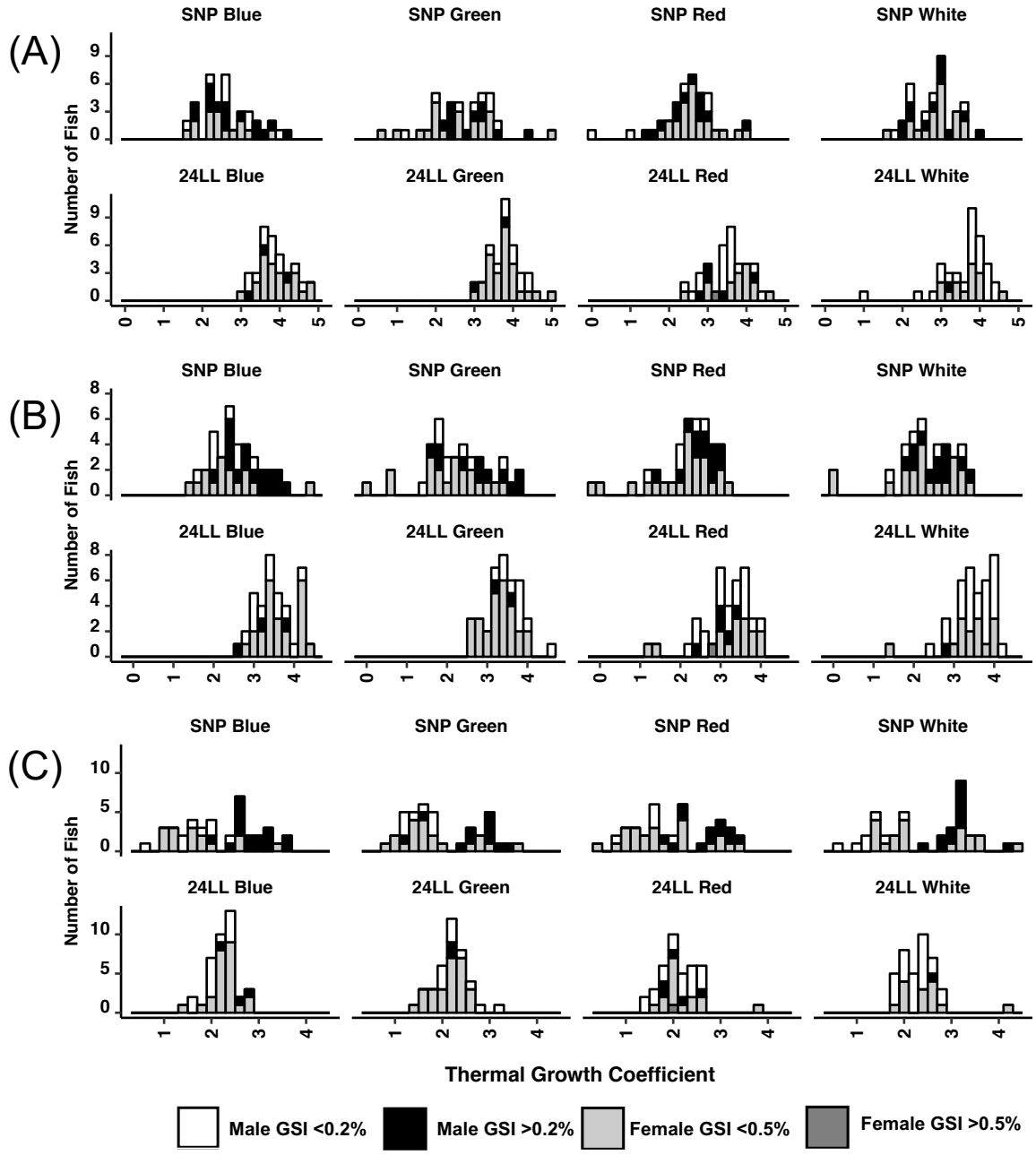

Figure 5.16. Thermal Growth Coefficient of male of male Atlantic salmon transferred to SW and exposed to simulated natural photoperiod (SNP) or continuous light (LL). Males are pooled from post-transfer photoperiod regime. A: 732 ºDays (SW), B: 1213 ºDays (SW); C: SNP 1937 ºDays (SW).

Table 5.6. Pearson product correlations for relationship between final GSI% and TGC and Weight during the trial.

		SNP		SNP-LL		LL		LL-SNP	
Metric and ºDays Relative to SW Transfer	**GSI%**	**Correlation**	**p-value**	**Correlation**	**p-value**	**Correlation**	**p-value**	**Correlation**	**p-value**
TGC -800 to -400 ºDays (FW)	**GSI**	0.08	0.49	-0.14	0.26	-0.05	0.69	0.06	0.57
TGC -400 to 0 ºDays (FW)	**GSI**	-0.09	0.44	0.23	**0.05**	0.14	0.24	-0.10	0.40
TGC 0 to 240 ºDays (SW)	**GSI**	0.16	0.18	0.40	**0.00**	-0.16	0.16	-0.13	0.23
TGC 240 to 732 ºDays (SW)	**GSI**	0.02	0.88	-0.12	0.32	-0.21	0.07	-0.20	0.07
TGC 732 to 1213 ºDays (SW)	**GSI**	0.29	**0.01**	0.38	**0.00**	-0.21	0.06	-0.11	0.35
TGC 1213 to 1937 ºDays (SW)	**GSI**	0.63	**0.00**	0.71	**0.00**	0.02	0.87	-0.48	**0.00**
-800 ºDays (FW)	**GSI**	0.12	0.30	-0.13	0.27	-0.04	0.74	0.00	0.97
-400 ºDays (FW)	**GSI**	0.14	0.24	-0.17	0.16	-0.04	0.71	0.02	0.85
Weight 0º Days (FW)	**GSI**	0.09	0.43	-0.11	0.37	0.00	0.98	-0.01	0.92
Weight 240 ºDays (SW)	**GSI**	0.16	0.17	0.11	0.35	-0.06	0.62	-0.08	0.49
Weight 732 ºDays (SW)	**GSI**	0.12	0.32	0.03	0.82	-0.13	0.26	-0.15	0.18
Weight 1213 ºDays (SW)	**GSI**	0.20	0.08	0.21	0.08	-0.19	0.11	-0.16	0.16
Weight 1937 ºDays (SW)	**GSI**	**0.46**	**0.00**	**0.55**	**0.00**	-0.17	0.15	**-0.32**	**0.00**

Female TGC

Female TGC in response to SNP and SNP-LL was broadly equivalent across all groups (Fig. 5.17A and B) and considerably more variable than under LL (Fig. 5.17C and D**).**

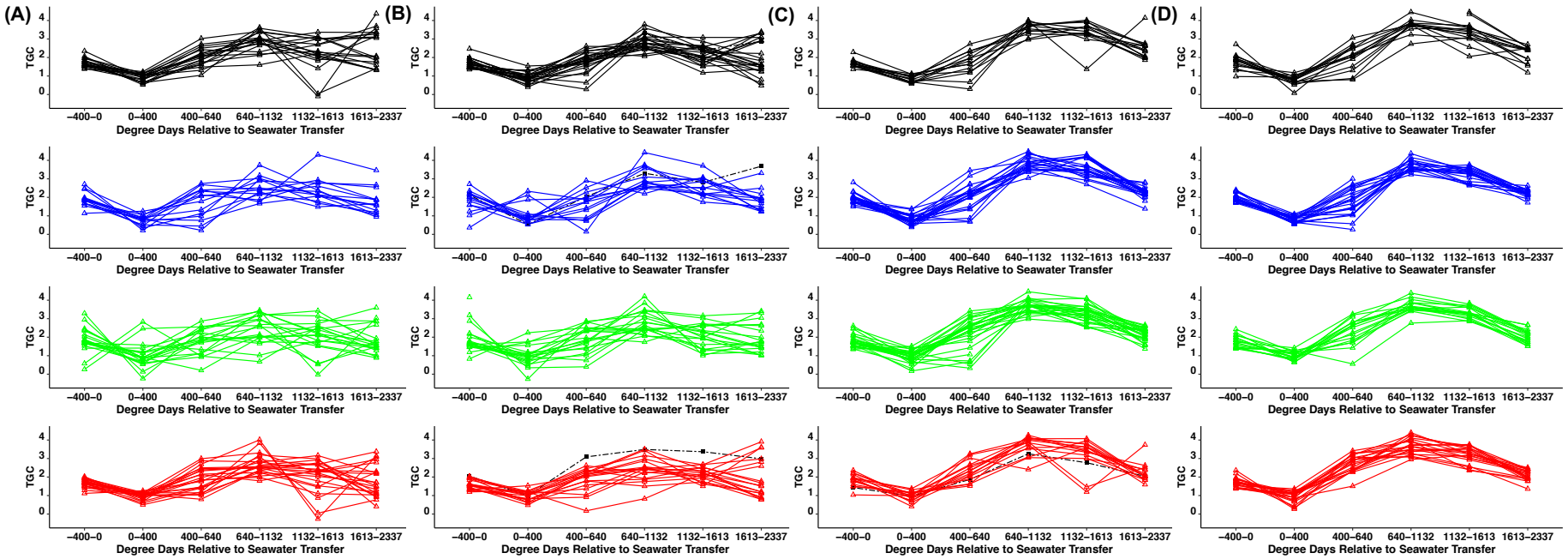

Figure 5.17 Individual Thermal growth coefficient (TGC) profile of Atlantic salmon transferred to SW and exposed to a simulated natural photoperiod (SNP) or switched to continuous light (LL) from 1213-1937 ºDays. Within each treatment females with a GSI >0.17 % are indicated by grey lines. (**A**) SNP Females; (**B**): SNP-LL Females; (**C**): LL Females; (**D**): LL-SNP Females. During the FW phase, fish were exposed to four different spectra (White; Blue; Green or Red) reflected by line colours.

Oogenesis

From the subset of female gonads examined, oocyte development was found to be in early primary growth (PG) phase (Fig. 5.18 A-L). Typically, the presence of cortical alveoli (CA) was observed in fish with a GSI above 0.5 %. From the samples processed, CA were found in one sample with a GSI of 0.17 %. To investigate this as a maturation indicator, individual TGC was plotted over time and those with a GSI higher than 0.17 % highlighted (Fig. 5.19). In fish exposed to White light during FW and a true LD "winter" higher GSI reflected higher TGC. Very early stage exogenous vitellogenesis was apparent in females with the highest GSI (Fig. 5.18N and O). All sections contained oocytes in early primary growth in addition to the later stages.

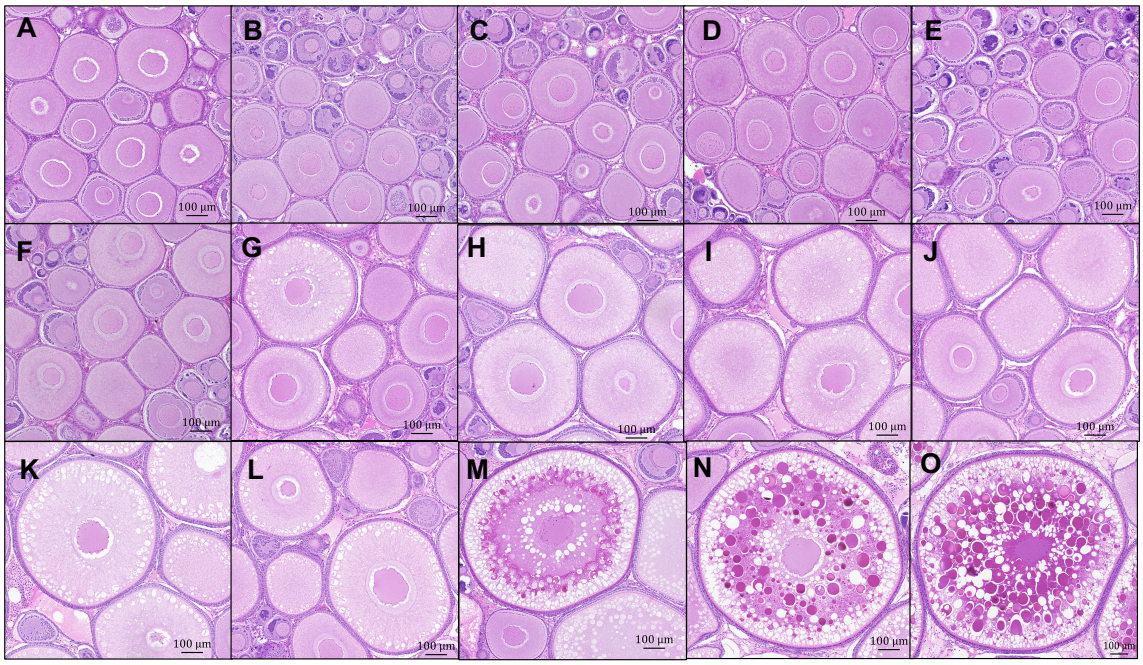

Stages of female oocyte development. Arranged in order of GSI. A: 0.08%; B: 0.11%; C:0.12%; D:0.15%; E:0.15%; F:0.18%; G:0.21%; H:0.22%; I:0.24%; J:0.25%; K:0.30%; L:0.31%; M:0.35%; N:0.50%; O:0.61%.

Figure 5.18. Histological examination of females according to GSI.

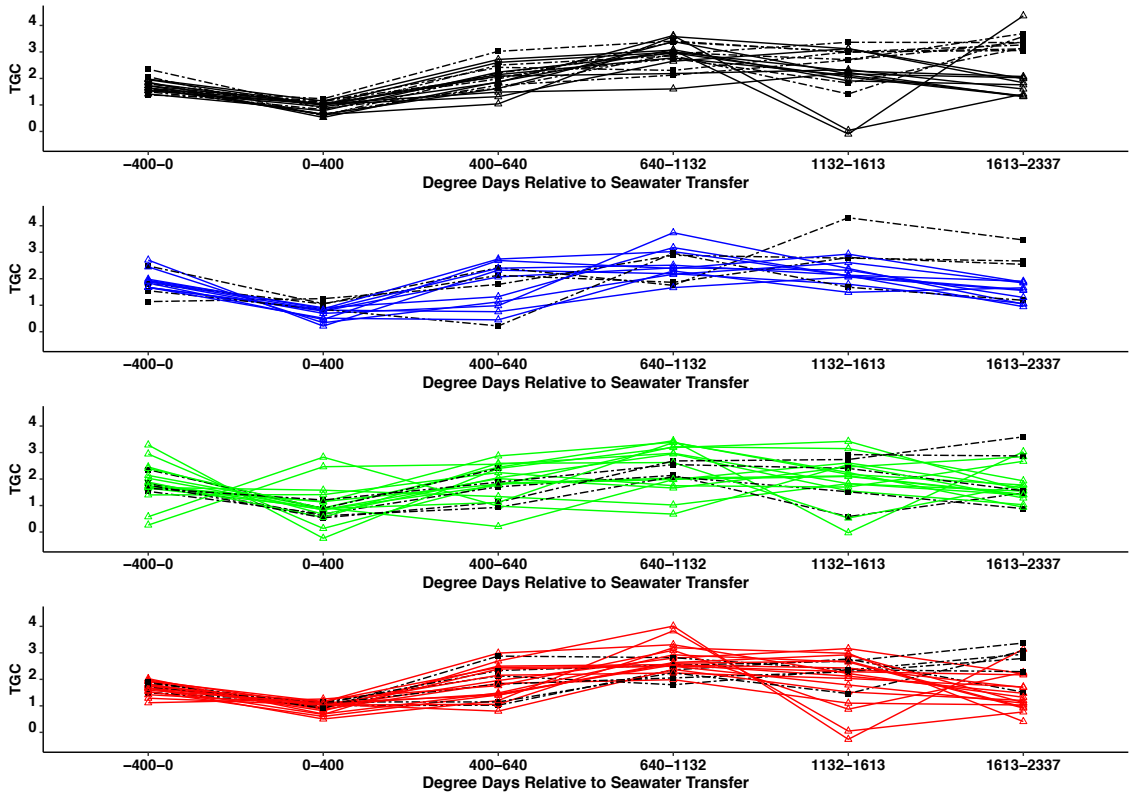

Figure 5.19. Individual Thermal Growth Coefficient (TGC) profile of female Atlantic salmon transferred to SW and exposed to a simulated natural photoperiod (SNP). Individual lines are based on repeat measures for individual fish. Fish with a GSI higher than 0.17 % are plotted as dashed lines for each treatment. Historic FW conditions are reflected by line colours.

Muscle Fibre

Progression Through Time

Growth altered the fibre diameter structure over time (Fig. 5.20). A reduction in fibre numbers per μm^2 from ~90 fibres in parr during freshwater and at the end of smoltification to ~45 μm^2 in fish exposed to SNP and ~28 μm^2 in fish exposed to continuous lighting (Data not shown).

During parr and smolt life stage no significant effects were seen on mean muscle fibre diameter between treatment (Fig. 5.20). A large increase in average diameter was seen after transfer to SW in all groups exposed to SNP and LL, fibres were the largest in the LL group and mean fibre diameter was significantly higher in the Green compared to the Blue and Red groups (Fig. 5.20B)

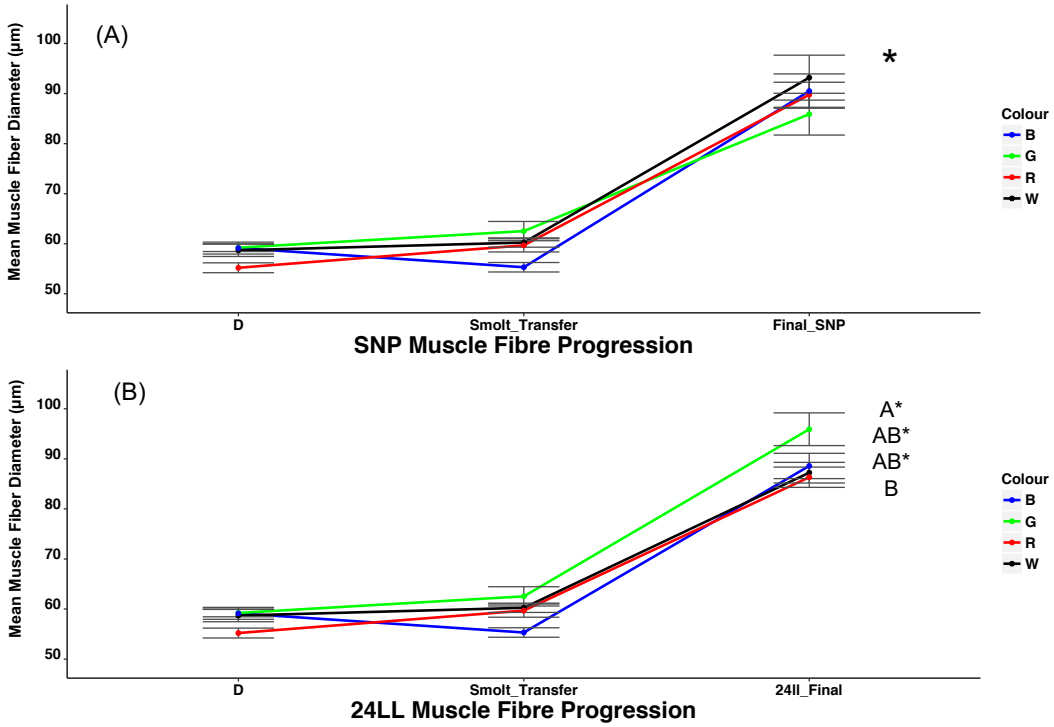

Figure 5.20. Muscle fibre size (Mean ± SEM, n = 3) of Atlantic salmon exposed during FW to four different spectra (White; Blue; Green or Red) indicated by line colours. Samples were collected from parr (sample point 'D') immediately prior to exposure to an out-of-season photoperiod regime (400 ºDays LD12:12 followed by 400 ºDays LL). Samples were then collected at smolt (sea transfer) and 1937 ºDays post-SW transfer (SW) exposed to **(A)** simulated natural photoperiod (SNP) or **(B)** continuous lighting (LL) using white light. Significant differences between treatments and time points are denoted by upper case superscripts (Linear-mixed effects model, P =<0.5).

Post-SW Transfer Muscle Fibre Recruitment

Following on-growing in SW fibre distribution changed in all treatments. The high number of small muscle fibres determined in the Blue treatment at the end of smoltification (chapter 4.4.2) was seen in the LL treatments with a larger cohort of fibres around 50 µm.

In the SNP treatment, such distribution was not detected. Small fibre recruitment (5^{th} quantile) between SNP groups was very consistent between treatments [p=0.86] (Table 5.7). Distribution comparisons between fish previously exposed to Blue, Red and White in FW and transferred to SNP in SW showed no significant difference between SNP-Blue and SNP-Red [p= 0.07], in addition no significant differences were seen between SNP-Red and SNP-White [p= 0.16]. Although significantly different

between SNP-Blue and SNP-White the p-value was high [p=0.04] compared to the contrasts against SNP-Green which were all <0.00 (Table 5.8). As seen in Fig 5.21A, B and D patterns observed were due to lower numbers of small fibres in the SNP-Green groups. No significant differences were observed between each quantile for any SNP group.

The distribution of muscle fibre in both the LL-Blue and LL-White were not significantly different [p=0.67] (Table 5.8). In contrast to results from fish exposed to SNP-Green, LL-Green displayed higher numbers of middle sized fibres compared to the other treatment groups (Fig. 5.23B). No significant differences were observed between quantiles in fish exposed to LL (Table 5.7).

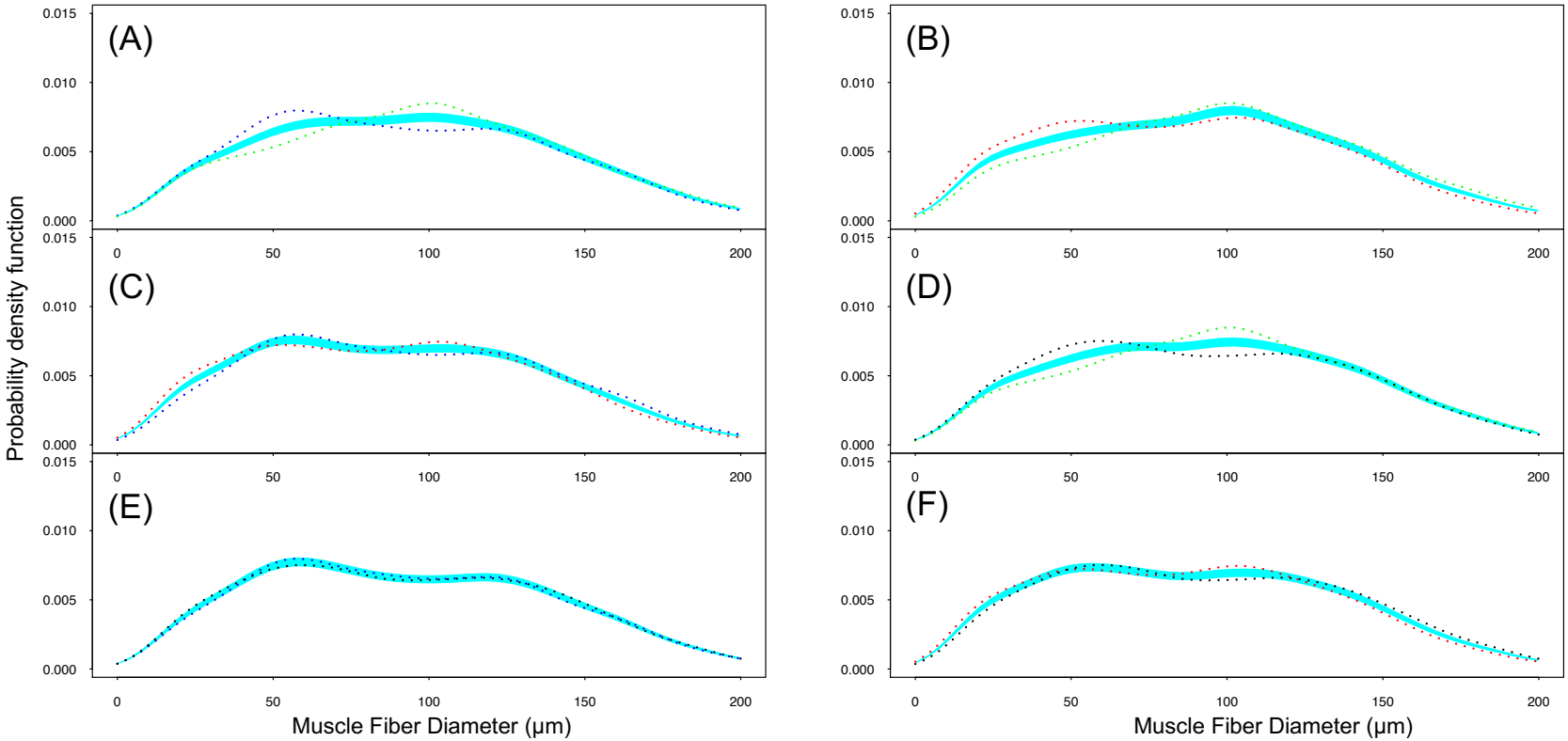

Figure 5.21. Muscle fibre distribution after rearing in seawater tanks for a period of 1937 ºDays (6 months) under a simulated natural photoperiod using white light. Atlantic salmon were exposed during FW to four different spectral compositions (White (black lines); Blue; Green or Red) indicated by line colour. Shaded area is combined probability density plot (PDF) for both treatments being contrasted. Coloured dashed lines are the PDF of each individual treatment. **(A)** Blue vs Green; **(B)** Green vs. Red; **(C)** Blue vs Red; **(D)** White vs Green; **(E)** Blue vs White; **(F)** Red vs White.

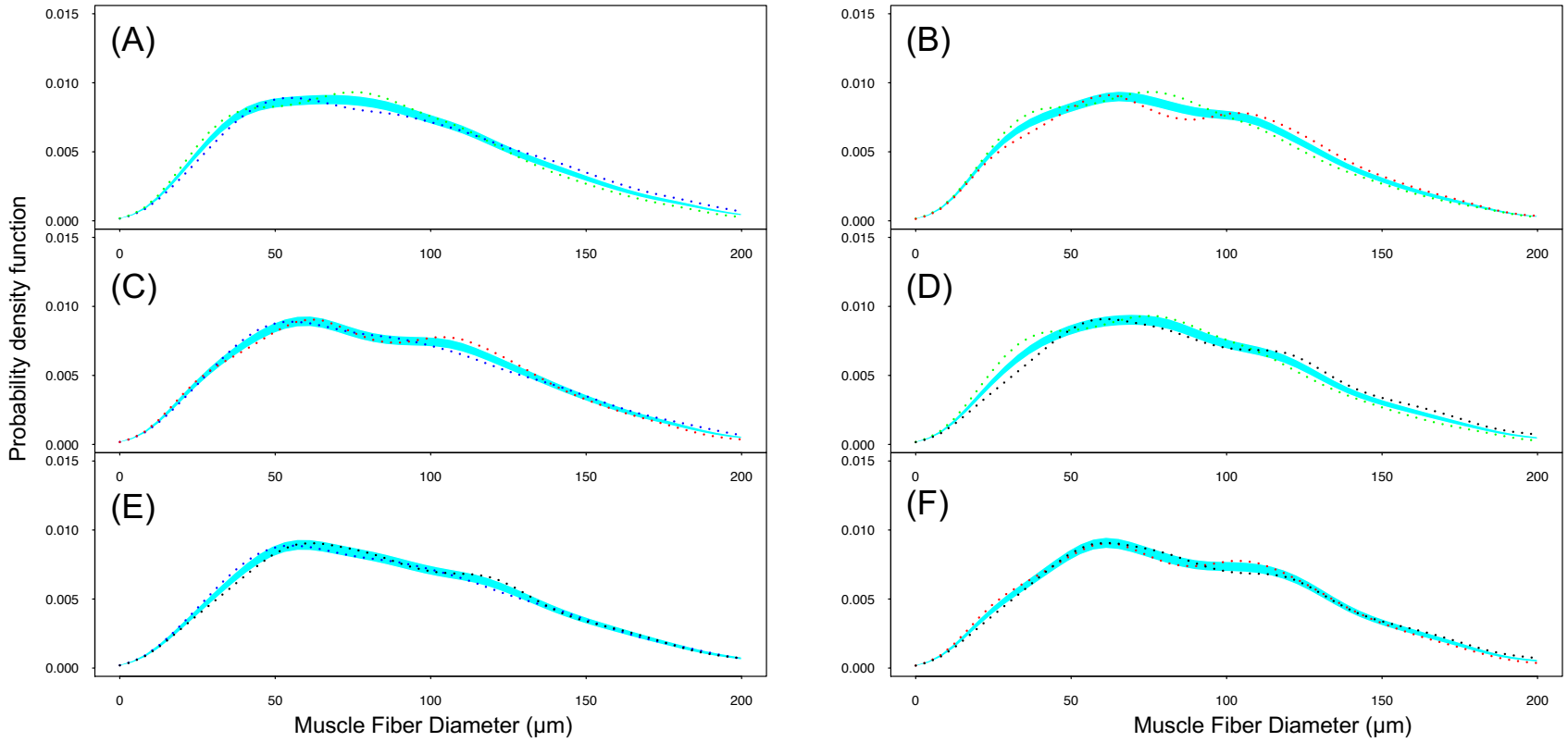

Figure 5.22. Muscle fibre distribution after rearing in seawater tanks for a period of 1937 ºDays (6 months) under a continuous white light immediately post-transfer. Atlantic salmon were exposed during the FW phase to four different spectra (White (black lines); Blue; Green or Red) indicated by line colours. Shaded area is combined probability density plot (PDF) for both treatments being contrasted. Coloured dashed lines are the PDF of each individual treatment. **(A)** Blue vs Green; **(B)** Green vs. Red; **(C)** Blue vs Red; **(D)** White vs Green; **(E)** Blue vs White; **(F)** Red vs White.

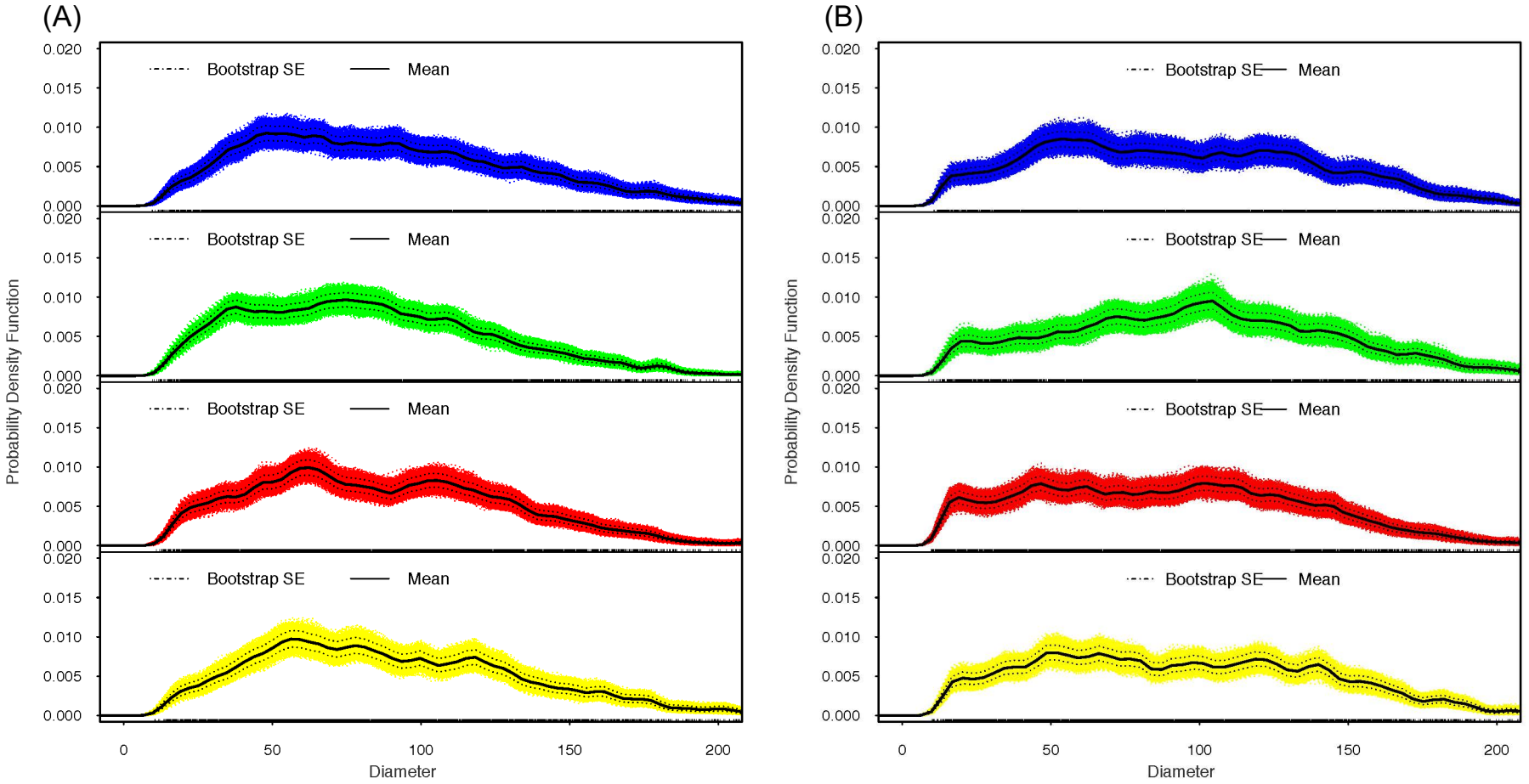

Figure 5.23. Variability band and mean (black line) of repeated bootstrapped probability density functions of muscle fibre diameter. Samples collected following subjection to either simulated natural photoperiod **(A)** or continuous **(B)** white light. During the FW phase, fish were exposed to four different spectra (White; Blue; Green or Red) indicated by line colours.

Table 5.7. Comparison of values determined from the percentiles of mean muscle fibre diameter in fish exposed to Blue (fB), Green (fG), Red (fR) and White (fW) during freshwater and smoltification and subsequently following exposure to either a simulated natural photoperiod (SNP) or continuous lighting (LL) using white light.

Sample Point	Percentile	Kruskall-Wallace *P*-value	Percentile for fB	S.E.M.	Percentile for fG	S.E.M.	Percentile for fR	S.E.M.	Percentile for fW	S.E.M.
SW SNP	**5%**	0.86	29.19	2.71	27.71	3.12	28.78	3.71	30.60	3.93
	10%	0.79	36.61	3.00	35.34	3.62	37.11	4.86	40.70	4.14
	50%	0.58	82.97	2.27	80.03	4.44	85.69	5.52	85.61	4.57
	95%	0.21	168.08	1.47	155.18	6.00	161.05	1.42	169.92	6.25
	99%	0.11	194.98	1.23	181.44	5.16	186.19	3.20	196.19	7.17
SW LL	**5%**	0.28	24.89	0.83	28.18	4.06	21.16	1.79	24.14	1.41
	10%	0.51	35.68	1.14	38.18	5.02	30.64	2.74	33.88	0.80
	50%	0.34	89.43	1.55	98.95	4.44	88.43	2.54	90.66	2.24
	95%	0.35	170.04	0.83	173.87	6.31	164.98	0.97	171.75	3.09
	99%	0.27	195.96	0.50	200.21	3.47	192.68	1.86	195.31	1.93

Table 5.8. Kolmogorov-Smirnov non-parametric bootstrap test for comparison of muscle fibre distribution between groups exposed to Blue (fB), Green (fG), Red (fR) and White (fW) treatment during freshwater and smoltification and subsequently exposed to either a simulated natural photoperiod (SNP) or continuous lighting (LL) using white light. Fish were sampled at the end of parr, at smolt transfer and trial termination.

Contrast: Treatment vs Treatment		**SW -SNP**		**SW – LL**	
		D	***P*-value**	**D**	***P*-value**
fB	**fG**	0.060	<0.000	0.081	<0.000
fB	**fR**	0.029	0.070	0.045	0.002
fB	**fW**	0.033	0.044	0.670	0.668
fG	**fR**	0.069	<0.000	0.10	<0.000
fG	**fW**	0.078	<0.000	0.080	<0.000
fR	**fW**	0.026	0.159	0.051	<0.000

Radiological Deformity

At the end of the trial, 1937 ºDays post-SW transfer, no significant differences in the percentage of individuals with at least one deformed vertebrae as assessed through x-ray were identified both within photoperiod or between photoperiods for any treatments (Fig. 5.24 and 5.25).

Results appear high due to including all fish with at least one deformed vertebrae. The threshold for concern is typically set at >5 deformed vertebrae per fish (Hansen et al., 2010). ~4% of fish in each group exhibited such a level with no significant differences between treatments (data not shown). Overall deformity levels are mid-range of the 12-73.3% reported in previous studies (Witten et al., 2006; Fjelldal et al., 2007, 2008).

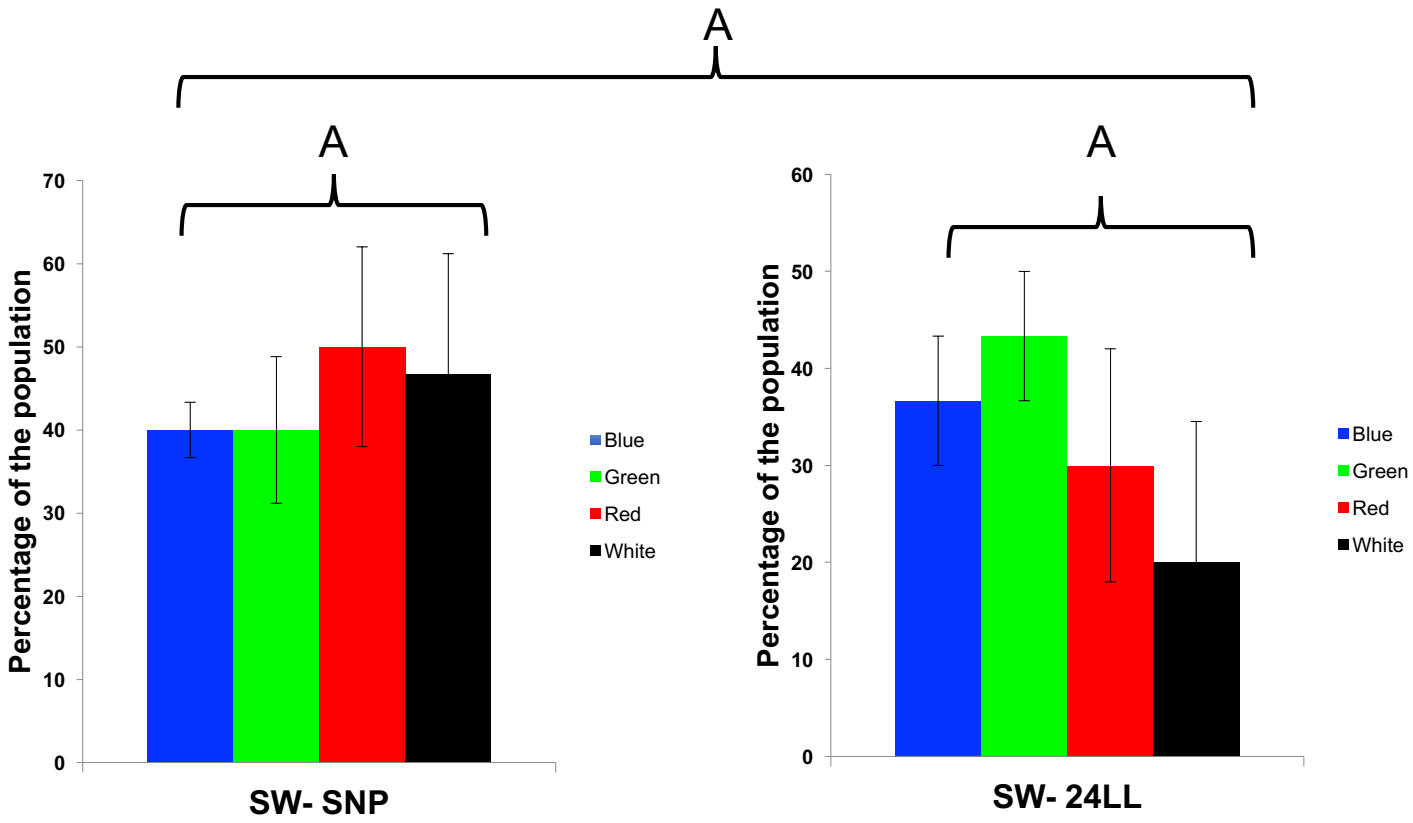

Figure 24. Comparison of Atlantic salmon with at least one deformed vertebrae between treatments following 16 weeks in sea water. Thirteen fish from each replicate based on FW photic history from with the SNP photoperiod or LL photoperiod were assessed using x-ray and classified according to Witten et al. (2009).

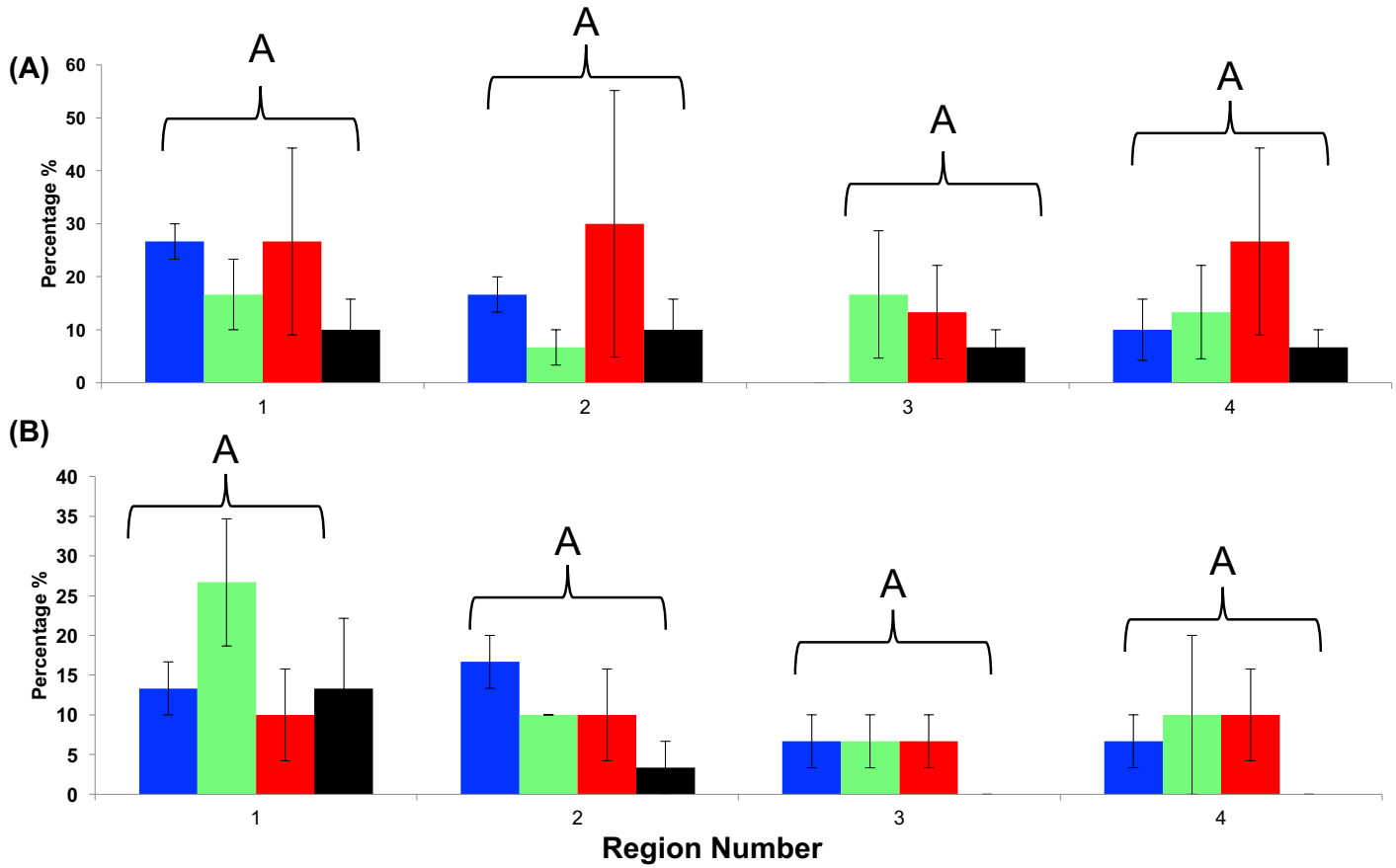

Figure 25. Comparison of Atlantic salmon with at least one deformed vertebrae between treatments following 16 weeks in sea water with deformities grouped by region. Thirteen fish from each replicate based on FW photic history from with the SNP photoperiod **(A)** or LL **(B)** photoperiod were assessed using x-ray and classified according to Witten et al. (2009).

5.4 Discussion

Results clearly showed that FW spectra had a lasting impact on post-transfer TGC, condition factor and bodyweight when transferred to SNP as SW development directly reflected the structure of weights observed during FW. Transferring to LL appeared to override differences evident at transfer between treatments and TGC, growth and muscle fibre development was positively influenced by LL. Changing photoperiods from hatchery to SW influenced pubertal recrudescence, which was higher (65 %) in post-smolts exposed to SNP compared to LL (15 %). Changing photoperiod after 4 months in SW resulted in a significant change in K for fish transferred from LL to SNP. GSI values increased in fish switched from SNP to LL and fish maintained under LL also exhibited a general increase in GSI suggestive of the start of recrudescence. Results provide new data for developing FW lighting regimes and for appropriate post-SW transfer photoperiods.

Effects of Spectral History on Post-SW Growth Performances Under Ambient Conditions

Growth during the freshwater developmental period for Atlantic salmon is low when compared to the increases seen during on-growing in seawater. However, the impact of this early phase on future growth potential is clearly seen in this trial. FW photic conditions resulted in long term growth effects in fish transferred to an ambient SNP photoperiod. Indeed, FW differences were maintained until the end of the trial in SW. Of the spectra tested, Blue compared favourably to the White control groups whereas Red light still had a negative effect on growth. Imsland et al. (2014) also demonstrated the importance of FW development growth reporting that stimulating growth during FW resulted in a 70-330 % higher weight after 14 months in SW. In addition, FW growth and SW performance were positively correlated in trials examining the effectiveness of restocking programs with heightened success ascribed to larger FW sizes (Connor et al., 2003; Miyakoshi et al., 2001) and in studies on Atlantic cod where supplementary lighting during early development led to enhanced growth which was still identifiable after 3 years in seawater (Imsland et al. 2007a).

Lasting differences in weights may be attributable to different growth trajectories between small and large fish. Red fish were significantly smaller at transfer than the Blue and White cohorts which performed better in SW. Growth trajectories

are sigmoidal in shape, accelerating throughout the juvenile stages before slowing at maturation (Dumas et al., 2010). Thus, smaller fish have a reduced trajectory compared to larger fish as absolute weight gain is greater in larger fish than smaller ones (Bureau et al., 2000). This effect is exacerbated by the low growth rates that occur when temperate ectotherm species experience seasonal temperature fluctuation such as in this trial. Post-transfer TGC was significantly higher than during the period between -400 to 0 ºDays of the smoltification regime and all SNP groups experienced a similar increase maintaining the population structure and serving to amplify earlier growth differences so that significantly lower values in the Red groups compared to the Blue for the period 240-732 ºDays and 732-1213 ºDays post SW transfer were seen.

In addition to TGC and BW, condition factor (K) showed significant differences based on FW history. K provides an accurate, non-lethal method of determining lipid content/energy reserves in immature salmon (Herbinger and Friars 1991). K reduced significantly following transfer to SW for all SNP groups with broadly equivalent changes between groups and the maintenance of pre-transfer structure. Nordgarden et al., 2003 reported a similar finding for fish exposed to SNP. K was significantly higher in both the Green and Red cohorts compared to the Blue and White treatments. Reductions in K are also a measure of SW readiness and the completion of smoltification (Bjornsson et al., 1989), and thus the current data may suggest that these groups were not as well SW adapted as Blue and White groups. The same contrasts were also apparent at 732 ºDays where the Green and Red groups had significantly higher K than the White group. Nutritional status, as reflected by K has can have important consequences for gated mechanisms which are suggested to influence decisions regarding pubertal recrudescence (Duston and Bromage 1988).

Effects of Photoperiods SNP and LL Post-SW Transfer on Growth

Exposing fish to LL immediately post-transfer resulted in a significantly higher TGC compared to SNP groups. Such was the impact that the decrease in condition factor seen in all SNP groups post-transfer was eradicated. While TGC under SNP was broadly equivalent, the response to LL was very different. All LL groups exhibited higher TGC compared to SNP as reported in many other trials (Imsland et al., 2007b; Porter et al., 1999; Oppedal et al., 1997; Saunders and Harmon 1988). The Red and Green groups, which performed the poorest during FW exhibited significantly higher

TGC than either the Blue or White treatments which performed best in FW. Interestingly, although smoltification in Red and Green may not have been advanced the additional K at transfer, suggestive of higher energy stores, may have helped fuel this growth. Following this initial enhanced period subsequent development occurred in concert with other LL treatments. The impact of this period was sufficient for significant differences in weights at transfer to be overcome and once this occurred no significant differences between treatments were seen at any future point in the trial.

The advancement in growth also reduced differences in K in contrast to fish exposed to SNP. Retardation of growth through periods of feed restriction (Stefansson et al., 2009) and other stressors such as high temperature (Nicieza and Metcalfe 1997), hypoxia (Foss and Imsland 2002) or high chemotherapeutant doses (Speare and Arsenault 1997) all showed enhanced growth rates upon a return to favourable conditions. Accelerated growth seen in the Red and Green group may then be considered as compensatory growth (CG) (Ali et al., 2003) initiated potentially as a response to the removal of prior stressful photic conditions. Growth retardation in FW in these groups may have stemmed from restricting feed intake either directly though poor prey visibility or as a result of photic conditions being directly stressful. In both *Oncorhynchus mykiss* (Karakatsouli et al., 2010) and red porgy *Pagrus pagrus* (Rotllant et al., 2003), reduced feed intake has been directly linked to photic conditions. It is intriguing why a similar response, albeit proportionally reduced, is not seen in the SNP treatment.

Atlantic salmon growth demonstrates considerably plasticity in response to genetic and environmental stimuli (Gjedrem 2012; Nicieza et al., 1994). The general overall observed increase in growth under LL as seen in this trial has been widely reported previously, as mentioned, and attributed to advances in growth cycles driven by postulated endogenous circannual rhythms (Nordgarden et al., 2003; Endal et al., 2000; Hansen et al., 1992; Krakenes et al., 1991; Saunders and Harmon 1988). Advancement sees enhanced spring and summer growth occurring out-of-season with similar end weights after a prolonged production cycle cited as evidence for this. However, increased feed appetite (Taranger et al., 1995), swimming activity (Herbert et al., 2011), or feed conversion (Totland et al., 2011) have also been shown to play an influential role. Continuous light stimulates feed intake (Nordgarden et al., 2003), increasing circulating IGF-1 and FGF2 hormone levels that stimulate somatic development (Chauvigné et al., 2003). Transferring fish to the opposing light regime

at 1213 ºdays post SW transfer for the LL treatment groups had no effect on weight although the duration was potentially too short to observe any statistically meaningful results. Changes in GSI do support though that the change in daylength in both groups was perceived. A significant drop in K was seen following switching from LL to SNP and as K is a proxy for nutrient/lipid status, changes support increased feed intake or feed conversion in response to LL.

Studies comparing harvest weights in groups where S1+ smolts were exposed from first sea winter to LL or SNP showed no significant differences in end weights (Nordgarden et al., 2003; Endal et al., 2000). Recorded TGC and K in the current trial were very similar to results by Nordgarden et al. (2003) examining 1SW S1+ smolts. However, a large discrepancy between start weights, ~120 g here vs. +1000 g in the previous trial, may affect long term results. Other studies have reported growth advantages attained in S1+ fish under LL continue through to harvest (Oppedal et al., 1997). A criticism of the current trial is the duration of 6 months in SW which was insufficient to determine if, over a production cycle, growth between the groups equalised. Periods of accelerated growth are typically followed by period of relative senescence owing to physiological growth restrictions (Morita and Fukuwaka 2006). Following periods of rapid growth underlying physiological homeostasis must be re-attained to ensure biological fitness. Rapid weight gain can impact or compromise swimming fitness (Munch and Conover 2003; Billerbeck and Lankford 2001), skeletal strength (Fjelldal et al., 2006; Arendt et al., 2001; Arendt 1997) and lead to reduced investment in existing protein structures (Morgan et al., 2000). No gross differences were observed between SNP and LL regarding vertebral deformity which suggests that bone growth was occurring within these physiological constraints. Re-attaining homeostasis requires time such that final BW between SNP and LL ends up the same over a prolonged production cycle (Nordgarden et al. 2003). Thus, instead of an advancement in endogenous seasonal rhythms, growth cycles may actually occur because of this required re-attainment of fitness.

Effects of Spectral History and SW Photoperiods on Muscle Fibre Recruitment and Development

The rate of somatic development stems from the relationship between protein synthesis, growth and protein degradation, the manifestation of which is muscle deposition (Houlihan et al., 1995; Houlihan et al., 1993). Whilst the rate is strongly

correlated to feed intake, the rate of degradation (Morgan et al., 2000) and structure of muscle fibre populations in terms of large and small fibres can also exert a large influence on growth (Arendt 1997).

At the end of the trial, muscle fibre populations in fish exposed to Green light during FW and transferred to SNP exhibited fewer small fibres (<50 μm) and more medium (~100 μm) fibres compared to the SNP-Blue, SNP-Red and SNP-White groups (Johnston et al., 1999). The Red and White showed significantly similar profiles. No significant differences were seen between the percentiles in either this group or the LL groups and showed that despite differences in weight, muscle structure was homogenous. Gross weight differences between SNP and LL are likely explained by the observed hypertrophy of existing fibres which reached maturity at ~200 μm as previously reported in salmonids owing to suggested diffusional constraints (Johnston et al., 1999; Suresh and Sheehan 1998). In response to continuous light, LL-White and LL-Blue showed similar distributions and population structure may reflect the close spectral output from the Blue and White LEDs. In each of the LL groups muscle fibre recruitment was similar to SNP, the low values that described the 5th percentile demonstrated that recruitment was still actively occurring. Seasonal growth profiles are proposed to occur through waves of recruitment followed by periods of hypertrophy (Johnston et al., 1999) however both hypertrophy and recruitment were shown in these groups. LL has been suggested to have a photostimulatory effect leading to enhanced MPC proliferation (Johnston et al., 2003). S1+ smolts exposed to LL for ~1 month prior to winter solstice experience a 40 day period of enhanced muscle fibre recruitment after which levels returned to those seen under SNP leading to growth benefits remaining (Johnston et al., 2003). The eradication of the structure of weights that can be observed in response to SNP is suggestive of photostimulation. In combination with a large cohort of small fibres in the Red and Green groups enhanced MPC proliferation augmented the advancement of seasonal growth profiles to remove differences in weight.

Small fibres though do not necessarily equate to future growth, changes in muscle fibre distribution similar to those seen here were reported to remain after a production cycle despite terminal weights being significantly similar (Johnston et al., 2004). Muscle fibre number though has the potential to influence post-harvest fillet quality and gaping (Johnston et al., 2000). Unfortunately, this trial could not proceed beyond 6 months in SW and was limited to a random selection from the LL and SNP

groups owing to constraints within the sampling method. A comparison of mature versus immature and also male vs female would have added further to the discussion and the influence of these variables is unknown. Following this trial to its conclusion and identifying the final weight and fibre number at harvest would also have contributed further to the discussion on growth physiology. In addition, feed intake has been linked to MPC proliferation (Chauvigné et al., 2003) and greater intake related to growth enhancement (Nordgarden et al., 2003) which due to technical constraints was also unable to be performed. In this trial, all fish were fed to the same percentage of BW and for the same hours and duration each day. Understanding the long-term influence of FW photic history on growth, feed intake and muscle structure would help to understand the action of LL on S0+ smolts.

Effects of Maturation and Gender on Growth in SW

Abrupt alterations in day length, rather than absolute duration, are capable of inducing seasonality and instigating developmental changes (Thrush et al., 1994; Duston and Bromage 1988). Just one female out of all the tanks was classed as maturing when using a threshold of 0.5 % as determined by Leclercq (personal comms). Maturation in males using a threshold of 0.2 % (GSI) (Leclercq et al., 2010) was significantly influenced by photoperiod regime. Prior to transfer, fish were maintained under LL and a transfer to SNP represented a change from long day to short day previously shown to induce maturation (Duncan et al., 2000; Taranger et al., 1999; Taranger et al., 1998) resulting in ~ 65 % male recruited. The use of a long day photoperiod, such as LL in this trial in both the hatchery and post-transfer is known to inhibit maturation (Taranger et al., 2010; Bromage et al., 1990; Bromage et al., 1982; Eriksson and Lundqvist 1980) resulting in approximately 15 % of the male stock classed as maturing. Both treatments were in line with those described by Taranger (1998) who reported a male maturation rate of 74 % compared to 16 % in S1+ stocks exposed to LL.

In the switched treatments, gross maturation rate was broadly similar however distinct changes in GSI were observed. A significant increase was apparent in gonadal development in the SNP-LL males compared to SNP as fish experienced LL-SNP-LL from the hatchery. Perception of changes in daylength are relative to previous photic conditions, photoperiods considered as ‘long’ such as 13.5:11.5 or LD18:6 can be perceived as short (Randall et al., 1998) and ‘short’ days LD 6:18, LD 8.5:15.5 can be perceived as long if the contrasting photoperiod is sufficiently different, i.e. LD 2:22 or

LD 1.5:22.5 in the case of short days perceived as long (Randall et al., 1998; Randall et al., 1991; Randall et al., 1987). Here the change from SNP to LL was 7 hours and clearly sufficient to provide a seasonal cue.

Pubertal recrudescence appears to be determined by a range of gated mechanisms and genetic inputs (Taranger et al., 2010) and whilst photic conditions may provide sufficient seasonal cues, suitable body size, fat reserves, and food intake constraints need to be met before progression can occur (Liu and Duston 2016; Sloat et al., 2014; Bromage et al., 2001; Thorpe et al., 1998). Early pubertal recrudescence, stimulated by enhanced GH and circulating sex steroids stimulate development during early gonadogenesis and thus comparatively higher growth, as seen here, and in other trials, (e.g. Kadri et al., 1996) occurs. Recent growth history as opposed to absolute body size may also play an important role in the decision to mature as seen in chum salmon *(Oncorhynchus keta*) (Morita and Fukuwaka 2006). Higher recrudescence in the LL group of fish exposed to Blue, Green and Red during FW was observed in this trial and unlike in the control treatment, these groups did not receive a true light dark photoperiod during smoltification. Whilst care must be given to any interpretation given how few individuals matured within these groups it may be possible that either spectrum or historic photic conditions led to this change.

Prolonged exposure to LL also resulted in differences between the LL and LL-SNP groups as GSI increased under LL as reported by Bromage et al. (2001). Interestingly, this was coupled with a continuation of K similar to the pre-switch level and while K in the cohort transferred from LL-SNP decreased, no rise in GSI was seen. The duration of supplementary lighting to prevent early maturation has received significant attention for S1 smolt cohorts (1 sea winter salmon), but little regarding S0+ smolts. Here, timings based on this trial would suggest an optimised regime of LL reduced to SNP at around 1200 ºDays post-transfer or once day length reaches 17 hours although results must be interpreted within context of the short duration of this trial. The maximum GSI from across the photoperiod groups was found in both the LL and LL-SNP groups and was accompanied with low BW suggesting pubertal anorexia and a reallocation of somatic resources to the gonads (Kadri et al., 1997). Such changes clearly demonstrate the importance of preventing maturation (McClure et al., 2007).

The impact of maturation on weight varied depending upon photoperiod stimulating growth under SNP and reducing growth under LL. A significant positive correlation in

response to SNP between final weight and GSI was seen compared to a negative correlation in the LL. Early prediction of maturation would be a useful tool for producers to identify and remove early maturing fish however metrics identified here do not seem suitable. Weight itself is a poor predictor of early maturation (Taranger et al., 1998) and the relationship between maturation status and weight/GSI was not found in this study until 1213 ºDays post SW transfer. Kadri et al. (1997) suggested that FL was more accurate however neither metric performed well at predicting future maturation status in the current trial. Despite immediate differences in TGC at SW transfer, correlation between TGC was also not sufficient to identify early maturation. Changes in TGC however suggested that the decision to mature occurs quickly once a stimulatory photoperiod is delivered. Correlations between TGC and maturation status were significant in the SNP to LL group, at the same point at which BW and FL were also suitable. Continuous light in this trial not only promoted extra growth but also reduced recruitment into maturation. Results were in accordance with those by Oppedal et al. (2003) who recorded reduced gonadal recrudescence in underyearling smolts exposed to LL from transfer.

In the present trial, no sexually dimorphic growth rates could be seen at any stage including during FW (results not shown). Results are in contrast to Leclercq et al. (2010) who reported sexual size dimorphism from an immature stage. Examination in that trial occurred from ~ 2 kg suggesting that dimorphic differences occur later in development and determining early maturing fish based on dimorphic growth can only be utilised later in the production cycle. The random distribution of maturing fish amongst the population suggests a genetic predisposition. Genetic, environmental, and biological factors work in concert to influence the timing of puberty (Sloat et al., 2014) and male Atlantic salmon are known to adopt different life strategies to ensure breeding success (Fleming 1996). Contributions by precocious parr on population genetics are demonstrably large, it is likely that ‘jacking’ may also play an important role in genetic diversity (Esteve 2005; Hutchings and Myers 1994).

Final oocyte maturation and expansion in female Atlantic salmon is concise, occurring in a two week window which sees GSI rise to around 25 % (Taranger et al., 2010). This brevity requires considerable preadaptation and a leading cohort of oocytes enter into secondary growth at least a year before spawning, notable by the presence of cortical alveoli (Andersson et al., 2009). Oocytes in both the SNP and LL treatments showed varying degrees of development with both primary and secondary growth

phases observed in some ovarian tissue. Histological examination showed that, of those tested, one sample had identifiable cortical alveoli at 0.17 %. This separation of higher TGC in females with a GSI >0.17 % was only seen in the White group. The White group however was the only group to experience a true light dark during S0+ induction and, although very speculative, may suggest that the use of low level lighting during the night stage of the 'winter' photoperiod in S0+ fish may inhibit early maturation. Further investigation into sexually dimorphic light responses are required.

Conclusions

This trial clearly showed that FW photic history can have a large impact on growth and development following transfer to seawater. Exposing S0+ post-smolts to different photoperiods induced changes in maturation as described in S1+ stocks albeit with changes occurring early following SW transfer. Using LL and suitable environmental conditions (temperature, light and feed), growth can occur at an increased rate. Cohorts that performed less well during FW exhibited immediate enhanced growth under LL such that no significant differences between FW treatments groups were apparent after 6 months at sea. The removal of these differences shows a photostimulatory influence from LL, the duration of this accelerated rate however cannot be determined from this trial. Muscle fibre data demonstrated key differences in structure between the LL and SNP groups. Underlying muscle fibre populations showed similar recruitment under continuous light to that seen under SNP suggesting that growth advantages may continue until harvest however this is speculative at this stage. Although previous studies have shown that at harvest SNP and LL cohorts exhibit similar final weights we identified a large number of males exhibiting pubertal recrudescence likely to lead to pubertal anorexia and reduced weights. Thus, based on these results the use of LL represents a win-win situation, maturation is decreased whilst growth, at least initially, is enhanced. As eluded to, timing of LL application should be carefully managed and here transferring S0+ smolts to LL for a period of 1200 ºDays post-transfer achieved both growth benefits and maintained GSI at very low levels.

6 Neural Activation in Photosensitive Brain Regions of Atlantic Salmon

This work was performed as a collaboration between the Institute of Aquaculture University of Stirling (UoS) and the Biology Department, University of Bergen (UoB). The second trial was performed at UoS and sample generation, timing, husbandry organised and performed by myself. The perfusion, insitu-hybridisation including all preparatory work for the RNA probes and analysis was performed by Mariann Eilertsen (ME) and Vidar Helvik UoB.

6.1 Introduction

In the previous chapters the downstream assimilation of photic conditions has been investigated in terms of physiological response. The initial signal driving such changes occurs through the activation of photoreceptors by incident light leads which conveys both visual and non-visual information to the brain. In addition to peripheral sensory organs such as the eyes, teleost fish have a broad range of directly photosensitive tissues including the pineal complex, the dermas and of increasing interest, the deep brain (Davies et al., 2010; Fernandes et al., 2013; Davies et al., 2015a; Garc'ia-Fernández et al., 2015). In the deep brain a considerable number of photoperception components have now been identified (Drivenes et al., 2003; Fernandes et al., 2012; Sandbakken et al., 2012; Eilertsen et al., 2014; Davies et al., 2015a; Hang et al., 2016). Changes in photoperiod induce distinct physiological processes and entrain developmental rhythms which drive ontogenic change in many species. Whilst the role of sensory organs such as the eye and pineal have defined links to visual and seasonal perception respectively, the specific functionality of non-visual photoreceptor networks is still poorly understood.

The characterisation and localisation of melanopsin to intrinsically photosensitive retinal ganglion cells in mammalian retina had major repercussions on the understanding of how circadian and pupillary reflexes occur in higher vertebrates (Peirson et al., 2009). In teleost's, a major advance regarding non-visual photoperception came from the characterisation of vertebrate ancient opsin (VA). Originally described in the horizontal and retinal ganglion cells of Atlantic salmon (Soni et al. 1998). VA opsin also is found in both the pineal and hypo / epithalmic brain regions (Davies et al. 2015b) where a defined function as a central photopigment for

non-visual extraretinal photoperception has been described (Philp et al. 2000). In the fishes, melanopsin-expressing cells in the preoptic area, likely in collaboration with other opsins, are responsible for light seeking behavior following exposure to darkness in zebrafish (*Danio rerio*) larvae lacking eyes and pineal glands (Fernandes et al., 2012).

Seasonal photoperception is also suggested to occur in other organs such as the saccus vasculosus (SV). In masu salmon (*Oncorhynchus masou*) stimulation of the SV with light leads to the upregulation of key genes regulating seasonal reproduction such as thyroid stimulating hormone (*TSHβ),* TSH receptor *TSHR,* common glycoproteins α-subunit (*CGA1)*, and type 2 iodothyronine deiodinase (*DIO2)* which converts the prohormone thyroxine (T4) into the bioactive hormone 3,3′,5-triiodothyronine (T3) and is suggested to play a central role in smoltification (Handeland et al., 2013). Expression of the opsins rhodopsin (RH1), short-wave sensitive SWS1, long wave sensitive (LWS) and opsin 5 (OPN4) have also been described in the SV (Nakane et al., 2013; Maeda et al., 2015) however it is not known what role these play. The clearest evidence of a role in seasonality is seen in VS excised males where compromised gonadal development is recorded (Nakane et al., 2013).

Identification of neuronal activation can be determined using the immediate-early gene *c-fos* (Bullitt 1990; Sheng and Greenberg 1990). Upregulation has been ascribed to brain activity in light stimulation experiments in mammals (Rusak et al., 1990; Schwartz et al., 1994) and fish (Moore and Whitmore 2014). Recently photosensitivity of the hindbrain cluster and hatching gland cells of halibut eggs (*Hippoglossus hippoglossus)* hatched through dark-induction has been identified using the co-localisation of melanopsins, VA opsin and *c-fos* (Eilertsen 2014). Elevated c-fos expression reflects distinct changes in neural activity in response to alterations in sensory input (Moore and Whitmore 2014). Zebrafish exhibit strong responses to changing photic conditions such as during light-dark transition determined by enhanced *c-fos* expression co-localised to brain regions with deep brain photoreceptors.

Seasonality in the Atlantic salmon (*Salmo salar*) is well described and influence by changes in diurnal photoperiods which entrain endogenous oscillators (Falcón et al., 2010). Changes in day length instigate physiological changes in growth, timing of smoltification, migration and maturation (McCormick et al., 1998; Bromage et al.,

2001; Stefansson et al., 2008). Given the influence of photoperiod, Atlantic salmon are an interesting species to study the underlying mechanisms of photo driven brain activity. The present study aimed firstly to determine the optimal time of exposure required to elicit neuronal expression of *c-fos* and VA and melanopsin. The trial then sought to determine differential responses in relation to stimulation by narrow bandwidth light on activation of photoreceptive brain regions.

6.2 Trial 1 - Activation Time Response of *C-fos*

6.2.1 Trial I -Materials and Methods

A Note on the Experimental Design of Both Trial I And Trial II

The aim of these trials was to identify whether light of specific spectral composition differentially stimulates the neural anatomy of the brain. In doing so, the trials aimed to provide a clear stimulation without any legacy from exposure to prior photic composition. Prior to stimulation, a period of acclimation in the tank system was delivered using white light LL consistent with that experienced in the hatchery and as is standard protocol within the salmon aquaculture production of out-of-season smolts. A period of darkness was then used to adapt the fish to a non-light environment prior to exposure to specific light sources. In adopting this approach, no clear day/night signal was provided. As reported in previous investigations in zebrafish, (see Carr and Whitemore, 2005), light serves to synchronise the oscillation of day and night circadian clocks. Whilst oscillations continue to occur in response to extended exposure to darkness, clock cycles become arrhythmic without a clear “on” signal to resynchonise the clock. The impact of the likely arrhythmicity induced through the extended LL and dark periods that fish experienced prior to sampling cannot be determined within the scope of these trials. Results thus must be determined with this in mind.

Fish Stocks and Rearing Conditions

Atlantic salmon parr were sourced from ILAB (Industry Laboratory), Bergen, Norway to perform the initial *c-fos* activation study to determine the optimal stimulation time (activation dynamics of *c-fos).* Fish were acclimatized in tanks at 12 degrees Celsius for 5 days LL before dark-adaption for 48 hours and subsequent exposure to White light (Fig. 1.A). Illumination was provided via two Viva-Lite® Full Spectrum Energy

Saving Bulbs (25W) (Vita-Lite, Germany) and measured to be 3.68 W/m^2 2 cm below the water surface (RAMSES ACC-VIS, TriOS Mess-und Datentechnik GmbH). No feed was delivered prior to and including the experimental period.

Experimental Design and Sampling

Fish were stimulated for 15, 30, 60 or 120 minutes of White light (Fig. 6.1). Sampling consisted in vascular perfusion following anesthesia with buffered MS-222 (50/mg^{-l}) with 4% paraformaldehyde as described in Sandbakken et al. (2012). In addition, a dark control was included. The brains, one per time point, were dissected out and prepared for *in situ* hybridization on cryo-sections (Sandbakken et al., 2012).

The ISH was carried out under similar conditions for all sampling points. The sampling followed the local animal care guidelines and was given ethical approval by the Norwegian Veterinary Authorities (Application number: 6918).

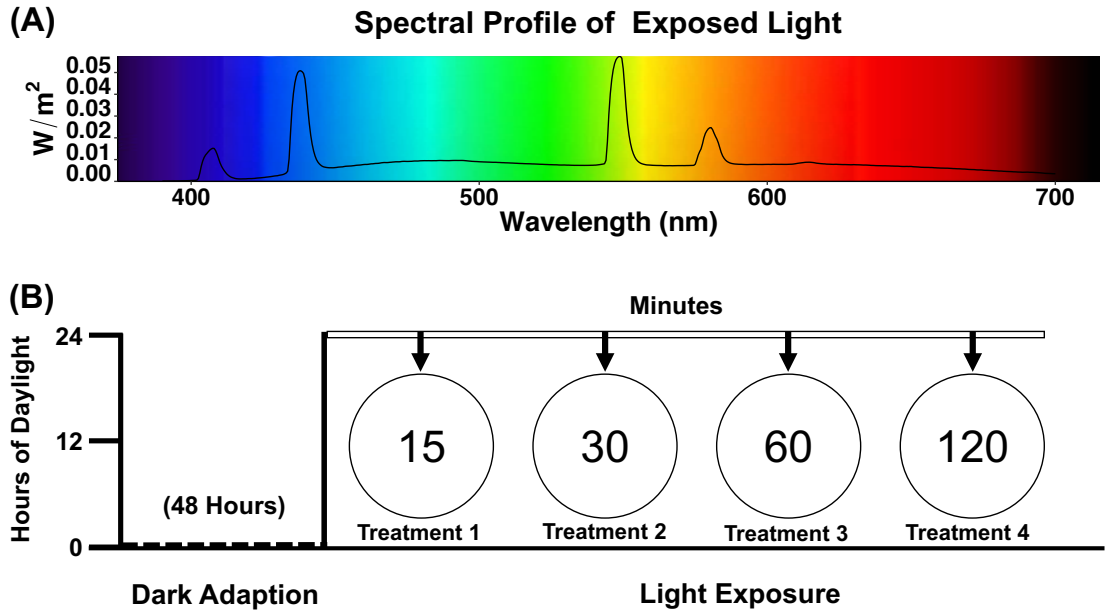

Figure 6.1. Trial I design to examine the optimal timing for sampling to visualise c-fos activity using an RNA probe and insitu-hybridisation. (A) Spectral profile of CFL lights B) following 48 hours of dark adaption samples were collected at 15, 30, 60 and 120 minutes.

Sample Processing

The Identification of *c-fos* paralogue genes, molecular cloning, synthesis of RNA probe for *c-fos*, melanopsin and VA opsin, *in situ* hybridization and Nissl staining were performed as described in chapter 2.4.7.

6.2.2 Trial I – Results

Throughout the trial there was no mortality in any tank

Activation Time Response of *c-fos*

Fish kept in darkness showed no expression of *c-fos* (Fig. 6.2A-B). Stimulation with light for 15 minutes did not result in any detectable *c-fos* expression by ISH (Fig. 6.2C-D). Expression levels of *c-fos* increased with the duration of the light stimulation (detectable but weak after 30 minutes (Fig. 6.2E-F), enhanced after 60 minutes (Fig. 6.2G, H) and very strong after 120 minutes (Fig. 6.2I, J). A light stimulation duration of 120 minutes was therefore selected for subsequent experiment and *c-fos* ISH analyses.

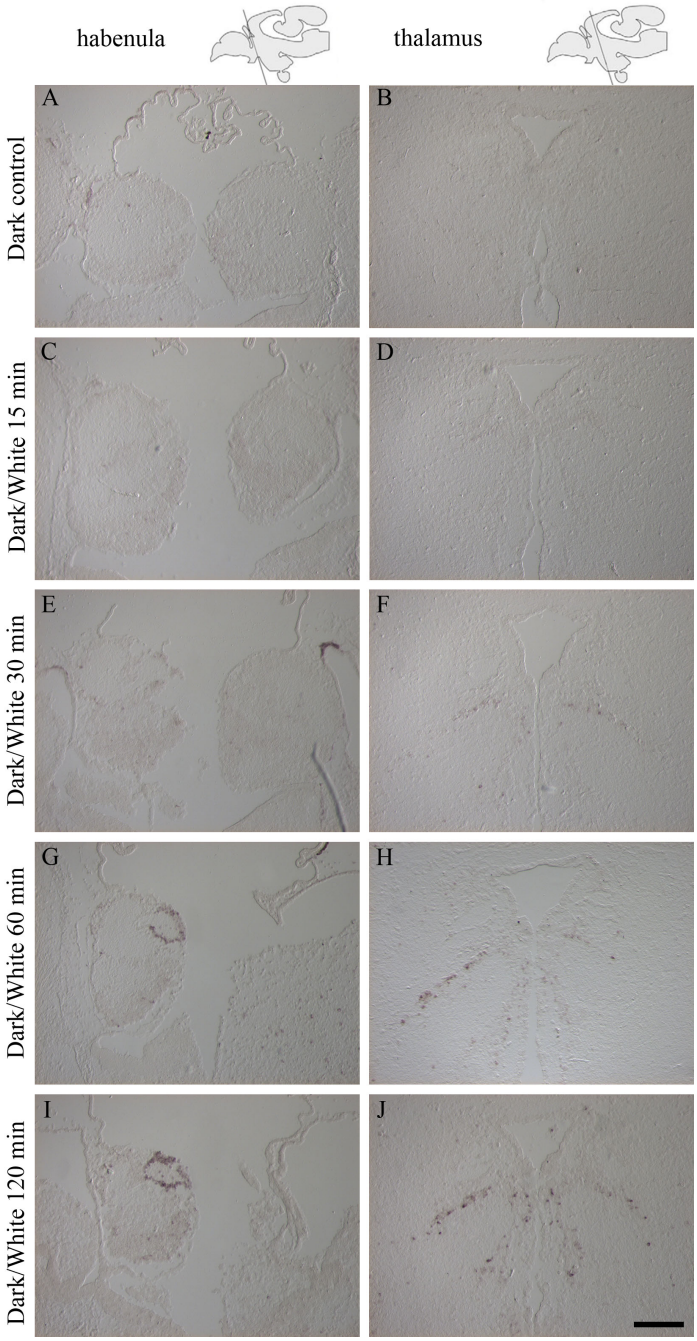

Figure 6.2. Activation of the immediate early gene *c-fos* after stimulation with white light was the strongest after 120 minutes of light exposure. In situ hybridization with c-fos is shown in the habenula (A, C, E, G, I) and thalamus (B, D, F, H, J) and schematic drawings indicate the plane of the cryo section. A-B: Dark control, no c-fos expression detected. C-D: Sampling after 15 minutes' exposure to white light, no c-fos expression detected. E-F: Sampling after 30 minutes' exposure, weak c-fos expression detected. G-H: Sampling after 60 minutes' exposure, strong c-fos expression detected. I-J: Sampling after 120 minutes' exposure, the strongest c-fos expression detected. Scale bar of 200 µm.

6.3 Trial II – Examination of the Influence of Spectrum on C-Fos Activation

6.3.1 Trial II – Materials and Methods

Fish Stocks and Rearing conditions

Atlantic salmon (parr) maintained under constant light since hatch were transferred into a recirculating aquaculture system (University of Stirling, UK) from Buckieburn Freshwater Research Facility (Stirling University, Stirling). Upon receipt 10 fish (mean weight 87g ± 14g) were stocked in each 300 liter tank (94cm outside diameter X 75 cm tall). Stocking density was 2.8 kg m^3. Water temperature was maintained at 11.5 ± 0.5ºC. Fish were unfed for the duration of the trial.

Experimental Design and Sampling

The experimental setup consisted of 5 tanks (10 fish / tank), 4 light treatments and a dark control. The experiment examined an on-response (dark to light) to four different spectral profiles. Fish were acclimated to 48 hours of darkness prior to being exposed to different narrow bandwidth light (Dark/White, Dark/Blue, Dark/Green, Dark/Red) for 120 minutes before sampling (Fig. 6.3E to H). An additional sample at 48 hours of darkness provided a dark adapted control (Fig. 6.3I). White light was provided using the same light source as in Trial I. Narrow bandwidth lights were delivered using computer-controlled LED units, supplied by Philips Lighting, producing either Blue ($\lambda_{(max)}$ 444 nm), Green ($\lambda_{(max)}$ 523 nm) or Red ($\lambda_{(max)}$ 632 nm) light. Light intensity was measured just below the water surface directly below the lamp using a single sensor channel Watts meter (Skye Instruments Ltd, UK) calibrated to National Physics Laboratory (UK) Standards. Intensity in each tank for all light treatments was calibrated to 5 W/m^2.

At each sampling, the first 5 fish randomly netted from each tank were anaesthetized and perfused as described for trial I. Due to time and cost restrictions, only one brain from each selection of five was used for analysis.

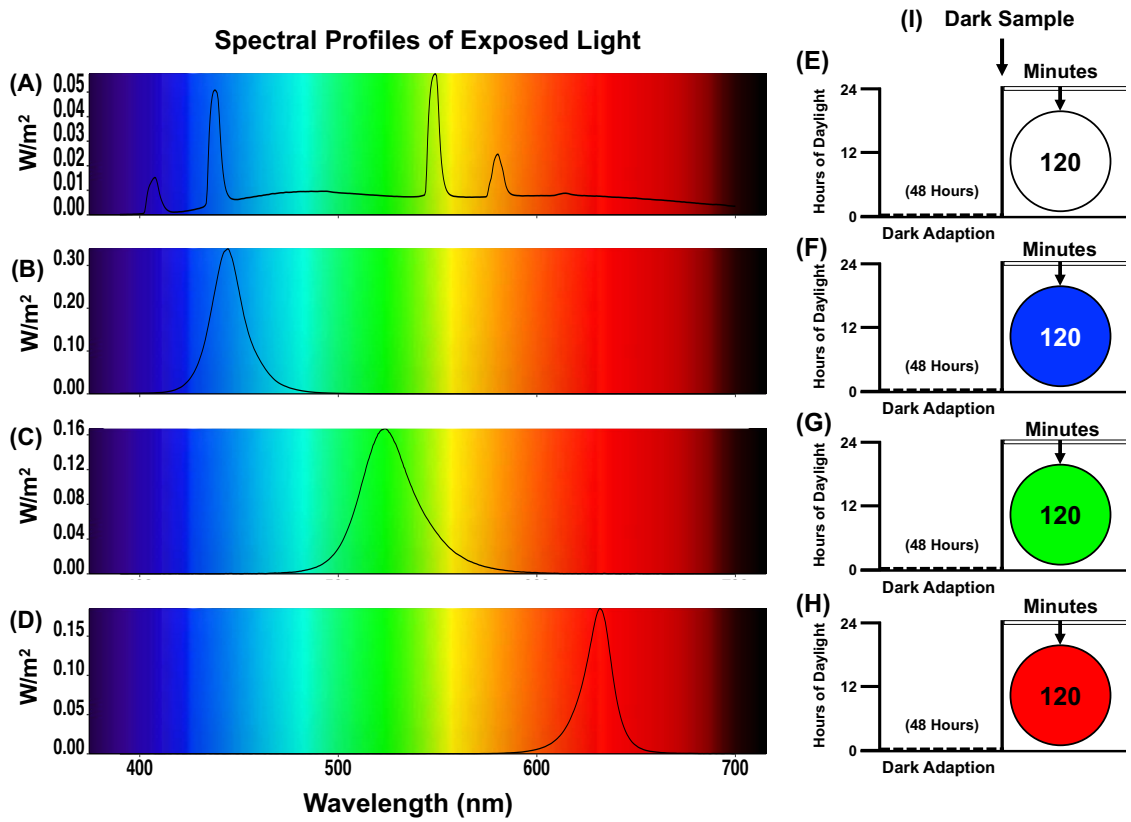

Figure 6.3. Trial II design and setup. Samples were collected Following 120 (E-H) minutes of exposure to four different spectra (A- White; B- Blue; C- Green; D- Red) and a dark control sample was collected following the dark adaption period.

In situ hybridization and Nissl staining

RNA probes, *in-situ* hybridization and Nissl staining used were as described in Trial I and described in chapter 2.4.7.

6.3.2 Trial II – Results

Throughout the trial there was no mortality in any tank

White Light Neural Activation

In the diencephalon, a characteristic ring of *c-fos* positive cells was located in dorsal parts of the left habenula (Fig. 6.4A.3). In addition, ventral parts of the habenula (Fig. 6.4A.3) and the suprachiasmatic nucleus (Fig. 6.4A.5) also expressed *c-fos*. Fig. 6.4B.3 shows a cell group expressing *c-fos* just ventral to the caudal parts of the habenula and in the same section *c-fos* positive cells can be seen in cells adjacent to

the third ventricle including the nucleus preopticus magnocellularis (Fig. 6.4B.5). Activated cells were also detected in both dorsal and ventral parts of the thalamus close to the third ventricle (Fig. 6.4C.3). In more caudal parts of the thalamus, a characteristic pattern of *c-fos* expression was observed (Fig. 6.4D.3) and in the hypothalamus, *c-fos* expression was located both in the nucleus anterior tuberis and in the nucleus lateralis tuberis (Fig. 6.4D.5). Positive cells have also been localised in tectum mesencephali, torus longitudinalis, torus semicircularis (Fig. 6.4E.3) and nucleus recessi lateralis (Fig. 6.4E.5). Off-response (light to dark) was also studied resulting in the same brain regions being activated although expression was in general weaker (data not shown).

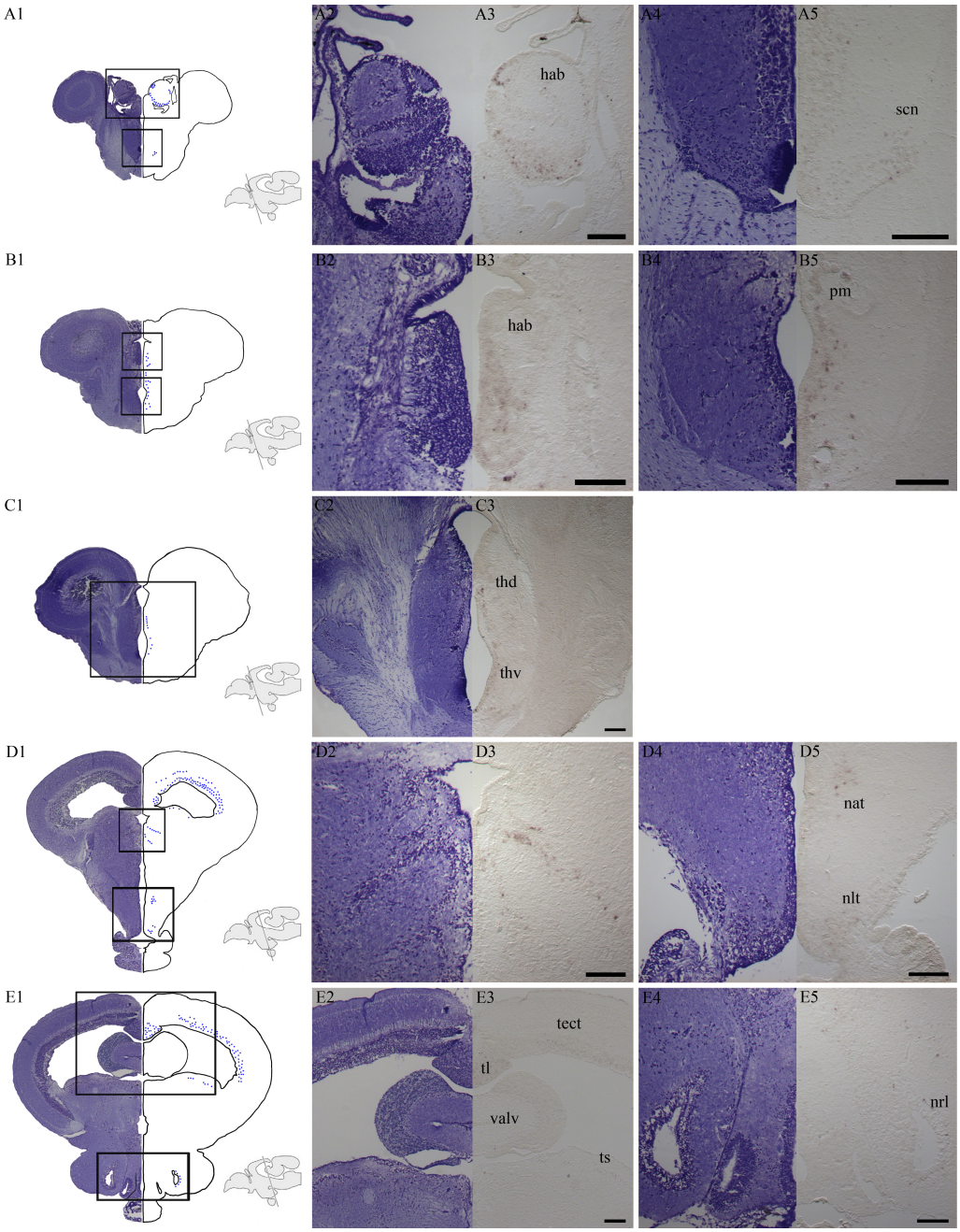

Figure 6.4. Activated brain regions after stimulation with white light for 120 minutes. A1-E1: Nissl-stained transverse sections at the equivalent level of *c-fos* expressing cells illustrated by blue dots in salmon, parr. Schematic drawings illustrate the level of the section. A2-E2, A4, B4, D4, E4: The Nissl-stained cell populations of interest with a higher magnification. A3-E3, A5, B5, D5, E5: *c-fos* expression at the same level and with the same high magnification. A1-3: Expression in a dorsal ring in the left habenula (hab) and in ventral parts of the habenula. A1, A4-5: *c-fos* expression in the

suprachiasmatic nucleus (scn). B1-3: A cell group expressing *c-fos* just ventral to the caudal habenula. B1, B4-5: Expression in cells close to the third ventricle and in the nucleus preopticus magnocellularis (pm). C1-3: Activated cells in the dorsal thalamus (thd) and ventral thalamus (thv) close to the third ventricle. D1-3: Expression of *c-fos* in caudal parts of the thalamus. D1, D4-5: In the hypothalamus, expression was seen in the nucleus anterior tuberis (nat) and nucleus lateralis tuberis (nlt). E1-3: Cells expressing *c-fos* were also localized in the tectum mesencephali (tect), torus longitudinalis (tl) and torus semicircularis (ts). E1, E4-5: Expression in the nucleus recessi lateralis (nrl). Scale bars of 200 µm.

Narrow Bandwidth Light Neural Activation

Although a number of samples and photic regimes were collected, only data from the following groups are presented. Dark-adapted fish were stimulated for 120 min with narrow bandwidth LED-light (Dark/Blue, Dark/Green and Dark/Red) and *c-fos* expression was compared against a dark control (Dark/Dark) (Fig. 6.5). Brains from control fish kept in darkness showed no or little *c-fos* expression (Fig. 6.5A, E, I, M, Q). In the left habenula (Fig. 6.5B-D), the ring of *c-fos* positive cells was detected in fish exposed to all three light spectra. In the ventral diencephalon expression of *c-fos* was detected in the preoptic area and in the suprachiasmatic nucleus for all colors (Fig. 6.5F-H). In the anterior part of the thalamus, expression was detected in the caudal habenula and dorsal thalamus for fish exposed to Blue (Fig. 6.5J) and Green light (Fig. 5K), while little expression was detected for Red (Fig. 6. 5L). In more caudal parts of the thalamus, the same characteristic expression pattern was observed for all colors (Fig. 6.5N-P). In the hypothalamus, expression of *c-fos* was detected in the nucleus anterior tuberis for all three colors (Fig. 6.5R-T) and in fish exposed Red light, strong expression was also seen in the nucleus lateralis tuberis (Fig. 6.5T).

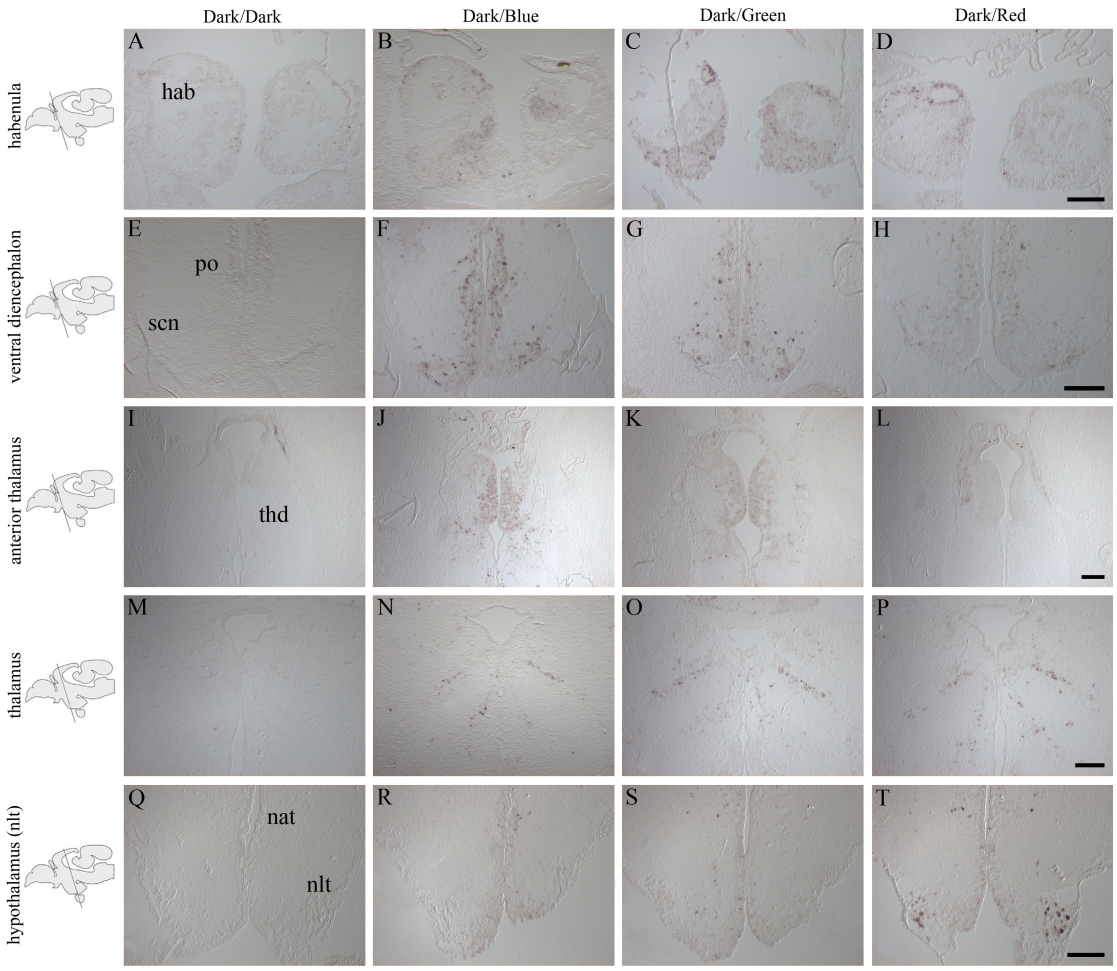

Figure 6.5. Comparison of c-fos positive signal in the brain of fish exposed to different narrow bandwidth light. Schematic drawings illustrate the plane of sections. A, E, I, M, Q, U: Control fish kept in darkness (Dark/Dark) showed no or little c-fos expression. B-D: A dorsal ring of c-fos positive cells was detected in the left habenula (hab) for all three spectra. F-H: In the ventral diencephalon, both the preoptic area (po) and superchiasmatic nucleus (scn) displayed c-fos expression. J-L: Expression of c-fos in the caudal habenula and dorsal thalamus (thd) for Blue (J) and Green (K), little expression in Red (L). N-P: Activated cells in caudal parts of the thalamus for all three spectra tested. R-T: In the hypothalamus, expression was detected in the nucleus anterior tuberis (nat) for the three spectra, in addition, a strong expression was detected in the nucleus lateralis tuberis (nlt) for fish exposed to Red light (T). Scale bars of 200 µm.

Localisation of Neural Activation and Deep Brain Photoreception

Results from exposure to all light conditions showed that C-fos and non-visual opsin stimulation occurred differentially across the tissue types examined. In the dorsal part of the left habenula, the characteristic ring of *c-fos* expression (Fig. 6.6A) was also detected for both melanopsin (Fig. 6.6B) and VA opsin (Fig. 6.6C). A similar small cluster of cells just ventral to caudal parts of the habenula was also detected for *c-fos* (Fig. 6.6D) and VA opsin (Fig. 6.6F) but not for melanopsin (Fig. 6.6E). In caudal parts of the thalamus, the same characteristic expression pattern was observed for *c-fos* (Fig. 6.6G) and VA opsin (Fig. 6.6I). In addition, low melanopsin signal was detected in the same brain region (Fig. 6.6H). In the hypothalamus, positive cells for both *c-fos* (Fig. 6.6J) and melanopsin (Fig. 6.6K), but not VA opsin (Fig. 6. 6L), was localised in the nucleus lateralis tuberis.

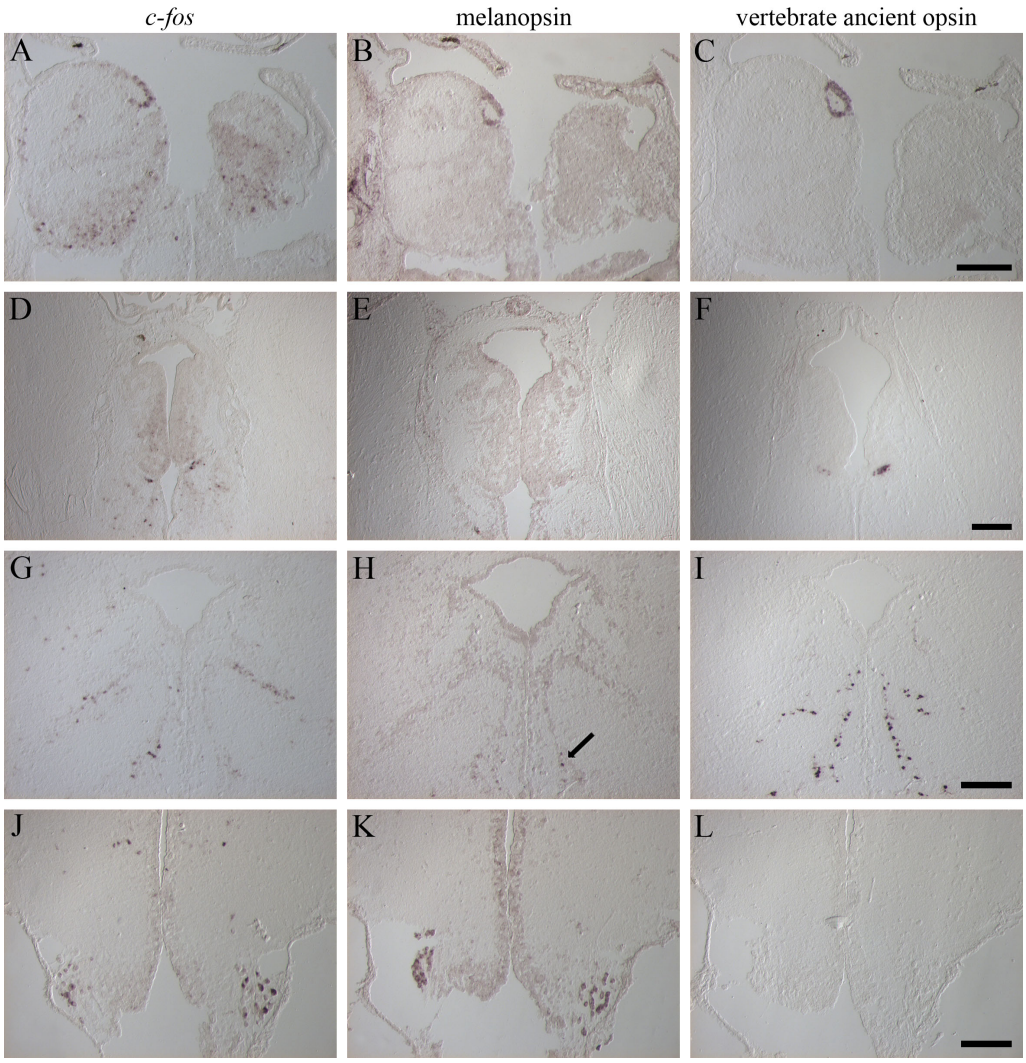

Figure 6.6. Comparison between specific brain regions in response to light exposure shows differential localisation of melanopsin, vertebrate ancient opsin (VA opsin) and c-fos activation. A-C: In the left habenula a similar ring of cells was seen for *c-fos* (A), melanopsin (B) and VA opsin (C). D-F: Ventral of the caudal habenula, a small cluster of cells was detected for *c-fos* (D) and VA opsin (F) but not for melanopsin (E). G-I: In the caudal thalamus, a similar expression pattern was seen for *c-fos* (G) and VA opsin (I) and some melanopsin positive cells (H) (see black arrow) were also detected. J-L: In the hypothalamus, the lateral cells of the nucleus lateralis tuberis expressed *c-fos* (J) after light activation and also melanopsin (K) but not VA opsin (L). Scale bars of 200 µm.

6.4 Discussion

The aim of this experimental chapter was to identify whether neuronal responses in Atlantic salmon parr varied in response to different narrow bandwidth light sources. Using the expression of the early immediate gene *c-fos* which undergoes both a rapid and transient upregulation in response to a variety of stimuli (Bullitt 1990; Sheng and Greenberg, 1990) and the co-localisation of two different opsins, a clear and localised upregulation was seen in different brain areas in response to different photic stimuli. Interestingly no such reaction was seen in the photosensitive pineal gland. Results suggest that different neuronal networks exhibit specific spectral sensitivities. The actions and potential implications of these findings raise interesting questions regarding the photic architecture of artificial lighting in the salmonid hatchery.

Following light exposure, the time response in the present study getting a strong *c-fos* positive signal in Atlantic salmon parr was 120 minutes. Results contrast to those discussed by Kovács (2008) who reported that the kinetics of the response to acute stimuli (e.g. vasopressin) induced peak *c-fos* mRNA expression after approximately 30 minutes and for protein (i.e. corticotrophin-releasing hormone) after 90 to 120 minutes. In accordance with this, studies in zebrafish responding to half-light/half-dark stimuli, medaka (*Oryzias latipes*) responding to mating stimuli, and goldfish to kainic acid also show peak *c-fos* mRNA expression after 30 minutes (Fujikawa et al., 2006; Lau et al., 2011; Okuyama et al., 2011). Here, *c-fos* expression after 30 minutes was present however the signal was weak and 120 minutes gave greater resolution. Our results are similar to those described in rainbow trout in response to kainic acid (Matsuoka et al., 1998) and Atlantic halibut brain where *c-fos* mRNA was detectable after 30 minutes following light exposure but reached a peak after 120 minutes (Eilertsen, 2014). The delay in elevated *c-fos* expression observed in the present study may be related to the impact of temperature on poikilothermic fishes.

The present study identified activation of distinct and specific brain regions in Atlantic salmon stimulated with light for 120 minutes. These regions included the habenula, suprachiasmatic nucleus, thalamus, hypothalamus, tectum, torus longitudinalis and torus semicircularis. Importantly, several of these brain regions also contain deep brain photoreceptors and co-express melanopsin and vertebrate ancient opsin suggesting a potential direct activation of these regions in response to light. Previous studies performed in adult zebrafish showed *c-fos* mRNA expression was

induced in many of the same specific and discrete brain regions in response to 30 minutes of exposure as identified here (Moore and Whitmore 2014). Several of these brain regions, such as the tectum and torus semicircularis, have retinal and pineal innervations (Ekstrzm and Meissl 1997). Differentiating between direct photostimulation and activation through photoreception in the retina or pineal is unfortunately beyond the scope of this trial. However, results showed little or no *c-fos* expression in the pineal organ (data not shown) even though the fish pineal organ is known to contain a photoreceptive circadian oscillator (Falcón et al., 2010). Results suggest that either retinal photoreception or direct photostimulation are responsible for the upregulation identified.

Comparing the expression pattern of *c-fos* with parallel Nissl stained sections allowed us to analyse the brain regions activated by light. These results, together with *c-fos* activation in regions that overlap with melanopsin or VA opsin or both, help to further elucidate the potential links between functional systems and physiological processes. It must be acknowledged however that such links can only be suggested and further functional studies are required.

Comparatively similar expression of VA opsin, melanopsin and *c-fos* expression was identified in a characteristic dorsal ring of the left habenula. Studies by Sandbakken et al. (2012) have shown that the melanopsin cell population in the habenula is co-localised with an asymmetric serotonergic cell group of the left habenula (Ebbesson et al., 1992). In salmonids, the left habenula is shown to receive the majority of the innervations from the parapineal organ and the flattened terminal field of the parapineal tract is shown to be located in the dorsal part (Yanez et al., 1996). Photoreceptors of the left habenula could be related to the assumed photoreceptive function of the parapineal organ as suggested by Sandbakken et al., (2012) and suggested to have a functional relationship to the limbic system (Yanez et al., 1996).

In this trial, significant activation was observed in the suprachiasmatic nucleus (SCN), an area where both retinal and pineal input is thought to be integrated (Holmqvist et al. 1994). The SCN is a major source for dopaminergic innervations of the pituitary in Atlantic salmon (Holmqvist and Ekström 1995). It has been shown that melanopsin positive cells in the SCN are co-localized with a dopaminergic cell population and it has been suggested that melanopsin positive cells in SCN play a role in the dopaminergic regulation of the pituitary function (Sandbakken et al., 2012).

Results are in accordance with activation seen in zebrafish exposed to a 30 minutes light pulse at night (Moore and Whitmore 2014).

The present study clearly demonstrated that *c-fos* is expressed after stimulation with light in the same thalamic regions as VA opsin e.g. anterior thalamus just ventral to the caudal habenula and in posterior parts where the VA opsin positive cells are spread caudally and laterally. In the caudal thalamus, melanopsin positive cells are also apparent laterally. In zebrafish, the deep brain VA opsin neurons have been suggested to have a role in time- and light-dependent physiology to adjust to environmental changes (Hang et al., 2015) and one can speculate if the activated thalamic population in salmon has a similar role. In adult zebrafish, the VA opsin positive cells of the thalamus appear from the anterior thalamic nucleus just ventral to the habenula and spread caudally and laterally to the intercalated thalamic nuclei. The VA opsin positive cells have been shown to all be GABAergic as *gad67* mRNA co-localise with *valop* mRNA and it has been suggested that this thalamic population may regulate light-avoidance behavior in zebrafish (Hang et al., 2014). Moreover, the thalamic VA opsin population in zebrafish has diurnal rhythmicity and it has been suggested that the thalamic cell group maximizes its photosensitivity diurnally to regulate neuronal activity in the thalamus during dawn and dusk (Hang et al., 2015). The thalamic population of VA opsin positive cells in salmon has been shown to have a similar pattern spanning caudally and laterally from the sub-habenula region terminating at the level of the posterior commissure (Philp et al., 2000).

The pituitary of teleost is known to be highly innervated with hypothalamic neurons (Terlou and Ekengren 1979; Ball 1981; Anglade et al., 1993) and present results revealed that cells in the NLT are activated after light stimulation. Interestingly, lateral cells of the NLT which are known to express melanopsin in salmon (Sandbakken et al., 2012) were activated in dark-adapted salmon stimulated with Red light. The melanopsin positive cells of the lateral NLT have been shown to be closely associated with cells expressing corticotropin releasing factor (CRF) and neuronal nitric oxide synthase (nNOS) and a possible functional link has been suggested (Sandbakken et al. 2012). A corresponding expression pattern of VA opsin is however not seen in this region. Localisation of opsins to distinct area may suggest a link between receptor functionality and spectral sensitivity however further work is required to confirm this.

Currently, there is a fundamental lack of information regarding the spectral sensitivity of the deep brain photoreceptor network. Results indicate clear effects of narrow bandwidth lights in the salmon brain although the global expression pattern of *c-fos* remained similar between light treatments. Despite the same gross areas exhibiting upregulation, differences in cell clusters were identified and raises interesting questions regarding the homogeneity of cell clusters between individual fishes. The most apparent difference between light treatments was in lateral cells of the nucleus lateralis tuberis where the neural activation was strong in fish exposed to Red light. Photopigments in the activated brain regions at both regional and cellular levels may be behind observations. Localisation to distinct regions as seen with melanopsins and VA opsin in the ring of cells in the dorsal habenula suggest a highly organised structure to receptor networks.

Differences in receptor stimulation may be a response to the transmission of light through the cranium and overlying tissues which has the effect of scattering shorter wavelengths increasing the prevalence of longer wavelengths (Migaud et al,. 2006). In addition, absorbance by pigments such as hemoglobin further impact the incident light received by the pineal and deep brain (Peirson et al., 2009). Spectral sensitivity may be tuned from an evolutionary need to accurately detect photoperiod based on the composition of transmitted light (Goldsmith 1990). Photic composition changes as the angle of the sun changes and greater absorption by ozone alters the spectrum, both intensity and the angle of irradiance changes significantly (Peirson et al., 2009). The resulting motif of photic composition provides a valuable indication of time which can be differentiated from intensity decreases during the day. Such spectral discrimination has been shown in the pineal gland of rainbow trout and goldfish (*Carassius auratus)* (Meissl and Yanez 1994). Results highlight the difficulty in dissecting the impact of light in fish and further studies are required to separate out these impacts further.

The diversity and number of photopigments in the deep brain is currently being elucidated with over 36 different opsins identified to date in the zebrafish (Hang et al., 2016). Four new pigment classes of nonvisual opsins have also been recently described in the zebra fish (Davies et al. 2015a). The new opsins were shown to be extensively expressed both in the eye and brain and were different both in shape and absorbance maxima of their spectra. These finding help to highlight the complexity of understanding neural networks and light stimulation. With the extra whole genome

duplication in salmonids (Allendorf and Thorgaard 1984) the potential diversity of nonvisual opsins in salmon are even greater and it will be of great interest to reveal the shape and spectral absorbance maxima of the salmon nonvisual opsins.

The main aim of this study was to elucidate the response to different narrow spectra. Differential responses to both Blue and Green, and Red light were determined potentially suggestive of functional divergence. When considering the results, it is perhaps beneficial to examine the trial design and the photoperiod history that the fish were exposed to. In both trial I and trial II fish were exposed to a period of 48 hours of darkness prior to application of light treatment. In trial II, prior to transferring into the experimental system fish were maintained in accordance to standard industry practice for out-of-season smolts, i.e. under LL. As has been identified in zebrafish a daily cue is required to keep the circadian transcriptome synchronised between individuals (Carr and Whitmore 2005). Whilst the circadian response was not the aim of this trial, and light conditions chosen in order to reduce rhythmicity it is likely that the fish were arrhythmic with regards transcriptomic output. The influence that this may have had is unclear given the small sample size. Further work is required to confirm results by processing more samples, in addition, repeating the trial with fish maintained under typical conditions exposed only to a change in light spectrum rather than photoperiod would help confirm results.

The determination of how spectral sensitivity occurs within the brain and subsequent links to functional processes would allow lights to be designed to fulfill biological requirements without exceeding them and this study provides a good initial starting point with which explore the neural responses further.

7 Differential Gene Expression in the Atlantic Salmon Pituitary Transcriptome in Response to Photic Conditions

7.1 Introduction

As incident light stimulates photoreceptive tissues in the Atlantic salmon, a vast array of neural responses occurs (Tombran-tink and Barnstable, 2008). These downstream light-induced signals act upon the visual processing centres and the photoneuroendocrine system (PNES) to drive broad physiological responses mediated through the endocrine system, mainly through the pituitary gland (Melmed 2010). In chapters three and four, the physiological response to both light spectrum and intensity during early freshwater (FW) development was discussed. The main findings from these previous studies were that exposure to Red light resulted in lower growth rates than either Blue, Green or broad spectrum white light. To determine whether the brain exhibits differential responses to narrow bandwidth light, the trial presented in chapter six was conducted to study neural activity through c-fos expression and the expression of two well described non-visual photoreceptor opsins, vertebrate ancient (*VA)* and *Opn4*. Whilst no differential c-fos expression was identified between spectrum, fish exposed to Red light exhibited a distinct upregulation of *VA* and *Opn4* in the nucleus lateralis tuberis (NLT) of the hypothalamus. The NLT is the link between the brain and the pituitary gland and is an important centre for the integration of photic information from the rest of the brain (Ebbesson et al.,, 2003; Holmqvistet al., 1979). Given the direct roles of the pituitary gland on many of the PNES responses, this chapter examines the response measured by gene expression of the pituitary gland of fish exposed to four different photic conditions.

One approach for examining gene expression is RNA-Seq that utilises high throughput sequencing, commonly known as next generation sequencing (NGS), to examine a snap shot of genes being transcribed, i.e. the transcriptome (Metzker 2010). Comparing transcriptomes allows differential gene responses to be identified and related to the effector - such as disease (Tacchi et al., 2011), pharmaceutical agents (Hampel et al., 2014), compromised nutrition (Morais et al., 2012) or in this case, photic conditions. Unlike previous studies that used microarray technology, NGS provides far greater depth and is considerably more sensitive in terms of both lowly expressed and differentially expressed genes (Marioni et al., 2008; Wang et al., 2009).

However, analysis of NGS data in salmonids is challenging due to a current lack of a high quality annotated reference genome (Sundaram et al., 2017). An additional challenge in salmonids is the complex genomic arrangement brought about by whole genome duplication events (Sundaram et al., 2017). One solution is to use denovo assemblies and compare the results with well annotated species (e.g. zebrafish). However, the approach needs to be used with caution as considerable subfunctionalisation has been identified in salmonids (Lien et al., 2016) and gene function may not necessarily be conserved (Warren et al., 2014). Despite this, NGS is an exciting tool with great potential (Sundaram et al., 2017).

Physiological development relies upon light for visual processes such as prey detection, predator avoidance and mate selection. Light also acts upon the non-visual photoreceptor networks to entrain endogenous clocks in salmonids that are responsible for seasonal developmental changes (Falcón et al., 2010). The perception of day night photoperiod is mediated through the production of melatonin (Falcón et al., 2007) and clock genes (Falcón, 1999). Circadian melatonin synthesis occurs through the cyclical expression of activator genes *Bmal* and *Clock* during the night and *Per* and *Cry* during the day; these genes regulate *Aanat2*, a key enzyme in melatonin production (Reppert and Weaver, 2002). Directly photosensitive, the pineal gland is considered as the major endocrine gland associated with melatonin production (Falcón et al., 2010). However, photoreceptors are also found localised to many other areas of the brain that co-occur with the production of distinct neurotransmitters (Hang et al., 2016). As yet, beyond suggestions of seasonal entrainment, these receptor networks have unknown functionality. The neuroanatomical arrangement of photoreceptive tissue in Chapter 6 appeared to exhibit specific spectral sensitivity, whether these distinct areas control distinct physiological processes is unknown (Hang et al., 2016). By understanding how the integration of photic signals through the visual and non-visual photoreceptor systems affect pituitary outputs, it may be possible to gain useful insights for designing lights targeted for specific production traits such as growth or synchronising seasonal entrainment.

The pituitary gland connects to the brain at the NLT via peptidogenic neurosecretory fibres that initiate hormonal cascades in the pituitary (Ebbesson et al., 2003). Specific hypothalamic neuroendocrine signals in the adenohypophysis are initiated via peripheral and/or tissue specific effects upstream and controlled via feedback loops (Ebbesson et al., 2003). Such systems allow the amplification of weak

signals into whole body responses. The pituitary gland is comprised of two anatomically discrete sections, the glandular adenohypophysis and the neurohypophysis. Hormones are produced and secreted in the adenohypophysis whilst the neurohypophysis is non-glandular (Peter et al., 1990), comprised of bundles of hypothalamic nerve fibres related to wider neural integration.

Homeostasis and ontogenic progression is regulated via pituitary hormone excretion that play a pivotal role in e.g. appetite (e.g. Growth Hormone (GH). (McLean and Donaldson, 1993; Wargelius et al., 2005), growth (e.g. GH) (Kling et al., 2012), smoltification (e.g. (Arnesen et al., 2003; Ebbesson et al., 2011), maturation (e.g. FSH, LH) (Andersson et al., 2013; Taranger et al., 2015), immune function (Esteban et al., 2013) and stress responses (e.g. ACTH) (Madaro et al., 2016; Pankhurst 2011). Secretions from the adenohypophysis are mediated through the actions of neurosecretory neurons from the NLT and putative dopaminergic neurons from the ventral pre-optic area (Holmqvist et al., 1994b). Hormones secreted act on membrane bound receptors such as G protein-coupled receptors (GPCRs) where binding of a ligand with the interaction domain on the receptor instigates an internal signal transduction cascade (Arshavsky et al., 2002) that lead to the upregulation of gene expression modulated by transcription factors. Upregulation requires accessing the requisite DNA though modification of the local chromatin structure, that is regulated through histone modification (Jenuwein and Allis, 2001). These processes increase protein production which, in the case of the adenohypophysis, increases the exocytosis of hormones (Orphanides and Reinberg, 2002). Whilst the adenohypophysis is involved with secretion, the neurohypophysis interprets and instigates neural signalling via the release of neurotransmitters such as glutamate and nitric oxide (NO).

Pathways moderated by the pituitary, frequently exhibit considerable overlap; hormones associated with growth i.e. growth hormone (GH) is also associated with stress (Pickering et al., 1991). In aquaculture, stress usually lead to reduced growth performance (Wendelaar et al., 1997), increased disease susceptibility (Barton et al., 1986) and reduced fecundity (Campbell, 1992). Stress responses lead to the modulation of immune responses and the pituitary also has significant involvement in these processes (Weyts et al., 1999). Plasma cortisol, regulated by the Hypothalamic-Pituitary-Interrenal axis (HPI), provides a generic proxy with which to gauge stress responses in fish (Pottinger 2010). Cortisol however also plays fundamental roles in

many aspects of salmon physiology and dissociating a stressor from basal physiology can be difficult. Cortisol acts as a ligand, binding both to mineralocorticoid (MR) and glucocorticoid (GR) receptors (Jiao et al., 2006) and receptor density has been shown to modulate tissue specific hormonal responses (Kiilerich et al., 2011). Control of the HPI axis occurs through negative feedback mechanisms derived from MR and GR receptors in the hypothalamus and pituitary (Bury and Sturm, 2007) whilst corticotropin releasing factor (CRF) binding proteins (CRF-BP) offer further control by reducing the bioavailability of CRF (Madaro et al., 2016).

The pituitary is considered as the master endocrine gland, initiating an array of endocrine pathways involved in ontogenic development and physiological homeostasis. It is thus the most relevant target with which to examine the influence of photic exposure on physiological responses. Despite light being used routinely to manipulate salmon physiology very little is known regarding differential light induced mechanisms. The aim of this trial was to identify broad changes in the transcriptome and relate these to light conditions. In doing so, it sought to characterise those genes that are most highly expressed and identify likely physiological roles. Two photic comparisons were used: light vs. dark and Blue vs. Red (spectral response). Data provides insights into the differential response to light, dark and the spectral response to Blue and Red light.

7.2 Materials and Methods

Fish Rearing and Husbandry

On the 10th of December, 2014, 260 Atlantic salmon (mean weight 95.9 ± 14.9 g) of the Aquagen strain were from were transferred from University of Stirling Hatchery, Scotland (56°N, 4°W) into a recirculating aquaculture system at the University of Stirling. Prior to transfer the fish were maintained under continuous (LL) white compact fluorescent lighting (CFL) (Philips Lighting, Eindhoven, NL) since hatching. Upon receipt, fish (40) were stocked into a holding tank (94 cm outside diameter x 75 cm tall with a working volume of 300 litres) and exposed to continual broad spectrum CFL lighting (Viva-Lite, Germany) at 5 W/m^2. Following 5 days of acclimation, fish were stocked into 4 tanks (10 fish per tank). Water temperature was maintained at 13.5 ± 1.0 °C for the duration of the trial. During holding, fish were fed a standard salmon diet

(Ewos Micro, Scotland) at the manufacturer's guideline of 1.1% BW^{-day}. Feed was delivered using an adapted Eheim twin screw feeders controlled through an in house feeding control system. Ammonia was below detectable limits throughout the trial, nitrite varied between 0.01 and 0.1 ppm and pH was maintained at 6.9 ± 0.2.

Experimental Design and Sampling

This trial sought to identify the response of continual exposure to four different photic conditions. As such the subjects and lighting conditions were chosen in order to remove circadian responses. By exposing fish to LL since hatch and then transferring them into the trial photic conditions the aim was reduce internal rhythms with results reflecting the impact of exposure to the wavelength/light condition being tested.

The experimental setup consisted of 4 tanks (10 fish / tank). Four treatment groups were sampled for analysis (Fig. 7.1): Dark group exposed to 48 hours of darkness achieved through the use of a light proof tank cover; White group exposed to 48 hours of darkness followed by 26 hours of 5 W/m^2 broad spectrum white light (Viva-lite, Germany); Blue group exposed to 48 hours of darkness followed by 26 hours of 5 W/m^2 Blue LED (Philips, NL); Red group exposed to 48 hours of darkness followed by 26 hours of 5 W/m^2 Red LED (Philips, NL). Photic composition for the White groups and LED lamps are as shown in Fig. 7.1A. Fish were unfed for the duration of the dark and light phase in experimental tanks.

Onset of light was staggered by 1 hour between treatments to ensure sufficient time for performing the sample and that each tank received the same number of hours of light exposure.

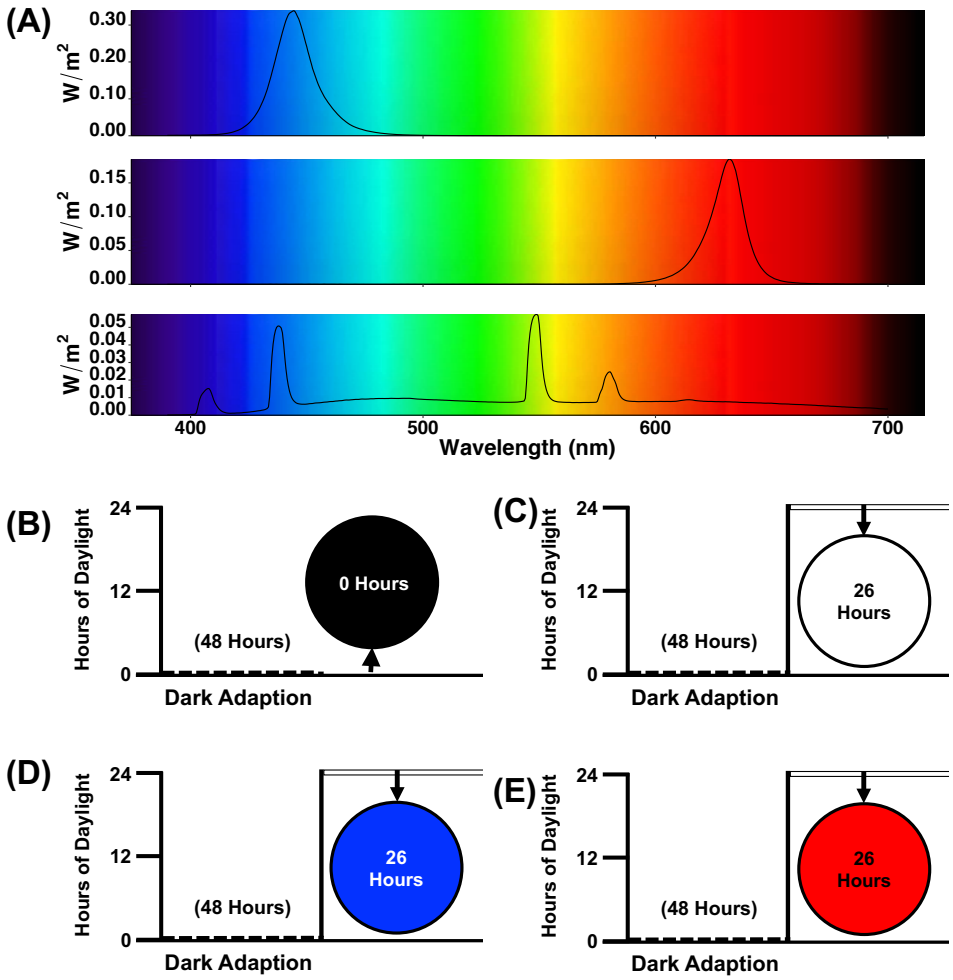

Figure 7.1. Light profiles of juvenile Atlantic salmon exposed to different photic conditions prior to sampling for comparative assessment of pituitary transcriptome. All fish received continuous white compact fluorescent (CFL) light since first feeding. All groups were exposed to 48 hours of darkness whereupon a dark-adapted sample (B) was collected. Lit tanks (C, D, E) then received 26 hours of 5 W/m^2 of either White (B), Blue (C) or Red (D) light.

All 10 fish per treatment group were sampled. Following the light treatments, fish were quickly hand netted into a black bucket in the dark to minimise exposure to extraneous light. The bucket was filled with buffered MS222 (50 mg/l) to initiate anaesthesia. Following anaesthesia blood was collected from the caudal vein using

heparinised needles. Whole blood was centrifuged at 1200 g for 15 mins at 4 °C and plasma aliquoted into replicate 1.5 mL Eppendorf tubes and stored at -70 °C.

Body weight and fork length was recorded following collection of blood and each fish was sexed. The brain and pituitary gland were dissected from the cranial cavity. Pituitary glands were placed in an RNA stabilisation solution at 4 °C for a period of 7 days and stored long term at -28 °C.

Transcriptome Library Preparation and Sequencing

From each group of ten fish, 5 males were selected for sequencing. Where more than 5 males were available a random number generator (Excel vs. 15.33, Microsoft, USA) was used to number samples and the lowest 5 numbers were selected.

Pituitary glands were extracted, sequenced and the bioinformatics performed as per chapter 2.4.8.

Comments on the Methodological approach

RNA-Seq transcriptome trials for salmonids are limited (Sundaram et al., 2017) and studies have typically used microarrays or PCR/qPCR for identifying known genes. RNA-Seq is an exciting new technology offering great power for the identification of new genes and expression pattern of known genes. Currently, beyond financial constraints, a major challenge occurs from the lack of a fully annotated genome (Sundaram et al., 2017). The Atlantic salmon genome is highly complex with large numbers of paralogues, autologues or subfunctionalisation (Lien et al., 2016). Thus, decisions are required regarding the bioinformatics approach i.e. the use of a poorly annotated genome vs. de novo transcripts. A major incentive for RNA-Seq is the ability to re-analyse data as the annotation improves. In this study, only genes present in the annotated genome are reported. This decision was based on described differences in library preparation used during the sequencing protocol. Results must be considered with this in mind in addition to the differences in library protocol which together prevent direct comparisons ‘between’ the light/dark (Li/Da) group and the Blue/Red (B/R) group being made.

Although the published transcriptome was used, there are still a number of uncharacterised genes within it. Where these genes occurred in the ten highest value lists the sequences were searched using BLASTn (NCBI) for similar transcripts. Where selected genes are annotated as PREDICTED, the closest match within the closest

species was used. Typically, this was from *Oncorhynchus mykiss*. The species of similarity is presented in each table to allow identification.

Comparative Lists

Analysis of the data occurred in three stages. Firstly, between each pair of conditions (i.e. dark vs light) a list was compiled of genes expressed in each condition based on a normalised fragments per kilobase per million (FPKM) value of >0. Gene reference (names) were used to compare lists to identify genes exclusively expressed in either condition (unique) and genes expressed in both conditions (shared).

From these lists, shared genes that were significantly differentially expressed between treatments were ranked in order of magnitude by two criteria; most highly expressed determined by absolute copy number, and most highly differentially expressed by fold change (FC); the ten highest values for each criterion are reported. In total six genes were found to be too highly expressed (reported as HIDATA) to allow computational normalisation and comparison. These are presented in a separate table.

Cortisol Analysis

Cortisol was analysed using an IBL Cortisol ELISA kit (RE50261, IBL, Germany) according to the manufacturer's instructions. Briefly, 20 µl of sample was mixed with 200 µL of conjugate enzyme and incubated for 60 minutes, the excess was washed off using wash buffer and 100 µL of TMB substrate solution was added to each well. Following 15 minutes of incubation a TMB stop solution was added and the optical density read using a spectrophotometer (model) at 450 nm. Recorded optical density was compared to a concentration gradient curve created at the same time and values extrapolated using the R/DRC package (Ritz et al., 2015).

7.3 Results

Differential Expression in Response to White Light and Dark

Gene expression was distinctly different between dark and light photic conditions (Fig. 7.2). Expressed genes were clustered into two broad clades. Values relating to row z-score are broadly similar between groups however the treatments did not cluster.

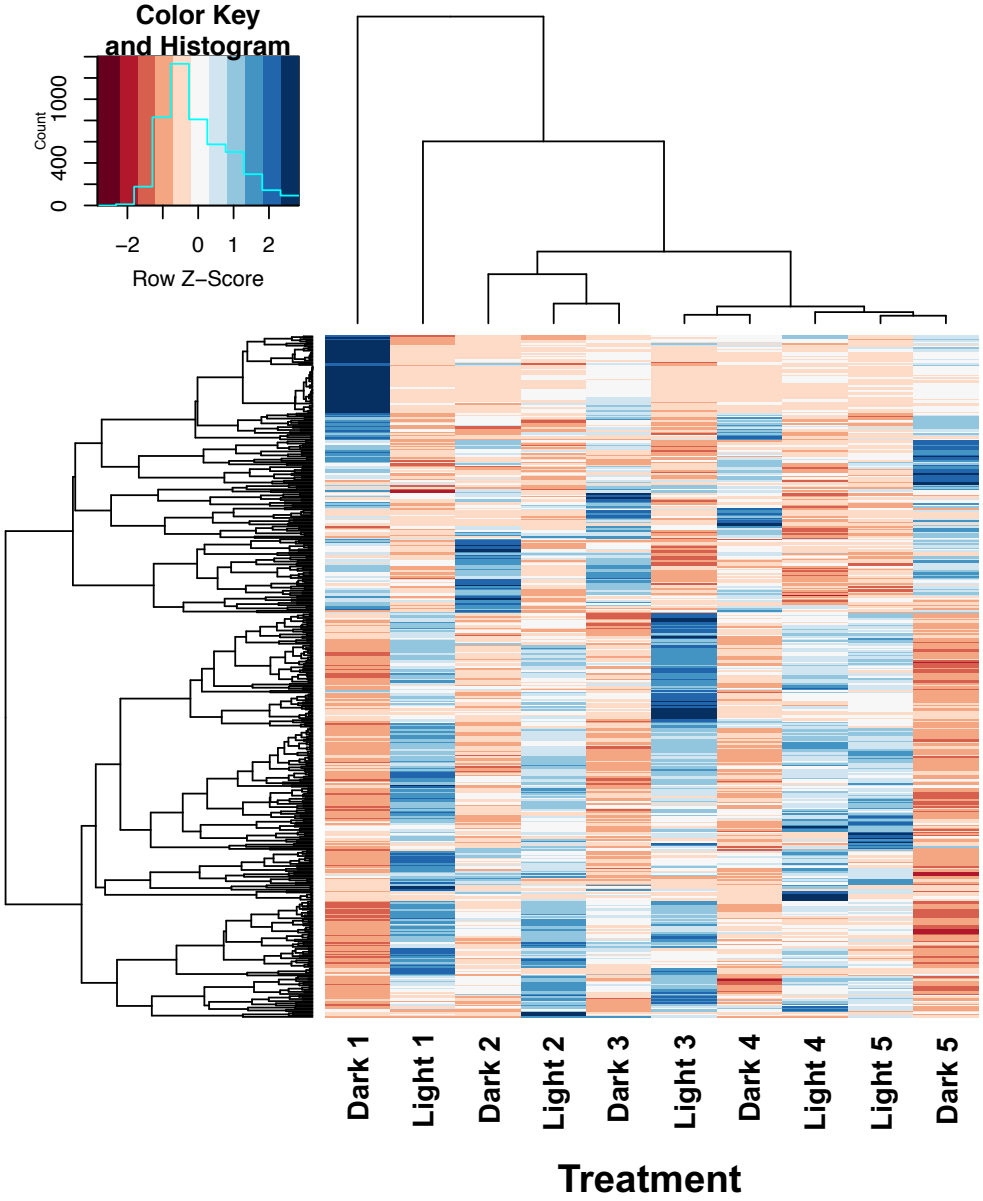

Figure 7.2. Overview of total gene expression in 10 individual pituitary glands in response to 26 hours of broad spectrum white light (Light 1 – Light 5) or 48 hours of darkness (Dark 1 – Dark 5). Colours from red to blue indicates the row z-score; blue indicates an increase in gene expression and red a decrease.

Expression and Significant Differences

In total, 46,907 annotated genes were identified in either the dark, light or both photic conditions. Of these 43,246 (93.6 %) were present under both conditions. 2,161 (4.6 %) were only present in dark and 1,499 (3.2 %) were only seen in response to light (Fig. 7.3A). The total number of significantly ($q<0.05$) differentially expressed genes in both treatments was similar (Fig. 7.3B), 380 were significantly differentially expressed in fish exposed to 48 hours of darkness and 378 significantly differentially expressed in fish exposed to 26 hours of broad spectrum white light.

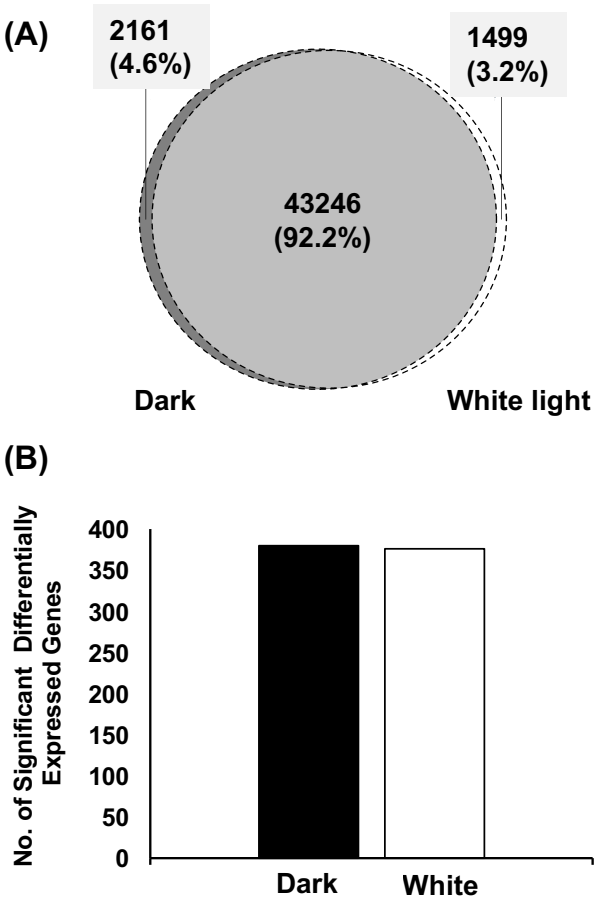

Figure 7.3. (**A)** Summary of all annotated genes detected by RNA-Seq. Genes unique to each condition are presented on the left and right circles and genes expressed in both conditions are presented in the middle. The Blue disk represents fish exposed to dark light for a period of 48 hours and the yellow disk is fish exposed to broad spectrum white light for 26 hours. Plot **(B)** shows the total number of differentially expressed in each condition.

Highest Copy Number – White Light vs. Dark light treatment

In fish exposed to 26 hours of broad spectrum white light, five of the ten highest expressed genes are associated with biosynthesis and modification of neuropeptides and initiation of cellular signalling (Table 7.1). Two genes associated with stress were identified (LOC106573597, *hs90a*) and the remaining genes are associated with neural generation (*gdn*) and photoreceptor functionality (*insm1* and LOC106575940). In fish exposed to dark for a period of 48 hours (Table 7.2), growth factors somatolactin and Pituitary alpha-2 glycoprotein hormone subunit precursor had the highest levels of expression, considerably higher than any of the top ten genes expressed in genes in response to white light. Genes involved in lipid homeostasis (*apoc1*) and glycolysis (LOC100194624) were recorded and genes involved in oxygen transfer (LOC106607372, LOC106607375, LOC100136576). One gene was uncharacterised with no significantly similar match detected by blast analysis. The other genes identified have roles in cellular sequestration.

Highest Fold Change – White Light vs. Dark

Genes that exhibited the highest comparative fold change in fish exposed to broad spectrum white light compared to dark (Table 7.3) have roles associated with post-translational modification, growth cofactor and stress responses. In dark conditions (Table 7.4), fold change was highest in cell signalling/communication and stress responses. Two genes involved in mitochondria function were also recorded. Two of the ten genes were predicted from similar sequences from *O. mykiss*.

Table 7.1. List of the highest differentially expressed genes in response to 26 hour period of broad spectrum white light derived from copy number. FC = Log_2 transformed fold change.

Gene ID	Dark FPKM	Light FPKM	FC log_2	q-value	Gene Description	Function
LOC106594053	507.94	**776.79**	0.61	0.002	Carboxypeptidase E-like	Biosynthesis of neuropeptides (Song and Fricker, 1995)
LOC106594914	519.41	**741.02**	0.51	0.010	Carboxypeptidase E-like	Biosynthesis of neuropeptides (Song and Fricker, 1995)
LOC106592880	497.99	**668.36**	0.42	0.036	Carboxypeptidase E-like	Biosynthesis of neuropeptides (Song and Fricker, 1995)
LOC106575940	131.45	**173.98**	0.40	0.044	Cytochrome P450 27C1	Catalyses 3,4-desaturation of retinoid (Kramlinger et al., 2016)
LOC106573597	122.79	**166.11**	0.44	0.028	Cold-inducible RNA-binding protein B-like	RNA chaperone in response to cold stress, osmotic stress, multifunctional (Zhu, Bührer, and Wellmann, 2016)
st1s3	123.76	**163.51**	0.40	0.031	Cytosolic sulfotransferase 3	Steroid catabolism / Post-translational modification (James, 2011)
insm1	84.91	**110.13**	0.38	0.044	Insulinoma-associated protein 1	Transcription factor involved in photoreceptor regeneration and differentiation (Forbes-Osborne, Wilson, and Morris, 2013; Lukowski, Ritzel, and Waskiewicz, 2006)

LOC106598617	78.38	**108.20**	0.47	0.016	Regulator of G-protein signalling 5-like	Modulation of G-protein signalling (Kimple, Bosch, Giguère, and Siderovski, 2011)
gdn	68.40	**94.42**	0.47	0.018	Glia-derived nexin	Neurite promoting factor released from glial cells in the pituitary (Sommer et al., 1987)
hs90a	50.38	**81.00**	0.69	>0.000	Heat shock protein HSP 90-alpha	Heat shock protein, stress response (Verleih et al., 2015)

Table 7.2. List of the highest differentially expressed genes in response to 48 hours of darkness derived from copy number. FC = Log_2 transformed fold change.

Gene ID	Dark FPKM	Light FPKM	FC log_2	q-value	Gene Description	Function
LOC100196589	**2903.29**	1539.60	-0.92	0.003	Somatolactin beta	Growth hormone like peptide, shows seasonal cycles with ovulation (Benedet, et al., 2008)
glha2	**2241.43**	1242.22	-0.85	<0.000	Pituitary alpha-2 glycoprotein hormone subunit precursor	Somatrotrophic factor (Kurata et al., 2012)
LOC100136589	**618.66**	387.19	-0.68	0.002	Metallothionein A	Cellular sequestration, high metal-binding ability, (Leggatt et al., 2017)
apoc1	**571.06**	407.38	-0.49	0.018	Apolipoprotein C-I	Systemic and local lipid homeostasis (Monnot et al., 1999)
LOC106607372	**555.52**	122.39	-2.18	<0.000	Haemoglobin subunit beta-like	Upregulate during immune responses (Dettleff et al.,, 2017)
LOC100136581	**502.50**	339.96	-0.56	0.015	Metallothionein B	Involved in cellular sequestration, high metal-binding ability, version B is an initiator of GH (Leggatt et al., 2017)
LOC106607375	**422.57**	108.63	-1.96	<0.000	Haemoglobin subunit alpha-4	Solute/oxygen transfer (Tacchi et al., 2011)

LOC106571169	**337.00**	254.67	-0.40	0.039	PREDICTED: Salmo salar uncharacterised uncharacterised	uncharacterised
LOC100194624	**302.07**	221.51	-0.45	0.030	PREDICTED: Salmo salar aldolase a, fructose-bisphosphate-1	Enzyme that splits fructose 1,6, biphosphate for glycolysis (Littlechild and Watson, 1993)
LOC100136576	**264.13**	61.68	-2.10	<0.000	Salmo salar beta globin (LOC100136576), mRNA	Oxygen transfer (Saha et al., 2014)

Table 7.3. List of the highest differentially expressed genes in response to 26 hours of broad spectrum white light derived from fold change. FC = Log_2 transformed fold change.

Gene ID	Dark FPKM	Light FPKM	FC log_2	q-value	Gene Description	Function
LOC106574533	0.36	4.26	**3.55**	0.000	LON peptidase N-terminal domain and RING finger protein 2-like	Protease- post translational modification (Harding et al., 2013)
LOC106588537	0.15	1.50	**3.36**	0.016	C-C chemokine receptor type 7-like	Chemokine- chemokine receptor signalling, interacts with immunoglobulin, identified in trout gills during infection (Castro et al., 2014)
LOC106569446	1.67	12.87	**2.95**	0.000	DNAJ homolog subfamily B member 5-like	Heatshock/chaperone, upregulated with diet induced stress (Sahlmann et al., 2013; Tacchi et al., 2011)
LOC106580476	9.71	68.18	**2.81**	0.001	Dual specificity protein phosphatase 2-like	Phosphatase for tyrosine, serine/threonine residues
LOC106575327	1.04	6.93	**2.74**	0.001	LON peptidase N-terminal domain and RING finger protein 2-like	Protease- post translational modification (Harding et al., 2013)
LOC106601023	0.42	2.46	**2.54**	0.001	Potassium voltage-gated channel subfamily H member 4-like	Voltage gated ion channel involved in neurotransmitter release

LOC106612125	0.47	2.65	**2.48**	0.001	Actin filament-associated protein 1-like 1	Inflammatory signalling in humans (Hoshi et al., 2017)
LOC106603336	1.09	5.93	**2.44**	0.001	coiled-coil domain-containing protein 61-like	Cell proliferation
LOC106565076	1.44	7.59	**2.40**	0.001	1,25-dihydroxyvitamin D (3) 24-hydroxylase, mitochondrial-like	Immune/inflammatory response
LOC106610051	0.30	1.52	**2.34**	0.003	PREDICTED: Salmo salar NADPH oxidase organizer 1-like (LOC106610051), mRNA	Mitochondria function

Table 7.4. List of the highest differentially expressed genes in response to 48 hours of darkness derived from copy number. FC = Log_2 transformed fold change.

Gene ID	Dark FPKM	Light FPKM	FC log_2	q-value	Gene Description	Function
LOC106602017	2.75	0.25	**3.48**	0.001	Multidrug resistance-associated protein 1-like	Drug resistance ABC transporter (Heumann et al., 2014)
prvt	17.93	2.14	**3.06**	0.001	Parvalbumin, thymic	Calcium binding protein (Hendrickson, et al., 2007)
LOC106609494	1.76	0.21	**3.05**	0.001	Semaphorin-3C-lik	Secretion membrane based (Moreno-Flores et al., 2003)
LOC106582674	3.57	0.65	**2.46**	0.005	Cytochrome c oxidase subunit NDUFA4-like	Mitochondria function
LOC106607872	1.43	0.27	**2.42**	0.011	Butyrophilin-like protein 1	Immune response (Bas et al., 2011)
LOC106596092	1.78	0.34	**2.40**	0.040	PREDICTED: Oncorhynchus mykiss heat shock protein family A (Hsp70) member 14 (hspa14), mRNA	Chaperone/ heatshock protein, involved in stress response
LOC106607373	235.73	45.14	**2.38**	0.001	Haemoglobin subunit alpha-like	Oxygen transfer (Saha et al., 2014)

LOC106592907	2.41	0.48	**2.33**	0.022	Regulator of G-protein signalling 11-like	Modulation of G-protein signalling (Kimple et al., 2011)
LOC106593041	3.67	0.77	**2.24**	0.010	PREDICTED: Oncorhynchus mykiss heat shock protein family A (Hsp70) member 14 (hspa14), mRNA	Hyperosmotic stress (Smith et al., 1999); Chaperone proteins (Takleet al., 2005)
ND1	3.49	0.76	**2.19**	<0.000	NADH dehydrogenase subunit 1	Mitochondria function

Differential Expression in Response to Blue and Red Light

Gene expression was broadly separated into two distinct clusters. Treatments showed differences in general expression but did not cluster together (Fig. 7.4).

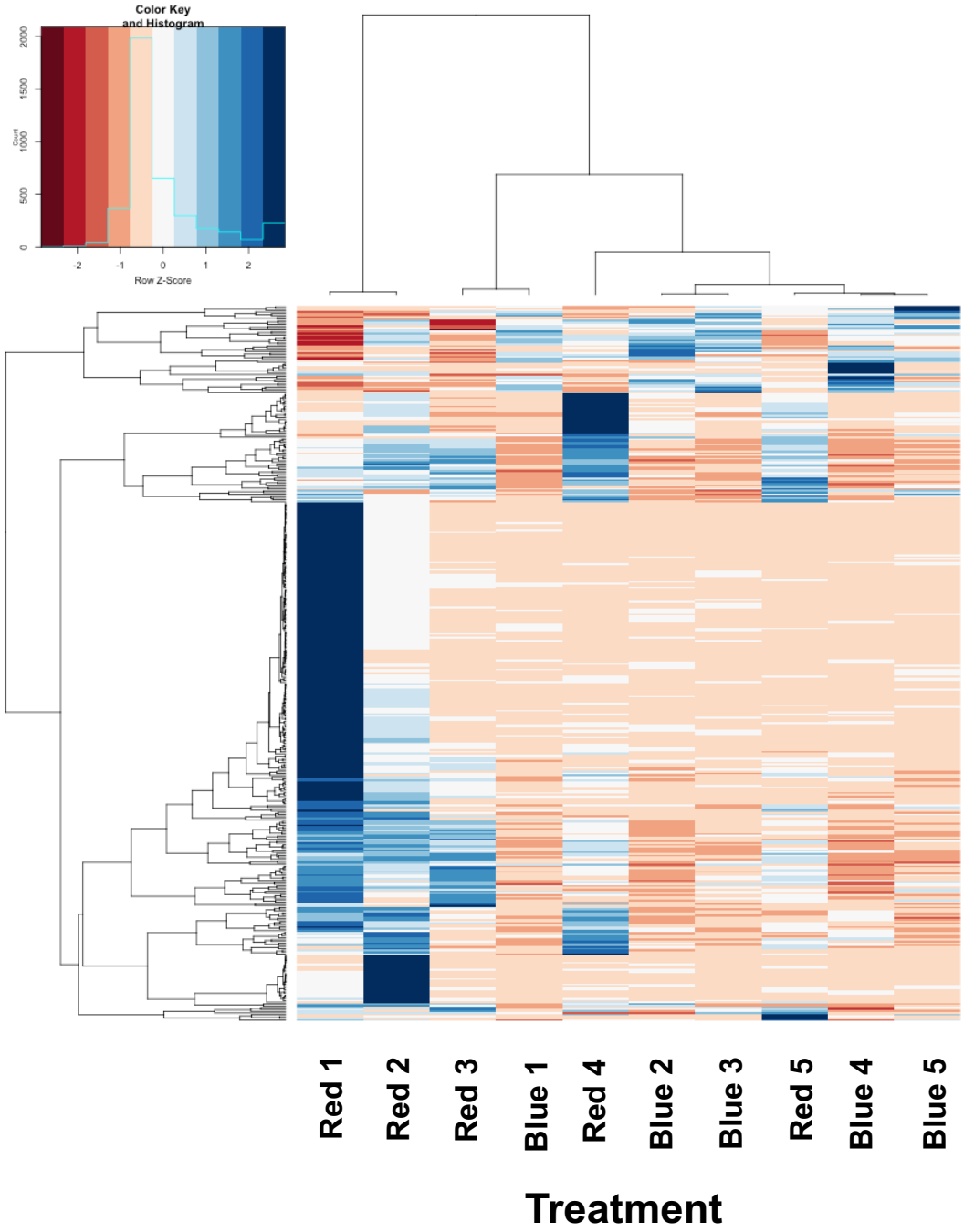

Figure 7.4 Overview of total gene expression in 10 individual pituitary glands in response to 26 hours of broad spectrum white light (Blue 1 – Blue 5) or 48 hours of darkness (Red 1 – Red 5). Colours from red to blue indicates the row z-score; blue indicates an increase in gene expression and red a decrease.

General Expression

In total 44,059 annotated genes were identified in response to either Blue and/or red. Of these 40,476 (91.9 %) were expressed in both groups. 1,246 (2.8 %) genes were only seen in response to Blue light whereas 2,337 (5.3 %) were only identified in the Red group (Fig. 7.5).

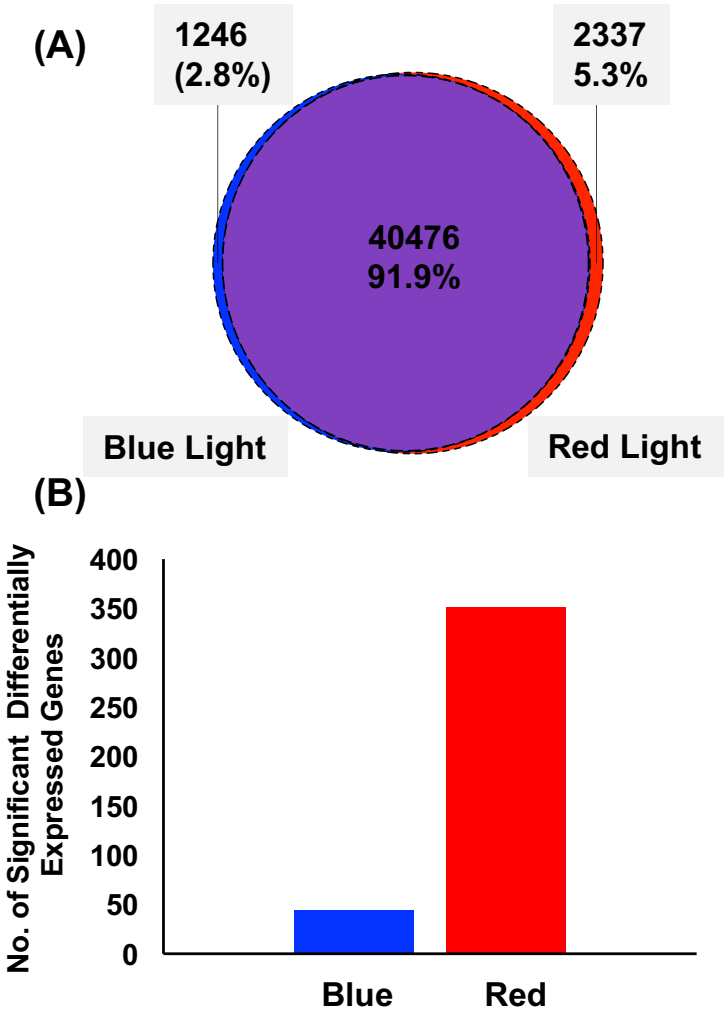

Figure 7.5 (**A)** Summary of all annotated genes expressed in Blue and Red light treatments. Genes unique to each condition are presented on the left and right of the Venn diagram and genes expressed in both conditions are presented in the middle. The Blue disk represents fish exposed to dark light for a period of 48 hours and the yellow disk is fish exposed to broad spectrum white light for 26 hours. Plot **(B)** shows the total number of differentially expressed in each condition.

Significantly Differentially Expressed Genes

Of the 40,476 shared genes, 44 were expressed significantly higher in fish exposed to Blue light than Red. In contrast 351 of the genes were significantly higher in response to Red light than Blue.

Highest Copy Number - Blue vs Red Light Treatment

Based on copy number, the highest expressed genes in the Blue light treatment (Table 7.5) consisted of genes associated with growth and metabolism, cellular signalling and axon guidance/differentiation. In contrast, fish exposed to Red light exhibited high expression of genes involved in oxygen and solute transfer and stress response (Table 7.6).

Highest Fold Change - Blue vs Red Light Treatment

Changes in response to Blue light showed a number of genes involved in secretory functions and cell communication (Table 7.7). In addition, genes involved in stress and the immune system were also significantly upregulated. Under Red light (Table 7.8), the highest significant fold changes occurred in genes relating to oxygen and nitric oxide (NO) signalling. Several genes associated with cellular proliferation and gene expression were seen. Two genes associated with stress responses were also recorded.

Table 7.5. List of the highest differentially expressed genes in response to 26 hours of Blue light derived from copy number. FC = Log_2 transformed fold change.

Gene ID	Blue FPKM	Red FPKM	FC log_2	q-value	Gene Description	Function
tshb	**1731.94**	1119.81	-0.63	0.004	Thyroid stimulating hormone, beta subunit	Metabolic processes mediated through the release of thyroid hormones
glha2	**1726.60**	1230.05	-0.49	0.030	Pituitary alpha-2 glycoprotein hormone subunit precursor	Growth factors (Kurata et al., 2012)
LOC106565094	**118.76**	75.65	-0.65	0.006	Contactin-2-like	Cell neural adhesion molecule, involved in axon extension and guidance (Linet al., 2012). Immune function
LOC106610795	**114.86**	78.28	-0.55	0.018	Glutaminyl-peptide cyclotransferase-like	Immune response (Morais et al., 2012)
gphb5	**76.79**	49.18	-0.64	0.012	Glycoprotein hormone beta 5	Thyrostimulin involved in the hypothalamic pituitary thyroid axis (identified in LJD deformities (Amoroso, 2016)
LOC106586335	**69.19**	51.47	-0.43	0.036	Isocitrate dehydrogenase [NADP] cytoplasmic-like	NADP generation Mitochondria function
LOC106585128	**66.50**	47.06	-0.50	0.025	Uncharacterized protein C8orf4 homolog	Thermal stress in rainbow trout (Verleih et al., 2015)

LOC106582267	**61.35**	43.87	-0.48	0.021	Neurogenic differentiation factor 1-like	Differentiation factor for neurogenesis (Lewis, 1996)
LOC106570190	**48.32**	9.72	-2.31	0.001	Type-4 ice-structuring protein-like	*LS-12* like, involved in lipid binding (Kiriake et al., 2016)
fkbp5	**45.71**	28.35	-0.69	0.013	FK506 binding protein 5	Glucocorticoid receptor (Jenkins et al., 2013)

Table 7.6. List of the highest differentially expressed genes in response to 26 hours of Red light derived from copy number. FC = Log_2 transformed fold change.

Gene ID	Blue FPKM	Red FPKM	FC log_2	q-value	Gene Description	Function
epd1					Ependymin-1	Upregulated during stress responses (Thornqvist, Hoglund, and Winberg, 2015)
LOC100136576	351.10	**788.89**	1.17	0.002	Beta globin	Oxygen transfer (Saha et al., 2014)
hbb1	159.16	**401.09**	1.34	0.001	Beta-globin	Oxygen transfer (Saha et al., 2014)
epd2	139.62	**286.26**	1.036	0.001	Ependymin-2	Upregulated during stress responses (Thornqvist et al., 2015)
LOC106601078	127.36	**216.44**	0.77	0.042	Haemoglobin subunit alpha-like	Oxygen transfer (Saha et al., 2014)
*xbp*1	78.69	**166.04**	1.08	0.049	X-box binding protein 1	Immune system transcription factor (Fujikawa et al., 2006)
LOC106601077	101.76	**165.91**	0.71	0.001	Haemoglobin subunit alpha	Oxygen transfer (Saha et al., 2014)
LOC106601072	76.45	**146.80**	0.94	0.001	Haemoglobin subunit alpha	Oxygen transfer (Saha et al., 2014)
LOC106601074	60.74	**128.44**	1.08	0.001	Haemoglobin subunit beta-1-like	Oxygen transfer (Saha et al., 2014)

LOC106601051	60.67	**105.27**	0.79	0.001	Haemoglobin beta-like	subunit	Oxygen transfer (Saha et al., 2014)

Table 7.7. List of the highest differentially expressed genes in response to 26 hours of Blue light derived from fold change. FC = Log_2 transformed fold change.

Gene ID	Blue FPKM	Red FPKM	FC log_2	q-value	Gene Description	Function
LOC106583605	1.58	0.26	**2.59**	0.032	Keratin, type II cytoskeletal 8-like	Intermediate filament proteins and components of the cytoskeleton (Schaffeld et al., 2002)
LOC106570190	48.32	9.72	**2.31**	0.001	Type-4 ice-structuring protein-like	*LS-12* like, involved in lipid (Kiriake et al., 2016)
LOC106597273	5.06	1.79	**1.50**	0.019	Tetraspanin-8-like	Protein binding, osmoregulation (Morais et al., 2012; Ronkin et al., 2015)
LOC106603336	1.71	0.75	**1.18**	0.032	Coiled-coil domain-containing protein 61-like	Cell proliferation (Ronkin et al., 2015)
LOC106560604	1.65	0.74	**1.17**	0.044	B-cell lymphoma 6 protein-like	Zincfinger transcription factor related to B-cells and immune responses (Sahlmann et al., 2013)
cldn18	3.78	1.70	**1.16**	0.037	Claudin 18	Tight junction gene, establish a paracellular barrier for controlling molecules between cells (Günzel and Yu, 2013)
LOC106603526	5.68	2.71	**1.06**	0.011	Protein BTG3-like	Stimulate transcription of Ig and T-cell receptors (Tadiso et al., 2011)

LOC106570785	15.36	7.39	**1.06**	0.003	Predicted GPI-anchored protein 58	Cell surface sodium channel expression (Nakano et al., 2010)
LOC106580519	17.92	9.18	**0.96**	0.013	Uncharacterized protein C8orf4 homolog	Thermal stress in rainbow trout (Verleih et al., 2015)
LOC106565346	25.94	13.40	**0.95**	0.001	Peptidyl-prolyl cis-trans isomerase FKBP5-like	Glucocorticoid receptor (Jenkins et al., 2013)

Table 7.8. List of the highest differentially expressed genes in response to 26 hours of Red light derived from fold change. FC = Log_2 transformed fold change.

Gene ID	Blue FPKM	Red FPKM	FC log_2	q-value	Gene Description	Function
prvt	1.52	94.017	**5.95**	0.001	Parvalbumin, thymic	Calcium binding protein (Hendrickson et al., 2007)
LOC106605334	0.046	2.50	**5.75**	0.033	Soluble guanylate cyclase 88E-like	NO signalling, primary activator of soluble guanylate cyclase (Derbyshire and Marletta, 2012)
LOC106580947	0.079	3.35	**5.41**	0.006	Soluble guanylate cyclase gcy-31-like	Oxygen and hypoxia sensing (Zimmer et al., 2009)
LOC106578192	0.76	27.76	**5.20**	0.001	Protein phosphatase methylesterase 1-like	Carboxymethylation to regulate cells (Ogris et al., 1999)
LOC106604839	0.78	26.17	**5.07**	0.001	Soluble guanylate cyclase 88E-like	NO signalling, primary activator of soluble guanylate cyclase (Derbyshire and Marletta, 2012)
LOC106571644	0.05	1.66	**4.93**	0.036	Homeobox protein Meis2-like	Cofactors for homeodomain proteins
LOC106588710	0.14	4.32	**4.91**	0.019	Ankyrin repeat and MYND domain-containing protein 2-like	MYND domain are associated with deacetylation gene regulation (Bower and Johnston, 2010)

LOC106603407	0.12	3.25	**4.74**	0.001	Pancreatic secretory granule membrane major glycoprotein GP2-like	Glycoproteins associated with ISAV response (Aspehaug et al., 2005)
LOC106610721	0.12	2.50	**4.40**	0.044	Actin, alpha skeletal muscle 2-like	Regulation of the stress axis HPI (Lovenberg et al., 1995)
LOC106608054	0.09	1.84	**4.30**	0.005	Trichohyalin-like	Upregulated in stress responses (Kocmarek et al., 2015)

Very Highly Expressed Genes

The algorithm CuffDiff (part of the tuxedo suit as previously detailed (Trapnell et al., 2012)) was used to determine differentially expressed genes. When performing this analysis, a known error occurs whereby genes that are very highly expressed result in saturation and therefore a reliable differential expression significance test cannot be performed. It is of course of great interest to review the expression of these genes, as they comprise a significant fraction of the RNA-Seq data set. These genes are annotated by CuffDiff with “HIDATA” and are presented for dark and light treatments (Table 7.9) and Blue vs Red groups (Table 7.10). The genes are associated with the major function of growth, osmoregulation and the prohormone proopiomelanocortin (POMC).

Table 7.9. List of genes CuffDiff was unable to differentiate between for fish exposed to 26 hours of broad spectrum white light and 48 hours of darkness that were reported as HIDATA

Gene ID	Gene	Photic Condition	Copy No.	Photic Condition	Copy No.	status	Description
ref.28707	LOC100136491	Dark	3959	Light	3002	HIDATA	Somatolactin
ref.4751	LOC100136580	Dark	14093	Light	12778	HIDATA	Prolactin
			14304		14960		Growth-hormone-prepeptide
ref.4807	LOC100136588	Dark		Light		HIDATA	
ref.9897	LOC100169856	Dark	2832	Light	3011	HIDATA	Proopiomelanocortin-B
ref.12224	LOC100510783	Dark	8236	Light	6738	HIDATA	Pro-opiomelanocortin-A1
ref.9483	LOC106607462	Dark	15713	Light	17366	HIDATA	Somatotropin-2

Table 7.10. List of genes CuffDiff was unable to differentiate between for fish exposed to 26 hours of Blue light and 26 hours of Red that were reported as HIDATA

Gene ID	Gene	Photic Condition	Copy No.	Photic Condition	Copy No.	status	Description
ref.28707	LOC100136491	Blue	2284	Red	2589	HIDATA	Somatolactin
ref.4751	LOC100136580	Blue	12002	Red	12328	HIDATA	Prolactin
			10946		9620		Growth-hormone-prepeptide
ref.4807	LOC100136588	Blue		Red		HIDATA	
ref.9897	LOC100169856	Blue	1155	Red	1281	HIDATA	Proopiomelanocortin-B
ref.12224	LOC100510783	Blue	6484	Red	7603	HIDATA	Pro-opiomelanocortin-A1
ref.9483	LOC106607462	Blue	12180	Red	8725	HIDATA	Somatotropin-2

Plasma Cortisol

Analysis of the plasma for cortisol showed no significant differences between groups [p=0.44] (Fig. 7.6A). No significant differences were identified for plasma cortisol between fish exposed to Blue and Red light despite there being a higher value in the Red [p=0.085] (Fig. 7.6B).

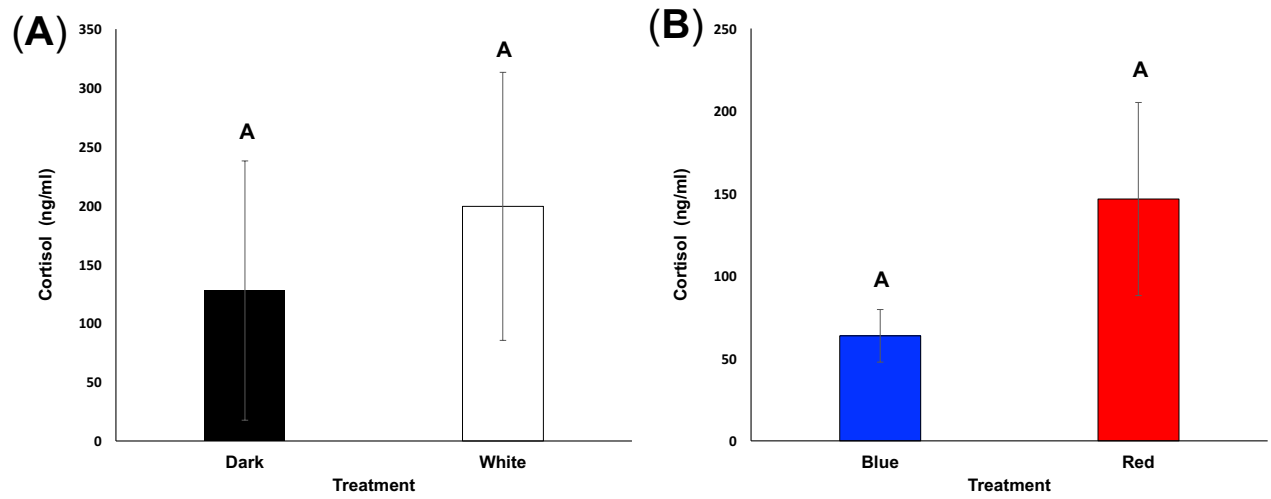

Figure 7.6 Plasma cortisol values from sequenced fish (n=5) exposed to A. dark for 48 hours or 26 hours of broad spectrum white light and B. Blue or Red light for 26 following a period of dark adaption of 48 hours (mean ± SD).

Known Circadian Pathways Genes – Dark vs. White Light

A gene ontology analysis was performed to determine functional pathways associated with expressed genes using the Kyoto Encyclopaedia of Genes and Genome (Kegg). Pathways identified using Kegg are frequently illustrated using mammalian pathways with genes from the organism of interest translocated into known systems. Almost all of the genes associated with the mammalian circadian pathway were identified within the transcriptome with the exception of melatonin receptor type 1 (MT1) and melatonin receptor type 2 (MT2) (Fig 7.7). Genes associated with circadian entrainment during the early night were significantly upregulated in response to darkness (red boxes)

whereas genes associated with daytime were significantly upregulated in broad spectrum white light.

Known Circadian Pathways Genes – Blue vs. Red

In response to Blue and Red light, most genes were present that are associated with the mammalian circadian pathway (Fig. 7.8). Red light led to a significant increase in genes associated with the early stages of night perception were identified within the transcriptome with the exception of melatonin receptor type 1 (MT1) and melatonin receptor type 2 (MT2). Genes associated with circadian entrainment during the early night were significantly upregulated in response to darkness (Red boxes) whereas genes associated with daytime were significantly upregulated in white light.

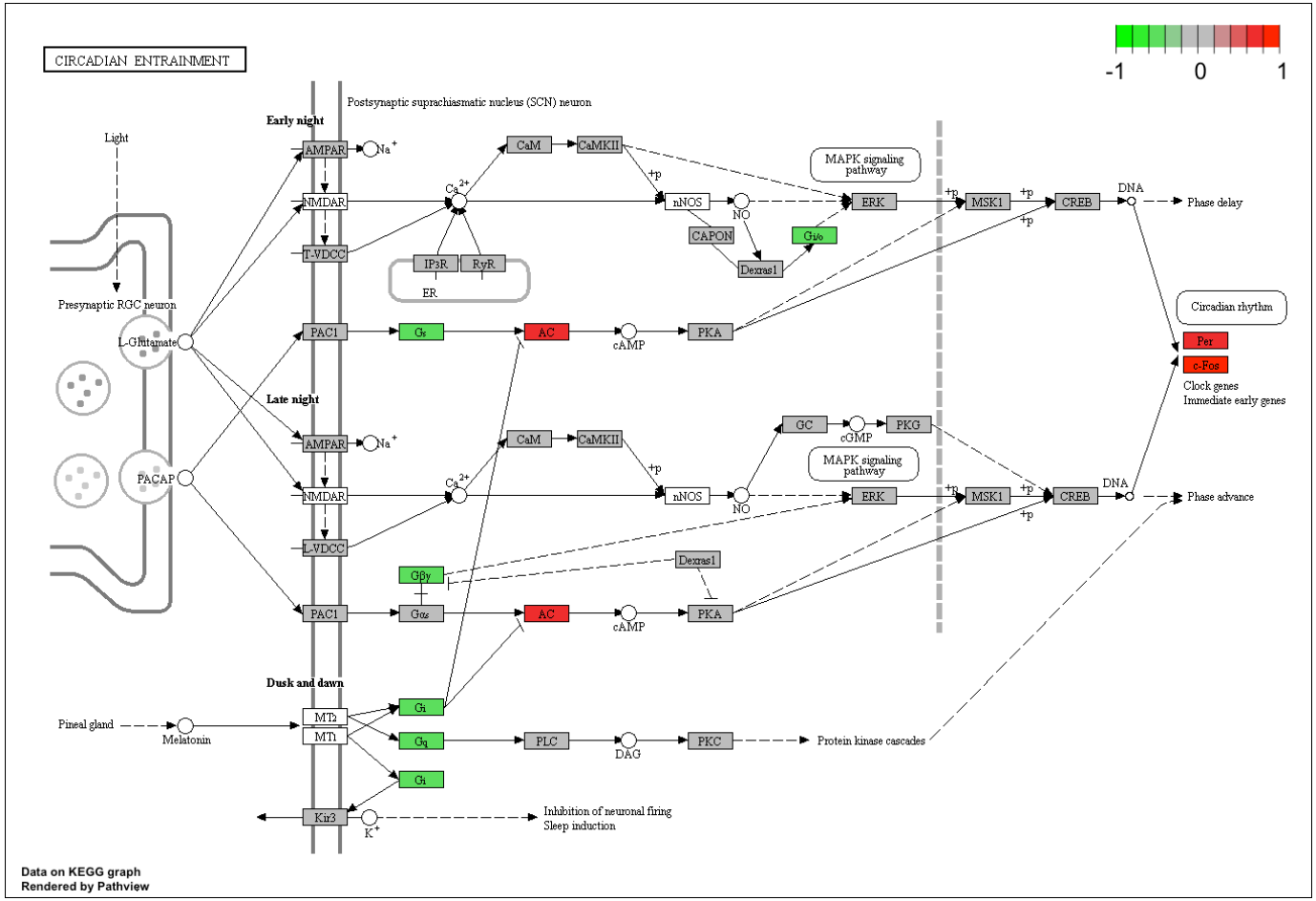

Figure 7.7. Regulation of genes associated with the circadian pathways. Green genes are those significantly upregulated in dark whereas red coloured genes are those significantly upregulated in light. Grey boxes show that the gene was detected, but no significant difference was detected.

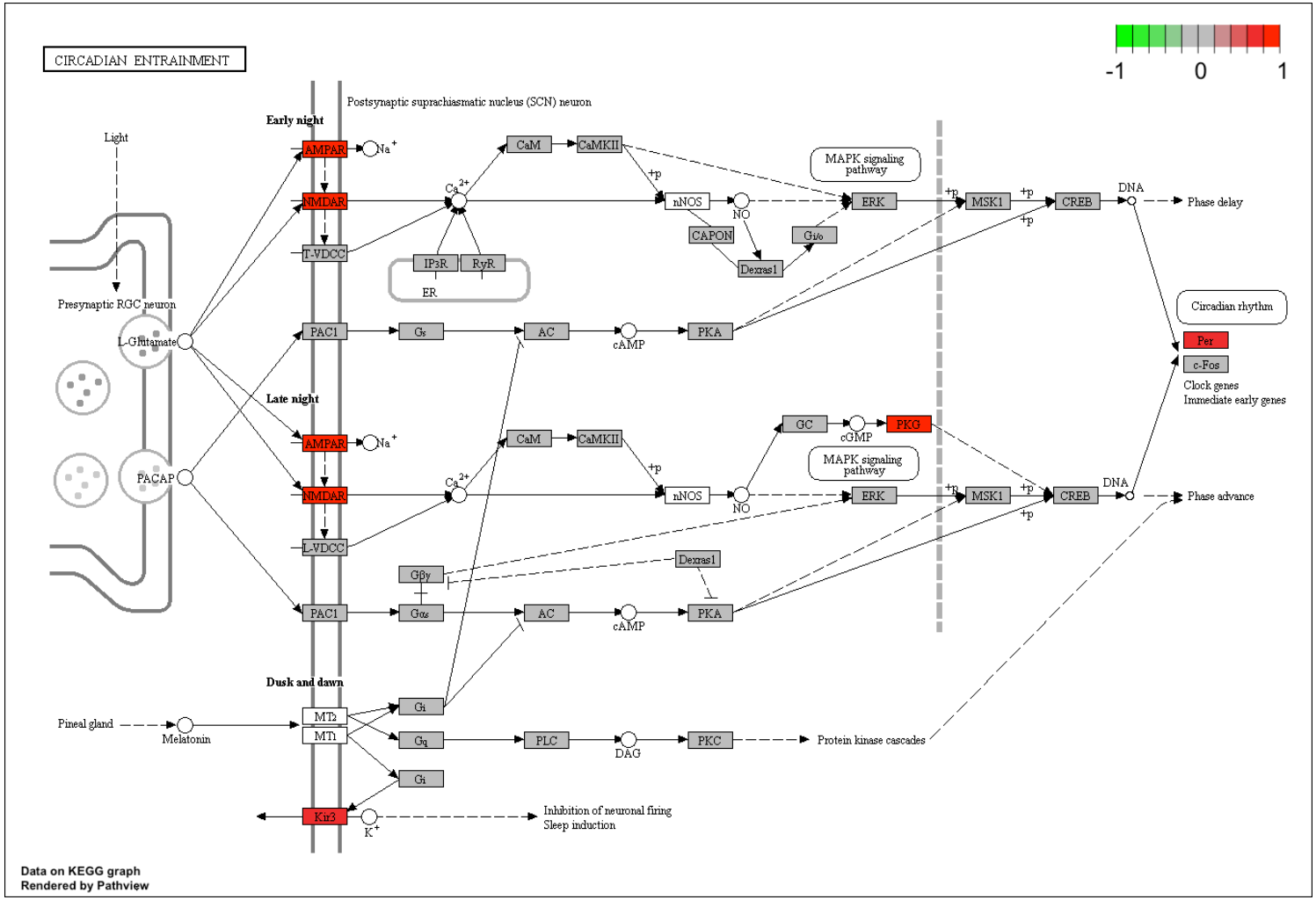

Figure 7.8. Regulation of genes associated with the circadian pathways in response to Blue and Red light. Genes significantly upregulated in Red are shown with red surrounding boxes. Grey boxes show that the gene was detected, but no significant difference was detected.

7.4 Discussion

The pituitary gland is a major component of the photoneuroendocrine system with a pivotal role in the initiation and regulation of endocrine responses from the perception and integration of neural photic information. To our knowledge, this study presents for the first time broad transcriptomic changes in response to photic conditions in Atlantic salmon. Using NGS we examined two photic extremes known to induce different neural responses in the deep brain using in-situ hybridization (Chapter 6). The aim was to determine how the transcriptome changes in response to 48 hours of darkness, 26 hours of broad spectrum white light, 26 hours of Blue light and 26 hours of Red light. Results showed significant changes in gene expression in all treatments. The highest expression and fold changes were identified and functions attributed based upon current published literature. A number of genes were expressed very highly, saturating the Cuffdiff algorithm and preventing direct comparisons. A generalised review of each group is presented and suggestions are made to describe observed differences.

Very Highly Expressed Genes

An ideal aspect of the pituitary gland is the ability to accurately select a very small area of tissue. As specific tissues have defined functions, expression is predominated by genes that facilitate that function (Ramsköld et al., 2009). It is not surprising then that the genes that where very highly expressed are representative of the fundamental functions of the pituitary gland, i.e. endocrine functions. Sequencing a specific amount of tissue with a high number of reads (80 gb per sample) resulted in saturation of the algorithm used to compile the differential expression. Six genes in total returned values as HIDATA and these genes accounted for 0.28 % of the total reads in the Light/Dark comparison and 0.29 % in the Blue/Red comparison. Data was unable to be normalised and thus significant differences in expression could not be determined.

Of the HIDATA genes, the majority were members of the cytokine superfamily which interact and dimerise with transmembrane-domain receptors to initiate cell signalling and behavioural changes (Karnitz and Abraham, 1995). Cytokines are involved in a wide range of somatic and metabolic pathways. Expression of prolactin was high in all treatments and higher value was recorded in response to dark compared to light whereas expression levels in both the Blue and Red groups was

broadly similar. Prolactin plays a key role in osmoregulation by regulating freshwater chloride cells (Sakamoto and McCormick, 2006). This function is inhibited by elevated growth hormone (GH) seen during the completion of smoltification which enhances the activity of seawater chloride cells (Sakamoto and McCormick 2006). High expression of somatolactin (SL) and GH prepropeptide were also present with similar copy numbers between all groups. SL also plays a role in osmoregulation, reducing the actions of GH in order to maintain osmotic balance (Ágústssonet al., 2003). In addition to osmoregulation, cytokines are involved in the complex balance of growth regulation. An opportunistic feeding strategy naturally results in periods of enforced fasting and gorging requiring complex manipulation of reserve to meet energetic and peptides demands (Kurata et al., 2012) and GH is a key regulator in this regard (Gac et al., 1993).

Remaining genes in the high data are from the proopiomelanocortin (POMC) family of which four isoforms have been identified in the pituitary (Valen et al., 2011). A key protein in the Hypothalamic-Pituitary-Adrenal axis, POMC, undergoes substantial post translation modification to form adrenocorticotropic hormone (ACTH), α and β melanocyte-stimulating-hormone, β-lipoprotein and smaller peptides derived from the subsequent modification of these derivatives (Schauer et al., 1994). Both *pomcb* and *pomca1* genes were present and transcript counts appeared to show a higher level of expression in the dark than the light and in the Red compared to the Blue treatment groups. Together these hormones represent some of the major peptides produced by the pituitary.

Dark vs, Light - Differential Gene Expression

The dark vs. light transcriptomes showed considerable variation regarding overall gene expression. A higher number of genes was seen only expressed in dark relative to the number only seen in light. Despite this, the numbers that were significantly differentially expressed between the two conditions was very similar at ~50 %. In response to broad spectrum white light conditions, many of the genes identified were associated with the transcription, and biosynthesis of neuropeptides and signalling. A number of genes associated with stress such as heat-shock protein alpha 90 and a cold-inducible RNA-binding protein are also upregulated during stressful conditions (Zhu et al., 2016). White light resulted in the upregulation of a neurite promoting factor which is released from glial cells, promoting neurite extension and supporting neural

development (Sommer et al., 1987). Given the structure of the pituitary and neurohypophysis, the presence of genes associated with neural development is not surprising.

Based on copy number, a significant increase in the expression of cytochrome P450 27C1 was seen in the light group. P450 27C1 until very recently was considered an orphan cytochrome with no described function. However, Kramlinger et al. (2016) demonstrated recently its ability to catalyse 3,4-dehydroretinal (vitamin A_2) from vitamin A_1. This conversion to vitamin A_2 and regeneration of all-trans retinal (A_1) to 11-*cis*-retinal are key processes in the functioning of the opsin/chromophore group in photoreceptors (Kramlinger et al., 2016). The pituitary is not known to be directly photosensitive and within our results (data not shown) no visual opsins were identified, however, a non-visual opsin gene, opsin-3 like, was identified in all four treatments (data not shown) although no differential expression was seen. Structurally, opn3 is very similar to encephalopsin or teleost multi tissue opsin (*tmt-opsin*) (Koyanagi et al., 2013) which has been identified in a large range of neural and non-neural tissue in zebrafish (Moutsaki et al., 2003). Interestingly *tmt-opsin* was not identified in our data, however this may be due to a lack of genome annotation. Opn-3 has been shown to be both photo-reversible and photo-interconvertible (Koyanagi et al., 2013) using vitamin A_2 as the chromophore. The presence of opn-3 like and P450 27C1, two of the key components in the phototransduction, was shown for the first time in the pituitary of Atlantic salmon. Further research is required to provide functional elucidation and to determine whether *Opn-3-like* is in fact *TMT-opsin*.

In fish exposed to 48 hours of darkness, the highest differentially expressed gene in terms of copy number was somatolactin (SL) beta, a growth hormone upregulated during gametogenesis (Benedet et al., 2008; Campbell et al., 2006; Planas et al., 1992). However, as with many of the somatotrophic factors, SL is also related to general growth (Company et al., 2001) and stress function (Rand-Weaver et al., 1993). In total, three genes associated with metabolic functions, SL, apolipoprotein C-1 and pituitary alpha-2 glycoprotein were significantly upregulated during the dark period suggesting a change in basal metabolism in response to dark conditions. Similar responses to light and darkness have been reported in salmonids regarding the release of the somatotrophins, prolactin and growth hormone, it is proposed that circadian growth cycles exist in salmonids (Leatherland et al., 1974) however as this trial examined a response to broad spectrum white and darkness as

opposed to circadian rhytmicity further work is required to confirm if the genes identified here exhibit such rhytmicity.

Examining the genes with the highest fold change between broad spectrum white light and dark revealed considerable numbers of proteases, cellular signalling genes, transcription factors and cell to cell signalling in response to broad spectrum white light. Elevated genes associated with stress and immune responses were also present. In darkness, a similar broad categorisation was identified with various genes associated with stress and membrane secretion. Of interest in the dark groups was the upregulation of parvalbumin (PV), a calcium binding protein (CaBPs) (Cheung et al., 1980) associated with the saccus vasculosus (Maeda et al., 2015) and nerve cells and a target for intracellular messengers (Cheung et al., 1980). Structural distribution of PV within the salmonid pituitary is not well documented, however the closely related CBP calretinin (CR) is extensively localised within the adenohypophysis, predominantly occurring in the proximal pars distalis (PPD) and rostral pars distalis (RPD), with little within the pars intermedia (Jadhao and Malz, 2007). The PPD and RPD are major centres for hypophysial function and as such the identification of PV in this area may suggest a permissive role in pituitary function (Jadhao and Malz, 2007).

The pituitary gland is a well-known integrator of neural information stimulated through the PNES via hypothalamic innervation and signalling. Almost all of the genes associated with the circadian entrainment pathway were identifiable in all groups with the exception of melatonin receptor type 1 (MT1) and 2 (MT2) which may stem from the challenges of using mammalian models against less well annotated species, i.e. differences may simply be due to the genes not being characterised yet. Results showed a significant upregulation of the circadian *Per* gene and also adenylate cyclase and an upregulation of the immediate early gene *c-fos* that is used as a marker for neural activity (Kovács 2008; Matsuoka et al., 1998). The initial pathway genes in each of the photic states related to changes in photic conditions, early night, late night, dusk and dawn, were also expressed significantly higher in the darkness. Result were as expected given that circadian entrainment occurs through the fluctuation of dark and light, with some genes responding to dark and some to light. The closeness to the mammalian pathway demonstrates how conserved circadian regulation is within vertebrates. The similarities in the number of genes significantly differentially expressed between light and dark was surprising and pointed to just how extreme these two photic conditions are in terms of basal physiological endocrine functions.

Blue vs Red

Whereas the number of genes that were significantly differently expressed between the fish exposed to 48 hours of darkness compared to those exposed to light, an 8-fold increase in significantly differentially expressed genes in response to Red light compared to Blue light was recorded. Thyroid stimulating hormone (TSH) was most highly differentially expressed in response to Blue light, in addition to glycoprotein hormone beta 5. Both of these hormones are involved in the regulation of metabolism and energy homeostasis through the hypothalamic-pituitary-thyroid axis (HPT axis) (Joseph-Bravo et al., 2015). Contactin-2 like and neurogenic differentiation factor 1-like were also seen to be upregulated which are involved in axon extension and guidance (Lin et al., 2012), and neurogenesis (Lewis 1996). A C8orf4 homolog was upregulated which has recently been linked to stress responses in rainbow trout (Verleih et al., 2015) and *gphb5* was seen which has also been implicated in immune responses (Morais et al., 2012) were also seen. Both the immune and endocrine system exhibit considerable cross-talk to ensure homeostasis with feedback from both systems initiating the regulation of cytokines and hormones (Weyts et al., 1999). It is not surprising then to see significant upregulation of genes related to both systems present.

In response to Red light, whilst two of the genes listed were associated with stress responses, *epd1* and *epd2* (Thornqvist et al., 2015) and immune function, *xbp1*, the rest of the genes are involved in the production of haemoproteins associated with oxygen transportation (Tacchi et al., 2011). The production of haemoglobin occurs not just in erythroid cells, but in a range of tissues sensitive to oxygen levels (Saha et al., 2014). Haemoproteins have been reported as being expressed previously in pituitary tissue (Kurata et al., 2012; Seear et al., 2010) in addition to mesangial, hepatocytes and retinal cells (Saha et al., 2014). Biagioli et al. (2009) reported finding both α and β-chain Hb transcripts in mouse brain located within subpopulations of dopamine and hippocampal astrocytes (Biagioli et al., 2009). The presence of local haemoproteins is suggested to ensure sufficient oxygen availability and in these results this is further supported by the upregulation of the soluble guanylate *gcy-31* with which BAG neurons perceive oxygen levels (Zimmer et al., 2009). The significant upregulation suggests a strict requirement for oxygen provision.

Examining the lists of genes upregulated by fold change in response to Blue light showed a general expression of genes associated with secretory cell mechanism

i.e. sodium channels, glucocorticoid receptor, transcription factors and protein binding genes. Results from the Red treatment were similar to those seen examining copy number. Interestingly, as in the dark treatment, parvalbumin was upregulated in response to Red light. In addition, a significant upregulation of the normally dark regulated *Per* was also seen. Sampling at night for circadian products typically takes place using Red light and these results contribute to the debate on the appropriateness of this method. Genes responsible for neural signalling using NO, hypoxia and oxygen sensing were also identified suggesting a highly active pituitary in response to Red light. MYND domain-containing protein is involved in the deacetylation of histones associated with gene transcription (Bower and Johnston, 2010) and expression was significantly higher than in fish exposed to Blue light. Red light clearly leads to a highly active pituitary.

General Comment on Results from Both Trials

In both the light vs dark and Red vs Blue treatments there is a failure for all individuals from each treatment to group together. A such, results show that there is greater variance in the individuals as opposed to that induced by the treatment. This may be due to the experimental design in which fish were taken from LL conditions, exposed to DD for an extended period and then exposed to a spectral condition. The experimental design was chosen to attempt to reduce circadian rhythmicity. However, results suggest that the trial design actually induced arrhythmicity which in turn resulted in clock associated elements becoming desynchronised (Carr and Whitmore, 2005). Care then must be taken when interpreting findings regarding the identification of clock regulated genes and caution applied to those genes determined as photicly entrained Such variation may also help to explain the variance observed within the cortisol results. Results help to highlight the complexity in conducting such studies and the requirement for ensuring extraneous impacts are minimised. In addition to the interesting findings this study helps to highlight the complexities involved in using NGS and provides evidence with which to help guide the design of future trials.

Conclusions

This study aimed to identify differential genes expression in the pituitaries of fish exposed to photic comparison of light and dark (light/dark response), and Blue and Red (spectral response). In total, 756 annotated genes were significantly differentially

expressed between the black and broad spectrum white light groups. This total number was roughly equally split between the conditions and shows that in response to either condition, a substantial change in regulation occurs. Indeed, analysing the top ten genes based on fold change and copy number shows contrasting gene sets. The response to light sees an upregulation of genes mainly involved in the glandular functions of the pituitary. In contrast, the gene lists for fish exposed to dark is predominantly associated with somatic pathways involved in growth. Results suggest that distinct physiological occur in darkness compared to light.

Light is used routinely throughout the production cycle to manipulate salmon physiology however very little is known regarding the light-induced mechanisms that impact upon physiology. In examining the impact of spectrum, 395 annotated genes in total were significantly differentially expressed. Of these, 351 were upregulated in response to Red light. Exposure to Red light resulted in a substantial upregulation of genes associated with stress responses. *Insitu*-hybridisation in Chapter 6 showed cells in the hypothalamus responded to Red light. CRF is produced as the initiator of the HPI axis to release CRF to stimulate the pituitary. Differential regulation of *crf-1*, a gene that is involved in the upregulation of cortisol through the production of ACTH was also seen in the Red group. The impact of ACTH is increased cortisol production, which, whilst not significant, was evident in this trial. Together, this suggests an adverse reaction to Red light. Gene's upregulated in response to Blue were generally associated with glandular function suggesting that Blue did not elicit such a response. This study is the first to examine the broad transcriptomic response to light and identify genes regulated by light and spectrum and represents an important step in beginning to build an understanding of the mechanisms behind physiological responses driven by light and distinct portions of the visible spectrum.

8 Discussion

The aim of this study was to investigate how photic conditions, intensity and spectrum, influence the physiological development of Atlantic salmon within a captive culture setting. Early freshwater development, smoltifciation and post-transfer lighting regimes are important for producers to ensure production cycles meet customer demand. In examining this, a range of biometrics were examined throughout each stage of the captive rearing cycle in order to determine from those tested the optimal photic conditions. Commercial production seeks to maxmise production rates, however the advancement of this must be sought in parallel to welfare considerations such as ocular and skeletal health. Combing these aims with a basal understanding of how the deep brain and pituitary respond to specific photic conditions, this thesis aimed to identify a framework for the design of successful artificial lighting systems.

Determination How Specific Spectrum and Intensity Parameters Impact Upon Growth Attributes During Freshwater Development

Early FW growth ultimately dictates the timing in which photothermal manipulation can be applied in order to induce smoltification. How parr growth is influenced by the photic environment is unexplored in reference to current commercial production systems. The present thesis sought to identify how spectrum and intensity impacts upon development during this ontogenic stage. Initial results clearly demonstrated that Atlantic salmon exhibit considerable tolerance to the wide range of intensities and spectra tested. Only small growth effects were detected between treatments. Collectively results suggested that low intensity lighting resulted in higher TGC values, regardless of spectrum. Findings may reflect the natural biology of juvenile salmon which use shelters to avoid predation and are therefore adapted for relatively dim light. Extrapolating the data further suggested that the optimal light intensity for parr growth was likely to be below 0.5 W/m^2. Interestingly, growth rates in the Green, Red and White were approximately equal for the 5 W/m^2 and 35 W/m^2 unlike in the Blue groups suggesting that different spectra have different optimal light thresholds for growth. Overall, exposure to Blue, Green or White resulted in broadly similar growth depending upon intensity. This broad preliminary look suggested that lower light intensity and the avoidance of red light, especially at high levels, should be used in future trials.

The design of the trial was heavily compromised owing to the incompatible desire of exploring many parameters with finite tank availability. To improve the data resolution, coded wire tags (CWT) were used to track individual fish. This is the first time that tags have been used in such a commercially focused trial (Personal comms. Northwest Marine Technology). Whilst tag recovery was challenging, results proved worthwhile. CWT tags thus provide a useful tool to follow fish from ~1g and could be used to follow a complete cycle from fry to harvest by supplementing the CWT with PIT tags once fish reach a suitable size.

Whereas trial I showed a broad response, trial II allowed the impact of spectrum to be tested using a robust trial design. Specific spectral responses have particular relevance to LED lighting as customised spectral profiles are easy to produce (Pimputkar et al., 2009). Parr development in all light treatments under 0.05 W/m^2 from ~1.5 g to ~40 g was considerably higher than at 0.5 W/m^2 reflectant of either improved water quality in the RAS or the use of lower light intensity. Low light intensity has been shown to reduce the territorial and aggressive behavior of parr (Valdimarsson and Metcalfe 2001) which likely reduces stress levels inhibiting feed intake and utilisation (Bernier and Peter 2001). Measurement of feed intake and FCR and the role of light intensity unfortunately could not be performed in this trial however this should be considered in future trials. TGC values were comparable to the 1.42 reported by Bendiksen et al., 2002 but lower than more recent results by Kolarevic et al., 2014 who reported 1.78 using a RAS system at 8 °C vs the 12 °C in this study. As TGC is calculated on body weight, the relationship between TGC and temperature is not truly linear (Jobling 2003) and as such temperature used during trials may have had an impact upon direct comparison.

Findings showed from those tested an optimal intensity for fry growth of 0.05 W/m^2. Support for this was also found in the trial on larger parr where SD was replaced with a single intensity decrease. As fish did not complete smoltification, growth may be considered to be in line with normal parr development. In that trial an extra 8% of growth was achieved. Such an improvement during parr development would allow out-of-season smoltification regimes to be induced sooner if required, increasing the window in which smolts can be produced. Based upon a production time similar to that seen here, smolts would be ready for SW transfer 1.5 days earlier for each percent, equivalent to 13 days in total. This ability to manipulate smolt timing, even by relatively small margins is highly applicable to industrial practice. Enhanced growth can also be

used to reduce final grow out time. An 8% increase in smolt weight based upon transfer to SW at the 98g in fish exposed to 0.04 W/m^2 instead of 87.7g in the 5 W/m^2 group (i.e. 8% less) would mean fish reach 4kg ~ 10 days earlier using the SGR from the trial 5. Achieving such gains in FW would offer flexibility for producers to make decisions later than is currently possible. Findings thus provide a significant starting point for light output from commercial lighting systems during early FW.

How Exposure to Narrow Spectrum Light Impacts Upon the Induction of Smoltification and the Duration of Seawater Adaptations

A significant finding from these trials with both scientific and commercial interest was that smoltification appeared to be impacted by light spectra. In both trial 4.1 and 4.3 Blue LED light advanced smoltification by 100-200 ºC. Changes in condition factor, NKAe and plasma chloride values were maintained serving to extend the smolt window. At the temperature these trials were conducted at, this represents a real time gain of 7 – 14 days. Such extension provides obvious benefits to production schedules. To explore these finding further and increase the resolution future studies could combine traditional metrics with newly developed metabolomic fingerprinting of smoltification developed by Dr. Simon Thain, TL Science Ltd. By combining the fingerprint with traditional metrics and the transcriptomic data from later in this study it may be possible to elucidate further the mechanisms behind these observations.

Examination of NKAe, and NKAα1a and NKAα1b every 100 ºDays in trial 4.3 showed a 300 ºDays period where NKAe is significantly elevated representing the smolt window. Early studies reported the duration to be around 420 ºDays in S1 fish (Sigholt et al., 1995) although more recently Handeland et al., 2004 showed that at 12 ºC the optimal duration is 250 ºDays. These later results are very similar to the results presented in this thesis and indicate that the biological constraints regarding SW adaptation in FW are remarkably conserved even in seasonally advanced smolts. Current guidance of 250 ºDays is predominantly based upon trials examining small in-season fish compared to large out-of-season fish as was the case here. In trial 4.3 peak NKAe was reached after ~350 degree days. Arnesen et al., (2003) demonstrated that although larger smolts of 75 grams have a shorter window for transfer, they cope better when transferred several weeks after NKAe has fallen as long as the temperature is above 9 ºC. Thus as long as NKAe has peaked transfer to SW should not drastically affect SW survival. Results presented here also show absolute size

seems to facilitate survival. Surprisingly, results from the SWC for fish exposed to no photoperiod cue at all survived. This is a major finding with potential to significantly change current smoltification protocols. If fish that are large enough survive SW with no cue, then the need for lighting protocols is negated. Further study is required to identify if this is the case and to benchmark appropriate performance metrics to determine the effectiveness of such practice.

The Role of Intensity on Smoltification and the Impacts on Seawater Adaptation

Commercial production of Atlantic salmon requires the predictable induction of smoltification. Lighting protocols must ensure synchronicity within the population however no guidelines are currently available to producers regarding day light intensity requirements or acceptable night time background light limits. Current protocols use true light and dark photoperiods to provide a strong cue (Handeland and Stefansson 2001). Here, replacement of the diurnal fluctuation with a single extended period of reduced light intensity (SubWin) resulted in smolt like adaptation occurring in all fish examined with adaptations most advanced in the lowest intensity treatment (0.04 W/m^2). Changes in intensity are thus clearly perceived by parr raising interesting questions regarding the extent to which this can be used to provide a seasonal cue for smoltification. Despite this, compared to the SD-L:D12:12 control, adaptations were incomplete, supporting the premise that a clear and sustained cue (i.e. repeated periods of true “dark”) is required to prevent desynchrony. Resulst are in line with previously studies (Thrush et al., 1994; Duston and Saunders 1995; Berge et al., 1995).

Adaptations, although incomplete, may have been initiated by the change in intensity between hatchery and RAS. Changes in winter light are suggested to account for circannual breeding rhythms in equatorial birds (Gwinner and Scheuerlein 1998). The description of a bistable non-visual photoreceptor by Peirson et al., 2009 provides a mechanism by which such detection may occur due to the high sensitivity to closely related bandwidths that it provides. This raises an interesting question regarding whether a spectral fluctuation could induce smoltification. Not only would this provide an alternative smoltification technique it may also help to elucidate the functional arrangement of photoreceptive tissue.

Smoltification fails to occur in response to LL (Stefansson et al., 2007). However, wild salmon parr will experience some night time illumination from the moon

and still smolt successfully inferring the presence of a night time maximum light threshold. Identifying this has important repercussions to mitigate potentially negative impacts from incident light from machinery and safety signage (Adatto et al. 2016) often present in RAS systems. Results show no such effect at 0.05 W.m^2. Indeed, parr acclimated to 5 W/m^2 prior to "winter" (short-day) smolt successfully when exposed to a repeated nighttime light level of 0.05 W/m^2 using a standard 400 ºDay regime. Finding raise the potential to use LL for smolt induction via diurnal changes in intensity to provide a SD seasonal cue. Such practice could allow feed to be delivered over the entire 24 hour period. Currently, feed is delivered in multiple small meals during the photophase (La Francois et al., 2010). Feeding in this manner gives rise to postprandial spikes in total ammonia (TAN) (Forsberg 1996) causing challenges for filtration systems. Continual feeding could help mitigate these spikes. Trial 4.2 also shows a positive impact on growth during exposure to 0.04 W/m^2 so benefits may be two-fold. A trial examining LL feeding and an intensity switch versus a traditional regime combined with TAN water quantification would be of particular benefit for investigating the suitability of such a regime in commercial systems.

A key question from this study is why smoltification was successful. Light values from 4.3 may have been below the threshold required to inhibit the innervation of the preoptic area by neural fibers required for relaying photoperiodic signals (Ebbessen et al., 2007). Alternatively, the intensity fluctuation may have provided sufficient cue. Understanding this question could allow the development of regimes using an intensity switch of suitable magnitude to induce smoltification. In 2015, 18 million smolts out of the 44.5 million produced in Scotland were grown in cage sites (ScottishGovernment, 2016). Such sites are restricted in terms of photoperiod augmentation to extending day length as ambient light, even on a cloudy day, is considerably higher in intensity that what can be created artificially. As such, sites are only used for S1 smolts (Douglas and Djamgoz 1990). If a photoperiod cue is perceived relative to the ambient conditions, an inverse regime whereby the nighttime is replaced with high intensity lighting compared to the daytime may be able to induce out-of-season smoltification. Findings from 4.1 show that any colour could be used to achieve this allowing the most efficient lights to be used to maximize light output.

<u>Assessment of the Long-Term Implications of Exposure to Narrow Spectrum Light on Welfare Traits Such As Vertebral Formation, Eye Structure and the Stress Axis</u>

The impact of photic conditions on animal welfare is of paramount importance. Encouragingly, no negative impact from narrow bandwidth or White LED could be identified in the present thesis. The tendency for Blue light to affect ocular health in humans (Taylor et al., 1992) was not seen, nor was any reaction to any of the other conditions tested. In previous studies, light intensity below 43 lux from a halogen lamp (~2.15 W/m^2) has been related to vertebral malformation during smoltification (Handeland et al., 2013). In the present trials 5 W/m^2 was applied during the photophase (4.1 and 4.3) and no impact was identified. No published studies have examined the impact of light intensity or spectrum on vertebral health during early parr development and encouragingly no significant differences between treatments was observed. Although appearing high, ~42% across the SNP groups and 34% across the LL groups when values closer to 20 % would be considered normal for this stage in diploid stock (Fjelldal et al., 2006), severity, using >5 deformed vertebrae as a threshold for concern (Hansen et al., 2010) was very low at ~4% of fish in each group A such, results fail to raise welfare concerns.

Although not severe, findings do support the suggestion that accelerating smoltification regimes can impact on vertebral health (Skilbrei and Hansen 2004). Considerable remodeling occurs during this stage and out-of-season regimes represent a real-time compression in calendar days compared to ambient conditions. The relationship between calendar days and degree days thus may not be truly linear. There is clearly a need to understand the effects of elevated water temperature during FW development to enable informed choices to be made regarding RAS operartion. Long term, vertebral problems can result in significant downgrading of fish at harvest, in addition to animal welfare concerns. It may be required to support this accelerated growth with supplementary higher nutrient packages to facilitate rapid bone development such as used with triploids (Fjelldall., 2015; Smedley et al., 2016).

Exposure to Red light had the largest negative impact on growth and thus suggests that this should be avoided. Natural exposure to red light is low and results may reflect a limited ability to tolerate such conditions. Compromised prey detection or a chronic stress response are likely candidates for these observations. Adverse photic conditions are known to heighten stress in salmon (Migaud et al., 2007) which is driven by responses is the HPI axis. Dissection of the constituent parts (brain, pituitary and head kidney) followed by qPCR of genes involved in the stress response, in combination with plasma cortisol would provide a good assessment of the animlas

physiological state (Madaro et al., 2015; Madaro et al., 2016) and should be considered for future trials. Although red light and the stress axis requires further elucidation, the transcriptomic response observed in the pituitary gland suggests a highly-activated transcriptome. Heightened activity at a major endocrine gland will undoubtedly stimulate a considerable number of downstream pathways leading to energetic costs and likely compromise growth. Reducing the diurnal variation induced through the experimental design in the transcriptomic and ISH trials and repeating the appropriate analysis could provide a very detailed overview of a broad range of responses to specific photic conditions and should be considered.

Explore the Impact of Long Term Exposure to Narrow Bandwidth Light on Somatic Growth and Muscle Structure

Examination of muscle fiber structure throughout parr, smoltification and for a period of on-growing demonstrated that exposing juvenile Atlantic salmon to different photic conditions in FW can have a lasting impact on the structure of muscle tissue. WHILST Salmon production aims to produce fish large fish quickly, fillets must be of a suitable quality and provide the consumer with a desirable product which has good mouth feel, health profiles and is attractive in colour. The potential for manipulating this through exposure to coloured light is highly intriguing. Muscle histology presents two opportunities, firstly for extending future growth through increasing latent growth capacity via the presence of greater numbers of small fibers; and secondly in improving the organoleptic properties of the product. Whilst the exact impact of muscle fibers on future development are debated, the improvement of gaping, fillet colour and mouth feel are not. Manipulating this is an exciting proposition and a truly novel result.

Fiber size and distribution data contribute to the discussion on why growth occurs in response to LL. In general, enhanced growth is purported to occur from the advancement of endogenous growth cycles (Duston and Bromage 1988; Nordgarden et al. 2003). However, Johnston et al. (2003) showed a direct photostimulatory action on muscle myoblasts. Results from trial 5 support both seasonal advancement and myoblast proliferation, enhanced growth was seen in all groups but the population structure was changed with compensatory growth occurring in the Green and Red that performed less well in FW. Examination of the muscle fiber structure prior to transfer showed higher numbers of small fibers in these groups which likely facilitated the enhanced growth. Continual recruitment also occurred in all groups exposed to LL

broadly equivalent to that seen in response to SNP. Growth cycles are suggested to arise though recruitment followed by hypertrophy however fish exposed to LL were actively recruiting suggesting that growth may continue at the rates observed. Determination of the feed intake and ultilisation is a substantial short falling of this trial as this would have helped understand better the mechianisms behind observed differences. Facility constraints and system design from the early 1970s did not allow an easy solution however the calculation of FCR is essential in growth trials and must be a priority in future studies.

Assessing growth using muscle fiber analysis was highly challenging and improvement in sampling power may help further studies examining growth. In future it is recommended to improve the automation of the process. Processing 12 fish (3/rep) took in excess of one month from sample collection to data analysis. The predominant time was spent manually tracing fibers. Future studies should aim to sample fish of an equivalent size to help minimise the likelihood of size induced variation which whilst not obvious may have impacted upon results. Whilst challenging, there is a strong case for performing “old fashioned” histological approaches instead of purely molecular analysis as linking molecular expression with cellular responses is difficult given the multitude of mediator mechanisms that regulate the production and actions of gene products. Considerable power can be gained from combing these techniques as shown by Johnston et al. 1999 who identified proliferation myoblasts in additions to structural changes allowing greater conclusions to be drawn and these should be considered in future.

Examine How Prior Photic History and Post-Transfer Photoperiod Regimes Impact Upon Seawater Growth and Sexual Maturation in Fish Transferred Out-Of-Season

Identifying the impact of prior photic history and post-transfer lighting regimes on growth was an important aim of this study and one that has received very little attention in the literature. In groups transferred to ambient photoperiod prior photic history had a lasting effect. The weight of smolts exposed to Red light was 11% lower than those raised under White light. Following 6 months in SW and exposure to SNP, this had increased to 19% and shows the detrimental effect that exclusive exposure to red light during FW can have. Post-transfer exposure to LL however led to accelerated growth in all groups as reported in previous studies (Hansen et al. 1992; Oppedal et al. 1997; U. Nordgarden et al. 2003).

Comparison of growth between cohorts in each light regime showed an increase of 22% in fish previously exposed to White, 25% in Blue, 43% Green and 44% in the Red in response to LL vs SNP. In seeking to identify if growth can be advanced later in the growth cycle, representatives from half of each replicate from each FW group were switched at ~4 months to the opposing photic regime (SNP to LL, and LL to SNP). Results show that photoperiod history plays an important permissive role to the extension of growth using LL. Following transfer, growth was remarkably constrained between the LL and LL-SNP and suggests that for late Q4/ early Q1 transferred smolts the application of additional light for 4 months following transfer has significant potential to enhance growth, in this case by an average of 30% whilst reducing maturation. Assuming this growth rate remains constant, the SGR calculated from the LL and SNP groups shows that LL fish will reach 5.0kg after 344 compared to 2.5 kg in response to SNP. Following fish for a complete growth cycle would help support these findings.

Whilst RAS systems are capable of producing large smolts and reducing on-growing times, manipulation of smolt production invariably leads to significant changes in photoperiods relative to ambient conditions. Imsland et al. 2014 reported that maturation in S0+ stock is becoming a problem in fish raised in RAS. Maximising growth increases the risk of physiological triggers being met early (Randall et al. 1998) as size McCormick et al. 2007), phase shifted photoperiod (Duston and Bromage 1988) and altered water temperatures (Pankhurst and King 2010) in ambient on-growing facilities provide final cues that initiate maturation. Smolts in this trial were transferred several months behind traditionally produced S0 smolts (Handeland et al., 2004), experiencing an immediate rising. Maturation was subsequently very high in males exposed to SNP (mean 73% compared to 13% under LL) suggesting both somatic thresholds and photoperiod were sufficient to initiate maturation.

Clearly, care is needed for the transfer of such fish as maturation in post-transfer smolts has a strong negative impact on production. Results here are the first time a post-SW transfer photoperiod regime for Q4 smolts has been examined. GSI data showed distinct responses to photoperiod with groups exposed to continuous LL increasing GSI compared to those changed to SNP after 4 months. Fish maintained under SNP also had a higher GSI than LL cohorts but lower than those switched to SNP-LL. Together this data strongly supports the model of decision windows that initiate maturation (Taranger et al., 2010). Based on the finding presented, research

is urgently required to develop suitable post SW transfer lighting protocols for fish transferred at different times of the year. Studies should take into account water temperature and hatchery photoperiod history in order to provide clear guidance for producers.

Identification of the Neural and Pituitary Response to Assimilated Light Perception in Response to Different Spectra

Results based upon the ISH and NGS trials provided a basic starting point to understanding the spectral specific neural responses. Results represent a significant advancement in this area of research. A restriction of the trial, and a deliberate one, was the use of animals with eyes and an intact pineal gland. As a result, observations were from a collective assimilation of all photoreceptive tissue and represent what would be perceived in a commercial environment. Such an approach is arguably more useful than using pinealectomised and enucleated subjects when considering the overall physiological response to narrow spectrum light.

The neuroanatomical arrangement of the brain and pituitary, and the central role that the pituitary gland plays in many light mediated axes, means that it is an ideal organ to attempt to identify whether observed differences in brain stimulation lead to changes in endocrine responses. Using high throughput sequencing (NGS), gene expression was intended to be related to photic composition. NGS is still very new in aquaculture with only a few papers released using this technique on salmonids (Harding et al. 2013; Hale et al. 2016; Dettleff et al. 2017). Expression patterns suggest that functions related to somatic development may be under light / dark regulation in agreeance with a considerable body of literature on both fish (Cowan et al. 2017) and higher vertebrates (Minors and Waterhouse 2013; Scheiermann et al. 2013). A differential response to Red and Blue also occurred with significantly more genes differentially expressed in response to Red light. A tentative, link between stress signal upregulation and Red light was apparent. Using genes associated with the stress response, *crfr1*, *pomcs*, *11βhsd2*, *grs* and *mr* such as identified in Madaro et al. 2015 could help to identify these mechanisms further. In exposing fish to the photic condition for 26 hours the aim was to mitigate early light shock/stress in response to switching lights on shown to cause stress behavior in other salmonids (Nemeth and Anderson 2011) however this may have compromised the homeogenous response of individuals

through the inadvertent induction of arrhythmic gene expression. Such an effect should be considered for future trials

Unfortunately, the ability to compare all groups directly was compromised through several mistakes resulting from inexperience. Future studies must ensure all samples are extracted on the same day and shipped together, even if relatively few samples are to be sequenced initially. In addition, library preparation should be performed on the same day by the same operator. The repeatability of NGS sequencing is very high (Marioni et al. 2008) and minimising differences in sample prep should enable comparisons between groups even if sequenced at different times.

General Summary

This thesis presents a considerable body of information with which to guide the development of lighting systems for the commercial production of Atlantic salmon. In summary, evidence suggest that lighting solutions need to be tailored to each stage of production in order to maximise desirable traits. Ultimately, successful production relies upon good husbandry and tank lighting must balance the requirement for manipulation with ease of use. The potential for shifting the timing of smoltification and extending the smolt window though the use of narrow bandwidth lights is exciting. The ability to use low level lighting for the scotophase of an out-of-season regime has important potential for smolt production in RAS and results regarding muscle structure deserves further investigation. Crucially, results show that post transfer light conditions clearly and dramatically influence both growth and maturation in Q4 smolts. Results in this thesis are both scientifically and commercially important.

9 References

Adams, C. E. 1989. Photoperiod and temperature effects on early development and reproductive investment in Atlantic salmon (*Salmo salar* L.). *Aquaculture* **79**, 403–409.

Adatto, I., Krug, L., and Zon, L. I. 2016. The Red Light District and Its Effects on Zebrafish Reproduction. *Zebrafish* **13**, 226-229.

Ágústsson, T., Sundell, K., Sakamoto, T., Ando, M., and Björnsson, B. T. 2003. Pituitary gene expression of somatolactin, prolactin, and growth hormone during Atlantic salmon parr-smolt transformation. *Aquaculture* **222**, 229–238.

Akasaki, I. 2007. Key inventions in the history of nitride-based blue LED and LD. *Journal of Crystal Growth* **300**, 2–10.

Ali, M. A. 1959. The occular structure, retinomotor and photo-behaviour responses of juvenille Pacific salmon. *Canadian Journal of Zoology* **37**, 965–996.

Ali, M. A. 1961. Histophysiological studies on the juvenile Atlantic salmon (Salmo salar) retina: II. Responses to light intensities, wavelenghts, temperatures, and continuous light or dark. *Canadian Journal of Zoology* **39**, 511–526.

Ali, M., Nicieza, A., and Wootton, R. J. 2003. Compensatory growth in fishes: A response to growth depression. *Fish and Fisheries* **4**, 147–190.

Allen, D. M., and Munz, F. W. 1983. Visual pigment mixtures and scotopic spectral sensitivity in rainbow trout. *Environmental Biology of Fishes* **8**, 185–190.

Allendorf, F. W., and Thorgaard, G. H. 1984. Tetraploidy and the evolution of salmonid fishes, In: Turner, B. J. (Ed.), *Evolutionary genetics of fishes,* Springer, New York*,* pp. 1–53.

Amoroso, G. 2016. Investigations of skeletal anomalies in triploid Atlantic salmon (Salmo salar L. 1758) in freshwater: with particular focus on lower jaw deformity (LJD). PhD Thesis, University of Tasmania.

Andersson, E., Nijenhuis, W., Male, R., Swanson, P., Bogerd, J., Lasse, G., and Schulz, R. W. 2009. General and comparative endocrinology pharmacological characterization, localization and quantification of expression of gonadotropin receptors in Atlantic salmon (*Salmo salar* L.) ovaries. *General and Comparative Endocrinology* **163**, 329–339.

Andersson, E., Schulz, R. W., Male, R., Bogerd, J., Patiña, D., Benedet, S., Norberg, B.,and Taranger, G. L. 2013. Pituitary gonadotropin and ovarian gonadotropin

receptor transcript levels: Seasonal and photoperiod-induced changes in the reproductive physiology of female Atlantic salmon (*Salmo salar*). *General and Comparative Endocrinology* **191**, 247–258.

Anglade, I., Zandbergen, T., and Kah, O. 1993. Origin of the pituitary innervation in the goldfish. *Cell and Tissue Research* **273**, 345–355.

Arendt, J. D. 1997. Adaptive intrinsic growth rates: an integration across taxa. *The Quarterly Review of Biology* **72**, 149.

Arendt, J., Wilson, D. S., and Stark, E. 2001. Scale strength as a cost of rapid growth in sunfish. *Oikos* **93**, 95–100.

Arnesen, A. M., Toften, H., Agustsson, T., Stefansson, S. O., Handeland, S. O., and Björnsson, B. T. 2003. Osmoregulation, feed intake, growth and growth hormone levels in 0+ Atlantic salmon (*Salmo salar* L.) transferred to seawater at different stages of smolt development. *Aquaculture* **222**, 167–187.

Arshavsky, V. Y., Lamb, T. D., and Pugh, E. N. 2002. G proteins and phototransduction. *Annual Review of Physiology* **64**, 153–187.

Aspehaug, V., Mikalsen, a. B. A. B., Snow, M., Biering, E., and Villoing, S. 2005. Characterization of the infectious salmon anemia virus fusion protein. *Journal of Virology* **79**, 12544-12553.

Austreng, E., Storebakken, T., and Åsgård, T. 1987. Growth rate estimates for cultured Atlantic salmon and rainbow trout. *Aquaculture* **60**, 157–160.

Baggerman, B. (1980). Photoperiodic and endogenous control of the annual reproductive cycle in teleost fishes. In: *Environmental Physiology of Fishes.* New York, NY: Plenum Press, 553–568.

Ball, J. N. 1981. Hypothalamic control of the pars distalis in fishes, amphibians, and reptiles. *General and Comparative Endocrinology* **44**, 135–170.

Bapary, M. A. J., Fainuulelei, P., and Takemura, A. 2009. Environmental control of gonadal development in the tropical damselfish *Chrysiptera cyanea*. *Marine Biology Research* **5**, 462–469.

Bapary, M. A. J., Amin, M. N., Takeuchi, Y., and Takemura, A. 2011. The stimulatory effects of long wavelengths of light on the ovarian development in the tropical damselfish, *Chrysiptera cyanea*. *Aquaculture* **314**, 188–192.

Barton, B. 2002. Stress in fishes: a diversity of responses with particular reference to changes in circulating corticosteroids. *Integrative and Comparative Biology* **42**, 517–525.

Barton, B., Schreck, C., and Barton, L. 1986. Effects of chronic cortisol administration and daily acute stress on growth, physiological conditions, and stress responses in juvenile rainbow trout. *Diseases of Aquatic Organisms* **2**, 173–185.

Barton, B. A., Schreck, C. B., Ewing, R. D., Hemmingsen, A. R., and Patiño, R. 1985. Changes in plasma cortisol during stress and smoltification in Coho Salmon, *Oncorhynchus kisutch*. *General and Comparative Endocrinology* **59**, 468–471.

Bas, A., Swamy, M., Abeler-Dörner, L., Williams, G., Pang, D. J., Barbee, S. D., and Hayday, A. C. 2011. Butyrophilin-like 1 encodes an enterocyte protein that selectively regulates functional interactions with T lymphocytes. *Proceedings of the National Academy of Sciences of the United States of America* **108**, 4376–4381.

Baver, S. B., Pickard, G. E., Sollars, P. J., and Pickard, G. E. 2008. Two types of melanopsin retinal ganglion cell differentially innervate the hypothalamic suprachiasmatic nucleus and the olivary pretectal nucleus. *The European Journal of Neuroscience* **27**, 1763–1770.

Beatty, D. D. 1966. A study of the succession of visual pigments in Pacific salmon (*Oncorhynchus*). *Canadian Journal of Zoology* **44**, 429–455.

Bellingham, J., Chaurasia, S. S., Melyan, Z., Liu, C., Cameron, M. A, Tarttelin, E. E., Iuvone, P. M., Hankins, M. W., Tosini, G. and Lucas, R. J. 2006. Evolution of melanopsin photoreceptors: discovery and characterization of a new melanopsin in nonmammalian vertebrates. *PLoS Biology* **4**, 254.

Bendiksen, E. Å., Jobling, M., and Arnesen, A. M. 2002. Feed intake of Atlantic salmon parr *Salmo salar* L. in relation to temperature and feed composition. *Aquaculture Research* **33**, 525–532.

Benedet, S., Björnsson, B., Taranger, G., and Andersson, E. 2008. Cloning of somatolactin alpha, beta forms and the somatolactin receptor in Atlantic salmon: seasonal expression profile in pituitary and ovary of maturing female broodstock. *Reproductive Biology and Endocrinology* **6**, 42-58.

Berge, A. I., Berg, A., Fyhn, H. J., Barnung, T., Hansen, T., and Stefansson, S. O. 1995. Development of salinity tolerance in underyearling smolts of Atlantic salmon (*Salmo salar*) reared under different photoperiods. *Canadian Journal of Fisheries and Aquatic Sciences* **52**, 243–251.

Bergheim, A., Drengstig, A., Ulgenes, Y., and Fivelstad, S. 2009. Production of Atlantic salmon smolts in Europe-Current characteristics and future trends. *Aquacultural*

Engineering **41**, 46–52.

Bernardos, R. L., Barthel, L. K., Meyers, J. R., and Raymond, P. A. 2007. Late-stage neuronal progenitors in the retina are radial Müller glia that function as retinal stem cells. *The Journal of Neuroscience: The Official Journal of the Society for Neuroscience* **27**, 7028–7040.

Bernier, N. J., and Peter, R. E. 2001. The hypothalamic-pituitary-interrenal axis and the control of food intake in teleost fish. *Comparative Biochemistry and Physiology - B Biochemistry and Molecular Biology* **129**, 639–644.

Berrill, I. K., Porter, M. J. R., Smart, A., Mitchell, D., and Bromage, N. R. 2003. Photoperiodic effects on precocious maturation, growth and smoltification in Atlantic salmon, *Salmo salar*. *Aquaculture* **222**, 239–252.

Berrill, I. K., Porter, M. J. R., and Bromage, N. R. 2006. The effects of daily ration on growth and smoltification in 0+ and 1+ Atlantic salmon (*Salmo salar*) parr. *Aquaculture* **257**, 470–481.

Biagioli, M., Pinto, M., Cesselli, D., Zaninello, M., Lazarevic, D., Roncaglia, P., Simone, R., Vlachouli, C., Plessy, C., Bertin, N., Beltrami, A., Kobayashi, K., Gallo, V., Santoro, C., Ferrer, I., Rivella, S., Beltrami, C.A., Carninci, P., Raviola, E. and Gustincich, S. 2009. Unexpected expression of alpha- and beta-globin in mesencephalic dopaminergic neurons and glial cells. *Proceedings of the National Academy of Sciences* **106**, 15454–15459.

Billerbeck, J. M., and Lankford, T. E. 2001. Evolution of intrinsic growth and energy acquisition rates. I. trade-offs with swimming performance in *Menidia menidia*. *Evolution* **55**, 1863–1872.

Bilton, H. T., Alderdice, D. F., and Schnute, J. T. 1982. Influence of time and size at release of juvenile Coho salmon (*Oncorhynchus kisutch*) on returns at maturity. *Canadian Journal of Fisheries and Aquatic Sciences* **39**, 426–447.

Björnsson, B. T. 1997. The biology of salmon growth hormone: from daylight to dominance. *Fish Physiology and Biochemistry* **17**, 9–24.

Björnsson, B. T., and Bradley, T. M. 2007. Epilogue: Past successes, present misconceptions and future milestones in salmon smoltification research. *Aquaculture* **273**, 384–391.

Björnsson, B. T., Taranger, G. L., Hansen, T., Stefansson, S. O., and Haux, C. 1994. The interrelation between photoperiod, growth hormone, and sexual maturation of adult Atlantic salmon (*Salmo salar*). *General and Comparative Endocrinology*

93, 70-81.

Blackburn, J., and Clarke, W. C. 1987. Revised procedure for the 24 hour seawater challenge test to measure seawater adaptability of juvenile salmonlds. *Canadian Technical Reports of Fisheries and Aquatic Sciences* **1515**, 1–35.

Boeuf, G., and Le Bail, P-Y. 1999. Does light have an influence on fish growth? *Aquaculture* **177**, 129–152.

Bostock, J., Lane, A., Hough, C., and Yamamoto, K. 2016. An assessment of the economic contribution of EU aquaculture production and the influence of policies for its sustainable development. *Aquaculture International* **24**, 699–733.

Boulton, M., Rózanowska, M., and Rózanowski, B. 2001. Retinal photodamage. *Journal of Photochemistry and Photobiology B: Biology* **64**, 144–161.

Bower, N. I., and Johnston, I. A. 2010. Discovery and characterization of nutritionally regulated genes associated with muscle growth in Atlantic salmon. *Physiological Genomics* **42A**, 114–130.

Bowler, C., Neuhaus, G., Yamagata, H., and Chua, N-H. 1994. Cyclic GMP and calcium mediate phytochrome phototransduction. *Cell* **77**, 73–81.

Bowmaker, J. K., and Kunz, Y. W. 1987. Ultraviolet receptors, tetrachromatic colour vision and retinal mosaics in the brown trout (*Salmo trutta*): Age-dependent changes. *Vision Research* **27**, 2101–2108.

Brodeur, J. C. 2003. Proliferation of myogenic progenitor cells following feeding in the sub-antarctic notothenioid fish *Harpagifer bispinis*. *Journal of Experimental Biology* **206**, 163–169.

Bromage, N., Duston, J., Randall, C., Brook, A., Thrush, M., Carrillo, M., and Zanuy, S. 1990. Photoperiodic control of teleost reproduction. *Photoperiodic Control of Teleost Reproduction* **342**, 620–626.

Bromage, N. R., Whitehead, C., and Breton, B. 1982. Relationships between serum levels of gonadotropin, oestradiol-17b, and vitellogenin in the control of ovarian development in the rainbow trout. II. Effects of alterations in environmental photoperiod. *General and Comparative Endocrinology* **47**, 366–376.

Bromage, N., Jones, J., Randall, C., Thrush, M., Davies, B., Springate, J., Duston, J., and Barker, G. 1992. Broodstock management, fecundity, egg quality and the timing of egg production in the rainbow trout (*Oncorhynchus mykiss*). *Aquaculture* **100**, 141–166.

Bromage, N., Porter, M., and Randall, C. 2001. The environmental regulation of maturation in farmed finfish with special reference to the role of photoperiod and melatonin. *Aquaculture* **197**, 63–98.

Buck, R. J. G., and Youngson, A. F. 1982. The downstream migration of precociously mature Atlantic salmon, *Salmo salar* L. parr in autumn; its relation to the spawning migration of mature adult fish. *Journal of Fish Biology* **20**, 279–288.

Bullitt, E. 1990. Expression of C-fos-like protein as a marker for neuronal activity following noxious stimulation in the rat. *Journal of Comparative Neurology* **296**, 517–530.

Bureau, D., Azevedo, P., Tapia-salazar, M., and Cuzon, G. 2000. Pattern and cost of growth and nutrient deposition in fish and shrimp: potential implications and applications. *Avances En Nutrición*, 111–140.

Bury, N. R., and Sturm, A. 2007. Evolution of the corticosteroid receptor signalling pathway in fish. *General and Comparative Endocrinology* **153**, 47–56.

Campbell, P. M., Pottinger, T. G., and Sumpter, J. P. 1992. Stress reduces the quality of gametes produced by rainbow trout. *Biology of Reproduction* **47**, 1140–1150.

Campbell, B., Dickey, J., Beckman, B., Young, G., Pierce, A., Fukada, H., and Swanson, P. 2006. Previtellogenic oocyte growth in salmon: relationships among body growth, plasma insulin-like growth factor-1, estradiol-17beta, follicle-stimulating hormone and expression of ovarian genes for insulin-like growth factors, steroidogenic-acute regulatory protein and receptors for gonadotropins, growth hormone, and somatolactin. *Biology of Reproduction* **75**, 34–44.

Carr, A. J. F. and Whitmore, D. 2005. Imaging of single light-responsive clock cells reveals fluctuating free-running periods. *Nature Cell Biology* **7**, 319.

Castro, R., Bromage, E., Abós, B., Pignatelli, J., González Granja, A., Luque, A., and Tafalla, C. 2014. CCR7 is mainly expressed in teleost gills, where it defines an IgD+IgM- B lymphocyte subset. *Journal of Immunology* **192**, 1257–1266.

Chauvigné, F., Gabillard, J. C., Weil, C., and Rescan, P. Y. 2003. Effect of refeeding on IGFI, IGFII, IGF receptors, FGF2, FGF6, and myostatin mRNA expression in rainbow trout myotomal muscle. *General and Comparative Endocrinology* **132**, 209–215.

Chellappa, S. L., Ly, J. Q. M., Meyer, C., Balteau, E., Degueldre, C., Luxen, A., Phillips, C., Cooper, H. M., and Vandewalle, G. 2014. Photic memory for executive brain responses. *Proceedings of the National Academy of Sciences of*

the United States of America **111**, 6087-6091.

Chen, S-C., Robertson, R. M., and Hawryshyn, C. W. 2014. Ontogeny of melanophore photosensitivity in rainbow trout (*Oncorhynchus mykiss*). *Biology Open* **3**, 1032–1036.

Cheng, C. L., Flamarique, I. N., Hárosi, F. I., Rickers-Haunerland, J., and Haunerland, N. H. 2006. Photoreceptor layer of salmonid fishes: transformation and loss of single cones in juvenile fish. *The Journal of Comparative Neurology* **495**, 213–235.

Cheung, W. Y. 1980. Calmodulin plays a pivotal role in cellular regulation. *Science* **207**, 19–27.

Cho, C. Y. 1992. Feeding systems for rainbow trout and other salmonids with reference to current estimates of energy and protein requirements. *Aquaculture* **100**, 107–123.

Clarke, L. A., and Sutterlin, A. M. 1985. Associative learning, short-term memory, and colour preference during first feeding by juvenile Atlantic salmon. *Canadian Journal of Zoology* **63**, 9–14.

Collin, J-P., Brisson, P., Falcon, J., and Voisin, P. 1986. Multiple cell types in the pineal: functional aspects. *Pineal and Retinal Relationships*, 15–32.

Colt, J. 2006. Water quality requirements for reuse systems. *Aquacultural Engineering* **34**, 143–156.

Company, R., Astola, A., Pendón, C., Valdivia, M. M., and Pérez-Sánchez, J. 2001. Somatotropic regulation of fish growth and adiposity: Growth hormone (GH) and somatolactin (SL) relationship. *Comparative Biochemistry and Physiology - C Toxicology and Pharmacology* **130**, 435–445.

Connor, W. P., Burge, H. L., Yearsley, J. R., and Bjornn, T. C. 2003. Influence of flow and temperature on survival of wild subyearling fall chinook salmon in the Snake River. *North American Journal of Fisheries Management* **23**, 362–375.

Cotter, D., O'Donovan, V., Drumm, A., Roche, N., Ling, E. N., and Wilkins, N. P. 2002. Comparison of freshwater and marine performances of all-female diploid and triploid Atlantic salmon (*Salmo salar* L.). *Aquaculture Research* **33**, 43–53.

Coughlin, D. J., and Hawryshyn, C. W. 1995. A cellular basis for polarized-light vision in rainbow trout. *Journal of Comparative Physiology A* **176**, 261–272.

Cowan, M., Azpeleta, C., and López-Olmeda, J. F. 2017. Rhythms in the endocrine system of fish: a review. *Journal of Comparative Physiology B*.

doi:10.1007/s00360-017-1094-5.

Crisp, D. T., and Hurley, M. A. 1991. Stream channel experiments on downstream movement of recently emerged trout, *Salmo trutta* L., and salmon, *S. salar* L.—11. Effects of constant and changing velocities and of day and night upon dispersal rate. *Journal of Fish Biology* **39**, 363–370.

Dalsgaard, J., Lund, I., Thorarinsdottir, R., Drengstig, A., Arvonen, K., and Pedersen, P. B. 2013. Farming different species in RAS in Nordic countries: Current status and future perspectives. *Aquacultural Engineering* **53**, 2–13.

Damsgård, B., and Arnesen, A. M. 1998. Feeding, growth and social interactions during smolting and seawater acclimation in Atlantic salmon, *Salmo salar* L. *Aquaculture* **168**, 7–16.

Darlington, T. K., Wager-Smith, K., Ceriani, M. F., Staknis, D., Gekakis, N., Steeves, T. D. L., Weitz, C. J., Takahashi, J. S., and Kay, S. A. 1998. Closing the circadian loop: CLOCK-induced transcription of its own inhibitors *per* and *tim*. *Science* **280**, 1599–1603.

Dartnall, H. J. A., Lander, M. R., and Munz, F. W. 1961. Periodic changes in the visual pigment of a fish, In: Christensen, B., and Buchmann, B. (Eds.), *Progress in Photobiology*. Elsevier, Amsterdam, pp. 203-213.

Daughaday, W. H., and Rotwein, P. 1989. Insulin-like growth factors I and II. Peptide, messenger ribonucleic acid and gene structures, serum, and tissue concentrations. *Endocrine Reviews* **10**, 68–91.

Davie, A., Minghetti, M., and Migaud, H. 2009. Seasonal variations in clock-gene expression in Atlantic salmon (*Salmo sala*r). *Chronobiology International* **26**, 379–395.

Davies, W. L., Hankins, M. W., and Foster, R. G. 2010. Vertebrate ancient opsin and melanopsin: divergent irradiance detectors. *Photochemical and Photobiological Sciences: Official Journal of the European Photochemistry Association and the European Society for Photobiology* **9**, 1444–1457.

Davies, W. I. L., Tamai, T. K., Zheng, L., Fu, J. K., Rihel, J., Foster, R. G., Whitmore, D., and Hankins, M. W. 2015. An extended family of novel vertebrate photopigments is widely expressed and displays a diversity of function. *Genome Research* **25**, 1666–1679.

Derbyshire, E. R., and Marletta, M. A. 2012. Structure and regulation of soluble guanylate cyclase. *Annual Review of Biochemistry* **81**, 533–559.

Dettleff, P., Moen, T., Santi, N., and Martinez, V. 2017. Transcriptomic analysis of spleen infected with infectious salmon anemia virus reveals distinct pattern of viral replication on resistant and susceptible Atlantic salmon (*Salmo salar*). *Fish and Shellfish Immunology* **61**, 187–193.

Dickhoff, W. W., Beckman, B. R., Larsen, D. A., and Moriyama, S. 1997. The role of growth in endocrine regulation of salmon smoltification. *Fish Physiology and Biochemistry* **17**, 231–236.

Dinno, A. 2016. Dunn's Test of Multiple Comparisons Using Rank Sums. Retrieved from https://cran.r-project.org/package=dunn.test

Doncaster, C. P., and Davey, A. J. H. 2007. Analysis of variance and covariance: how to choose and construct models for the life sciences. *Cambridge University Press, Cambridge*.

Douglas, R. H., and Djamgoz, M. B. A. 1990. *The Visual System of Fish*. Chapman and Hall, Torquay.

Doyle, W. L., and Gorecki, D. 1961. The so-called chloride cell of the fish gill. *Physiological Zoology* **34**, 81–85.

Drivenes, Ø., Søviknes, A. M., Ebbesson, L. O. E., Fjose, A., Seo, H-C., and Helvik, J. V. 2003. Isolation and characterization of two teleost melanopsin genes and their differential expression within the inner retina and brain. *Journal of Comparative Neurology* **456**, 84–93.

Dumas, A., France, J., and Bureau, D. 2010. Modelling growth and body composition in fish nutrition: Where have we been and where are we going? *Aquaculture Research* **41**, 161–181.

Dumas, A., France, J., and Bureau, D. P. 2007. Evidence of three growth stanzas in rainbow trout (*Oncorhynchus mykiss*) across life stages and adaptation of the thermal-unit growth coefficient. *Aquaculture* **267**, 139–146.

Duncan, N. J., and Bromage, N. 1998. The effect of different periods of constant short days on smoltification in juvenile Atlantic salmon (*Salmo salar*). *Aquaculture* **168**, 369–386.

Duncan, N. J., Selkirk, C., Porter, M., Hunter, D., Magwood, S., and Bromage, N. 2000. The effect of altered photoperiods on maturation of male and female Atlantic salmon (*Salmo salar*), observations of different responses and mechanisms. In: Norberg, B., Kjesbu, O. S., Taranger, G. L., Andersson, E., and Stefansson, S. O. (Eds.), *International Symposium on the Reproductive Physiology of Fish*.

Bergen, Norway.

Dunn, J. F., and Johnston, I. A. 1986. Metabolic constraints on burst-swimming in the Antarctic teleost *Notothenia neglecta*. *Marine Biology* **91**, 433–440.

Duston, J., and Bromage, N. 1988 The entrainment and gating of the endogenous circannual rhythm of reproduction in the female rainbow trout (*Salmo gairdneri*). *Journal of Comparative Physiology A* **164**, 259–268.

Duston, J., and Saunders, R. L. 1990. The entrainment role of photoperiod on hypoosmoregulatory and growth-related aspects of smolting in Atlantic salmon (*Salmo salar*). *Canadian Journal of Zoology* **68**, 707–715.

Duston, J., and Saunders, R. L. 1992. Effect of 6-, 12-, and 18-month photoperiod cycles on smolting and sexual maturation in juvenile Atlantic salmon (*Salmo salar*). *Canadian Journal of Fisheries and Aquatic Sciences* **49**, 2273–2280.

Duston, J., and Saunders, R. L. 1995. Advancing smolting to autumn in age 0+ Atlantic salmon by photoperiod, and long-term performance in sea water. *Aquaculture* **135**, 295–309.

Duston, J., and Saunders, R. L. 1997. Life histories of Atlantic salmon altered by winter temperature and summer rearing in fresh- or sea-water. *Environmental Biology of Fishes* **50**, 149–166.

Duston, J., Saunders, L., and Knox, D. E. 1991. Effects of increases in freshwater temperature on loss of smolt characteristics in Atlantic salmon (*Salmo salar*). *Canadian Journal of Fisheries and Aquatic Sciences* **48**, 164–169.

Ebbesson, L. O. E., Holmqvist, B., Östholm, T., and Ekström, P. 1992. Transient serotonin-immunoreactive neurons coincide with a critical period of neural development in Coho salmon (*Oncorhynchus kisutch*). *Cell and Tissue Research* **268**, 389–392.

Ebbesson, L. O. E., Ekström, P., Ebbesson, S. O. E., Stefansson, S. O., and Holmqvist, B. 2003. Neural circuits and their structural and chemical reorganization in the light-brain-pituitary axis during parr-smolt transformation in salmon. *Aquaculture* **222**, 59–70.

Ebbesson, L. O. E., Ebbesson, S. O. E., Nilsen, T. O., Stefansson, S. O., and Holmqvist, B. 2007. Exposure to continuous light disrupts retinal innervation of the preoptic nucleus during parr-smolt transformation in Atlantic salmon. *Aquaculture* **273**, 345–349.

Ebbesson, L. O. E., Nilsen, T. O., Helvik, J. V., Tronci, V., and Stefansson, S. O. 2011.

Corticotropin-releasing factor neurogenesis during midlife development in salmon: Genetic, environmental and thyroid hormone regulation. *Journal of Neuroendocrinology* **23**, 733–741.

Edwards, D. 2016. *Plant Bioinformatics Methods and Protocols*. *Methods and Protocols*. Springer, New York.

Eilertsen, M., Drivenes, Ø., Edvardsen, R. B., Bradley, C. A., Ebbesson, L. O. E., and Helvik, J. V. 2014. Exorhodopsin and melanopsin systems in the pineal complex and brain at early developmental stages of Atlantic halibut (*Hippoglossus hippoglossus*). *Journal of Comparative Neurology* **522**, 4003–4022.

Ekström, P., Foster, R. G., Korf, H. W., and Schalken, J. J. 1987. Antibodies against retinal photoreceptor-specific proteins reveal axonal projections from the photosensory pineal organ in teleosts. *The Journal of Comparative Neurology* **265**, 25–33.

Ekstrzm, P., and Meissl, H. 1997. The pineal organ of teleost fishes. *Reviews in Fish Biology and Fisheries* **7**, 199–284.

Elliott, J. M., and Hurley, M. A. 1997. A functional model for maximum growth of Atlantic Salmon parr, *Salmo salar*, from two populations in northwest England. *Functional Ecology* **11**, 592–603.

Ellis, T., Yildiz, H. Y., López-Olmeda, J., Spedicato, M. T., Tort, L., Øverli, Ø., and Martins, C. I. M. 2012. Cortisol and finfish welfare. *Fish Physiology and Biochemistry* **38**, 163–188.

Endal, H. P., Taranger, G. L., Stefansson, S. O., and Hansen, T. 2000. Effects of continuous additional light on growth and sexual maturity in Atlantic salmon, *Salmo salar*, reared in sea cages. *Aquaculture* **191**, 337–349.

Eriksson, L., and Lundqvist, H. 1980. Photoperiod entrains ripening by its differential effect in salmon. *Naturwissenschaften* **67**, 202–203.

Eriksson, L., and Lundqvist, H. 1982. Circannual rhythms and photoperiod regulation of growth and smolting in Baltic salmon (Salmo salar L.). *Aquaculture* **28**, 113–121.

Erwin, D. H., Laflamme, M., Tweedt, S. M., Sperling, E. A., Pisani, D., and Peterson, K. J. 2011. The Cambrian conundrum: early divergence and later ecological success in the early history of animals. *Science* **334**, 1091–1097.

Esteban, M. Á., Cuesta, A., Chaves-Pozo, E., and Meseguer, J. 2013. Influence of melatonin on the immune system of fish: a review. *International Journal of*

Molecular Sciences **14**, 7979–7999.

Esteve, M. 2005. Observations of spawning behaviour in Salmoninae: *Salmo*, *Oncorhynchus* and *Salvelinus*. *Reviews in Fish Biology and Fisheries* **15**, 1-21.

Falcón, J. 1999. Cellular circadian clocks in the pineal. *Progress in Neurobiology* **58**, 121–162.

Falcón, J., Galarneau, K. M., Weller, J. L., Ron, B., Chen, G., Coon, S. L., and Klein, D. C. 2001. Regulation of arylalkylamine N-acetyltransferase-2 (AANAT2, EC 2.3. 1.87) in the fish pineal organ: evidence for a role of proteasomal proteolysis. *Endocrinology* **142**, 1804–1813.

Falcón, J., Gothilf, Y., Coon, S. L., Boeuf, G., and Klein, D. C. 2003. Genetic, temporal and developmental differences between melatonin rhythm generating systems in the teleost fish pineal organ and retina. *Journal of Neuroendocrinology* **15**, 378–382.

Falcón, J., Besseau, L., Sauzet, S., and Boeuf, G. 2007. Melatonin effects on the hypothalamo-pituitary axis in fish. *Trends in Endocrinology and Metabolism* **18**, 81–88.

Falcón, J., Migaud, H., Muñoz-Cueto, J. A, and Carrillo, M. 2010. Current knowledge on the melatonin system in teleost fish. *General and Comparative Endocrinology* **165**, 469–82.

FAO.org. 2017. Fisheries and aquaculture software. FishStat Plus - Universal software for fishery statistical time series.

Ferguson, H. W. 1989. *Systemic pathology of fish. A text and atlas of comparative tissue responses in diseases of teleosts.* Iowa State University Press, Ames, Iowa.

Fernandes, A. M., Fero, K., Arrenberg, A. B., Bergeron, S. A., Driever, W., and Burgess, H. A. 2012. Deep brain photoreceptors control light-seeking behavior in zebrafish larvae. *Current Biology* **22**, 2042–2047.

Fernandes, A. M., Fero, K., Driever, W., and Burgess, H. A. 2013. Enlightening the brain: linking deep brain photoreception with behavior and physiology. *Bioessays* **35**, 775–779.

FishFarmingExpert.com. (n.d.). Producer set to double smolt size. Retrieved July 19, 2017, from http://www.fishfarmingexpert.com/news/producer-set-to-double-smolt-size

Fjelldal, P. G., Hansen, T. J. and Berg, A. E. 2007. A radiological study on the

development of vertebral deformities in cultured Atlantic salmon (Salmo salar, L.). *Aquaculture* **273**, 721–728.

Fjelldal, P. G., Hansen, T., and Huang, T. S. 2011. Continuous light and elevated temperature can trigger maturation both during and immediately after smoltification in male Atlantic salmon (*Salmo salar*). *Aquaculture* **321**, 93–100.

Fjelldal, P. G., Grotmol, S., Kryvi, H., Gjerdet, N. R., Taranger, G. L., Hansen, T., Porter, M. J., and Totland, G. K. 2004. Pinealectomy induces malformation of the spine and reduces the mechanical strength of the vertebrae in Atlantic salmon, *Salmo salar*. *Journal of Pineal Research* **36**, 132–139.

Fjelldal, P. G., Lock, E. J., Grotmol, S., Totland, G. K., Nordgarden, U., Flik, G., and Hansen, T. 2006. Impact of smolt production strategy on vertebral growth and mineralisation during smoltification and the early seawater phase in Atlantic salmon (*Salmo salar*, L.). *Aquaculture* **261**, 715–728.

Fjelldal, P. G., Hansen, T., Breck, O., Sandvik, R., Waagbø, R., Berg, A., Ørnsrud, R. 2008. Supplementation of dietary minerals during the early seawater phase increase vertebral strength and reduce the prevalence of vertebral deformities in fast growing under-yearling Atlantic salmon (Salmo salar L.) smolt. *Aquaculture. Nutrition* **15**, 366–378.

Flamarique, I., and Hawryshyn, C. 1996. Retinal development and visual sensitivity of young Pacific Sockeye salmon (*Oncorhynchus nerka*). *The Journal of Experimental Biology* **199**, 869–882.

Flamarique, I. N., and Browman, H. I. 2001. Foraging and prey-search behaviour of small juvenile rainbow trout (*Oncorhynchus mykiss*) under polarized light. *The Journal of Experimental Biology* **204**, 2415–2422.

Fleming, I. A. 1996. Reproductive strategies of Atlantic salmon: ecology and evolution. *Fisheries, Reviews in Fish Biology and Fisheries* **6**, 349–416.

Folkedal, O., Torgersen, T., Nilsson, J., and Oppedal, F. 2010. Habituation rate and capacity of Atlantic salmon (*Salmo salar*) parr to sudden transitions from darkness to light. *Aquaculture* **307**, 170–172.

Folmar, L. C., and Dickhoff, W. 1980. The parr-smolt transformation (smoltification) and seawater adaptation in salmonids. A review of selected literature. *Aquaculture* **21**, 1-37.

Folmar, L., and Dickhoff, W. 1981. Evaluation of some physiological parameters as predictive indices of smoltification. *Aquaculture* **23**, 309–324.

Forbes-Osborne, M. A., Wilson, S. G., and Morris, A. C. 2013. Insulinoma-associated 1a (*Insm1a*) is required for photoreceptor differentiation in the zebrafish retina. *Developmental Biology* **380**, 157–171.

Forsberg, O. I. 1996. Ammonia excretion rates from post-smolt Atlantic salmon, *Salmo salar* L., in land-based farms. *Aquaculture Research* **27**, 937–944.

Forseth, T., Hurley, M. A., Jensen, A. J., and Elliott, J. M. 2001. Functional models for growth and food consumption of Atlantic salmon parr, *Salmo salar*, from a Norwegian river. *Freshwater Ecology* **46**, 173–186.

Foskett, J. K., and Scheffey, C. 1982. The chloride cell: definitive identification as the salt-secretory cell in teleosts. *Science* **215**, 164–166.

Foss, A., and Imsland, A. K. 2002. Compensatory growth in the spotted wolffish *Anarhichas minor* (Olafsen) after a period of limited oxygen supply. *Aquaculture Research* **33**, 1097–1101.

Foster, R. G., Follett, B. K., and Lythgoe, J. N. 1985. Rhodopsin-like sensitivity of extra-retinal photoreceptors mediating photoperiodic response in quail. *Nature* **313**, 50–52.

Fraser, N. H. C., and Metcalfe, N. B. 1997. The costs of becoming nocturnal: feeding efficiency in relation to light intensity in juvenile Atlantic Salmon. *Functional Ecology* **11**, 385–391.

Freitag, A. R., Thayer, L. R., Leonetti, C., Stapleton, H. M., and Hamlin, H. J. 2015. Effects of elevated nitrate on endocrine function in Atlantic salmon, *Salmo salar*. *Aquaculture* **436**, 8–12.

Frisch, K. von 1911. Beiträge zur Physiologie der Pigmentzellen in der Fischhaut. *Pflüger's Archiv Für Die Gesamte Physiologie Des Menschen Und Der Tiere* **138**, 319–387.

Fujikawa, Y., Kozono, K., Esaka, M., Iijima, N., Nagamatsu, Y., Yoshida, M., and Uematsu, K. 2006. Molecular cloning and effect of c-fos mRNA on pharmacological stimuli in the goldfish brain. *Comparative Biochemistry and Physiology - Part D: Genomics and Proteomics* **1**, 253–259.

Gac, F. Le, Blaise, O., Fostier, A., Bail, P. Le, Loir, M., Mourot, B., and Weil, C. 1993. Growth hormone (GH) and reproduction: a review. *Fish Physiology and Biochemistry* **11**, 219–232.

Garcia de Leaniz, C., Fleming, I.A., Einum, S., Verspoor, E., Jordan, W.C., Consuegra, S., Aubin-Horth, N., Lajus, D., Letcher, B.H., Youngson, A.F., Webb, J.H.,

Vollestad, L.A., Villanueva, B., Ferguson, A., Quinn, T.P. 2007. A critical review of adaptive genetic variation in Atlantic salmon: implications for conservation. *Biol. Rev*. **82,** 173–211.

García-Fernández, J. M., Cernuda-Cernuda, R., Davies, W. I. L., Rodgers, J., Turton, M., Peirson, S. N., Follett, B. K., Halford, S., Hughes, S., Hankins, M. W., and Foster, R. G. 2015. The hypothalamic photoreceptors regulating seasonal reproduction in birds: a prime role for VA opsin. *Frontiers in Neuroendocrinology* **37**, 13–28.

Gesto, M., Hernández, J., López-Patiño, M. A., Soengas, J. L., and Míguez, J. M. 2015. Is gill cortisol concentration a good acute stress indicator in fish? A study in rainbow trout and zebrafish. *Comparative Biochemistry and Physiology - Part A: Molecular and Integrative Physiology* **188**, 65–69.

Ginetz, R. M., and Larkin, P. A. 1973. Choice of colors of food items by rainbow trout (*Salmo gairdneri*). *Journal of the Fisheries Board of Canada* **30**, 229–234.

Gjedrem, T. 2012. Genetic improvement for the development of efficient global aquaculture: A personal opinion review. *Aquaculture* **344–349**, 12–22.

Gjerde, B. 1984. Response to individual selection for age at sexual maturity in Atlantic salmon. *Aquaculture* **38**, 229–240.

Goldsmith, T. H. 1990. Optimization, constraint, and history in the evolution of eyes. *The Quarterly Review of Biology* **65**, 281–322.

Good, C., Weber, G. M., May, T., Davidson, J., and Summerfelt, S. 2016. Reduced photoperiod (18 h light vs. 24 h light) during first-year rearing associated with increased early male maturation in Atlantic salmon *Salmo salar* cultured in a freshwater recirculation aquaculture system. *Aquaculture Research* **47**, 3023–3027.

Grant, J. W. A., Steingrímsson, S. Ó., Keeley, E. R., and Cunjak, R. A. 1998. Implications of territory size for the measurement and prediction of salmonid abundance in streams. *Canadian Journal of Fisheries and Aquatic Sciences* **55**, 181–190.

Graves, S., Piepho, H-P., Selzer, L., and Dorai-Raj, S. 2015. multcompView: Visualizations of Paired Comparisons. Retrieved from https://cran.r-project.org/package=multcompView

Günzel, D., and Yu, A. S. L. 2013. Claudins and the modulation of tight junction permeability. *Physiological reviews* **93**, 525-569

Gustafson-Marjanen, K. I., and Dowse, H. B. 1983. Seasonal and diel patterns of emergence from the redd of Atlantic salmon (*Salmo salar*) fry. *Canadian Journal of Fisheries and Aquatic Sciences* **40**, 813–817.

Gwinner, E., and Scheuerlein, A. 1998. Seasonal changes in day-light intensity as a potential zeitgeber of circannual rhythms in equatorial Stonechats. *Journal of Ornithology* **139**, 407–412.

Hale, M. C., McKinney, G. J., Thrower, F. P., and Nichols, K. M. 2016. RNA-seq reveals differential gene expression in the brains of juvenile resident and migratory smolt rainbow trout (*Oncorhynchus mykiss*). *Comparative Biochemistry and Physiology - Part D: Genomics and Proteomics* **20**, 136–150.

Halford, S., Pires, S. S., Turton, M., Zheng, L., González-Menéndez, I., Davies, W. L., Peirson, S. N., García-Fernández, J. M., Hankins, M. W., and Foster, R. G. 2009. VA opsin-based photoreceptors in the hypothalamus of birds. *Current Biology* **19**, 1396–1402.

Hampel, M., Bron, J. E., Taggart, J. B., and Leaver, M. J. 2014. The antidepressant drug Carbamazepine induces differential transcriptome expression in the brain of Atlantic salmon, *Salmo salar*. *Aquatic Toxicology* **151**, 114–123.

Handeland, S. O., and Stefansson, S. O. 2001. Photoperiod control and influence of body size on off-season parr–smolt transformation and post-smolt growth. *Aquaculture* **192**, 291–307.

Handeland, S. O., Berge, Å., Björnsson, B. T., Lie, O., and Stefansson, S. O. 2000. Seawater adaptation by out-of-season Atlantic salmon (*Salmo salar* L.) smolts at different temperatures. *Aquaculture* **181**, 377–396.

Handeland, S. O., Björnsson, B. T., Arnesen, A. M., and Stefansson, S. O. 2003. Seawater adaptation and growth of post-smolt Atlantic salmon (*Salmo salar*) of wild and farmed strains. *Aquaculture* **220**, 367–384.

Handeland, S. O., Porter, M., Björnsson, B. T., and Stefansson, S. O. (2003). Osmoregulation and growth in a wild and a selected strain of Atlantic salmon smolts on two photoperiod regimes. *Aquaculture* **222**, 29–43.

Handeland, S. O., Wilkinson, E., Sveinsbø, B., McCormick, S. D., and Stefansson, S. O. 2004. Temperature influence on the development and loss of seawater tolerance in two fast-growing strains of Atlantic salmon. *Aquaculture* **233**, 513–529.

Handeland, S. O., Imsland, A. K., Ebbesson, L. O. E., Nilsen, T. O., Hosfeld, C. D.,

Baeverfjord, G., Espmark, Å., Rosten, T., Skilbrei, O. T., Hansen, T., Gunnarsson, G. S., Breck, O., and Stefansson, S. O. 2013. Low light intensity can reduce Atlantic salmon smolt quality. *Aquaculture* **384–387**, 19–24.

Handeland, S. O., Imsland, A. K., Björnsson, B. T., Stefansson, S. O., and Porter, M. 2013. Physiology during smoltification in Atlantic salmon: effect of melatonin implants. *Fish Physiology and Biochemistry* **39**, 1079–1088.

Hang, C. Y., Kitahashi, T., and Parhar, I. S. 2014. Localization and characterization of val-opsin isoform-expressing cells in the brain of adult zebrafish. *Journal of Comparative Neurology* **522**, 3847–3860.

Hang, C. Y., Kitahashi, T., and Parhar, I. S. 2015. Brain area-specific diurnal and photic regulation of val-opsinA and val-opsinB genes in the zebrafish. *Journal of Neurochemistry* **133**, 501–510.

Hang, C. Y., Kitahashi, T., and Parhar, I. S. 2016. Neuronal organization of deep brain opsin photoreceptors in adult teleosts. *Frontiers in Neuroanatomy* **10**, 48.

Hansen, T., Stefansson, S., and Taranger, G. L. 1992. Growth and sexual maturation in the Atlantic salmon, *Salmo salar* L., reared in sea cages at two different light regimes. *Aquaculture And Fisheries Management* **23**, 275–280.

Hansen, T., Fjelldal, P. G., Yurtseva, A. and Berg, A. 2010. A possible relation between growth and number of deformed vertebrae in Atlantic salmon (Salmo salar L.). *Journal of Applied Ichthyology* **26**, 355–359.

Hansen, T., Remen, M., Sambraus, F., and Fjelldal, P. G. 2015. A report on overripe female and spent male Atlantic salmon (*Salmo salar*) in August. *Aquaculture* **444**, 114–116.

Harding, L. B., Schultz, I. R., Goetz, G. W., Luckenbach, J. A., Young, G., Goetz, F. W., and Swanson, P. 2013. High-throughput sequencing and pathway analysis reveal alteration of the pituitary transcriptome by 17α-ethynylestradiol (EE2) in female Coho salmon, *Oncorhynchus kisutch*. *Aquatic Toxicology* **142–143**, 146–163.

Harosi, F. I., and Hashimoto, Y. 1983. Ultraviolet visual pigment in a vertebrate: a tetrachromatic cone system in the dace. *Science* **222**, 1021–1023.

Hattar, S., Liao, H-W., Takao, M., Berson, D. M., and Yau, K-W. 2002. Melanopsin-containing retinal ganglion cells: architecture, projections, and intrinsic photosensitivity. *Science* **295**, 1065–1070.

Hawryshyn, C. W., Arnold, M. G., Chaisson, D. J., and Martin, P. C. 1989. The

ontogeny of ultraviolet photosensitivity in rainbow trout (*Salmo gairdneri*). *Visual Neuroscience* **2**, 247–254.

Hawryshyn, C. W., Ramsden, S. D., Betke, K. M., and Sabbah, S. 2010. Spectral and polarization sensitivity of juvenile Atlantic salmon (*Salmo salar*): phylogenetic considerations. *The Journal of Experimental Biology* **213**, 3187–3197.

He, W., Cowan, C. W., and Wensel, T. G. 1998. RGS9, a GTPase accelerator for phototransduction. *Neuron* **20**, 95–102.

Hendrickson, A., Yan, Y. H., Erickson, A., Possin, D., and Pow, D. 2007. Expression patterns of calretinin, calbindin and parvalbumin and their colocalization in neurons during development of Macaca monkey retina. *Experimental Eye Research* **85**, 587–601.

Herbert, N. A., Kadri, S., and Huntingford, F. A. 2011. A moving light stimulus elicits a sustained swimming response in farmed Atlantic salmon, *Salmo salar* L. *Fish Physiology and Biochemistry* **37**, 317–325.

Herbinger, C. M., and Friars, G. W. 1991. Correlation between condition factor and total lipid content in Atlantic salmon, *Salmo salar* L., parr. *Aquaculture and Fisheries Management* **22**, 527–529.

Heumann, J., Carmichael, S. N., Bron, J. E., and Sturm, A. 2014. Isolation and characterisation of four partial cDNA sequences encoding multidrug resistance-associated proteins (MRPs) in the salmon louse *Lepeophtheirus salmonis* (Krøyer, 1837). *Aquaculture* **424–425**, 207–214.

Hiroi, J., and McCormick, S. D. 2012. New insights into gill ionocyte and ion transporter function in euryhaline and diadromous fish. *Respiratory Physiology and Neurobiology* **184**, 257–268.

Hoar, W. S. 1976. Smolt transformation: evolution, behavior, and physiology. *Journal of the Fisheries Research Board Canada* **33**, 1233–1252.

Hoar, W. S. 1988. The physiology of smolting salmonids. In: Hoar, W. S., and Randall, D. J. (Eds.), *Fish Physiology* **11**, 275–343. Academic Press, New York.

Hoge F., Vodacek A., Swift R., Yungel J., and Blough N. 1995. Inherent optical properties of the ocean: retrieval of the absorption coefficient of chromophoric dissolved organic matter from airborne laser spectral fluorescence measurements. *Appl. Opt*. **34**, 7032-7038.

Holloway, A. C., and Leatherland, J. F. 1998. Neuroendocrine regulation of growth hormone secretion in teleost fishes with emphasis on the involvement of gonadal

sex steroids. *Reviews in Fish Biology and Fisheries* **8**, 409–429.

Hollway, G. E., Bryson-Richardson, R. J., Berger, S., Cole, N. J., Hall, T. E., and Currie, P. D. 2007. Whole-somite rotation generates muscle progenitor cell compartments in the developing zebrafish embryo. *Developmental Cell* **12**, 207–219.

Holmqvist, B. I., and Ekström, P. 1995. Hypophysiotrophic systems in the brain of the Atlantic salmon. Neuronal innervation of the pituitary and the origin of pituitary dopamine and nonapeptides identified by means of combined carbocyanine tract tracing and immunocytochemistry. *Journal of Chemical Neuroanatomy* **8**, 125–145.

Holmqvist, B. I., Östholm, T., and Ekström, P. 1992. Retinohypothalamic projections and the suprachiasmatic nucleus of the teleost brain. In: Ali, M. A. (Ed.), *Rhythms in fishes*. Plenum Press, New York, pp 394–418.

Holmqvist, B. I., Östholm, T., and Ekström, P. 1994. Neuroanatomical analysis of the visual and hypophysiotropic systems in Atlantic salmon (*Salmo salar*) with emphasis on possible mediators of photoperiodic cues during parr-smolt transformation. *Aquaculture* **121**, 1–12.

Hoshi, Y., Uchida, Y., Tachikawa, M., Ohtsuki, S., and Terasaki, T. 2017. Actin filament-associated protein 1 (AFAP-1) is a key mediator in inflammatory signaling-induced rapid attenuation of intrinsic P-gp function in human brain capillary endothelial cells. *Journal of Neurochemistry* **141**, 247–262.

Houlihan, D. F., Mathers, E. M., and Foster, A. 1993. Biochemical correlates of growth rate in fish. In: Rankin, J. C., and Jensen, F. B. (Eds.), *Fish Ecophysiology.* Chapman and Hall, London, 45–71).

Houlihan, D. F., Carter, C. G., and McCarthy, I. D. 1995. Protein synthesis in fish. In: Hochachka, P. W., and Mommsen, T. P. (Eds.), *Biochemistry and Molecular Biology of Fishes* **4**, 191–220. Elsevier Biomedical, Amsterdam.

Hutchings, J. A., and Myers, R. A. 1994. The evolution of alternative mating strategies in variable environments. *Evolutionary Ecology* **8,** pp 256–268.

Hutchings, J.A., Jones, M.E.B., 1998. Life history variation and growth rate thresholds for maturity in Atlantic salmon, Salmo salar. *Can J. Fish. Aquatic. Science* **55**, 22–47.

Imsland, A. K., Foss, A., Koedijk, R., Folkvord, A., Stefansson, S. O., and Jonassen, T. M. 2007. Persistent growth effects of temperature and photoperiod in Atlantic

cod *Gadus morhua*. *Journal of Fish Biology* **71**, 1371–1382.

Imsland, A. K., Våge, K. A., Handeland, S. O., and Stefansson, S. O. 2011. Growth and osmoregulation in Atlantic salmon (*Salmo salar*) smolts in response to different feeding frequencies and salinities. *Aquaculture Research* **42**, 469–479.

Imsland, A. K., Handeland, S. O., and Stefansson, S. O. 2014. Photoperiod and temperature effects on growth and maturation of pre- and post-smolt Atlantic salmon. *Aquaculture International* **22**, 1331–1345.

Isaksson, O. G. P., Lindahl, A., Nilsson, A., and Isgaard, J. 1987. Mechanism of the stimulatory effect of growth hormone on longitudinal bone growth. *Endocrine Reviews* **8**, 426–438.

Isoldi, M. C., Rollag, M. D., de Lauro Castrucci, A. M., and Provencio, I. 2005. Rhabdomeric phototransduction initiated by the vertebrate photopigment melanopsin. *Proceedings of the National Academy of Sciences of the United States of America* **102**, 1217–1221.

Jadhao, A. G., and Malz, C. R. 2007. Localization of calcium-binding protein (calretinin, 29 kD) in the brain and pituitary gland of teleost fish: An immunohistochemical study. *Neuroscience Research* **59**, 265–276.

Jaillon, O., Aury, J-M., Brunet, F., Petit, J-L., Stange-Thomann, N., Mauceli, E., Bouneau, L., Fischer, C., Ozouf-Costaz, C., Bernot, A., Nicaud, S., Jaffe, D., Fisher, S., Lutfalla, G., Dossat, C., Segurens, B., Da Silva, C., Salanoubat, M., Levy, M., Boudet, N., Castellano, S., Anthouard, V., Jubin, C., Castelli, V., Katinka, M., Vacherie, B., Biémont, C., Skalli, Z., Cattolico, L., Poulain, J., de Berardinis, V., Cruaud, C., Duprat, S., Brottier, P., Coutanceau, J-P., Gouzy, J., Parra, G., Lardier, G., Chapple, C., McKernan, K. J., McEwan, P., Bosak, S., Kellis, M., Volff, J-N., Guigó, R., Zody, M. C., Mesirov, J., Lindblad-Toh, K., Birren, B., Nusbaum, C., Kahn, D., Robinson-Rechavi, M., Laudet, V., Schachter, V., Quétier, F., Saurin, W., Scarpelli, C., Wincker, P., Lander, E. S., Weissenbach, J., and Roest Crollius, H. 2004. Genome duplication in the teleost fish *Tetraodon nigroviridis* reveals the early vertebrate proto-karyotype. *Nature* **431**, 946–957.

James, M. O. 2011. Steroid catabolism in marine and freshwater fish. *Journal of Steroid Biochemistry and Molecular Biology* **127**, 167–175.

Jenkins, S. A., Ellestad, L. E., Mukherjee, M., Narayana, J., Cogburn, L. A., and Porter, T. E. 2013. Glucocorticoid-induced changes in gene expression in embryonic anterior pituitary cells. *Physiological Genomics* **45**, 422–433.

Jensen, A. J., Heggberget, T. G., and Johnsen, B. O. 1986. Upstream migration of adult Atlantic salmon, *Salmo salar* L., in the River Vefsna, northern Norway. *Journal of Fish Biology* **29**, 459–465.

Jenuwein, T., and Allis, C. D. 2001. Translating the histone code. *Science* **293**, 1074–1080.

Jiao, B., Huang, X., Chan, C. B., Zhang, L., Wang, D., and Cheng, C. H. K. 2006. The co-existence of two growth hormone receptors in teleost fish and their differential signal transduction, tissue distribution and hormonal regulation of expression in seabream. *Journal of Molecular Endocrinology* **36**, 23–40.

Jobling, M. 2003. The thermal growth coefficient (TGC) model of fish growth: A cautionary note. *Aquaculture Research* **34**, 581–584.

Johnsson, J. I., and Björnsson, B. T. 1994. Growth hormone increases growth rate, appetite and dominance in juvenile rainbow trout, *Oncorhynchus mykiss*. *Animal Behaviour* **48**, 177-186.

Johnston, C. E., and Saunders, R. L. 1981. Parr–smolt transformation of yearling Atlantic salmon (*Salmo salar*) at several rearing temperatures. *Canadian Journal of Fisheries and Aquatic Sciences* **38**, 1189–1198.

Johnston, I. A. 1991. Muscle action during locomotion: a comparative perspective. *Journal of Experimental Biology* **160**, 167–185.

Johnston, I. A. 1999. Muscle development and growth: potential implications for flesh quality in fish. *Aquaculture* **177**, 99–115.

Johnston, I. A, Strugnell, G., McCracken, M. L., and Johnstone, R. 1999. Muscle growth and development in normal-sex-ratio and all-female diploid and triploid Atlantic salmon. *The Journal of Experimental Biology* **202**, 1991–2016.

Johnston, I. A., Alderson, R., Sandham, C., Dingwall, A., Mitchell, D., Selkirk, C., Nickell, D., Baker, R., Robertson, B., Whyte, D., and Springate, J. 2000. Muscle fibre density in relation to the colour and texture of smoked Atlantic salmon (*Salmo salar* L.). *Aquaculture* **189**, 335–349.

Johnston, I. A, McLay, H. A, Abercromby, M., and Robins, D. 2000. Early thermal experience has different effects on growth and muscle fibre recruitment in spring- and autumn-running Atlantic salmon populations. *The Journal of Experimental Biology* **203**, 2553–2564.

Johnston, I. A., Manthri, S., Smart, A., Campbell, P., Nickell, D., Alderson, R. 2003. Plasticity of muscle fibre number in seawater stages of Atlantic salmon in

response to photoperiod manipulation. *Journal of Experimental Biology* **206**, 3425–3435.

Johnston, I. A, Manthri, S., Alderson, R., Smart, A., Campbell, P., Nickell, D., Robertson, B., Paxton, C. G., and Burt, M. L. 2003. Freshwater environment affects growth rate and muscle fibre recruitment in seawater stages of Atlantic salmon (*Salmo salar* L.). *The Journal of Experimental Biology* **206**, 1337–1351.Johnston, I. A., Li, X., Vieira, V. L. A., Nickell, D., Dingwall, A., Alderson, R., Campbell, P., and Bickerdike, R. 2006. Muscle and flesh quality traits in wild and farmed Atlantic salmon. *Aquaculture* **256**, 323–336.

Johnston, I. A, Manthri, S., Bickerdike, R., Dingwall, A., Luijkx, R., Campbell, P., Nickell, D., and Alderson, R. 2004. Growth performance, muscle structure and flesh quality in out-of-season Atlantic salmon (*Salmo salar*) smolts reared under two different photoperiod regimes. *Aquaculture* **237**, 281–300.

Johnston, I. A, Bower, N. I., and Macqueen, D. J. 2011. Growth and the regulation of myotomal muscle mass in teleost fish. *The Journal of Experimental Biology* **214**, 1617–1628.

Johnstone, D. L., O'Connell, M. F., Palstra, F. P., and Ruzzante, D. E. 2013. Mature male parr contribution to the effective size of an anadromous Atlantic salmon (*Salmo salar*) population over 30 years. *Molecular Ecology* **22**, 2394–2407.

Jones, J. W., and King, G. M. 1952. The spawning of the male Salmon parr (*Salmo salar* Linn. juv.). *Journal of Zoology* **122**, 615–619.

Jonsson, B., and J. Rudd-Hansen. 1985. Water temperature as the primary influence of timing of seaward migrations of Atlantic salmon (Salmo salar) smolts. *Canadian Journal of Fisheries and Aquatic Sciences* **42**, 593-595.

Joseph-Bravo, P., Jaimes-Hoy, L., and Charli, J-L. 2015. Regulation of TRH neurons and energy homeostasis-related signals under stress. *Journal of Endocrinology* **224**, R139--R159.

Joseph-Bravo, P., Jaimes-Hoy, L., Uribe, R-M., and Charli, J-L. 2015. 60 years of neuroendocrinology: TRH, the first hypophysiotropic releasing hormone isolated: control of the pituitary--thyroid axis. *Journal of Endocrinology* **226**, T85-T100.

Juell, J-E., and Fosseidengen, J. E. 2004. Use of artificial light to control swimming depth and fish density of Atlantic salmon (*Salmo salar*) in production cages. *Aquaculture* **233**, 269–282.

Juell, J-E., Oppedal, F., Boxaspen, K., and Taranger, G. L. 2003. Submerged light

increases swimming depth and reduces fish density of Atlantic salmon *Salmo salar* L. in production cages. *Aquaculture Research* **34**, 469–478.

Julian, D., Ennis, K., and Korenbrot, J. I. 1998. Birth and fate of proliferative cells in the inner nuclear layer of the mature fish retina. *The Journal of Comparative Neurology* **394**, 271–282.

Kadri, S., Mitchell, D. F., Metcalfe, N. B., Huntingford, F. A., and Thorpe, J. E. 1996. Differential patterns of feeding and resource accumulation in maturing and immature Atlantic salmon, *Salmo salar*. *Aquaculture* **142**, 245–257.

Kadri, S., Metcalfe, N. B., Huntingford, F. A., John, E., and Mitchell, D. F. 1997. Early morphological predictors of maturity in one-sea-winter Atlantic salmon. *Aquaculture International* **5**, 41–50.

Kadri, S., Thorpe, J. E., and Metcalfe, N. B. 1997. Anorexia in one-sea-winter Atlantic salmon (*Salmo salar*) during summer, associated with sexual maturation. *Aquaculture* **151**, 405–409.

Kalleberg, H. 1958. Observations in a streamtank of territoriality and competition in juvenile salmon and trout. *Report of Institute of Freshwater Research, Drottningholm* **39**, 55–98.

Kamermans, M., and Hawryshyn, C. 2011. Teleost polarization vision: how it might work and what it might be good for. *Philosophical Transactions of the Royal Society of London. Series B, Biological Sciences* **366**, 742–756.

Karakatsouli, N., Papoutsoglou, S. E., Pizzonia, G., Tsatsos, G., Tsopelakos, A., Chadio, S., Kalogiannis, D., Dalla, C., Polissidis, A., and Papadopoulou-Daifoti, Z. 2007. Effects of light spectrum on growth and physiological status of gilthead seabream *Sparus aurata* and rainbow trout *Oncorhynchus mykiss* reared under recirculating system conditions. *Aquacultural Engineering* **36**, 302–309.

Karakatsouli, N., Papoutsoglou, E. S., Sotiropoulos, N., Mourtikas, D., Stigen-Martinsen, T., and Papoutsoglou, S. E. 2010. Effects of light spectrum, rearing density and light intensity on growth performance of scaled and mirror common carp *Cyprinus carpio* reared under recirculating system conditions. *Aquacultural Engineering* **42**, 121–127.

Karnitz, L. M., and Abraham, R. T. 1995. Cytokine receptor signaling mechanisms. *Current Opinion in Immunology* **7**, 320–326.

Kasahara, M., Naruse, K., Sasaki, S., Nakatani, Y., Qu, W., Ahsan, B., Yamada, T., Nagayasu, Y., Doi, K., Kasai, Y., Jindo, T., Kobayashi, D., Shimada, A., Toyoda,

A., Kuroki, Y., Fujiyama, A., Sasaki, T., Shimizu, A., Asakawa, S., Shimizu, N., Hashimoto, S-I., Yang, J., Lee, Y., Matsushima, K., Sugano, S., Sakaizumi, M., Narita, T., Ohishi, K., Haga, S., Ohta, F., Nomoto, H., Nogata, K., Morishita, T., Endo, T., Shin-I, T., Takeda, H., Morishita, S., and Kohara, Y. 2007. The medaka draft genome and insights into vertebrate genome evolution. *Nature* **447**, 714–719.

Keenleyside, M. H. A. 1962. Skin-diving observations of Atlantic salmon and brook trout in the Miramichi River, New Brunswick. *Journal of the Fisheries Board of Canada* **19**, 625–634.

Kiilerich, P., Milla, S., Sturm, A., Valotaire, C., Chevolleau, S., Giton, F., Terrien, X., Fiet, J., Fostier, A., Debrauwer, L., and Prunet, P. 2011. Implication of the mineralocorticoid axis in rainbow trout osmoregulation during salinity acclimation. *Journal of Endocrinology* **209**, 221–235.

Kimple, A. J., Bosch, D. E., Giguère, P. M., and Siderovski, D. P. 2011. Regulators of G-protein signaling and their Gα substrates: promises and challenges in their use as drug discovery targets. *Pharmacological Reviews* **63**, 728–749.

King, H. R., Lee, P. S., and Pankhurst, N. W. 2004. Photoperiod-induced precocious male sexual maturation in Atlantic salmon (*Salmo salar*). *Fish Physiology and Biochemistry* **28**, 427–428.

Kiriake, A., Ohta, A., Suga, E., Matsumoto, T., Ishizaki, S., and Nagashima, Y. 2016. Comparison of tetrodotoxin uptake and gene expression in the liver between juvenile and adult tiger pufferfish, *Takifugu rubripes*. *Toxicon* **111**, 6–12.

Kirk, J. T. O. 1976. Yellow substance (gelbstoff) and its contribution to the attenuation of photosynthetically active radiation in some inland and coastal south-eastern Australian waters. *Marine and Freshwater Research* **27**, 61–71.

Klein, D. C. 1985. Photoneural regulation of the mammalian pineal gland. In: Evered, D., and Clark, S. (Eds.), Photoperiodism, melatonin, and the pineal. *Ciba Foundation Symposium* **117**, pp. 38–56. Pittman Press, London.

Klein, D. C., Auerbach, D. A., Namboodiri, M. A. A., and Wheler, G. H. T. 1981. Indole metabolism in the mammalian pineal gland. *The Pineal Gland* **1**, 199–227.

Kling, P., Jönsson, E., Nilsen, T. O., Einarsdottir, I. E., Rønnestad, I., Stefansson, S. O., and Björnsson, B. T. 2012. The role of growth hormone in growth, lipid homeostasis, energy utilization and partitioning in rainbow trout: interactions with leptin, ghrelin and insulin-like growth factor I. *General and Comparative*

Endocrinology **175**, 153–162.

Klinger, D., and Naylor, R. 2012. Searching for solutions in aquaculture: charting a sustainable course. *Annual Review of Environment and Resources* **37**, 247–276.

Kocmarek, A. L., Ferguson, M. M., and Danzmann, R. G. 2015. Co-localization of growth QTL with differentially expressed candidate genes in rainbow trout. *Genome* **58**, 393–403.

Kolarevic, J., Selset, R., Felip, O., Good, C., Snekvik, K., Takle, H., Ytteborg, E., Bæverfjord, G., Åsgård, T., and Terjesen, B. F. 2013. Influence of long term ammonia exposure on Atlantic salmon (*Salmo salar* L.) parr growth and welfare. *Aquaculture Research* **44**, 1649–1664.

Kolarevic, J., Baeverfjord, G., Takle, H., Ytteborg, E., Reiten, B. K. M., Nergård, S., and Terjesen, B. F. 2014. Performance and welfare of Atlantic salmon smolt reared in recirculating or flow through aquaculture systems. *Aquaculture* **432**, 15–25.

Komourdjian, M. P., Saunders, R. L., and Fenwick, J. C. 1976. Evidence for the role of growth hormone as a part of a 'light-pituitary axis' in growth and smoltification of Atlantic salmon (*Salmo salar*). *Canadian Journal of Zoology* **54**, 544–551.

Koumans, J. T. M., Akster, H. A., Booms, G. H. R., Lemmens, C. J. J., and Osse, J. W. M. 1991. Numbers of myosatellite cells in white axial muscle of growing fish: *Cyprinus carpio* L. (teleostei). *American Journal of Anatomy* **192**, 418–424.

Kovács, K. J. 2008. Measurement of immediate-early gene activation- c-fos and beyond. *Journal of Neuroendocrinology* **20**, 665–672.

Koyanagi, M., Takada, E., Nagata, T., Tsukamoto, H., and Terakita, A. 2013. Homologs of vertebrate Opn3 potentially serve as a light sensor in nonphotoreceptive tissue. *Proceedings of the National Academy of Sciences* **110**, 4998–5003.

Kråkenes, R., Hansen, T., Stefansson, S. O., and Taranger, G. L. 1991. Continuous light increases growth rate of Atlantic salmon (*Salmo salar*) postsmolts in sea cages. *Aquaculture* **95**, 281–287.

Kramlinger, V. M., Nagy, L. D., Fujiwara, R., Johnson, K. M., Phan, T. T. N., Xiao, Y., Enright, J. M., Toomey, M. B., Corbo, J. C., and Guengerich, F. P. 2016. Human cytochrome P450 27C1 catalyzes 3,4-desaturation of retinoids. *FEBS Letters* **590**, 1304–1312.

Kristensen, T., Åtland, Å., Rosten, T., Urke, H. A., and Rosseland, B. O. 2009.

Important influent-water quality parameters at freshwater production sites in two salmon producing countries. *Aquacultural Engineering* **41**, 53–59.

Kurata, Y., Kimura, Y., Yamanaka, Y., Ishikawa, A., Okamoto, H., Masaoka, T., Nagoya, H., Araki, K., Moriyama, S., Hirano, H., and Mori, T. 2012. Effects of growth hormone on the salmon pituitary proteome. *Journal of Proteomics* **75**, 1718–1731.

Lamb, T. D. 2013. Evolution of phototransduction, vertebrate photoreceptors and retina. *Progress in Retinal and Eye Research* **36**, 52–119.

Lau, B. Y. B., Mathur, P., Gould, G. G., and Guo, S. 2011. Identification of a brain center whose activity discriminates a choice behavior in zebrafish. *Proceedings of the National Academy of Sciences* **108**, 2581–2586.

Leaniz, C. G. de, Fraser, N., and Huntingford, F. 1993. Dispersal of Atlantic salmon fry from a natural redd: evidence for undergravel movements? *Canadian Journal of Zoology* **71**, 1454–1457.

Leatherland, J. F., McKeown, B. A., and John, T. M. 1974. Circadian rhythm of plasma prolactin, growth hormone, glucose and free fatty acid in juvenile kokanee salmon, *Oncorhynchus nerka*. *Comparative Biochemistry and Physiology Part A: Physiology* **47**, 821–828.

Leclercq, E., Taylor, J. F., Hunter, D., and Migaud, H. 2010a. Body size dimorphism of sea-reared Atlantic salmon (*Salmo salar* L.): Implications for the management of sexual maturation and harvest quality. *Aquaculture* **301**, 47–56.

Leclercq, E., Migaud, H., Taylor, J. F., and Hunter, D. 2010b. The use of continuous light to suppress pre-harvest sexual maturation in sea-reared Atlantic salmon (*Salmo salar* L.) can be reduced to a 4-month window. *Aquaculture Research* **41**, 709–714.

Leclercq, E., Taylor, J. F., Sprague, M., and Migaud, H. 2011. The potential of alternative lighting-systems to suppress pre-harvest sexual maturation of 1+ Atlantic salmon (*Salmo salar*) post-smolts reared in commercial sea-cages. *Aquacultural Engineering* **44**, 35–47.

Leggatt, R. A., Biagi, C. A., Sakhrani, D., Dominelli, R., Eliason, E. J., Farrell, A. P., and Devlin, R. H. 2017. Fitness component assessments of wild-type and growth hormone transgenic coho salmon reared in seawater mesocosms. *Aquaculture* **473**, 31–42.

Lenth, R. V. 2016. Least-squares means: The R Package lsmeans. *Journal of*

Statistical Software **69**, 1–33.

Levine, J. S., and MacNichol, E. F. 1979. Visual pigments in teleost fishes: effects of habitat, microhabitat, and behavior on visual system evolution. *Sens Processes* **3**, 95–131.

Lewis, J. 1996. Neurogenic genes and vertebrate neurogenesis. *Current Opinion in Neurobiology* **6**, 3–10.

Lewis, W. M., and Morris, D. P. 1986. Toxicity of nitrite to fish: a review. *Transactions of the American Fisheries Society* **115**, 183–195.

Liao, P. B., and Mayo, R. D. 1972. Salmonid hatchery water reuse systems. *Aquaculture* **1**, 317–335.

Lien, S., Koop, B. F., Sandve, S. R., Miller, J. R., Kent, M. P., Nome, T., Hvidsten, T. R., Leong, J. S., Minkley, D. R., Zimin, A., Grammes, F., Grove, H., Gjuvsland, A., Walenz, B., Hermansen, R. A., von Schalburg, K., Rondeau, E. B., Di Genova, A., Samy, J. K. A., Olav Vik, J., Vigeland, M. D., Caler, L., Grimholt, U., Jentoft, S., Våge, D. I., de Jong, P., Moen, T., Baranski, M., Palti, Y., Smith, D. R., Yorke, J. A., Nederbragt, A. J., Tooming-Klunderud, A., Jakobsen, K. S., Jiang, X., Fan, D., Hu, Y., Liberles, D. A., Vidal, R., Iturra, P., Jones, S. J. M., Jonassen, I., Maass, A., Omholt, S. W., and Davidson, W. S. 2016. The Atlantic salmon genome provides insights into rediploidization. *Nature* **533**, 200–205.

Lin, J. F., Pan, H. C., Ma, L. P., Shen, Y. Q., and Schachner, M. 2012. The cell neural adhesion molecule contactin-2 (TAG-1) is beneficial for functional recovery after spinal cord injury in adult zebrafish. *PLoS ONE* **7**, e52376

Littlechild, J. A., and Watson, H. C. 1993. A data-based reaction mechanism for type I fructose bisphosphate aldolase. *Trends in Biochemical Sciences* **18**, 36–39.

Liu, Q., and Duston, J. 2016. Preventing sexual maturation in Arctic charr by 24h light overwinter and suppressing somatic growth. *Aquaculture* **464**, 537–544.

Livak, K. J., and Schmittgen, T. D. 2001. Analysis of relative gene expression data using real-time quantitative PCR and the 2(-Delta Delta C(T)) Method. *Methods San Diego Calif* **25**, 402–408.

Loncoman, C., Gutiérrez, L., Strobel, P., Alarcón, P., Contreras, C., Conejeros, I., and Morera, F. 2015. Application of a real-time PCR assay to detect BK potassium channel expression in samples from Atlantic salmon (*Salmo salar*) and Rainbow trout (*Oncorhynchus mykiss*) acclimated to freshwater **220**, 215–220.

Lovenberg, T. W., Chalmers, D. T., Liu, C., and De Souza, E. B. 1995. CRF2 alpha

and CRF2 beta receptor mRNAs are differentially distributed between the rat central nervous system and peripheral tissues. *Endocrinology* **136**, 4139–42.

Lubin, R. T., Rourke, A. W., and Saunders, R. L. 1991. Influence of photoperiod on the number and ultrastructure of gill chloride cells of the Atlantic salmon (*Salmo salar*) before and during smoltification. *Canadian Journal of Fisheries and Aquatic Sciences* **48**, 1302–1307.

Lucas, R. J., Peirson, S. N., Berson, D. M., Brown, T. M., Cooper, H. M., Czeisler, C. A, Figueiro, M. G., Gamlin, P. D., Lockley, S. W., O'Hagan, J. B., Price, L. A. L., Provencio, I., Skene, D. J., and Brainard, G. C. 2014. Measuring and using light in the melanopsin age. *Trends in Neurosciences* **37**, 1–9.

Lukowski, C. M., Ritzel, R. G., and Waskiewicz, A. J. 2006. Expression of two insm1-like genes in the developing zebrafish nervous system. *Gene Expression Patterns* **6**, 711–718.

Lundqvist, H., McKinnell, S., Fängstam, H., and Berglund, I. 1994. The effect of time, size and sex on recapture rates and yield after river releases of *Salmo salar* smolts. *Aquaculture* **121**, 245–257.

Luo, W., and Brouwer, C. 2013. Pathview: An R/Bioconductor package for pathway-based data integration and visualization. *Bioinformatics* **29**, 1830–1831.

MacCrimmon, H. R., and Gots, B. L. 1979. World distribution of Atlantic salmon, *Salmo salar*. *Journal of the Fisheries Board of Canada* **36**, 422–457.

Macqueen, D. J., and Johnston, I. A. 2014. A well-constrained estimate for the timing of the salmonid whole genome duplication reveals major decoupling from species diversification. *Proceedings of the Royal Society of London B* **281**, 20132881.

Macqueen, D. J., Robb, D. H. F., Olsen, T., Melstveit, L., Paxton, C. G. M., and Johnston, I. A. 2008. Temperature until the “eyed stage” of embryogenesis programmes the growth trajectory and muscle phenotype of adult Atlantic salmon. *Biology Letters* **4**, 294–298.

Madaro, A., Olsen, R. E., Kristiansen, T. S., Ebbesson, L. O. E., Nilsen, T. O., Flik, G., and Gorissen, M. 2015. Stress in Atlantic salmon: response to unpredictable chronic stress. *Journal of Experimental Biology* **218**, 2538–2550.

Madaro, A., Olsen, R. E., Kristiansen, T. S., Ebbesson, L. O. E., Flik, G., and Gorissen, M. 2016. A comparative study of the response to repeated chasing stress in Atlantic salmon (*Salmo salar* L.) parr and post-smolts. *Comparative Biochemistry and Physiology Part A: Molecular and Integrative Physiology* **192**, 7–16.

Maeda, R., Shimo, T., Nakane, Y., Nakao, N., and Yoshimura, T. 2015. Ontogeny of the saccus vasculosus, a seasonal sensor in fish. *Endocrinology* **156**, 4238–4243.

Mano, H., and Fukada, Y. 2007. A median third eye: pineal gland retraces evolution of vertebrate photoreceptive organs. *Photochemistry and Photobiology* **83**, 11–18.

Marioni, J. C., Mason, C. E., Mane, S. M., Stephens, M., and Gilad, Y. 2008. RNA-seq: an assessment of technical reproducibility and comparison with gene expression arrays. *Genome Research* **18**, 1509–1517.

Marty, C., and Beall, E. 1989. Modalités spatio-temporelles de la dispersion d'alevins de saumon Atlantique (*Salmo salar* L.) à l'emergence. *Revue Des Sciences de l'eau* **2**, 831–846.

Matsuoka, I., Fuyuki, K., Shoji, T., and Kurihara, K. 1998. Identification of c-fos related genes and their induction by neural activation in rainbow trout brain. *Biochimica et Biophysica Acta - Gene Structure and Expression* **1395**, 220–227.

Max, M., and Menaker, M. 1992. Regulation of melatonin production by light, darkness, and temperature in the trout pineal. *Journal of Comparative Physiology A: Neuroethology, Sensory, Neural, and Behavioral Physiology* **170**, 479–489.

Mayer, I., Bornestaf, C., and Borg, B. 1997. Melatonin in non-mammalian vertebrates: physiological role in reproduction? *Comparative Biochemistry and Physiology Part A: Physiology* **118**, 515–531.

McClure, C. A., Hammell, K. L., Moore, M., Dohoo, I. R., and Burnley, H. 2007. Risk factors for early sexual maturation in Atlantic salmon in seawater farms in New Brunswick and Nova Scotia, Canada. *Aquaculture* **272**, 370–379.

Mccormick, S. D. 1993. Methods for non biopsy and measurement of Na+, K+-ATPase activity. *Canadian Journal of Aquatic Sciences* **50**, 9–11.

McCormick, S. D. 1995. 11 Hormonal Control of Gill Na+, K+-ATPase and Chloride Cell Function. *Fish Physiology* **14**, 285–315.

McCormick, S. D. 2012. Smolt Physiology and Endocrinology. In: McCormick, S. D., Farrell, A. P., and Brauner, C. J. (Eds.), *Fish Physiology* **32**. Academic Press, Waltham, USA.

McCormick, S. D., and Naiman, R. J. 1984. Osmoregulation in the brook trout *Salvelinus fontinalis* - II. Effects of size, age and photoperiod on seawater survival and ionic regulation. *Comparative Biochemistry and Physiology Part A: Physiology* **79A**, 17–28.

McCormick, S. D., and Saunders, R. L. 1987. Preparatory physiological adaptations for marine life in salmonids: osmoregulation, growth and metabolism. *American Fisheries Society Symposium*, 211–229.

Mccormick, S. D., Saunders, R. L., Henderson, E. B., and Harmon, P. R. 1987. Photoperiod control of parr-smolt transformation in Atlantic salmon (*Salmo salar*): changes in salinity tolerance, gill Na+, K+-ATPase activity, and plasma thyroid hormones. *Canadian Journal of Fisheries and Aquatic Sciences* **44**, 1462-1468.

McCormick, S. D., Björnsson, B. T., Moriyama, S., Carey, J. B., and O'Dea, M. 1995. Plasma growth hormone (GH), insulinlike growth factor I (IGF-I), cortisol and thyroid hormones during environmental manipulation of the parr-smolt transformation of Atlantic salmon. *American Zoologist* **75**.

McCormick, S. D., Hansen, L. P., Quinn, T. P., and Saunders, R. L. 1998. Movement, migration, and smolting of Atlantic salmon (*Salmo salar*). *Canadian Journal of Fisheries and Aquatic Sciences* **55**, 77–92.

McCormick, S. D., Cunjak, R. A., Dempson, B., O'Dea, M. F., and Carey, J. B. 1999. Temperature-related loss of smolt characteristics in Atlantic salmon (*Salmo salar*) in the wild. *Canadian Journal of Fisheries and Aquatic Sciences* **56**, 1649–1657.

McCormick, S. D., Shrimpton, J. M., Moriyama, S., and Björnsson, B. T. 2007. Differential hormonal responses of Atlantic salmon parr and smolt to increased daylength: A possible developmental basis for smolting. *Aquaculture* **273**, 337–344.

McCormick, S. D., Regish, A. M., and Christensen, A. K. 2009. Distinct freshwater and seawater isoforms of Na+/K+-ATPase in gill chloride cells of Atlantic salmon. *The Journal of Experimental Biology* **212**, 3994–4001.

McLean, E., and Donaldson, E. M. 1993. The role of growth hormone in the growth of poikilotherms. In: Schreibman, M. P., Scanes, C. G., and Pang, P. K. T. (Eds.), *The Endocrinology of Growth, Development, and Metabolism in Vertebrates*, pp. 43–71. Academic Press, San Diego.

Mehta, N., and Cheng, H-Y. M. 2013. Micro-managing the circadian clock: The role of microRNAs in biological timekeeping. *Journal of Molecular Biology* **425**, 3609–3624.

Meissl, H., and Ekström, P. 1988. Dark and light adaptation of pineal photoreceptors. *Vision Research* **28**, 49–56.

Meissl, H., and Yanez, J. 1994. Pineal photosensitivity. A comparison with retinal

photoreception. *Acta Neurobiologiae Experimentalis* **54**, 19-29.

Melmed, S. 2010. *The pituitary, 3rd Edition*. Elsevier, Amsterdam.

Metzker, M. L. 2010. Sequencing technologies - the next generation. *Nature Reviews Genetics* **11**, 31–46.

Migaud, H., Taylor, J. F., Taranger, G. L., Davie, A., Cerdá-Reverter, J. M., Carrillo, M., Hansen, T., and Bromage, N. R. 2006. A comparative ex vivo and in vivo study of day and night perception in teleosts species using the melatonin rhythm. *Journal of Pineal Research* **41**, 42–52.

Migaud, H., Cowan, M., Taylor, J., and Ferguson, H. W. 2007. The effect of spectral composition and light intensity on melatonin, stress and retinal damage in post-smolt Atlantic salmon, *Salmo salar*. *Aquaculture* **270**, 390–404.

Migaud, H., Davie, A., Martinez Chavez, C. C., and Al-Khamees, S. 2007. Evidence for differential photic regulation of pineal melatonin synthesis in teleosts. *Journal of Pineal Research* **43**, 327–335.

Migaud, H., Davie, A., and Taylor, J. F. 2010. Current knowledge on the photoneuroendocrine regulation of reproduction in temperate fish species. *Journal of Fish Biology* **76**, 27–68.

Minors, D. S., and Waterhouse, J. M. 2013. *Circadian rhythms and the human*. Butterworth-Heinemann, UK.

Mitchell, D. F. 1986. The effect of light intensity on the growth and behaviour of cultured juvenile Atlantic salmon (*Salmo salar* L.). M. Sc. thesis, University of Stirling, Scotland, UK.

Miyakoshi, Y., Nagata, M., and Kitada, S. 2001. Effect of smolt size on postrelease survival of hatchery-reared Masu salmon *Oncorhynchus masou. Fisheries Science* **67**, 134–137.

Mommsen, T. P., Vijayan, M. M., and Moon, T. W. 1999. Cortisol in teleosts: dynamics, mechanisms of action, and metabolic regulation. *Reviews in Fish Biology and Fisheries* **9**, 211–268.

Mommens, M., Naeve, I., Brunsvik, Per, and Tveiten, H. 2016. Land-based Atlantic salmon (*Salmo salar*) broodstock production for an out-of-season pathogen-free egg production. In: *European Aquaculture Society Conference, Edinburgh, 21st September 2016*.

Monnot, M. J., Babin, P. J., Poleo, G., Andre, M., Laforest, L., Ballagny, C., and Akimenko, M. A. 1999. Epidermal expression of apolipoprotein E gene during fin

and scale development and fin regeneration in zebrafish. *Developmental Dynamics : An Official Publication of the American Association of Anatomists* **214**, 207–215.

Monteith, J. L., and Unsworth, M. H. 2013a. Properties of gases and liquids. In: Monteith, J. L., and Unsworth, M. H., (Eds.), *Principles of Environmental Physics, 4th Edition*, pp. 5–23. Academic Press, Boston.

Monteith, J. L., and Unsworth, M. H. (2013b). Radiation Environment. In: Monteith, J. L., and Unsworth, M. H., (Eds.), *Principles of Environmental Physics, 4th Edition*, pp. 49–79. Academic Press, Boston.

Moore, H. A., and Whitmore, D. 2014. Circadian rhythmicity and light sensitivity of the zebrafish brain. *PLoS One* **9**, e86176.

Morais, S., Taggart, J. B., Guy, D. R., Bell, J., and Tocher, D. R. 2012. Hepatic transcriptome analysis of inter-family variability in flesh n-3 long-chain polyunsaturated fatty acid content in Atlantic salmon. *BMC Genomics* **13**, 410.

Moran, D. 2010. Carbon dioxide degassing in fresh and saline water. I: Degassing performance of a cascade column. *Aquacultural Engineering* **43**, 29–36.

Morel, A., Gentili, B., Claustre, H., Babin, M., Bricaud, A., Ras, J., and Tièche, F. 2007. Optical properties of the “clearest” natural waters. *Limnology and Oceanography* **52**, 217–229.

Moreno-Flores, M. T., Martín-Aparicio, E., Martín-Bermejo, M. J., Agudo, M., McMahon, S., Avila, J., Díaz-Nido, J., and Wandosell, F. 2003. Semaphorin 3C preserves survival and induces neuritogenesis of cerebellar granule neurons in culture. *Journal of Neurochemistry* **87**, 879–890.

Morgan, I. J., Mccarthy, I. D., and Metcalfe, N. B. 2000. Life-history strategies and protein metabolism in overwintering juvenile Atlantic salmon: growth is enhanced in early migrants through lower protein turnover. *Journal of Fish Biology* **56**, 637–647.

Morita, K., and Fukuwaka, M. 2006. Does size matter most? The effect of growth history on probabilistic reaction norm for salmon maturation. *Evolution* **60**, 1516–1521.

Moriya, Y., Itoh, M., Okuda, S., Yoshizawa, A. C., and Kanehisa, M. 2007. KAAS: An automatic genome annotation and pathway reconstruction server. *Nucleic Acids Research* **35**, 182–185.

Mørkøre, T., and Rørvik, K-A. 2001. Seasonal variations in growth, feed utilisation and

product quality of farmed Atlantic salmon (*Salmo salar*) transferred to seawater as 0+smolts or 1+smolts. *Aquaculture* **199**, 145–157.

Mortensen, A., and Damsgård, B. 1998. The effect of salinity on desmoltification in Atlantic salmon. *Aquaculture* **168**, 407–411.

Moutsaki, P., Whitmore, D., Bellingham, J., Sakamoto, K., David-Gray, Z. K., and Foster, R. G. 2003. Teleost multiple tissue (tmt) opsin: A candidate photopigment regulating the peripheral clocks of zebrafish? *Molecular Brain Research* **112**, 135–145.

Munch, S. B., and Conover, D. O. 2003. Rapid growth results in increased susceptibility to predation in Menidia menidia. *Evolution; International Journal of Organic Evolution* **57**, 2119–2127.

Mure, L. S., Cornut, P-L., Rieux, C., Drouyer, E., Denis, P., Gronfier, C., and Cooper, H. M. 2009. Melanopsin bistability: a fly's eye technology in the human retina. *PLoS One* **4**, e5991.

Myers, R. A., Hutchings, J. A., and Gibson, R. J. 1986. Variation in male parr maturation within and among populations of Atlantic salmon, *Salmo salar*. *Canadian Journal of Fisheries and Aquatic Sciences* **43**, 1242–1248.

Nakane, Y., Ikegami, K., Iigo, M., Ono, H., Takeda, K., Takahashi, D., Uesaka, M. Kimijima, M., Hashimoto, R., Arai, N., Suga, T., Kosuge, K., Abe, T., Maeda, R., Senga, T., Amiya, N., Azuma, T., Amano, M., Abe, H., Yamamoto, N., and Yoshimura, T. 2013. The saccus vasculosus of fish is a sensor of seasonal changes in day length. *Nature Communications* **4**, 1–7.

Nakano, Y., Fujita, M., Ogino, K., Saint-Amant, L., Kinoshita, T., Oda, Y., and Hirata, H. 2010. Biogenesis of GPI-anchored proteins is essential for surface expression of sodium channels in zebrafish Rohon-Beard neurons to respond to mechanosensory stimulation. *Development* **137**, 1689–1698.

Nakatani, Y., Takeda, H., Kohara, Y., and Morishita, S. 2007. Reconstruction of the vertebrate ancestral genome reveals dynamic genome reorganization in early vertebrates. *Genome Research* **17**, 1254–1265.

Near, T. J., Eytan, R. I., Dornburg, A., Kuhn, K. L., Moore, J. A., Davis, M. P., Wainwright, P. C., Friedman, M., and Smith, W. L. 2012. Resolution of ray-finned fish phylogeny and timing of diversification. *Proceedings of the National Academy of Sciences* **109**, 13698–13703.

Nemeth, R. S., and Anderson, J. J. 2011. Response of juvenile Coho and Chinook

salmon to strobe and mercury vapor lights. *North American Journal of Fisheries Management* **12**, 684-692.

Nicieza, A. G., and Metcalfe, N. B. 1997. Growth compensation in juvenile Atlantic salmon: Responses to depressed temperature and food availability. *Ecology* **78**, 2385–2400.

Nicieza, A. G., Reyes-Gavilán, F. G., and Braña, F. 1994. Differentiation in juvenile growth and bimodality patterns between northern and southern populations of Atlantic salmon (*Salmo salar* L.). *Canadian Journal of Zoology* **72**, 1603–1610.

Nilsen, T. O., Ebbesson, L. O. E., Madsen, S. S., McCormick, S. D., Andersson, E., Björnsson, B. T., Prunet, P., and Stefansson, S. O. 2007. Differential expression of gill Na+,K+-ATPase alpha- and beta-subunits, Na+,K+,2Cl- cotransporter and CFTR anion channel in juvenile anadromous and landlocked Atlantic salmon Salmo salar. *The Journal of Experimental Biology* **210**, 2885–2896.

Nordgarden, U., Oppedal, F., Taranger, G. L., Hemre, G., and Hansen, T. 2003. Seasonally changing metabolism in Atlantic salmon (*Salmo salar* L.) I – Growth and feed conversion ratio. *Aquaculture Nutrition* **9**, 287–293.

Nordgarden, U., Ørnsrud, R., Hansen, T., and Hemre, G. I. 2003. Seasonal changes in selected muscle quality parameters in Atlantic salmon (*Salmo salar* L.) reared under natural and continuous light. *Aquaculture Nutrition* **9**, 161–168.

Ogris, E., Du, X., Nelson, K. C., Mak, E. K., Yu, X. X. Lane, W. S.,and Pallas, D. C. 1999. A protein phosphatase methylesterase (PME-1) is one of several novel proteins stably associating with two inactive mutants of protein phosphatase 2A. *Cell* **18**, 1089–1098.

Okuyama, T., Suehiro, Y., Imada, H., Shimada, A., Naruse, K., Takeda, H., Kubo, T., and Takeuchi, H. 2011. Induction of c-fos transcription in the medaka brain (*Oryzias latipes*) in response to mating stimuli. *Biochemical and Biophysical Research Communications* **404**, 453–457.

Oppedal, F., Lasse Taranger, G., Juell, J-E., Fosseidengen, J. E., and Hansen, T. 1997. Light intensity affects growth and sexual maturation of Atlantic salmon (*Salmo salar*) postsmolts in sea cages. *Aquatic Living Resources* **10**, 351–357.

Oppedal, F., Taranger, G. L., Juell, J-E., and Hansen, T. 1999. Growth, osmoregulation and sexual maturation of underyearling Atlantic salmon smolt *Salmo salar* L. exposed to different intensities of continuous light in sea cages. *Aquaculture Research* **30**, 491–499.

Oppedal, F., Taranger, G. L., and Hansen, T. 2003. Growth performance and sexual maturation in diploid and triploid Atlantic salmon (*Salmo salar* L.) in seawater tanks exposed to continuous light or simulated natural photoperiod. *Aquaculture* **215**, 145–162.

Oppedal, F., Berg, A., Olsen, R. E., Taranger, G. L., and Hansen, T. 2006. Photoperiod in seawater influence seasonal growth and chemical composition in autumn sea-transferred Atlantic salmon (*Salmo salar* L.) given two vaccines. *Aquaculture* **254**, 396–410.

Oppedal, F., Juell, J-E., and Johansson, D. 2007. Thermo- and photoregulatory swimming behaviour of caged Atlantic salmon: implications for photoperiod management and fish welfare. *Aquaculture* **265**, 70–81.

Orphanides, G., and Reinberg, D. 2002. A unified theory of gene expression. *Cell* **108**, 439–451.

Palczewski, K., Kumasaka, T., Hori, T., Behnke, C. A., Motoshima, H., Fox, B. A., Le Trong, I., Teller, D. C., Okada, T., Stenkamp, R. E., Yamamoto, M., and Miyano, M. 2000. Crystal structure of rhodopsin: AG protein-coupled receptor. *Science* **289**, 739–745.

Panda, S., Nayak, S. K., Campo, B., Walker, J. R., Hogenesch, J. B., and Jegla, T. 2005. Illumination of the melanopsin signaling pathway. *Science* **307**, 600–604.

Pankhurst, N. W. 2011. The endocrinology of stress in fish: an environmental perspective. *General and Comparative Endocrinology* **170**, 265–275.

Pankhurst, N. W. and Porter, M. J. R. (2003). Cold and dark or warm and light: variations on the theme of environmental control of reproduction. *Fish Physiology and Biochemistry* **28**, 385–389.

Pankhurst, N. W., Ludke, S. L., King, H. R., and Peter, R. E. 2008. The relationship between acute stress, food intake, endocrine status and life history stage in juvenile farmed Atlantic salmon, *Salmo salar*. *Aquaculture* **275**, 311–318.

Pankhurst, N. W., and King, H. R. 2010. Temperature and salmonid reproduction: implications for aquaculture. *Journal of Fish Biology* **76**, 69–85.

Parker, A. R. 2011. On the origin of optics. *Optics and Laser Technology* **43**, 323–329.

Parkyn, D. C., Hawryshyn, C. W., and Columbia, B. 2000. Spectral and ultraviolet-polarisation sensitivity in juvenile salmonids: a comparative analysis using electrophysiology. *Journal of Experimental Biology* **203**, 1173–1191.

Pat, W., Stone, G., and Johnston, I. A. 2005. *Environmental physiology of animals, 2nd*

Edition. *Blackwell Science, Oxford, UK*. Retrieved from http://www.worldcat.org/oclc/53307700

Pedersen, P. B., von Ahnen, M., Fernandes, P., Naas, C., Pedersen, L-F., and Dalsgaard, A. J. T. 2015. Room for all? Particulate surface area and bacterial activity in RAS. In: *3rd NordicRAS Workshop on Recirculating Aquaculture Systems*. Norway.

Peirson, S. N., Halford, S., and Foster, R. G. 2009. The evolution of irradiance detection: melanopsin and the non-visual opsins. *Philosophical Transactions of the Royal Society B: Biological Sciences* **364**, 2849–2865.

Pertea, M., Kim, D., Kim, D., Pertea, G. M., Leek, J. T., and Salzberg, S. L. 2016. Transcript-level expression analysis of RNA-seq experiments with HISAT , StringTie and Ballgown. *Nature Protocols* **11**, 1650–1667.

Peter, R. E., Yu, K-L, Marchant, T. A., and Rosenblum, P. M. 1990. Direct neural regulation of the teleost adenohypophysis. *Journal of Experimental Zoology* **256**, 84–89.

Pfaffl, M. W. 2001. A new mathematical model for relative quantification in real-time RT-PCR. *Nucleic Acids Research* **29**, e45.

Philp, A. R., Garcia-Fernandez, J. M., Soni, B. G., Lucas, R. J., Bellingham, J., and Foster, R. G. 2000. Vertebrate ancient (VA) opsin and extraretinal photoreception in the Atlantic salmon (*Salmo salar*). *Journal of Experimental Biology* **203**, 1925–1936.

Pickering, A. D., Pottinger, T. G., Sumpter, J. P., Carragher, J. F., and Le Bail, P. Y. 1991. Effects of acute and chronic stress on the levels of circulating growth hormone in the rainbow trout, *Oncorhynchus mykiss*. *General and Comparative Endocrinology* **83**, 86–93.

Pimputkar, S., Speck, J. S., DenBaars, S. P., and Nakamura, S. 2009. Prospects for LED lighting. *Nature Photonics* **3**, 180–182.

Pinheiro, J., Bates, D., DebRoy, S., Sarkar, D., and R Core Team. 2016. nlme: Linear and Nonlinear Mixed Effects Models. Retrieved from http://cran.r-project.org/package=nlme

Planas, J. V, Swanson, P., Rand-Weaver, M., and Dickhoff, W. W. 1992. Somatolactin stimulates in vitro gonadal steroidogenesis in coho salmon, *Oncorhynchus kisutch*. *General and Comparative Endocrinology* **87**, 1–5.

Porter, M. J. R., Duncan, N., Mitchell, D., and Bromage, N. R. 1999. The use of cage

lighting to reduce plasma melatonin in Atlantic salmon (*Salmo salar*) and its effects on the inhibition of grilsing. *Aquaculture* **176**, 237–244.

Porter, M. J. R., Duncan, N., Handeland, S. O., Stafansson, S. O., and Bromage, N. R. 2001. Temperature, light intensity and plasma melatonin levels in juvenile Atlantic salmon. *Journal of Fish Biology* **58**, 431–438.

Pottinger, T. G. 2010. A multivariate comparison of the stress response in three salmonid and three cyprinid species: evidence for inter-family differences. *Journal of Fish Biology* **76**, 601–621.

R Core Team. 2016. R: A Language and Environment for Statistical Computing. Vienna, Austria. Retrieved from https://www.r-project.org/

Rader, R. B., Belish, T., Young, M. K., and Rothlisberger, J. 2007. The scotopic visual sensitivity of four species of trout: a comparative study. *Western North American Naturalist* **67**, 524–537.

Ramsköld, D., Wang, E. T., Burge, C. B., and Sandberg, R. 2009. An abundance of ubiquitously expressed genes revealed by tissue transcriptome sequence data. *PLoS Computational Biology* **5**, e1000598.

Rand-Weaver, M., Pottinger, T. G., and Sumpter, J. P. 1993. Plasma somatolactin concentrations in salmonid fish are elevated by stress. *Journal of Endocrinology* **138**, 509–515.

Randall, H., and Hoar D. J. 1988. Yolk Absorbtion In embryonic and Larval Fishes. The Physioligy Of Developing Fish. *Fish larval physiology* **11***,* 407-446*.*

Randall, C. F., Duston, J., and Bromage, N. R. 1987. Photoperiodic history and the entrainment of the annual cycle of reproduction in the female rainbow trout, *Salmo gairdneri*. In: Idler, D. R., Crim, L. W., and Walsh, J. M. (Eds.). *Proceedings of 3rd International Symposium on the Reproductive Physiology of Fish.* St. Johns, Newfoundland, 310*.*

Randall, C. F., Bromage, N. R., Thrush, M. A., and Davies, B. 1991. Photoperiodism and melatonin rhythms in salmonid fish. In: Scott, A. P., Sumpter, J., Kime, D., and Roffe, M. (Eds.), *Proceedings of 4th International Symposium on Reproductive Physiology of Fish* **91**, 136-138.

Randall, C. F., Bromage, N. R., Duston, J., and Symes, J. 1998. Photoperiod-induced phase-shifts of the endogenous clock controlling reproduction in the rainbow trout: a Circannual Phase-Response Curve. *Journal of Reproduction and Fertility* **112**, 399–405.

Reinecke, M., Björnsson, B. T., Dickhoff, W. W., McCormick, S. D., Navarro, I., Power, D. M., and Gutiérrez, J. 2005. Growth hormone and insulin-like growth factors in fish: where we are and where to go. *General and Comparative Endocrinology* **142**, 20–24.

Reppert, S. M., and Weaver, D. R. 2002. Coordination of circadian timing in mammals. *Nature* **418**, 935–941.

Richardson, J. 1836. Fauna Boreali, *The fish* **3**. Bentley, London.

Ritz, C., Baty, F., Streibig, J. C., and Gerhard, D. 2015. Dose-response analysis using R. *PLoS ONE* **10**, e0146021.

Roberts, N. W., and Needham, M. G. 2007. A mechanism of polarized light sensitivity in cone photoreceptors of the goldfish *Carassius auratus*. *Biophysical Journal* **93**, 3241–3248.

Ronkin, D., Seroussi, E., Nitzan, T., Doron-Faigenboim, A., and Cnaani, A. 2015. Intestinal transcriptome analysis revealed differential salinity adaptation between two tilapiine species. *Comparative Biochemistry and Physiology - Part D: Genomics and Proteomics* **13**, 35–43.

Rotllant, J., Tort, L., Montero, D., Pavlidis, M., Martinez, M., Wendelaar Bonga, S. E., and Balm, P. H. M. 2003. Background colour influence on the stress response in cultured red porgy *Pagrus pagrus*. *Aquaculture* **223**, 129–139.

Rowe, R. W. D., and Goldspink, G. 1969. Muscle fibre growth in five different muscles in both sexes of mice: I. Normal mice. *Journal of Anatomy* **104**, 519–530.

Rowe, D. K., Thorpe, J. E., and Shanks, A. M. 1991. Role of fat stores in the maturation of male Atlantic salmon (*Salmo salar*) parr. *Canadian Journal of Fisheries and Aquatic Sciences* **48**, 405–413.

Rozenboim, I., Biran, I., Uni, Z., and Halevy, O. 1999. The involvement of monochromatic light in growth, development and endocrine parameters of broilers. *Poultry Science* **78**, 135–138.

Rozenboim, I., Biran, I., Chaiseha, Y., Yahav, S., Rosenstrauch, A., Sklan, D., and Halevy, O. 2004. The effect of a green and blue monochromatic light combination on broiler growth and development. *Poultry Science* **83**, 842–845.

RSPCA. 2015. RSPCA Welfare standards for Farmed Atlantic Salmon. RSPCA [Leaflet] .

Rusak, B., Robertson, H. A., Wisden, W., and Hunt, S. P. 1990. Light pulses that shift rhythms induce gene expression in the suprachiasmatic nucleus. *Science* **248**,

1237–1240.

Sabbah, S., Troje, N. F., Gray, S. M., and Hawryshyn, C. W. 2013. High complexity of aquatic irradiance may have driven the evolution of four-dimensional colour vision in shallow-water fish. *The Journal of Experimental Biology* **216**, 1670–1682.

Saha, D., Patgaonkar, M., Shroff, A., Ayyar, K., Bashir, T., and Reddy, K. V. R. 2014. Hemoglobin Expression in Nonerythroid Cells: Novel or Ubiquitous? *International Journal of Inflammation*, **803237**.

Sahlmann, C., Sutherland, B. J. G., Kortner, T. M., Koop, B. F., Krogdahl, Å., and Bakke, A. M. 2013. Early response of gene expression in the distal intestine of Atlantic salmon (*Salmo salar* L.) during the development of soybean meal induced enteritis. *Fish and Shellfish Immunology* **34**, 599–609.

Sakai, Y., Ohtsuki, H., Kasagi, S., Kawamura, S., and Kawata, M. 2016. Effects of light environment during growth on the expression of cone opsin genes and behavioral spectral sensitivities in guppies (*Poecilia reticulata*). *BMC Evolutionary Biology* **16**, 106.

Sakamoto, T., and McCormick, S. D. 2006. Prolactin and growth hormone in fish osmoregulation. *General and Comparative Endocrinology* **147**, 24–30.

Sandbakken, M., Ebbesson, L., Stefansson, S., and Helvik, J. V. 2012. Isolation and characterization of melanopsin photoreceptors of Atlantic salmon (*Salmo salar*). *The Journal of Comparative Neurology* **520**, 3727–3744.

Saunders, R. L., and Harmon, P. R. 1988. Extended daylength increases postsmolt growth of Atlantic salmon. *World Aquaculture* **19**, 72–73.

Saunders, R. L., Henderson, E. B., and Harmon, P. R. 1985. Effects of photoperiod on juvenile growth and smolting of Atlantic salmon and subsequent survival and growth in sea cages. *Aquaculture* **45**, 55–66.

Schaffeld, M., Haberkamp, M., Braziulis, E., Lieb, B., and Markl, J. 2002. Type II keratin cDNAs from the rainbow trout: Implications for keratin evolution. *Differentiation* **70**, 292–299.

Scharrer, E. 1964. Photo-neuro-endocrine systems: general concepts. *Annals of the New York Academy of Sciences* **117**, 13–22.

Schauer, E., Trautinger, F., Köck, A., Schwarz, A., Bhardwaj, R., Simon, M., Ansel, J. C., Schwarz, T., and Luger, T. A. 1994. Proopiomelanocortin-derived peptides are synthesized and released by human keratinocytes. *Journal of Clinical Investigation* **93**, 2258-2262.

Scheiermann, C., Kunisaki, Y., and Frenette, P. S. 2013. Circadian control of the immune system. *Nature Reviews Immunology* **13**, 190-198.

Schroeder, A. M., and Colwell, C. S. 2013. How to fix a broken clock. *Trends in Pharmacological Sciences* **34**, 605–619.

Schwartz, W. J., Takeuchi, J., Shannon, W., Davis, E. M., and Anonin, N. 1994. Temporal regulation of light-induced Fos and Fos-like protein expression in the ventrolateral subdivision of the rat suprachiasmatic nucleus. *Neuroscience* **58**, 573–583.

Seear, P. J., Carmichael, S. N., Talbot, R., Taggart, J. B., Bron, J. E., and Sweeney, G. E. 2010. Differential gene expression during smoltification of Atlantic salmon (*Salmo salar* L.): A first large-scale microarray study. *Marine Biotechnology* **12**, 126–140.

Sekhon, J. S. 2011. Multivariate and propensity score matching software with automated balance optimization: the matching package for R. *Journal of Statistical Software* **42**, 1–52.

Shcherbakov, D., Knörzer, A., Espenhahn, S., Hilbig, R., Haas, U., and Blum, M. 2013. Sensitivity differences in fish offer near-infrared vision as an adaptable evolutionary trait. *PloS One* **8**, e64429.

Sheng, M., and Greenberg, M. E. 1990. The regulation and function of c-fos and other immediate early genes in the nervous system. *Neuron* **4**, 477–485.

Sheridan, M. A. 1989. Alterations in lipid metabolism accompanying smoltification and seawater adaptation of salmonid fish. *Aquaculture* **82**, 191–203.

Sigholt, T., Staurnes, M., Jakobsen, H. J., and Åsgård, T. 1995. Effects of continuous light and short-day photoperiod on smolting, seawater survival and growth in Atlantic salmon (*Salmo salar*). *Aquaculture* **130**, 373–388.

Sigholt, T., Åsgård, T., and Staurnes, M. 1998. Timing of parr-smolt transformation in Atlantic salmon (*Salmo salar*): Effects of changes in temperature and photoperiod. *Aquaculture* **160**, 129–144.

Skilbrei, O. T., and Hansen, T. 2004. Effects of pre-smolt photoperiod regimes on post-smolt growth rates of different genetic groups of Atlantic salmon (*Salmo salar*). *Aquaculture* **242**, 671–688.

Sloat, M. R., Fraser, D. J., Dunham, J. B., Falke, J. A., Jordan, C. E., McMillan, J. R., and Ohms, H. A. 2014. Ecological and evolutionary patterns of freshwater maturation in Pacific and Atlantic salmonines. *Reviews in Fish Biology and*

Fisheries **24**, 689–707.

Smith, R. C., and Baker, K. S. 1981. Optical properties of the clearest natural waters (200-800 nm). *Applied Optics* **20**, 177–184.

Smith, T. R., Tremblay, G. C., and Bradley, T. M. 1999. Hsp70 and a 54 kDa protein (Osp54) are induced in salmon (*Salmo salar*) in response to hyperosmotic stress. *Journal of Experimental Zoology* **284**, 286–298.

Sommer, J., Gloor, S. M., Rovelli, G. F., Hofsteenge, J., Nick, H., Meier, R., and Monard, D. 1987. cDNA sequence coding for a rat glia-derived nexin and its homology to members of the serpin superfamily. *Biochemistry* **26**, 6407–6410.

Song, L., and Fricker, L. D. 1995. Purification and characterization of carboxypeptidase D, a novel carboxypeptidase E-like enzyme, from bovine pituitary. *Journal of Biological Chemistry* **270**, 25007–25013.

Soni, B. G., and Foster, R. G. 1997. A novel and ancient vertebrate opsin. *FEBS Letters* **406**, 279–283.

Soni, B. G., Philp, A. R., Foster, R. G., and Knox, B. E. 1998. Novel retinal photoreceptors. *Nature* **394**, 27–28.

Sontag, C. 1971. Spectral sensitivity studies on the visual system of the praying mantis, *Tenodera sinensis*. *The Journal of General Physiology* **57**, 93–112.

Speare, D. J., and Arsenault, G. J. 1997. Effects of intermittent hydrogen peroxide exposure on growth and columnaris disease prevention of juvenile rainbow trout (*Oncorhynchus mykiss*). *Canadian Journal of Fisheries and Aquatic Sciences* **54**, 2653–2658.

Stefansson, S. O., and Hansen, T. J. 1989. The effect of spectral composition on growth and smolting in Atlantic salmon (*Salmo salar*) and subsequent growth in sea cages. *Aquaculture* **82**, 155–162.

Stefansson, S. O., Naevdal, G., and Hansen, T. 1989. The influence of three unchanging photoperiods on growth and parr-smolt transformation in Atlantic salmon, *Salmo salar* L. *Journal of Fish Biology* **35**, 237–247.

Stefansson, S. O., Berge, Å. I., and Gunnarsson, G. S. 1998. Changes in seawater tolerance and gill Na+,K+-ATPase activity during desmoltification in Atlantic salmon kept in freshwater at different temperatures. *Aquaculture* **168**, 271–277.

Stefansson, S. O., Nilsen, T. O., Ebbesson, L. O. E., Wargelius, A., Madsen, S. S., Björnsson, B. T., and McCormick, S. D. 2007. Molecular mechanisms of continuous light inhibition of Atlantic salmon parr–smolt transformation.

Aquaculture **273**, 235–245.

Stefansson, S. O., Bjornsson, B. T. H., Ebbesson, L. O. E., and Mccormick, S. D. 2008. Smoltification. In: Finn, R., and Kapoor, B. (Eds.), *Fish Larval Physiology,* 639-681. Science Publishers, New Hampshire, USA.

Stefansson, S. O., Imsland, A. K., and Handeland, S. O. 2009. Food-deprivation, compensatory growth and hydro-mineral balance in Atlantic salmon (*Salmo salar*) post-smolts in sea water. *Aquaculture* **290**, 243–249.

Stenkamp, D. L. 2007. Neurogenesis in the Fish Retina. *International Review of Cytology* **259**, 173–224.

Stickland, N. C. 1983. Growth and development of muscle fibres in the rainbow trout (*Salmo gairdneri*). *Journal of Anatomy* **137**, 323–333.

Stradmeyer, L., and Thorpe, J. E. 1987. Feeding behaviour of wild Atlantic salmon, *Salmo salar* L., parr in mid-to late summer in a Scottish river. *Aquaculture Research* **18**, 33–49.

Strand, Å., Alanärä, A., Staffan, F., and Magnhagen, C. 2007. Effects of tank colour and light intensity on feed intake, growth rate and energy expenditure of juvenile Eurasian perch, *Perca fluviatilis* L. *Aquaculture* **272**, 312–318.

Summerfelt, S. T., Zühlke, A., Kolarevic, J., Reiten, B. K. M., Selset, R., Gutierrez, X., and Terjesen, B. F. 2015. Effects of alkalinity on ammonia removal, carbon dioxide stripping, and system pH in semi-commercial scale water recirculating aquaculture systems operated with moving bed bioreactors. *Aquacultural Engineering* **65**, 46–54.

Sumpter, J. P. 1990. General concepts of seasonal reproduction. In *Reproductive Seasonality in Teleosts: Environmental Influences.* Boca Raton, FL: CRC Press, 13–31.

Sundaram, A., Tengs, T., and Grimholt, U. 2017. Issues with RNA-seq analysis in non-model organisms: A salmonid example. *Developmental and Comparative Immunology* **75**, 38-47.

Suresh, A. V, and Sheehan, R. J. 1998. Muscle fibre growth dynamics in diploid and triploid rainbow trout. *Journal of Fish Biology* **52**, 570–587.

Tacchi, L., Bron, J. E., Taggart, J. B., Secombes, C. J., Bickerdike, R., Adler, M. A., Takle, H., and Martin, S. A. M. 2011. Multiple tissue transcriptomic responses to *Piscirickettsia salmonis* in Atlantic salmon (*Salmo salar*). *Physiological Genomics* **43**, 1241–1254.

Tadiso, T. M., Krasnov, A., Skugor, S., Afanasyev, S., Hordvik, I., and Nilsen, F. 2011. Gene expression analyses of immune responses in Atlantic salmon during early stages of infection by salmon louse (*Lepeophtheirus salmonis*) revealed bi-phasic responses coinciding with the copepod-chalimus transition. *BMC Genomics* **12**, 141.

Takle, H., Baeverfjord, G., Lunde, M., Kolstad, K., and Andersen, Ø. 2005. The effect of heat and cold exposure on HSP70 expression and development of deformities during embryogenesis of Atlantic salmon (*Salmo salar*). *Aquaculture* **249**, 515–524.

Taranger, G. L., and Hansen, T. 1993. Ovulation and egg survival following exposure of Atlantic Salmon, *Salmo salar* L., broodstock to different water temperatures. *Aquaculture and Fisheries Management* **24**, 151–156.

Taranger, G. L., Haux, C., Stefansson, S. O., Bjornsson, B. T., Walther, B. T., and Hansen, T. 1998. Abrupt changes in photoperiod affect age at maturity, timing of ovulation and plasma testosterone and oestradiol-17 beta profiles in Atlantic salmon, *Salmo salar*. *Aquaculture* **162**, 85–98.

Taranger, G. L., Haux, C., Hansen, T., Stefansson, S. O., Björnsson, B. T., Walther, B. T., and Kryvi, H. 1999. Mechanisms underlying photoperiodic effects on age at sexual maturity in Atlantic salmon, *Salmo salar*. *Aquaculture* **177**, 47–60.

Taranger, G. L., Carrillo, M., Schulz, R. W., Fontaine, P., Zanuy, S., Felip, A., Weltzien, F-A., Dufour, S., Karlsen, Ø., Norberg, B., Andersson., E., and Hansen, T. 2010. Control of puberty in farmed fish. *General and Comparative Endocrinology* **165**, 483–515.

Taranger, G. L., Muncaster, S., Norberg, B., Thorsen, A., and Andersson, E. 2015. Environmental impacts on the gonadotropic system in female Atlantic salmon (*Salmo salar*) during vitellogenesis: Photothermal effects on pituitary gonadotropins, ovarian gonadotropin receptor expression, plasma sex steroids and oocyte growth. *General and Comparative Endocrinology* **221**, 86-93.Tatsumi, R., Anderson, J. E., Nevoret, C. J., Halevy, O., and Allen, R. E. 1998. HGF/SF is present in normal adult skeletal muscle and is capable of activating satellite cells. *Developmental Biology* **194**, 114–128.

Taylor, H. R., West, S., Munoz, B., Rosenthal, F. S., Bressler, S. B., and Bressler, N. M. 1992. The long-term effects of visible light on the eye. *Archives of Ophthalmology* **110**, 99–104.

Taylor, S. M., Loew, E. R., and Grace, M. S. 2015. Ontogenic retinal changes in three ecologically distinct elopomorph fishes (Elopomorpha:Teleostei) correlate with light environment and behavior. *Visual Neuroscience* **32**, E005.

Terjesen, B. F., Summerfelt, S. T., Nerland, S., Ulgenes, Y., Fjæra, S. O., Megård Reiten, B. K., Selset, R., Kolarevic, J., Brunsvik, P., Bæverfjord, G., Takle, H., Kittelsen, A. H., and Åsgård, T. 2013. Design, dimensioning, and performance of a research facility for studies on the requirements of fish in RAS environments. *Aquacultural Engineering* **54**, 49–63.

Terlou, M., and Ekengren, B. 1979. Nucleus praeopticus and nucleus lateralis tuberis of *Salmo salar* and *Salmo gairdneri*: Structure and relationship to the hypophysis. *Cell and Tissue Research* **197**, 1–21.

The Scottish Government. 2016. Marine Scotland Science: Scottish fish farm production survey 2015. Retrieved July 31, 2017, from http://www.gov.scot/Resource/0050/00505162.pdf

The Scottish Government. 2017. Aquaculture. Retrieved June 16, 2017, from http://www.gov.scot/Topics/marine/Fish-Shellfish.

Thisse, C., and Thisse, B. 2008. High-resolution in situ hybridization to whole-mount zebrafish embryos. *Nature Protocols* **3**, 59–69.

Thorarensen, H., Kubiriza, G. K., and Imsland, A. K. 2015. Experimental design and statistical analyses of fish growth studies. *Aquaculture* **448**, 483–490.

Thornqvist, P-O., Hoglund, E., and Winberg, S. 2015. Natural selection constrains personality and brain gene expression differences in Atlantic salmon (*Salmo salar*). *Journal of Experimental Biology* **218**, 1077–1083.

Thorpe, J.E. 1994. Salmonid fishes and the estuarine environment. *Estuaries* **17**, 73-93.

Thorpe, J.E., 2007. Maturation responses of salmonids to changing developmental opportunities. *Marine Ecology – Prog. Ser*. **335**, 285–288.

Thorpe, J. E., Morgan, R. I. G., Pretswell, D., and Higgins, P. J. 1988. Movement rhythms in juvenile Atlantic salmon, *Salmo salar* L. *Journal of Fish Biology* **33**, 931–940.

Thorpe, J. E., Talbot, C., Miles, M. S., Rawlings, C., and Keay, D. S. 1990. Food consumption in 24 hours by Atlantic salmon (*Salmo salar* L.) in a sea cage. *Aquaculture* **90**, 41–47.

Thorpe, J. E., Mangel, M., Metcalfe, N. B., and Huntingford, F. A. 1998. Modelling the

proximate basis of salmonid life-history variation, with application to Atlantic salmon, *Salmo salar* L. *Evolutionary Ecology* **12**, 581–599.

Thrush, M. A., Duncan, N. J., and Bromage, N. R. 1994. The use of photoperiod in the production of out-of-season Atlantic salmon (*Salmo salar*) smolts. *Aquaculture* **121**, 29–44.

Tombran-tink, J., and Barnstable, C. J. 2008. *Visual transduction and non-visual light perception*. Totowa, N.J.: Humana Press.

Totland, G. K., Fjelldal, P. G., Kryvi, H., Løkka, G., Wargelius, A., Sagstad, A., Hansen, T., and Grotmol, S. 2011. Sustained swimming increases the mineral content and osteocyte density of salmon vertebral bone. *Journal of Anatomy* **219**, 490–501.

Trapnell, C., Hendrickson, D. G., Sauvageau, M., Goff, L., Rinn, J. L., and Pachter, L. 2012. Differential analysis of gene regulation at transcript resolution with RNA-seq. *Nature Biotechnology* **31**, 46–53.

Ullmann, J. F. P., Gallagher, T., Hart, N. S., Barnes, A. C., Smullen, R. P., Collin, S. P., and Temple, S. E. 2011. Tank color increases growth, and alters color preference and spectral sensitivity, in barramundi (*Lates calcarifer*). *Aquaculture* **322–323**, 235–240.

Valdimarsson, S. K., and Metcalfe, N. B. 2001. Is the level of aggression and dispersion in territorial fish dependent on light intensity? *Animal Behaviour* **61**, 1143–1149.

Valen, R., Jordal, A. E. O., Murashita, K., and Rønnestad, I. 2011. Postprandial effects on appetite-related neuropeptide expression in the brain of Atlantic salmon, *Salmo salar*. *General and Comparative Endocrinology* **171**, 359–366.

Van Rijn, J., Tal, Y., and Schreier, H. J. 2006. Denitrification in recirculating systems: Theory and applications. *Aquacultural Engineering* **34**, 364–376.

Venugopal, V., and Shahidi, F. 1996. Structure and composition of fish muscle. *Food Reviews International* **12**, 175–197.

Vera, L. M., and Migaud, H. 2009. Continuous high light intensity can induce retinal degeneration in Atlantic salmon, Atlantic cod and European sea bass. *Aquaculture* **296**, 150–158.

Vera, L. M., Davie, A., Taylor, J. F., and Migaud, H. 2010. Differential light intensity and spectral sensitivities of Atlantic salmon, European sea bass and Atlantic cod pineal glands ex vivo. *General and Comparative Endocrinology* **165**, 25–33.

Verleih, M., Borchel, A., Krasnov, A., Rebl, A., Korytář, T., Kühn, C., and Goldammer,

T. 2015. Impact of thermal stress on kidney-specific gene expression in farmed regional and imported rainbow trout. *Marine Biotechnology* **17**, 576–592.

Villamizar, N., Vera, L., Foulkes, N. and Javier, S.V. 2013. Effect of Lighting Conditions on Zebrafish Growth and Development. *Zebrafish*. **11**, 173-181.

Wall, T., and Bjerkas, E. 1999. A simplified method of scoring cataracts in fish. *Bulletin of the European Association of Fish Pathologists* **19**, 162–165.

Walls, G. L. 1942. The vertebrate eye and its adaptive radiation. Cranbrook Institute of Science, Bloomfield Hills, USA.

Wang, Z., Gerstein, M., and Snyder, M. 2009. RNA-Seq: a revolutionary tool for transcriptomics. *Nature Reviews Genetics* **10**, 57–63.

Wańkowski, J. W. J. 1981. Behavioural aspects of predation by juvenile Atlantic salmon (*Salmo salar* L.) on particulate, drifting prey. *Animal Behaviour* **29**, 557–571.

Wargelius, A., Fjelldal, P. G., Benedet, S., Hansen, T., Björnsson, B. T., and Nordgarden, U. 2005. A peak in gh-receptor expression is associated with growth activation in Atlantic salmon vertebrae, while upregulation of igf-I receptor expression is related to increased bone density. *General and Comparative Endocrinology* **142**, 163–168.

Warren, I. A, Ciborowski, K. L., Casadei, E., Hazlerigg, D. G., Martin, S., Jordan, W. C., and Sumner, S. 2014. Extensive local gene duplication and functional divergence among paralogs in Atlantic salmon. *Genome Biology and Evolution* **6**, 1790–1805.

Warton, D. I., and Hui, F. K. C. 2011. The arcsine is asinine: The analysis of proportions in ecology. *Ecology* **92**, 3–10.

Wedemeyer, G. A., Saunders, R. L., and Clarke, W. C. 1980. Environmental factors affecting smoltification and early marine survival of anadromous salmonids. *Marine Fisheries Review* **42**, 1-14.

Wendelaar Bonga, S. E. 1997. The stress response in fish. *Physiological Reviews* **77**, 591-625.

Weyts, F. A. A., Cohen, N., Flik, G., and Verburg-van Kemenade, B. M. L. 1999. Interactions between the immune system and the hypothalamo-pituitary-interrenal axis in fish. *Fish and Shellfish Immunology* **9**, 1–20.

Wheeler, T. G. 1982. Color vision and retinal chromatic information processing in teleost: A review. *Brain Research Reviews* **4**, 177–235.

Wickham, H. 2009. *ggplot2: Elegant graphics for data analysis*. Springer-Verlag, New York.

Wickham, H., and Francois, R. 2016. dplyr: A grammar of data manipulation. Retrieved from https://cran.r-project.org/package=dplyr

Widmaier, E. P., Raff, H., and Strang, K. T. 2008. *No Human Physiology: The mechanims of body function, 11th edition*. McGraw-Hill Higher Education, New York.

Winter, B. 2013. A very basic tutorial for performing linear mixed effects analyses. *arXiv Preprint arXiv:1308.5499*.

Winter, B. 2015. A very basic tutorial for performing linear mixed effects analyses: Tutorial 2.

Witten, P. E., Obach, A., Huysseune, A., Baeverfjord, G. 2006. Vertebrae fusion in AtaIntic salmon (Salmo salar): development, aggravation and pathways of containment. *Aquaculture* **258**, 164–172.

Witten, P. E., Gil-Martens, L., Huysseune, A., Takle, H., & Hjelde, K. 2009. Towards a classification and an understanding of developmental relationships of vertebral body malformations in Atlantic salmon (*Salmo salar*). *Aquaculture* **295**, 6–14.

Wood, A. W., Duan, C., and Bern, H. A. 2005. Insulin-like growth factor signaling in fish. *International Review of Cytology* **243**, 215-285.

Yamanome, T., Mizusawa, K., Hasegawa, E-I., and Takahashi, A. 2009. Green light stimulates somatic growth in the barfin flounder *Verasper moseri*. *Journal of Experimental Zoology. Part A, Ecological Genetics and Physiology* **311**, 73–79.

Yanez, J., Meissl, H., and Anadon, R. 1996. Central projections of the parapineal organ of the adult rainbow trout (*Oncorhynchus mykiss*). *Cell and Tissue Research* **285**, 69–74.

Yau, K-W., and Hardie, R. C. 2009. Phototransduction motifs and variations. *Cell* **139**, 246–264.

Yu, G., Wang, L-G., Han, Y., and He, Q-Y. 2012. clusterProfiler: an R package for comparing biological themes among gene clusters. *OMICS: A Journal of Integrative Biology* **16**, 284–287.

Zhu, X., Bührer, C., and Wellmann, S. 2016. Cold-inducible proteins CIRP and RBM3, a unique couple with activities far beyond the cold. *Cellular and Molecular Life Sciences* **73**, 3839–3859.

Zimmer, M., Gray, J. M., Pokala, N., Chang, A. J., Karow, D. S., Marletta, M. A.,

Hudson, M. L., Morton, D. B., Chronis, N., and Bargmann, C. I. 2009. Neurons detect increases and decreases in oxygen levels using distinct guanylate cyclases. *Neuron* **61**, 865–879.

Zydlewski, J. D., McCormick, S. D., and Shrimpton, J. M. 1997. Temperature effects on osmoregulatory physiology of juvenile anadromous fish. In: Wood, C. M., and MacDonald, D. G. (Eds.), *Global Warming: Implications for Freshwater and Marine Fish* **69**, 279-301. Society for Experimental Biology Seminar Series, Cambridge University Press, Cambridge.